社会的・職業能力育成プログラムに資する認知・脳科学的エビデンス情報提供基盤の構築

平成 26 年度～平成 30 年度

私立大学戦略的研究基盤形成支援事業

研 究 成 果 報 告 書

令和元年 5 月

学校法人梅檀学園 東北福祉大学
感性福祉研究所 健康科学研究センター
研究代表者　小川 誠二

「研究成果報告書によせて」

東北福祉大学 感性福祉研究所
健康科学研究センター
特任教授　小川誠二

最近に於ける脳科学の著しい進歩の内で、機能的 MRI (fMRI) は脳活動がマクロな機能ネットワークを組んで進む事を示してきた。 我々は、さらに教育の場で意味のあるヒトの特性（社会性、知能、情動など）や職業適性などにつき、心理データと fMRI データを統合することによってそれらの心理・行動特性の脳内表現を求め、教育現場での活動に資する事を目指し、平成 26 年度採択の私立大学戦略的研究基盤形成支援事業として「社会的・職業能力育成プログラムに資する認知・脳科学エビデンス情報提供基盤の構築」をそのプロジェクトとした。昨今の教育現場には、教育者らの実践の妥当性や、学習者の行動について認知・脳科学研究の知見・エビデンスから検討しようとする動向があり、本事業の取り組みは、このような教育現場に焦点を合わせて、認知・脳科学的基盤技術の提供を目指す極めて重要な事業である。

心の働きやそれを司る脳の機能は、教育や訓練、職業、成人までに形成されたパーソナリティ特性等に依存して、適応的に変化すると考えられる。この変化は認知・脳機能の最たる特徴（可塑性）であり、本研究では、教育・職業・パーソナリティ等の要因がいかにして認知・脳機能をダイナミックに変容させるかを、大学在籍期間の数年にわたって追跡する縦断研究と、年齢や職業経験の点で異なる集団間の変動を比較する横断研究とを統合して問題を理解する努力がなされてきた。

更に、これまでの認知・脳科学研究の成果は、個々人に共通する法則性・全体的傾向に着目したものであるのに対して、ケース（個人）をいかに理解するかに着目しなければならない教育現場に役立てるべく、個々人の社会的・職業的能力の定量的な推定・理解・育成を志向した研究を展開した。

上記の研究目的に沿い、その企画実行により、ヒトの各種心理・行動特性を総合的に評価した心理指標のセットとそれに対応する MRI データからなる中規模のデータベースの構築、さらに心理指標を表現する脳部位とネットワークからなるテンプレート（TFU template）の作成が完了した。さらに、それらを用いたヒト特性推定器・職業適性推定器の開発と、その推定器による縦断的可塑性の検出を可能にしたことから、“個々人”に焦点を当てる本研究事業の目標に沿うことができた。得られた成果が大学等の教育機関・高齢者福祉施設・医療機関での社会的・職業能力育成プログラムの改善支援などへつながることを期待している。

目　次

序文　「研究成果報告書」によせて

Ⅰ　年度別活動報告

Ⅱ　研究成果の概要

Ⅲ　外部評価

Ⅳ　研究業績

Ⅰ　年度別活動報告

平成26年度　健康科学研究センター年次報告

1．諸　言

健康科学研究センターは、本学感性福祉研究所が平成20-24年度の５年間に亘って実施した文部科学省私立大学戦略的研究基盤形成支援事業によるプロジェクト「児童青年期精神障害および高齢者関連疾患における先進的個別化予防システムの構築に関する研究」の主体として、既存の感性福祉研究センターと並列して設置された組織である。研究期間の終了に伴い、当該プロジェクトは解散となったが、同センター所属であった本学の研究者は、プロジェクトを契機に研究所に構築された設備・備品、学内外施設との交流や情報ネットワークを含む研究基盤を活用し、引き続きグループ体制で研究に取組んでいた。

そのような流れの中、児童青年期精神障害研究グループとMRI研究グループの元メンバー有志が中心となって、大学の役割である教育や社会貢献活動に寄与できるような新しい研究をしようという機運が徐々に高まり、今後の研究の方向性について模索を続けた。その結果、MRI研究と心理学的研究を統合的に行う事によって、人間の志向・特性・潜在能力といった、我国ではこれまで質問紙への回答や面接結果などから特定されてきた項目について、その背景となっている脳機能の特徴という生物学的根拠を提供できるのでは、という着想を得た。

近年は、タクシー運転手や楽器演奏者、運動選手、棋士など、訓練を受けることによって社会的に確立した職業人における各種の身体能力と脳機能の特徴との対応を明らかにする研究が、国際紙にもしばしば登場している。大学の教育機関としての特徴を活かし、教育の過程で生じる様々な能力の変化と脳機能の変化とを並行して捉えてゆくことは可能であり、上記のような職業人における各種能力と脳機能特性との対応に関する知見を基に、被教育者の社会的適性が推断できるようになることも期待できる。

そこで、平成26年度文部科学省私立大学戦略的研究基盤形成支援事業による助成を受け、「社会的・職業能力育成プログラムに資する認知・脳科学的エビデンス情報提供基盤の構築」という課題を掲げた新しいチームが発足した。プロジェクトへ参加する研究者は、小川誠二特任教授を代表者とする総勢23名の厳選されたメンバーとなった。研究期間は、平成26-30年度の５年間であり、初年度は主に研究設備の設置などを含む準備期間とされた。このため、本稿では、まず研究プロジェクトの全体像について申請時の構想調書等を基に述べ、次いで26年度の進捗状況を報告する。

2．研究プロジェクトの概要

(1) 研究プロジェクトの位置付け

本プロジェクトは、大学の中心テーマである「感性の涵養」・「福祉社会を担う人材の養成」を実現するための社会的・職業能力育成プログラムを定量的に評価し、最適化する課題に答える１つのアプローチとして認知・脳科学的エビデンスを提供する基盤を構築するものである。これは、大学教育に資することはもちろん、研究対象（大学生から高齢者まで）を変えていくことで地域社会における職業選択・人材選択の有益な手がかりとなりうる。そして、本研究で提供される情報提供基盤は当該研究期間の終了後も成長し続けるものとなることが期待できる。大学等の教育機関における社会的・職業能力育成プログラムのもたらす効果の測定・評価は、教育・学習の質を保証する上で極めて有効であり、プログラムの効果を学習者に定量的に示すことは学習意欲の向上へとつながる。また、本プロジェクトは、プログラムの効果を示す新たな客観的評価基準として認知機能とそれを実現する脳機能の測定結果を提供するものである。この課題の実現に向けて、数年にわたる変化を視野に入れた定期測定及び若年者と高齢者を対象とした横断研究を展開する。認知課題及び質問紙の成績、脳活動・脳内ネットワーク・脳構造の時間的変化を通して、

教育や職業経験により成熟が認められる側面並びに社会的・職業能力が育成されていく過程を捉え、教育現場や職業選択の際の一助となる情報提供基盤につなげていく。

(2) 研究内容の概要

①個人の認知・脳機能の変動からみた社会的・職業的能力の推定

教育・スポーツ・音楽等の来歴が社会的能力・職業適性に及ぼす影響を認知機能指標と客観的な脳活動・構造指標から評価する指針を提案し、教育現場へのフィードバックを行う。特定の教育や文化活動の影響下にある個人の安静時 / 刺激時脳活動・脳形態を定期的に計測し、脳固有の情報と性格検査・社会的スキル尺度・職業適性検査等および新規に作成する認知課題との相関を分析すると共に個人の性格特性をも予測する。期間ごとにデータを整理し、認知機能と脳機能ネットワークの強度・分布を関連づけて検討する。異なる教育を受けている集団間の比較も行う。

②加齢や職業により発達する社会的・職業的能力の同定

加齢や職業経験・業種が認知機能・脳構造 / 機能に与える影響を定量化し、成熟した認知・脳機能を特定し、職業選択サポートの一助となる情報提供を目指す。社会生活で生じる様々な認知・感情を喚起させる心理課題、社会的スキル尺度・職業適性検査を年齢や業種の異なる集団に課して脳機能・形態計測を行う。加齢や職業経験に伴う課題成績変化、脳構造・機能等の脳固有の情報からわかる潜在的変化から、対象者の社会的・職業能力を同定する。

③パーソナリティや精神障害を反映する客観的指標の提案

精神障害と関連するパーソナリティを保持する人を対象とした実験的研究から客観的評価の難しい精神障害を予測する認知・脳機能マーカーを創出し、予防ケアや円滑な社会生活、就業支援を促す技術基盤の形成を目指す。精神障害関連パーソナリティ特性の強い群と弱い群を対象に認知課題中 / 安静下の脳活動計測・構造計測を行う。群間での認知課題成績、脳活動・構造の差異を比較する。

④認知・脳機能の高精度測定法・データ分析方法の開発

実験の精度・妥当性を高めるため、装置のアップデート、信号 / 雑音比を改善する測定シーケンスとデータ処理プログラムの開発、高速測定法の実用化、速い応答特性を持つ fMRI 信号測定法の開発、脳機能計測時に課す心理課題の最適化等の技術革新に取り組む。

3．研究の学術的な特色と意義

(1) 認知・脳機能の中期・長期的変化を捉える縦断・横断研究によるマトリクス的アプローチ

本研究の特色は、個人の認知機能・脳機能を、A: 大学在籍期間の数年にわたる長期的時間スケールで追跡計測する縦断研究、B: 加齢や職業経験という点で異なる集団での変動、精神障害等と関連するパーソナリティ特性の強弱という点で異なる集団での変動を比較する横断研究を統合したマトリクス的アプローチにある。従来、教育経験や職業経験に伴って適応的に変化する認知機能、さらには脳機能を大学在籍期間の数年間にわたり縦断的に調べる研究は皆無に等しかったが、本プロジェクトでは多数の被験者を対象とした長期にわたる定期計測を実現することができる。さらに、縦断研究が難しい数十年単位といったライフスパンでの認知・脳機能変化をも捉えるために若年者と高齢者を対象に横断研究を行うことで、人の認知・脳機能変化を包括的に測定・評価することが可能となる。すでに若年者と高齢者を対象とした社会的認知に関する研究に着手し、着実にノウハウが確立されており、実現可能性は極めて高い。

(2) 教育効果・職業経験・パーソナリティへの着目

近年の認知・脳科学研究では言語習得に伴う認知・脳機能変化が着目されているが、社会の中で適応的に行動する人々の理解と育成に向けては、教育・職業・パーソナリティ等の人間行動の広範にわたり影響を与える要因に着目することが必須である。このため、対象者の生活環境・職業経験の情報、可能な限り多くの心理指標（社会的スキル・パーソナリティに関する質問紙と認知心理学実験）と MRI による脳機能画像・構造画像・脳内ネットワーク解析を組み合わせ、各指標の因果・相関関係を統計学的手法により抽出し、社会的・職業能力データベース作成を進めていく。

(3) 個々人の脳機能を総合的に計測するための MRI 測定・データ分析法の確立

本プロジェクトでは従来の MRI 計測の時空間分解能を飛躍的に（時間分解能：従来の約十数倍、空間分解度：従来の約二十数倍）向上させた測定技術を用いることで個人の脳の特性を正確に捉えることができる。さらに脳皮質、白質、賦活量等の構造・機能データといった異なる時空間特性をもつ多次元情報を統合的に扱える MRI 測定・分析プロセスを構築することで複雑な認知と脳の関係について包括的に理解するための道筋を示す。

4．期待される成果

(1) 社会的・職業的能力への教育効果を定量化でき、さらに定期測定により教育効果の発現に要する期間等の評価指針を提供できる。

(2) 個人が成熟したと考える職業的能力、施設関係者等のサポート側が必要と考える職業的能力を認知機能と脳機能の両面から定量化し、情報提供する仕組みを構築できる。

(3) 精神障害と関連するパーソナリティ特性の強い群と弱い群との違いを、認知課題成績や脳活動、脳内ネットワークにおける 3 尺度の違いとして表現し、精神障害や社会生活への影響を予測する客観的尺度を提供できる。

(4) 脳活動データの精度向上と短時間測定が可能となり、個人の fMRI 測定から得られる情報内容・量ともに飛躍的に向上させられる。また速い応答信号の検出により脳機能ダイナミックスの情報が取得できる。fMRI の分野を進展させ、従来の時間限界を超えた新たな認知・脳機能計測法を提供する。

5．研究組織

統括：小川誠二（東北福祉大学・特任教授）

グループ A「先端的 fMRI 測定法の開発」:

成烈完（東北福祉大学・特任准教授）、姜大勲（東北福祉大学・特任研究員）、亀井裕孟（東北福祉大学・特任研究員）、加藤和夫（東北学院大学・准教授）

グループ B －①「加齢・職業経験の異なる集団の認知・脳機能を比較する横断研究」:

藤井俊勝（東北福祉大学・教授）、庭野賀津子（東北福祉大学・准教授）、河村孝幸（東北福祉大学・准教授）、田邊素子（東北福祉大学・講師）、幕内充（国立障害者リハビリテーションセンター・室長）、奥田次郎（京都産業大学・准教授）、月浦崇（京都大学・准教授）、阿部修士（京都大学・特定准教授）、姜東植（琉球大学・准教授）

グループ B －②「パーソナリティの異なる集団の認知・脳機能を比較する横断研究」:

浅野弘毅（東北福祉大学・教授）、小松紘（東北福祉大学・教授）、松江克彦（東北福祉大学・教授）、滝井泰孝（東北福祉大学・教授）

グループ C「個人の認知・脳機能変動を追跡計測する縦断研究」:

坪川宏（東北福祉大学・教授）、大城泰造（東北福祉大学・准教授）、曽根稔雅（東北福祉大学・講師）、河地庸介（東北福祉大学・特任講師）、山本絵里子（東京大学・研究員）

6．平成26年度の進捗

(1) 取組の内容

縦断研究においての心理・行動データ収集分析はグループC、横断研究での心理・行動及びMRIデータ収集分析はグループB、縦断研究のMRIデータ収集分析及び神経回路網などの推定プログラムの作成はグループAで主に担当しながら、役割の分担を可変的に行うなどの有機的な連携のもとで研究を進めている。具体的な実施内容は以下のとおりである。

①職業適性や社会的能力の可塑性・発達を捉えるのに有効と考えられる心理測度（質問紙・認知課題等）の選定。

②脳の機能及び構造計測を実現するためのMRI装置のアップグレード、マルチモーダルなMRI（機能・構造）画像を収集するための測定方法とMRI画像データ解析法の選定、および予備実験と既存のデータによる選定した解析法の検証。

③横断研究の実施に向けて、職業適性や社会的能力の検討に適した被験者群の設定（年齢の違い、音楽、業種、芸術等の特定スキルの有無で分類した被験者群）とfMRI実験課題の設定。

(2) 成果の公表状況

①論文

Sung Y., Choi U.-S., Ogawa S., Invariance of functional characteristics to task difference at low-level and high-level areas in the ventral visual pathway. J. Behavioral and Brain Science. vol. 4, 402 411.

Chung J.-Y., Sung Y., Ogawa S., Evaluation of the contribution of signals originating from large blood vessels to signals of functionally specific brain areas. BioMed Research International (in press).

Kang D., Sung Y., Kang C.-K., Fast imaging techniques for fMRI: consecutive multi-shot echo planar imaging accelerated with GRAPPA technique. BioMed Research International (in press)

②国際学会発表

Kang D., Sung Y., Shioiri S., Ogawa S., Estimation of functional specificity of visual areas by a transverse relaxation profile. The 10th Asia-Pacific conference on Vision, Takamatsu, Japan, July 19-22, 2014.

Sung Y., Chung J.-Y., Ogawa S., Effects of signals originating from large blood vessels on BOLD signals of the fusiform face area. The 44th society for neuroscience meeting, Washington DC, USA, November 15-19, 2014

Choi u・S., Sung Y., Kim Y.-B., Cho Z.-H., Yoon H., Ogawa S., Functional differences in processing preferred and non-preferred stimuli at object selective areas. The 44th society for neuroscience meeting, Washington DC, USA, November 15-19, 2014

平成27年度　健康科学研究センター年次報告

1．諸　言

健康科学研究センターは、平成26年度文部科学省私立大学戦略的研究基盤形成支援事業による助成を受け、「社会的・職業能力育成プログラムに資する認知・脳科学的エビデンス情報提供基盤の構築」という課題を掲げた研究チームとして、新たなスタートを切った。研究期間は平成26-30年度の５年間、プロジェクトへ参加する研究者は、小川誠二特任教授を代表者とする総勢23名の厳選されたメンバーである。研究設備の整備や機器類の購入・設置、また予備実験の実施などプロジェクト全体の準備を終え、本年度より本格的な研究を開始した。本プロジェクトの概要や研究の特色・意義、研究組織等については、年報16号の同報告、あるいは本プロジェクトのWebサイト（http://www.tfu.ac.jp/research/gp2014_01/index.html）を参照されたい。

研究を遂行するにあたっては、同センターがこれまで委託され実施した私立大学戦略的研究基盤形成支援事業等の実施期間に指摘された様々な事項や、同事業等の最終評価結果に留意し、今後に向けて次の事柄を研究者全員の合意の下に実施した。

1．研究倫理・コンプライアンスの習得を徹底するため、研究者全員にCITI JAPAN PROGRAMによるｅラーニングの受講を義務付け、合格者のみに研究の実施を許可するものとした。
2．研究費等の執行状況をより明白にするため、学外研究者への支払いは精査の上で必要最低限とした。
3．当初の研究計画書に記載のない研究補助者（ポストドクター等）の採用は控えた。
4．人的資源を有効に活用し、情報共有によるプロジェクト全体の活性化を図る観点から、各研究者の活動を研究グループ内のテーマに限定することなく、グループ間で有機的に協働することとした。
5．研究成果だけでなく、研究全体の計画やそれを実現するための体制について助言を得るために、期間全体で２回（研究開始後１年、４年）、学外の有識者による外部評価を実施することとした。

上記５の通り、本年度は第一回の外部評価実施年度に相当し、平成28年２月に実施した。以下、本年度の事業進捗状況について述べる。

2．平成27年度経過

(1) 事業の流れ

1）外部評価

以下の要領で、東北福祉大学以外の機関に所属する有識者３名の外部評価委員による書面審査と実地審査が行われた。

①書面審査

事前に送付する評価票に基づき、本事業で取り組んでいる研究の意義・方法・成果について以下の５つの視点から評価頂いた。

ⅰ．研究プロジェクトの意義・新規性
ⅱ．研究計画の妥当性
ⅲ．研究方法の妥当性
ⅳ．進捗状況
ⅴ．今後の展望

②実地審査

日時：平成28年２月13日（土）午前10：00～

場所：東北福祉大学 感性福祉研究所２階 大会議室

次第：

10：00　開　　会

開会挨拶　　副所長　松江 克彦

Ⅰ．外部評価委員の紹介

外部評価委員　　出江 紳一（東北大学大学院 医学系研究科　教授）

外部評価委員　　松岡 和生（岩手大学 人文社会科学部　教授）

外部評価委員　　福永 雅喜（自然科学研究機構 生理学研究所　准教授）

Ⅱ．本事業の取り組みについて（報告）

研究代表者　小川 誠二

12：00　昼　食（ランチミーティング）

Ⅲ．研究施設（MRI）の紹介

Ⅳ．外部評価委員による評価ならびに助言

15：00　閉　　会

閉会挨拶　　研究代表者　小川 誠二

なお、外部評価結果は「４．外部評価の結果（最終評価票より）」の通りである。

２）コアメンバー会議

下記の要領で実施された。

平成27年５月27日（16：00－17:30）　…　出席者（敬称略）　小川、坪川、藤井、成、河地、岩田

平成27年７月８日（16：00－17:30）　…　出席者（敬称略）　小川、坪川、藤井、成、河地

平成27年９月９日（16：00－17:30）　…　出席者（敬称略）　小川、成、河地、押江、岩田

平成27年11月11日（16：00－17:30）　…　出席者（敬称略）　小川、坪川、藤井、成、河地、押江、岩田

平成27年12月16日（16：00－17:30）　…　出席者（敬称略）　小川、坪川、成、河地、押江、岩田

平成28年１月20日（16：00－17:30）　…　出席者（敬称略）　小川、坪川、成、押江、岩田

平成28年３月23日（16：00－17:30）　…　出席者（敬称略）　小川、坪川、藤井、成、押江、岩田

(2) 経費執行状況

平成27年度における、研究費執行状況は、以下のとおりである。

	予算額［千円］	実績額［千円］	執行率
研究費	27,152	25,774	95%

(3) グループ別進捗状況

Ⅰ．グループＡ

テーマ：「先端的 fMRI 測定法の開発」

研究者：成烈完（東北福祉大学・特任准教授）、姜大勲（東北福祉大学・特任研究員）、亀井裕孟（東北福祉大学・特任研究員）、加藤和夫（東北学院大学・准教授）

研究の状況：

大学在籍期間中の教育・訓練による脳の可塑的変化を計測するためのマルチモーダルなMRI（機能・構造）画像を収集した。前年度設定しておいた解析方法により収集した画像データから社会性・学習に関連する脳の部位の同定と機能ネットワークの推定を行った。

これにより、社会的・心理的指標を反映する脳のテンプレートの作成が出来た。このテンプレートをベースとして、脳の可塑的変化を縦断的に追跡できる。また、特定の訓練（音楽・運動・認知）に伴う脳の可塑的変化を調べた。また、機能的高分解能の測定方法により脳のミクロ的な機能活動の検出をも試みた。

（測定期間：2015年4月－2016年3月、被験者数：206名（のべ309名））

Ⅱ．グループB

テーマ：①「加齢・職業経験の異なる集団の認知・脳機能を比較する横断研究」 ②「パーソナリティの異なる集団の認知・脳機能を比較する横断研究」

研究者：藤井俊勝（東北福祉大学・教授）、庭野賀津子（東北福祉大学・教授）、河村孝幸（東北福祉大学・准教授）、田邊素子（東北福祉大学・准教授）、幕内充（国立障害者リハビリテーションセンター・室長）、奥田次郎（京都産業大学・准教授）、月浦崇（京都大学・准教授）、阿部修士（京都大学・特定准教授）、姜東植（琉球大学・准教授）、浅野弘毅（東北福祉大学・教授）、小松紘（東北福祉大学・特任教授）、松江克彦（東北福祉大学・教授）、滝井泰孝（東北福祉大学・教授）

研究の状況：

現代の複雑化した社会の中で、どのように人々が職業を選択し、適応的に生きているか明らかにすることは、学術的に重要であるだけでなく、人間社会の今後の方向性を占っていく上でも重要な課題である。本年度は、保育士を目指して実習に行くグループと実習に行かないグループで乳幼児の顔を見たときの脳活動の変化をfunctional MRIを用いて同定した。

具体的には、（研究1）46名の学生に対して、快・不快・どちらでもない表情の乳幼児の顔をみせ、fMRIを施行した。併せて、性格特性を評価した。その結果、不快な表情をみているときに、良心（誠実さ）のスコアと眼窩前頭皮質のBold signalに負の相関がみられた。（研究2）21名の実習経験学生と25名の実習未経験学生を対象に実習期間前後のfMRIを施行した（刺激は上記（1）と同様）。実習経験学生のグループのみで、実習後に、不快な顔に対して右扁桃体の活動低下が認められ、すべてのタイプの顔に対して左紡錘状回の活動低下が認められた。

今年度はこれらの知見を基に、実際に働いている保育士の専門性を明らかにすべく、fMRIを用いた検討を重ねていく予定である。

Ⅲ．グループC

テーマ：「個人の認知・脳機能変動を追跡計測する縦断研究」

研究者：河地庸介（東北福祉大学・特任講師）、大城泰造（東北福祉大学・准教授）、曽根稔雅（東北福祉大学・講師）、坪川宏（東北福祉大学・教授）、山本絵里子（東京大学・研究員）

研究の状況：

大学在籍期間中の教育・訓練による脳の可塑的変化及び職業適性に関する心理データを行動実験、心理検査および質問紙で計測を行った。また、得られたデータをもとに種々の認知機能間の関係性について相関分析・重回帰分析・共分散構造分析などの解析方法を用いて検討を行った。

従来十分に検討されていなかった一般知能・情動知能・職業適性（能）の独立性と関連性を推定することができた。また、教育・訓練の影響を受ける認知・心理変数を導出するために特定の認知課題（実行機能・メタ認知関連）による行動実験を行った。

（測定期間：2015年４月－現在、被験者数：236名（のべ487名））

3．業績

（論文）

1．Sung Y, Kawachi, Y, Choi U-S, Kang D, Ogawa S. Modality dependent sensitivity in evaluating brain prasticity. Report of Kannsei Fukushi Research Institute（in press）

2．Nazari　Z, Kang D, Kawachi Y, Sung Y, Ogawa S, Hierarchical clustering of fMRI Data. Report of Kannsei Fukushi Research Institute（in press）

3．Choi US, Sung Y, Hong Sujin, Chung JY, Ogawa S, Structural and functional plasticity specific to musical training with wind instruments. Front. Hum. Neurosci. 9 : 597. doi: 10.3389/fnhum.2015.00597

4．Chung JY. Sung Y. Ogawa S. Evaluation of the contribution of signals originating from large blood vessels to signals of functionally specific brain areas. Biomed Res Int. vol. 2015; 2015: 234345.（H26年度投稿論文の H27年度掲載）

5．Kang D. Sung Y. Kang C.-K. Fast imaging techniques for fMRI: consecutive multi-shot echo planar imaging accelerated with GRAPPA technique. Biomed Res Int. vol. 2015; 2015: 394213.（H26年度投稿論文の H27年度掲載）

6．阿部千裕・河地庸介・坪川宏・成烈完・小川誠二．一般知能と主観的実行機能の関連性．感性福祉研究所年報（in press）

（国際学会）

1．Sung Y, Microscopic functional structures seen through fMRI signals. BIT's 6th annual world congress of neurotalk-2015, Hanzhou, China, May 22-24, 2015.

2．Choi U-S, Sung Y., Chung J-Y, Ogawa S. Brain plasticity seen in musicians of wind instruments. 21st annual meeting of the Organization for Human Brain Mapping, Hawaii, USA, Jun 14-18, 2015.

3．Kang D, Sung Y, Shioiri S. Ogawa S, Investigation of microscopic functional specificity for attention in peripheral visual field. 21st annual meeting of the Organization for Human Brain Mapping, Hawaii, USA, Jun 14-18, 2015.

4．Sung Y, Kang D, Ogawa S, Robustness of microscopic functional structures estimated by dynamic magnetic susceptibility change. The 21st annual meeting of the Organization for Human Brain Mapping, Hawaii, USA, Jun 14-18, 2015.

5．Sung Y, Yoon H, Choi U-K, Ogawa S, Regional difference in characteristics for top-down modulation in the ventral visual stream. The 45th annual meeting of the Society for Neuroscience, Chicago, USA, Oct 17-21, 2015.

6．Sung Y, Kang D, Ogawa S, Morphological changes in cortical microstructure of the brain by short-term training. The 45th annual meeting of the Society for Neuroscience, Chicago, USA, Oct 17-21, 2015.

7．Ogawa S, Macro-scale structure and function of the brain visualized by MRI, Gachon Univ. NRI Symposium, Incheon, Korea, Feb 24, 2016

（国内学会）

1．小川誠二 「fMRI の昨今」、熊本大学イメージングセンターセミナー、５月７日、熊本

2．小川誠二 「MRI でみる脳機能活動の幾つかの側面」、東芝開発研究センターセミナ、６月19日、川崎

3．小川誠二 「機能的 MRI の開発と発展」、東京慈恵会医科大学総合医科学研究センター創立20周年記念シンポジウム　基調講演、11月４日、東京

4．小川誠二 「MRI によるマクロスケールでの脳の構造と機能の可視化」、理研光量子工学研究センター、2016年１月15日、和光

5．Niwano K, Ito A, Tanabe M, Sato Y, Fujii T. Relationship between regional brain responses to infant faces and personality traits in young female adults. 31st International Congress of Psychology, July 24-29, 2016, Yokohama, Japan.

6．Tanabe M, Ito A, Niwano K, Sato Y, Fujii T. Correlations between the brain responses of nulliparous females when viewing infants' facial expressions and their personality. 31st International Congress of Psychology, July 24-29, 2016, Yokohama, Japan.

7．Ito A, Niwano K, Tanabe M, Sato Y, Fujii T. The effect of childcare training on the perception of infant's emotional facial expression. 31st International Congress of Psychology, July 24-29, 2016, Yokohama, Japan.

４．外部評価の結果（最終評価票より）

(1) 評価委員氏名：出江　紳一（東北大学大学院 医学系研究科 教授）

①研究プロジェクトの意義・新規性

社会的・職業的能力を脳科学により推定することをそれらの育成プログラムに役立てるというビジョンは重要であり、かつ新規性がある。

②研究計画の妥当性

心理指標、脳機能画像の予備実験、データ収集、中間評価、ブラッシュアップという流れ、ならびに項目ごとの研究計画は妥当であると考える。

③研究方法の妥当性

方法として、心理行動特性のパターンと脳機能画像のパターン（脳ネットワーク）を対応させ、それらの可塑的変化を捉える構成となっており、妥当であると考える。なお、可塑的変化を誘導する介入の個々のセッションにおける短期効果と、セッションの繰り返しによる長期効果の関係を明らかにする方法を加えることにより、より質の高い研究になると思われる。

④進捗状況

心理学的研究、MRI 研究のそれぞれですでに100名以上のデータが取得・解析されており、順調な進捗状況であると考える。

⑤今後の展望

今後の縦断的研究の成果に期待する。

⑥総評

意義、新規性の高い研究である。研究計画ならびに方法は妥当であり、予定に合致した成果が上がっている。

⑦メモ（自由記載。評価対象とはせず、今後の研究推進の一助とする）

評価資料に倫理委員会の承認書がみられなかった。被験者の多くは、在学学生であると推測されるため、倫理委員会、該当すれば利益相反委員会などの審査結果を開示する必要があると考える。

(2) 評価委員氏名：松岡　和生（岩手大学 人文社会科学部 教授）

①研究プロジェクトの意義・新規性

本研究プロジェクトは、教育効果、職業キャリア訓練、パーソナリティ等の要因がいかにして認知・脳機能をダイナミックに変容させるかを、心理・行動データ及びMRI脳機能データにより計測・評価するものであり、そのために本研究では、年齢や職業経験などの点で異なる集団間を比較する横断的研究と大学在籍期間の数年にわたって追跡する縦断研究が行なわれる。

本研究では人間能力の社会性に焦点が当てられ、その個人差とその可塑性（訓練、変化の可能性）に着眼点がある。そこに脳レベルでのエビデンスを与えるという点で、大きな特徴を有する研究になっている。その意義は大きく、学術的、社会的な貢献度の高い極めて重要な研究である。

具体的には、以下のような点に意義、新規性が認められる。

・従来、取り扱いが難しいとされている心理・行動課題への応答及びMRIの脳機能測定における個人差を検証しようとしている点
・個々人の能力・資質の訓練可能性、可塑性に対する着眼：ポジティブ心理学でいうところの人間の「強み（strength)」の育成・成長を見据えている点
・方法的には、①従来、質問紙尺度研究（自己報告、自己意識レベル）にとどまっている個人の性格や資質を、脳構造や脳機能の個人差から捉え直すことができる。②脳構造解析（VBM解析による）と脳機能解析（fMRIによる）の統合アプローチの採用されており、脳構造・機能データを統合的に扱うMRI測定・分析プロセスを構築されれば、その応用的な価値は高い。③安静状態脳活動の機能的結合（=DMN）の個人差データがベースとなっているが、Resting State fMRIの先端的データ解析を適用した研究として注目できる。
・実社会に活用可能な社会的コンテクストにおける個人の能力の違い（個人差）を脳ベースで捉えようとしている点、いわゆる「社会脳」研究の進展に寄与できる研究である。
・近年、国の施策として、国民総幸福量が注目され、幸福度指標に対する社会の関心が高くなっている。人の幸福感あるいはウェルビーイングの研究において、脳機能レベルでのエビデンスを提供できるという点で、大きな貢献が期待される。
・本研究PJのように同一集団の多数の大学生を対象に、数年間にわたって縦断的に心理・行動的データとMRI計測に基づく脳構造／機能データを大規模に収集するような研究の実施は容易なことではないことから、その研究成果に対する期待は学術的、社会的にも大きいと考える。

②研究計画・方法の妥当性、

同一集団を対象とし、縦断的に行動、認知能力、人格特性、社会性等の変化を脳構造／機能レベルと対応させ、さらに、異なる年齢（若年者と高齢者）・属性・能力をもつ集団に対する横断研究を組み入れた手法によって検討する方法は、画期的な手法であり、研究目的を達成する上で、極めて妥当で有望な方法

である。

心理指標に関して、本研究で採用されているIQ（知能指数）, EQ（情動知能指数）、社会的スキル、EF（実行機能）、職業適性検査、及び主観的幸福感は、心理指標としての妥当性が学人されている標準化された指標であり、認知・社会的能力を査定するうえで適切な選択と思われる。社会性に関わる19個の質問紙尺度も本研究の関心領野をカバーしており、考え得る範囲で、本研究で考慮すべき側面を網羅する指標が含まれており、社会性及び職業適性と脳構造／機能との関連を見ていく上で妥当である。

③進捗状況

H.27年度までの研究で、計画通り心理指標データの収集済みであり、今年度研究では、職業適性や社会的能力の予測力のデータも示されている。心理・行動指標間の関係性について共分散構造分析等の統計手法によって確認していく作業は今度の課題である。MRIデータに関しては、脳構造データとしてはVBM、脳機能データとしてはResting State fMRIを使った計測が進められている。いずれも大きな成果が期待できる解析手法である。心理指標との関連に関して基礎的な検討が行われ、すでにいくつかの研究成果が得られており、計画にそって研究は順調に進展していると評価できる。心理指標と安静期脳活動のネットワークとの関連については、社会的・情動的心理データ80項目中53項目のネットワークの同定されている。また、社会性関連心理指標に対応する脳部位及びネットワークについても、たとえば、行動抑制・活性化システム（欲求、報酬）、あるいは、自己成長主導（積極的行動、計画性、変化への準備）に関連する脳部位とネットワークのHub脳部位が同定されているおり、今後の研究に繋がる成果として評価したい。

長期・中期・短期的な可塑的変化の検証では、①長期的な可塑性変化として、中学・高校からの継続的吹奏楽経験者に対するMRI解剖・機能画像の測定、②中期的な可塑的変化としては、大学期間中（22ヶ月間）の学生１ケースの解析、③短期的な可塑的変化では、１）認知課題を用いた学習効果の検討と２）大学生、４週間の保育実習前後の赤ちゃんの顔に対する脳活動変化が検討され、いずれも興味深い知見が得られている。

④今後の展望

・本研究プロジェクトは、いうまでもなく、その成果はきわめて直接的な社会貢献に結びつくものと思われる。個々人の知的能力や性格、資質あるいはそれらを変容させうる教育効果、訓練効果に脳構造／機能レベルでエビデンスを与える手法が確立されるならば、心理学、認知科学、脳科学の分野だけでなく、大学教育、職業キャリア教育、科学や芸術における創造的能力の開発、本人に自覚されない隠された能力の発見、スポーツ、芸術、音楽におけるトレーニング効果への応用等、その波及効果は広範囲に及ぶことが予想される。また、人生の各段階での生活の質、ウィールビイングや健康長寿の問題に対しても寄与し得る研究になる。

  知性の心理学・認知科学研究への波及効果も考えられる。知能検査に始まる心理学における知性研究は、近年、多重知能理論、社会的知能やサクセスフルインテリジェンス、情動知能、心の理論など、人の知性を捉える枠組みが社会性や情動性にまで広がっている。人間の知的能力の本質的特徴とは何か、社会的・職業的な実践場面において真に必要とされる知的能力とは何か、という問いのもとで展開されてきた諸研究であるが、いずれもその実証的なエビデンスは心理・行動レベルにとどまっている。本研究はこうした人間の知性と感性の理解のための新たな次元の研究へと進む突破口になり得るといっても大げさではないかもしれない。

・パーソナリティ等の心理学における査定研究の分野への波及効果も大きいと思われる。心理学における

個人の性格や資質の研究は、その多くが心理検査や質問紙調査によって行われている。特に、社会的な心理・行動特性に関する研究は、質問紙尺度研究が一般的である。本研究において、脳構造／機能の量的データベースによって、生物学的なエビデンスを容易に提供できることになれば、従来の研究スタイルに大きな変化をもたらす可能性がある。

⑤総評

学術的、社会的な貢献度の高い極めて重要な研究プロジェクトである。研究目的を達成するための研究計画、方法は妥当で、現時点で、研究、データ収集はほぼ計画通りに進行している。一部、すでに先行して進められている部分もあり、研究は順調に進んでいる。研究成果は、社会的にもインパクトが大きいものになると予想されるので、今後の研究成果を期待したい。

⑥メモ（自由記載。評価対象とはせず、今後の研究推進の一助とする）

・今後の研究で、新しい認知・行動能力次元との対応等、追加していくことは可能か、あるいはその必要性はないか？　⇒　担当者説明により、今後追加されて検討予定になっているいくつかの認知・行動次元について確認することができた。
・長期・中期・短期的な可塑的変化の検証の研究に関して：今年度までの研究で、興味深い知見が得られているが、今後は具体的にどのような課題での検討が予定されているか、確認しておきたい。⇒いくつかの研究計画について説明を受けた。
・パターン認知・ラーニングアルゴリズムの開発が進んでいるようだが、これを、個々人の社会性・職業特性または在学期間中の教育・訓練によって発達した機能の推定に利用するということだが、具体的にはどのように適用されることになるのか？
・研究施設、装置を見学させていただき、データ収集の様子などについても説明を受けましたが、本事業の規模を考えると、実際の心理データの収集やMRI撮像データの収集等に対応するための人員は十分ではないように感じました。

(3) 評価委員氏名：福永 雅喜（自然科学研究機構 生理学研究所 准教授）

①研究プロジェクトの意義・新規性

専門的な知識や技能を習得し各分野で活躍が期待される人材の育成は、大学等の高等教育課程に期待される大きな役割である。しかし、その一方、養成課程の検証に応用しうる認知・脳科学的根拠を備えた指標は、これまで十分に検討されていなかった。このような背景のなか、本研究課題は、人材育成の現場において欠くことの出来ない社会的能力・職業能力の獲得、向上をサポートする養成プログラムを前提に、個人が備え持つ認知・心理的素因（パーソナリティ）の寄与、教育・訓練を通じた学習効果による認知機能の変容を、種々のバッテリーによる心理・行動指標とニューロイメージング手法を用いたその神経基盤探索にてアプローチを試みる。本研究の発展は、養成プログラムに対する脳科学的根拠に基づく評価系の創出と、プログラムへの最適化に供与しうる情報提供につながるものであり、従来の研究に類を見ないものであるとともに、本システムを応用することで、ニューロイメージング測定から個々人の社会的・職業的能力の推定を行おうとする挑戦的プロジェクトでもある。本プロジェクトは、ニューロイメージング計測により裏付けされた認知・脳科学的エビデンスのもと、社会的・職業能力育成プログラムの効果・価値を高める基盤構築を掲げており、その意義は明確である。

②研究計画の妥当性

種々のバッテリーによる心理、行動指標にニューロイメージング手法を応用し認知・脳科学的根拠にもとづいてその神経基盤を同定することは、それらの画像指標をもとにヒトの社会性・職業的能力を定量的に評価する上で必要不可欠なステップである。また、社会能力・職業能力的観点から、これらの心理・行動・画像指標により得られる情報が、教育を受けることで如何に変容するかを明らかにするためには、短期・中期・長期的な効果への言及が望まれるが、本研究では、それぞれの段階に対応する縦断的研究および横断的研究が計画されている。個別の認知機能に限定せず、大局的な認知・行動・心理特性の変容を含めた追跡研究として本学の学部学生を対象とする本研究は、被験者が受ける教育課程や職種における統制の観点からも適切であると思われる。５年間の研究計画の前半より計測を開始し、３年目の中間的なデータマイニングから、計測、解析系のリファインを行い、プロジェクト後半の継続したデータ収集と分析法・定量指標の確立へ展開する本研究計画は妥当なものであると思われる。

③研究方法の妥当性

認知・行動・心理特性を構成する機能要素の集合が、社会的能力・職業的能力を表現するとのコンセプトを考えると、現在のところ、これらの能力を包括的に捉えうる単独の質問紙、心理指標は存在しない。従って、既存の手法の相互関係解析をもとに評価要素を再カテゴライズし、これらのカテゴリーに対応する課題実験から客観的に社会的能力・職業的能力を推定できるか検証すること、またこれらの機能要素が教育効果を経て変容する過程の追跡を実施するために、これまで広く普及し応用が進められている心理・行動指標を網羅的に収集する研究スタイルはきわめて妥当である。

一方、ニューロイメージングによる神経基盤探索のために応用される Voxel based Morphometry（VBM）、Resting state fMRI（rsfMRI）、Diffusion tensor imaging（DTI）は、ヒト脳を対象とした構造的、機能的情報抽出の手法として広く応用が進められている。単に、ある特定の脳領域に局在する脳活動のみにフォーカスせず、脳全体を対象としたネットワーク構造として脳機能を捉えようとする本研究は、社会的能力・職業的能力という大局的な認知・行動・心理特性を捉えるためには適切なアプローチである。

④進捗状況

平成26年度から５年間の事業期間に対し、約２年が経過した現時点において、初年度に計画されたデータ収集に使用される心理指標の選定、MRI 装置のアップグレードおよびニューロイメージング計測手法の選定と最適化、予備実験が終了し、今年度からは縦断的研究に供される大学低年次学生を対象とした計測が開始されている。心理指標では計測項目に対する被験者数に差異があるものの総数200名を越えるサンプル収集が、同様にニューロイメージング計測もすでに200名近いサンプルの収集が完了しており、当初の年次計画に沿いプロジェクトが進んでいるものと思われる。

また、収集された多彩な心理指標から、指標間の関連分析も進められており、平成28年度以降に計画されているデータマイニングにおいて必要と予想される、膨大なデータからの効率的な情報圧縮（情報の dimensional reduction）の初期検討も開始されている。とくに社会性に関する指標では、再カテゴライズされた認知・心理指標と脳イメージングから収集された灰白質容積から、それらに相関がある脳領域が一部同定され、TFU Template として rsfMRI での機能的な脳ネットワーク検出に応用されていることは、心理指標計測および脳イメージング計測グループが十分な連携をもって研究が推進されていることを示すものと思われる。一方、社会的能力・職業的能力を端的に検出するためには、特定の事象を対象にその前後比較を想定した横断的研究が必要となるが、中期的事象として吹奏楽経験者、短期的事象として実習経験者の脳変化を捉えることに成功しており、今後の研究への基盤整備が進んでいるものと思われる。以上

より、現段階での達成状況は良好であると考えられる。

⑤今後の展望

すでに本研究で収集された行動・認知・心理指標およびニューロイメージングデータの解析が進められ、両者を統合する形で結果が報告されていることは、これまで2年間の研究が順調に遂行されていることを示している。今回の研究プロジェクトでも重要な部分を占める縦断的研究に関しては、サンプル収集が肝要であるため、今後も一貫したデータ収集を継続して行っていただきたいし、本研究プロジェクトで蓄積されるデータは、多彩な指標を備える画像データとして、非常に価値の高いものになると思われる。研究プロジェクト後半は、システマティックに収集された膨大な情報から、社会的能力・職業的能力推定に有用な要素を如何に抽出するかがキーとなるため、データ解析へのさらなる注力を期待したい。

⑥総評

本研究プロジェクトは、人材の育成という高等教育課程に期待される役割を、認知・脳科学的エビデンスに裏付けられた客観的な情報から評価し、その教育・育成の効果・価値を高めるための基盤構築を掲げており、その成果は、高い社会的還元性を持つものである。現在までの研究計画、実施状況をみると、当初の予定どおり成果が得られているものと思われる。今後の研究の発展を期待したい。

⑦メモ（自由記載。評価対象とはせず、今後の研究推進の一助とする）

個別の認知・行動・心理特性とニューロイメージングデータとの関連解析はすでに開始されており、一部、結果も得られている。事前評価の資料では、関連解析の次段階で計画されている定量的指標作成、分析手法の確立にあたって、パターン認識、マシンラーニングの手法を応用するとのことであるが、これらは、収集されるデータに合わせた最適化も重要になると思われます。データ収集完了を待たずに、逐次的に検証を継続することが肝要ですので、これらにリソースが確保されることを望みます。

平成28年度　健康科学研究センター活動報告

1．はじめに

本戦略研究も愈々３年目を迎える。研究の内容はもとより、予算の使い方や費用対効果はどうか、人的リソースを含む研究資源の有効活用ができているかなどを謙虚に振り返り、最終的な目標に向かって新たな一歩を踏み出すことが必要であろう。本稿では、その節目の年を迎えるにあたり、研究計画全体の進捗について概観したい。

2．これまでの状況

近年の教育現場では、経験豊かな教育者らの実践の妥当性や、学習者の行動を理解するための枠組みについてエビデンスを与えるべく認知・脳科学研究に期待が寄せられている。他方、認知・脳科学研究者も得られた知見を教育の現場や実生活に還元することを意識し、研究対象として社会的相互作用等の高次の主観的体験を扱うようになった。しかし、研究成果が充分に教育現場で活かされているとはいえないのが現状である。その一因は、教育現場ではそれぞれ異なるケース（個人）をみており、研究ではケースに共通する法則性・全体的傾向をみているという視座の違いにある。そこで本研究では、認知・脳科学的エビデンスに基づいて個々人を評価できる情報提供基盤を形成することを目指している。

平成28年度は、個人の認知・脳科学的評価を実現するための根幹となる数百人の100項目以上の心理データを内包する脳機能マップ・ネットワークの作成を行った。これにより個々人の多様性を特徴づけるのに必要とされる数々の心理・認知的特性が、脳内マップ・ネットワークという形で定量的かつ客観的に表現されうることが示された。特に、新たに追加した認知検査（職業適性能）・質問紙（パーソナリティ特性等）を含む全ての心理データと脳機能データを利用したデータ分析を行い、昨年度から作成している社会的・心理的指標を反映する脳機能マップ・ネットワークのバージョンアップを行った。

これを受け、上述の認知・脳科学的エビデンス情報をもとに個々人を評価する基盤の形成に着手した。具体的には、脳機能ネットワークと心理測定データに加えて新たに機械学習法を導入することで、“ヒト特性推定器（仮称）”を開発した。データ処理過程を自動化し、1回の MRI データを入力することで、個々人の知能指数、情動知能指数、社会性などのヒト特性を多段階に推定することが出来る。この開発により、個々人の行動に共通する法則性等の全体的傾向ではなく、脳内マップ・ネットワークという客観的データに基づいて一人一人がどういった特性を強く、あるいは弱く持つのかという評価ができ、一個人がどのような教育を必要とするのか、といった教育指針を得ることも可能となろう。

3．コアメンバー会議

下記の要領で実施された。

平成28年４月13日（17：00－18：30）　出席者（敬称略）小川、坪川、藤井、成、河地
平成28年５月18日（16：00－17：30）　出席者（敬称略）小川、坪川、藤井、成、河地、押江、岩田
平成28年７月27日（16：00－17：30）　出席者（敬称略）小川、坪川、藤井、成、河地、押江、岩田、小川
平成28年９月２日（16：00－17：30）　出席者（敬称略）小川、坪川、藤井、成、河地、押江、岩田、小川
平成28年12月12日（16：00－17：30）　出席者（敬称略）小川、藤井、成、押江、岩田、小川
平成29年２月15日（16：00－17：30）　出席者（敬称略）小川、坪川、藤井、成、河地、押江、小川

4．平成28年度 経過報告会

日時：平成29年 3 月21日（火）15：00～

場所：東北福祉大学 感性福祉研究所 2 階 大会議室

出席者（敬称略）小川、小松、坪川、庭野、藤井、大城、成、田邊、伊藤、河地、曽根、姜

報告会次第：

開　　会	
開会挨拶・研究概要説明	小川誠二
グループ報告	
・グループ 2（職業関連実験　等）	伊藤文人
	小松　紘
・グループ 3（心理実験　等）	河地庸介
・グループ 1（MRI 実験　等）	成　烈完
閉　　会	

5．経費執行状況

平成28年度における、研究費執行状況は、以下のとおりである。

	予算額［千円］	実績額［千円］	執行率
研究費	27,791	26,837	97%

6．今後の方針

現在は、“ヒト特性推定器（仮称）”を用いて、就労による訓練効果が推定可能かを評価するために、就労者（例えば、医療、福祉系・一般事務系等）の MRI データを収集している。その結果、推定器は、就労者が従事する職業に必要となるヒト特性を高評価でき、就労に伴う訓練効果を的確に推定できることが明らかになりつつある。今後は、“ヒト特性推定器（仮称）”の最適化や調整を進めていくことで、社会的能力・職業的能力の習得を目指す教育効果が個人に及ぼす影響を高精度推定し、個人の特性に寄り添う形で種々の職業適性の涵養を促す指針の提供を目指す。

本事業では、ある一時点での個人評価のみならず、日々成長していく個々人の評価の必要性を視野に入れて、数年間にわたる大学教育が個々人に及ぼす影響の推定に取り組んでいる。昨年度は、継続する課題として、これまでに心理・MRI 測定に参加した研究協力者（本学学生）を対象に、2 か月－ 3 ヶ月に 1 回程度のペースで定期的に脳機能・構造計測を行った。さらに 4 年間の大学教育課程を90％以上終えた 4 年生の一部の学生を対象に、心理測定と脳機能測定を行った。さらに本年度はデータの集積に伴い、部分的に縦断的データ解析に着手した。本縦断研究のデータとヒト特性推定器を組み合わせることで得られる成果は、大学での教育指導が個々人に与える影響についての定量的なエビデンスとなり、個人単位で最良と思われる教育指導の提供が実現できる。

上述の他、脳機能ネットワークのさらなる拡充のために注意機能、実行機能、メタ認知機能に関する行動計測を行っている。既に、因子分析・共分散構造分析などの多変量解析技術を用いて、多種多様な認知機能データを支える基本機能要素間のデータ構造をモデル化した。また、教育による脳機能変化を捉えること、さらには既存の fMRI データによる脳機能ネットワークの拡充を目指して、論理的思考能力を評価する fMRI 実験パラダイムを作成して実験を行っている。さらに、fMRI の技術開発を通して、可塑的な

脳機能変化に関連するミクロ的なメカニズムの解明を行うために、MRIによるT1またはスピン密度の計測を行っている。

7．業績

（原著論文）

1．Nazari Z., Inamine M., Sugama Y., Kang D., Kawachi Y., Sung Y., Ogawa S.（in press）Evaluation of characteristics of resting state fMRI data by Machine Learning. *Report of Kansei Fukushi Research Institute*, 18.

2．Kang D., Sung Y., Ogawa S.（in press）Realization of a Longitudinal Relaxation Time Measurement with High Spatial Resolution. *Report of Kansei Fukushi Research Institute*, 18.

3．Sung Y., Kang D., Kawachi Y., Ogawa S.（in press）Detection of fast MRI signals by an EEG-like stimulus scheme and multi-voxel pattern analysis. *Report of Kansei Fukushi Research Institute,* 18.

4．大友ゆき・河地庸介・阿部千裕・成烈完・小川誠二（印刷中）メタ認知と自己成長主導性の関連性. 感性福祉研究所年報 , 18.

5．Sone T., Kawachi Y., Abe C., Otomo Y., Sung Y., Ogawa S.（in press）Attitude and Practice of Physical Activity and Social Problem-Solving Ability among University Students. *Environmental Health and Preventive Medicine*.

6．河地庸介（2016）．脳活動からみる芸術鑑賞・制作 *臨床美術ジャーナル*，5（1），75-81.

7．Kawachi, Y.（2016）Visual Mislocalization of Moving Objects in an Audiovisual Event. *PLoS ONE* 11（4）: e0154147. doi:10.1371/journal.pone.0154147

8．Choi U.-S., Sung Y., Ogawa S.（2017）Steady-state and dynamic network modes for perceptual expectation. *Scientific Reports* 7, doi:10.1038/srep40626.

9．Abe, C., Kawachi, Y., Sung, Y., Ogawa, S.（In press）. The effects of short-term practice on executive functions, *Tohoku Psychologica Folia*.

（国際学会発表）

1．Ito A, Kawachi Y Kawasaki I, Fujii T. Age-related reduction of cognitive dissonance. 31st International Congress of Psychology（ICP2016）July 24-29, 2016, Yokohama, Japan

2．Ito A, Niwano K, Tanabe M, Sato Y, Fujii T. The effect of childcare training on the perception of infant’s emotional facial expressin. 31st International Congress of Psychology（ICP2016）July 24-29, 2016, Yokohama, Japan

3．Tanabe M, Niwano K, Ito A, Sato Y, Fujii T. Correlations between the brain responses of nulliparous females when viewing infants’facial expressions and their personality. 31st International Congress of Psychology（ICP2016）July 24-29, 2016, Yokohama, Japan

4．Fujii T, Ito A, Jenkins R, Sanders J, Yoshida K, Murakami Y, Sakai S, Tanabe M. The effect of wearing a medical mask and sunglasses on perceiver’s impression. 31st International Congress of Psychology（ICP2016）July 24-29, 2016, Yokohama, Japan

5．Sung Y., Choi U.-S., Ogawa S., Interaction between high and low level areas and the temporal window for repetition suppression. The 22st annual meeting of the Organization for Human Brain Mapping, Geneva, Switzerland, Jun 26-30, 2016.

6．Sung Y., Kang D., Ogawa S., A challenge for sub - millisecond fMRI. The 44th annual meeting of the

Japanese Society for Magnetic Resonance In Medicine, Omiya, Japan, Sep 9-11, 2016.

7．Kang D., Sung Y., Ogawa S., Comparison of voxel-based morphometry and T 1 absolute value. The 44th annual meeting of the Japanese Society for Magnetic Resonance In Medicine, Omiya, Japan, Sep 9-11, 2016.

8．Sung Y., Kang D., Kawachi Y., Ogawa S., Brain plasticity changes by playing wind instruments and piano. The 46th annual meeting of the Society for Neuroscience, SanDiego, USA, Oct 12-16, 2016.

（国内学会発表）

1．河地庸介・阿部千裕・成烈完・松江克彦・小川誠二 統合失調型パーソナリティの個人差が注意の下位機能間の相互作用に及ぼす影響．第46回日本臨床神経生理学会学術大会，福島，2016年10月．

2．阿部千裕・河地庸介・成烈完・松江克彦・小川誠二 実行機能と統合失調型パーソナリティの関係．第46回日本臨床神経生理学会学術大会 , 福島，2016年10月．

3．大友ゆき・阿部千裕・河地庸介・成烈完・松江克彦・小川誠二 統合失調型パーソナリティ傾向におけるメタ記憶の特徴．第46回日本臨床神経生理学会学術大会，福島，2016年10月．

平成29年度　健康科学研究センター活動報告

1．はじめに

健康科学研究センターは、次年度に最終年度を迎える『平成26年度採択私立大学戦略的研究基盤形成支援事業「社会的・職業能力育成プログラムに資する認知・脳科学的エビデンス情報提供基盤の構築」』の完遂に向けて精力的に研究を展開している。本稿では、認知・脳科学的エビデンス情報提供基盤の要となる“ヒト特性推定器（仮称）”の改良・発展を中心とした研究進捗状況を概観した上で最終年度に達成すべき目標について述べる。

2．これまでの状況

昨今の教育現場では、経験豊かな教育者らの実践の妥当性や、学習者の行動について認知・脳科学研究の知見・エビデンスから検討しようとする動向がある。このような動向は教育現場に限らず、精神医学等の心を最たる問題とする医療現場（Yahata et al., 2016, *Nature Communications*）や消費者の購買行動の正確な予測を目標とするビジネスの現場でも盛んである（応用脳科学コンソーシアム http://www.keieiken.co.jp/can/）。本事業の取り組みは高まる関心をよそにほぼ手つかずの領域であった教育現場に焦点を合わせて、認知・脳科学的基盤技術の提供を目指す極めて重要な事業である。

従来の認知・脳科学研究の成果は、個々人に共通する法則性・全体的傾向に着目したものであり、ケース（個人）をいかに理解するかに着目しなければならない教育現場にその成果を還流することは困難であった。本事業が提供を目指す情報提供基盤はこうした状況を克服するべく、個々人の社会的・職業的能力の定量的な推定・理解・育成を志向したものとなっている。本事業で開発した、その情報提供基盤が“ヒト特性推定器（仮称）”である（Fig. 1－4，Sung et al., 2018, *Frontiers in Neuroscience*）。本推定器は脳機能ネットワークと心理測定データに加えて新たに機械学習法を導入することで作成された。データ処理過程を自動化し、1回のMRIデータを入力しただけで、個々人の知能指数、情動知能指数、社会性などのヒト特性を多段階に推定することが出来る。

平成29年度は、“ヒト特性推定器”を用いて、就労による訓練に伴って向上していると考えられる社会的能力・職業的能力を推定・評価するために、就労者（例えば、医療、福祉・一般事務系等）のMRIデータを収集した。この就労者のデータを入力として“ヒト特性推定器”を適用したところ、就労者の職業に深く関連し、高いと想定される社会的能力を概ね正しく推定することができた。このように“ヒト特性推定器”による社会的能力の推定結果の妥当性について確認がなされている。さらに職業適性に特化した推定器を作成するために、前年度までに蓄積してきた脳機能ネットワークデータに、新たに職業適性検査のデータを組み合わせて機械学習法を適用し、“職業適性推定器”を作成した。19種の職業群に関する適性を多段階で推定することができる。現在、得られた知見を論文化し、国際研究専門誌への投稿を行っている。

これまで蓄積されてきた心理測定データは、知能検査・職業適性検査を除くとその多くは質問紙によるデータであった。結果として、研究協力者が自分自身で意識できる側面を測定してきたとも言える。当然ながら、ヒトの心理・行動は必ずしも意識化できない側面も多く存在する。そこで本事業では、教育による認知・脳機能変化のうち意識化・言語化しにくい部分を含めてより多方面から捉えるために、種々の認知機能のうち特に重要と考えられる機能について質問紙ではなく行動実験による検討を始めた。具体的には、論理的思考に関するfMRI実験、実行機能・メタ認知・注意機能・意思決定機能の各々について100名程度の学生の参加を募って行動実験を行った。

さらに、前年度までの参加者の縦断的側面をとらえるために同一参加者を対象にデータ収集を継続して行い、データ解析作業を行っている。最終年度に卒業する研究協力者（本学学生）のデータを取得することで、認知行動的変化（認知能力、社会的能力およびパーソナリティ等）および脳機能・構造変化の両面から大学における社会的・職業能力の育成効果を推定できる。

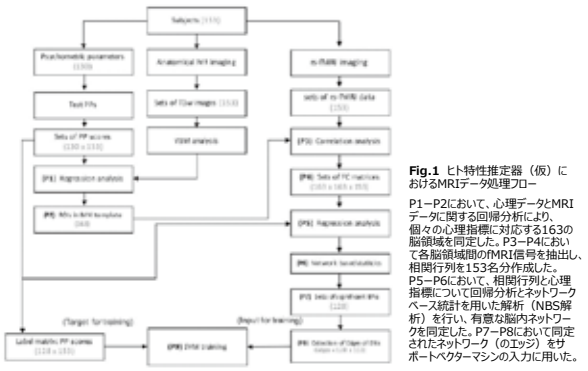


Fig.1 ヒト特性推定器（仮）におけるMRIデータ処理フロー

P1−P2において、心理データとMRIデータに関する回帰分析により、個々の心理指標に対応する163の脳領域を同定した。P3−P4において各脳領域間のfMRI信号を抽出し、相関行列を153名分作成した。P5−P6において、相関行列と心理指標について回帰分析とネットワークベース統計を用いた解析（NBS解析）を行い、有意な脳内ネットワークを同定した。P7−P8において同定されたネットワーク（のエッジ）をサポートベクターマシンの入力に用いた。

Sung Y-W, Kawachi Y, Choi U-S, Kang D, Abe C, Otomo Y and Ogawa S (2018) A Set of Functional Brain Networks for the Comprehensive Evaluation of Human Characteristics. *Front. Neurosci.* 12:149. doi: 10.3389/fnins.2018.00149

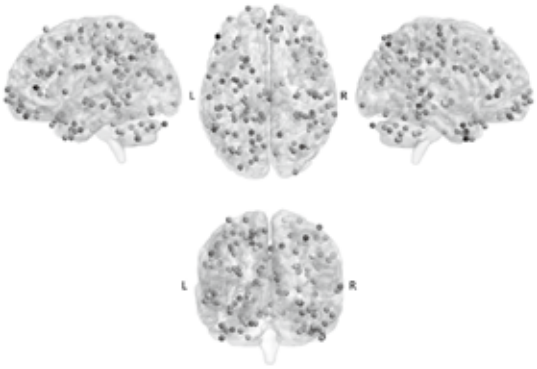


Fig.2 96個の心理指標との回帰分析により同定された163個の関連領域脳マップ

Sung Y-W, Kawachi Y, Choi U-S, Kang D, Abe C, Otomo Y and Ogawa S (2018) A Set of Functional Brain Networks for the Comprehensive Evaluation of Human Characteristics. *Front. Neurosci.* 12:149. doi: 10.3389/fnins.2018.00149

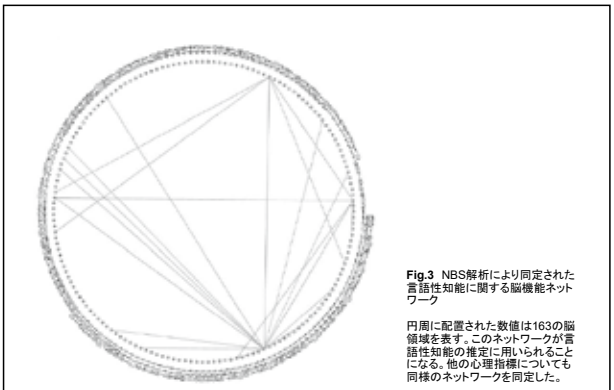


Fig.3 NBS解析により同定された言語性知能に関する脳機能ネットワーク

円周に配置された数値は163の脳領域を表す。このネットワークが言語性知能の推定に用いられることになる。他の心理指標についても同様のネットワークを同定した。

Sung Y-W, Kawachi Y, Choi U-S, Kang D, Abe C, Otomo Y and Ogawa S (2018) A Set of Functional Brain Networks for the Comprehensive Evaluation of Human Characteristics. *Front. Neurosci.* 12:149. doi: 10.3389/fnins.2018.00149

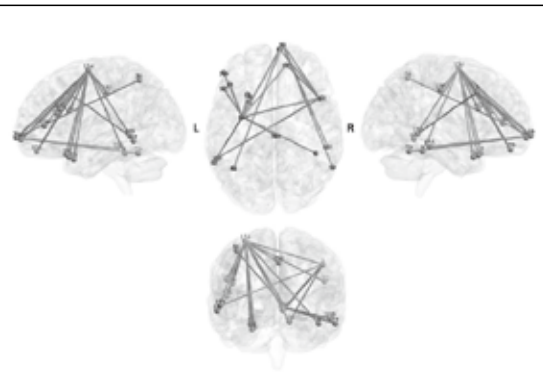


Fig.4 NBS解析による言語性知能に関する脳機能ネットワークの3次元ビュー

Sung Y-W, Kawachi Y, Choi U-S, Kang D, Abe C, Otomo Y and Ogawa S (2018) A Set of Functional Brain Networks for the Comprehensive Evaluation of Human Characteristics. *Front. Neurosci.* 12:149. doi: 10.3389/fnins.2018.00149

3．コアメンバー会議

下記の要領で実施された。

平成29年 6 月15日（18：00－19：00）出席者（継承略）小川、藤井、成、押江、小川

平成30年 1 月24日（18：00－19：00）出席者（敬称略）小川、成、河地、押江、小川

平成30年 3 月 7 日（18：00－19：00）出席者（敬称略）小川、藤井、成、河地、小川

4．平成29年度　経過報告会

日時：平成30年 3 月 7 日（水）17：00－18：00

場所：東北福祉大学 感性福祉研究所 2 階　小会議室

出席者（敬称略）小川、藤井、成、河地

報告会次第：

開　　会

開会挨拶・研究概要説明　小川誠二

研究進捗報告

・社会性に関連する心理指標、IQ、EQ、職業適性に関連する心理データベース作成

・MRI データ（構造データ及び機能データ）ベースの作成

・MRI データと心理データによるヒト特性評価器の作製

閉　　会

5．経費執行状況

平成29年度における、研究費執行状況は、以下のとおりである。

	予算額［千円］	実績額［千円］	執行率
研究費	25,548	22,011	86%

6．今後の方針

本事業の特色は、集団の一般的傾向ではなく個人に、ある一時点ではなく大学生活における日々の成長過程に着目して認知・脳科学的研究を展開している点である。昨年度までに同一の研究協力者に対して２か月―３か月に１回程度のペースで定期的に脳機能・構造計測を行ってきた。その協力者の多くは来年度卒業を迎え、大学生活の４年間を捉える縦断データが完成することになる。この貴重な縦断データから大学における社会的・職業能力の育成効果を抽出することが最終年度の最重要課題である。一個人の受けた大学教育、大学生活の中での種々の経験、それらの何が社会的・職業能力を育む糧となったのか、その手がかりを見つけ出し、教育現場にフィードバックすることを目指す。

縦断研究から得られる時間的変化のデータ、さらには本年度着手した fMRI 実験および種々の行動実験データ、さらには白質 MRI データを認知・脳科学的データベースを拡充し、ヒト特性推定器・職業適性推定器に適用することで個々人の社会的・職業的能力推定のさらなる精度の向上を目指す。将来的に個々の学生の特性に適した社会的・職業能力の涵養を促す教育・指導方針を考える契機を教育現場へ提供することを目指す。

7．業績

（原著論文）

1．Nazari Z., Inamine M., Sugama Y., Kang D., Kawachi Y., Sung Y., Ogawa S.（2017）Evaluation of characteristics of resting state fMRI data by Machine Learning. *Report of Kansei Fukushi Research Institute* 18, 281-284.

2．Kang D., Sung Y., Ogawa S.（2017）Realization of a Longitudinal Relaxation Time Measurement with High Spatial Resolution. *Report of Kansei Fukushi Research Institute* 18, 285-288.

3．Sung Y., Kang D., Kawachi Y., Ogawa S.（2017）Detection of fast MRI signals by an EEG-like stimulus scheme and multi-voxel pattern analysis. *Report of Kansei Fukushi Research Institute* 18, 275-280.

4．大友ゆき・河地庸介・阿部千裕・成烈完・小川誠二（2017）メタ認知と自己成長主導性の関連性．感性福祉研究所年報 18, 293-299.

5．Sone T., Kawachi Y., Abe C., Otomo Y., Sung Y., Ogawa S.（2017 Attitude and practice of physical activity and social problem-solving ability among university students. Environ Health Prev Med. 22,

18 doi: 10.1186/s12199-017-0625-8.
6．Kang D, Sung Y, Shioiri S.（2018）Estimation of physiological sources of nonlinearity in blood oxygenation level-dependent contrast signals. Magn Reson Imaging 46, 121-129.
7．Sung Y, Kawachi Y, Choi U-K, Kang D, Abe C, Otomo Y and Ogawa S（2018）A Set of Functional Brain Networks for the Comprehensive Evaluation of Human Characteristics. *Front. Neurosci.* 12:149. doi: 10.3389/fnins.2018.00149.
8．Sung Y., Kang D., Kawachi Y., Ogawa S（in press）Comparison of resting state fMRI signals depending on participants' conditions under MRI measurements. *Report of Kansei Fukushi Research Institute.*
9．Nazari Z., Inamine M., Kang D., Kawachi Y., Sung Y., Ogawa S（in press）Classifying resting state fMRI data using an unsupervised neural network. *Report of Kansei Fukushi Research Institute.*
10. 大友ゆき・河地庸介・阿部千裕・成烈完・小川誠二（in press）統合失調型パーソナリティ特性と自閉症スペクトラム特性のメタ認知における差異．感性福祉研究所年報
11. 阿部千裕・河地庸介（in press）．実行機能を構成する要素に関する研究動向と課題，感性福祉研究所年報，19.

（国際学会発表）

1．Ogawa S: On some approaches of fMRI. The 22st annual meeting of the Organization for Human Brain Mapping, Vancouver, Canada, Jun 26-26, 2017.
2．Sung Y, Kang D, Kawachi Y, Ogawa S: Brian maps reflected in different imaging modalities. The 22st annual meeting of the Organization for Human Brain Mapping, Vancouver, Canada, Jun 26-26, 2017.
3．Sung Y, Kang D, Ogawa S: Measurement of task-induced high frequency band signals by ultra-high temporal resolution imaging, the 25th annual meeting of International Society for Magnetic Resonance Imaging, Hawaii, USA

（国内学会発表）

1．阿部千裕・河地庸介　短期的訓練が実行機能に及ぼす影響．日本感性福祉学会第17回大会，宮城，2017年10月
2．大友ゆき・阿部千裕・河地庸介　メタ認知と自己成長主導性の関連性．日本感性福祉学会第17回大会，宮城，2017年10月
3．阿部千裕・河地庸介・北村康宏・成烈完・小川誠二　報酬を導く意思決定方略への依存 －アイオワギャンブリング課題を用いた検討．日本基礎心理学会第36回大会，大阪，2017年12月

（書籍）

河地庸介（2017）．VBM・DTI 坂田省吾・山田冨美雄（編）生理心理学と精神生理学 第Ⅰ巻 基礎（pp.142-147）北大路書房．

健康科学研究センター　平成30年度　活動報告

1．はじめに

『平成26年度採択私立大学戦略的研究基盤形成支援事業「社会的・職業能力育成プログラムに資する認知・脳科学的エビデンス情報提供基盤の構築」』は、大学在籍期間の数年にわたって個人の変化を追跡する縦断研究と、職業経験や性格特性等の種々の点で異なる集団間の差異を比較検討する横断研究を統合したマトリクス的アプローチを採用した研究を展開してきた。本年は本事業の最終年度であり、縦断データが完成するとともに、これまでの研究成果をまとめるべく精力的に研究に取り組んできた。本稿では、縦断データの分析状況を含め、現在に至るまでの研究成果および今後の課題について報告する。

2．これまでの状況

今日の教育現場ではエビデンスに基づいた教育が求められており、その一環として経験豊かな教育者らの実践や、学習者の行動理解について心理学・脳科学研究の知見・エビデンスに基づいて捉え直そうという動きが盛んとなっている。その一方で、個々人に共通する法則性・全体的傾向を捉えようとする研究アプローチは、個々人の特異性に着目することが必要不可欠である教育現場が求めるものを提供することは困難であった。そこで、本事業では個々人に焦点を当てた社会的・職業的能力の定量的な推定・理解・育成を志向し、個々人を認知・脳科学的に評価できる情報提供基盤を形成するべく、研究を展開してきた。

上述の教育現場の要請に応えるため本事業で開発した情報提供基盤が“ヒト特性推定器（仮称）”である（Sung et al., 2018, *Frontiers in Neuroscience*）。本推定器は脳機能ネットワークと心理測定データに加えて機械学習法を導入して作成されており、１回のMRIデータから個々人の知能指数や情動知能指数、社会性等のヒト特性を多段階推定できる。さらに、職業適性に特化した推定器として開発した“職業適性推定器”では19種の職業群に関する適性を多段階で推定することを可能とした（Sung et al., 2018, *Human Brain Mapping*）。

平成30年度は最終年度であり、初年度より蓄積してきた縦断データの収集が概ね完了した。50名程度の卒業する研究協力者（本学学生）を対象にした縦断的データ分析を行った。その結果、種々の心理特性（職業適性等）に関連する脳機能ネットワークにおける経時的変化の検出に成功した。さらに、同研究協力者らの初年度および最終年度の心理測定データを比較・検討したところ、社会的スキル、自己概念の明確性、情動知能といった心理特性が初年度と比較して向上しており、一方で統合失調型パーソナリティ傾向といった社会的にネガティブな側面として捉えられることが多い心的特性については初年度と比較して低下する傾向が示された。今後さらに大学で受けた教育の違い（具体的には学部・学科の違い等）が経時変化に影響を及ぼしているかの詳細な検討を引き続き行う予定である。

また研究協力者のヒト特性をより多面的に捉えるための測定法・測定指標を作製するべく行動実験を実施してきた。１つは、学習者の効率的な学習に重要とされるメタ認知機能に関する実験結果について新たに線形混合モデルによる分析を行った。この取り組みにより、従来考慮できていなかった交絡要因（実験刺激の種類等）の影響を除外してメタ認知機能をより精緻に測定することが可能となった。さらに、適応的な社会生活を支えるとされ、発達障害との関連が指摘されている実行機能に関する新たな測定法を提案した。本測定法は、実行機能の３要素（更新・切替・抑制）の相互作用を想定しており、今後様々な年齢の測定対象者に適用できるように改訂を行っていく予定である。

3．コアメンバー会議

下記の要領で実施された。

平成30年４月26日（17：00－19：00）　出席者（敬称略）小川、坪川、成、押江、河地
平成30年５月30日（14：00－15：00）　出席者（敬称略）小川、坪川、成、押江、河地
平成30年７月２日（16：00－17：00）　出席者（敬称略）小川、坪川、成、押江、河地
平成30年８月22日（16：00－17：00）　出席者（敬称略）小川、坪川、成、押江、河地
平成30年11月16日（15：00－16：00）　出席者（敬称略）小川、坪川、成、押江、河地
平成31年１月18日（15：00－16：00）　出席者（敬称略）小川、坪川、成、押江、河地
平成31年２月14日（15：00－16：00）　出席者（敬称略）小川、坪川、成、押江、河地

4．経費執行状況

平成30年度における、研究経費執行状況は、以下のとおりである。

	予算額［千円］	実績額［千円］	執行率
研究費	15,826	12,015	75.9％

5．今後の方針

今後は収集を終えた縦断データに基づいて、大学における社会的・職業能力の育成効果の抽出を行うとともに、一個人の受けた大学教育・大学生活の中での種々の経験の何が社会的・職業能力を育む糧となったのかの検討を行う形で本事業を纏め上げる。本事業において作製されたヒト特性推定器については、個々人のヒト特性を表現する指標の妥当性・信頼性の評価とヒト特性に関するMRI測定の限界についての評価を行い、また職業適性推定器については、多様な職業分野ごとに勤務年数の多いエキスパートの脳機能測定データの活用を行っていくことで、推定精度のさらなる向上を目指す。

来年度は、本事業の成果を発展的に活用することを意識して、超高齢社会で生活する地域の人々の認知機能に焦点を当てた研究を展開していく。とりわけ加齢に伴う通常の認知機能変化・軽度認知障害（Mild Cognitive Impairment: MCI）・認知症（主としてアルツハイマー型認知症）をターゲット分野として、多様な脳機能・構造指標および心理指標を用いて中高年の脳機能・構造画像および心理特性データベースを作成し、ヒト特性推定器の対象範囲の拡大を目指す。そのため、「介護老人保健施設せんだんの丘」との共同研究を中心とした研究体制の確立、データ計測・分析方法の選定、研究協力者の選定など研究フレームワークの構築を着実に進める。

6．業績

（原著論文）

1．Sung Y., Kawachi Y., Choi U.-S., Kang D., Abe C., Otomo Y., Ogawa S.（2018）Estimation of vocational aptitudes using functional brain networks. *Human Brain Mapping*, 39（9）, 3636-3651.

2．Sung Y, Kawachi Y, Choi U.-S., Kang D, Abe C, Otomo Y, Ogawa S.（2018）A Set of Functional Brain Networks for the Comprehensive Evaluation of Human Characteristics. *Front Neurosci*, 12（149）, doi:10.3389/fnins.2018.00149.

3．Sung Y., Kawachi Y., Ogawa S.（in press）Comparison of multichannel head array coils for fMRI experiments. *Report of Kansei Fukushi Research Institute*, 20.

4．Otomo Y., Kawachi Y., Sung Y., Ogawa S.（in press）A linear-mixed effect model analysis of the

effect of schizotypal personality traits on confidence in reality monitoring. *Tohoku Psychologica Folia*, 77.

（国際学会発表）

1．Kang D., Sung Y., Shioiri S. Estimation of physiological sources of nonlinearity in bold signals. The 26th annual meeting of International Society for Magnetic Resonance Imaging, Paris, France, Jun 16-21, 2018.

2．Sung Y., Kawachi Y., Ogawa S. Functional specificity of resting-state fMRI signals. The 24th annual meeting of the Organization for Human Brain Mapping, Singapole, Jun 17-21, 2018.

3．Sung Y, Kawachi Y, Otomo Y, Ogawa S. Occupational abilities and function networks estimated through resting state fMRI. The 45th annual meeting of the Society for Neuroscience, San Diego, USA, Nov 3-7, 2018.

（国内学会発表）

1．阿部千裕・河地庸介 実行機能ネットワークの同定．日本心理学会第82回大会，宮城，2018年 9 月.

2．阿部千裕・河地庸介 実行機能ネットワークテストの考案．日本認知心理学会第16回大会，大阪，2018年 9 月.

3．Sung Y., Ogawa S. Modality-dependent functional specificity in resting-state fMRI signals. 第46回日本磁気共鳴医学会大会，金沢，2018年 9 月.

4．大友ゆき・河地庸介 線形混合モデルでみるメタ記憶．日本感性福祉学会第18回大会，宮城，2018年11月.

5．大友ゆき・河地庸介 パーソナリティ特性が既学習判断（Judgment of Learning: JOL）に及ぼす影響．東北心理会第72回大会，岩手，2018年11月.

6．成烈完・河地庸介・大友ゆき・小川誠二 脳機能ネットワークによるヒト特性変化の推定．第21回日本ヒト脳機能マッピング学会，東京，2019年 3 月.

7．Sung Y., Kawachi Y., Otomo Y., Ogawa S. Estimation of specific functional brain areas relecting individual characteristics. 第21回日本ヒト脳機能マッピング学会，東京，2019年 3 月.

8．Kikuchi Y., Sung Y., Ogawa S. Quantification method of brain networks and estimation of network measure. 第21回日本ヒト脳機能マッピング学会，東京，2019年 3 月.

II　研究成果の概要

（様式 2）

法人番号	041001
プロジェクト番号	S1411001

平成26年度～平成30年度「私立大学戦略的研究基盤形成支援事業」
研究成果報告書概要

1 学校法人名 梅檀学園 2 大学名 東北福祉大学

3 研究組織名 東北福祉大学感性福祉研究所 健康科学研究センター

4 プロジェクト所在地 宮城県仙台市青葉区国見ケ丘 6-149-1

5 研究プロジェクト名 社会的・職業能力育成プログラムに資する認知・脳科学的エビデンス情報提供基盤の構築

6 研究観点 研究拠点を形成する研究

7 研究代表者

研究代表者名	所属部局名	職名
小川誠二	感性福祉研究所	特任教授

8 プロジェクト参加研究者数 23 名

9 該当審査区分 理工・情報 生物・医歯 (人文・社会)

10 研究プロジェクトに参加する主な研究者

研究者名	所属・職名	プロジェクトでの研究課題	プロジェクトでの役割
小川 誠二	東北福祉大学・特任教授	社会的・職業能力育成プログラムに資する認知・脳科学的エビデンス情報提供基盤の構築	研究統括
坪川 宏	東北福祉大学・教授	社会的・職業能力育成プログラムに資する認知・脳科学的エビデンス情報提供基盤の構築	個人の認知・脳機能変動を追跡計測する縦断研究
大城 泰造	東北福祉大学・准教授	社会的・職業能力育成プログラムに資する認知・脳科学的エビデンス情報提供基盤の構築	個人の認知・脳機能変動を追跡計測する縦断研究
曽根 稔雅	東北福祉大学・講師	社会的・職業能力育成プログラムに資する認知・脳科学的エビデンス情報提供基盤の構築	個人の認知・脳機能変動を追跡計測する縦断研究
河地 庸介	東北福祉大学・准教授	社会的・職業能力育成プログラムに資する認知・脳科学的エビデンス情報提供基盤の構築	個人の認知・脳機能変動を追跡計測する縦断研究
藤井 俊勝	東北福祉大学・教授	社会的・職業能力育成プログラムに資する認知・脳科学的エビデンス情報提供基盤の構築	加齢・職業経験の異なる集団の認知・脳機能を比較する横断研究
河村 孝幸	東北福祉大学・准教授	社会的・職業能力育成プログラムに資する認知・脳科学的エビデンス情報提供基盤の構築	加齢・職業経験の異なる集団の認知・脳機能を比較する横断研究
庭野 賀津子	東北福祉大学・教授	社会的・職業能力育成プログラムに資する認知・脳科学的エビデンス情報提供基盤の構築	加齢・職業経験の異なる集団の認知・脳機能を比較する横断研究
田邊 素子	東北福祉大学・准教授	社会的・職業能力育成プログラムに資する認知・脳科学的エビデンス情報提供基盤の構築	加齢・職業経験の異なる集団の認知・脳機能を比較する横断研究
浅野 弘毅	東北福祉大学・教授	社会的・職業能力育成プログラムに資する認知・脳科学的エビデンス情報提供基盤の構築	パーソナリティの異なる集団の認知・脳機能を比較する横断研究
小松 紘	東北福祉大学・名誉教授	社会的・職業能力育成プログラムに資する認知・脳科学的エビデンス情報提供基盤の構築	パーソナリティの異なる集団の認知・脳機能を比較する横断研究
松江 克彦	東北福祉大学・教授	社会的・職業能力育成プログラムに資する認知・脳科学的エビデンス情報提供基盤の構築	パーソナリティの異なる集団の認知・脳機能を比較する横断研究
滝井 泰孝	東北福祉大学・教授	社会的・職業能力育成プログラムに資する認知・脳科学的エビデンス情報提供基盤の構築	パーソナリティの異なる集団の認知・脳機能を比較する横断研究

法人番号	041001
プロジェクト番号	S1411001

成　烈完	東北福祉大学・特任准教授	社会的・職業能力育成プログラムに資する認知・脳科学的エビデンス情報提供基盤の構築	先端的fMRI 測定法の開発
姜　大勲	東北福祉大学・特任研究員	社会的・職業能力育成プログラムに資する認知・脳科学的エビデンス情報提供基盤の構築	先端的fMRI 測定法の開発
亀井　裕孟	東北福祉大学・特任研究員	社会的・職業能力育成プログラムに資する認知・脳科学的エビデンス情報提供基盤の構築	先端的fMRI 測定法の開発
（共同研究機関等）			
山本　絵里子	東京大学・研究員	次世代脳機能イメージングセンター（“個”の理解のための脳機能計測・評価を志向する）の構築	個人の認知・脳機能変動を追跡計測する縦断研究
幕内　充	国立障害者リハビリテーションセンター・室長	次世代脳機能イメージングセンター（“個”の理解のための脳機能計測・評価を志向する）の構築	加齢・職業経験の異なる集団の認知・脳機能を比較する横断研究
奥田　次郎	京都産業大学・教授	次世代脳機能イメージングセンター（“個”の理解のための脳機能計測・評価を志向する）の構築	加齢・職業経験の異なる集団の認知・脳機能を比較する横断研究
月浦　崇	京都大学・教授	次世代脳機能イメージングセンター（“個”の理解のための脳機能計測・評価を志向する）の構築	加齢・職業経験の異なる集団の認知・脳機能を比較する横断研究
阿部　修士	京都大学・特定准教授	次世代脳機能イメージングセンター（“個”の理解のための脳機能計測・評価を志向する）の構築	加齢・職業経験の異なる集団の認知・脳機能を比較する横断研究
姜　東植	琉球大学・准教授	次世代脳機能イメージングセンター（“個”の理解のための脳機能計測・評価を志向する）の構築	加齢・職業経験の異なる集団の認知・脳機能を比較する横断研究
加藤　和夫	東北学院大学・教授	次世代脳機能イメージングセンター（“個”の理解のための脳機能計測・評価を志向する）の構築	先端的fMRI 測定法の開発

＜研究者の変更状況（研究代表者を含む）＞

旧

ﾌﾟﾛｼﾞｪｸﾄでの研究課題	所属・職名	研究者氏名	プロジェクトでの役割

（変更の時期：平成　　年　　月　　日）

新

変更前の所属・職名	変更（就任）後の所属・職名	研究者氏名	プロジェクトでの役割

法人番号	041001
プロジェクト番号	S1411001

11 研究の概要（※ 項目全体を10枚以内で作成）

（1）研究プロジェクトの目的・意義及び計画の概要

昨今の教育現場では、経験豊かな教育者らの実践の妥当性や、学習者の行動について認知・脳科学研究の知見・エビデンスから検討しようとする動向がある。このような動向は教育現場に限らず、精神医学等の心を最たる問題とする医療現場や消費者の購買行動の正確な予測を目標とするビジネスの現場でも盛んである。本プロジェクトの取り組みは高まる関心をよそにほぼ手つかずの領域であった教育現場に焦点を合わせて、認知・脳科学的基盤技術の提供を目指す極めて重要な事業である。

従来の認知・脳科学研究の成果は、人々に共通する法則性・全体的傾向に着目したものであり、ケース（個人）をいかに理解するかに着目しなければならない教育現場にその成果を還流することは困難であった。本プロジェクトが提供を目指す情報提供基盤はこうした状況を克服するべく、個々人の社会的・職業的能力の定量的な推定・理解・育成を志向したものとなっている。本プロジェクトでは、教育・職業・パーソナリティ等の要因がいかにして認知・脳機能をダイナミックに変容させるかを、大学在籍期間の数年にわたって追跡する縦断研究と、年齢や職業経験の点で異なる集団間の変動、また精神障害と関連するパーソナリティ特性の強弱の点で異なる集団の変動を比較する横断研究を統合したマトリクス的アプローチにより明らかにする。得られた成果を大学等の教育機関・高齢者福祉施設・医療機関へ情報提供し、社会的・職業能力を育成する教育プログラムの改善支援へつなげていく。

認知・脳機能の中期・長期的変化を捉える縦断・横断研究によるマトリクス的アプローチ

本プロジェクトの特色は、個人の認知機能・脳機能を①大学在籍期間の数年にわたる長期的時間スケールで追跡計測する縦断研究、②加齢や職業経験という点で異なる集団での変動、精神障害等と関連するパーソナリティ特性の強弱という点で異なる集団での変動を比較する横断研究を統合したマトリクス的アプローチにある。従来、教育経験や職業経験に伴って適応的に変化する認知機能、さらには脳機能を大学在籍期間の数年間にわたり縦断的に調べる研究は皆無に等しかったが、本プロジェクトでは多数の研究協力者を対象とした長期にわたる定期計測を実現することができる。さらに、縦断研究が難しい数十年単位といったライフスパンでの認知・脳機能変化をも捉えるために様々な年代の研究協力者を対象に横断研究を行うことで、人の認知・脳機能変化を包括的に測定・評価することが可能となる。

教育効果・職業経験・パーソナリティへの着目

近年の認知・脳科学研究では言語習得に伴う認知・脳機能変化が着目されているが、社会の中で適応的に行動する人々の理解と育成に向けては、教育・職業・パーソナリティ等の人間行動の広範にわたり影響を与える要因に着目することが必須である。このため、対象者の生活環境・職業経験の情報、可能な限り多くの心理指標（社会的スキル・パーソナリティに関する質問紙と認知心理学実験）と MRI による脳機能画像・構造画像・脳内ネットワーク解析を組み合わせ、各指標の因果・相関関係を統計学的手法により抽出し、社会的・職業能力データベース作成を進めていく。

個々人の脳機能を総合的に計測するための MRI 測定・データ分析法の確立

本プロジェクトでは従来の MRI 計測の時空間分解能を飛躍的に（時間分解能：従来の約十数倍、空間分解度：従来の約二十数倍）向上させた測定技術を用いることで個人の脳の特性を正確に捉えることができる。さらに脳皮質、白質、賦活量等の構造・

法人番号	041001
プロジェクト番号	S1411001

機能データといった異なる時空間特性をもつ多次元情報を統合的に扱える MRI 測定・分析プロセスを構築することで複雑な認知と脳の関係について包括的に理解するための道筋を示す。

（2）研究組織

１．研究者等の役割分担・責任体制

本プロジェクトでは、教育・訓練・職業・パーソナリティ等の要因による認知・脳機能の長期的変化の客観的計測・評価を目標に、fMRI（BOLD）の開発者である小川誠二特任教授を中心とし、三つのサブグループの連携による統合的な研究を進める。サブグループ A は、大学生を対象に大学在籍期間にわたって個人の認知・脳機能変動を追跡計測する縦断研究を行う。サブグループ B は、加齢や職業の点で異なる集団及び精神障害と関連するパーソナリティの強弱の点で異なる集団間の認知・脳機能変化を比較する横断研究を行う。サブグループ C は、fMRI 技術の改良・更新とともに、新しい fMRI 現象の探索並びに fMRI 技術の開発を行う。各グループは研究者の所属機関にかかわらず有機的に連関し、職業適性や能力育成の問題に直面する諸機関・施設等の現場の意見を踏まえ、多数の心理測度・脳計測を組み合わせて定量化することで、個人がもつ能力の発見や既存の育成プログラムの抱える諸問題の解決につながりうる有益な情報の獲得を目指して研究を展開した。

２．研究者・RA の人数等の動向

研究者は、小川誠二特任教授を交えて研究開始段階から定期的に打ち合わせをし、適切に研究が遂行された。研究補助者は本学学生・大学院生を中心として 26 年度 12 名、27 年度 11 名、28 年度 12 名、29 年度 16 名、30 年度 14 名としを採用した。うち、1 名は平成 29 年度特任研究員として、1 名は平成 30 年度特任研究員として採用された。

３．研究支援体制

感性福祉研究所の事務局スタッフを中心に施設・設備・購入物品等の維持・管理が行われ、事務作業等による研究者の時間的・精神的負担は大幅に軽減された。また、研究遂行上の問題は速やかに解決されるよう、全学的な支援が継続的に行われた。

（3）研究施設･設備等

研究施設である感性福祉研究所の使用総面積は 4,092 m^2 であり、約 150 名の研究者が利用している。本プロジェクトに関連して、のべ約 1100 人の大学生・大学院生・社会人が研究協力者として参加している。

平成 26 年度に研究装置として感性福祉研究所内の「磁気共鳴撮影装置（MRI）」がアップグレードされた。研究設備として「MRI 対応脳波計」、「MRI 対応眼球運動計測装置」が設置された。31 年 3 月末現在の延べ利用時間は以下の通りである。

1）磁気共鳴撮影装置(MRI)‥‥‥‥‥約 1860 時間

2）MRI 対応脳波計‥‥‥‥‥‥‥‥約 267 時間

3）MRI 対応眼球運動計測装置‥‥‥‥‥‥‥‥‥‥‥‥‥‥‥‥約 273 時間

（4）研究成果の概要　※下記、13及び14に対応する成果には下線及び＊を付すこと。

１．教育効果・職業経験・パーソナリティに着目したヒト特性測定指標の作成

教育･職業･パーソナリティ等の要因によって影響を受ける個人のヒト特性を総合的に評価するための礎となる認知機能測定用の各種質問紙･心理検査･行動指標（社会的能力、知能、情動、パーソナリティ、職業適性、生活習慣等のおよそ 200 個のヒト特性要素）を作成した。併せて種々のヒト特性と関連づける脳構造･機能画像データベースを作成するための撮像シークエンス（VBM: Voxel Based Morphometry, DWI: Diffusion Weighted Imaging, rs-fMRI: resting-state fMRI）を最適化した。

法人番号	041001
プロジェクト番号	S1411001

ヒト特性の構成要素間の関連性を理解するために、心理検査および種々の心理尺度による測定データについて共分散構造分析等の多変量解析法を適用した検討を行った（論文*4, *13,*15; 学会発表*42）。その検討の中で職業適性を予測するにあたっては、元来の知能も重要であるが、知能とは独立に個々人が大学で修める学業成績がより重要となるといった職業適性における大学教育の影響が明らかになってきている。

また教育による認知・脳機能変化のうち意識化・言語化しにくい部分を含めてより多方面から捉えるために、種々の認知機能のうち特に重要と考えられる機能について質問紙ではなく行動実験による検討を行った（論文*3,*17,*21; 学会発表*37,*38,*43）。検討の 1 つとして、社会に出て適応的に生活していくために特に重要と目される論理的思考に着目した。論理的思考が大学教育の中で養われることで脳機能の変化として顕現していくことを検討するために、論理的思考を要する課題遂行中の fMRI 実験を行い、前頭前野での論理的思考関連部位が同定できた。次に、近年高次機能障害におけるリハビリテーションなどの領域で注目されている実行機能に着目した検討も行った。実行機能は独立 3 要素（情報の更新・心的な構えの切替・反応の抑制）より構成されていると考えられてきたが、要素間の相関や脳機能ネットワークの重複が確認されている。そこで各要素のみならず要素間の相互作用を含めた実行機能要素を捉えるために実行機能ネットワークテストを考案し、実行機能を包括的に評価するためのツールとなることが期待される。

２．認知・脳機能変化を捉える縦断・横断研究によるマトリクス的アプローチ

２．１．縦断研究について

本プロジェクトでの縦断研究を着実に進めるため、先駆けて学習・訓練により形成されるヒト特性が脳組織・機能における可塑的変化として顕現されるかを MRI 測定により確認した（論文*22, *25; 学会発表*26）。これにより、学習・訓練の結果として脳に可塑的な変化が起きることを本プロジェクトにおける実験環境で確認ができ、数年にわたる追跡測定へのエビデンスを得ることが出来た。また、職業等の経験が脳組織・機能へ顕現されうることについての根拠を得ることができた。

上述の研究を踏まえ、個々人の認知・脳機能を大学在籍期間の数年にわたる長期的スパンで追跡計測する縦断研究に着手した。約 300 名の研究協力者から開始し、約 50 名の研究協力者が 3 年半にわたり継続的に認知・脳計測に参加した。縦断的データ分析を行った結果、種々の心理特性（職業適性等）に関連する脳機能ネットワークにおける経時的変化の検出に成功した（学会発表*31,*32,*33）。さらに、同研究協力者らの初年度および最終年度の心理測定データを比較・検討したところ、社会的スキル、自己概念の明確性、情動知能といった心理特性が初年度と比較して向上しており、一方で統合失調型パーソナリティ傾向といった社会的にネガティブな側面として捉えられることが多い心的特性については初年度と比較して低下する傾向が示された。今後、大学で受けた教育の違い（具体的には学部・学科の違い等）により経時変化に影響を及ぼしているかの詳細な検討を引き続き行う。

さらに、ヒト特性における可塑的変化に必要となる学習・訓練の時間限界を検討するために、知能等とは独立に人間の行動や意思を制御しているとされる実行機能を対象に、短期的な学習・訓練による機能向上の検討を行った（論文*14; 学会発表*41）。先行研究では実行機能の学習・訓練が効果を発するには1ヶ月程度の集中的な訓練が必要とされてきたが、本プロジェクトでは 20 分程度の訓練であっても長期訓練とほぼ同様の機能の改善・向上が示された。本結果は学習内容に応じた効率のよい学習・訓練期間の設定に有益な示唆を与える。

法人番号	041001
プロジェクト番号	S1411001

２．２．横断研究について

職業経験やパーソナリティ特性の異なる集団での認知・脳機能変動を比較する横断研究については、本学学生の就職状況を勘案して事務職、保育士、看護師、リハビリテーション関連職に就く職業従事者 100 余名を対象として横断研究データ収集を行った。当該データは、3. に述べる「ヒト特性推定器」「職業適性推定器」の推定結果の妥当性の確認に用いられた。

職業従事者に関する横断研究に関連して、保育課程に在籍し保育実習に参加する学生と保育実習に参加しない学生を対象として実習の有無による認知・脳機能変化を特定するための fMRI 研究を実施した（学会発表*10,*12,*13,*14,*15）。その結果、実習参加後に乳幼児の泣いている表情に対する扁桃体・上側頭溝の活動が有意に低下することがわかった。この結果は、保育実習という学習・訓練が脳活動の変化として顕現することを示した。

パーソナリティ特性の強弱の点で異なる集団での認知・脳機能変動を比較する横断研究も実施された。学習者の効率的な学習に重要とされるメタ認知機能（自分の認知に関する認知）に着目した研究（論文*2; 学会発表*39,*40）では、自分自身が学習内容を想起できるか否か（既学習判断）といった予測的評価は、記憶機能等の認知的能力のみを反映しているとは言い切れず、神経症傾向・外向性・開放性・誠実性・調和性といったパーソナリティ特性が関係していることが、既学習判断の個人差、記憶項目における判断の差異を変数として組み込んだ線形混合モデルによる新たな分析で明らかにされた。

また大学での休学・退学理由となりうる精神障害に関連する統合失調型パーソナリティ特性等に着目して研究を展開した。研究では、統合失調症の前駆段階ともされる統合失調型パーソナリティ特性について特性強群と特性弱群を設定し、上述の認知機能指標に加えて注意機能・実行機能・メタ認知機能・ソースモニタリング機能測定を行った。その結果、健常者であっても特性強群では、統合失調症患者にみられるような機能低下が確認された（論文*6; 学会発表*44,*45,*46）。精神障害の発症予測の補助手段になりうるこれらの指標とストレスコーピング指標や幸福感尺度等を関連づけて評価することで、学生へよりきめ細やかな心理的・教育的配慮ができる可能性がある。

３．個々人のヒト特性を総合的に評価するためのデータ分析法の創出

３．１．ヒト特性の多面的評価を可能にする推定器の構築

縦断研究の一環として得られた脳皮質・白質・賦活量等の構造・機能データといった異なる時空間特性をもつ多次元脳データ、約 200 個のヒト特性要素に関する心理測定データを統合的に扱えるデータ分析プロセス（「ヒト特性推定器」と呼称））（論文*9;学会発表*6, *9;その他*1）を構築した。

具体的には、162 名の研究協力者に対して知能検査（WAIS-III）を実施するとともに、質問紙により情動知能を含む 130 の心理特性の測定を実施した。また同一の実験参加者に MRI 測定を行い、解剖画像および安静時脳活動データを収集した。その後、上述の心理データと解剖画像について VBM（voxel based morphometry）を行い、個々の心理指標に対応する 163 の脳領域を示すマップ（TFU テンプレート）を同定した。各脳領域について安静時脳活動（信号）を抽出して、脳領域間の相関行列を実験参加者の人数分作成した。次に相関行列と心理指標について回帰分析とネットワークベース統計量を用いた解析（Network-based statistics 解析）を行い、心理指標との関連が有意な 111 の脳内ネットワークを同定した。同定されたネットワーク（のエッジ）を機械学習アルゴリズムの 1 つである SVM（support vector machine）の入力に使用し、正解データとして心理特性データを使用して、入力情報に基づいて心理指標データを推定できる関数を求めた。機械学習の結果、求められた関数（分類器）を

法人番号	041001
プロジェクト番号	S1411001

用いることで、新たな個人の脳画像データのみから当該個人の心理特性の推定が可能となった。この推定器により、MRI により得られる脳のデータ（測定時間約 13 分）だけで、社会性、IQ、EQ、パーソナリティ 5 特性、職業適性を 8 段階または 3 段階で評価でき、学習・訓練の効果の評価が可能になった。本プロジェクトのように1研究の中でこれだけ多岐にわたるヒト特性要素を扱ったマップは世界的に類を見ないものである。

３．２．職業従事者データを用いた「ヒト特性推定器」の妥当性の検証

２．２．で述べた職業従事者の MRI データから、「ヒト特性推定器」を利用して職業適性の推定を行った。その結果、保育・リハビリ・看護の職業に従事する研究協力者の職業適性レベルは、事務職に就労している研究協力者より有意に高く推定されることが確認できた。本知見は「ヒト特性推定器」の職業適性評価の妥当性を保証するものであり、学習・訓練による職業適性の変化をこの推定器により追跡可能であることを示している。

３．３．職業適性の多面的評価を可能にする推定器の構築

「ヒト特性推定器」のために蓄積してきた脳機能ネットワークデータおよび他機関が提供する脳構造データに、新たに厚生労働省編 一般職業適性検査（General Aptitude Test Battery: GATB）のデータを組み合わせて、新たに機械学習法を適用し、“職業適性推定器”を作成した（論文*8; 学会発表*4, *26）。19 種の職業群に関する適性を3段階で推定することができる。実際に、5～10 年の経験のある二つの職種群（看護関連職種と事務関連職種）に属する研究協力者に対して MRI データから職業適性推定器を利用し職業適性を推定した。その結果、職種の違いが脳機能ネットワークに反映されていることが確認できた。

３．４．ヒト特性・職業適性の可塑的変化の推定

ヒト特性推定器と職業適性推定器を用いて MRI データから各個人の約3年間の可塑的変化の推定を 12 名のデータを用いて行った。その結果、看護関連職に関連する脳機能ネットワークでの可塑的変化が事務関連職に関連する脳機能ネットワークでの可塑的変化より多いことが確認でき、本学の教育課程による可塑的変化の可能性が示唆された。

３．５．fMRI/MRI 測定法の改良：脳の可塑的変化に関するミクロ的なメカニズムの解明

脳内の樹状突起や棘突起等のミクロ的な変化を計測するための測定方法を作製した。組織または機能的な変化を T1 コントラスト測定法により計測した。楽器演奏経験などの訓練により、関連機能部位の T1 の変化を計測することができた（論文*22; 学会発表*19,*22,*26）。また、マクロな脳機能・形態測定からミクロな機能情報を推定する測定方法を作製し、測定を行った（論文*23,*26; 学会発表*23,*26,*27,*28,*29）。これらの結果はヒト特性が脳内で顕現するメカニズムの解明と「ヒト特性推定器」の性能向上へつながると期待できる。

３．６．fMRI/MRI 測定法の改良：脳機能の動特性

高速 MRI 測定法および刺激パラダイムの改良により脳活動の動的信号、動的ネットワークの検出を試みた（学会発表*17,*18,*25,*30）。これにより fMRI で数十ミリ秒の速さで生じる神経活動の検出可能性を示した（論文*12）。また、脳活動信号のフィードフォワードとフィードバック伝達を fMRI で捉えることに成功した（論文*16）。これらの結果は、脳ネットワークの動特性の解明に貢献でき、「ヒト特性推定器」の精度向上に寄与するものと考える。

＜優れた成果が上がった点＞

大学教育、職業適性、社会的能力に焦点を当てた約 200 にも達するヒト特性を扱って、100 名単位の fMRI/MRI による脳データと組み合わせたデータベース（TFU テンプレート）を作製した。当該データベースは世界的にも類を見ない情報量をもつ。今後縦断研究データが含まれることにより、個人の認知・脳機能の成長にまで対応できる先駆的なデータベースとなる。

また、1 回の脳計測のみで多様なヒト特性を客観的に評価できるデータ分析プロセスである「ヒト特性推定器」を作製した。作製にあたり、ヒト特性データと脳データを統合するという世界

法人番号	041001
プロジェクト番号	S1411001

的に例の少ない最新の手法を用いており、学術的に意義深い。さらに、個々人の職業適性の推定に特化した「職業適性推定器」をも作製し、発表することができた。これら推定器により、従来研究のように一般的傾向ではなく、個人を評価できるという点で教育・臨床場面での応用が期待できる。

＜課題となった点＞

本プロジェクトにおける研究結果・成果における限界と課題は以下のようにまとめられる。

(1) 今回のデータベースの元となる 153 名のデータサンプルを用いて、統計的に有意な結果を得ることが出来た。しかし、このデータサンプルが日本全体のデータに対してどの程度の代表性を表すかについて検討を行う必要がある。また、最近の国内外の動向及び精度の向上の観点から、より規模の大きいデータベースへの拡張の必要性も検討する必要がある。さらに、心理指標同士の相関を検討して、各心理指標で構成されるヒト特性空間を総合的に現す新たな心理指標の作成についての検討も必要である。

(2) 縦断研究により可塑的変化が確認できたものの、測定のために使用したデータのサンプルサイズが小さいために大学の教育カリキュラムなどと可塑的変化の関連を解明するまでには至らなかった。10 回以上の繰り返し測定データについてのみ分析を行ったが、繰り返し測定の回数が少ないデータについても可塑的変化の検出が出来るように分析方法を検討する必要がある。また、この研究成果の発展を図る上で、今後新たな研究計画の策定をも検討する必要がある。

(3) 質問紙などの心理測定と resting-state fMRI により同定された脳機能ネットワークの機能的選択性などの比較検討のために task fMRI またはメタ分析による検討が必要である。しかし、課題作成などの限界とメタ分析のための既存の task fMRI によるデータベースの不足などから、現段階での比較検討は困難であるため、今後、長期的な視野のもと検討方法などを計画していく必要がある。その一環として、現在、task-applied resting state fMRI パラダイムを考案して、通常の resting-state fMRI 測定と同様な条件で持続的に課題（パズル課題、実行機能課題など）を与えながら fMRI データを得ることにより task 時の脳機能ネットワークを同定する実験を遂行している。

(4) 脳機能ネットワークの同定で用いた 163 個の脳部位のセットにおける個々の脳部位は特定の心理特性を表現するものであり、同定されたネットワークの機能的特性を理解する上で有用である。しかし、その脳部位セットは脳全体を均一にカバーするものではなかった。より均一な脳部位セットを作成するために task fMRI データなどを追加して同定精度の比較を行う必要がある。

(5) 職業適性・能力の脳機能ネットワークの同定では、関連する心理・行動指標の数が少なかったことなどから、他の研究グループが作製した既存の脳部位のセットを組み合わせて構成した 272 個からなる脳部位のセットを用いた。TFU template の 163 個の脳部位セットと比較検討の上、二つを統合することをも検討する必要がある。

(6) 同定された各脳機能ネットワークは統計的に有意に関連する心理指標を表しているが、必ずしもそのネットワークが関連するヒト特性を処理するための機能的活動に参加するとは限らない。この問題を解決するための方法を検討中である。

法人番号	041001
プロジェクト番号	S1411001

(7) ヒト特性推定器の場合の推定精度約 30％と職業適性・能力推定器の推定精度約 60％はチャンスレベルに比べて優位に高い精度であり、個人データの場合は複数の繰り返し測定時に有意な結果が出せる。このような点を踏まえれば実用的に応用できるが、より性能の向上が必要であり、そのための研究を継続している。MRI データだけで設計した推定器の精度は約 80％であり、追跡測定においては有効であると考えられるが、心理特性推定を含む精度の向上のためのさらなる努力が要求される。

＜自己評価の実施結果と対応状況＞

本プロジェクトは、教育・訓練・職業・パーソナリティ等の要因による個人の認知・脳機能の長期的変化の客観的計測・評価を目標に掲げて推進された。その結果、個人の認知・脳機能を客観的に計測・評価するための「ヒト特性推定器」および「職業適性推定器」を開発することに成功した。さらには、当該推定器を用いて就業・教育によるヒト特性および職業適性の可塑的変化の検出が可能となった。以上から、本プロジェクトの目標である“個々人に焦点を当てた社会的・職業的能力の定量的な推定・理解・育成を志向し、個々人を評価できる認知・脳科学的知見からの情報提供基盤の形成”が概ね達成できたと言える。

今回の自己評価は、「目標」・「現状」・「効果が上がっている事項・課題事項」・「改善の方向性」等の観点から本学の内部質保証定期点検・評価の形で行われたものであるとともに、月に 1 回程度のペースで開催するメンバーミーティングにおける進捗状況報告でも随時行われてきたものである。このような自己評価は、外部有識者 3 名による外部評価委員会による高い評価によって支持されている。したがって各グループの研究成果やプロジェクト全体の目標達成度が、社会的インパクトも含めて中立的・客観的に評価されたと考えられる。

＜外部（第三者）評価の実施結果と対応状況＞

３名の外部評価委員（出江紳一教授（東北大学大学院医学系研究科）、松岡和生教授（岩手大学人文社会科学部）、福永雅喜准教授（自然科学研究機構生理学研究所））により、平成 28 年 2 月には書面審査と実地審査、平成 31年 3 月には書面審査が行われた。いずれの外部評価においても、総評として、高い社会的還元性・貢献度がある研究プロジェクトであり、学術的な意義・新規性も高い。研究方法も妥当であり、当初の研究目標は達成されているとの評価を受けた。

＜研究期間終了後の展望＞

今後は収集を終えた縦断データに基づいて、大学における社会的・職業能力の育成効果のさらなる抽出を行うとともに、一個人の受けた大学教育・大学生活の中での種々の経験の何が社会的・職業能力を育む糧となったのかの検討を行う形で本プロジェクトを纏め上げる。本プロジェクトにおいて作製されたヒト特性推定器については、個々人のヒト特性を表現する指標の妥当性・信頼性の評価とヒト特性に関する MRI 測定の限界についての評価、また職業適性推定器については、多様な職業分野ごとに勤務年数の多いエキスパートの脳機能測定データの活用を行っていくことで、推定精度のさらなる向上を目指す。

令和元年度は、本プロジェクトの成果を発展的に活用することを意識して、超高齢化する地域社会で生活する人々の認知機能に焦点を当てた研究を展開していく。とりわけ加齢に伴う通常の認知機能変化・軽度認知障害（Mild Cognitive Impairment:

法人番号	041001
プロジェクト番号	S1411001

MCI）・認知症（主としてアルツハイマー型認知症）をターゲット分野として、多様な脳機能・構造指標および心理指標を用いて中高年の脳機能・構造画像および心理特性データベースを作成し、ヒト特性推定器の対象範囲の拡大を目指す。そのため、「介護老人保健施設せんだんの丘」との共同研究を中心とした研究体制の確立、データ計測・分析方法の選定、研究協力者の選定など研究フレームワークの構築を着実に進める。

＜研究成果の副次的効果＞

本プロジェクトで構築した新たなデータ分析プロセス「ヒト特性推定器」「職業適性推定器」により、個々人が自分自身では自覚することの難しい社会的能力、職業適性、知能、情動知能、パーソナリティ等のヒト特性を推定して、個人が自分自身を知るための資料・エビデンスを提供するサービス、また企業における人材管理・育成の補助サービス等につながる可能性が見いだされた。今後当該サービスの提供を行う共同開発企業を募ることを視野に活動範囲を広げる。

12 キーワード（当該研究内容をよく表していると思われるものを8項目以内で記載してください。）

（1）社会的能力 （2）職業適性 （3）大学教育
（4）fMRI （5）脳機能ネットワーク （6）可塑性
（7）機械学習 （8）「ヒト特性推定器」

13 研究発表の状況（研究論文等公表状況。印刷中も含む。）
上記、11(4)に記載した研究成果に対応するものには＊を付すこと。

＜雑誌論文＞

1 Sung, Y., Kawachi, Y., Ogawa, S. (in press) Comparison of multichannel head array coils for fMRI experiments. *Report of Kansei Fukushi Research Institute*,20,153-157.

*2 Otomo, Y., Kawachi, Y., Sung, Y., Ogawa S. (2019) A linear-mixed effect model analysis of the effect of schizotypal personality traits on confidence in reality monitoring. *Tohoku Psychologica Folia*, 77, 83-90.

*3 阿部千裕・河地庸介（2018）実行機能を構成する要素に関する研究動向と課題．感性福祉研究所年報, 19, 149-156.

*4 小松紘（2018）理解とパーソナリティの研究ー文章理解への性格特性の影響．感性福祉研究所年報, 19, 115-127.

5 Nazari, Z., Inamine, M., Sugama, Y., Kang, D., Kawachi, Y., Sung, Y., Ogawa, S. (2018) Classification of Resting State fMRI Data by an Unsupervised Neural Network. *Report of Kansei Fukushi Research Institute*, 19, 135-139.

*6 大友ゆき・河地庸介・阿部千裕・成烈完・小川誠二（2018）統合失調型パーソナリティ特性と自閉症スペクトラム特性のメタ認知における差異．感性福祉研究所年報, 19, 157-165.

7 Sung, Y., Kang, D., Kawachi, Y., Ogawa, S. (2018) A Comparison of Resting State fMRI Signals Depending on Participant's Conditions under MRI Measurements. *Report of Kansei Fukushi Research Institute*, 19, 129-134.

*8 Sung, Y., Kawachi, Y., Choi, U.-S., Kang, D., Abe, C., Otomo, Y., Ogawa, S. (2018) Estimation of vocational aptitudes using functional brain networks. *Human Brain Mapping*, 39(9), 3636-3651.

法人番号	041001
プロジェクト番号	S1411001

*9 Sung, Y., Kawachi, Y., Choi, U.-S., Kang, D., Abe, C., Otomo, Y., Ogawa, S. (2018) A Set of Functional Brain Networks for the Comprehensive Evaluation of Human Characteristics. *Front Neurosci*, 12:149, doi: 10.3389/fnins.2018.00149

10 Nazari, Z., Inamine, M., Sugama, Y., Kang, D., Kawachi, Y., Sung, Y., Ogawa, S. (2017) Evaluation of characteristics of resting state fMRI data by Machine Learning. *Report of Kansei Fukushi Research Institute*, 18, 281-284.

11 Kang, D., Sung, Y., Ogawa, S. (2017) Realization of a Longitudinal Relaxation Time Measurement with High Spatial Resolution. *Report of Kansei Fukushi Research Institute*, 18, 285-292.

*12 Sung, Y., Kang, D., Kawachi, Y., Ogawa, S. (2017) Detection of fast MRI signals by an EEG-like stimulus scheme and multi-voxel pattern analysis. *Report of Kansei Fukushi Research Institute*, 18, 275-280.

*13 大友ゆき・河地庸介・阿部千裕・成烈完・小川誠二（2017）メタ認知と自己成長主導性の関連性. 感性福祉研究所年報, 18, 293-299.

*14 Abe, C., Kawachi, Y., Sung, Y., Ogawa, S. (2017). The effects of short-term practice on executive functions. *Tohoku Psychologica Folia*, 75, 15-21.

*15 Sone, T., Kawachi, Y., Abe, C., Otomo, Y., Sung, Y., Ogawa, S. (2017) Attitude and Practice of Physical Activity and Social Problem-Solving Ability among University Students. *Environmental Health and Preventive Medicine*, 22:18, doi: 10.1186/s12199-017-0625-8

*16 Choi, U.-S., Sung, Y., Ogawa, S. (2017) Steady-state and dynamic network modes for perceptual expectation. *Scientific Reports* 7, doi:10.1038/srep40626.

*17 Kawachi, Y. (2016) Visual Mislocalization of Moving Objects in an Audiovisual Event. *PLoS ONE* 11(4): e0154147. doi:10.1371/journal.pone.0154147

18 河地庸介 (2016). 脳活動からみる芸術鑑賞・制作 臨床美術ジャーナル, 5(1), 75-81.

19 Sung, Y., Kawachi, Y, Choi, U.-S., Kang, D., Ogawa, S. (2016) Modality dependent sensitivity in evaluating brain plasticity. *Report of Kansei Fukushi Research Institute*, 17, 271-277.

*20 Nazari, Z., Kang, .D, Kawachi, Y., Sung, Y., Ogawa, S. (2016) Hierarchical clustering of fMRI Data. *Report of Kansei Fukushi Research Institute*, 17, 279-285.

*21 阿部千裕・河地庸介・坪川宏・成烈完・小川誠二 (2016) 一般知能と主観的実行機能の関連性. 感性福祉研究所年報, 17, 287-292.

*22 Choi, U.-S., Sung, Y., Hong Sujin, Chung, J.Y., Ogawa, S. (2015) Structural and functional plasticity specific to musical training with wind instruments. *Front. Hum. Neurosci.* 9: 597. doi: 10.3389/fnhum.2015.00597

*23 Chung, J.Y., Sung, Y., Ogawa, S. (2015) Evaluation of the contribution of signals originating from large blood vessels to signals of functionally specific brain areas. *Biomed Res Int.*, 2015; 2015: 234345.

*24 Kang, D., Sung, Y., Kang, C.-K. (2015) Fast imaging techniques for fMRI: consecutive multi-shot echo planar imaging accelerated with GRAPPA technique. *Biomed Res Int.*, 2015; 2015: 394213.

*25 Sung, Y., Kawachi, Y., Kang, D., Ogawa, S. (2015) Evaluation of differences in brain plasticity with individual characteristics by MRI. *Report of Kansei Fukushi Research Institute*, 16, 35-242.

*26 Sung, Y., Choi, U.-S., Ogawa, S. (2014) Invariance of functional characteristics to task difference at low-level and high-level areas in the ventral visual pathway. *J. Behavioral and Brain Science*, 4, 402-411.

法人番号	041001
プロジェクト番号	S1411001

＜図書＞

1 河地庸介（2018）VBM・DTI　山田冨美雄・坂田省吾（編）生理心理学と精神生理学 第 I 巻　北大路書房

2 櫻井研三・河地庸介（2018）剰余変数の概念と実験者関連の剰余変数　坂上貴之他（編）基礎心理学実験法ハンドブック　朝倉書店

3 河地庸介・櫻井研三（2018）被験者関連の剰余変数　坂上貴之他（編）基礎心理学実験法ハンドブック　朝倉書店

4 河地庸介・櫻井研三（2018）実験方法・装置関連の剰余変数　坂上貴之他（編）基礎心理学実験法ハンドブック　朝倉書店

＜学会発表＞

（国際学会）

1 Kang, D., Sung, Y., Shioiri, S. Estimation of physiological sources of nonlinearity in bold signals. The 26th annual meeting of International Society for Magnetic Resonance Imaging, Paris, France, July 17-21, 2018

2 Sung, Y., Kawachi, Y., Ogawa, S. Functional specificity of resting-state fMRI signals. The 22th annual meeting of the Organization for Human Brain Mapping, Singapore, July 17-21, 2018

3 Sung, Y., Ogawa, S. Modality-dependent functional specificity in resting-state fMRI signals. The 46th annual meeting of the Japanese Society for Magnetic Resonance In Medicine, Kanazawa, Japan, Sep 18-20, 2018

*4 Sung, Y., Kawachi, Y., Otomo, Y., Ogawa, S. Occupational abilities and function networks estimated through resting state fMRI. The 45th annual meeting of the Society for Neuroscience, San Diego, USA, Nov 3-7, 2018

5 Ogawa, S. On some approaches of fMRI. The 22st annual meeting of the Organization for Human Brain Mapping, Vancouver, Canada, June 25-29, 2017

*6 Sung Y., Brain profile seen by functional networks and human traits. The 2nd International Neuroscience Symposium, Incheon, Korea, May 24, 2017.

7 Sung, Y., Kang, D., Ogawa, S. Measurement of task-induced high frequency band signals by ultrahigh temporal resolution imaging. The 25th annual meeting of International Society for Magnetic Resonance Imaging, Hawaii, USA, April 22-27, 2017

8 Sung, Y., Kang, D., Kawachi, Y., Ogawa, S. Brian maps reflected in different imaging modalities. The 22st annual meeting of the Organization for Human Brain Mapping, Vancouver, Canada, June 25-27, 2017

*9 Sung, Y., Kang, D., Kawachi, Y., Kang, D., Abe, C., Otomo, Y., Ogawa S. Functional brain networks reflecting human characteristics. The 45th annual meeting of the Society for Neuroscience, Washington DC, USA, Oct. 11-15, 2017

*10 Niwano, K., Ito, A., Tanabe, M., Sato, Y., Fujii, T. An fMRI study of the relationship between neuroticism and neural responses to infant emotional faces. 15th European Congress of Psychology, Amsterdam, Netherlands, July 12-14, 2017

11 Ito, A., Kawachi, Y., Kawasaki, I., Fujii, T. Age-related reduction of cognitive dissonance. 31st International Congress of Psychology (ICP2016) July 24-29, 2016, Yokohama, Japan

*12 Ito, A., Niwano, K., Tanabe, M., Sato, Y., Fujii, T. The effect of childcare training on the perception of infant's emotional facial expression. 31st International Congress of Psychology (ICP2016), Yokohama, Japan, July 24-29, 2016

法人番号	041001
プロジェクト番号	S1411001

*13 Niwano, K., Ito, A., Tanabe, M., Sato, Y., Fujii, T. Relationship between regional brain responses to infant faces and personality traits in young female adults. 31st International Congress of Psychology (ICP2016), Yokohama, Japan, July 24-29, 2016

*14 Niwano, K., Ito, A., Tanabe, M., Sato, Y., Fujii, T. Behavioral inhibition system relates to the responses of the dorsal anterior cingulate cortex and the orbitofrontal cortex to infant emotional faces. The 39th Annual Meeting of JNS, Yokohama, Japan, July 20-22, 2016

*15 Tanabe, M., Niwano, K., Ito, A., Sato, Y., Fujii, T. Correlations between the brain responses of nulliparous females when viewing infants' facial expressions and their personality. 31st International Congress of Psychology (ICP2016), Yokohama, Japan, July 24-29, 2016

16 Fujii, T., Ito, A., Jenkins, R., Sanders, J., Yoshida, K., Murakami, Y., Sakai, S., Tanabe, M. The effect of wearing a medical mask and sunglasses on perceiver's impression. 31st International Congress of Psychology (ICP2016), Yokohama, Japan, July 24-29, 2016

*17 Sung, Y., Choi, U.-S., Ogawa, S., Interaction between high and low level areas and the temporal window for repetition suppression. The 22st annual meeting of the Organization for Human Brain Mapping, Geneva, Switzerland, Jun 26-30, 2016.

*18 Sung, Y., Kang, D., Ogawa, S., A challenge for sub‐millisecond fMRI. The 44th annual meeting of the Japanese Society for Magnetic Resonance In Medicine, Omiya, Japan, Sep 9-11, 2016.

*19 Kang, D., Sung, Y., Ogawa, S., Comparison of voxel-based morphometry and T1 absolute value. The 44th annual meeting of the Japanese Society for Magnetic Resonance In Medicine, Omiya, Japan, Sep 9-11, 2016.

20 Sung, Y., Kang, D., Kawachi, Y., Ogawa, S., Brain plasticity changes by playing wind instruments and piano. The 46th annual meeting of the Society for Neuroscience, SanDiego, USA, Oct 12-16, 2016.

21 Sung, Y., Microscopic functional structures seen through fMRI signals. BIT's 6th annual world congress of neurotalk-2015, Hanzhou, China, May 22-24, 2015.

*22 Choi, U.-S., Sung, Y., Chung J.Y., Ogawa, S. Brain plasticity seen in musicians of wind instruments. 21st annual meeting of the Organization for Human Brain Mapping, Hawaii, USA, Jun 14-18, 2015.

*23 Kang, D., Sung, Y., Shioiri, S., Ogawa, S. Investigation of microscopic functional specificity for attention in peripheral visual field. 21st annual meeting of the Organization for Human Brain Mapping, Hawaii, USA, Jun 14-18, 2015.

24 Sung, Y., Kang, D., Ogawa, S., Robustness of microscopic functional structures estimated by dynamic magnetic susceptibility change. The 21st annual meeting of the Organization for Human Brain Mapping, Hawaii, USA, Jun 14-18, 2015.

*25 Sung, Y., Yoon, H., Choi, U.-K., Ogawa, S. Regional difference in characteristics for top-down modulation in the ventral visual stream. The 45th annual meeting of the Society for Neuroscience, Chicago, USA, Oct 17-21, 2015

*26 Sung, Y., Kang, D., Ogawa, S. Morphological changes in cortical microstructure of the brain by short-term training. The 45th annual meeting of the Society for Neuroscience, Chicago, USA, Oct 17-21, 2015

*27 Ogawa S., Macro-scale structure and function of the brain visualized by MRI, Gachon Univ. NRI Symposium, Incheon, Korea, Feb 24, 2016

*28 Kang, D., Sung, Y., Shioiri, S., Ogawa, S., Estimation of functional specificity of visual areas by a transverse relaxation profile. The 10th Asia-Pacific conference on Vision, Takamatsu, Japan, July 19-22, 2014.

法人番号	041001
プロジェクト番号	S1411001

*29 Sung, Y., Chung, J.Y., Ogawa, S. Effects of signals originating from large blood vessels on BOLD signals of the fusiform face area. The 44th society for neuroscience meeting, Washington DC, USA, November 15-19, 2014

*30 Choi, U.-S., Sung, Y., Kim ,Y.-B., Cho, Z.-H., Yoon, H., Ogawa, S., Functional differences in processing preferred and non-preferred stimuli at object selective areas. The 44th society for neuroscience meeting, Washington DC, USA, November 15-19, 2014

（国内学会）

*31 成烈完・河地庸介・小川誠二 脳機能ネットワークによるヒト特性変化の推定．第 21 回日本ヒト脳機能マッピング学会，東京，2019 年 3 月．

*32 Sung Y, Kawachi Y, Ogawa S. Estimation of specific functional brain areas reflecting individual characteristics. The 21st Congress of Japan Human Brain Mapping Society, Tokyo, Japan, Mar 15-16, 2019

*33 Kikuchi Y, Sung Y, Ogawa S. Quantification method of functional brain networks and estimation of network measure. The 21st Congress of Japan Human Brain Mapping Society, Tokyo, Japan, Mar 15-16, 2019

34 小川誠二、「あなたのことはあなたの脳に訊け」は可能か？。豊田理化学研究所　懇話会招待講演、2019 年 2 月

35 小川誠二, Challenges in fMRI.　第４６回日本磁気共鳴医学会大会、特別講演、2018 年 9 月

36 小川誠二、Some Challenges in fMRI.　東北大学 Neuro Global 国際共同大学院サマースクール, 講演，2018 年 9 月

*37 阿部千裕・河地庸介 実行機能ネットワークの同定．日本心理学会第 82 回大会，宮城, 2018 年 9 月

*38 阿部千裕・河地庸介 実行機能ネットワークテストの考案．日本認知心理学会第 16 回大会，大阪, 2018 年 9 月

*39 大友ゆき・河地庸介　線形混合モデルでみるメタ記憶．日本感性福祉学会第 18 回大会，宮城, 2018 年 11 月

*40 大友ゆき・河地庸介 パーソナリティ特性が既学習判断（Judgment of Learning: JOL）に及ぼす影響．東北心理学会第 72 回大会，岩手, 2018 年 11 月

*41 阿部千裕・河地庸介 短期的訓練が実行機能に及ぼす影響．日本感性福祉学会第 17 回大会，宮城, 2017 年 10 月

*42 大友ゆき・阿部千裕・河地庸介 メタ認知と自己成長主導性の関連性．日本感性福祉学会第 17 回大会，宮城, 2017 年 10 月

*43 阿部千裕・河地庸介・北村康宏・成烈完・小川誠二 報酬を導く意思決定方略への依存ーアイオワギャンブリング課題を用いた検討．日本基礎心理学会第 36 回大会，大阪, 2017 年 12 月

*44 河地庸介・阿部千裕・成烈完・松江克彦・小川誠二 統合失調型パーソナリティの個人差が注意の下位機能間の相互作用に及ぼす影響．第 46 回日本臨床神経生理学会学術大会，福島, 2016 年 10 月．

*45 阿部千裕・河地庸介・成烈完・松江克彦・小川誠二 実行機能と統合失調型パーソナリティの関係．第 46 回日本臨床神経生理学会学術大会，福島, 2016 年 10 月．

*46 大友ゆき・阿部千裕・河地庸介・成烈完・松江克彦・小川誠二 統合失調型パーソナリティ傾向におけるメタ記憶の特徴．第 46 回日本臨床神経生理学会学術大会，福島, 2016 年 10 月．

47 小川誠二　「MRI によるマクロスケールでの脳の構造と機能の可視化」理研光量子工学研究

法人番号	041001
プロジェクト番号	S1411001

セミナー, 2016 年 1 月，和光.

48 小川誠二 「機能的 MRI の開発と発展」東京慈恵会医科大学総合医科学研究センター創立 20 周年記念シンポジウム 基調講演, 2015 年 11 月，東京.

49 小川誠二 「MRI でみる脳機能活動の幾つかの側面」東芝開発研究センターセミナ, 2015 年 6 月，川崎.

50 小川誠二 「fMRI の昨今」熊本大学イメージングセンターセミナー, 2015 年 5 月，熊本.

＜研究成果の公開状況＞（上記以外）

シンポジウム・学会等の実施状況、インターネットでの公開状況等

＜既に実施しているもの＞

https://www.tfu.ac.jp/research/gp2014_01/index.html
https://www.tfu.ac.jp/research/gp/2014_01.html

＜これから実施する予定のもの＞

14 その他の研究成果等

*1. A program manual for Estimator of Human Characteristics.
上記 11（4）にて述べた、1 回の MRI 測定から得られる脳データからヒト特性を総合的に評価することの出来る「ヒト特性推定器」（ソフトウェア）の操作マニュアル

法人番号	041001
プロジェクト番号	S1411001

15 「選定時」及び「中間評価時」に付された留意事項及び対応

＜「選定時」に付された留意事項＞

該当なし

＜「選定時」に付された留意事項への対応＞

該当なし

＜「中間評価時」に付された留意事項＞

該当なし

＜「中間評価時」に付された留意事項への対応＞

該当なし

（様式1）

法人番号	41001
プロジェクト番号	S1411001

16 施設・装置・設備・研究費の支出状況（実績概要） （千円）

年度・区分		支出額	内訳						
			法人負担	私学助成	共同研究機関負担	受託研究等	寄付金	その他（　　）	備考
平成26年度	施設	0	0	0	0	0	0		
	装置	0	0	0	0	0	0		
	設備	143,154	54,830	88,324	0	0	0		
	研究費	12,968	7,141	5,827	0	0	0		
平成27年度	施設	0	0	0	0	0	0		
	装置	0	0	0	0	0	0		
	設備	0	0	0	0	0	0		
	研究費	25,774	13,990	11,784	0	0	0		
平成28年度	施設	0	0	0	0	0	0		
	装置	0	0	0	0	0	0		
	設備	0	0	0	0	0	0		
	研究費	26,813	15,269	11,544	0	0	0		
平成29年度	施設	0	0	0	0	0	0		
	装置	0	0	0	0	0	0		
	設備	0	0	0	0	0	0		
	研究費	22,011	10,011	12,000	0	0	0		
平成30年度	施設	0	0	0	0	0	0		
	装置	0	0	0	0	0	0		
	設備	0	0	0	0	0	0		
	研究費	12,012	6,463	5,549	0	0	0		
総額	施設	0	0	0	0	0	0	0	
	装置	0	0	0	0	0	0	0	
	設備	0	0	0	0	0	0	0	
	研究費	99,578	52,874	46,704	0	0	0	0	
総計		99,578	52,874	46,704	0	0	0	0	

17 施設・装置・設備の整備状況 （私学助成を受けたものはすべて記載してください。）

《施　設》（私学助成を受けていないものも含め、使用している施設をすべて記載してください。） （千円）

施設の名称	整備年度	研究施設面積	研究室等数	使用者数	事業経費	補助金額	補助主体
東北福祉大学 感性福祉研究所	－	4,092㎡	42室	約150名	0	0	－

（様式1）

法人番号	41001
プロジェクト番号	S1411001

※ 私学助成による補助事業として行った新増築により、整備前と比較して増加した面積

0 ㎡

《装置・設備》（私学助成を受けていないものは、主なもののみを記載してください。） （千円）

装置・設備の名称	整備年度	型　番	台　数	稼働時間数	事業経費	補助金額	補助主体
（研究装置）				h			
				h			
				h			
				h			
				h			
（研究設備）							
f－MRI対応磁気共鳴撮影装置㏌ップグレードロ	平成26年度	Tim4Gアップグレード"MAGNETOM SkyraFit"	一式	1,860.25 h	119,988	74,032	私学助成
MRI対応EEG測定装置	平成26年度	BP-E32B16SYS	一式	266.5 h	14,850	9,162	私学助成
MRI対応眼球測定システム	平成26年度	ELM-CORE 他	一式	272.5 h	8,316	5,130	私学助成
				h			
				h			
（情報処理関係設備）							
				h			
				h			
				h			
				h			
				h			

18 研究費の支出状況 （千円）

年　度	平成　26　年度			
小科目	支出額	積算内訳		
		主な使途	金　額	主な内容
教育研究経費支出				
消耗品費	2,219	実験消耗品、解析ソフト、光学メディア等	1,735・336・148	実験消耗品、解析ソフト、光学メディア等
光熱水費	0		0	
通信運搬費	0		0	
印刷製本費	6	ポスター印刷代	6	ポスター印刷代
旅費交通費	1,411	研究打ち合わせ旅費、学会発表旅費、fMRI Training講習旅費	462・136・813	研究打ち合わせ旅費、学会発表旅費、fMRI Training講習旅費
報酬・委託料	1,265	被験者謝金、英文校正等	312・953	被験者謝金、英文校正等
（　　）	0		0	
計	4,901		4,901	
アルバイト関係支出				
人件費支出	361	研究補助	303	時給 710円，年間時間数 427.5時間
（兼務職員）			58	時給 730円，年間時間数 79.5時間
				実人数 15人
教育研究経費支出	0		0	
計	361		361	
設備関係支出（1個又は1組の価格が500万円未満のもの）				
教育研究用機器備品	7,706	MRI用プロジェクター、パソコン等	4,968・2,738	MRI用プロジェクター、パソコン等
図　書	0		0	
計	7,706		7,706	
研究スタッフ関係支出				
リサーチ・アシスタント	0			
ポスト・ドクター	0			
研究支援推進経費	0			
計	0			

（様式1）

法人番号	41001
プロジェクト番号	S1411001

（千円）

年　度	平成　27　年度			
小科目	支出額	積算内訳		
		主な使途	金額	主な内容
教育研究経費支出				
消耗品費	7,693	解析ソフト、質問紙、実験消耗品	6,051・675・967	解析ソフト、質問紙、実験消耗品
光熱水費	0		0	
通信運搬費	248	研究参加同意書配送料	248	研究参加同意書配送料
印刷製本費	10	研究参加同意書印刷代、学会ポスター印刷代	10	研究参加同意書印刷代、学会ポスター印刷代
旅費交通費	2,424	学会発表旅費、研究打合せ旅費等	1,194・1,230	学会発表旅費、研究打合せ旅費等
報酬・委託料	4,722	被験者謝金、ライセンス料等	4,084・638	被験者謝金、ライセンス料等
（修繕費）	70	備品修理費	70	備品修理費
計	15,167		15,167	
アルバイト関係支出				
人件費支出	2,702	研究補助	410	時給 710円，年間時間数 578時間
（兼務職員）			1,451	時給 730円，年間時間数 1988.5時間
			631	時給 750円，年間時間数 841時間
			63	時給 800円，年間時間数 78.5時間
			147	時給 820円，年間時間数 179.5時間
				実人数 19人
教育研究経費支出	0		0	
計	2,702		2,702	
設備関係支出（1個又は1組の価格が500万円未満のもの）				
教育研究用機器備品	7,879	MRI画像管理システム、プロジェクターレンズ等	3,240・4,639	MRI画像管理システム、プロジェクターレンズ等
図書	26	MRI・脳認知行動等に関する書籍	26	MRI・脳認知行動等に関する書籍
計	7,905		7,905	
研究スタッフ関係支出				
リサーチ・アシスタント	0			
ポスト・ドクター	0			
研究支援推進経費	0			
計	0			

（千円）

年　度	平成　28　年度			
小科目	支出額	積算内訳		
		主な使途	金額	主な内容
教育研究経費支出				
消耗品費	2,224	MRI関連消耗品、心理検査紙、検査用電子部品等	797・531・896	MRI関連消耗品、心理検査紙、検査用電子部品等
光熱水費	0		0	
通信運搬費	11	研究関連機器運搬費	11	研究関連機器運搬費
印刷製本費	331	出版掲載料、質問紙等印刷費、複写費	323・6・2	論文出版費、質問紙等印刷費、複写費
旅費交通費	2,202	国際学会参加費、国内学会参加費、研究打合せ等	758・105・1,339	国際学会参加費、国内学会参加費、研究打合せ等
報酬・委託料	5,596	研究協力謝金、ライセンス料等	5,306・290	研究協力謝金、ライセンス料等
（　　）				
計	10,364		10,364	
アルバイト関係支出				
人件費支出	4,667	研究補助	396	時給　730円，年間時間数　543時間
（兼務職員）			2,258	時給　750円，年間時間数　3011時間
			1,271	時給　770円，年間時間数　1651時間
			459	時給　820円，年間時間数　559.5時間
			283	時給　840円，年間時間数　336.5時間
				実人数　26人
教育研究経費支出	0		0	
計	4,667		4,667	
設備関係支出（1個又は1組の価格が500万円未満のもの）				
教育研究用機器備品	11,753	MRI用表面コイル/ポータブル脳波計測システム等	4,957・6,796	MRI用表面コイル/ポータブル脳波計測システム等
図書	29	心理関連図書、MRI関連図書	21・8	心理関連図書、MRI関連図書
計	11,782		11,782	
研究スタッフ関係支出				
リサーチ・アシスタント	0			
ポスト・ドクター	0			
研究支援推進経費	0			

法人番号	41001
プロジェクト番号	S1411001

計	0			

（千円）

年　度	平成　29　年度			
小科目	支出額	積算内訳		
		主な使途	金額	主な内容
教育研究経費支出				
消耗品費	5,474	解析用ソフト、質問紙、記録メディア	4,968・169・337	解析用ソフト、質問紙、記録メディア
光熱水費	0		0	
通信運搬費	17	研究機器運搬	17	研究機器運搬
印刷製本費	277	論文出版費、文献複写費	269・8	論文出版費、文献複写費
旅費交通費	3,552	国際学会参加旅費、研究打合せ旅費、国内学会参加旅費	2,515・559・478	国際学会参加旅費、研究打合せ旅費、国内学会参加旅費
報酬・委託料	4,517	研究協力謝金、英文校正費、学会参加費	3864・653	研究協力謝金、英文校正費等
（　　）				
計	13,837		13,837	
アルバイト関係支出				
人件費支出	2,933	研究補助	856	時給　750円，年間時間数　1,141時間
（兼務職員）			963	時給　770円，年間時間数　1,250時間
			478	時給　780円，年間時間数　612.5時間
			569	時給　800円，年間時間数　711時間
			26	時給　840円，年間時間数　31.5時間
			41	時給　870円，年間時間数　48時間
教育研究経費支出	0		0	実人数　16人
計	2,933		2,933	
設備関係支出（1個又は1組の価格が500万円未満のもの）				
教育研究用機器備品	5,241	MRI用ヘッドコイル/レーザープリンタ等	4,968・273	MRI用ヘッドコイル/レーザープリンタ等
図　書	0		0	
計	5,241		5,241	
研究スタッフ関係支出				
リサーチ・アシスタント	0			
ポスト・ドクター	0			
研究支援推進経費	0			
計	0			

（千円）

年　度	平成　30　年度			
小科目	支出額	積算内訳		
		主な使途	金額	主な内容
教育研究経費支出				
消耗品費	1,632	解析用ソフトウェア、検査用紙、実験消耗品	1272・202・158	解析用ソフトウェア、検査用紙、実験消耗品
光熱水費	0			
通信運搬費	10	研究機器運搬	10	研究機器運搬
印刷製本費	15	学会発表用ポスター	15	学会発表用ポスター
旅費交通費	2,202	国際学会参加費・研究打ち合わせ旅費・国内学会参加費	1341・544・317	国際学会参加費、研究打ち合わせ旅費、国内学会参加費
報酬・委託料	2,951	研究協力者金・学会参加費・英文校正	2232・582・137	研究協力謝金・学会参加費・英文校正
（修繕費）	74	備品修理費	74	備品修理費
計	6,884		6,884	
アルバイト関係支出				
人件費支出	3,360	研究補助	1,154	時給　780円，年間時間数　1480.5時間
（兼務職員）			1,656	時給　800円，年間時間数　2070時間
			444	時給　820円，年間時間数　541.5時間
			48	時給　870円，年間時間数　55時間
			58	時給　890円，年間時間数　65時間
				実人数　14　人
教育研究経費支出	0		0	
計	3,360		3,360	
設備関係支出（1個又は1組の価格が500万円未満のもの）				
教育研究用機器備品	1,768	MRI解析用デスクトップPC/心理検査・解析用ノートPC/認知検査・刺激提示用デスクトップPC	838・480・450	MRI解析用デスクトップPC/心理検査・解析用ノートPC/認知検査・刺激提示用デスクトップPC
図　書	0		0	
計	1,768		1,768	
研究スタッフ関係支出				
リサーチ・アシスタント	0			

法人番号	41001
プロジェクト番号	S1411001

ポスト・ドクター	0			
研究支援推進経費	0			
計	0			

Ⅲ 外部評価

平成 26 年度採択私立大学戦略的研究基盤形成支援事業
第 1 回 外部評価委員会

日　時：　平成 28 年 2 月 13 日　(土)
午前 10：00　～
場　所：　感性福祉研究所　大会議室

次　　第

開　　会　　(10：00～)
開会挨拶　　副所長　　松江 克彦

Ⅰ．外部評価委員の紹介
外部評価委員　　出江 紳一（東北大学大学院 医学系研究科　教授）
外部評価委員　　松岡 和生（岩手大学 人文社会科学部　教授）
外部評価委員　　福永 雅喜（自然科学研究機構 生理学研究所　准教授）

Ⅱ．本事業の取り組みについて（報告）
研究代表者　小川 誠二

昼　食（ランチミーティング）　　(12：00～)

Ⅲ．研究施設（MRI）の紹介

Ⅳ．外部評価委員による評価ならびに助言

閉　　会　　(15：00)
閉会挨拶　　研究代表者　　小川 誠二

私立大学戦略的研究基盤形成支援事業（H26－H31）

：社会的・職業能力育成プログラムに資する認知・脳科学的エビデンス情報提供基盤の構築

外部評価（2016年2月13日）用資料

研究代表者：小川誠二

目次

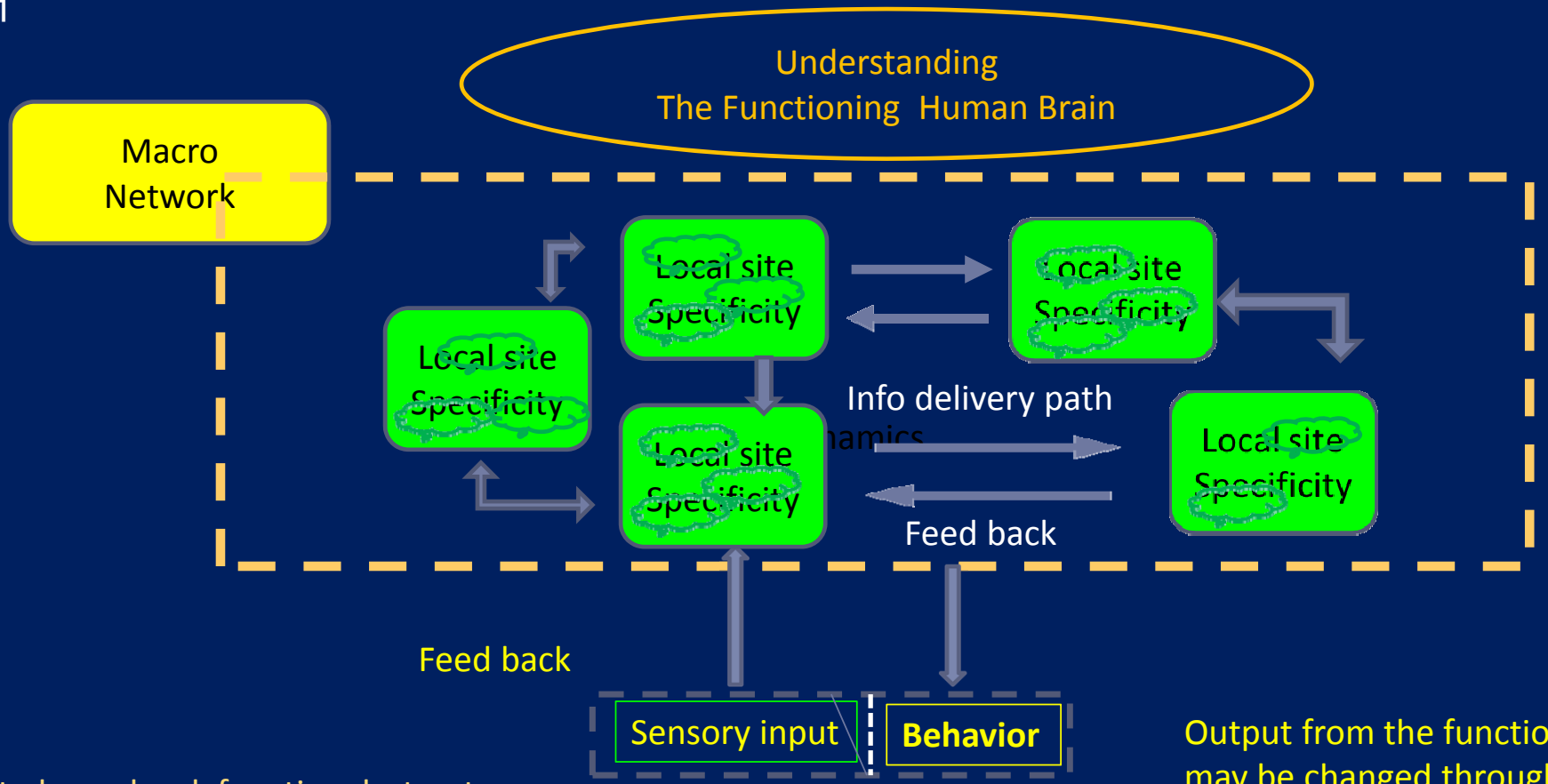
1. 経緯
2. 目的
3. 研究計画
4. 研究体制
5. 研究方法
6. 結果（進捗状況）
7. まとめ
8. 今後の課題

１．背景

・本研究は、学習・訓練などによる知識・技能などの獲得は脳の神経回路機能における何らかの可塑的変化を意味する（図１）、という作業仮説をヒトで検証するものである。

・近年のNeuroimaging technology（表１）の発展と前回の戦略プロジェクト（H20-H24）で得られた結果（聴覚野と視覚野での信号処理系の可塑性と音楽などの学習による脳活動・組織の変化）をもとに、大学教育期間中の学習・訓練などによる脳の機能的・構造的変化を経時的に計測する計画を立てた。

図1



Need to know local functional structures (functionally organized submodules) with their specificities, and intra- and inter-site Interaction, forming Network

Output from the functional network that may be changed through plasticity of neural system

図1

可塑性計測のためのMRI技術

表1

１）機能的MRI（fMRI）－task-based fMRI:
外因または内因的な刺激による脳の時空間的な機能的特性を検索
２）機能的MRI－resting state fMRI
無刺激時の脳の活動、主に、機能ネットワークの検索
３）構造的MRI（灰白質volume, thickness,白質のAnisotropy）
神経細胞やspineの密度のmacroな計測
４）構造的高分解度MRI（ Axonal connections や cortical submodules の変化、T1, T2*の脳内分布の局所的変化）

２．目的

社会的・職業能力育成プログラムに資する認知・脳科学的エビデンス情報の収集とそれらの応用法を提供する基盤の構築を目的とし、MRI測定による個々人の社会的・職業的能力の推定を目指す。

３．研究計画（コンセプト・年次計画）

ヒトの心理・活動などを総称するものをヒト行動と呼ぶことにする。

ヒト行動が顕現（representation）するために、基本的な心理及び脳機能要素の集合体 (set of basis) が存在すると考える。この基本要素の組み合わせによって、社会性（社会的能力）、職業適性（職業的能力）が表現できるとする。

例えば、目的志向的なヒト行動は注意・知覚・記憶・言語などの必須となる認知機能要素 (cognitive functional modules) とこれらの認知機能要素のヴァリエーションと組み合わせによる実行注意・プランニング・意思決定などの中核となる実行機能要素（Executive functional modules）により支えられる。このような認知機能要素と実行機能要素が基本機能要素になり得る。

社会的能力・職業的能力の測定のために

A. 互いに独立な基本機能要素の同定から社会・職業的機能の同定（bottom-up approach）

:(1) 互いに独立な認知機能要素の同定　(2) 基本認知機能要素のsub-setからなる中核となる実行機能要素の同定　(4) 社会・職業的機能の同定

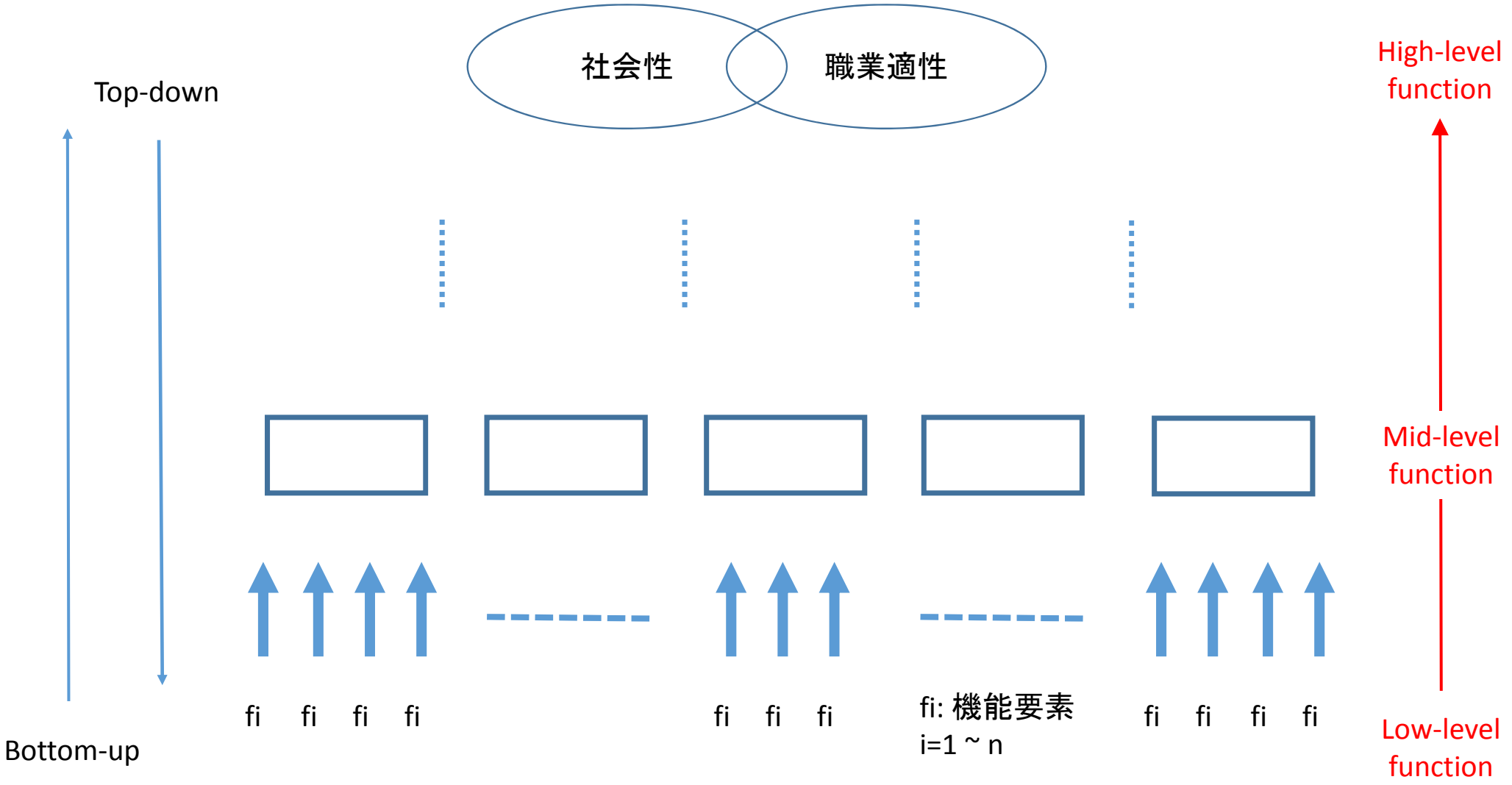
B. 社会・職業特性から行動基本要素の推定（top-down approach）

C. 各レベルの機能（要素）に対する short/mid/long-term plasticity の測定

を行う必要がある（図2）。

*A, B　は主として横断的研究、C は縦断的研究となる。

図2


社会性
職業適性
Top-down
Bottom-up
High-level function
Mid-level function
Low-level function
fi fi fi fi
fi fi fi
fi fi fi fi
fi: 機能要素
i=1 ~ n

（1）心理学的研究

質問紙・心理検査などの下位項目および心理実験データは各種基本機能要素（注意・記憶・感情・言語・知識など）を反映するものと仮定し

A. 各種心理指標の測定とその下位項目の定義から基本機能（要素）を推定、クラスタリングなどによりグループ化

B. 社会・職業的能力に関連する機能を課題ベースの実験により推定

C. 下位項目または上位項目に関連する心理・行動課題への訓練によるshort/mid/long-term plasticityの測定

を行う。

（２）MRI study

各種心理指標（認知・行動・思考・感情・知識・知能など）を測定する質問紙・心理テストなどの下位項目が脳に反映されると仮定し
解剖・機能画像の収集と

A. 心理指標の各下位項目に関連する脳の部位を同定
   各部位の機能的特性の同定
   各下位項目に対する機能的ネットワークの同定
B. 課題ベースの実験により社会的・職業的特性に関連する脳の機能部位とネットワークの推定
C. 下位項目または上位項目に関連する心理・行動課題への訓練により変化する脳の部位またはネットワークの推定による脳のmid/short-term plasticityの測定

を行う。

（3）社会性・職業特性推定プログラムの開発

心理・MRIデータからなるデータベースをもとに

パターン認知・マシンラーニングなどによる個々人の社会性・職業特性または大学在籍期間中教育・訓練によって発達した機能の推定を行う。

（4）年次計画

次のような年度別の研究計画に従って研究を行う（図３）

１）H２６年度：大学生を対象とした縦断研究を行うための認知課題・MRI測定方法・データ分析法の選定・予備実験、若年者・高齢者を対象とした横断研究への着手、認知・脳機能測定パラダイムの向上と創出。

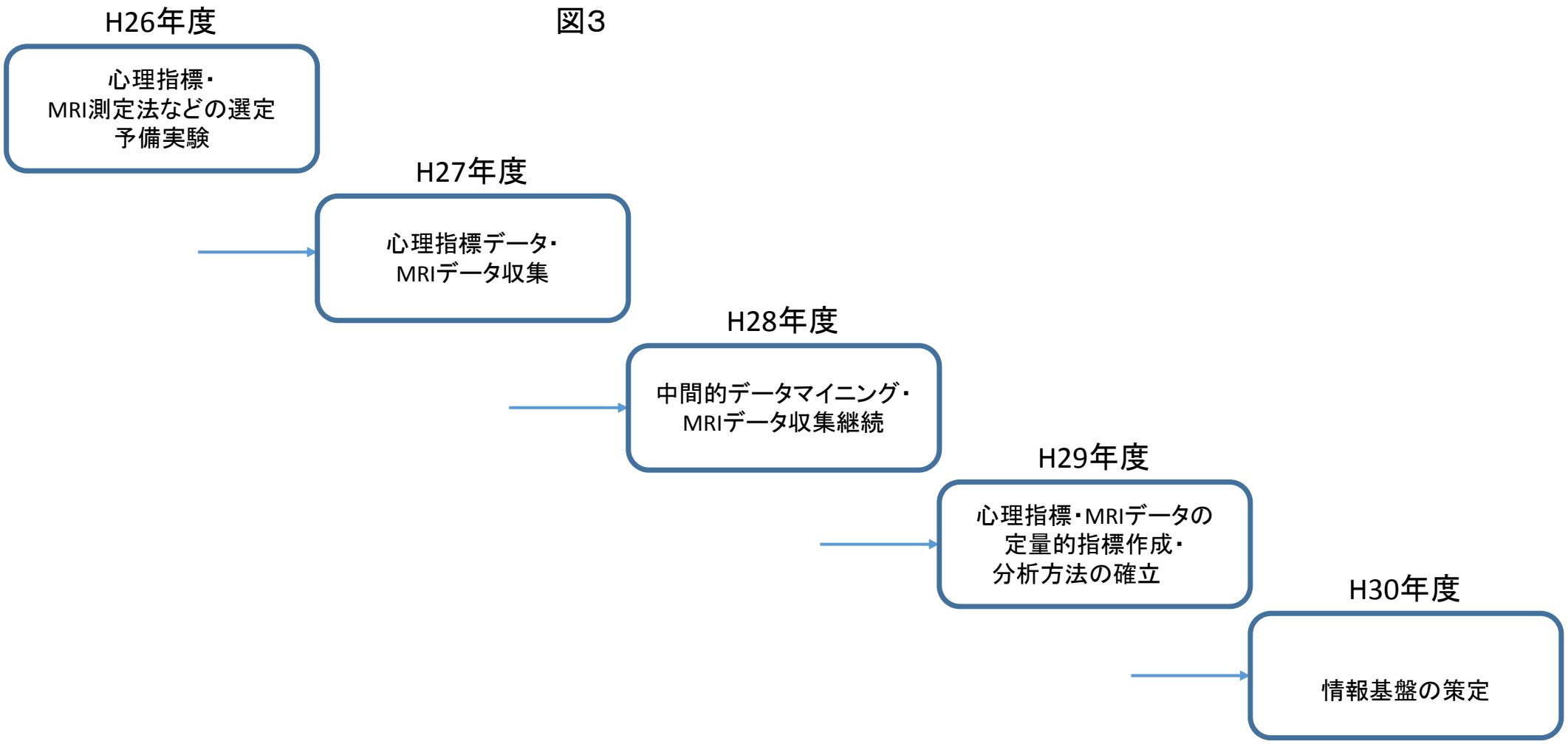
２）H２７年度：社会的・職業能力推定のための認知・脳機能の長期変動を捉える縦断データ収集への着手、職業経験により発達する社会的・職業能力同定の横断研究への着手、MRI測定・データ処理法の改良・開発。

３）H２８年度：中間的データマイニング：教育・訓練課程、加齢・職業と相関する可塑性の検出・評価。認知・脳機能モデルの推定。測定方法・データ分析法の評価。

４）H２９年度：認知・脳計測による定量的指標の作成、新たなデータ分析法の確立。測定・分析過程のルーチン化。

５）H３０年度：研究全体のまとめ・教育・職業による認知・脳機能変化に関する情報基盤（データベース）の策定。

図3


H26年度
心理指標・
MRI測定法などの選定
予備実験
H27年度
心理指標データ・
MRIデータ収集
H28年度
中間的データマイニング・
MRIデータ収集継続
H29年度
心理指標・MRIデータの
定量的指標作成・
分析方法の確立
H30年度
情報基盤の策定

４．研究体制

一つのプロジェクトになっているが、効率的に研究を遂行するために3つのワーキンググループ(図4)を基本として研究を行う。ただし、グループは完全に独立ではなく、グループメンバーは課題遂行時に能動的に協調しあう。

H26-27年度は主にグループ1と3によるデータ測定（分析）が行われる。H28-30年度にはグループ2から提供される情報に基づき、さらなるデータマイニングと情報基盤策定を行う （図５、６）。

グループ1： MRI測定・データ分析関連

グループ2： 教育課程・職業分析関連

グループ3： 心理指標データ収集・分析

図4

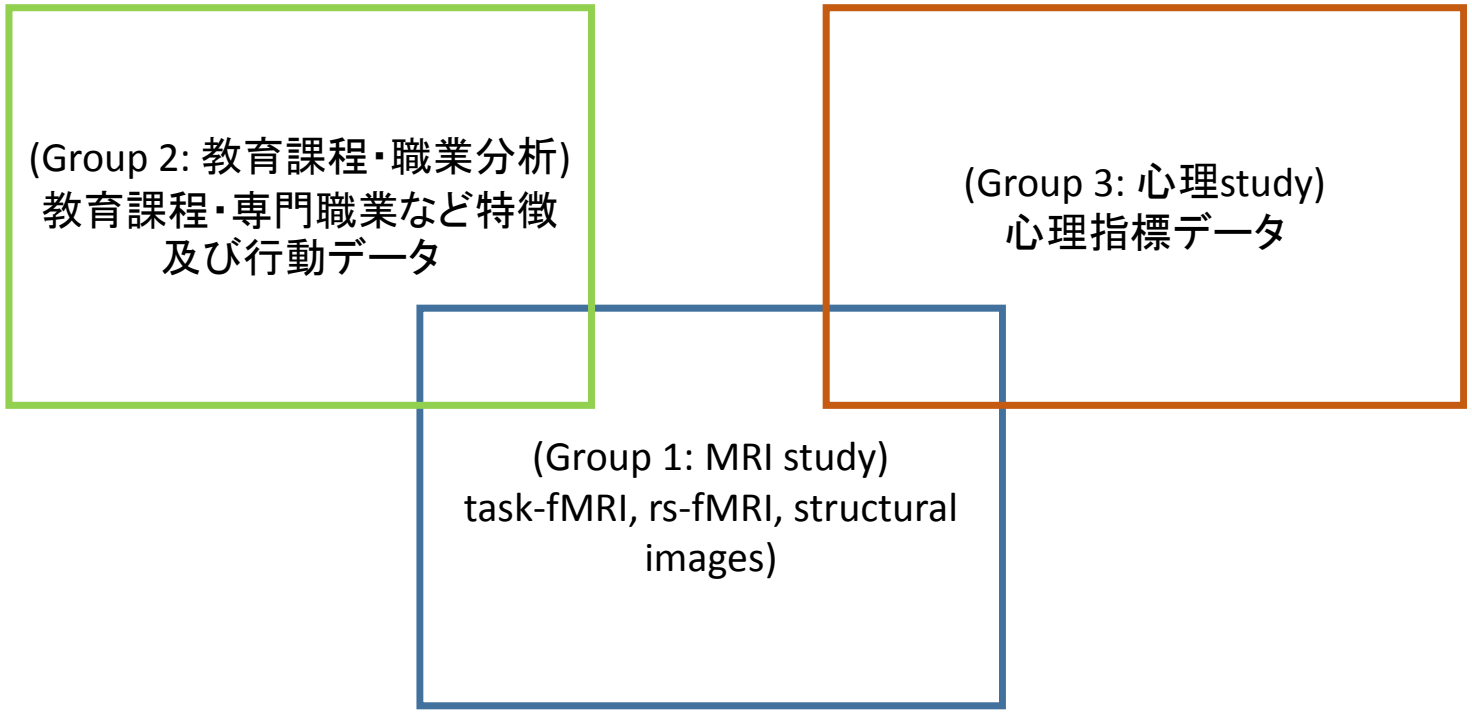

(Group 2: 教育課程・職業分析)
教育課程・専門職業など特徴
及び行動データ
(Group 3: 心理study)
心理指標データ
(Group 1: MRI study)
task-fMRI, rs-fMRI, structural
images)

図5

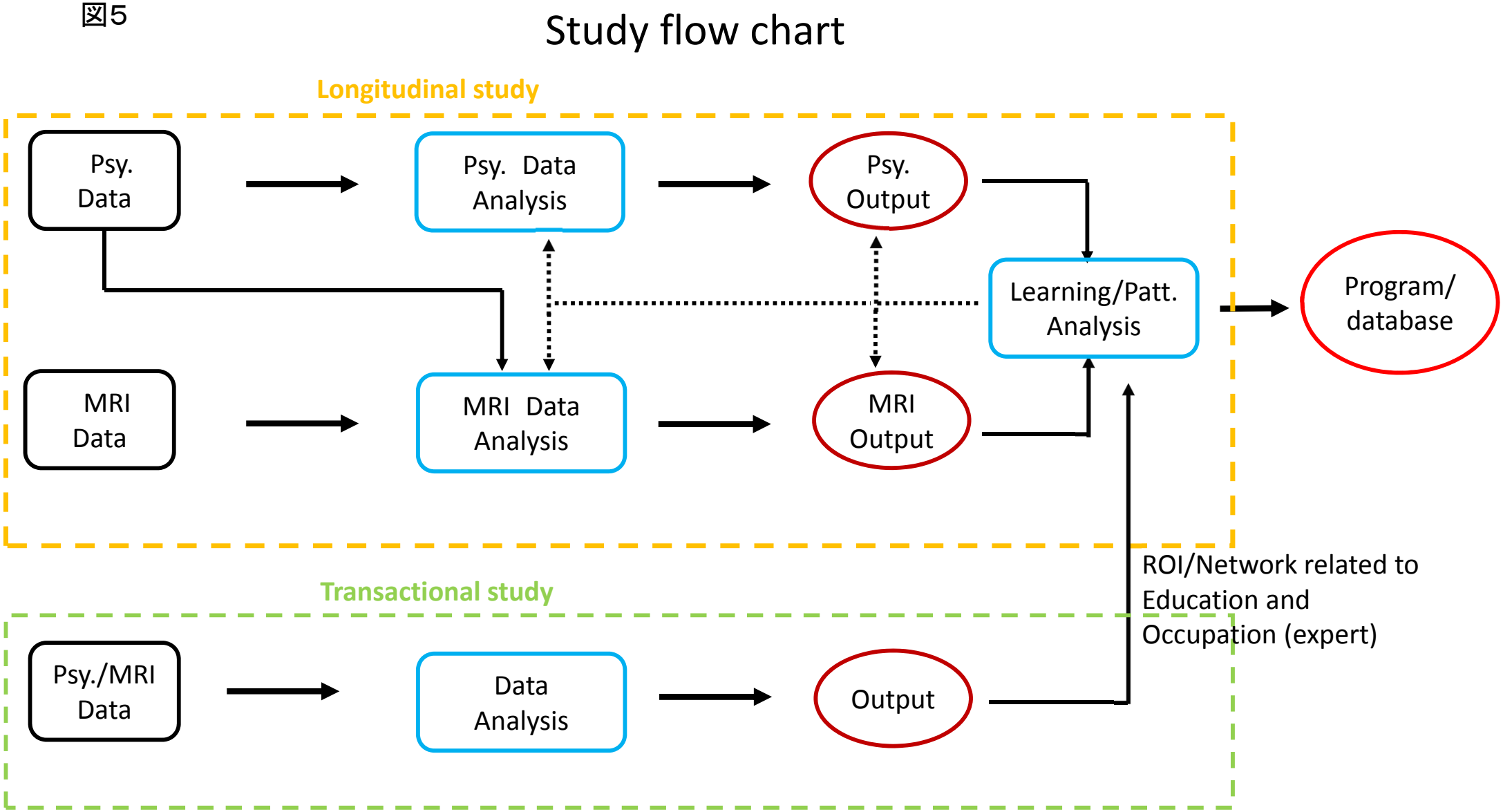
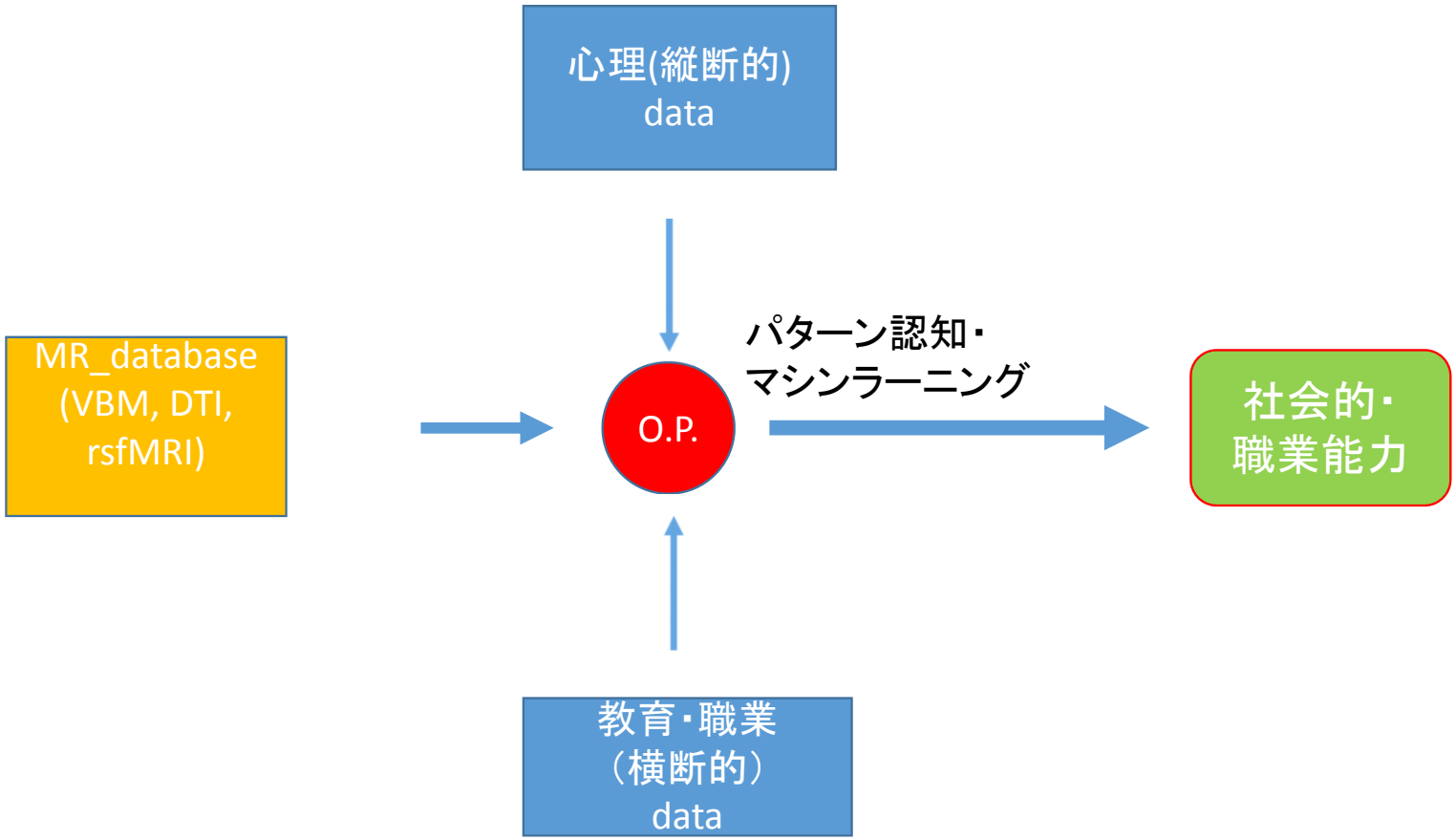

Study flow chart
Longitudinal study
Psy. Data
Psy. Data Analysis
Psy. Output
Learning/Patt. Analysis
Program/ database
MRI Data
MRI Data Analysis
MRI Output
ROI/Network related to Education and Occupation (expert)
Transactional study
Psy./MRI Data
Data Analysis
Output

図6


心理(縦断的)
data
MR_database
(VBM, DTI,
rsfMRI)
O.P.
パターン認知・
マシンラーニング
社会的・
職業能力
教育・職業
（横断的）
data

５．研究方法

大学１、２年生を卒業まで、MRIを１０－１６回（心理データの場合は２－３回）測定することにより、脳の可塑的変化を計測する。また、短期的訓練などにより可塑的変化の起きる脳部位・ネットワークを同定するためのtask-based fMRI実験を行う。

(1) 心理 study

(2) MRI study

(3) 可塑性・認知study

(4) パターン認知study

（1）心理学的研究

1）心理指標の種類：

社会性関連・WAIS・情動知能・職業適性・パーソナリティ・健康習慣等

その他の質問紙　例）成人用エフォートフル・コントロール尺度・自我同一性尺度,自意識尺度など

2）データ収集方法

社会性・感情・パーソナリティに関する質問紙および職業適性検査（集団式）

WAIS（個別式：被験者1名につきテスター1～2名）

3）被験者数

質問紙：236名； WAIS：158名； EQS：136名； 職業適性：105名

※1月28日現在(欠損データを含む)

４）データ分析

心理指標の項目間の独立性・関連性を検討するために、相関分析・重回帰分析・因子分析などを行った。H27年度は上位項目間での関連を調べた。

- 各種心理指標、社会性、IQ、EQ、職業適性間について相関分析・重回帰分析を行った。
- 職業適性検査データから被験者群の各職業に対する適性の分布を調べた。
- 心理指標の上位項目について因子分析によりクラスタリングを行った。
- 心理指標の上位項目について意味による分類を行った。

(2) MRI study

[被験者]

大学1、2年生　187名（2016年1月28日現在）

[MRI 測定]

1）MRI装置

Siemense MRI scanner Skyra fit, 20ch matrix coil (head 16 ch, neck4 ch)

2）解剖画像：3D T1 image by MPRAGE, 1x1x1 mm^3

3）拡散強調画像（DTI）：b=0, b=900, directions 30, average 2

4）fMRI画像(resting state):

(Condition: Eye Open)

multi-band GE-EPI, TR 1000ms, 34 slices, 3.4x3.4x3.4 mm^3,

480 volumes

(データ分析)

１２月時点で、心理指標（社会性関連）とMRIデータの両方が収集された１２０名に対して行った。１２０名に対しては脳部位とネットワークの同定、また、１２０名中９１名はIQデータが、９９名はEQデータが収集されていたため、それぞれにネットワーク同定を行った。

灰白質容積（VBM）：SPM(www.fil.ion.ucl.ac.uk/**spm**)

Resting state fMRI:

DPABI (rfmri.org/dpabi) for Preprocessing

GraphVar (www.fmri.org/GraphVar) for network analysis

BrainNet Viewer (www.nitrc.or/projects/) for network view

Rosenbach ROIs for template (Rosenbach et al., Science 2010)

６．結果

[1]心理 study

[2]MRI study

[3]可塑性・認知機能 study

[4]パターン認知 study

[1]心理学的研究

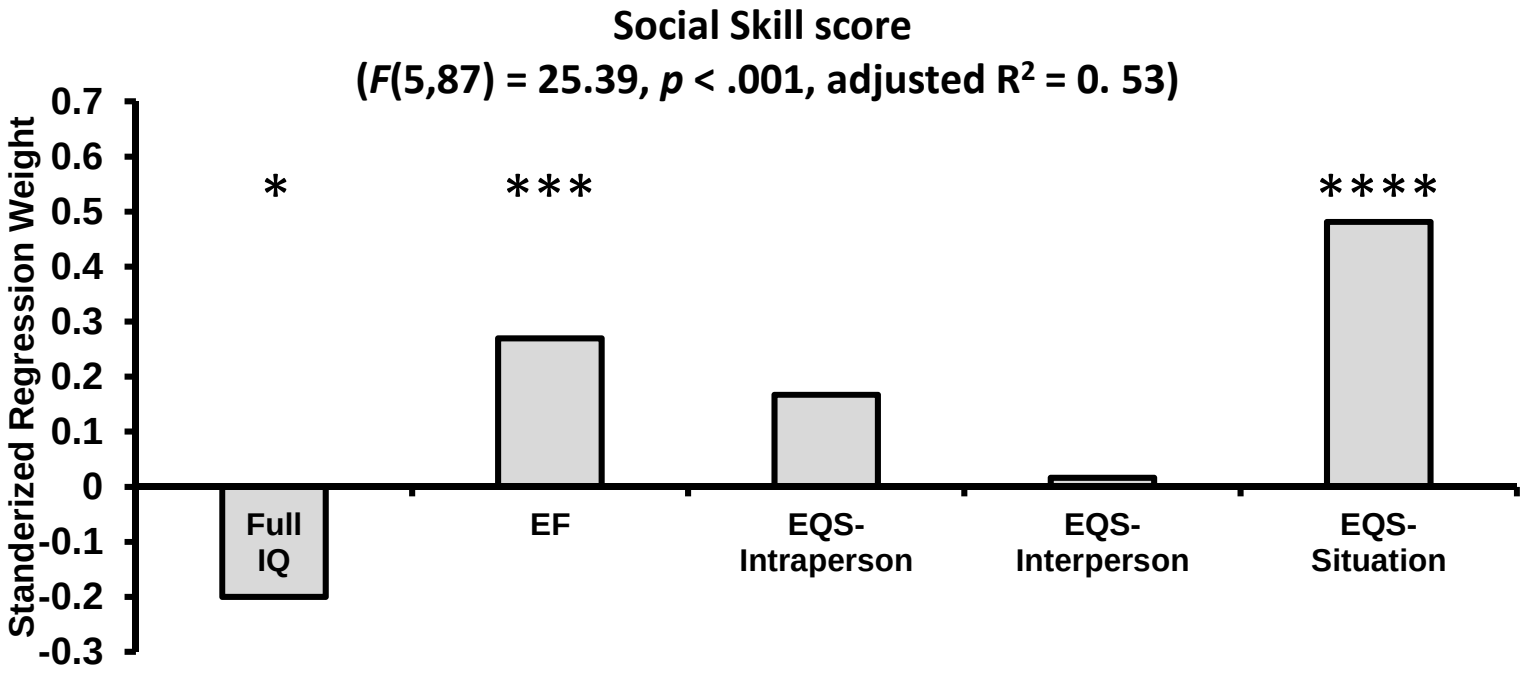
- IQ項目はいずれも職業適性と有意な相関があった。
- 社会的能力とIQとの有意な相関はなかった。
- EQの各項目は社会的能力と有意な相関があった。
- 実行機能 (EF) は、EQ（状況対応）と Full IQ とともに社会的能力を予測し、また、流動性IQとともに職業適性を予測する。
- 主観的幸福感はEF、EQ、社会的能力と有意な相関があった。
- 職業適性の分布は測定対象群の職業に対する傾向を示した。
- 社会性に関連する 19 個の上位項目は測定データをもとに 4 つのグループ、定義をもとに 9 つのグループに分類できた。

IQ・職業適性・EF・EQ・SQに関する相関分析

Measure	Full IQ	VIQ	PIQ	CIQ	FIQ	職業適性	EF	EQS-Intraperson	EQS-Interperson	EQS-Situation	Social Skill
Full IQ	-	.847**	.820**	.769**	.779**	.646**	.176	.074	-.068	.079	-.054
VIQ		-	.393**	.906**	.511**	.434**	.144	-.005	-.155	-.015	-.124
PIQ			-	.360**	.802**	.666**	.157	.124	.039	.143	.024
CIQ				-	.434**	.396**	.113	-.004	-.114	-.024	-.114
FIQ					-	.636**	.215*	.145	-.004	.176	.051
職業適性						-	.405**	.383**	.288*	.411**	.220
EF							-	.442**	.113	.289**	.481**
EQS-Intraperson								-	.674**	.738**	.613**
EQS-Interperson									-	.634**	.426**
EQS-Situation										-	.619**
Social Skill											-

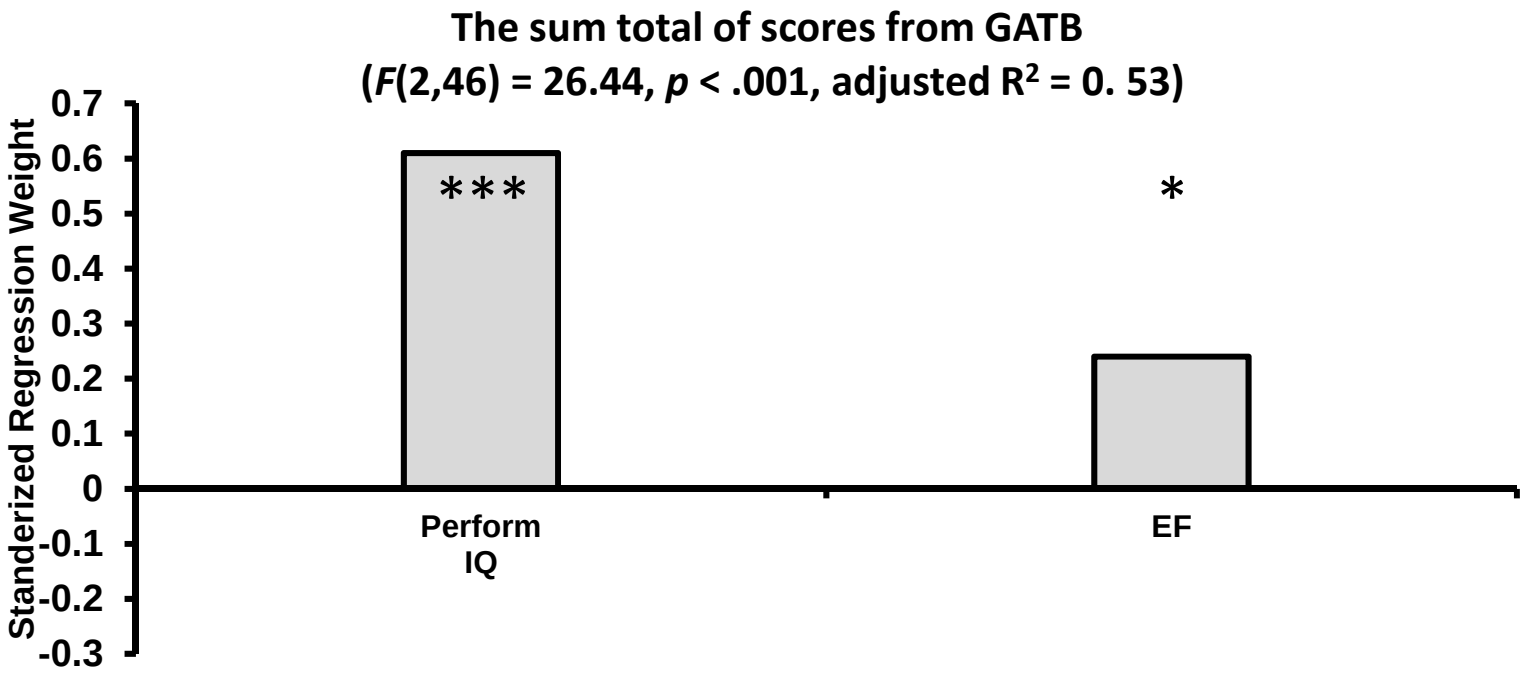
IQ: Intelligence quotient; VIQ: Verbal IQ; PIQ; Performance IQ; CIQ: Crystalized IQ; FIQ: Fluid IQ;
EF: Executive Functions; EQS: Emotional Quotient Scale

社会的スキルに関する階層的重回帰分析



* The variance inflation factor (VIF) for each independent variable was less than 3.50, and was confirmed not to be problematic.

職業適性に関する階層的重回帰分析



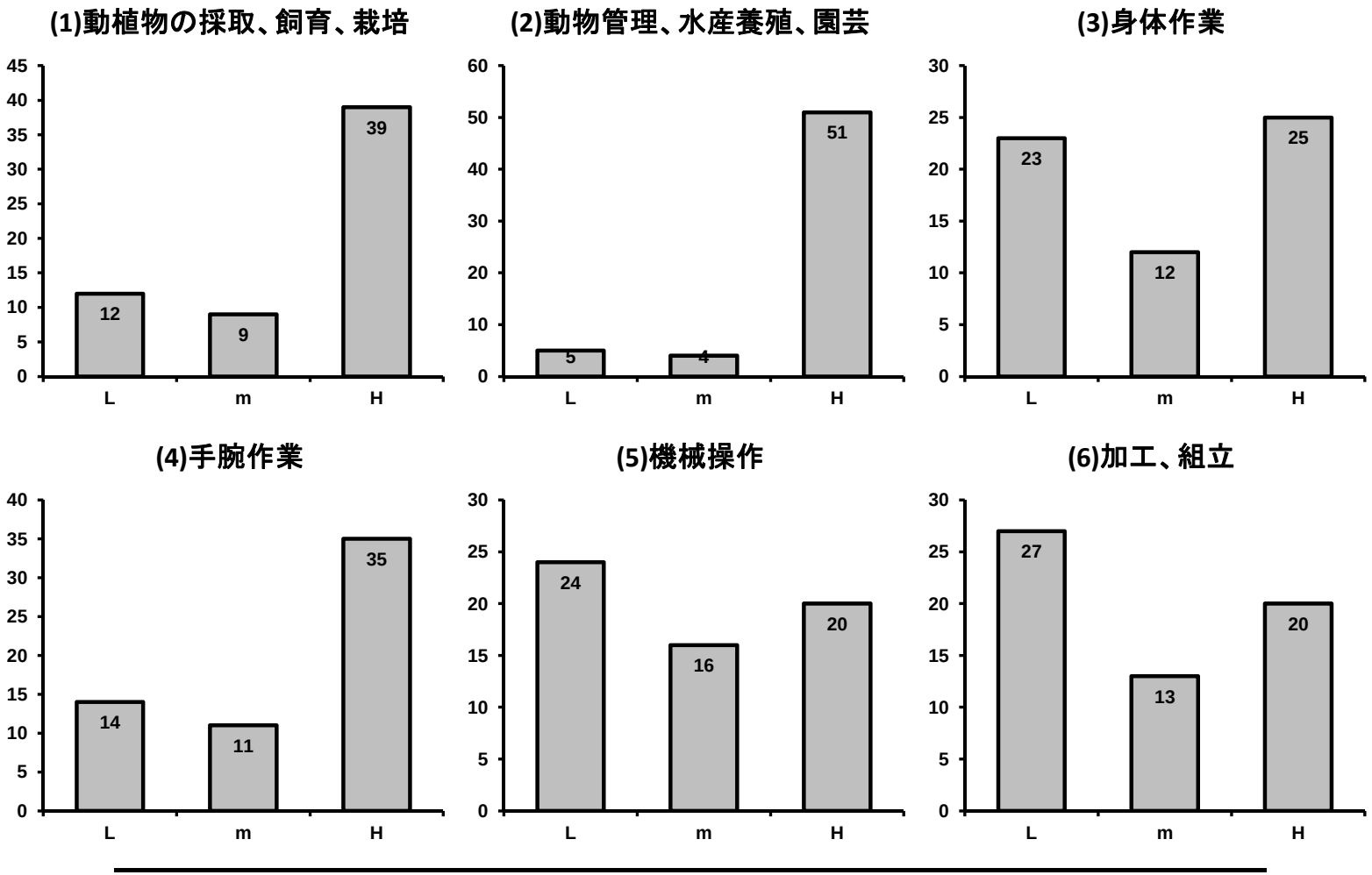
* The variance inflation factor (VIF) for each independent variable was less than 1.17, and was confirmed not to be problematic.

諸能力と主観的幸福感に関する相関分析

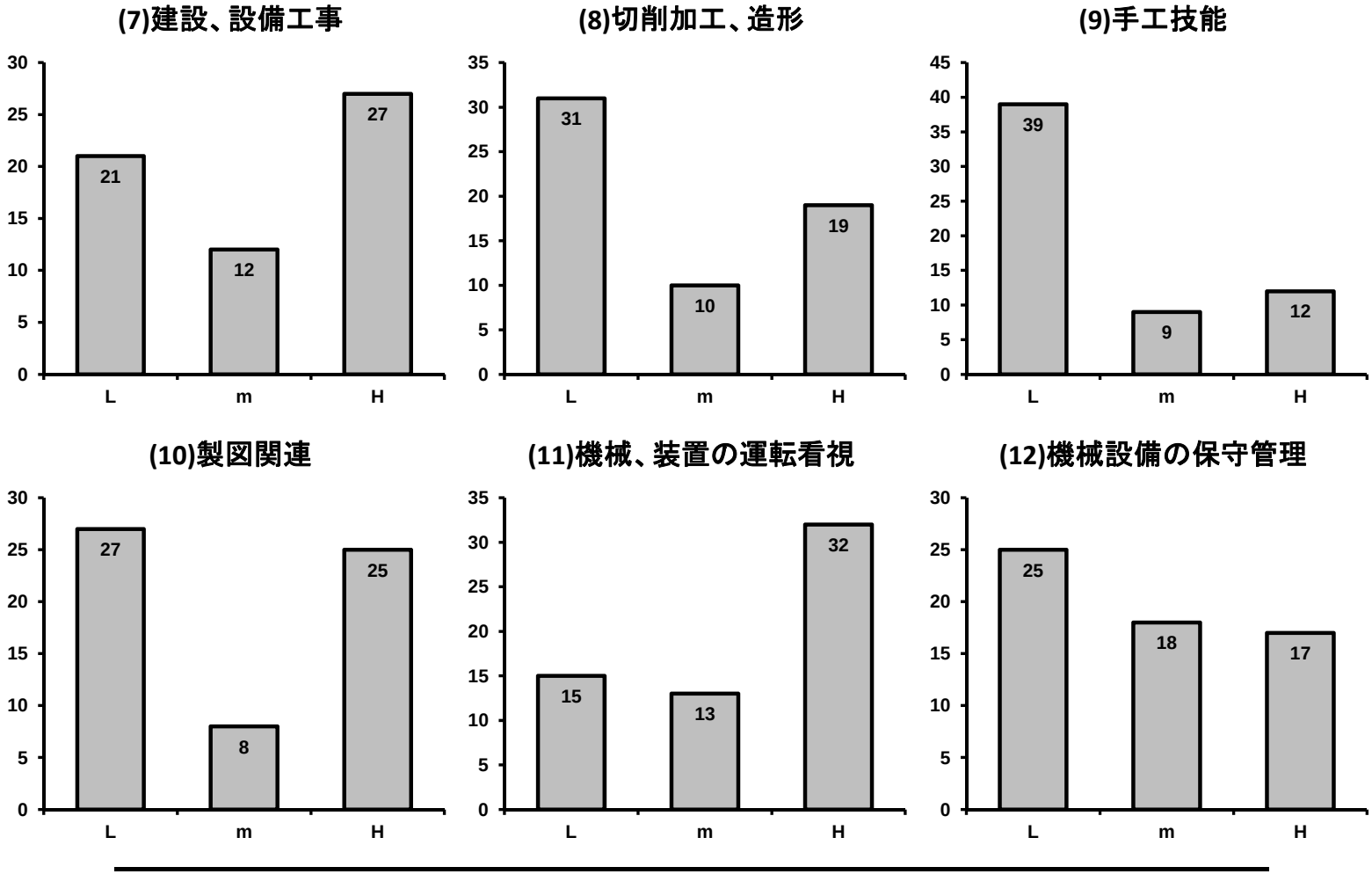
Measure	Full IQ	VIQ	PIQ	CIQ	FIQ	職業適性	EF	EQS-Intraperson	EQS-Interperson	EQS-Situation	Social Skill	Subjective Happiness
Full IQ	-	.847**	.820**	.769**	.779**	.646**	.176	.074	-.068	.079	-.054	-.012
VIQ		-	.393**	.906**	.511**	.434**	.144	-.005	-.155	-.015	-.124	-.145
PIQ			-	.360**	.802**	.666**	.157	.124	.039	.143	.024	.128
CIQ				-	.434**	.396**	.113	-.004	-.114	-.024	-.114	-.139
FIQ					-	.636**	.215*	.145	-.004	.176	.051	.055
職業適性						-	.405**	.383**	.288*	.411**	.220	.200
EF							-	.442**	.113	.289**	.481**	.254**
EQS-Intraperson								-	.674**	.738**	.613**	.332**
EQS-Interperson									-	.634**	.426**	.209*
EQS-Situation										-	.619**	.346**
Social Skill											-	.535**
Subjective Happiness												-

IQ: Intelligence quotient; VIQ: Verbal IQ; PIQ; Performance IQ; CIQ: Crystalized IQ; FIQ: Fluid IQ;
EF: Executive Functions; EQS: Emotional Quotient Scale

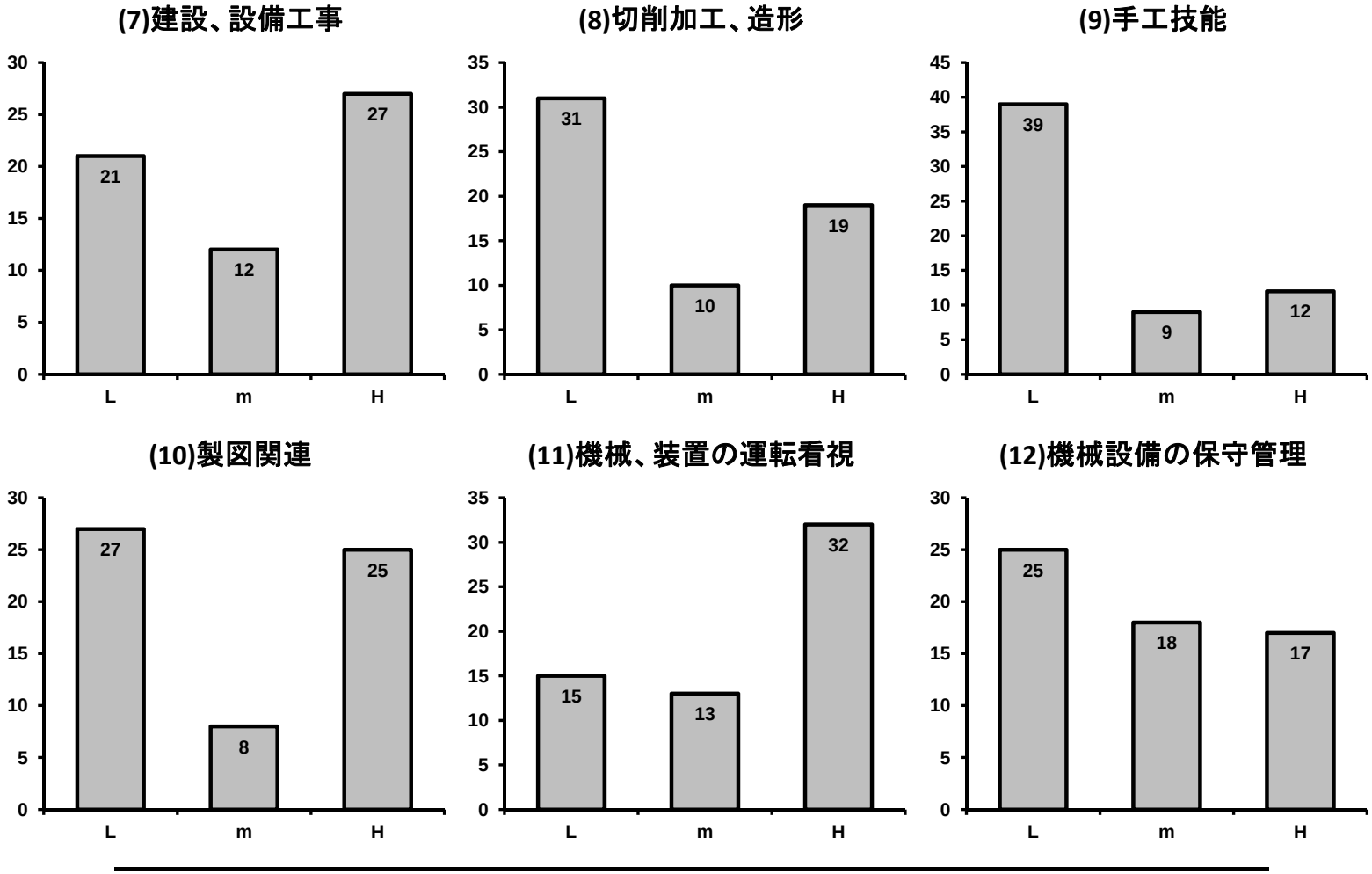
職業適性ヒストグラム


(1)動植物の採取、飼育、栽培
45
40
35
30
25
20
15
10
5
0
12
9
39
L
m
H
(2)動物管理、水産養殖、園芸
60
50
40
30
20
10
0
5
4
51
L
m
H
(3)身体作業
30
25
20
15
10
5
0
23
12
25
L
m
H
(4)手腕作業
40
35
30
25
20
15
10
5
0
14
11
35
L
m
H
(5)機械操作
30
25
20
15
10
5
0
24
16
20
L
m
H
(6)加工、組立
30
25
20
15
10
5
0
27
13
20
L
m
H

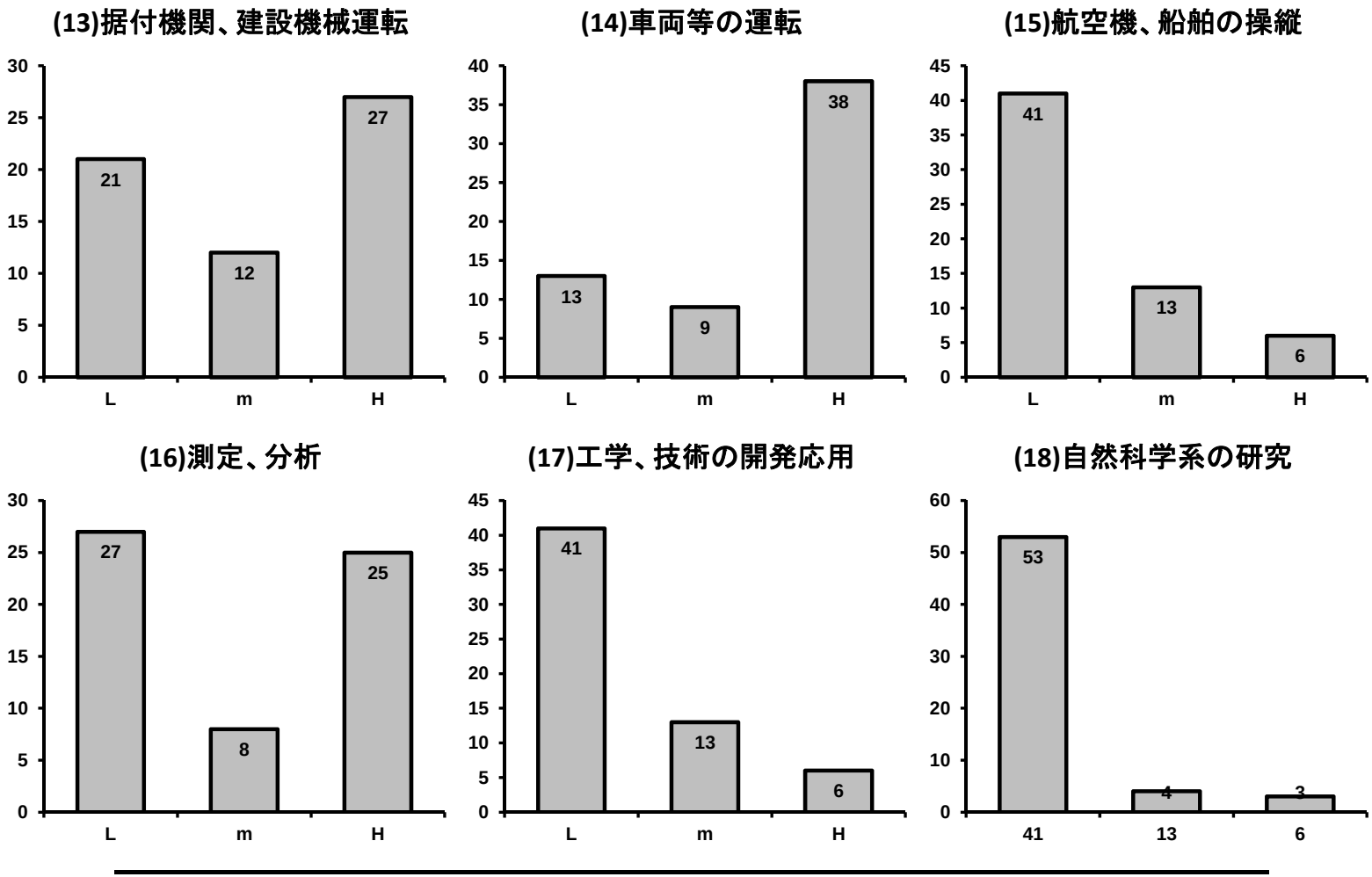
職業適性ヒストグラム


(7)建設、設備工事
30
25
20
15
10
5
0
21
12
27
L
m
H
(8)切削加工、造形
35
30
25
20
15
10
5
0
31
10
19
L
m
H
(9)手工技能
45
40
35
30
25
20
15
10
5
0
39
9
12
L
m
H
(10)製図関連
30
25
20
15
10
5
0
27
8
25
L
m
H
(11)機械、装置の運転看視
35
30
25
20
15
10
5
0
15
13
32
L
m
H
(12)機械設備の保守管理
30
25
20
15
10
5
0
25
18
17
L
m
H

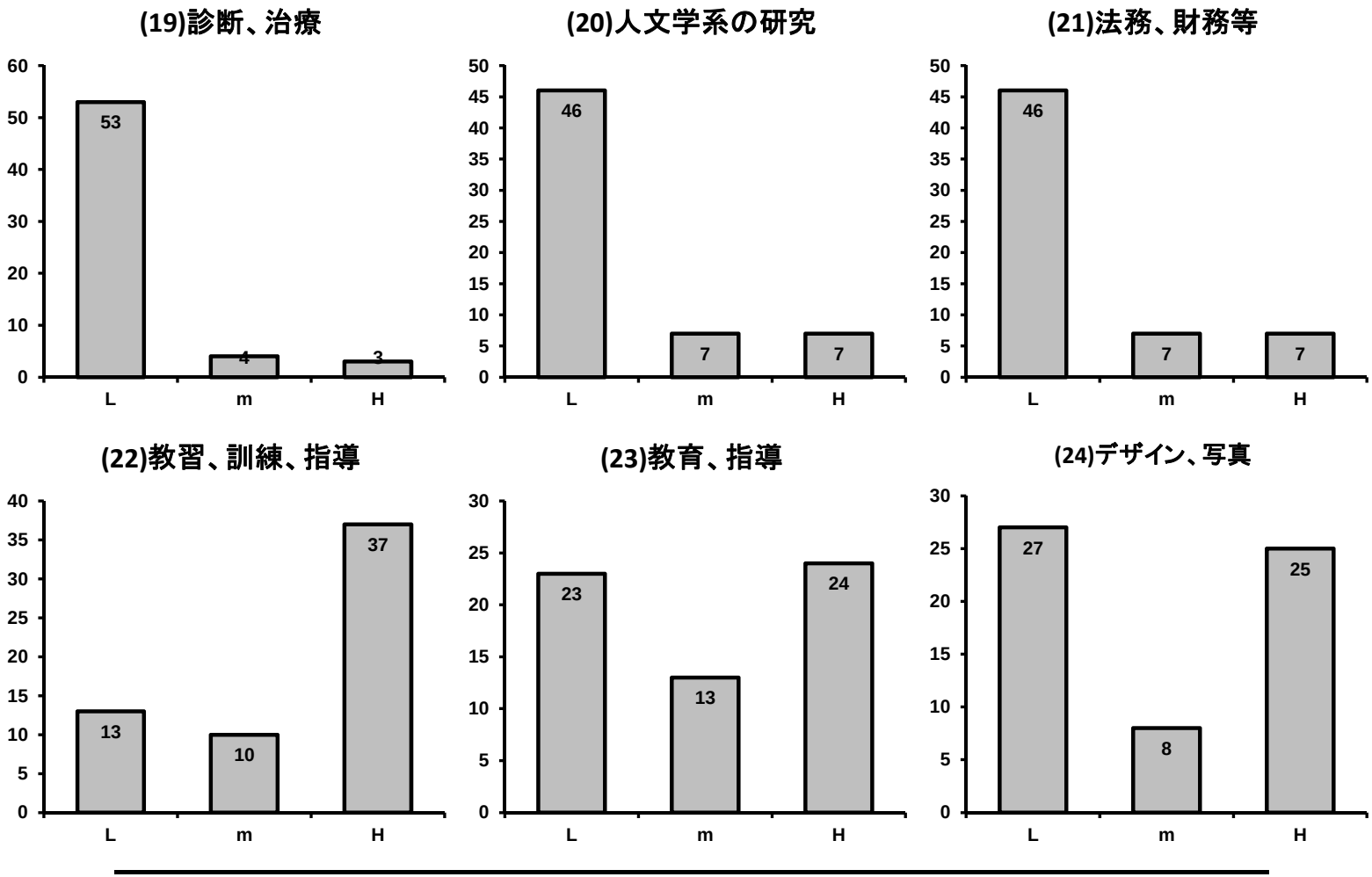
職業適性ヒストグラム


(7)建設、設備工事
30
25
20
15
10
5
0
21
12
27
L
m
H
(8)切削加工、造形
35
30
25
20
15
10
5
0
31
10
19
L
m
H
(9)手工技能
45
40
35
30
25
20
15
10
5
0
39
9
12
L
m
H
(10)製図関連
30
25
20
15
10
5
0
27
8
25
L
m
H
(11)機械、装置の運転看視
35
30
25
20
15
10
5
0
15
13
32
L
m
H
(12)機械設備の保守管理
30
25
20
15
10
5
0
25
18
17
L
m
H

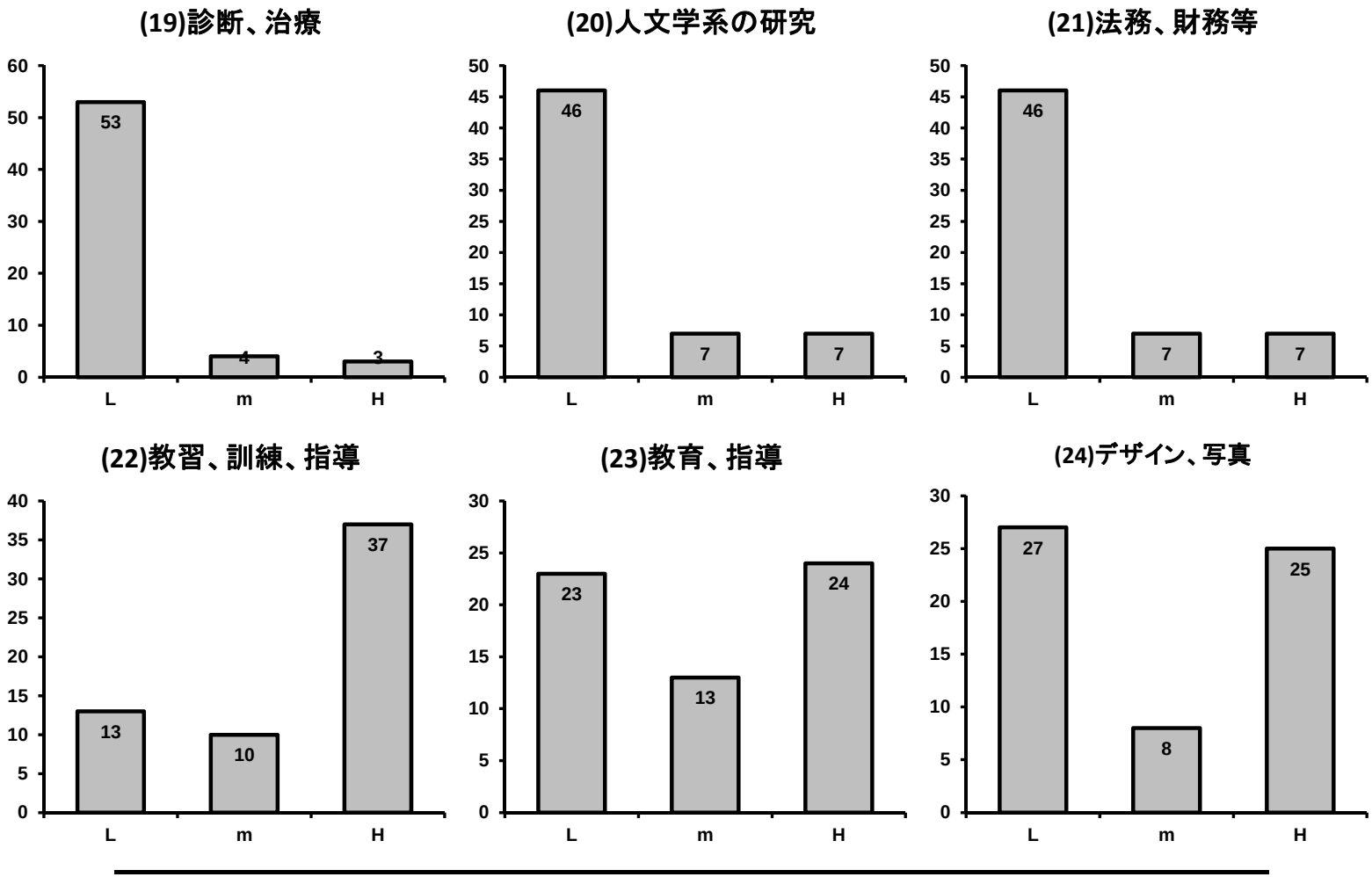
職業適性ヒストグラム


(13)据付機関、建設機械運転
30
25
20
15
10
5
0
21
12
27
L
m
H
(14)車両等の運転
40
35
30
25
20
15
10
5
0
13
9
38
L
m
H
(15)航空機、船舶の操縦
45
40
35
30
25
20
15
10
5
0
41
13
6
L
m
H
(16)測定、分析
30
25
20
15
10
5
0
27
8
25
L
m
H
(17)工学、技術の開発応用
45
40
35
30
25
20
15
10
5
0
41
13
6
L
m
H
(18)自然科学系の研究
60
50
40
30
20
10
0
53
4
3
41
13
6

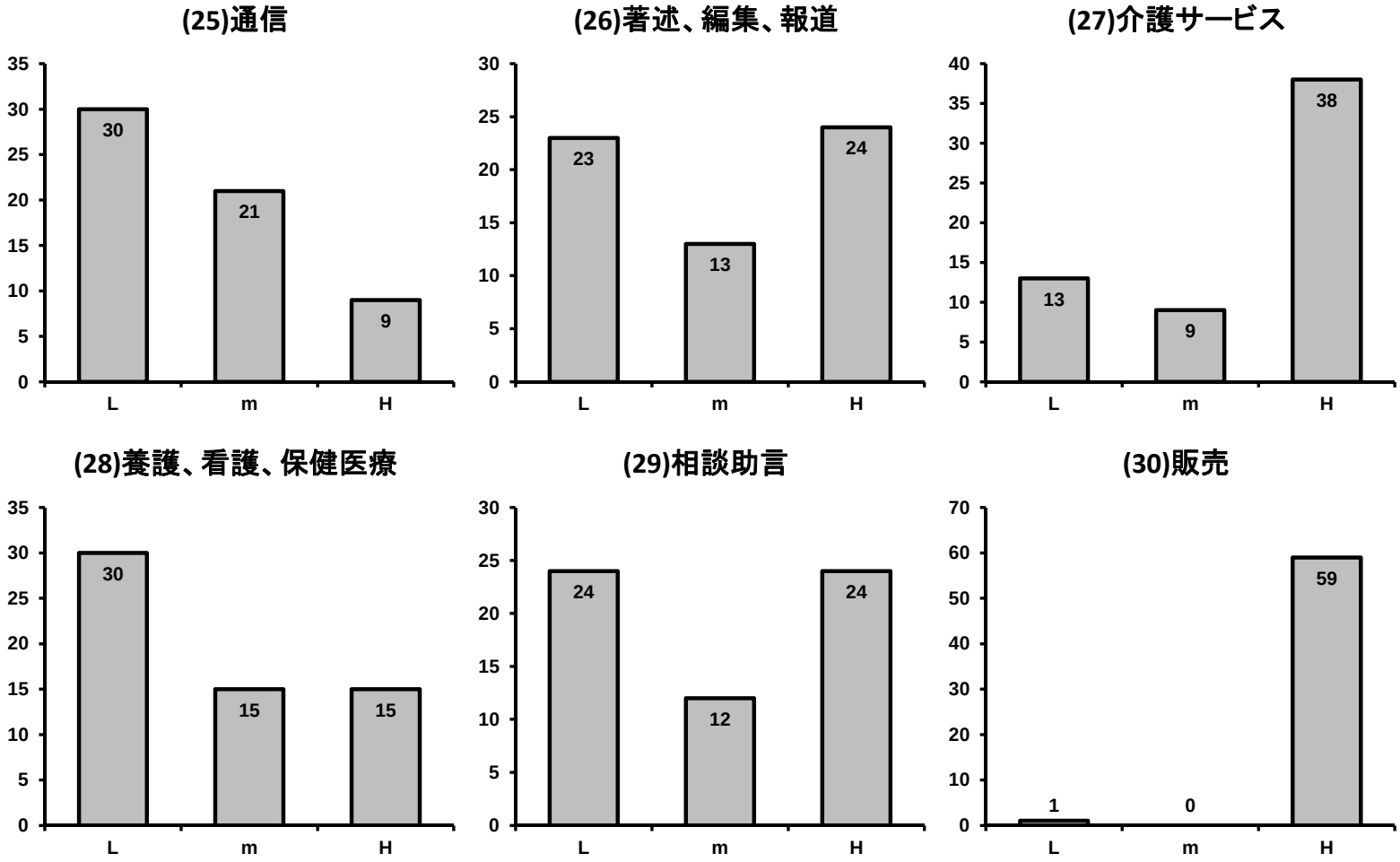
職業適性ヒストグラム


(19)診断、治療
60
50
40
30
20
10
0
53
4
3
L
m
H
(20)人文学系の研究
50
45
40
35
30
25
20
15
10
5
0
46
7
7
L
m
H
(21)法務、財務等
50
45
40
35
30
25
20
15
10
5
0
46
7
7
L
m
H
(22)教習、訓練、指導
40
35
30
25
20
15
10
5
0
13
10
37
L
m
H
(23)教育、指導
30
25
20
15
10
5
0
23
13
24
L
m
H
(24)デザイン、写真
30
25
20
15
10
5
0
27
8
25
L
m
H

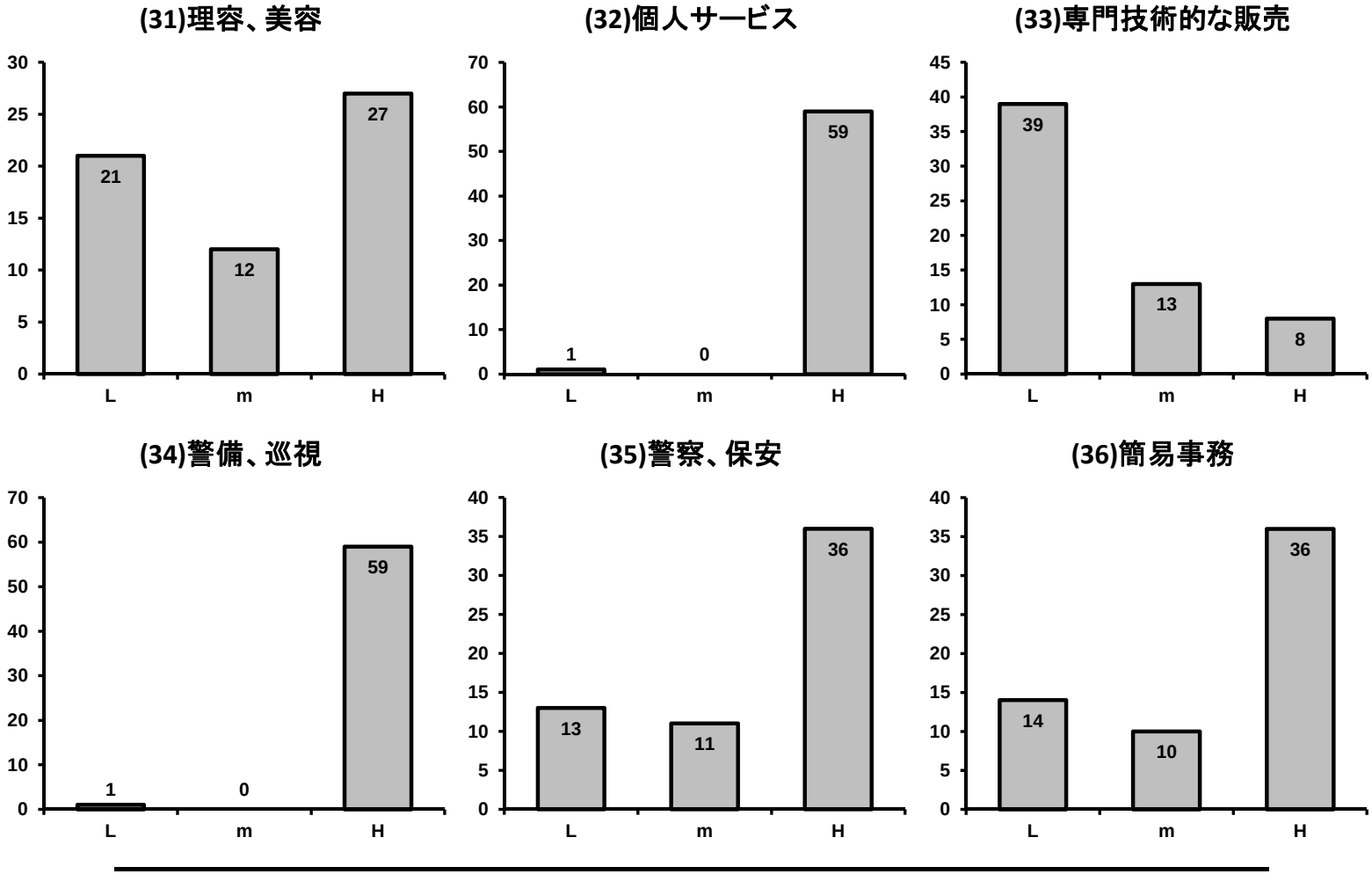
職業適性ヒストグラム


(19)診断、治療
60
50
40
30
20
10
0
53
4
3
L
m
H
(20)人文学系の研究
50
45
40
35
30
25
20
15
10
5
0
46
7
7
L
m
H
(21)法務、財務等
50
45
40
35
30
25
20
15
10
5
0
46
7
7
L
m
H
(22)教習、訓練、指導
40
35
30
25
20
15
10
5
0
13
10
37
L
m
H
(23)教育、指導
30
25
20
15
10
5
0
23
13
24
L
m
H
(24)デザイン、写真
30
25
20
15
10
5
0
27
8
25
L
m
H

職業適性ヒストグラム

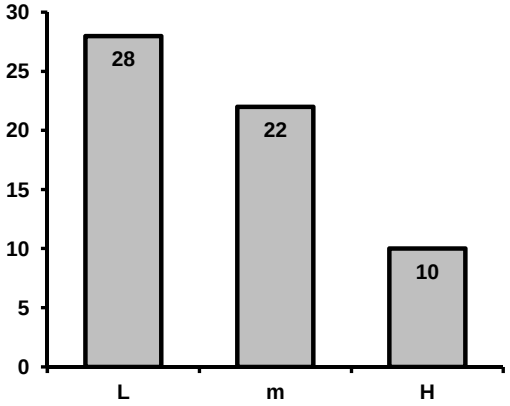

(25)通信
35
30
25
20
15
10
5
0
30
21
9
L
m
H
(26)著述、編集、報道
30
25
20
15
10
5
0
23
13
24
L
m
H
(27)介護サービス
40
35
30
25
20
15
10
5
0
13
9
38
L
m
H
(28)養護、看護、保健医療
35
30
25
20
15
10
5
0
30
15
15
L
m
H
(29)相談助言
30
25
20
15
10
5
0
24
12
24
L
m
H
(30)販売
70
60
50
40
30
20
10
0
1
0
59
L
m
H

職業適性ヒストグラム

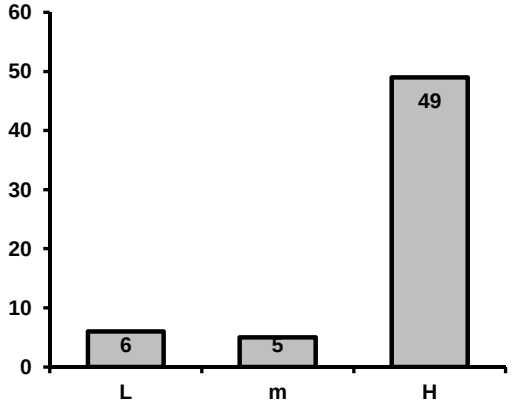

(31)理容、美容
30
25
20
15
10
5
0
21
12
27
L
m
H
(32)個人サービス
70
60
50
40
30
20
10
0
1
0
59
L
m
H
(33)専門技術的な販売
45
40
35
30
25
20
15
10
5
0
39
13
8
L
m
H
(34)警備、巡視
70
60
50
40
30
20
10
0
1
0
59
L
m
H
(35)警察、保安
40
35
30
25
20
15
10
5
0
13
11
36
L
m
H
(36)簡易事務
40
35
30
25
20
15
10
5
0
14
10
36
L
m
H

職業適性ヒストグラム

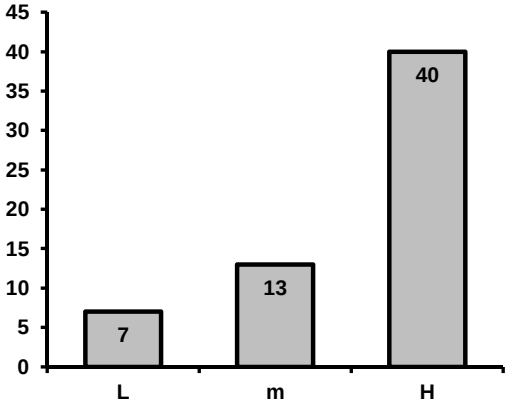
(37)事務機器操作



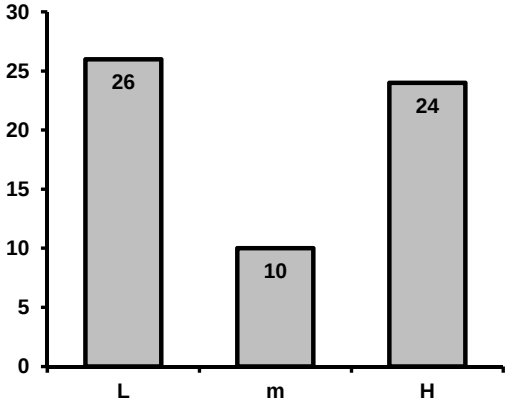
(38)一般事務



(39)経理、会計



(40)専門企画



質問紙得点に関する因子分析結果

尺度名	因子負荷量 Ⅰ	Ⅱ	Ⅲ	Ⅳ
自尊感情尺度	**0.91**	−0.17	−0.03	0.11
主観的幸福感尺度 (Subjective Happiness Scale: SHS)	**0.90**	−0.15	0.02	−0.12
Brief Core Schema Scale	**−0.89**	0.06	0.10	0.04
人生に対する満足尺度 The Satisfaction with Life Scale (SWLS)	**0.76**	−0.07	−0.05	−0.06
状態・特性不安尺度	**0.53**	0.15	−0.17	0.09
自我同一性尺度	**−0.52**	−0.31	0.05	−0.13
Ego-Resiliency尺度	**0.42**	0.20	0.35	−0.09
自閉スペクトラム指数 Autism-Spectrum Quotient	0.21	**−0.96**	−0.10	0.10
統合失調型パーソナリティ尺度Schizotypal Personality Questionnaire-Brief	0.05	**−0.73**	0.28	0.02
Shyness尺度	−0.25	**−0.72**	0.14	0.07
社会的スキル尺度	0.17	**0.48**	0.28	0.22
認知された自己有能感尺度（Perceived Competence Scale for Adolescence）	0.40	**0.44**	0.14	−0.06
自己概念の明確性尺度	0.01	**0.42**	−0.32	0.16
TALE(The Thinking About Life Experiences)尺度	−0.12	−0.01	**0.69**	0.11
自意識 (self-consciousness) 尺度	0.00	−0.32	**0.67**	−0.02
Behavioral Inhibitory System(BIS)/Behavioral Activate System (BAS) 尺度	0.00	0.16	**0.45**	−0.44
自己成長主導性尺度Ⅱ（Personal Growth Initiative Scale-II）	0.16	0.11	**0.45**	0.16
成人用エフォートフル・コントロール＊尺度	−0.10	−0.08	−0.03	**1.00**
Social Problem-Solving Inventory-Revised (SPSI-R)	0.14	0.05	0.15	**0.62**

Ⅰ.自己感情　Ⅱ.社会性
Ⅲ.セルフモニタリング　Ⅳ.問題解決能力

	Ⅰ	Ⅱ	Ⅲ	Ⅳ
Ⅰ	1	0.74	0.15	0.59
Ⅱ		1	0.03	0.56
Ⅲ			1	−0.02
Ⅳ				1

定義による質問紙分類

①認知された自己有能感尺度
①自尊感情尺度

② Ego-Resiliency尺度

③自我同一性尺度
③自意識 (self-consciousness) 尺度
③自分自身への注意をむける傾向を自意識として測定
③自己概念の明確性尺度
③ Brief Core Schema Scale

④ Shyness尺度
④状態・特性不安尺度

⑤成人用エフォートフル・コントロール＊尺度
⑤ BIS/BAS 尺度
⑤自己成長主導性尺度Ⅱ
⑤ Social Problem-Solving Inventory-Revised(SPSI-R)

⑥社会的スキル尺度

⑦TALE尺度

⑧統合失調型パーソナリティ尺度
⑧自閉スペクトラム指数

Summary

- ヒトの行動を表現し得る代表的な心理指標である社会的能力、IQ、EQ、職業適性間の関係の推定ができた。
- 職業適性にはIQとEQがともに影響している。
- 社会的能力には主にEQが影響している。
- 心理指標における上位階層の分析ができた。
- 実行機能は社会的能力と職業適性に関連していることが分かった。教育・訓練内容と実行機能との相関が分かれば、実行機能の測定により可塑的変化の推定が可能であると思われる。

（心理データ分析における限界と対策）

- 今回の分析では、心理データの測定途中のため、各心理指標の被験者数が揃ってない。被験者数を揃えて分析しなおす必要がある。
- 上位項目間の関連性の分析に加えて、下位項目間の独立性・関連性の分析も行う必要がある。
- 下位・上位項目における独立性を評価し、独立項目からなる基本要素の集合体(set of basis)を求める必要がある。
- 縦断的データ分析のために３－４年間の教育期間中に受ける教育・訓練の内容ごとに被験者群の分類と各心理指標に対する検討が必要である。
- これらの分析はH28年度から行われる予定である。

[2]MRI　study

(1) 灰白質容積（VBM）

１）VBM:　心理データ（社会的・情動的）と相関してVBMが変化する脳マップ（６１項目下位項目＋１９上位項目）を作成した。８０項目のなかで６１項目に対するROIが同定できた（Correlation analysis, p = 0.001, uncorrected, Cluster threshold 70）。複数のROIが同定された項目もあったので、同定されたROIsは１５８であった。

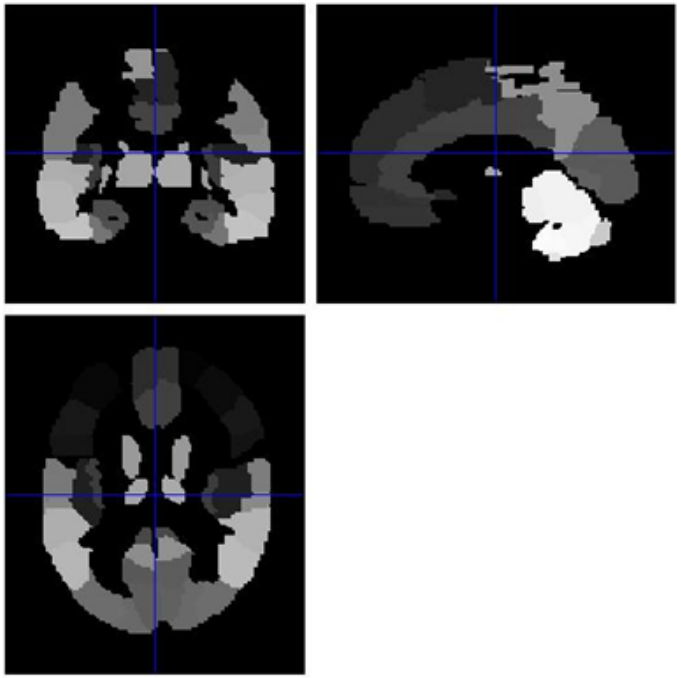
２）VBMによる脳マップから心理データ（社会的・情動的）を表現する脳の１５８のROIsからなるtemplate（TFU template）を作った。

＊Resting state fMRI によるネットワーク同定にはすでに確認された機能をもとに検証をするため、Rosenbach Templateを使用したので、比較のためRosenbach Templateを表示した。

ROIが大きいのでpartial volume effect
により検出感度が低いと思われ
使用しなかった。
機能的ROIsからのDosenbach templateと
本研究で作成したTFU templateとの比較
のために表示した。

Anatomical ROIs: 116

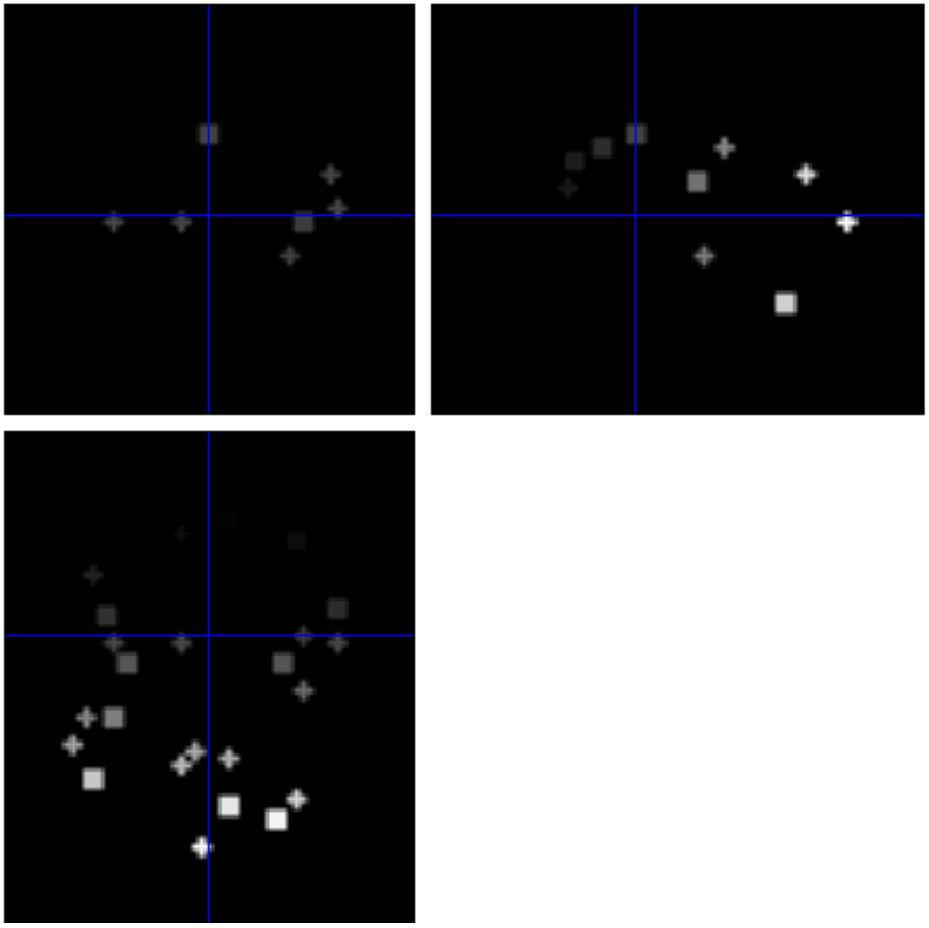
AAL template
ROIs



Functional ROIs: 160

Dosenbach template
ROIs: 5mm sphere

Grayscale で　ROIの違いを表している



Rosenbach template
: location of 160 ROIs

1_vmPFC_R
2_mPFC
3_aPFC_L
4_vmPFC_R
5_vmPFC_L
6_vmPFC_L
7_vmPFC_R
8_ACC_R
9_vlPFC_R
10_sup frontal_R
11_sup frontal_L
12_inf temporal_R
13_inf temporal_L
14_post cingulate_R
15_fusiform_R
16_precuneus_L
17_post cingulate_L
18_inf temporal_L
19_occipital_L
20_post cingulate_L
21_precuneus_R
22_precuneus_R
23_post cingulate_L
24_post cingulate_R
25_precuneus_L
26_post cingulate_L
27_angular gyrus_R

28_angular gyrus_L
29_precuneus_R
30_IPS_L
31_occipital_L
32_occipital_R
33_occipital_L
34_occipital_L
35_aPFC_R
36_aPFC_L
37_vent aPFC_R
38_vent aPFC_L
39_vlPFC_R
40_dlPFC_R
41_ACC_L
42_dlPFC_R
43_vPFC_L
44_dlPFC_L
45_dFC_R
46_dFC_R
47_dFC_L
48_IPL_L
49_IPL_R
50_post parietal_L
51_IPL_L
52_IPL_L
53_IPL_R
54_IPS_L
55_IPS_R

56_aPFC_R
57_vPFC_R
58_ACC_L
59_vFC_R
60_ant insula_R
61_dACC_R
62_ant insula_L
63_basal ganglia_L
64_mFC
65_vFC_L
66_basal ganglia_L
67_basal ganglia_R
68_vFC_L
69_mid insula_R
70_thalamus_L
71_thalamus_L
72_thalamus_R
73_mid insula_R
74_mid insula_L
75_basal ganglia_R
76_post insula_L
77_temporal_R
78_post cingulate_L
79_fusiform_R
80_precuneus_R
81_parietal_R
82_temporal_R
83_parietal_L

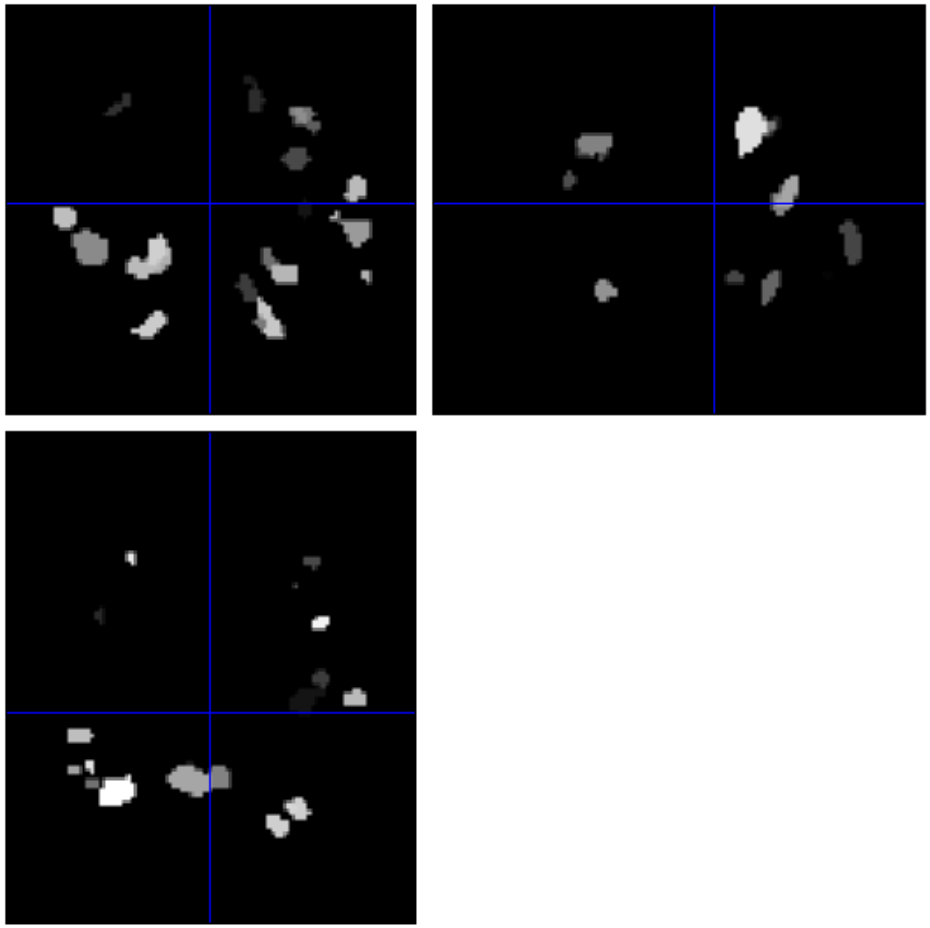
Rosenbach template
: location of 160 ROIs

84_sup temporal_R	112_parietal_R	140_post occipital_R
85_angular gyrus_L	113_post insula_R	141_post occipital_R
86_temporal_L	114_parietal_R	142_post occipital
87_TPJ_L	115_parietal_L	143_lat cerebellum_L
88_frontal_R	116_parietal_L	144_lat cerebellum_L
89_dFC_R	117_post parietal_L	145_inf cerebellum_L
90_vFC_L	118_temporal_L	146_lat cerebellum_L
91_pre-SMA_R	119_temporal_L	147_med cerebellum_L
92_vFC _R	120_sup parietal_R	148_inf cerebellum_L
93_SMA	121_occipital_L	149_inf cerebellum_R
94_frontal_R	122_occipital_L	150_med cerebellum_L
95_precentral gyrus_R	123_occipital_R	151_lat cerebellum_R
96_mid insula_L	124_temporal_R	152_med cerebellum_R
97_precentral gyrus_L	125_occipital_L	153_inf cerebellum_L
98_parietal_L	126_occipital_R	154_med cerebellum_L
99_precentral gyrus_R	127_occipital_R	155_inf cerebellum_R
100_precentral gyrus_L	128_occipital_R	156_med cerebellum_R
101_precentral gyrus_R	129_occipital_R	157_med cerebellum_R
102_parietal_L	130_occipital_L	158_inf cerebellum_L
103_mid insula_R	131_occipital_L	159_inf cerebellum_L
104_mid insula_L	132_occipital_R	160_inf cerebellum_R
105_temporal_R	133_occipital_R	
106_parietal_L	134_occipital_R	
107_parietal_L	135_post occipital_L	
108_parietal_R	136_post occipital_R	
109_parietal_L	137_post occipital_R	
110_precentral gyrus_L	138_post occipital_L	
111_temporal_L	139_post occipital	

Psychological data based
Functional ROIs: 158

TFU template
ROIs

Grayscale で　ROIの違いを
表している



TFU template
: location of 160 ROIs

1	Precuneus
2	Inferior Frontal Gyrus
3	Middle Frontal Gyrus
4	Cerebellar Tonsil
5	Superior Frontal Gyrus
6	Superior Frontal Gyrus
7	Declive
8	Superior Frontal Gyrus
9	Inferior Frontal Gyrus
10	Cingulate Gyrus
11	Superior Frontal Gyrus
12	Precuneus
13	Precentral Gyrus
14	Precentral Gyrus
15	Insula
16	Lentiform Nucleus
17	Posterior Cingulate
18	Lingual Gyrus
19	Cuneus
20	Superior Frontal Gyrus
21	Postcentral Gyrus
22	Superior Temporal Gyrus
23	Precentral Gyrus
24	Cuneus
25	Precuneus
26	Precuneus
27	Superior Frontal Gyrus
28	Inferior Frontal Gyrus

29	Sub-Gyral
30	Precuneus
31	Postcentral Gyrus
32	Cuneus
33	Postcentral Gyrus
34	Medial Frontal Gyrus
35	Middle Occipital Gyrus
36	Sub-Gyral
37	Superior Temporal Gyrus
38	Inferior Frontal Gyrus
39	Culmen
40	Precuneus
41	Postcentral Gyrus
42	Middle Frontal Gyrus
43	Inferior Frontal Gyrus
44	Lingual Gyrus
45	Culmen
46	Middle Temporal Gyrus
47	Precentral Gyrus
48	Middle Frontal Gyrus
49	Middle Frontal Gyrus
50	Medial Frontal Gyrus
51	Paracentral Lobule
52	Supramarginal Gyrus
53	Inferior Parietal Lobule
54	Cuneus
55	Precuneus
56	Middle Frontal Gyrus
57	Inferior Parietal Lobule

58	Precuneus
59	Precuneus
60	Inferior Parietal Lobule
61	Superior Parietal Lobule
62	Middle Frontal Gyrus
63	Fusiform Gyrus
64	Declive
65	Inferior Temporal Gyrus
66	Precentral Gyrus
67	Middle Temporal Gyrus
68	Parahippocampal Gyrus
69	Inferior Frontal Gyrus
70	Parahippocampal Gyrus
71	Middle Temporal Gyrus
72	Middle Frontal Gyrus
73	Precentral Gyrus
74	Middle Frontal Gyrus
75	Postcentral Gyrus
76	Culmen
77	Middle Occipital Gyrus
78	Precuneus
79	Inferior Parietal Lobule
80	Precuneus
81	Medial Frontal Gyrus
82	Insula
83	Inferior Frontal Gyrus
84	Culmen
85	Superior Temporal Gyrus
86	Superior Temporal Gyrus

TFU template
: location of 160 ROIs

87	Precuneus
88	Inferior Parietal Lobule
89	Precuneus
90	Medial Frontal Gyrus
91	Anterior Cingulate
92	Caudate
93	Precuneus
94	Middle Frontal Gyrus
95	Superior Temporal Gyrus
96	Superior Temporal Gyrus
97	Paracentral Lobule
98	Parahippocampal Gyrus
99	Insula
100	Superior Temporal Gyrus
101	Supramarginal Gyrus
102	Posterior Cingulate
103	Superior Temporal Gyrus
104	Middle Temporal Gyrus
105	Superior Temporal Gyrus
106	Parahippocampal Gyrus
107	Lentiform Nucleus
108	Culmen
109	Culmen
110	Middle Temporal Gyrus
111	Sub-Gyral
112	Precentral Gyrus
113	Postcentral Gyrus
114	Superior Temporal Gyrus
115	Sub-Gyral

116	Superior Temporal Gyrus
117	Cerebellar Tonsil
118	Uvula
119	Middle Frontal Gyrus
120	Inferior Frontal Gyrus
121	Culmen
122	Precuneus
123	*
124	Cerebellar Tonsil
125	Middle Occipital Gyrus
126	Middle Frontal Gyrus
127	Thalamus
128	Middle Temporal Gyrus
129	Superior Frontal Gyrus
130	Middle Occipital Gyrus
131	Superior Temporal Gyrus
132	Fusiform Gyrus
133	Precentral Gyrus
134	*
135	Precuneus
136	Postcentral Gyrus
137	Parahippocampal Gyrus
138	Middle Frontal Gyrus
139	Superior Frontal Gyrus
140	Declive
141	Lentiform Nucleus
142	Precentral Gyrus
143	Superior Frontal Gyrus
144	Middle Frontal Gyrus

145	Declive
146	Parahippocampal Gyrus
147	Inferior Frontal Gyrus
148	Inferior Frontal Gyrus
149	Superior Frontal Gyrus
150	Middle Frontal Gyrus
151	Precuneus
152	Precuneus
153	Cuneus
154	Middle Temporal Gyrus
155	Culmen
156	Culmen
157	Cerebellar Tonsil
158	Precuneus

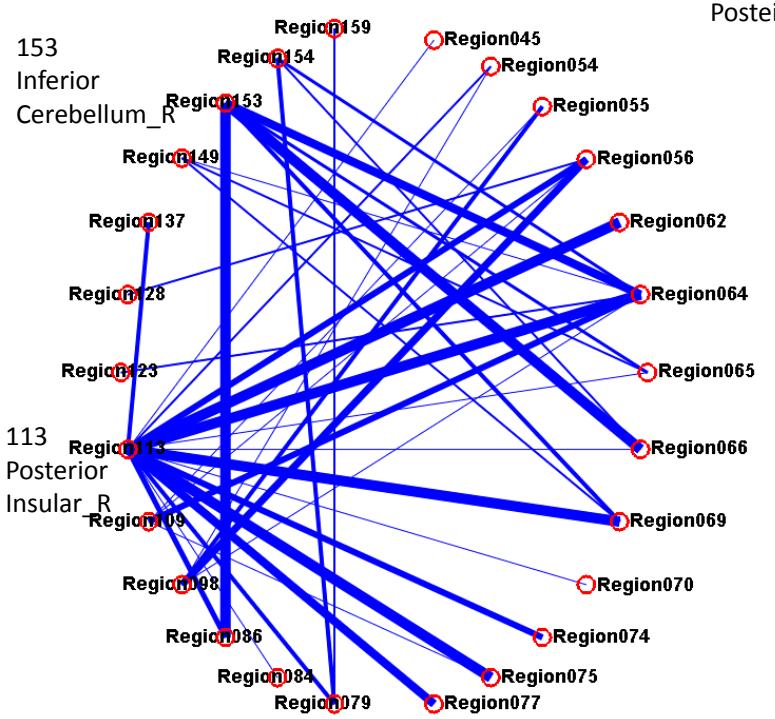
（２）Resting state network

１）Resting state fMRI:心理データ（社会的・情動的、IQ(WAIS）、EQ）と相関してRosenbach ROIs からなる脳ネットワークを同定し(Correlation analysis, p = 0.001, Uncorrected)。社会的・情動的心理データの８０項目のうち５３項目に対するネットワークが同定できた。

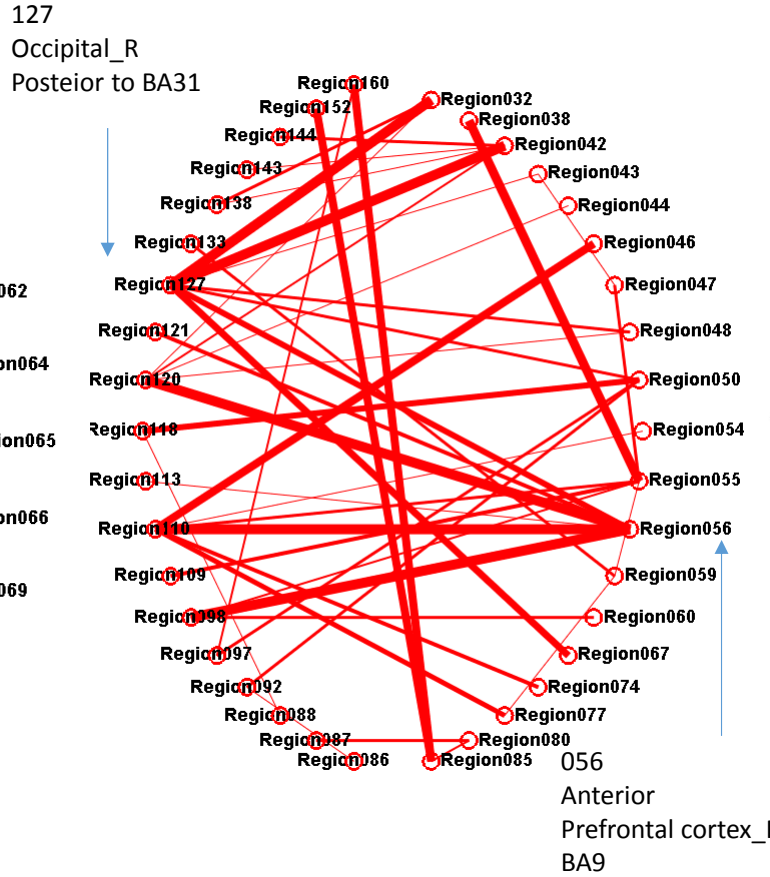
２）全てのネットワークを示すことができないので、社会性に関連する心理指標では同定されたネットワークの一部、特に、nodeとedgeの多いものを例として示す。また、IQとEQについては各項目についてしめす。

社会性に関連する心理指標項目の例

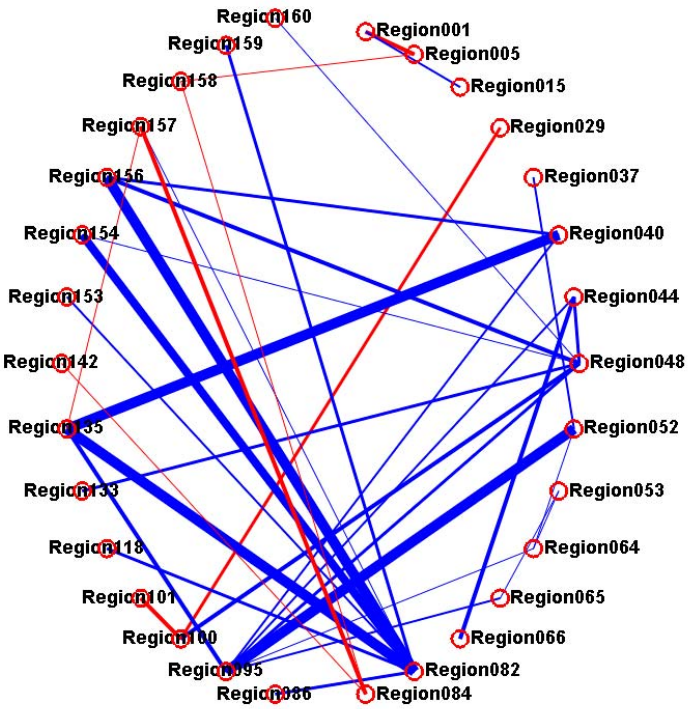
全体的自己評価



積極性vs罪悪感



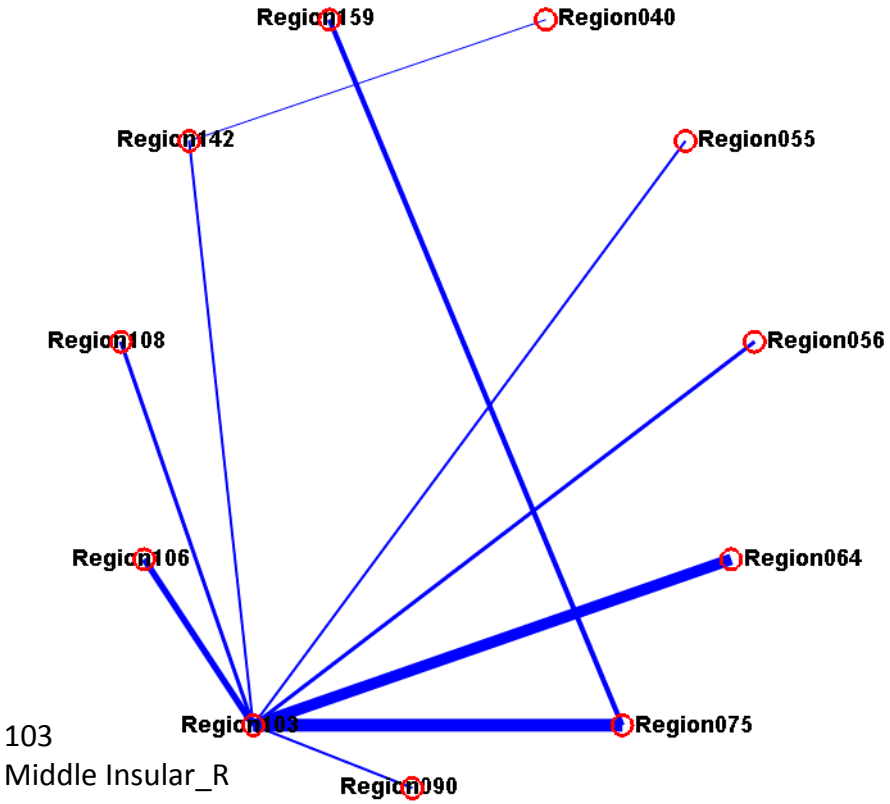
自己継続機能



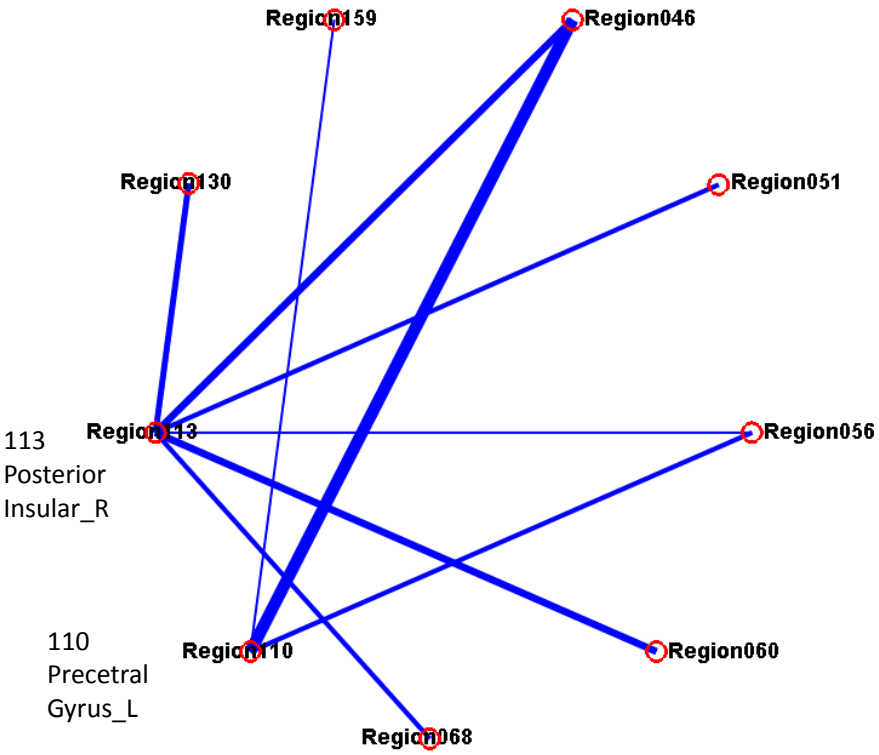
赤：項目データと正の相関を示すedge, 青：項目データと正の相関を示すedge; 線の太さは相関の強さ+1~-1

各種IQに関連するネットワークの例

言語性IQ



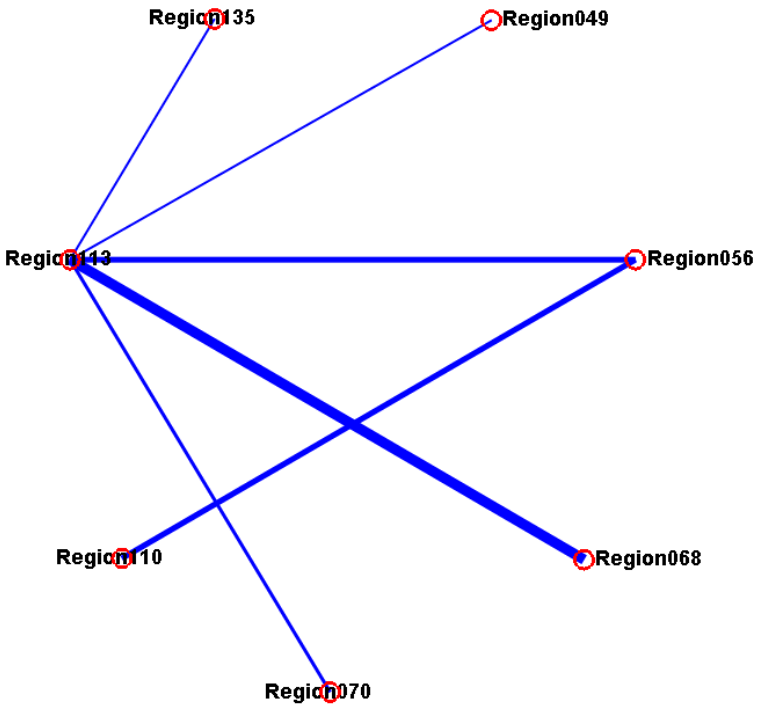
動作性IQ



赤：項目データと正の相関を示すedge, 青：項目データと正の相関を示すedge; 線の太さは相関の強さ+1~-1

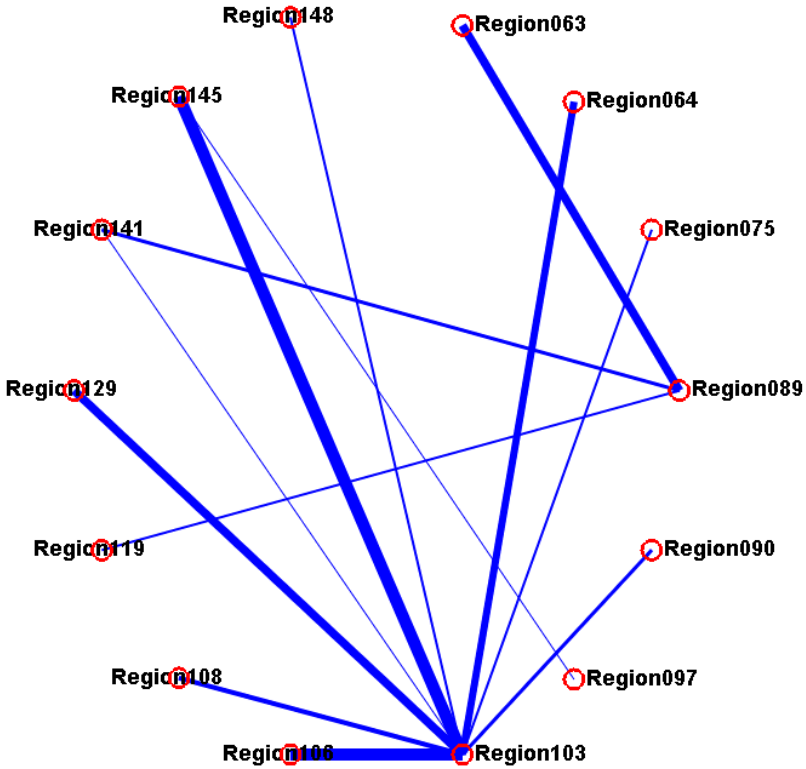
各種IQに関連するネットワークの例

流動性（Fluid）IQ



113
Posterior
Insular_R

結晶性（Crystalized）IQ



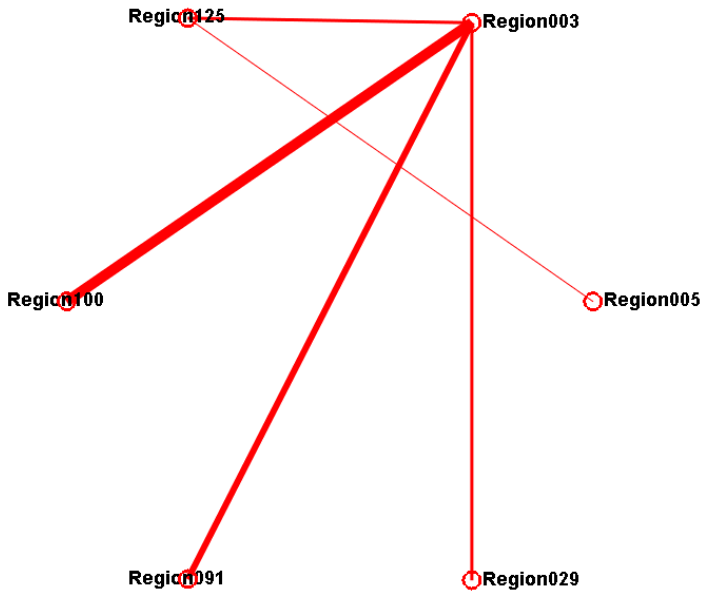
103
Middle Insular_R

赤：項目データと正の相関を示すedge, 青：項目データと正の相関を示すedge; 線の太さは相関の強さ+1~-1

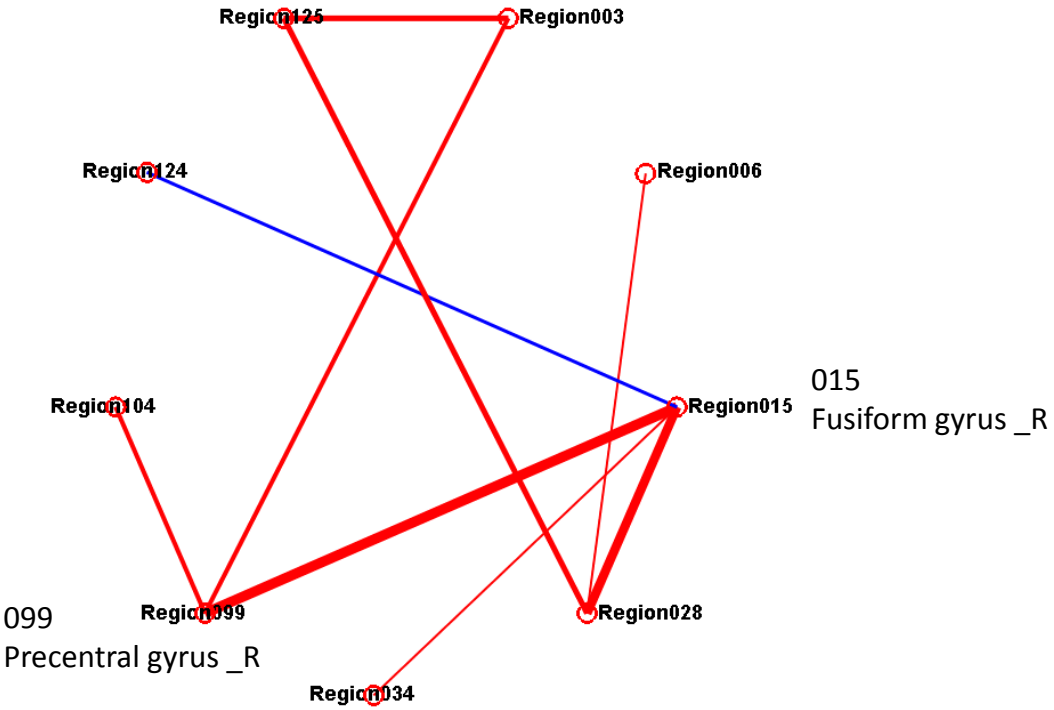
各種IQに関連するネットワークの例

自己対応EQ

003
Anterior Prefrontal cortex _L
BA9



対人対応EQ



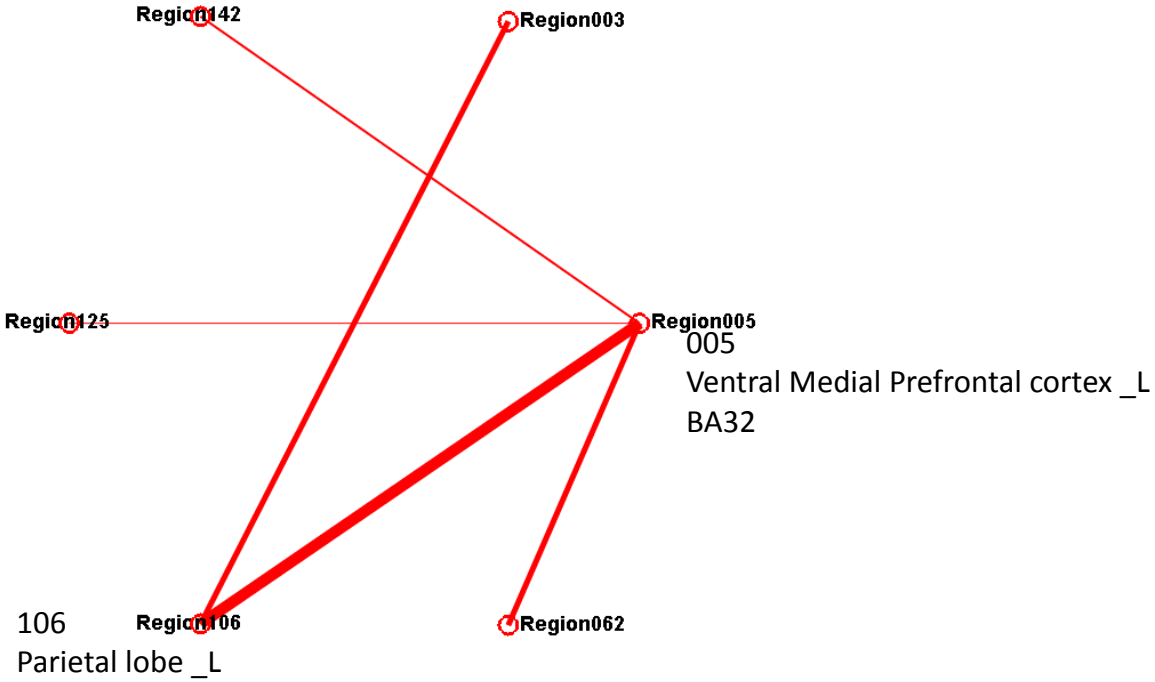
015
Fusiform gyrus _R

099
Precentral gyrus _R

赤：項目データと正の相関を示すedge, 青：項目データと正の相関を示すedge; 線の太さは相関の強さ+1~-1

各種IQに関連するネットワークの例

状況対応EQ



赤：項目データと正の相関を示すedge, 青：項目データと正の相関を示すedge; 線の太さは相関の強さ+1~-1

（3）同定された脳部位・ネットワークの機能的特性

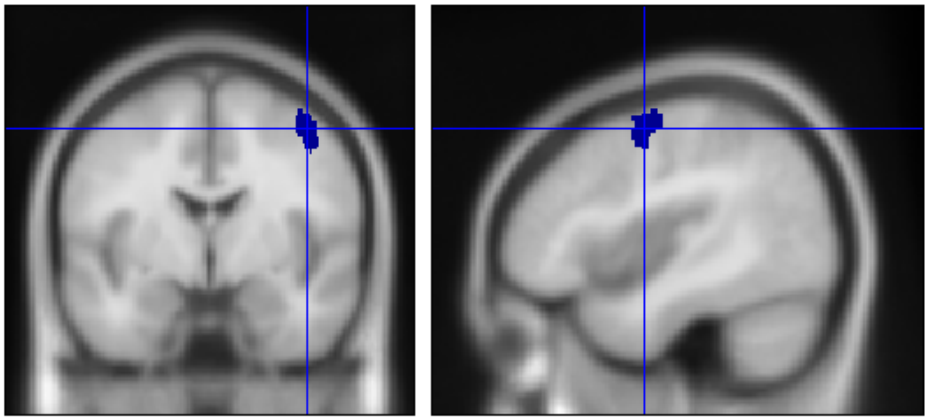
教育・訓練に関わる重要な要素であると思われる社会性関連心理指標の上位項目に対する脳部位及びネットワークを機能的な側面から検討した（Rosenbach ROIs から求めたネットワークだけを対象にした）。

（心理指標関連の部位・ネットワークの例1）

Behavior Inhibitory and Activate System:次の四つの下位項目からなる

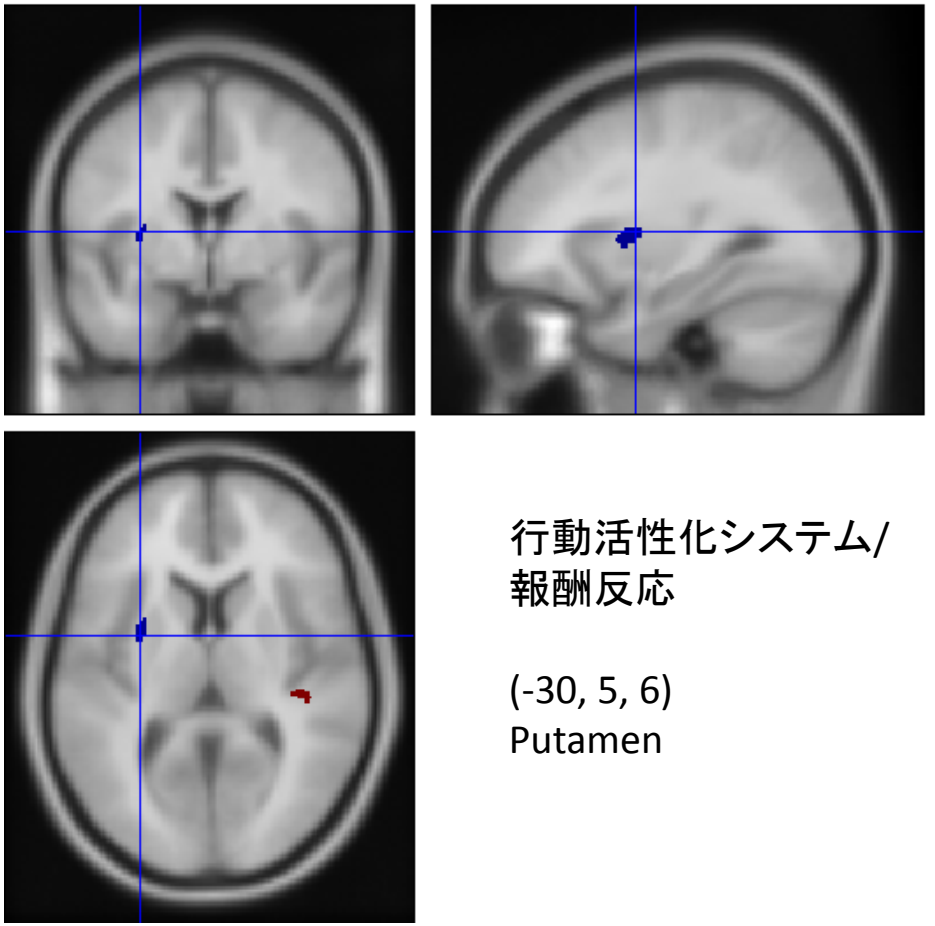
・行動制御システム
・行動活性化システム/欲求動因
・行動活性化システム/報酬動因
・行動活性化システム/報酬反応

Behavior Inhibitory and Activate System:下位項目に関連する脳部位の例



行動制御システム

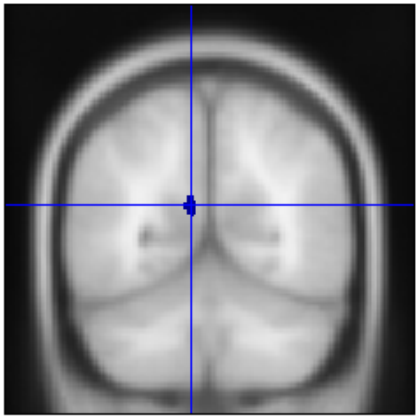
(43, -3, 52)
Right Precentral Gyrus
BA6

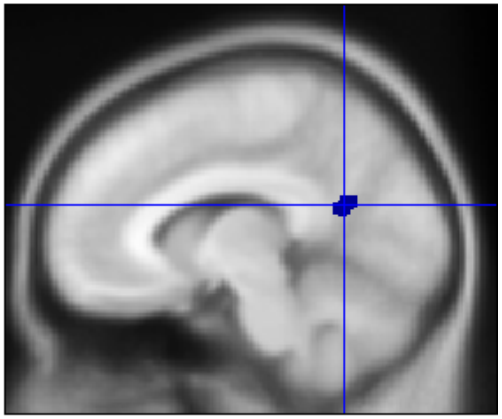


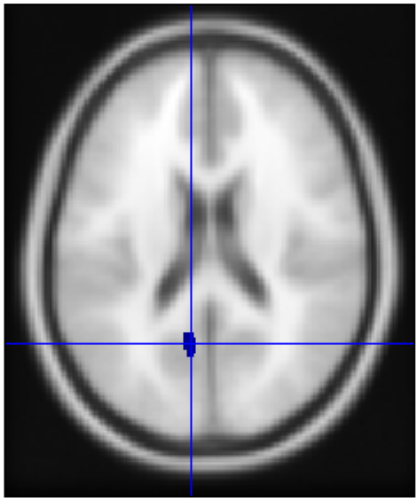
行動活性化システム/
報酬反応

(-30, 5, 6)
Putamen

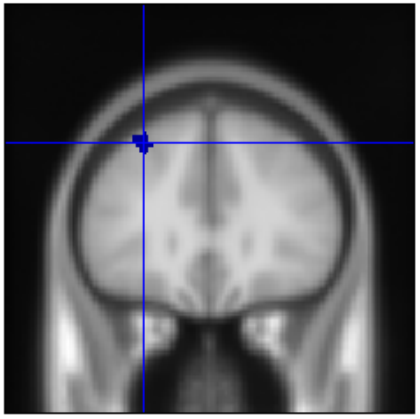
Behavior Inhibitory and Activate System:下位項目に関連する脳部位の例

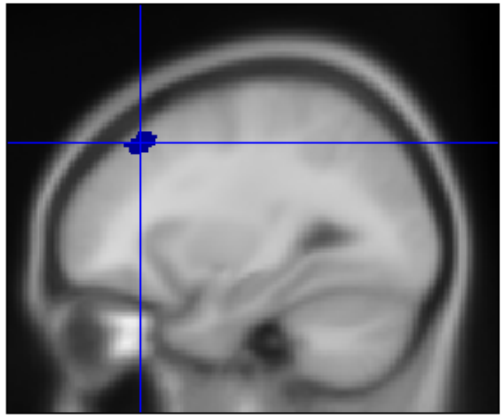


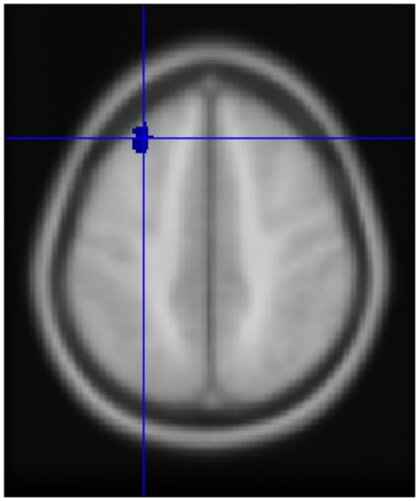




行動活性化システム
/欲求動因
(-8, -59, 20)
Left Posterior Cingulate
Cortes
BA 23/30





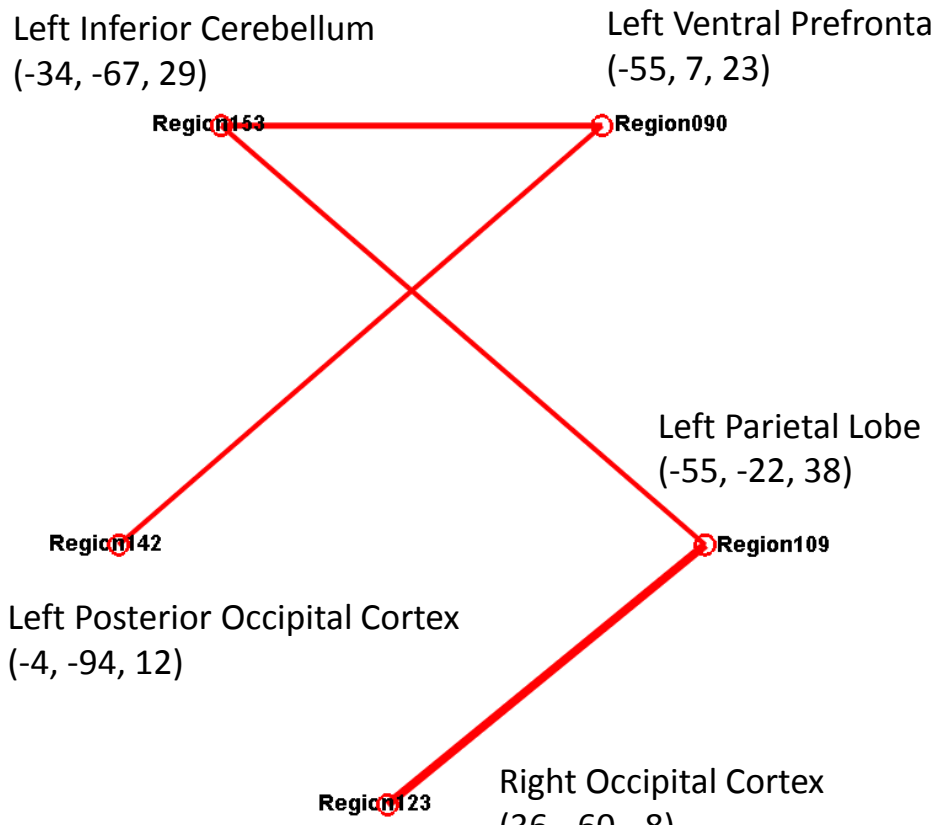


行動活性化システム/
報酬反応

(-30, 35, 48)
Left Middle Frontal Gyrus
BA9

Behavior Inhibitory and Activate System:下位項目に関連する脳部位の例

行動制御システム
p=0.001, uncorrected



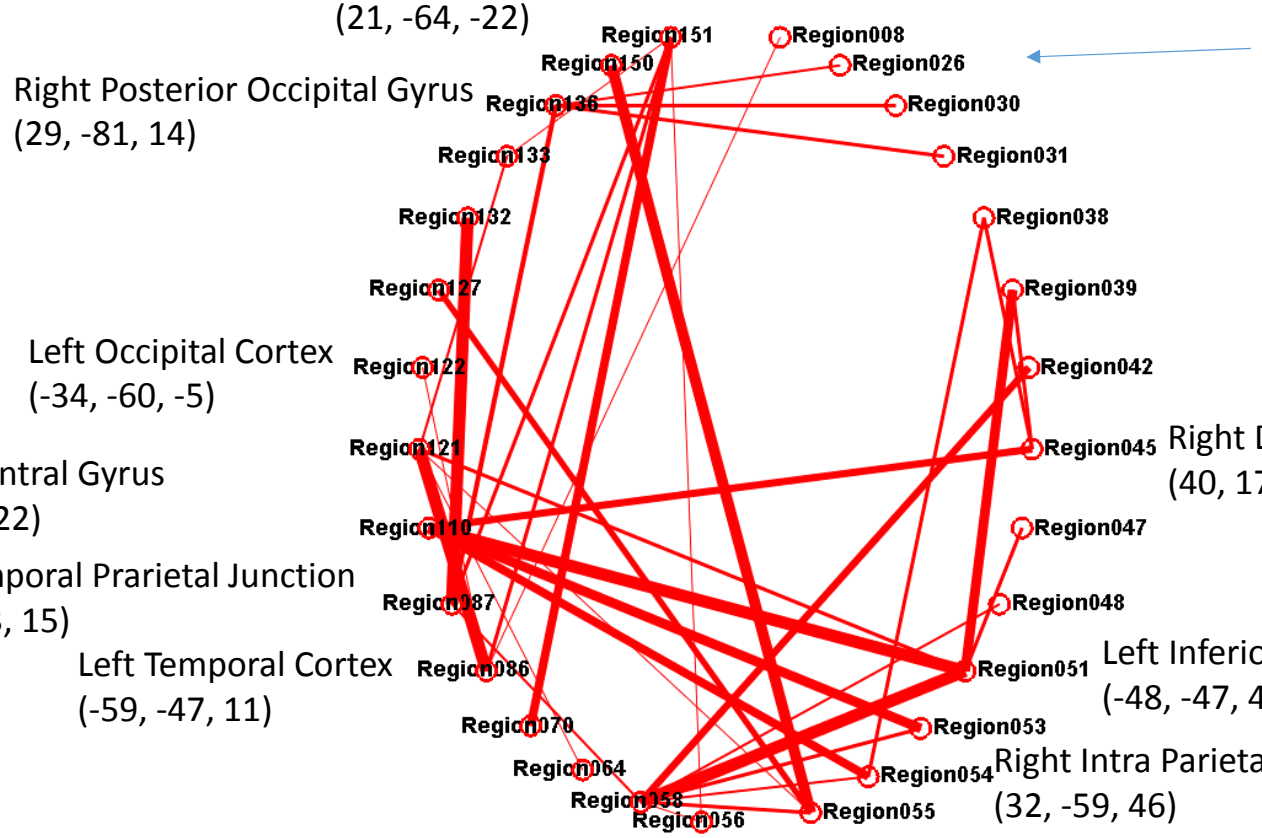
行動活性化システム
p=0.001, uncorrected

No networks

Behavior Inhibitory and Activate System:下位項目に関連する脳部位の例

行動活性化システム /欲求動因,
p = 0.001

Hubs with more than 3 edges



Right Lateral Cerebellum
(21, -64, -22)

Right Posterior Occipital Gyrus
(29, -81, 14)

Left Posterior Cingulate Cortex

Left Occipital Cortex
(-34, -60, -5)

Left Precentral Gyrus
(-54, -22, 22)

Left Temporal Prarietal Junction
(-52, -63, 15)

Left Temporal Cortex
(-59, -47, 11)

Right Dorsal Prefrontal Cortex
(40, 17, 40)

Left Inferior Parietal Lobe
(-48, -47, 49)

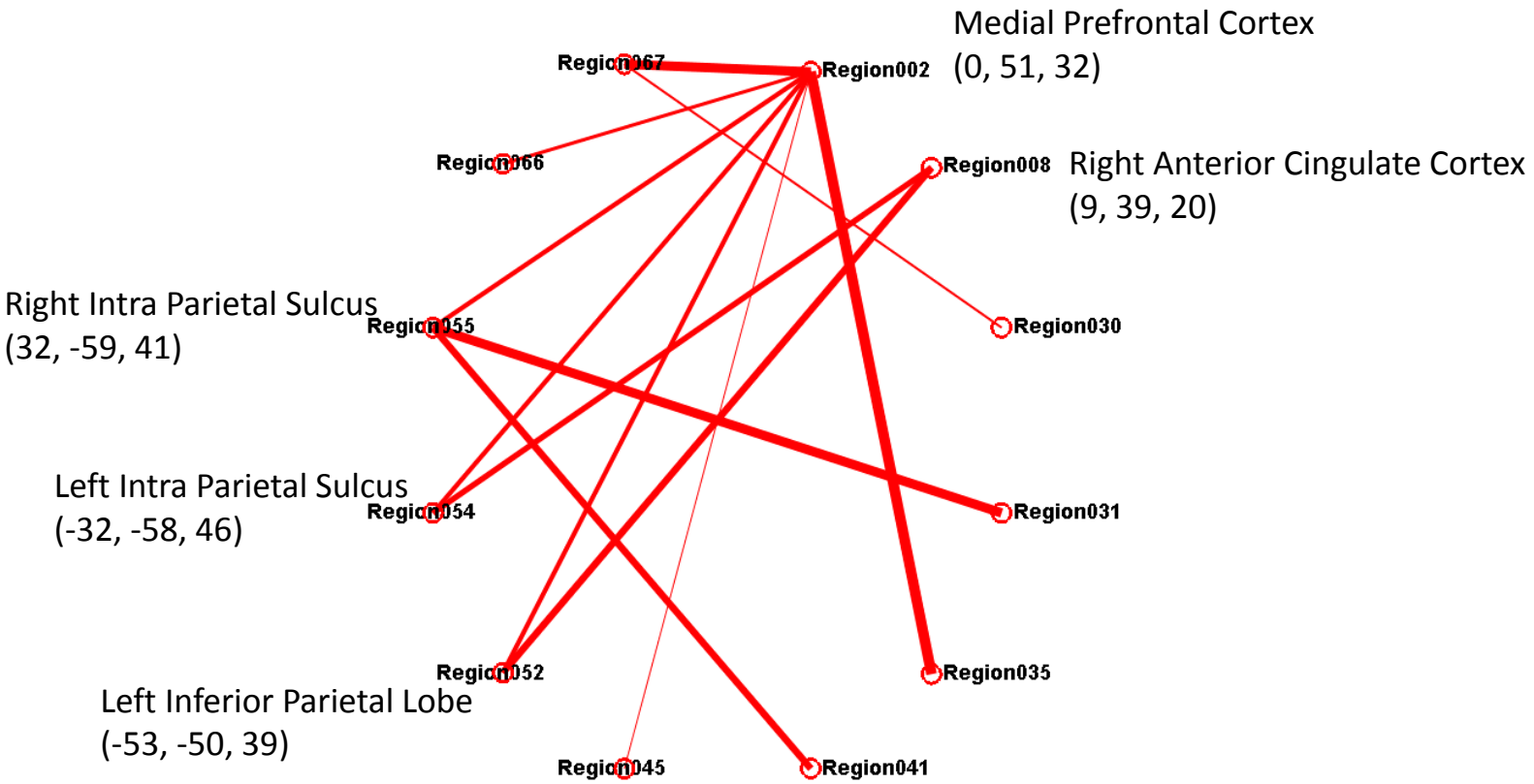
Right Intra Parietal Sulcus
(32, -59, 46)

Left Anterior Cingulate Cortex
(-2, 30, 27)

Right Intra Parietal Sulcus
(32, -59, 41)

Behavior Inhibitory and Activate System:下位項目に関連する脳部位の例

行動活性化システム/報酬反応
P = 0.001



Summary

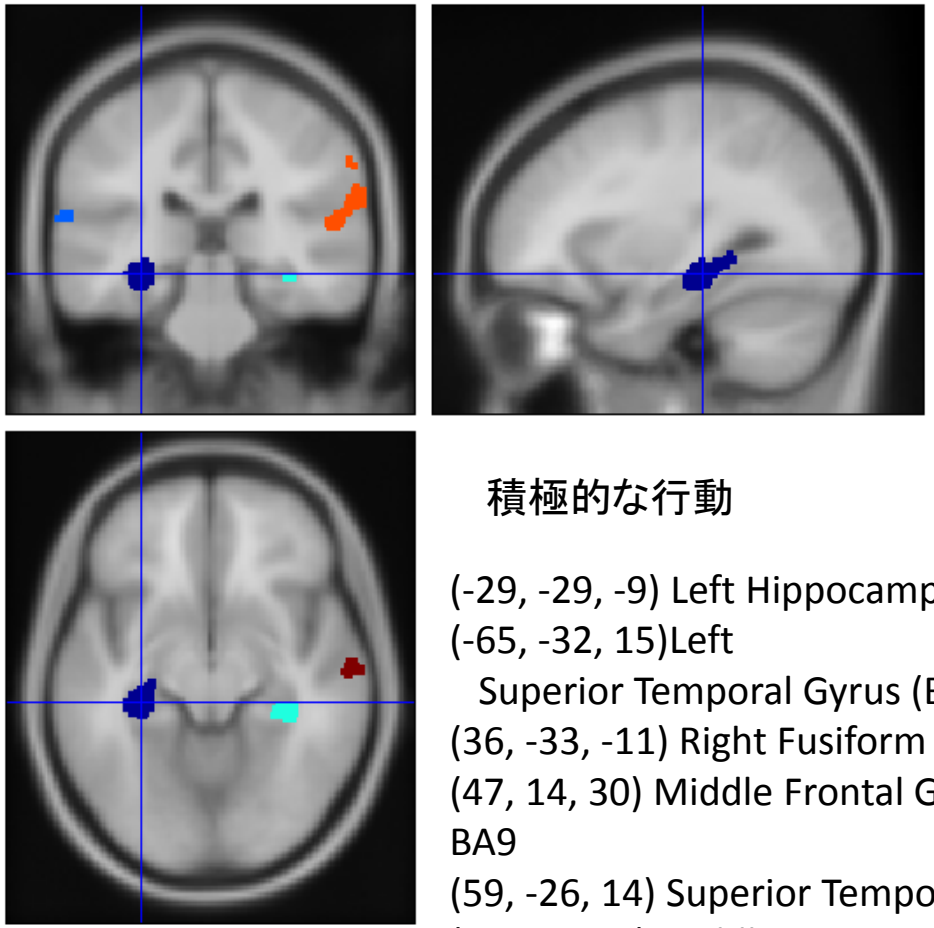
行動抑制・活性化システム（ Behavior Inhibitory and Activate System ）の下位項目に関連して同定された脳の各部位（Precentral gyrus/BA6, Putamen, PCC, Middle Frontal Cortexなど）とネットワークのHub脳部位（Inferior Cerebellum, Ventral Prefrontal Cortex, Parietal Lobe, Dorsal Prefrontal Cortex, Intra Parietal Sulcus, ACC, Precentral Gyrus/BA6, Temporal Parietal Junction, Middle Frontal Cortex）はそれぞれ Performance monitoring, Error detection, Short-term memory, Sustained attention, Decision making, Design of goal-directed behavior などの 行動関連機能を表している。

（心理指標関連脳部位・ネットワークの例２）

Personal Growth Initiative:次の四つの下位項目からなる

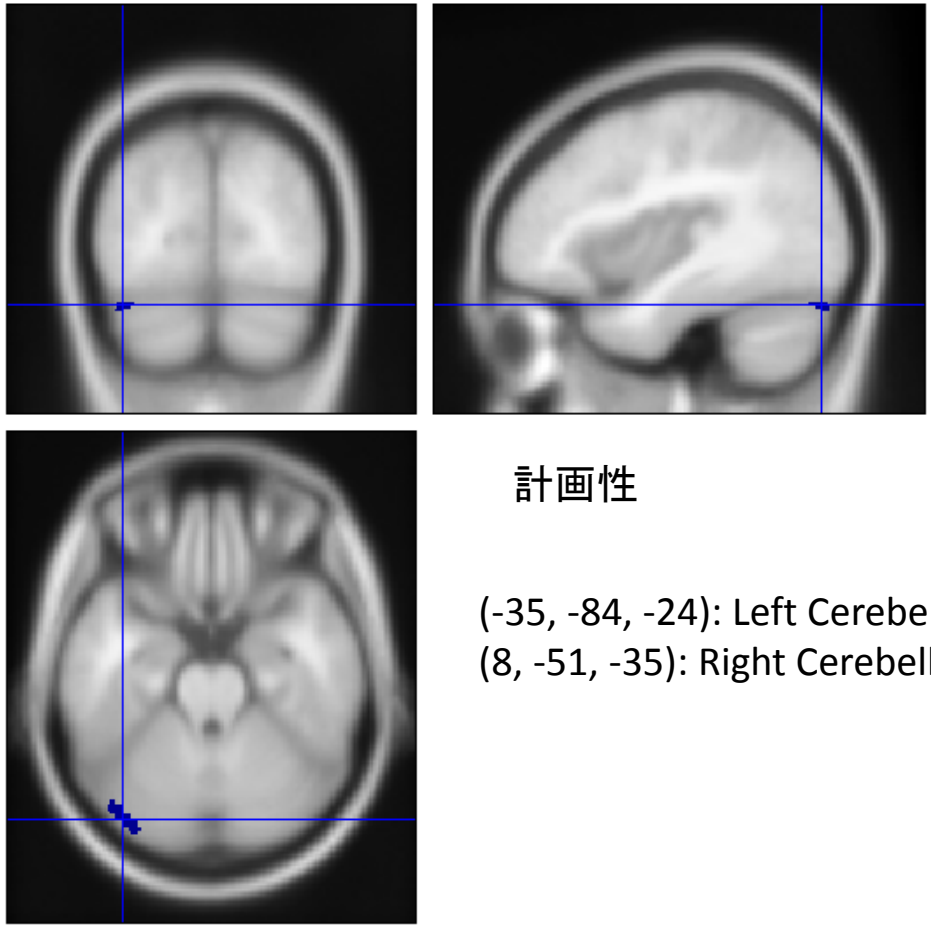
・積極的行動
・計画性
・変化への準備
・資源の活用

Personal Growth Initiative:下位項目に関連する脳部位の例



積極的な行動

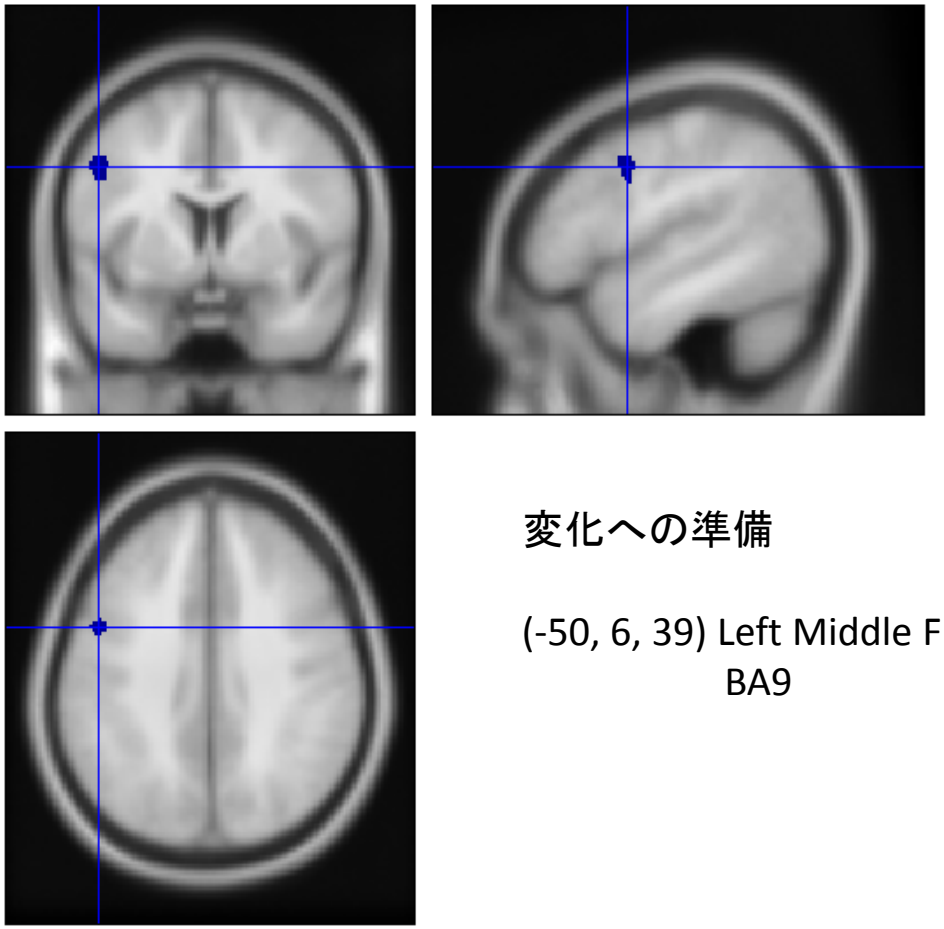
(-29, -29, -9) Left Hippocampus
(-65, -32, 15)Left
Superior Temporal Gyrus (BA42)
(36, -33, -11) Right Fusiform Gyrus
(47, 14, 30) Middle Frontal Gyrus
BA9
(59, -26, 14) Superior Temporal Gyrus
(64, -17, -6) Middle temporal Gyrus



計画性

(-35, -84, -24): Left Cerebellum
(8, -51, -35): Right Cerebellum

Personal Growth Initiative:下位項目に関連する脳部位の例



資源の活用
p=0.001, uncorrected

No Maps

変化への準備

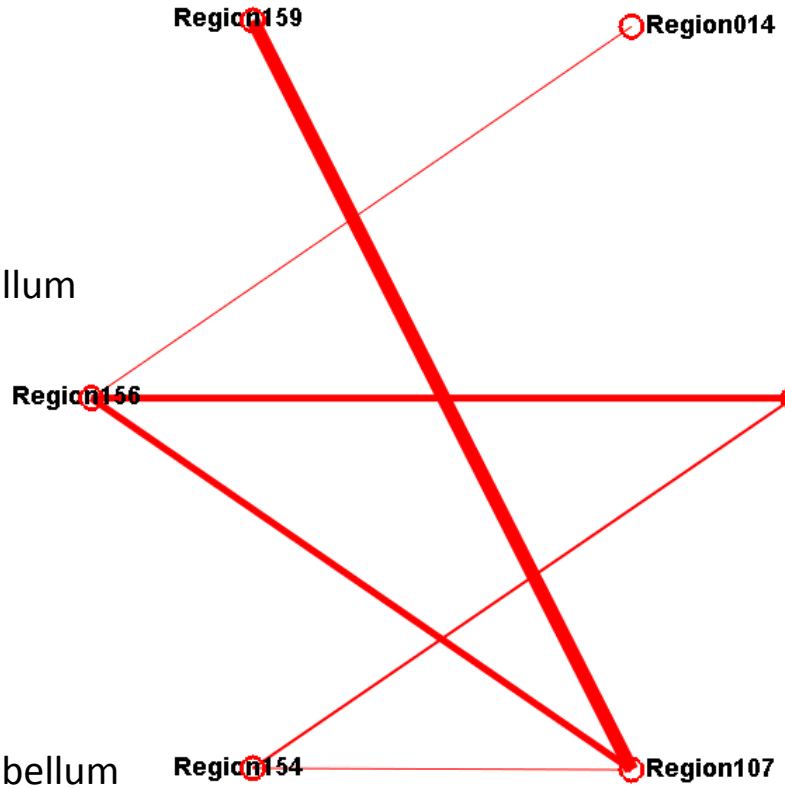
(-50, 6, 39) Left Middle Frontal Gyrus
BA9

Personal Growth Initiative:下位項目に関連する脳部位の例

積極的行動
p=0.001, uncorrected

Left Inferior Cerebellum
(-6, -79, -33)

Right Posterior Cingulate Gyrus
(1, -26, 31)



Right Middle Cerebellum
(5, -75, -11)

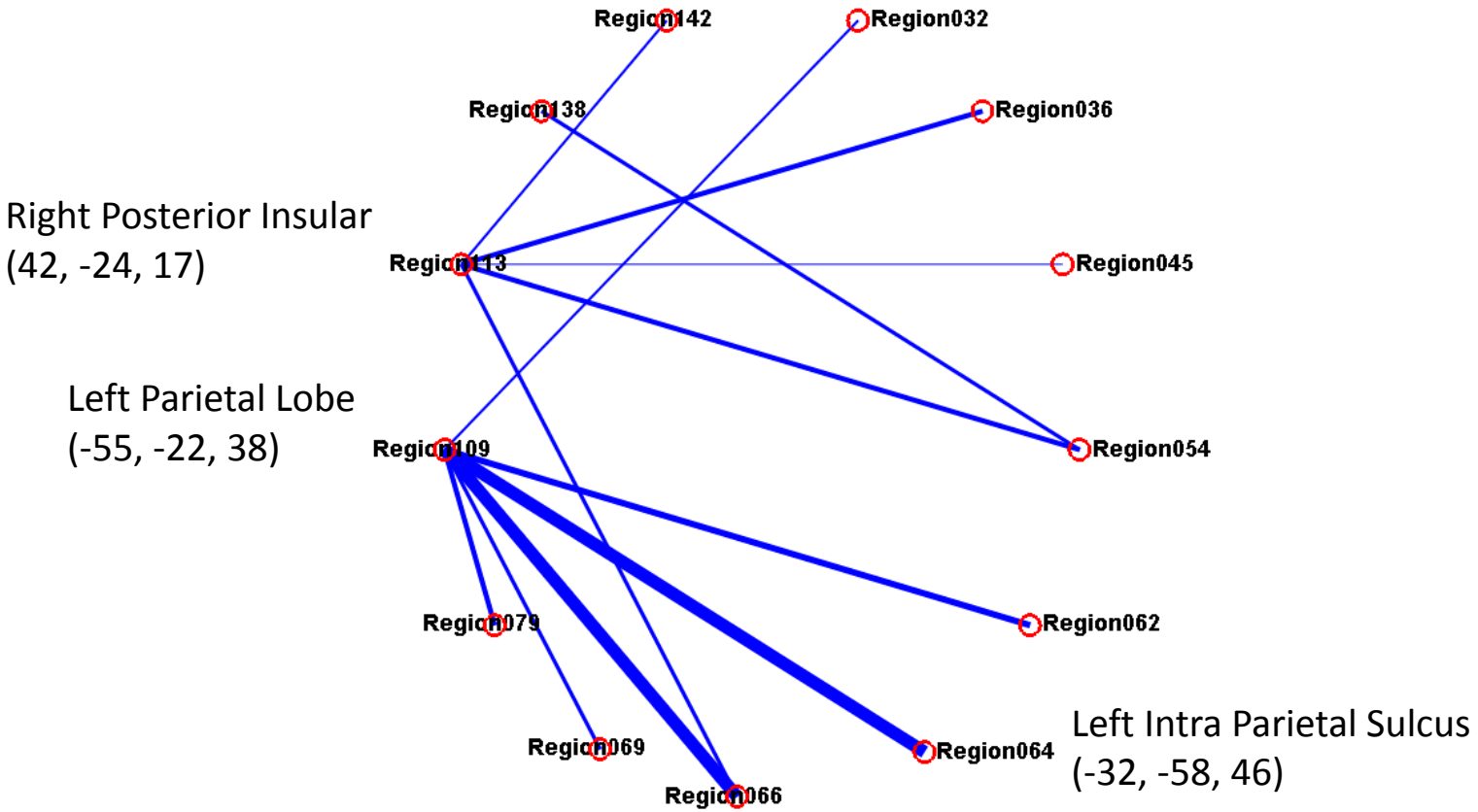
Left Middle Insular
(-42, -3, 11)

Left Parietal Lobe
(-47, -18, 50)

Left Middle Cerebellum
(-11, -72, -14)

Personal Growth Initiative:下位項目に関連する脳部位の例

計画性
p=0.001, uncorrected



Right Posterior Insular
(42, -24, 17)

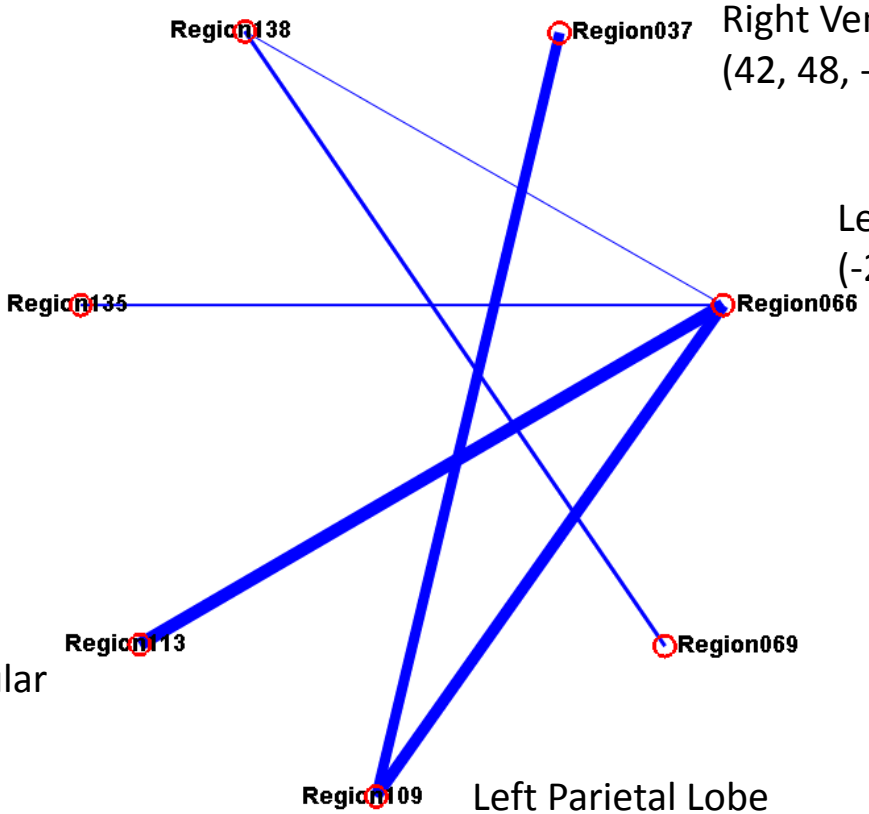
Left Parietal Lobe
(-55, -22, 38)

Left Intra Parietal Sulcus
(-32, -58, 46)

Left Basal Ganglia
(-20, 6, 7)

Personal Growth Initiative:下位項目に関連する脳部位の例

変化への準備
p=0.001, uncorrected



Right Ventral Anterior Prefrontal Cortex
(42, 48, -3)

Left Basal Ganglia
(-20, 6, 7) Putamen

Right Posterior Insular
(42, -24, 17)

Left Parietal Lobe
(-55, -22, 38)

Summary

自己成長主導（personal growth initiative）の下位項目に関連する脳部位（Hippocampus, Superior Temporal Gyrus/BA42, Fusiform Gyrus, Middle Frontal Gyrus/BA9, Middle temporal Gyrus, Cerebellum) とネットワークのHub脳部位（ Insular, Cerebellum, Parietal Lobe, Putamen）はBehavior, Perception, Memoryなど行動・外部からの情報の収集に関連する機能を表している。

（MRIデータ分析における限界と対策）

・　今回の分析では、MRIデータと心理データがともに収集されてない被験者があったので、社会性に関する心理指標と、IQとEQに関する心理指標に対応する脳部位・ネットワークの同定に用いられたデータサンプル数が異なった。

・　職業適性に関するデータ分析は１２月の時点でサンプル数がIQサンプルより少なかったので行われなかった。

・　データ分析における心理指標間の比較または統合は行われなかった。

・　Resting state fMRI data のネットワーク分析ではtemplateを使用したがシードベースの分析も必要である。

・　DTIの分析は分析に時間がかかり、H28年度から始める予定である。

・今回までのMRIデータ分析では、心理指標下位項目に対して独立性を検討しないで使用した。また、VBMの解析では正の相関だけで脳部位の同定を行った。

・今後、独立性の検討と心理指標のcategorization などを行いそれに対応する脳部位とネットワークを同定して行く必要がある。このような過程を通して、最終的に、３－４年間の可塑的変化を計測するための基盤（template）の作成が完成する。今後１年にかけてその作業を行う予定である。

・　脳部位の検出ができなった心理指標の下位項目については課題ベースfMRI実験により脳部位・ネットワークの同定を行う必要がある。

・縦断的データ分析のために３－４年間の教育期間中に受ける教育・訓練の内容ごとに被験者群の分類と各心理指標に対応する脳部位・ネットワークの初期値に対する分析も必要である。

[3] 可塑性・認知機能 study

（１）長期的な可塑的変化

（２）中期的な可塑的変化

（３）短期的な可塑的変化―１

（４）短期的な可塑的変化－２

（１）長期的な可塑的変化

大学在籍中の学生で、中学・高校時代に吹奏学部で演奏して、演奏を続けている人を対象にMRI解剖・機能画像を測定した。

（被験者）

実験群：１４名

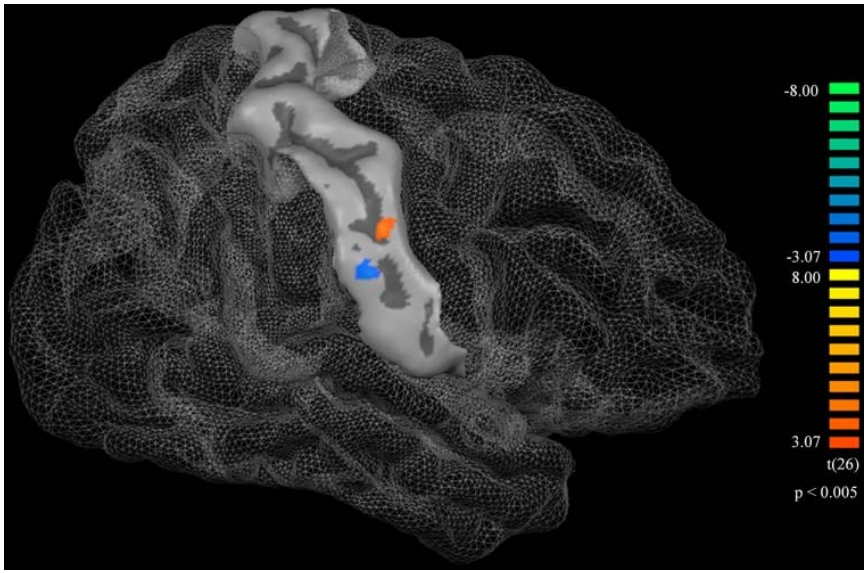
制御群：１４名

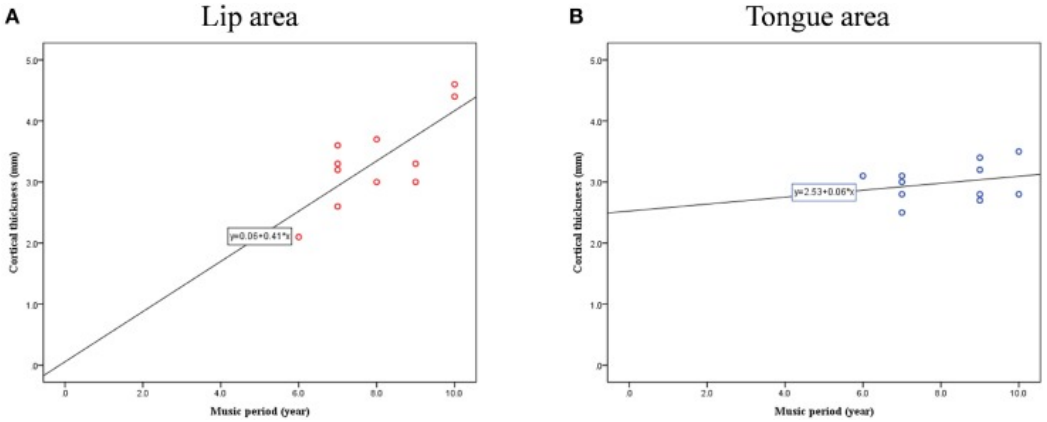
（結果）

実験群と制御群との差がある脳部位はLip area tongue areaであった。

演奏期間に対しては、Lip area のcortical thickness が正の相関を示した。

Long-term plasticity: Music training by wind instruments for 7 – 10 years;
Lip areas showed changes in cortical thickness. (Ogawa et al. 2015)





A surface atlas showing of the postcentral gyrus and a cortical thickness difference map. The orange represents the area in which the music playing group had greater cortical thickness than the non-music playing group. The blue represents the area in which the music playing group had less cortical thickness than the non-music playing group. Both thicker and thinner areas were statistically significant ($p < 0.005$, corrected).

Correlation between cortical thickness and musical training years in lip- (A) and tongue-related (B) brain areas. Significant and positive high correlations between the thickness and years of musical training ($r = 0.761$, $p = 0.006$ by Pearson correlation; Figure A).

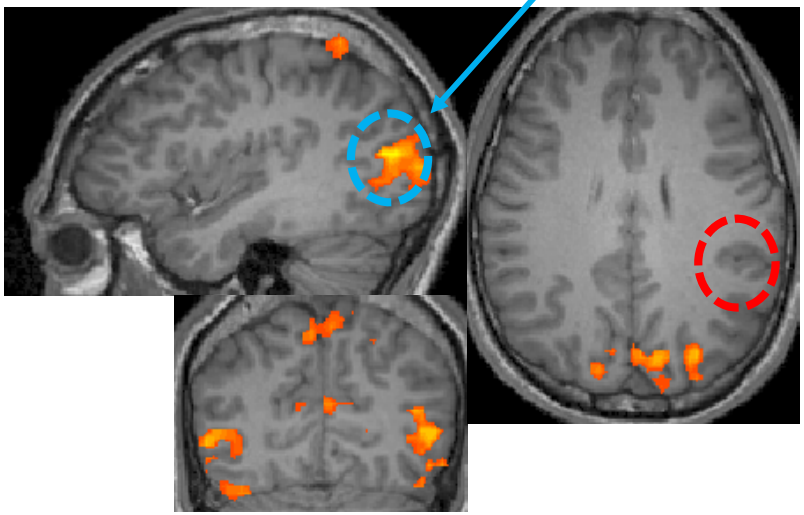
（２）中期的な可塑的変化

大学期間中の学生（１例）を２２ヶ月間解剖画像を９回測定し、VBMの変化がある脳部位を同定した。その脳部位をシードにしたresting state ネットワークを同定した。２２ヶ月後のネットワークでは新しい脳部位が加わっていることが分かった。

Resting state network: new area involved after 22 months University life

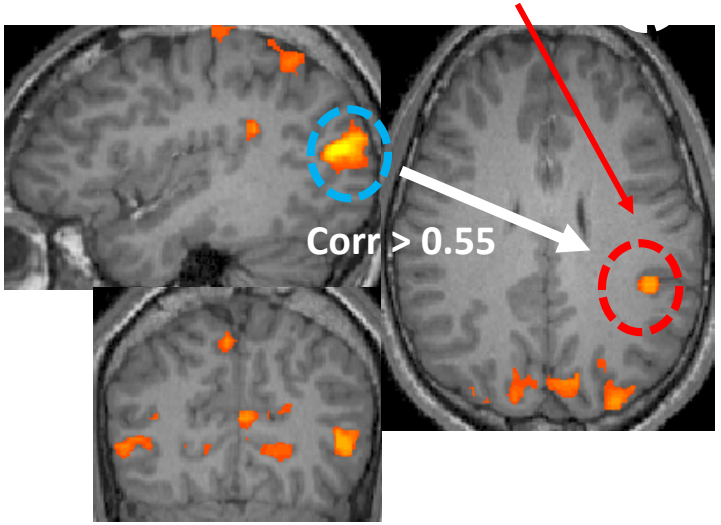
0 Month

A seed area :
showed a change
at gray matter volume



After 22 Months

New correlation found



BA 40

（３）短期的な可塑的変化ー１

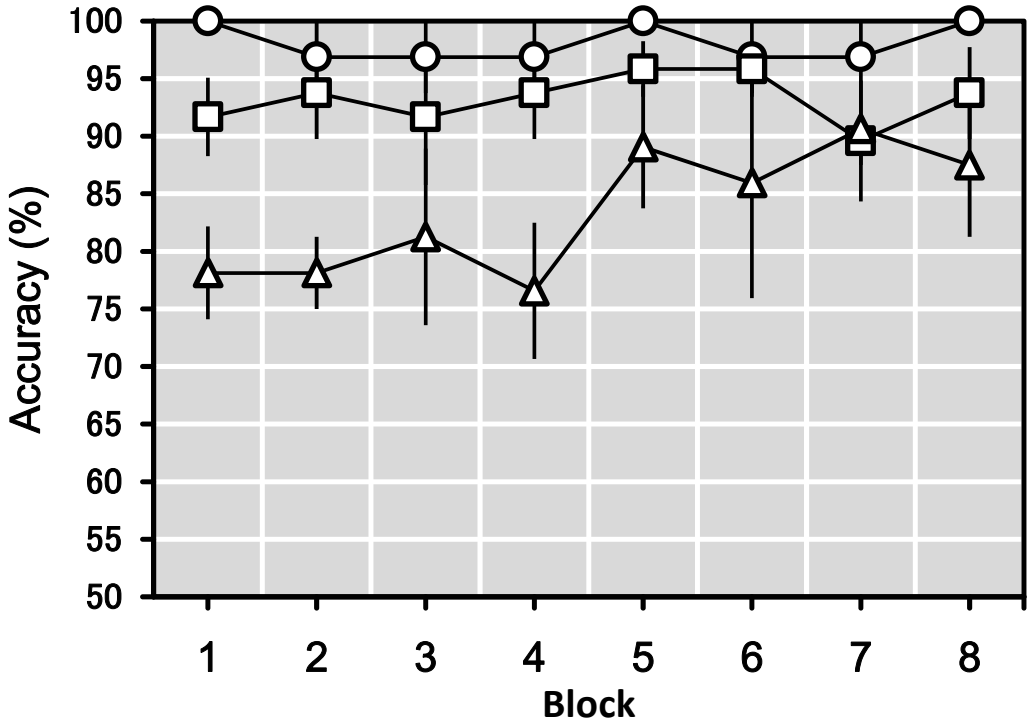
Short-term training による実行機能の可塑的変化について、下記 3 つの構成要素に対応する課題を用いて検討した。

Updating: ワーキングメモリーの情報の追加や削除
Shifting: 構え（mental set）・課題の切り替え
Inhibition: 反応の抑制

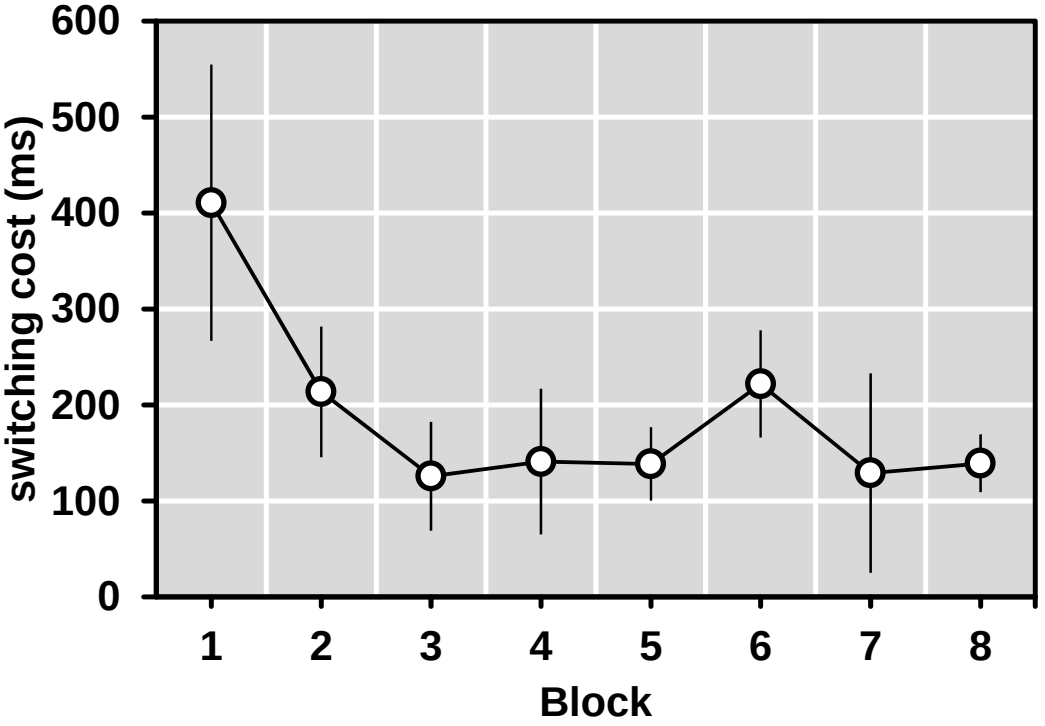
（結果と考察）

いずれの課題でもブロック数を追うごとに学習の効果が見られた。今後課題間転移の効果や学習効果の個人差の詳細な検討を行う必要がある。

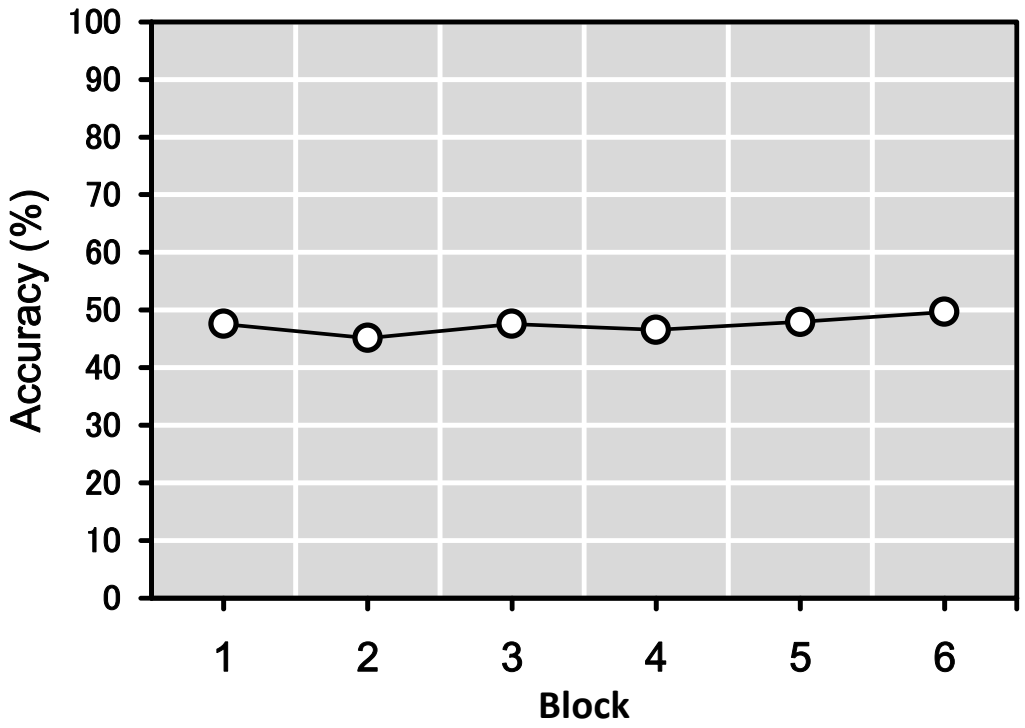
Updating: Keep track task

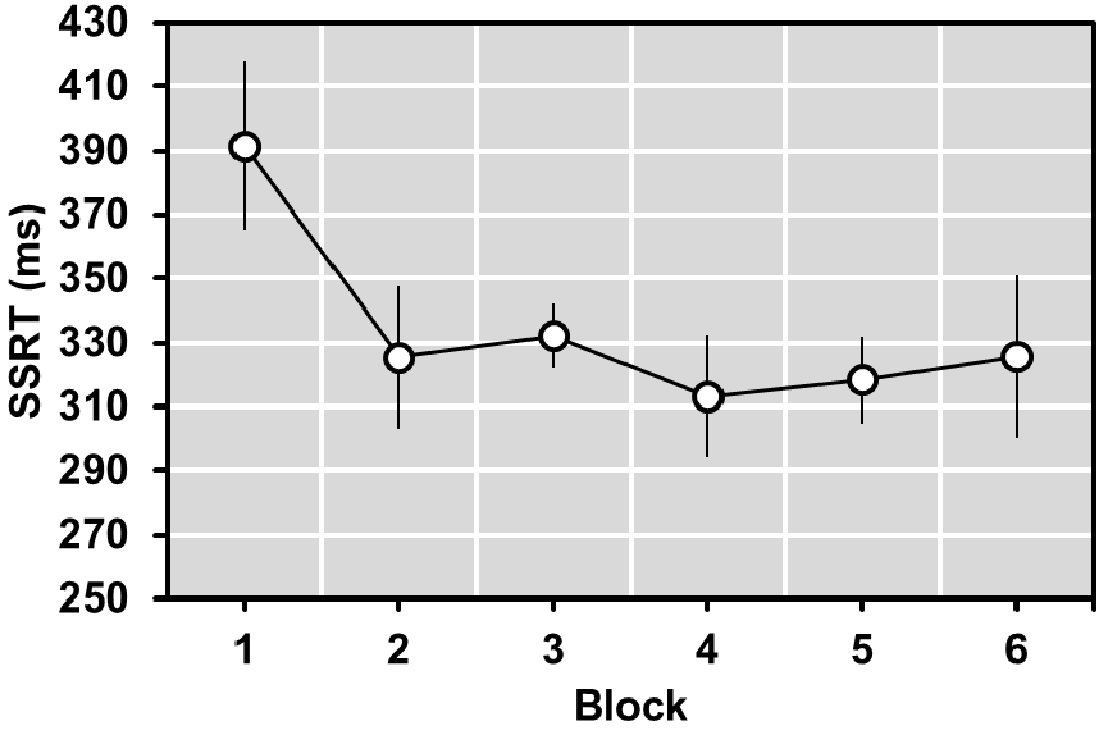


Shifting: category switch task



Inhibition: stop signal task





SSRT: stop signal response time
(反応を抑制するまでの時間)

（３）短期的な可塑的変化－２

大学在籍の学生で、４週間の保育実習前後の赤ちゃんの顔に対する脳活動の変化を見た。

（被験者）

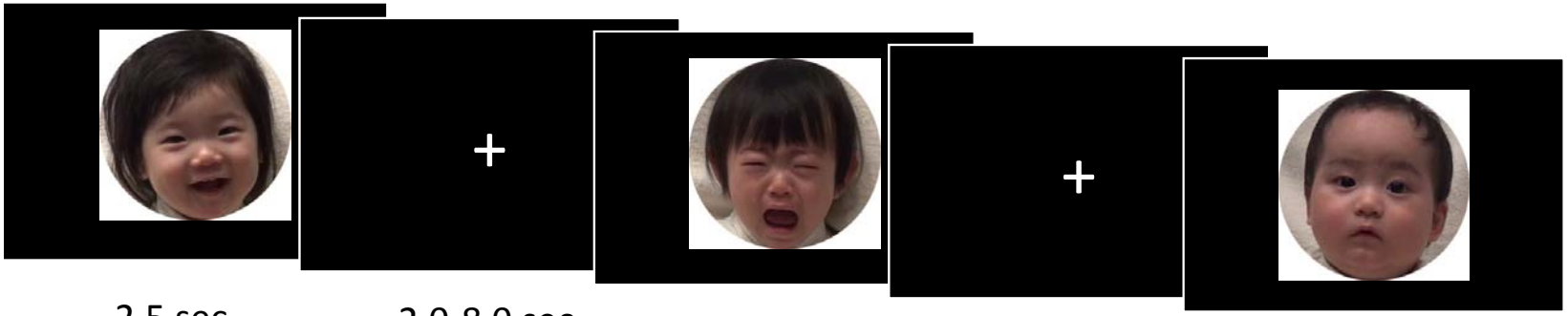
実験群（実習参加者）：２５名

制御群（不参加者）：２５名

（結果）

保育実習参加者において、顔刺激に対する脳活動が、Left Fusiform Gyrus, Amigdala で実験前後の差があった。

Methods



2.5 sec 2.0-8.0 sec

Subjects

Experimental group: 25 participants (age range, 20-21 years; mean age, 20.13 years)

Control group: 21 participants (age range, 20-21 years; mean age, 20.14 years).

Stimuli

Seventy-two positive, neutral, negative facial images of four infants.

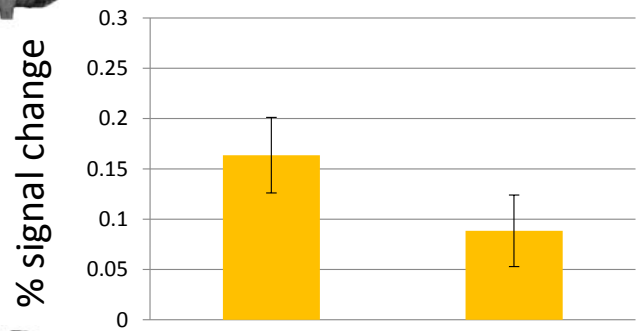
Task

The subjects rated each face based on how positive or negative it was using a 8-point scale.

ROI analysis (experimental group)

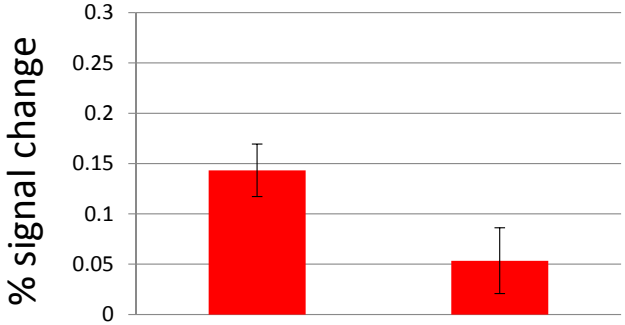


Left amygdala
P = 0.051



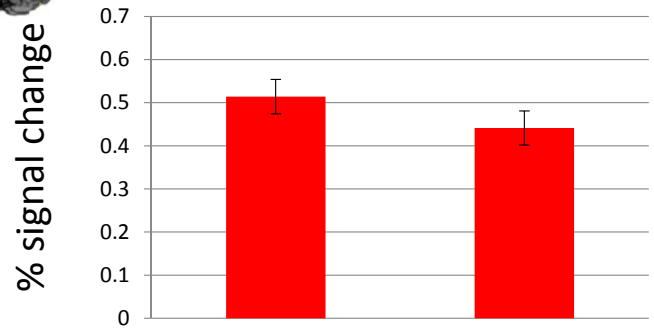


Right amygdala
P < 0.05



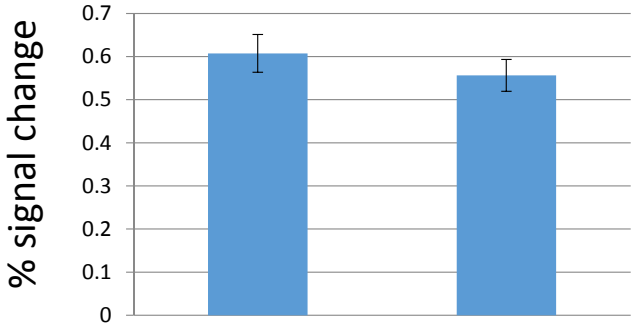


Left fusiform
P < 0.05

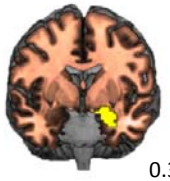




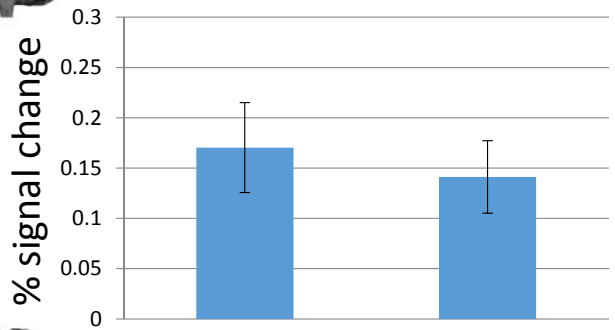
Right fusiform
P = 0.137



ROI analysis (control group)

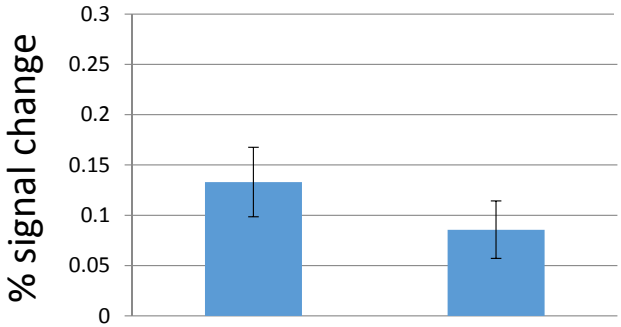


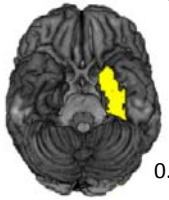
Left amygdala
P = 0.335



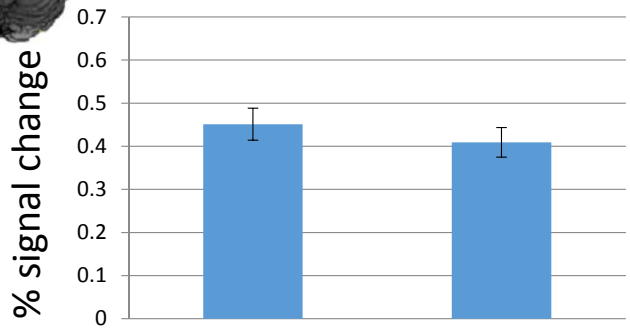


Right amygdala
P = 0.189



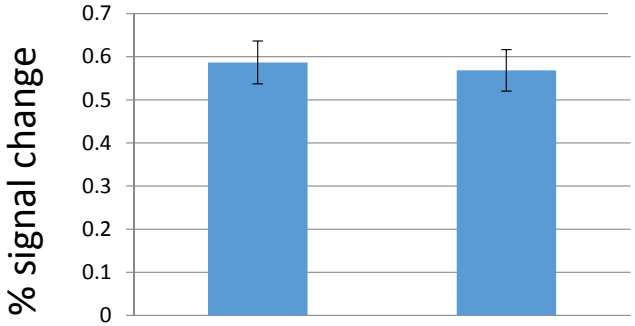


Left fusiform
P = 0.288





Right fusiform
P = 0.687



[4] パターン認知 study

(1) The Aim of the current research is applying the Density Based SVM cluster the MRI/fMRI data.

(2) The Density Based SVM was used to classify resting state fMRI data of 26 subjects with 116 ROIs of AAL template (13 for eye open, 13 for eye closed). We used the normal SVM and our developed Density Based SVM for this classification and finally we found that DBSVM was better than Linear SVM.

Classification accuracy is as follows:

Linear SVM	Linear DBSVM	RBF SVM	RBF DBSVM
76%	84%	88%	88%

7. まとめ

(1) H26年度での研究、MRIアップグレード、MRI測定方法とパラメータの設定、予備実験、心理指標のための質問紙の準備などを計画通りに終えて、H27年度から本実験を始めた。

(2) 教育・訓練による脳の可塑的変化を検出する上で必要な心理・脳データ基盤を作るための心理データ とMRIデータを収集した。

(3) MRI解剖画像により、心理指標に関連する脳部位を同定し、心理指標を表現する脳のtemplate(ROIs とネットワーク)を作成した。

(4) MRI機能画像により、心理指標に関連する脳ネットワークを同定した（一部の心理指標（社会性）についてはネットワークtemplateが作成できた）。

（５） 脳の長期的な可塑的変化への実証データを得た。また、中・短期的な可塑的変化に対する実証データを得るための予備実験を行った。また、パターン認知のアルゴリズムの開発とテストを行った。

（６） H26-27年度の研究はおもに、横断的研究に相当する。３－４年間のMRI・心理データ収集による縦断研究はH28年度後半から分析をして行く予定である。

（７） 横断的研究において職業の専門家に対する測定は脳templateの機能的な特性を分析し、本大学の教育・職業に関連する代表的な職業について行う。

（８） H26－２７年度の研究において、機能的データ基盤のために必要なデータが計画どおり収集できたこと、また、データ分析により、脳部位・ネットワークのtemplateのような基盤ができたことから、計画どおりに研究が進んだことになる。また、一部の心理データとMRIデータ分析においては次年度（H28）から計画しているデータマイニングに入ったことになる。

研究進捗状況

H26年度

心理指標・
MRI測定法などの選定
予備実験

H27年度

心理指標データ・
MRIデータ収集

H28年度

中間的データマイニング・
MRIデータ収集継続

H29年度

心理指標・MRIデータの
定量的指標作成・
分析方法の確立

H30年度

情報基盤の策定

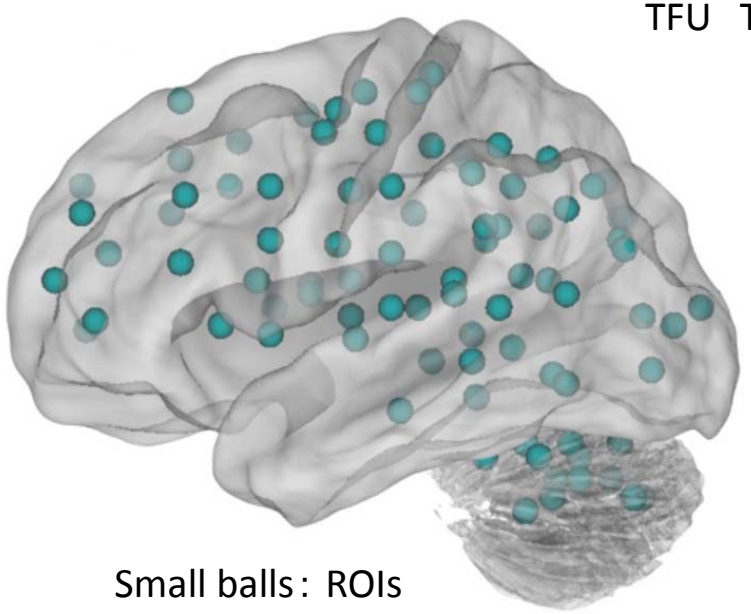
可塑性検出（縦断データ）のための基盤作成
（心理指標による横断的データ収集完了
横断的MRIデータ収集完了
心理指標に対する脳マップの同定）

(9)H26-27年度の研究結果のプロジェクト全体における意義・展望

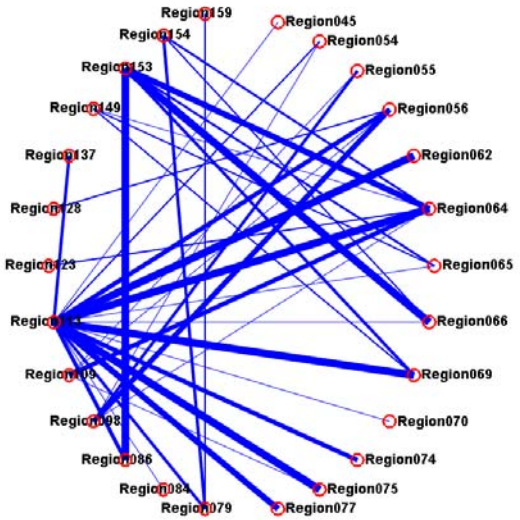
(A)TFU templateの意義

Templateは機能的役割が同定された脳部位・ネットワークからなるものであり、ヒトの行動を表す心理指標が脳へ投射されたものである。これは、プロジェクト遂行におけるデータ基盤となる。H27年度までの研究では、templateの作成のための心理・MRIデータの収集と分析ができた。また、収集したデータをもとに独自のtemplate (TFU template)が作成できた。H28年度からはより完成度(精度)の高いものに改良して行く予定である。

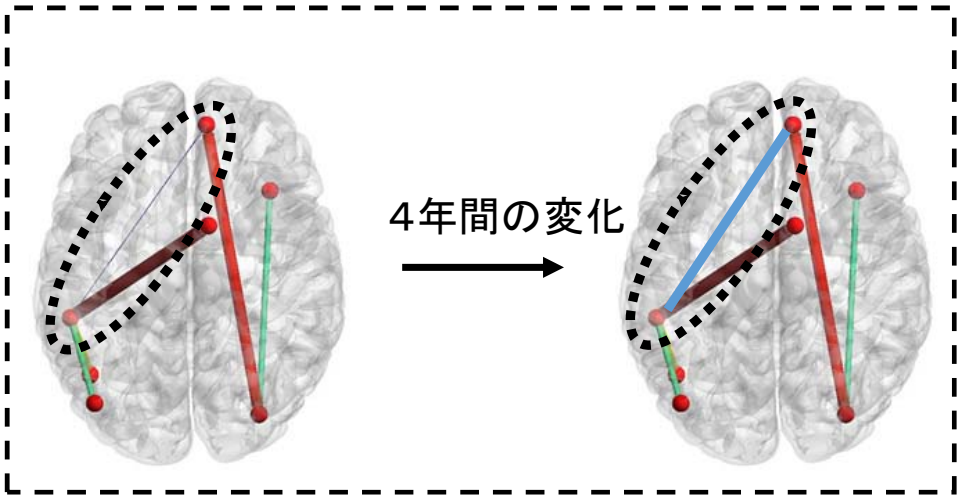
TFU Template



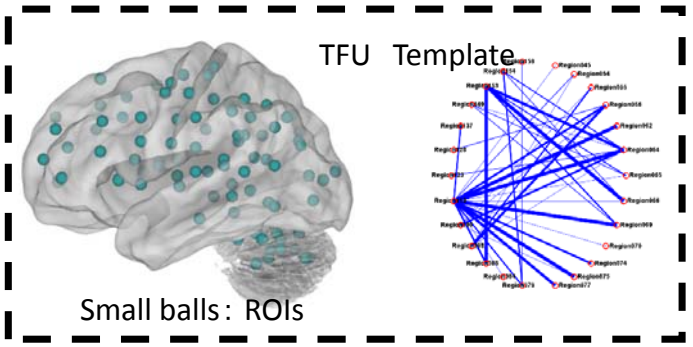
Small balls: ROIs



（B）学習・訓練効果の評価への利用
被験者の固有の心理活動の可塑的変化をtemplate をベースに推定できる。
ある人の脳を計測して、特定のネットワークの変化が分かれば、そのネットワークがどの心理指標に対応するかを templateから検索できる。例えば、それが行動制御であれば、その人は4年間の教育・訓練により、行動制御について何らかの変化があったと推測できる。H28年度からの研究はそのためのMRI測定の継続、推定方法の開発を行う予定である。

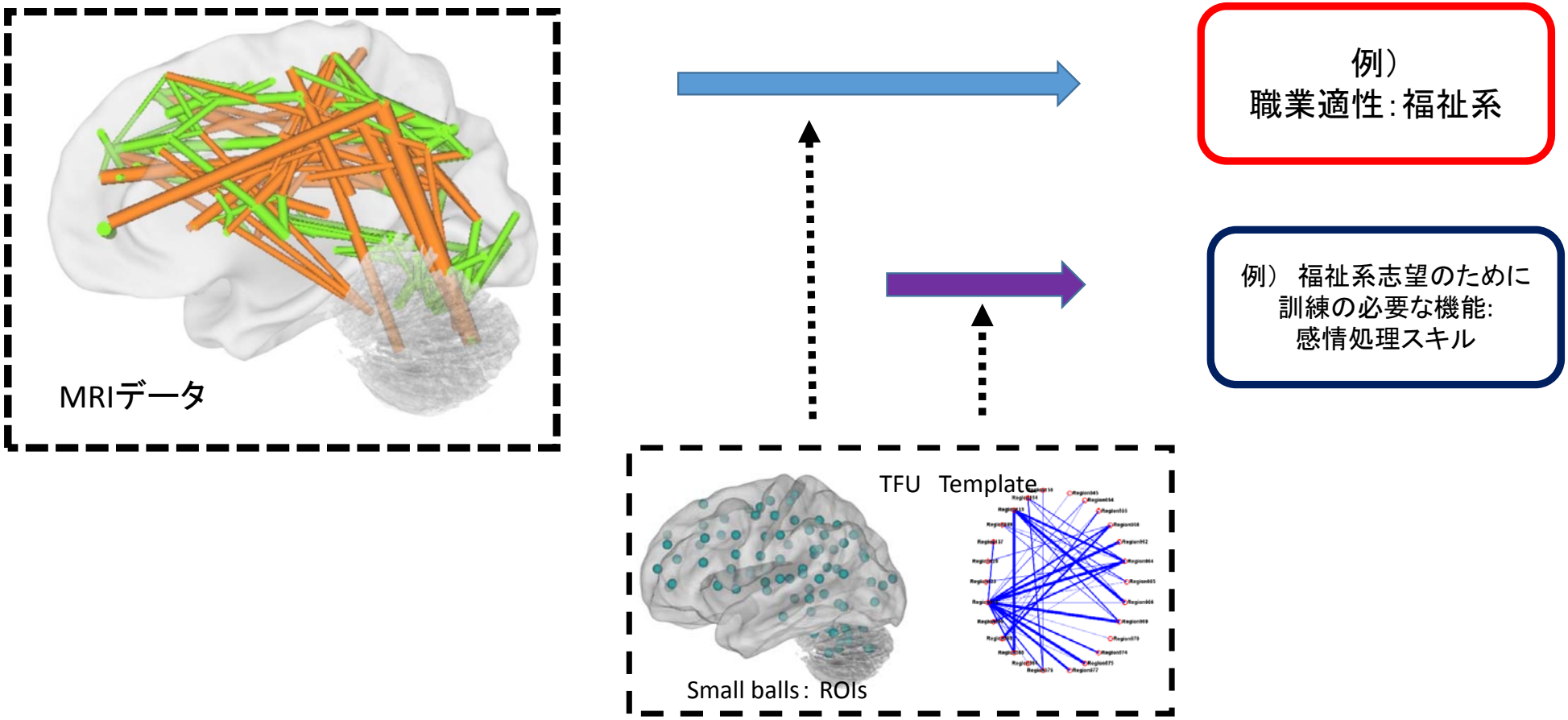


（例）
心理指標
（行動制御）



（C） 職業能力評価・支援への利用

一回のMRI測定から、TFU Templateより、その人の職業適性（例えば、福祉系）を推定することができる。
また、その人の職業適性が他の職種（例えば、技術職）と推定されたにも関わらず、本人が福祉系を志望する場合にトレーニングする必要のある機能（例えば、感情処理スキル）の推定などができる。H28年度からはそのためのデータマイニングとアルゴリズムの開発を行っていく予定である。



８．今後の課題

（１）MRIデータ収集の継続

（２）心理・MRIデータ分析の継続

（３）認知機能実験またはメタ分析により心理指標と関連する脳部位・ネットワークの機能的役割の推定

（４）中・短期的に可塑的変化を示す脳部位・ネットワークの同定

（５）心理指標に関連する脳マップ（template）の完成

（６）パターン認知・ラーニングアルゴリズムの開発

(7) 脳のミクロ的の変化を計測し、可塑的変化のメカニズムを解明

(8) Microscopic structure 測定

脳の可塑的変化がどのようなメカニズムによって起きるかを調べるために、ミクロ的な機能・構造変化が計測できる次のようなMRI測定方法の準備・テストなどをH27年度までに行った。H28年度からそれらを用いて実験を開始する予定である。

1）T1ρ測定用のMRIシーケンスの作成

2）MR Spectroscopy （^{1}H と^{31}P）の　セットアップ

3）定量的T1の測定テスト

4）Functional DTI 予備実験

評　価　票

評価委員氏名　　松岡　和生

1. 研究プロジェクトの意義・新規性

本研究プロジェクトは，教育効果，職業キャリア訓練，パーソナリティ等の要因がいかにして認知・脳機能をダイナミックに変容させるかを，心理・行動データ及びＭＲＩ脳機能データにより計測・評価するものであり，そのために本研究では，年齢や職業経験などの点で異なる集団間を比較する横断的研究と大学在籍期間の数年にわたって追跡する縦断研究が行なわれる。

本研究では人間能力の社会性に焦点が当てられ，その個人差とその可塑性（訓練，変化の可能性）に着眼点がある。そこに脳レベルでのエビデンスを与えるという点で，大きな特徴を有する研究になっている。その意義は大きく，学術的，社会的な貢献度の高い極めて重要な研究である。

具体的には，以下のような点に意義，新規性が認められる。

- 従来，取り扱いが難しいとされている心理・行動課題への応答及びＭＲＩの脳機能測定における個人差を検証しようとしている点
- 個々人の能力・資質の訓練可能性，可塑性に対する着眼：ポジティブ心理学でいうところの人間の「強み(strength)」の育成・成長を見据えている点
- 方法的には，□従来，質問紙尺度研究（自己報告，自己意識レベル）にとどまっている個人の性格や資質を，脳構造や脳機能の個人差から捉え直すことができる。□脳構造解析（VBM 解析による）と脳機能解析（ｆMRI による）の統合アプローチの採用されており，脳構造・機能データを統合的に扱う MRI 測定・分析プロセスを構築されれば，その応用的な価値は高い。□安静状態脳活動の機能的結合（=DMN）の個人差データがベースとなっているが，Resting State fMRI の先端的データ解析を適用した研究として注目できる。
- 実社会に活用可能な社会的コンテクストにおける個人の能力の違い（個人差）を脳ベースで捉えようとしている点，いわゆる「社会脳」研究の進展に寄与できる研究である。
- 近年，国の施策として，国民総幸福量が注目され，幸福度指標に対する社会の関心が高くなっている。人の幸福感あるいはウェルビーイングの研究において，脳機能レベルでのエビデンスを提供できるという点で，大きな貢献が期待される。
- 本研究ＰＪのように同一集団の多数の大学生を対象に、数年間にわたって縦断的に心理・行動的データとＭＲＩ計測に基づく脳構造／機能データを大規模に収集するような研究の実施は容易なことではないことから，その研究成果に対する期待は学術的，社会的にも大きいと考える。

２．研究計画の妥当性、3. 研究方法の妥当性

同一集団を対象とし，縦断的に行動，認知能力，人格特性，社会性等の変化を脳構造／機能レベルと対応させ，さらに，異なる年齢（若年者と高齢者）・属性・能力をもつ集団に対する横断研究を組み入れた手法によって検討する方法は, 画期的な手法であり, 研究目的を達成する上で, 極めて妥当で有望な方法である。

心理指標に関して，本研究で採用されている IQ（知能指数）, EQ（情動知能指数），社会的スキル，EF(実行機能)，職業適性検査，及び主観的幸福感は，心理指標としての妥当性が学人されている標準化された指標であり，認知・社会的能力を査定するうえで適切な選択と思われる。社会性に関わる 19 個の質問紙尺度も本研究の関心領野をカバーしており，考え得る範囲で，本研究で考慮すべき側面を網羅する指標が含まれており, 社会性及び職業適性と脳構造／機能との関連を見ていく上で妥当である。

４．進捗状況

H.27 年度までの研究で，計画通り心理指標データの収集済みであり，今年度研究では，職業適性や社会的能力の予測力のデータも示されている。心理・行動指標間の関係性について共分散構造分析等の統計手法によって確認していく作業は今度の課題である。MRI データに関しては, 脳構造データとしては VBM，脳機能データとしては Resting State fMRI を使った計測が進められている。いずれも大きな成果が期待できる解析手法である。心理指標との関連に関して基礎的な検討が行われ，すでにいくつかの研究成果が得られており，計画にそって研究は順調に進展していると評価できる。心理指標と安静期脳活動のネットワークとの関連については，社会的・情動的心理データ 80 項目中 53 項目のネットワークの同定されている。また，社会性関連心理指標に対応する脳部位及びネットワークについても，たとえば，行動抑制・活性化システム（欲求，報酬），あるいは，自己成長主導（積極的行動，計画性，変化への準備）に関連する脳部位とネットワークの Hub 脳部位が同定されているおり，今後の研究に繋がる成果として評価したい。

長期・中期・短期的な可塑的変化の検証では，□長期的な可塑性変化として，中学・高校からの継続的吹奏楽経験者に対する MRI 解剖・機能画像の測定，□中期的な可塑的変化としては，大学期間中（22 ヶ月間）の学生 1 ケースの解析，□短期的な可塑的変化では，1)認知課題を用いた学習効果の検討と 2)大学生, 4 週間の保育実習前後の赤ちゃんの顔に対する脳活動変化が検討され，いずれも興味深い知見が得られている。

５．今後の展望

本研究プロジェクトは，いうまでもなく，その成果はきわめて直接的な社会貢献に結びつくものと思われる。個々人の知的能力や性格，資質あるいはそれらを変容させうる教育効果，訓練効果に脳構造／機能レベルでエビデンスを与える手法が確立されるならば，心理学，認知科学，脳科学の分野だけでなく，大学教育，職業キャリア教育，科学や芸術における創造的能力の開発，本人に自覚されない隠された能力の発見，スポーツ，芸術，音楽におけるトレーニング効果への応用等，その波及効果は広範囲に及ぶことが予想される。また，人生の各段階での生活の質，ウィールビイングや健康長寿の問題に対しても寄与し得る研究になる。

知性の心理学・認知科学研究への波及効果も考えられる。知能検査に始まる心理学における知性研究は，近年，多重知能理論，社会的知能やサクセスフルインテリジェンス，情動知能，心の理論など，人の知性を捉える枠組みが社会性や情動性にまで広がっている。人間の知的能力の本質的特徴とは何か，社会的・職業的な実践場面において真に必要とされる知的能力とは何か，という問いのもとで展開されてきた諸研究であるが，いずれもその実証的なエビデンスは心理・行動レベルにとどまっている。本研究はこうした人間の知性と感性の理解のための新たな次元の研究へと進む突破口になり得るといっても大げさではないかもしれない。

パーソナリティ等の心理学における査定研究の分野への波及効果も大きいと思われる。心理学における個人の性格や資質の研究は，その多くが心理検査や質問紙調査によって行われている。特に，社会的な心理・行動特性に関する研究は，質問紙尺度研究が一般的である。本研究において，脳構造／機能の量的データベースによって，生物学的なエビデンスを容易に提供できることになれば，従来の研究スタイルに大きな変化をもたらす可能性がある。

6．総評

学術的，社会的な貢献度の高い極めて重要な研究プロジェクトである。研究目的を達成するための研究計画，方法は妥当で，現時点で，研究，データ収集はほぼ計画通りに進行している。一部，すでに先行して進められている部分もあり，研究は順調に進んでいる。研究成果は，社会的にもインパクトが大きいものになると予想されるので，今後の研究成果を期待したい。

評　価　票

評価委員氏名　出江　紳一

1. 研究プロジェクトの意義・新規性

社会的・職業的能力を脳科学により推定することをそれらの育成プログラムに役立てるというビジョンは重要であり、かつ新規性がある。

2. 研究計画の妥当性

心理指標、脳機能画像の予備実験、データ収集、中間評価、ブラッシュアップという流れ、ならびに項目ごとの研究計画は妥当であると考える。

3. 研究方法の妥当性

方法として、心理行動特性のパターンと脳機能画像のパターン（脳ネットワーク）を対応させ、それらの可塑的変化を捉える構成となっており、妥当であると考える。なお、可塑的変化を誘導する介入の個々のセッションにおける短期効果と、セッションの繰り返しによる長期効果の関係を明らかにする方法を加えることにより、より質の高い研究になると思われる。

4. 進捗状況

心理学的研究、MRI 研究のそれぞれですでに１００名以上のデータが取得・解析されており、順調な進捗状況であると考える。

5. 今後の展望

今後の縦断的研究の成果に期待する。

6. 総評

意義、新規性の高い研究である。研究計画ならびに方法は妥当であり、予定に合致した成果が上がっている。

評　価　票

評価委員氏名　　福永 雅喜

1. 研究プロジェクトの意義・新規性

専門的な知識や技能を習得し各分野で活躍が期待される人材の育成は、大学等の高等教育課程に期待される大きな役割である。しかし、その一方、養成課程の検証に応用しうる認知・脳科学的根拠を備えた指標は、これまで十分に検討されていなかった。このような背景のなか、本研究課題は、人材育成の現場において欠くことの出来ない社会的能力・職業能力の獲得、向上をサポートする養成プログラムを前提に、個人が備え持つ認知･心理的素因（パーソナリティ）の寄与、教育･訓練を通じた学習効果による認知機能の変容を、種々のバッテリーによる心理・行動指標とニューロイメージング手法を用いたその神経基盤探索にてアプローチを試みる。本研究の発展は、養成プログラムに対する脳科学的根拠に基づく評価系の創出と、プログラムへの最適化に供与しうる情報提供につながるものであり、従来の研究に類を見ないものであるとともに、本システムを応用することで、ニューロイメージング測定から個々人の社会的・職業的能力の推定を行おうとする挑戦的プロジェクトでもある。本プロジェクトは、ニューロイメージング計測により裏付けされた認知･脳科学的エビデンスのもと、社会的・職業能力育成プログラムの効果・価値を高める基盤構築を掲げており、その意義は明確である。

2. 研究計画の妥当性

種々のバッテリーによる心理、行動指標にニューロイメージング手法を応用し認知・脳科学的根拠にもとづいてその神経基盤を同定することは、それらの画像指標をもとにヒトの社会性・職業的能力を定量的に評価する上で必要不可欠なステップである。また、社会能力・職業能力的観点から、これらの心理・行動・画像指標により得られる情報が、教育を受けることで如何に変容するかを明らかにするためには、短期・中期・長期的な効果への言及が望まれるが、本研究では、それぞれの段階に対応する縦断的研究および横断的研究が計画されている。個別の認知機能に限定せず、大局的な認知・行動・心理特性の変容を含めた追跡研究として本学の学部学生を対象とする本研究は、被験者が受ける教育課程や職種における統制の観点からも適切であると思われる。５年間の研究計画の前半より計測を開始し、３年目の中間的なデータマイニングから、計測、解析系のリファインを行い、プロジェクト後半の継続したデータ収集と分析法･定量指標の確立へ展開する本研究計画は妥当なものであると思われる。

なお、種々の心理･行動指標、教育･技能習得、ニューロイメージングの３つのグループの強固な連携のもと、各段階における縦断的および横断的研究が計画され実施されていることがうかがい知れた。

3. 研究方法の妥当性

認知・行動・心理特性を構成する機能要素の集合が、社会的能力・職業的能力を表現するとのコンセプトを考えると、現在のところ、これらの能力を包括的に捉えうる単独の質問紙、心理指標は存在

しない。従って、既存の手法の相互関係解析をもとに評価要素を再カテゴライズし、これらのカテゴリーに対応する課題実験から客観的に社会的能力・職業的能力を推定できるか検証すること、またこれらの機能要素が教育効果を経て変容する過程の追跡を実施するために、これまで広く普及し応用が進められている心理・行動指標を網羅的に収集する研究スタイルはきわめて妥当である。

一方、ニューロイメージングによる神経基盤探索のために応用される Voxel based Morphometry (VBM)、Resting state fMRI (rsfMRI)、Diffusion tensor imaging (DTI)は、ヒト脳を対象とした構造的、機能的情報抽出の手法として広く応用が進められている。単に、ある特定の脳領域に局在する脳活動のみにフォーカスせず、脳全体を対象としたネットワーク構造として脳機能を捉えようとする本研究は、社会的能力・職業的能力という大局的な認知・行動・心理特性を捉えるためには適切なアプローチである。

なお、事前評価用資料および委員会にて、おおむね研究方法は妥当であるとの認識を得た。本研究プロジェクトでは、学習による知識や技能の習得を、認知･心理的素因の可塑的変化とし、これが社会的･職業的能力向上の本質と捉えている。個人が備え持つ各職種への適性が、能力向上のパフォーマンスに関与することは容易に予想されるため、本プロジェクトで収集された種々の指標と職業適性に関する検討をさらに推進させることが重要であると思われた。また、ニューロイメージンググループは、高度な脳計測技術を有しており、本研究プロジェクトで検出される脳の可塑的な構造的・機能的変化が、どのような脳微細構造（microstructure）に由来するかを探求する生物物理化学的メカニズムに対するアプローチも合わせて推進されることを期待したい。

4. 進捗状況

平成 26 年度から 5 年間の事業期間に対し、約 2 年が経過した現時点において、初年度に計画されたデータ収集に使用される心理指標の選定、MRI 装置のアップグレードおよびニューロイメージング計測手法の選定と最適化、予備実験が終了し、今年度からは縦断的研究に供される大学低年次学生を対象とした計測が開始されている。心理指標では計測項目に対する被験者数に差異があるものの総数 200 名を越えるサンプル収集が、同様にニューロイメージング計測もすでに 200 名近いサンプルの収集が完了しており、当初の年次計画に沿いプロジェクトが進んでいるものと思われる。

また、収集された多彩な心理指標から、指標間の関連分析も進められており、平成 28 年度以降に計画されているデータマイニングにおいて必要と予想される、膨大なデータからの効率的な情報圧縮（情報の dimensional reduction）の初期検討も開始されている。とくに社会性に関する指標では、再カテゴライズされた認知･心理指標と脳イメージングから収集された灰白質容積から、それらに相関がある脳領域が一部同定され、TFU Template として rsfMRI での機能的な脳ネットワーク検出に応用されていることは、心理指標計測および脳イメージング計測グループが十分な連携をもって研究が推進されていることを示すものと思われる。一方、社会的能力・職業的能力を端的に検出するためには、特定の事象を対象にその前後比較を想定した横断的研究が必要となるが、中期的事象として吹奏楽経験者、短期的事象として実習経験者の脳変化を捉えることに成功しており、今後の研究への基盤整備が進んでいるものと思われる。以上より、現段階での達成状況は良好であると考えられる。

5. 今後の展望

すでに本研究で収集された行動・認知・心理指標およびニューロイメージングデータの解析が進め

られ、両者を統合する形で結果が報告されていることは、これまで 2 年間の研究が順調に遂行されていることを示している。今回の研究プロジェクトでも重要な部分を占める縦断的研究に関しては、サンプル収集が肝要であるため、今後も一貫したデータ収集を継続して行っていただきたいし、本研究プロジェクトで蓄積されるデータは、多彩な指標を備える画像データとして、非常に価値の高いものになると思われる。研究プロジェクト後半は、システマティックに収集された膨大な情報から、社会的能力・職業的能力推定に有用な要素を如何に抽出するかがキーとなるため、データ解析へのさらなる注力を期待したい。

なお、委員会での質疑にて、本研究プロジェクトが教育･養成分野に大きな波及効果を生み出す可能性を再認識した。継続したデータ収集と、膨大な情報から、社会的能力・職業的能力推定に有用な要素を的確に抽出するデータマイニングを強力に推進していただきたい。

本研究プロジェクトの遂行には、横断的研究、縦断的研究とも継続したデータ収集が必須である。また、心理･行動指標は網羅的な採取が必要で有り、ニューロイメージング計測においても、新たな脳計測パラメータの収集に計測手法の追加が予想されること、種々の熟練度を有する被験者を対象にした横断的研究には、縦断的研究で収集する安静時データに加え、課題実験も計画されていることから、データ収集に必要なマンパワーが不足することが想定される。継続したデータ収集に加え、逐次的なデータ評価が、長期的な研究には重要であるので、それぞれのプロジェクトの担当者が、データ解析にも十分な時間が割けるようなサポート体制が整備されることを望みたい。

6. 総評

本研究プロジェクトは、人材の育成という高等教育課程に期待される役割を、認知･脳科学的エビデンスに裏付けられた客観的な情報から評価し、その教育･育成の効果・価値を高めるための基盤構築を掲げており、その成果は、高い社会的還元性を持つものである。現在までの研究計画、実施状況をみると、当初の予定どおり成果が得られているものと思われる。

なお、事前資料においても、本プロジェクトの意義とその成果が教育分野に及ぼす効果は大きいとの印象であったが、実際に研究の当事者らと議論を交わすことで、良好な実施状況を確認できた。今後の研究の発展を期待したい。

平成 26 年度採択私立大学戦略的研究基盤形成支援事業
第 2 回 外部評価委員会

1. 第 2 回外部評価について

(1)外部評価委員

下記のとおり、平成 27 年度に実施した第 1 回外部評価委員会の際と同じ委員に評価を頂くこととした。

○ 出江 紳一（東北大学大学院 医学系研究科　教授）

○ 松岡 和生（岩手大学 人文社会科学部　教授）

○ 福永 雅喜（自然科学研究機構 生理学研究所　准教授）

(2) 審査方法

【書面審査】

平成 31 年 3 月 19 日　評価資料を外部評価委員に送付

令和元年 5 月 20 日までに、別添のとおり、外部評価委員 3 名から書面による評価がなされ、これを第 2 回外部評価結果とした。

※評価資料送付の際、各委員宛て実地審査の必要性の有無についてあわせて確認したところ、全員から評価資料のみ審査は十分であり、実地審査の必要はないと回答があったため、第 2 回外部評価は書面審査とした。

2. 審査結果

別添、評価票のとおり

私立大学戦略的研究基盤形成支援事業（H26-H30）

社会的・職業的能力育成プログラムに資する認知・脳科学的エビデンス情報提供基盤の構築

研究代表者: 小川 誠二

外部評価資料

目 次

第一部

本研究事業の概要と一次外部評価までの要約

Ⅰ．背景

Ⅱ．目的

Ⅰ．研究計画

Ⅱ．研究成果(1)

Ⅲ．まとめ

第二部

一次外部評価後から現在

Ⅰ．研究成果(2)

Ⅱ．まとめ

Ⅲ．今後の課題

第一部　本研究事業の概要と一次外部評価までの要約

I. 背 景

本研究は、

学習・訓練などによる知識・技能などの獲得は脳の神経回路機能における何らかの可塑的変化を意味する

という作業仮説をヒトで検証するものである。

近年のNeuroimaging technologyの発展と
前回の戦略プロジェクト(H20-H24)で得られた結果をもとに
（聴覚野と視覚野での信号処理系の可塑性と音楽などの学習による脳活動・組織の変化）

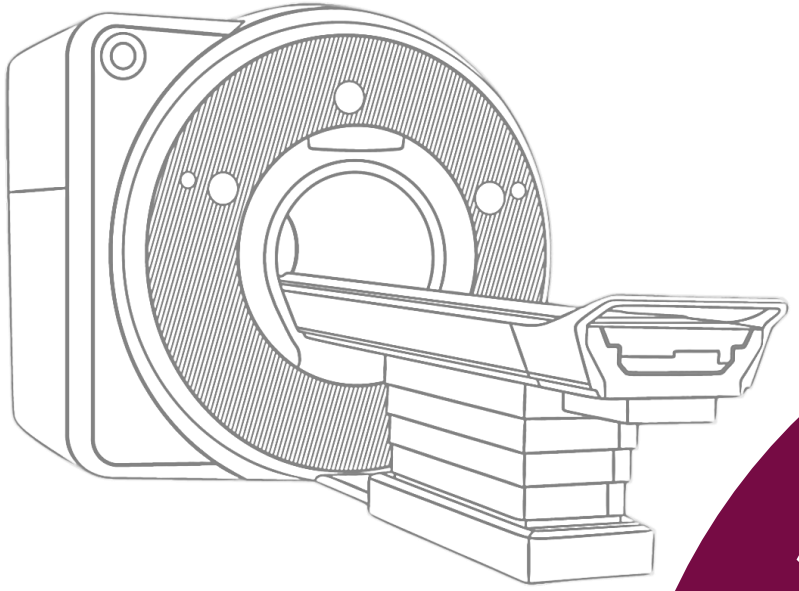
大学教育期間中の学習・訓練などによる脳の機能的・構造的変化を経時的に計測する

計画を立てた。

Ⅱ. 目 的

社会的・職業能力育成プログラムに資する
認知・脳科学的エビデンス情報の収集

それらの応用法を提供する基盤の構築



MRI測定による
個々人の社会的・職業的能力の推定
を目指す



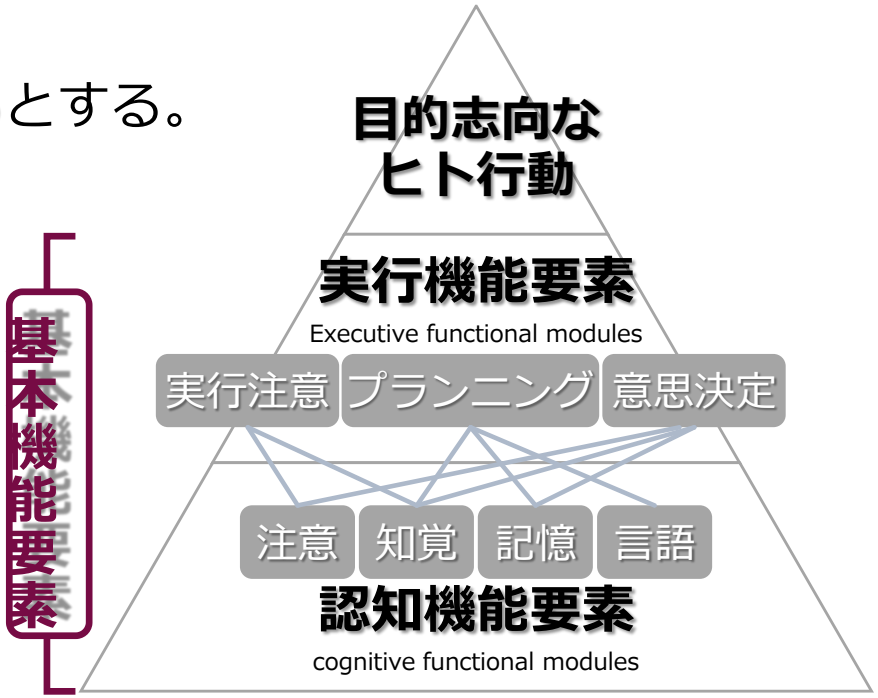
Ⅲ. 研 究 計 画

ヒトの心理・活動などを総称するものをヒト行動と呼ぶことにする。

ヒト行動が脳内で顕現 (representation)するために
基本的な心理及び脳機能要素の集合体(set of basis)が存在すると考える。

この基本要素の組み合わせによって
社会性(社会的能力)・職業適性(職業的能力)が表現できるとする。

目的志向的なヒト行動は、注意・知覚・記憶・言語などの
必須となる**認知機能要素 (cognitive functional modules)** と
これらの認知機能要素のバリエーションと組み合わせによる
実行注意・プランニング・意思決定などの中核となる
実行機能要素(Executive functional modules)により支えられる。
このような認知機能要素と実行機能要素が
基本機能要素により説明でき得る。



Ⅲ. 研 究 計 画

社会的能力・職業的能力の測定に向けて

A **互いに独立な基本機能要素の同定から社会・職業的機能の同定 (bottom-up approach)**

(1)互いに独立な認知機能要素の同定
(2)基本認知機能要素のsub-setからなる中核となる実行機能要素の同定
(3)社会・職業的機能の同定

B **社会・職業特性から行動基本要素の推定 (top-down approach)**

C **各レベルの機能(要素)に対する short/mid/long-term plasticityの測定**

※A, Bは主として横断的研究、C は縦断的研究となる。

Ⅲ. 研 究 計 画

1 心理学的研究

質問紙・心理検査などの下位項目および心理実験データは
各種**基本機能要素(注意・記憶・感情・言語・知識など)を反映する**ものと仮定し、以下のことを行う。

A | 各種心理指標の測定とその下位項目の定義から
基本機能(要素)を推定、**クラスタリングなどによりグループ化**

B | 社会・職業的能力に関連する機能を**課題ベースの実験により推定**

C | 下位項目または上位項目に関連する心理・行動課題への
訓練によるshort/mid/long-term plasticityの測定

Ⅲ. 研 究 計 画

② MRI study

各種心理指標(認知・行動・思考・感情・知識・知能など)を測定する
質問紙・心理テストなどの下位項目が脳に反映されると仮定し
解剖・機能画像の収集と以下のことを行う。

A
心理指標の各下位項目に関連する**脳の部位を同定**
各部位の**機能的特性の同定**
各下位項目に対する**機能的ネットワークの同定**

B
課題ベースの実験により社会的・職業的特性に関連する
脳の機能部位とネットワークの推定

C
下位項目または上位項目に関連する心理・行動課題への
訓練により変化する脳の部位またはネットワークの推定による
脳のmid/short-term plasticityの測定

Ⅲ. 研 究 計 画

③ 社会性・職業特性推定プログラムの開発

心理・MRIデータからなるデータベースをもとに
パターン認知・マシンラーニングなどによる**個々人の社会性・職業特性**
または大学在籍期間中教育・訓練によって発達した機能の推定を行う。



Ⅲ. 研 究 計 画

H26 年度
- 大学生を対象とした縦断研究を行うための認知課題・MRI測定方法・データ分析法の選定・予備実験
- 若年者・高齢者を対象とした横断研究への着手
- 認知・脳機能測定パラダイムの向上と創出

心理指標・MRI測定法などの選定 予備実験

H27 年度
- 社会的・職業能力推定のための認知・脳機能の長期変動を捉える縦断データ収集への着手
- 職業経験により発達する社会的・職業能力同定の横断研究への着手
- MRI測定・データ処理法の改良・開発

心理指標データ・MRIデータ収集

H28 年度
- 中間的データマイニング
  ：教育・訓練課程、加齢・職業と相関する可塑性の検出・評価
- 認知・脳機能モデルの推定
- 測定方法・データ分析法の評価

中間的データマイニング・MRIデータ収集継続

H29 年度
- 認知・脳計測による定量的指標の作成
- 新たなデータ分析法の確立
- 測定・分析過程のルーチン化

心理指標・MRIデータの定量的指標作成・分析方法の確立

H30 年度
- 研究全体のまとめ
- 教育・職業による認知・脳機能変化に関する情報基盤(データベース)の策定

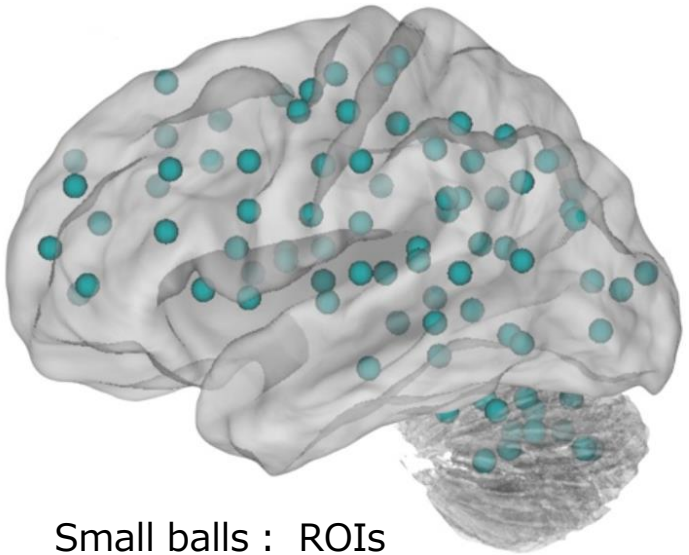
情報基盤の策定

Ⅳ. 研 究 成 果 (1)

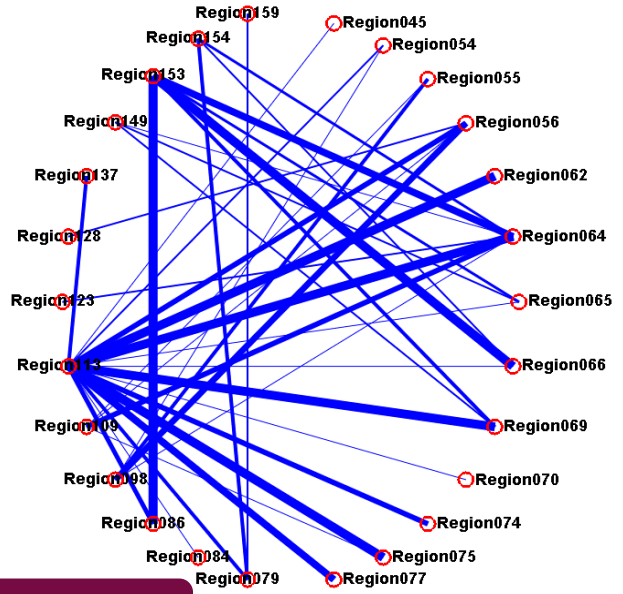
TFU template:
本事業により収集したデータをもとに独自に作成したtemplate(一部の心理指標：社会性)

Templateは機能的役割が同定された脳部位・ネットワークからなるものであり
ヒトの行動を表す心理指標が脳へ投射されたものである。
これは、**プロジェクト遂行におけるデータ基盤**となる。

H27年度までの研究では、**templateの作成のための心理・MRIデータの収集と分析ができた。**



Small balls： ROIs



TFU Template

V. ま と め

1. H26年度での研究として、MRIアップグレード、MRI測定方法とパラメータの設定、予備実験、心理指標のための質問紙の準備などを計画通りに終えて、**H27年度から本実験**を始めた。

2. 教育・訓練による脳の可塑的変化を検出する上で必要な心理・脳データ基盤を作るための**心理データとMRIデータを収集**した。

3. MRI解剖画像により、心理指標に関連する脳部位を同定し、心理指標を表現する**脳部位のセット(ROIs)を作成**した。

4. MRI機能画像により、**心理指標に関連するネットワークを同定**した。一部の心理指標(社会性)については**脳のtemplate（ROIs とネットワーク）**が作成できた。

V. ま と め

5 脳の**長期的な可塑的変化への実証データを得た**。また、中・短期的な可塑的変化に対する実証データを得るための**予備実験**を行った。
また、**パターン認知のアルゴリズムの開発とテスト**を行った。

6 H26-27年度の研究において、機能的データ基盤のために必要なデータが計画通り収集できたこと、また、データ分析により、脳部位・ネットワークのtemplateのような基盤ができたことから、計画通りに研究が進んだことになる。
また、一部の心理データとMRIデータ分析においてはH28年度から計画している**データマイニングに入った**ことになる。

V. まとめ

H26 年度
・大学生を対象とした縦断研究を行うための認知課題・MRI測定
データ分析法の選定・予備実験
・若年者・高齢者を対象とした横断研究への着手
・認知・脳機能測定パラダイムの向上と創出

完　了

心理指標・
測定法などの選定
予備実験

**心理・脳MRI
データベース
の作成**

H27 年度
・社会的・職業能力推定のための認知・脳機能の長
縦断データ収集への着手
・職業経験により発達する社会的職業能力測定の横断
・MRI測定・データ処理法の改良・開発

完　了

心理指標データ・
MRIデータ収集

一次外部評価時

H28 年度
・中間的データマイニング
：教育・訓練課程、加齢・職業と相関する可塑性の検出・評価
・認知・脳機能モデルの推定
・測定方法・データ分析法の評価

中間的データマイニング・
MRIデータ収集継続

H29 年度
・認知・脳計測による定量的指標の作成
・新たなデータ分析法の確立
・測定・分析過程のルーチン化

心理指標・MRIデータの
定量的指標作成・
分析方法の確立

H30 年度
・研究全体のまとめ
・教育・職業による認知・脳機能変化に関する情報基盤(データベース)の策定

情報基盤の策定

第二部　一次外部評価後から現在

Ⅰ. 研 究 成 果 (2)

社会的能力・職業的能力の測定に向けて（H28－現在）

Ⅰ

1．心理指標と関連する脳部位・ ネットワークの機能的役割の推定
2．心理指標に関連する脳マップ（template）の完成
3．パターン認知・ラーニングアルゴリズムの開発

Ⅱ

1．参加者の固有の認知・脳機能の可塑的変化の推定

Ⅲ

1．職業適性関連脳ネットワークの同定
2．職業推定器の開発

Ⅳ

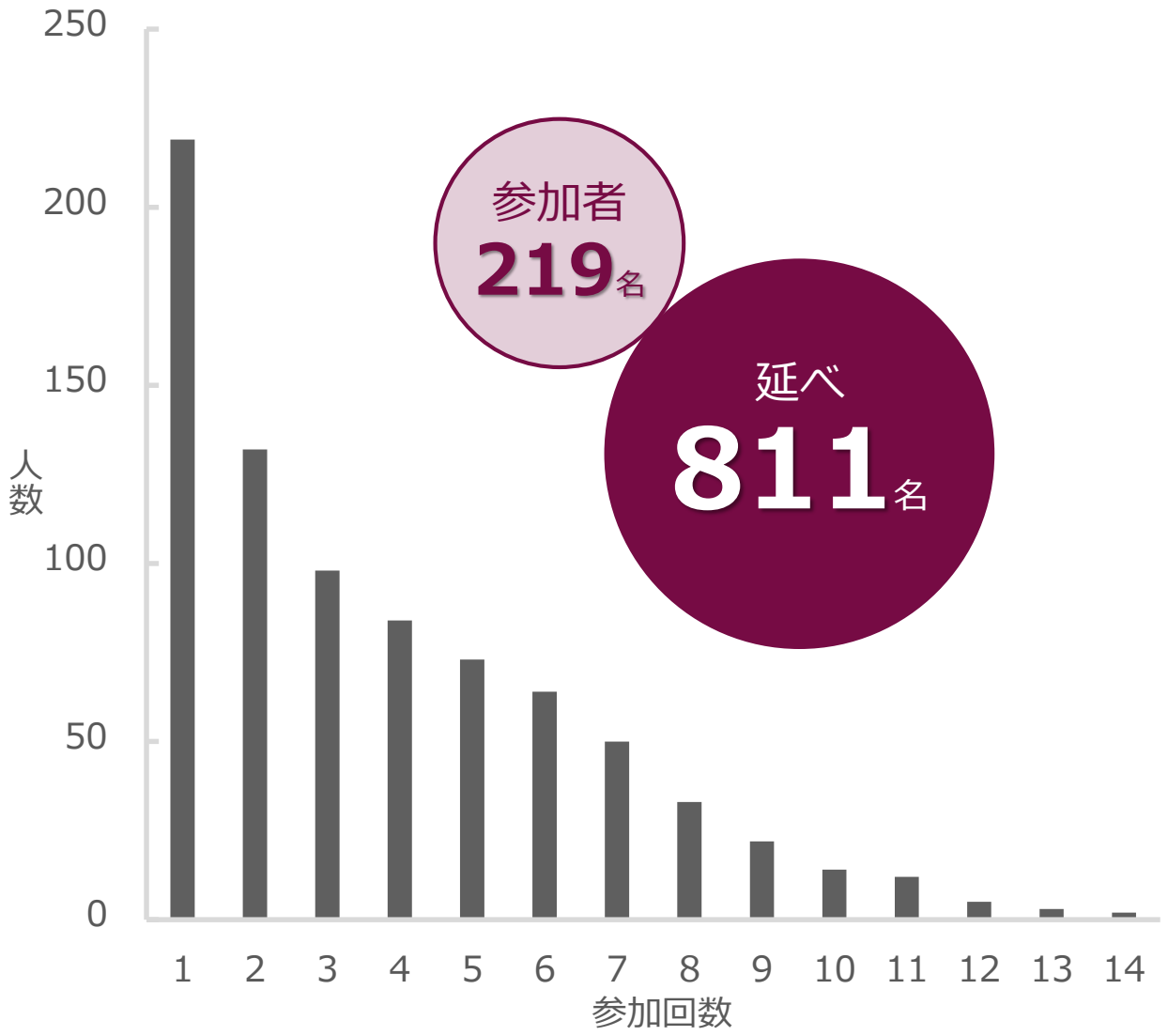
1．推定器の性能改善

Ⅰ. 研 究 成 果 (2)

MRI縦断計測参加者延数（～2019.2.現在）

MRI
縦断測定
参加延数

1回	**219**名	8回	**33**名
2回	**132**名	9回	**22**名
3回	**98**名	10回	**14**名
4回	**84**名	11回	**12**名
5回	**73**名	12回	**5**名
6回	**64**名	13回	**3**名
7回	**50**名	14回	**2**名



参加者
219名

延べ
811名

Ⅰ. 研究成果(2)

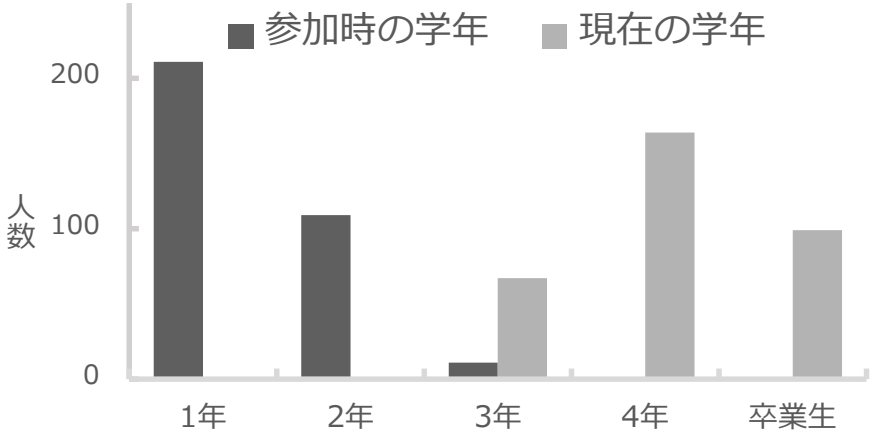
心理検査研究協力者数（～2019.2.現在）

平均年齢
18.9歳
(SD ±0.93)

性別
男性
114名
女性
217名

参加時の学年
1年**221**名
2年**109**名
3年**11**名

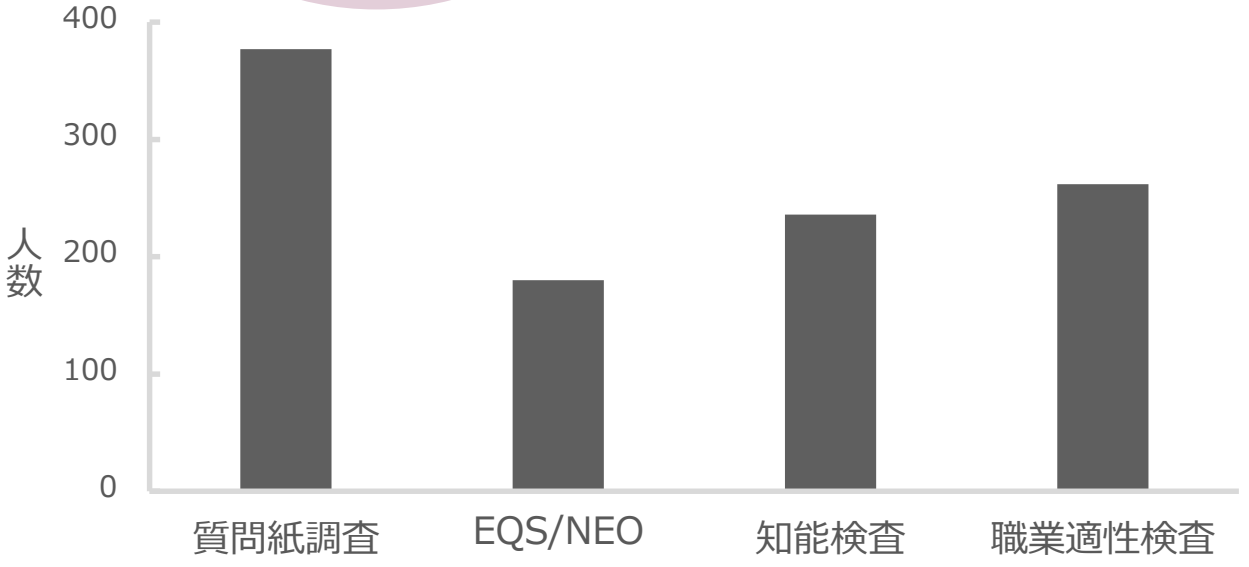
現在の学年
2年**1**名
3年**67**名
4年**164**名
卒業生**99**名



心理検査別参加数
質問紙調査 **327**名
(うち縦断**54**名)
EQS/NEO **180**名
(うち縦断**37**名)
知能検査 **236**名
職業適性検査 **262**名
(うち縦断**44**名)

参加者
331名

延べ
1005名



Ⅰ. 研 究 成 果 (2)

実施した心理検査

1 自己有能感
2 エフォートフル・コントロール
3 自我同一性
4 BIS/BAS
5 自尊感情
6 シャイネス
7 社会的スキル
8 自意識
9 自己概念の明確性
10 Thinking About Life Experiences
11 エゴ・レジリエンス
12 社会的問題解決
13 Brief Core Schema
14 自己成長主導性
15 主観的幸福感
16 人生に対する満足感
17 状態・特性不安
18 統合失調型パーソナリティ
19 自閉スペクトラム傾向
20 健康習慣
21 抑うつ
22 メタ認知
23 情動知能（EQS）
24 パーソナリティ5因子(NEO-PI-R)

質問紙調査



職業適性検査



厚生労働省編一般職業適性検査（GATB）

多種多様な職業分野において仕事を遂行するうえで必要とされる代表的な9つの能力(適性能)を測定することで、能力面からみた職業についての情報を提供することを目的としている

行動実験



1 Judgment of Learning
2 Source monitoring
3 実行機能関連課題
4 意思決定関連課題
5 VAST etc…

知能検査



WAIS-Ⅲ

Ⅰ. 研 究 成 果 (2)

Ⅰ　1．心理指標と関連する脳部位・ ネットワークの機能的役割の推定

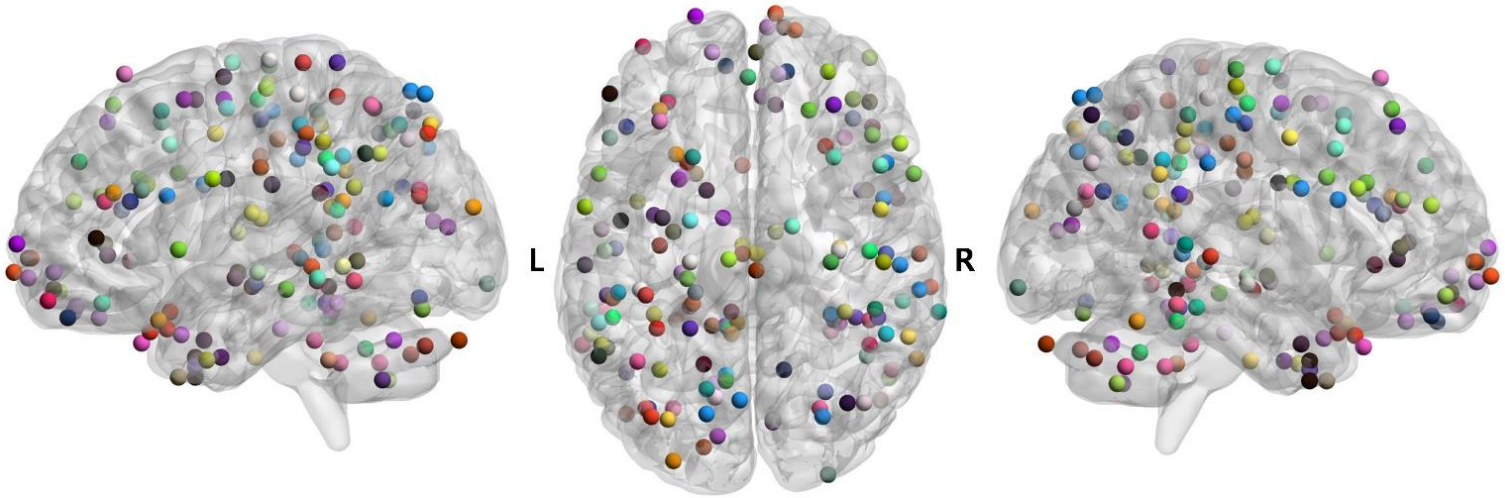
前回の外部評価後タスクfMRI、メタ分析などにより脳部位の同定を進めてきたが、タスク作製における限界と社会性に関わる機能部位のデータベースの不足などから**VBMによる脳部位の同定**を行うことにした。

1) Social Quotient(SQ), Intelligence Quotient (IQ), Emotion Quotient(EQ)についての心理指標と相関のある脳部位の同定をVBMで行った。

2) 130個の心理指標の中96個の指標に対する脳部位が同定され、そのなかで重複するものを除いて163個の脳部位が最終的なTFU脳部位のセットとしてまとまった(p<0.05, FWE corrected)。

Ⅰ. 研 究 成 果 (2)

心理指標と関連する脳部位の同定



同定脳部位：163ROIs(SQ, IQ, EQ)

Ⅰ. 研 究 成 果 (2)

心理指標と関連する脳部位の同定

#	Region	MNI Coordinates			Psychometric Parameters
		x	y	z	
1	MFG_R	31	18	48	Cognitive competence
2	SFG_R	16	-7	69	Cognitive competence
3	MFG_ope_R	48	15	40	Cognitive competence
4	MFG_ope_L	-29	39	-16	Cognitive competence
5	MTG_L	-57	-37	-7	Cognitive competence
6	IPG_L	-49	-40	35	Social competence with friends of the same sex
7	PoCG_R	44	-16	56	Social competence with friends of the same sex
8	FG_R	44	-41	-21	Social competence with friends of the same sex
9	FG_L	-36	-74	-18	Social competence with friends of opposite sex
10	IPG_R	50	-46	36	General self-worth
11	PoCG_R	50	-17	49	Perceived Competence Scale for Adolescence
12	IFG_orb_L	-38	58	-15	Inhibitory Control
13	MFG_L	-29	38	20	Inhibitory Control
14	MTG_R	44	-50	11	Inhibitory Control
15	MTG_L	-52	-37	-8	Inhibitory Control
16	MFG_L	-32	35	23	Activation Control
17	MOG_L	-27	-92	18	Activation Control
18	IFG_orb_L	-26	19	-22	Activation Control
19	AG_L	-32	-59	37	Attentional Control
20	SPG_L	-15	-66	47	Japanese version of Effortful Control (EC) scale for adults
21	MTG_R	69	-38	6	Japanese version of Effortful Control (EC) scale for adults
22	SPG_L	-15	-75	58	Trust vs. Mistrust
23	SPG_L	-3	-70	59	Trust vs. Mistrust
24	SMG_R	62	-30	35	Trust vs. Mistrust
25	FG_R	33	-42	-19	Intimacy vs. Isolation
26	Calc_L	-11	-83	11	Intimacy vs. Isolation
27	Calc_R	9	-78	13	Intimacy vs. Isolation
28	MFG_L	-25	10	56	Intimacy vs. Isolation
29	Hipp_L	-20	-35	-3	Japanese version of Rasmussen's Ego Identity Scale (REIS)
30	IFG_orb_R	10	70	-5	Japanese version of Rasmussen's Ego Identity Scale (REIS)
31	PrCG_R	48	-1	44	Behavioral Inhibition System (BIS)
32	SPG_L	-8	-63	45	BAS / Driver
33	PrCG_R	30	-20	68	BAS / Driver
34	Cu_L	-8	-61	21	BAS / Reward
35	TP_Inf_R	41	6	-38	BAS / Fun Seeking
36	SPG_L	-21	-44	69	BAS / Fun Seeking
37	IPG_L	-51	-32	39	BAS / Fun Seeking
38	FG_R	39	-40	-16	BAS / Fun Seeking
39	SFG_orb_R	13	65	0	Rosenberg Self Esteem Scale (RSES)
40	Hipp_R	-19	-31	0	Difficulty in expressing opinions
41	Cu_R	9	-77	19	Japanese version of Jones and Russell's Social Reticence Scale for college students
42	PoCG_L	-37	-32	69	Beginning social skills
43	MOG_L	-37	-73	22	Beginning social skills
44	SFG_L	-21	-5	53	Advanced social skills
45	SMG_L	-54	-42	32	Advanced social skills
46	SFG_orb_R	17	64	0	Skills for dealing with feelings
47	IPG_L	-49	-33	44	Skills for dealing with feelings
48	PoCG_L	-32	31	71	Skill alternatives to aggression
49	PoCG_L	-47	-31	47	Skills for dealing with stress
50	PoCG_L	-39	-30	58	Planning skills
51	PrCG_L	-21	-20	70	Planning skills
52	Hipp_R	33	-16	-8	Planning skills
53	SMA_L	-7	-19	60	Kikuchi's Scale of Social Skills (KiSS-18)
54	IPG_R	46	-37	52	Public self-consciousness
55	SFG_L	-15	6	56	Private self-consciousness
56	TP_Mid_R	54	3	-29	Private self-consciousness
57	ACC_R	10	37	1	Private self-consciousness
58	MFG_R	31	37	48	Japanese Version of the Self-Concept Clarity (SCC) Scale
59	FG_R	44	-41	-15	Self-Continuity Function Subscale
60	MTG_R	-60	-50	-8	Self-Continuity Function Subscale

Ⅰ. 研 究 成 果 (2)

心理指標と関連する脳部位の同定

#	Region	MNI Coordinates x	y	z	Psychometric Parameters
61	SPG_L	-12	-69	42	Directing-Behavior Function Subscale
62	MOG_R	42	-71	35	Directing-Behavior Function Subscale
63	SOG_L	-54	-54	37	Japanese version of the TALE(Thinking About Life Experiences) Scale
64	FG_R	33	-15	-35	Decision Making (DM)
65	SPG_L	-29	-77	47	Decision Making (DM)
66	SMG_R	58	-47	31	Decision Making (DM)
67	MTG_R	66	-29	2	Impulsivity／Carelessness Style (ICS)
68	IFG_orb_R	28	22	-26	Impulsivity／Carelessness Style (ICS)
69	RectusG_L	-2	15	-19	Impulsivity／Carelessness Style (ICS)
70	IPG_L	-35	-76	44	Impulsivity／Carelessness Style (ICS)
71	IFG_orb_L	-22	16	-25	Impulsivity／Carelessness Style (ICS)
72	IFG_orb_L	-54	12	3	Avoidance Style (AS)
73	IFG_orb_L	-24	11	-27	Japanese version of the Social Problem-Solving Inventory-Revised (SPSI-R)
74	SOG_R	28	-67	25	Positive-Self (PS)
75	MFG_L	-44	29	20	Positive-Self (PS)
76	FG_L	-36	-73	-14	Positive-Self (PS)
77	Cerebellum_L	-44	-60	-43	Negative-Other (NO)
78	PCC_L	-6	-46	20	Positive-Other (PO)
79	ITG_R	61	-55	-21	Positive-Other (PO)
80	MFG_R	7	65	-7	Japanese version of the Brief Core Schema Scale (JBCSS)
81	Cerebellum_L	-21	-36	-29	Planfulness
82	Cerebellum_R	52	-59	-37	Planfulness
83	Cerebellum_R	30	-45	-37	Planfulness
84	SOG_R	26	-73	25	Planfulness
85	SOG_L	-27	-73	24	Planfulness
86	IPG_L	-40	-56	54	Planfulness
87	MFG_orb_R	44	54	-12	Readiness for change
88	MFG_R	38	39	22	Readiness for change
89	Cerebellum_R	51	-62	-43	Readiness for change
90	SFG_L	-20	18	52	Using resource
91	Cerebellum_L	-26	-41	-36	Japanese version of the Personal Growth Initiative Scale-II (PGIS-II)
92	Th_L	-2	-14	16	Subjective Happiness Scale (SHS)
93	Th_R	3	-17	14	Subjective Happiness Scale (SHS)
94	Cerebellum_R	48	-70	-34	The Satisfaction with Life Scale (SWLS)
95	Cerebellum_L	-44	-75	-31	The Satisfaction with Life Scale (SWLS)
96	Hipp_L	-32	-14	-10	The Satisfaction with Life Scale (SWLS)
97	IPG_L	-34	-39	41	State Anxiety (A-State)
98	IPG_R	35	-38	47	State Anxiety (A-State)
99	TP_Inf_L	-40	2	-36	Trait Anxiety (A-Trait)
100	Putamen_L	-27	-9	-5	Disorganization
101	MTG_L	-51	-51	-1	Disorganization
102	IFG_Med_R	3	56	-11	Disorganization
103	IFG_Tri_R	44	38	5	Disorganization
104	TP_Mid_L	-19	12	-42	Social skill
105	FG_R	31	-41	-10	Attention switching
106	IFG_Tri_L	-50	41	7	Attention switching
107	TP_Inf_R	43	6	-35	Attention switching
108	TP_Inf_R	52	6	-42	Attention switching
109	SFG_L	-19	69	5	Attention to detail
110	SFG_L	-9	-4	56	Attention to detail
111	Cerebellum_L	-12	-64	-29	Attention to detail
112	IFG_Tri_R	50	16	22	Communication
113	PrCG_R	49	3	26	Communication
114	Cerebellum_R	43	-54	-32	Imagination
115	SFG_Med	0	47	34	Imagination
116	PCC_L	-7	-44	17	Verbal IQ
117	PreCu_R	13	-59	44	Performance IQ
118	SFG_Med_R	11	48	-17	Full scale IQ
119	IFG_Med_R	5	40	-21	Full scale IQ
120	SFG_Med_L	-13	56	-5	Full scale IQ

心理指標と関連する脳部位の同定

#	Region	MNI Coordinates x	y	z	Psychometric Parameters
121	PHG_L	-24	-24	-25	Full scale IQ
122	PCC_L	-7	-44	-16	Full scale IQ
123	PCC_L	-13	-43	9	Fluid intelligence
124	IFG_Tri_R	45	29	-1	Crystallized intelligence
125	SPG_L	-16	-57	53	Crystallized intelligence
126	PCC_L	-6	-38	23	Crystallized intelligence
127	TP_Sup_R	35	25	-30	Verbal Comprehension
128	SFG_orb_L	-8	51	-21	Similarities
129	SFG_orb_R	14	49	-19	Similarities
130	Hipp_L	-22	-26	-11	Arithmetic
131	IFG_Tri_R	45	26	28	Arithmetic
132	PrCG_R	60	12	30	Arithmetic
133	SFG_R	22	35	54	Arithmetic
134	PrCG_L	-31	-4	64	Information
135	SMG_L	-59	-21	26	Information
136	PCC_L	-4	-42	18	Comprehension
137	SPG_L	-33	-44	57	Picture Completion
138	Hipp_R	30	-39	3	Digit Symbol
139	PoCG_R	55	-21	52	Digit Symbol
140	SOG_R	27	-76	39	Digit Symbol
141	PCC_L	-8	-43	9	Block Design
142	IFG_Tri_L	-50	25	24	Matrix Reasoning
143	IOG_R	29	-97	-9	Matrix Reasoning
144	PoCG_R	49	-20	62	Picture Arrangement
145	SMG_L	-53	-50	25	Emotional awareness
146	PoCG_R	62	-17	36	Self-efficacy
147	SMG_R	47	-40	24	Perseverance
148	Cerebellum_L	-16	-87	-29	Impulse control
149	PCC_M_L	-2	-17	32	Impulse control
150	PCC_M_R	3	-23	42	Impulse control
151	IFG_Tri_R	55	23	26	Patience
152	MFG_R	29	49	20	Patience
153	PrCG_L	-59	0	28	Patience
154	PrCG_L	-46	-5	28	Sharing positive emotion
155	ITG_R	56	-34	-16	Sharing negative emotion
156	MFG_R	38	32	17	Voluntary support
157	MTG_L	-48	-15	-9	Voluntary support
158	Th_R	10	-9	9	Decision making
159	MTG_L	-57	-46	-3	Decision making
160	ITG_L	-34	-3	-35	Optimism
161	MTG_L	-53	-8	-7	Group consideration
162	SPG_R	36	-71	52	Adaptability
163	MTG_L	-52	-16	-5	Situational awareness

Ⅰ. 研 究 成 果 (2)

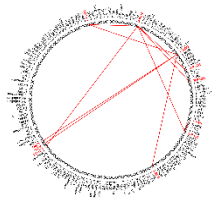
Ⅰ　1．心理指標と関連する脳部位・ ネットワークの機能的役割の推定

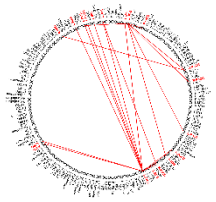
3) TFU脳部位セット(163ROIs)をもとにした**脳ネットワークの同定**を行った。

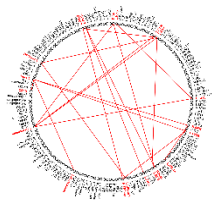
4) 心理指標130個に対して128個の脳ネットワークが同定され、
重複するものを除いて最終的に116個の心理指標に対する脳ネットワークが
TFUの脳ネットワークセットとしてまとまった(p<0.005, NBS corrected)。

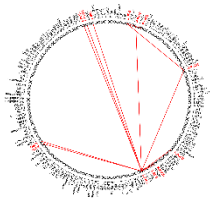
Ⅰ. 研 究 成 果 (2)

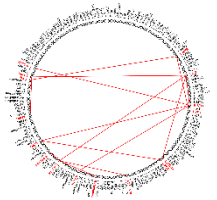
心理指標と関連するネットワークの同定

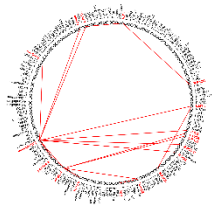
SQ 01 

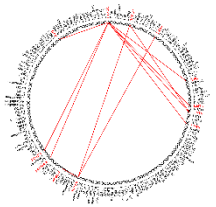
SQ 02 

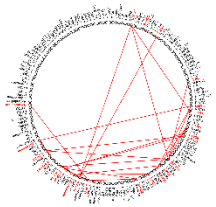
SQ 05 

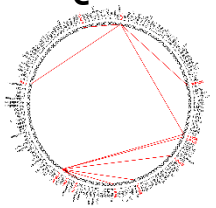
SQ 06 

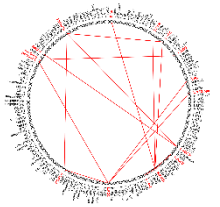
..... SQ 78  82/78

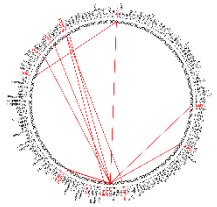
IQ 01 

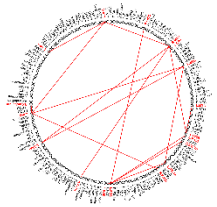
IQ 02 

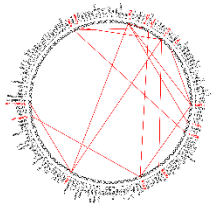
IQ 03 

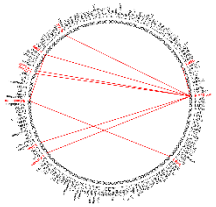
IQ 05 

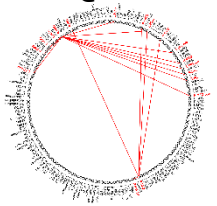
..... IQ 18  17/18

EQ 01 

EQ 02 

EQ 03 

EQ 04 

..... EQ 34  29/34

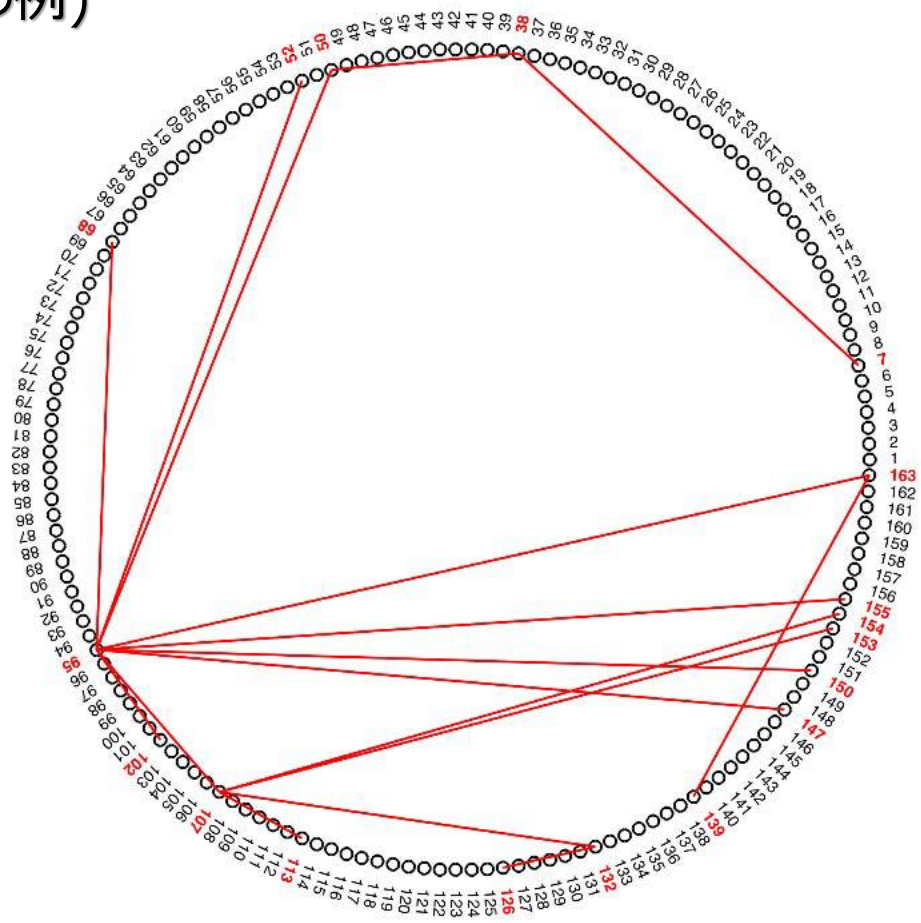
Total 128 networks

(Under revision)

Ⅰ. 研 究 成 果 (2)

心理指標と関連するネットワークの同定 (言語性IQの例)

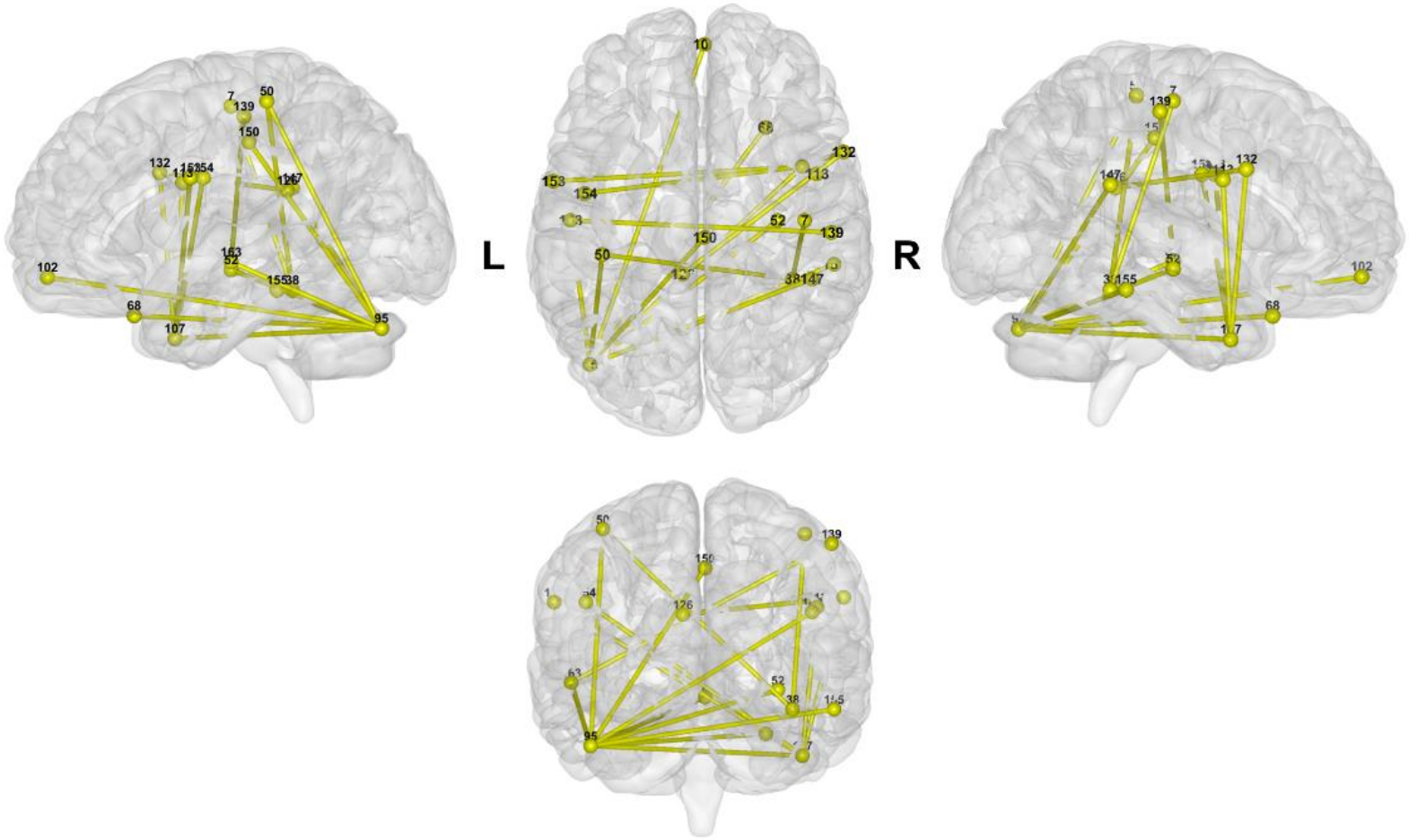
#	Region	MNI coordinates x	y	z	Brodmann area	Psychometric parameters
7	PoCG_R	44	−16	56	BA 4	Social competence with friends of the same sex
38	FG_R	39	−40	−16	BA 37	BAS/fun seeking
50	PoCG_L	−39	−30	58	BA 40	Planning skills
52	Hipp_R	33	−16	−8	BA 28	Planning skills
68	IFG_orb_R	28	22	−26	BA 47	Impulsivity/Carelessness Style(ICS)
95	Cerebellum_L	−44	−75	−31	Pyramis_L	The Satisfaction with Life Scale(SWLS)
102	IFG_Med_R	3	56	−11	BA 10	Disorganization
107	TP_Inf_R	43	6	−35	BA 38	Attention switching
113	PrCG_R	49	3	26	BA 6	Communication
126	PCC_L	−6	−38	23	BA 23	Crystallized intelligence
132	PrCG_R	60	12	30	BA 9	Arithmetic
139	PoCG_R	55	−21	52	BA 2	Digit symbol
147	SMG_R	47	−40	24	BA 13	Perseverance
150	PCC_M_R	3	−23	42	BA 31	Impulse control
153	PrCG_L	−59	0	28	BA 6	Patience
154	PrCG_L	−46	−5	28	BA 6	Sharing positive emotion
155	ITG_R	56	−34	−16	BA 20	Sharing negative emotion
163	MTG_L	−52	−16	−5	BA 22	Situational awareness



Brain map of the functional network for the psychometric parameter “verbal intelligence quotient (VIQ).” (A) Two-dimensional view of the network.

Ⅰ. 研 究 成 果 (2)

心理指標と関連するネットワークの同定



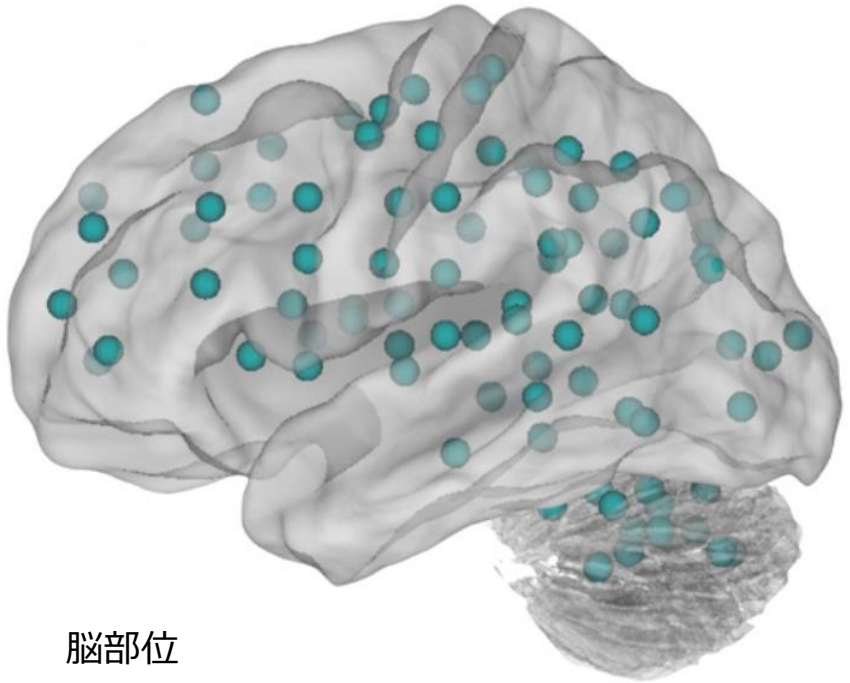
Brain map of the functional network for the psychometric parameter “verbal intelligence quotient (VIQ)” (B) Three-dimensional view of the network.

Ⅰ. 研 究 成 果 (2)

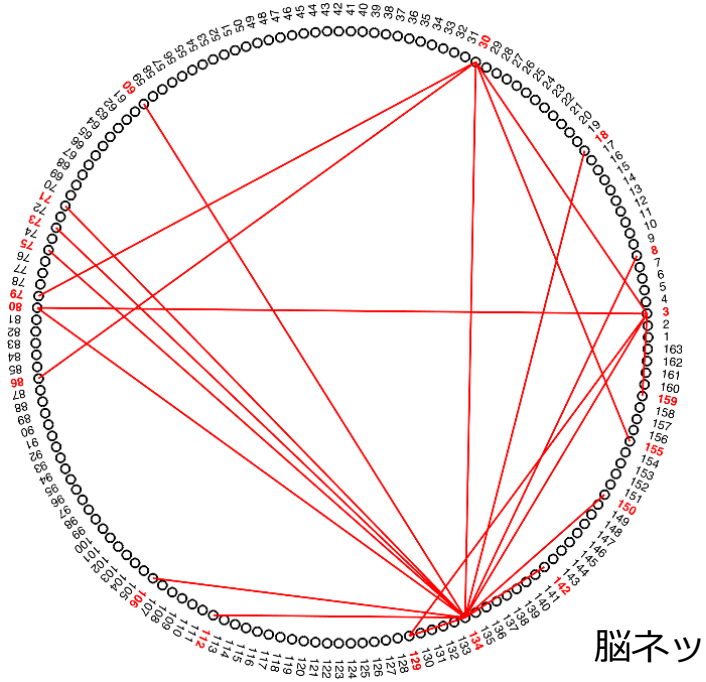
Ⅰ 2. 心理指標に関連する脳マップ（template）の完成

TFU-templateが完成した。

TFU-Templateは機能的役割が同定された脳部位・ネットワークからなるものであり、ヒトの行動を表す心理指標（SQ, IQ, EQ）が脳へ投射されたものである。



脳部位



脳ネットワーク

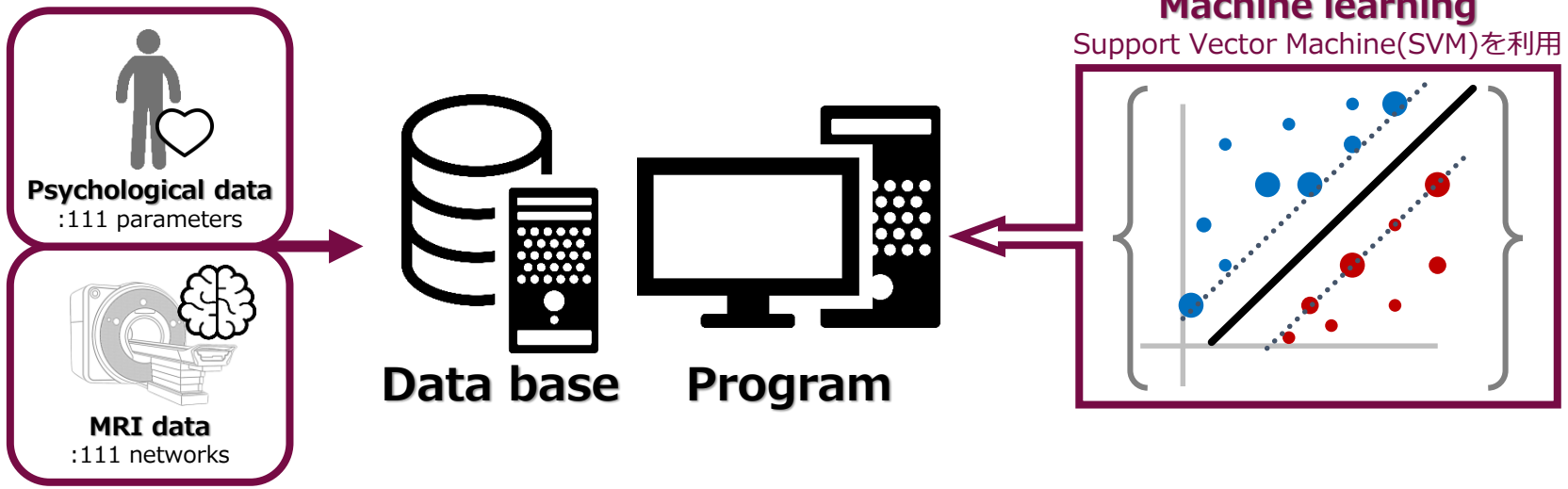
Ⅰ. 研 究 成 果 (2)

Ⅰ 3. パターン認知・ラーニングアルゴリズムの開発

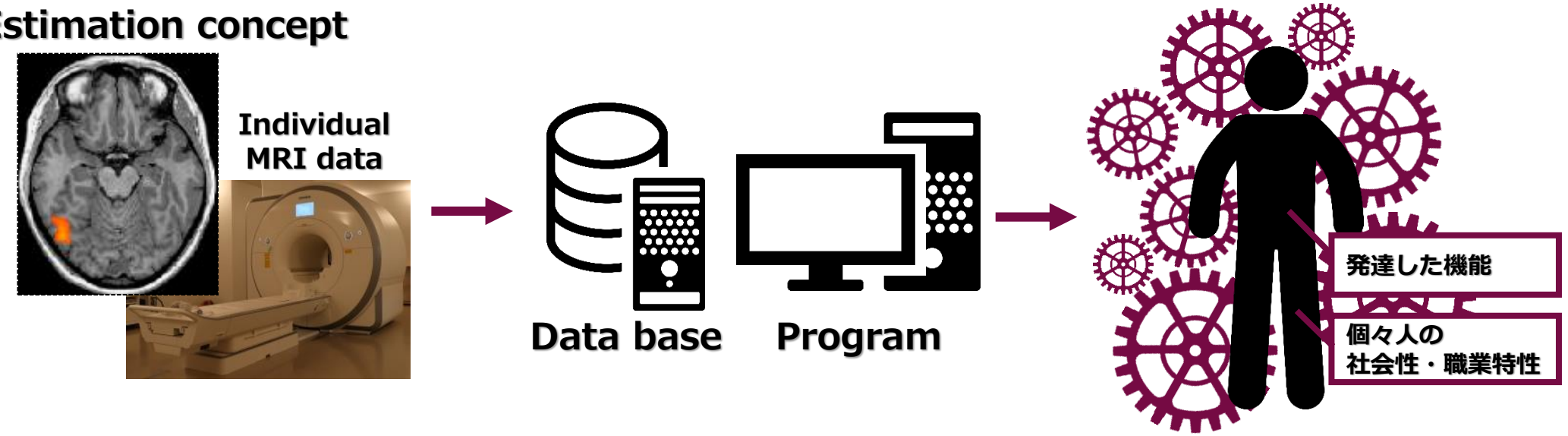
- 心理指標を８段階にして**ラーニングアルゴリズム(multi-class classifier)**を設計。
- ラーニングアルゴリズムはmulti-class Support Vector Machine (SVM)を利用。
- 脳ネットワークごとに一つのmulti-class SVM classifierを設計。
- 脳ネットワークのセット(128個)から123個の脳ネットワークに対して significant accuracy(>12.5%)を有するclassifierが設計できた。
  (SQに対して78、IQに対して17、EQに対して28のclassifier)
- 重複を除いて111個のSVM classifier(SQ:70, IQ:15, EQ:26)のセットとして まとまった。
- 設計されたSVM classifierで**111項目の心理指標が推定可能**になった。

Ⅰ. 研 究 成 果 (2)

Training Concept

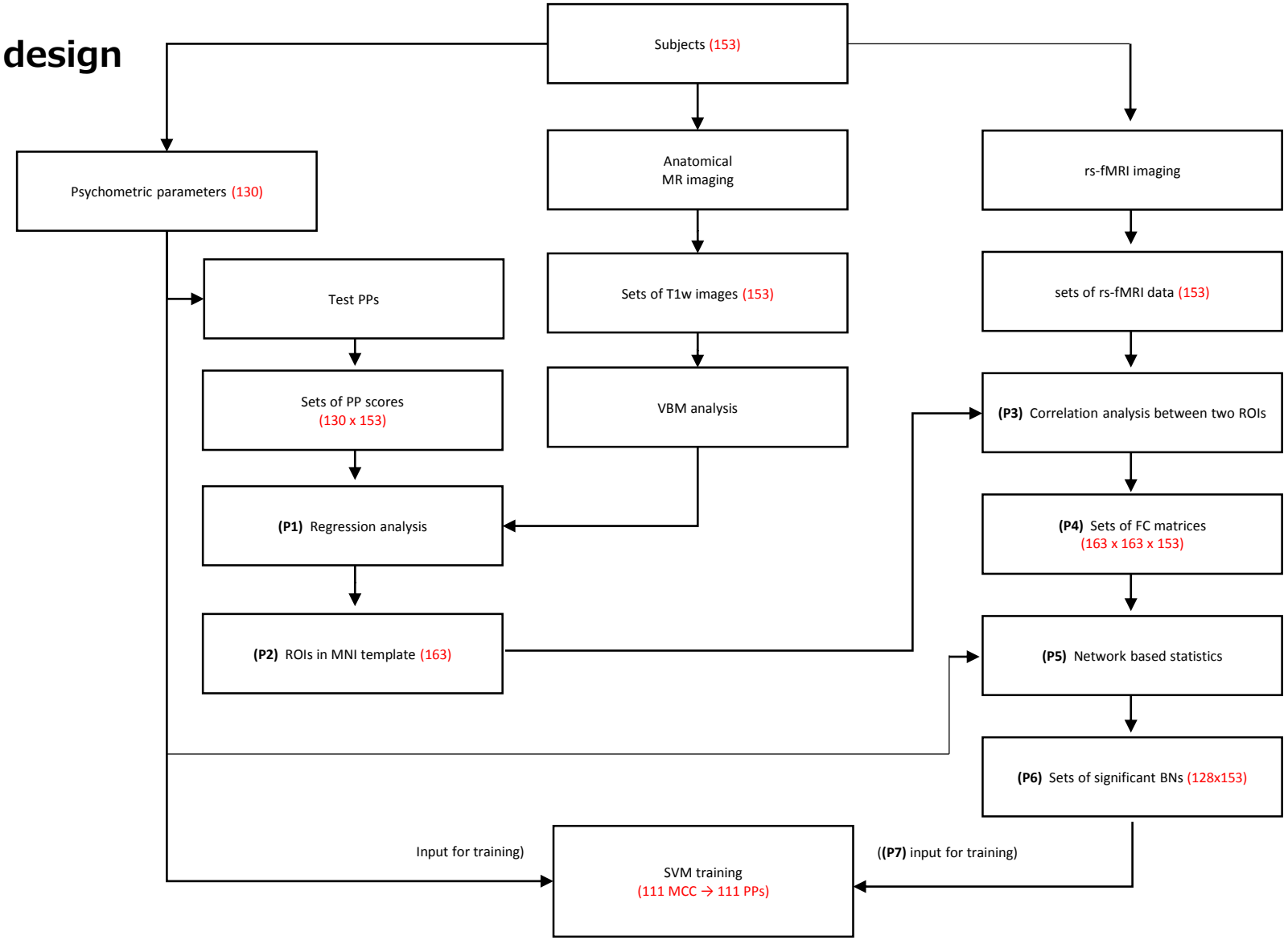


Estimation concept



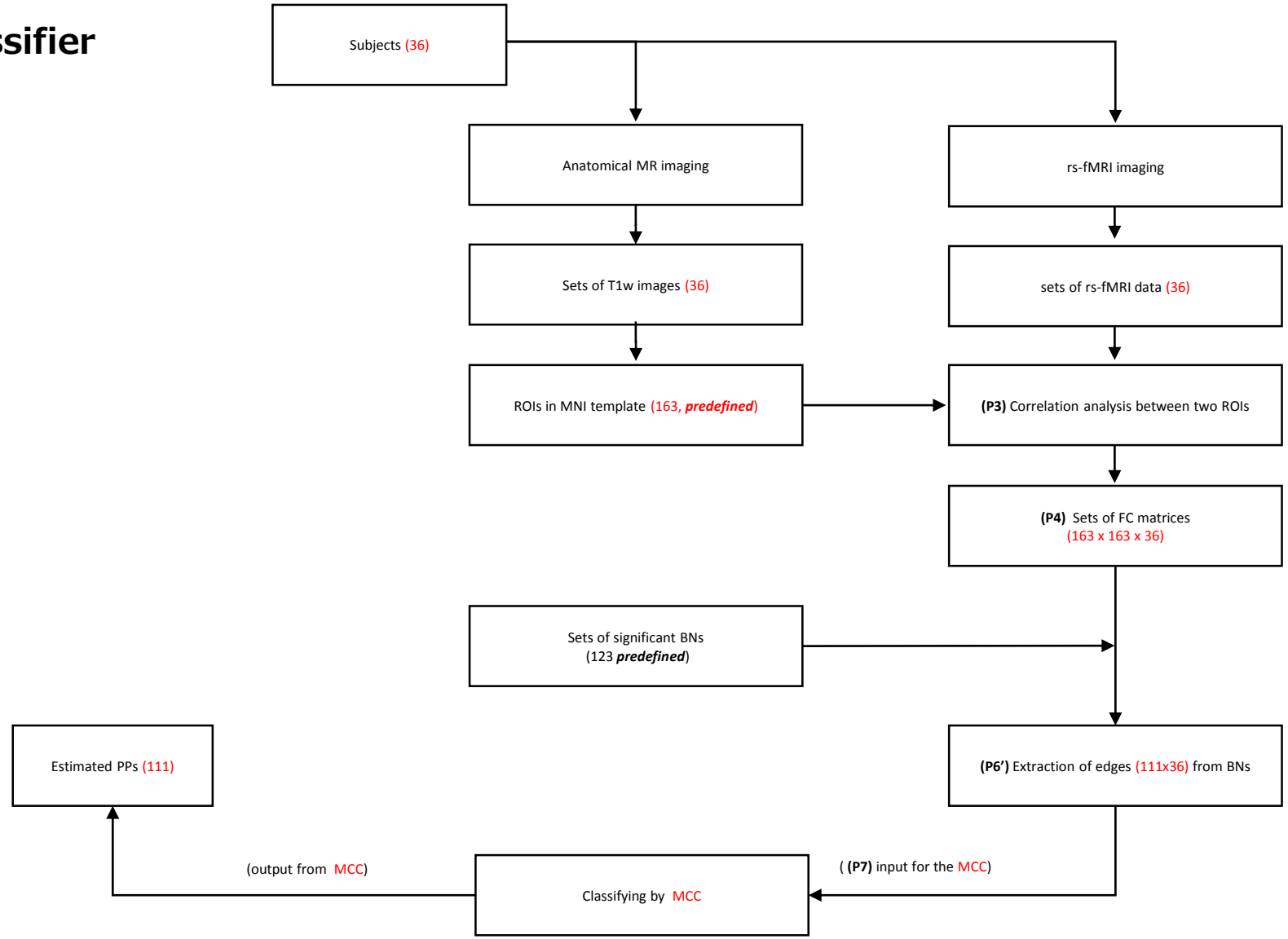
Training flow for SVM classifier design

Diagrams of data flow for the primary experiment. Brain areas are identified by psychometric parameters and MRI data by regression analysis. fMRI signals are extracted from the ROIs, and the correlation matrix is constructed . Regression analysis and network based statistics (NBS) analysis were performed for the correlation matrices of 153 subjects, and significant brain networks are identified. Inputs to the SVM classifiers are determined from the edges of the identified functional networks. Scores of psychometric parameters are estimated by classifiers and compared with psychologically measured scores to calculate accuracy. Numbers and letters in the parenthesis stand for specific information obtained after the processing at each step. PP, psychometric parameter; SVM, support vector machine; rs-Fmri, resting-state functional MRI; FC, functional connectivity; BN, brain network; MCC, multiple class classifiers; T1w, T1 weighted.



Estimation flow from SVM classifier

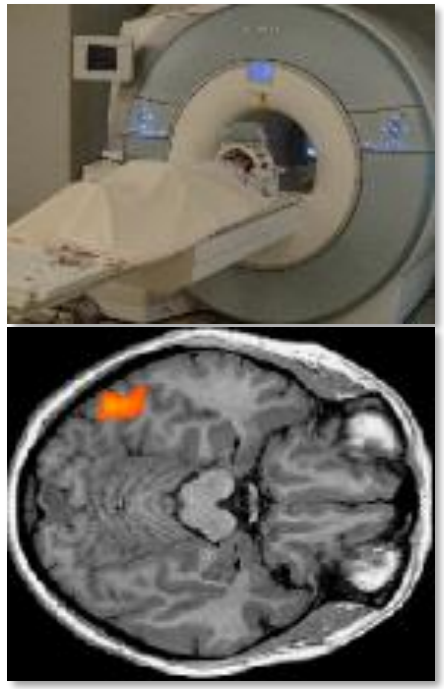
Diagrams of data flow for the test of trained SVM classifier. Bypassing the regression analyses used during training, fMRI signals are extracted from the ROIs, and the edges of functional networks are calculated for input into the SVM classifiers. Scores of psychometric parameters are estimated by the classifiers.



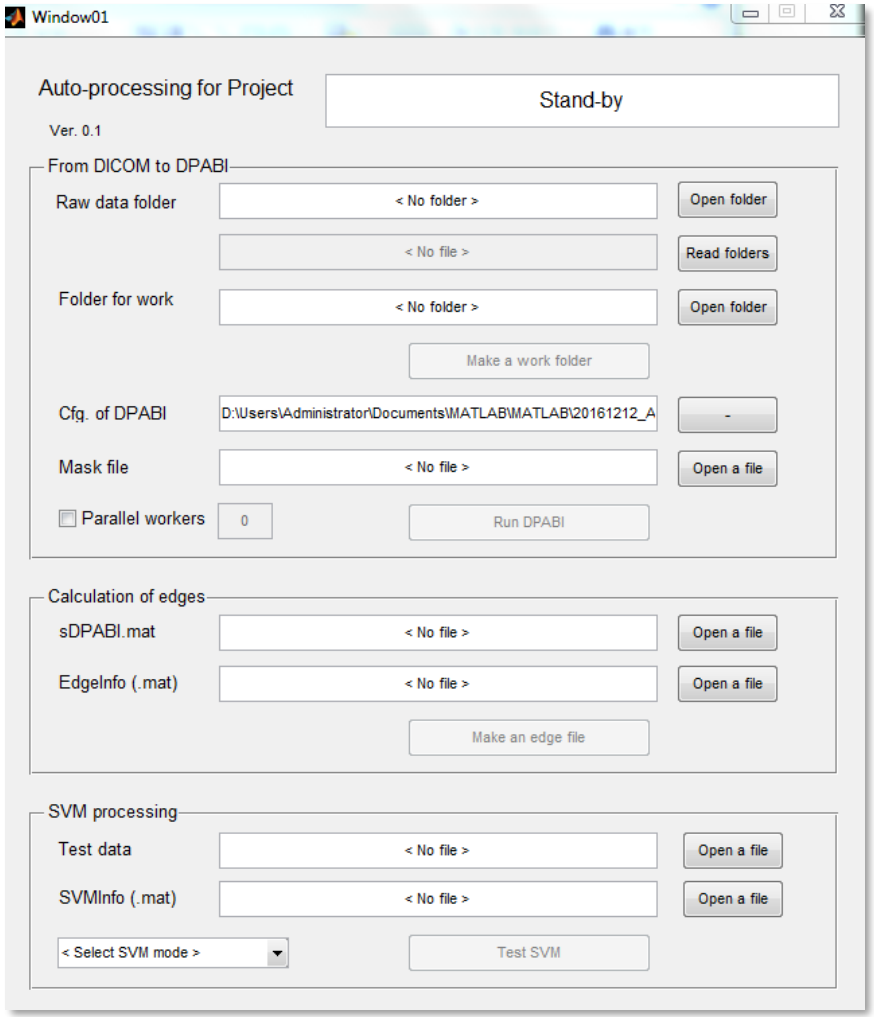
Ⅰ. 研 究 成 果 (2)

Final form of the estimator for human characteristics (SQ, IQ, EQ): User Interface

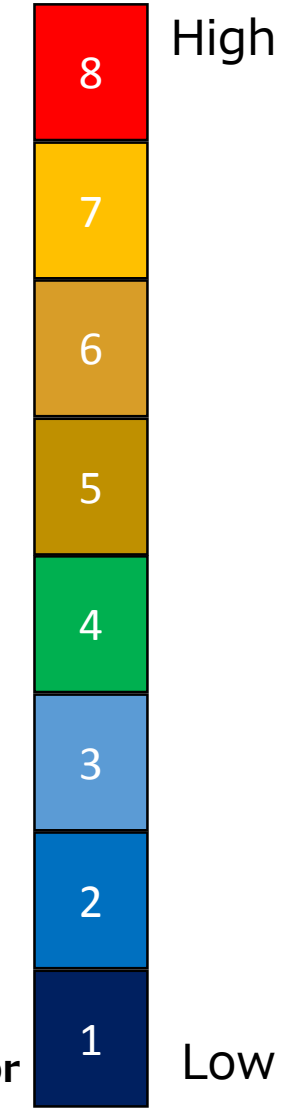
MRIデータの格納場所を指定するだけで
心理指標の推定結果を出力できるプログラム



Individual MRI data



GUI of the estimator for human characteristics



Scores of psychometric parameters estimated by the estimator

Ⅰ. 研 究 成 果 (2) - Interim summary

Ⅰ

1．心理指標と関連する脳部位・ ネットワークの機能的役割の推定
2．心理指標に関連する脳マップ（template）の完成
3．パターン認知・ラーニングアルゴリズムの開発

心理指標を反映する**脳部位・ネットワークデータベースの構築**

このデータベースに基づいた**脳マップの完成**

MRIデータから心理指標が推定できる
心理指標推定器(ヒト特性推定器)の開発

以上が完了した。

Ⅰ. 研 究 成 果 (2)

Ⅱ　1．参加者の固有の認知・脳機能の可塑的変化の推定

大学における教育・経験による個々人の脳および心理活動の変化を検討するために**縦断研究**として卒業年次の心理測定および約3年にかけて定期的なMRIデータの収集を行った。

心理測定による可塑的変化

1) **短期可塑的変化**
課題による心理測定(実行機能課題)で数十分間の訓練により、認知機能への変化が起きていることが確認できた。

2) **長期可塑的変化**
約30ヶ月以上経過した心理検査結果と初回実施時の結果の比較から心理特性の変化を検出できた。

※これらの心理機能・特性変化は脳機能の変化の顕在であると考えられる。

Ⅰ. 研 究 成 果 (2)

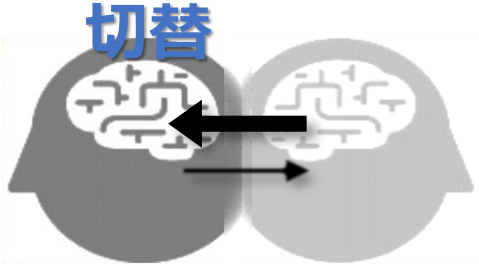
Ⅱ 1． 参加者の固有の認知・脳機能の可塑的変化の推定

短期可塑的変化

20～30分間の訓練による実行機能変化

実行機能：自分の思考や行動を支える3つの心的機能からなるとされている





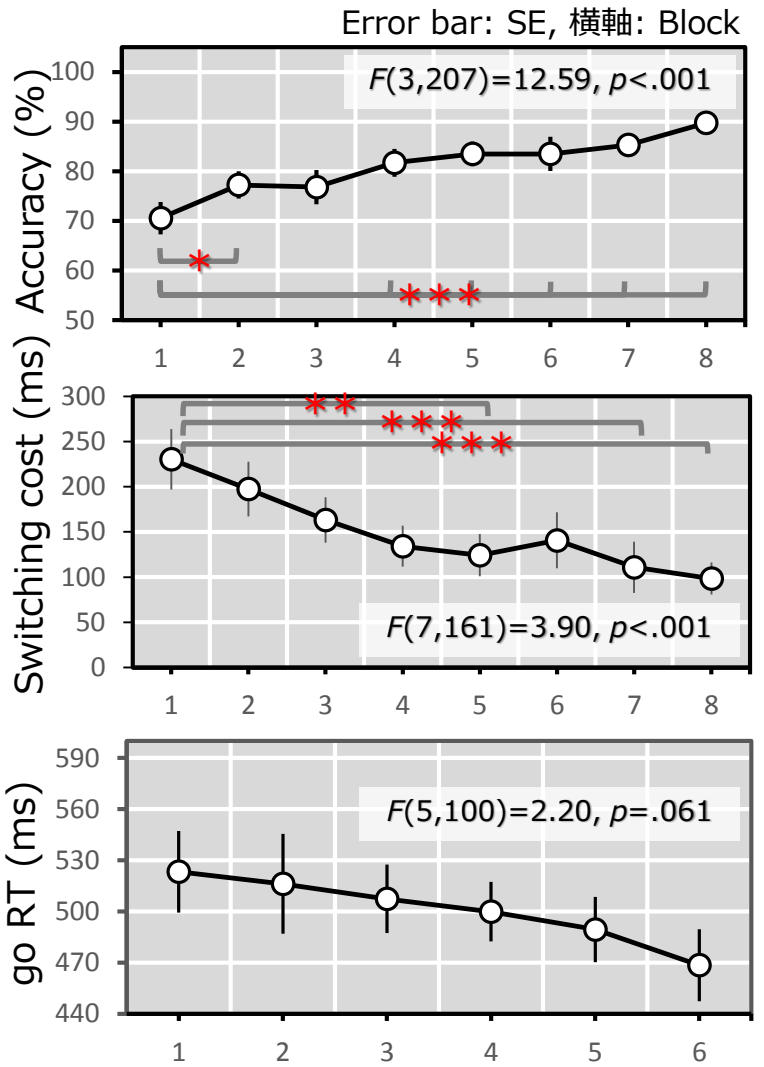


課題成績向上率

約18%
課題成績向上

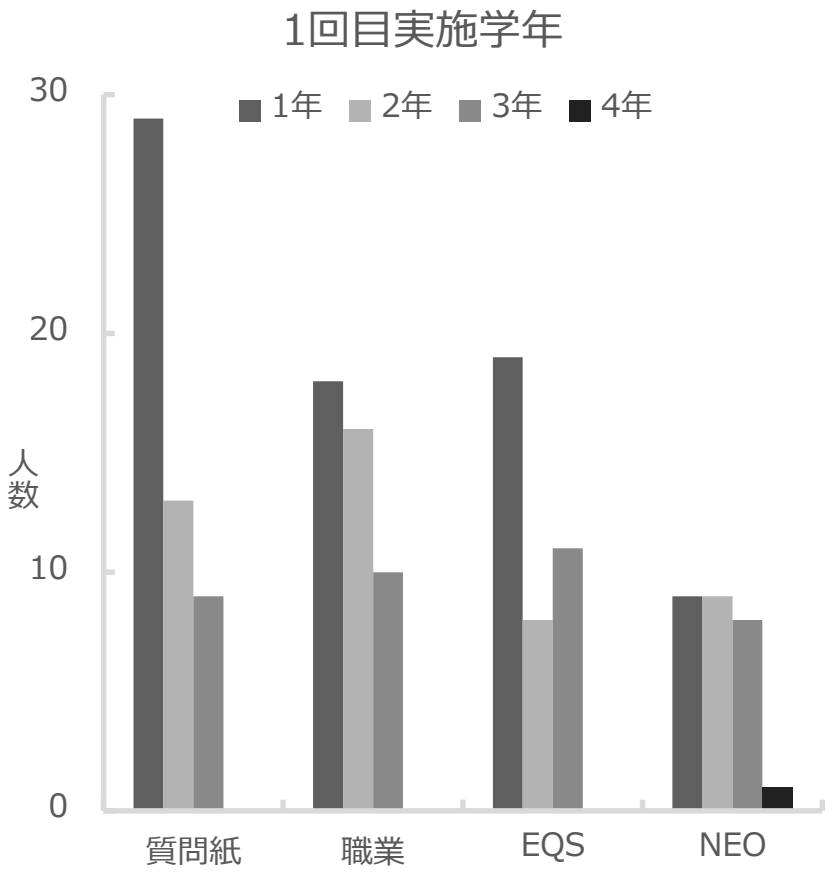
約57%
課題成績向上

約10%
課題成績向上

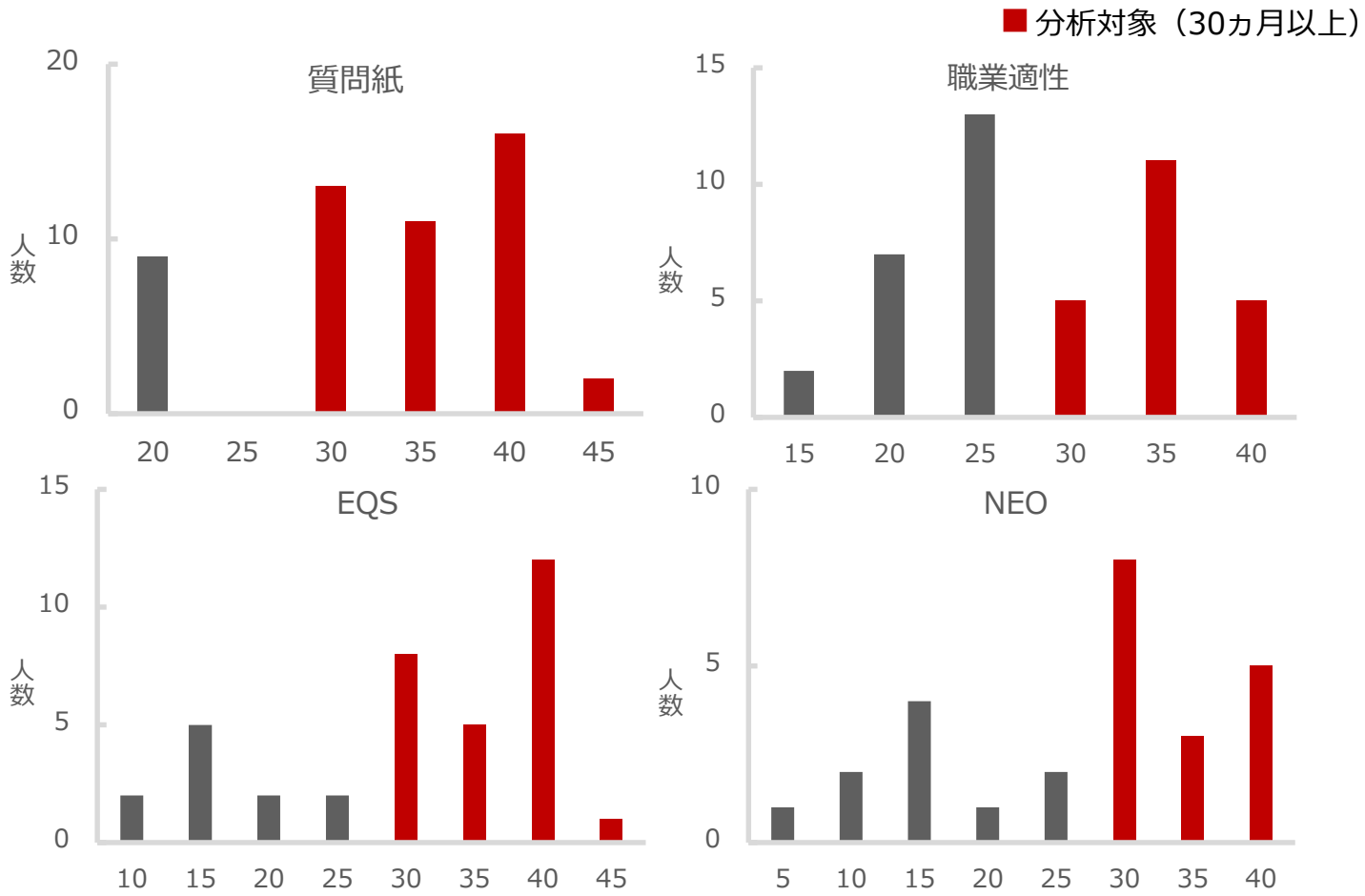


Ⅰ. 研 究 成 果 (2)

長期可塑的変化



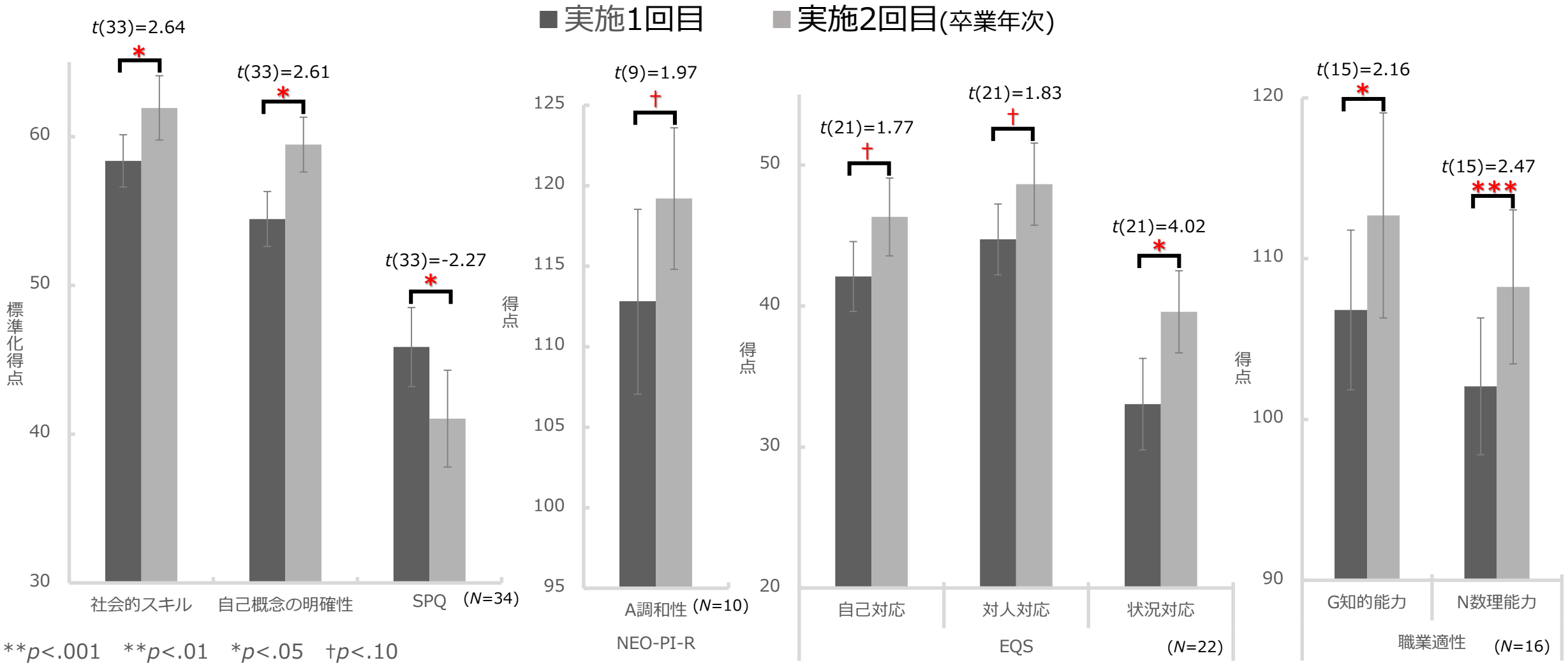
実施時期の分布



Ⅰ. 研 究 成 果 (2)

Ⅱ 1．参加者の固有の認知・脳機能の可塑的変化の推定

長期可塑的変化　初回検査から30か月以上経過後の心理特性の比較



***p<.001　**p<.01　*p<.05　†p<.10

Ⅰ. 研 究 成 果 (2)

Ⅱ　1．参加者の固有の認知・脳活動の可塑的変化の推定

MRIによる長期可塑的変化

1）推定器によるレベルの推定

2）推定レベルと時間の相関($p<0.1$)

3）各参加者の変化心理特性の数の評価

4）各心理特性に対する可塑的変化を示す参加者の数

※画像調整が完了したMRI縦断計測10回以上の参加者**12名**が分析対象

Ⅰ. 研 究 成 果 (2) - Interim summary

Ⅱ

１．被験者の固有の心理活動の可塑的変化の推定

参加者の**可塑的変化の推定**。
- 参加者によって変化のあるパラメータが異なった。
- 参加者によって可塑的な変化が生じる方向の差異が見られた。

変化と大学生活などとの相関についてはまだ**検討が必要**である。

以上の知見を得た。

Ⅰ. 研 究 成 果 (2)

Ⅲ 1. 職業適性関連脳ネットワークの同定

GATBの19個の職業適性の各々に対応する脳ネットワークが推定できた。

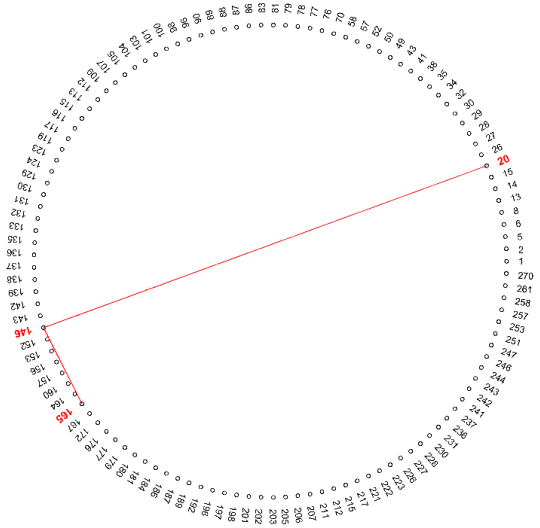
Job No.	適性能類型
Job 1	(M) Plant culture/Animal breeding
Job 2	(GV) Animal training and service/Aquaculture/Gardening
Job 3	(KM) Physical works in Mechanical/Plants/Animals
Job 4	(PM) Hand work
Job 5	(KFM) Industrial machine manipulation
Job 6	(PKM) Manufacture/Assembly
Job 7	(SPM) Cutting/Molding/Construction/Installation
Job 8	(SPF) Barber/Beauty services
Job 9	(NSP) Drawing and architecture design/Laboratory technology
Job 10	(GQM) Nursing/Therapy/Specialized teaching services/Quality control/Security management
Job 11	(GNS) Engineering technology/Physical sciences/Medical sciences
Job 12	(GVN) Social research/Law/Social service/Mathematics and statistics
Job 13	(GVQ) General office work/Educational and library services
Job 14	(SP) Design and visual arts
Job 15	(GQK) Clerical machine operation/Communicator
Job 16	(GM) Nursing-care services
Job 17	(GNQ) General sales/Accounting
Job 18	(GQ) Hospitality/Security services
Job 19	(QK) Clerical handling

Ⅰ. 研 究 成 果 (2)

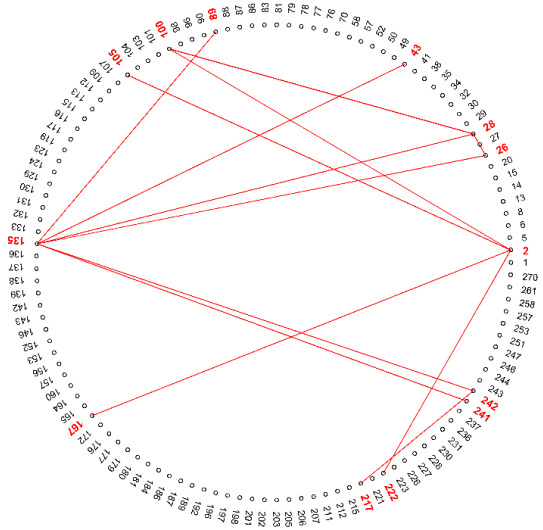
Ⅲ 1．職業適性関連脳ネットワークの同定

各職業適性と機能的結合(度)との回帰分析により、
各職業適性に対応する脳ネットワークが見出された。

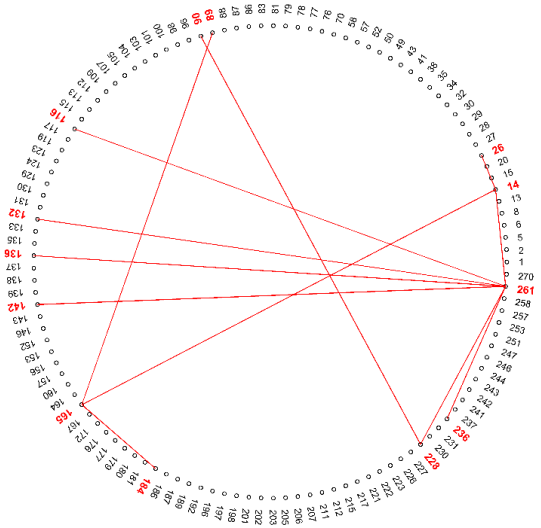
各脳ネットワークは全272の脳部位セットの一部の脳部位をつなぐ形で構成されている。



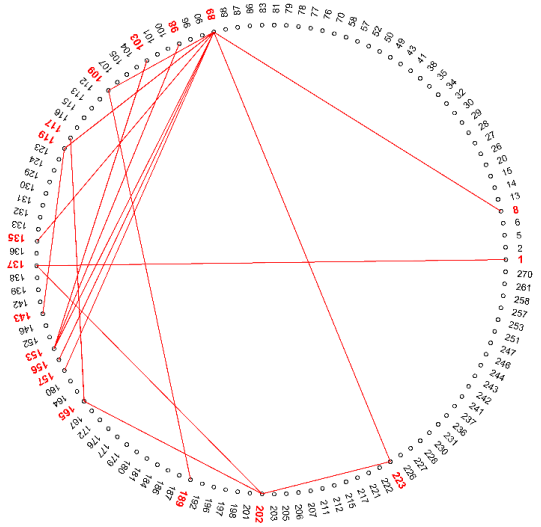
Job01



Job02



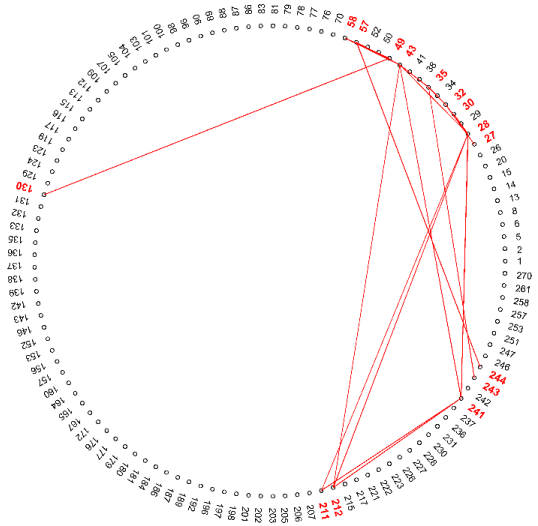
Job03



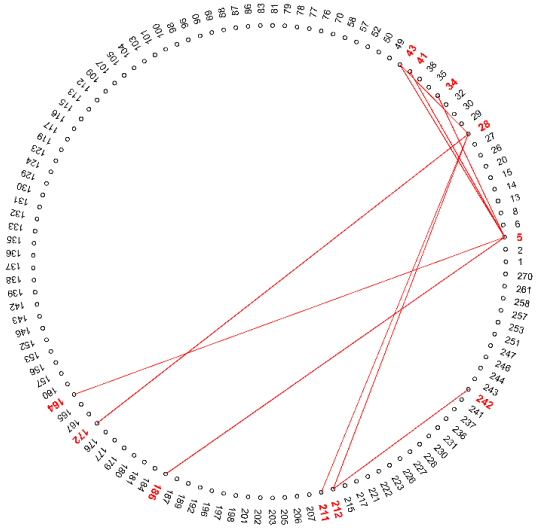
Job04

Ⅰ. 研 究 成 果 (2)

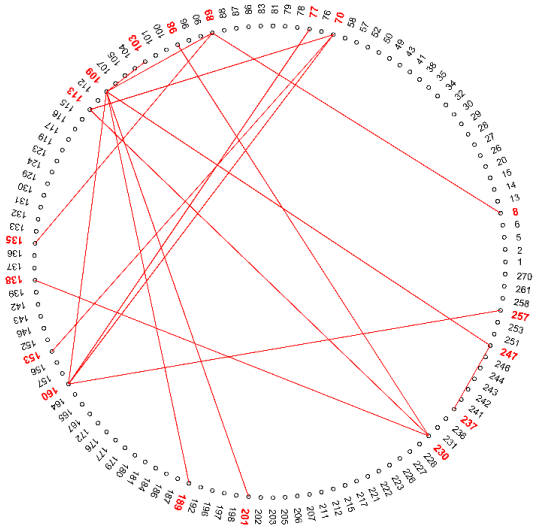
Ⅲ 1．職業適性関連脳ネットワークの同定



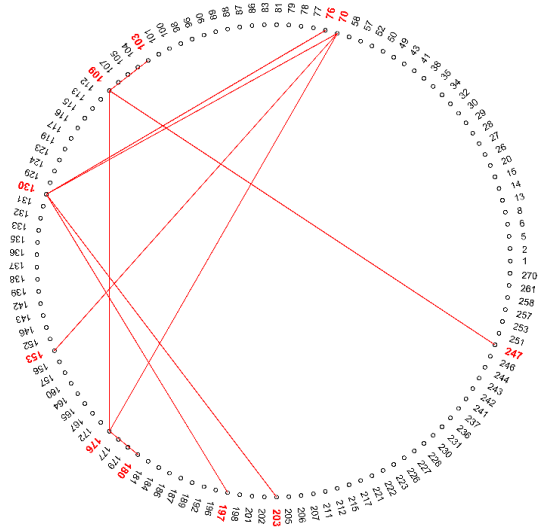
Job05



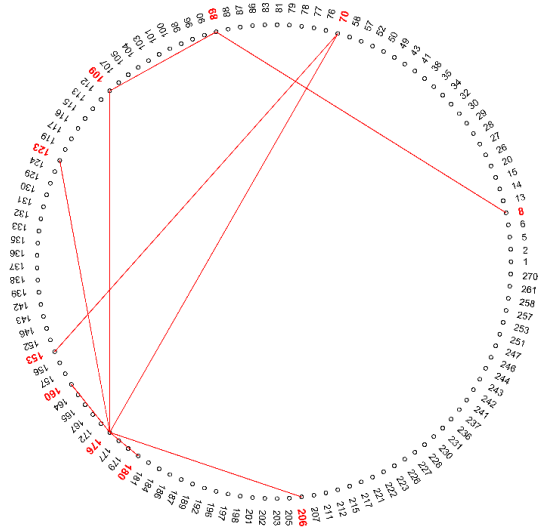
Job06



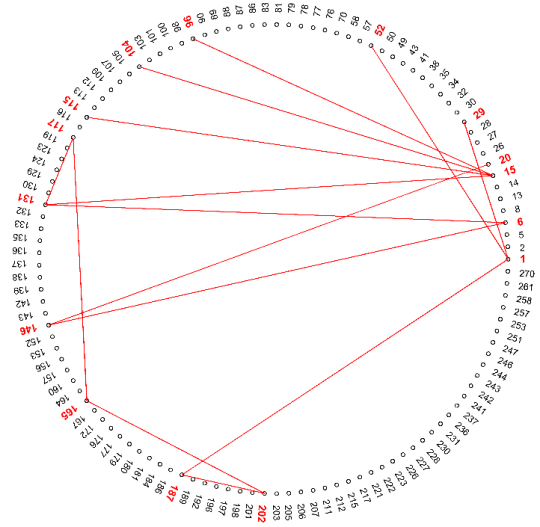
Job07



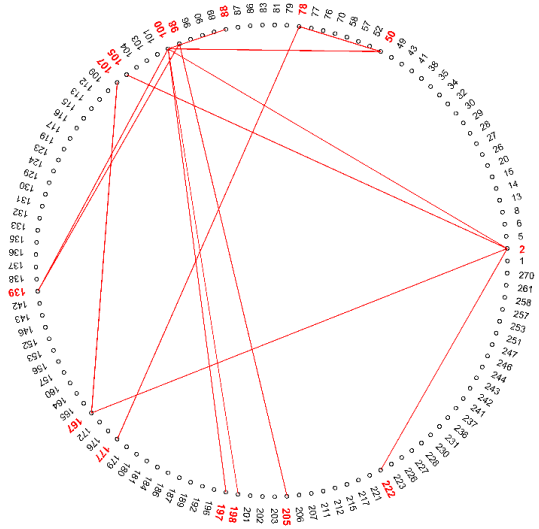
Job08



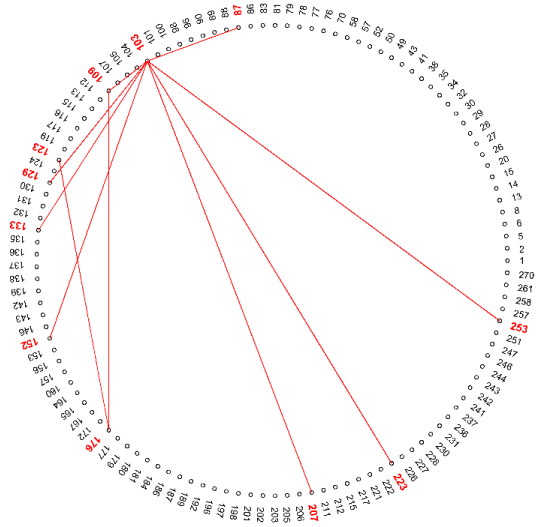
Job09



Job10



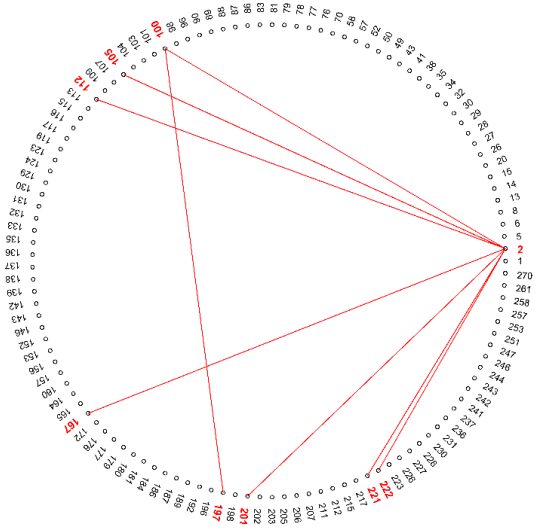
Job11

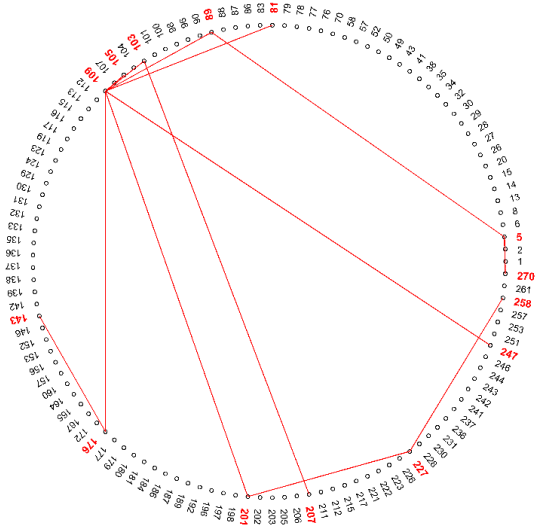


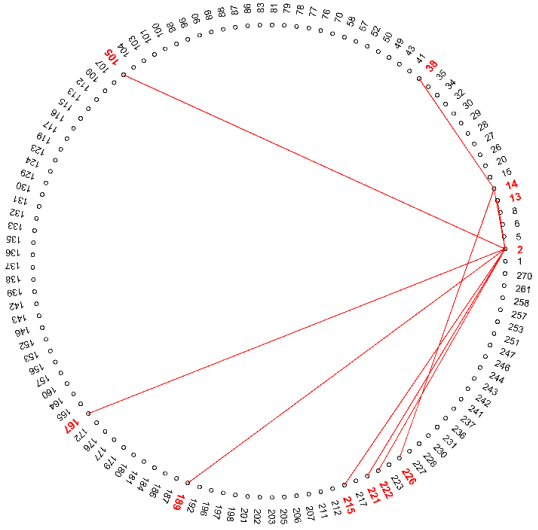
Job12

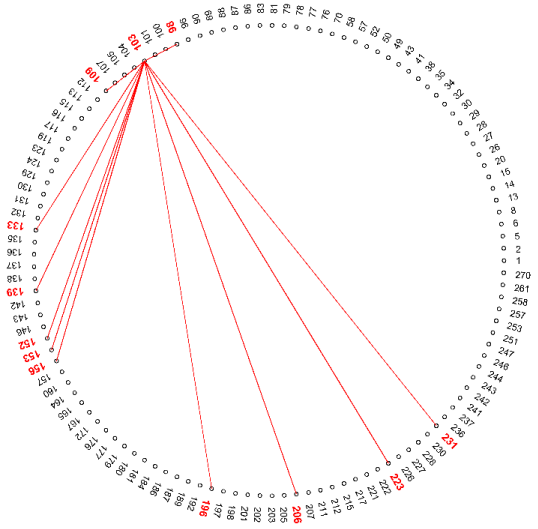
Ⅰ. 研 究 成 果 (2)

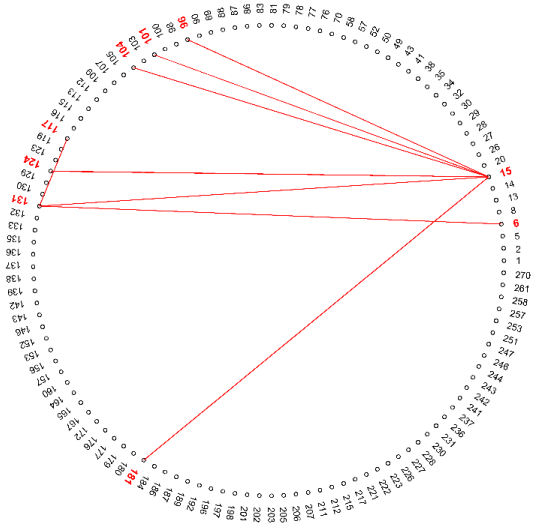
Ⅲ 1．職業適性関連脳ネットワークの同定

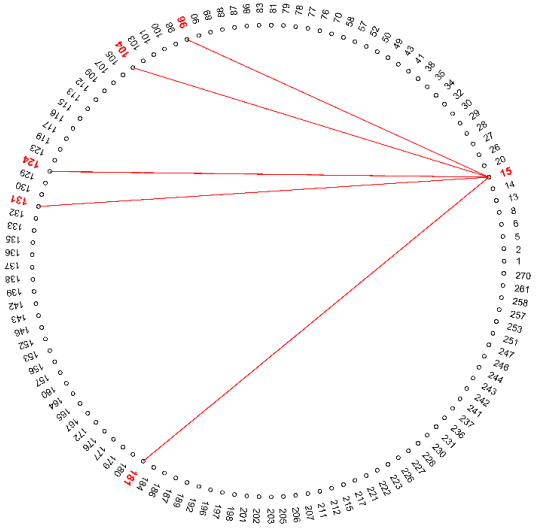

Job13

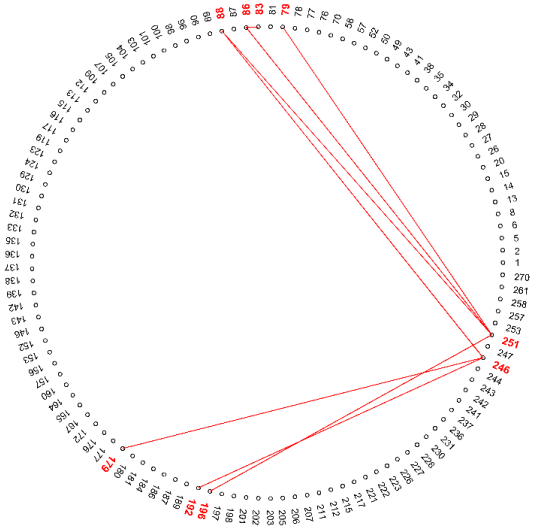

Job14


Job15


Job16


Job17


Job18


Job19

Ⅰ. 研 究 成 果 (2)

Ⅲ 1. 職業適性関連脳ネットワークの同定

#	ROI numbers in 19 networks	ROI-belonging Job Network	Brain Region	MNI Coordinates		
				x	y	z
1	1	Job04,10	'vmPFC'	6	64	3
2	2	Job02,11,13,15	'aPFC'	29	57	18
3	5	Job06,14	'aPFC'	-25	51	27
4	6	Job10,17	'vmPFC'	9	51	16
5	8	Job04,07,09	'aPFC'	27	49	26
6	13	Job15	'vmPFC'	8	42	-5
7	14	Job03,15	'ACC'	9	39	20
8	15	Job10,17,18	'vlPFC'	46	39	-15
9	20	Job01,10	'sup frontal'	-16	29	54
10	26	Job02,03	'ant insula'	38	21	-1
11	27	Job05	'dACC'	9	20	34
12	28	Job02,05,06	'ant insula'	-36	18	2
13	29	Job10	'dFC'	40	17	40
14	30	Job05	'basal ganglia'	-6	17	34
15	32	Job05	'frontal'	58	11	14
16	34	Job06	'dFC'	44	8	34
17	35	Job05	'dFC'	60	8	34
18	38	Job15	'basal ganglia'	-20	6	7
19	41	Job06	'pre-SMA'	10	5	51
20	43	Job02,05,06	'SMA'	0	-1	52
21	49	Job05	'precentral gyrus'	-44	26	49
22	50	Job11	'parietal'	-26	28	54
23	52	Job10	'precentral gyrus'	-54	29	23
24	57	Job05	'thalamus'	-12	-12	6
25	58	Job05	'thalamus'	11	-12	6
26	70	Job07,08,09	'post insula'	42	-24	17
27	76	Job08	'post insula'	-30	-28	9
28	77	Job07	'parietal'	-24	-30	64
29	78	Job11	'temporal'	51	-30	5
30	79	Job19	'post parietal'	-41	-31	48

#	ROI numbers in 19 networks	ROI-belonging Job Network	Brain Region	MNI Coordinates		
				x	y	z
31	81	Job14	'fusiform'	54	-31	-18
32	83	Job19	'temporal'	-53	-37	13
33	86	Job19	'sup parietal'	34	-39	65
34	87	Job12	'precuneus'	8	-40	50
35	88	Job11,19	'IPL'	-41	-40	42
36	89	Job02,03,04,07,09,14	'parietal'	58	-41	20
37	90	Job03	'post cingulate'	28	241	3
38	96	Job10,17,18	'IPL'	54	-44	43
39	98	Job04,07,11,16	'lat cerebellum'	-28	-44	-25
40	100	Job02,11,13	'sup temporal'	42	-46	21
41	101	Job17	'IPL'	-48	-47	49
42	103	Job04,07,08,12,14,16	'temporal'	-59	-47	11
43	104	Job10,17,18	'IPL'	-53	-50	39
44	105	Job02,11,13,14,15	'precuneus'	5	-50	33
45	107	Job11	'IPL'	44	-52	47
46	109	Job04,07,08,09,12,14,16	'lat cerebellum'	-24	-54	-21
47	112	Job13	'precuneus'	-6	-56	29
48	113	Job07	'lat cerebellum'	-34	-57	-24
49	115	Job10	'post cingulate'	-11	-58	17
50	116	Job03	'IPS'	32	-59	41
51	117	Job04,10,17	'angular gyrus'	51	-59	34
52	119	Job04	'occipital'	36	-60	-8
53	123	Job09,12	'temporal'	46	-62	5
54	124	Job17,18	'angular gyrus'	-48	-63	35
55	129	Job12	'occipital'	19	-66	-1
56	130	Job05,08	'med cerebellum'	1	-66	-24
57	131	Job10,17,18	'inf cerebellum'	-34	-67	-29
58	132	Job03	'precuneus'	11	-68	42
59	133	Job12,16	'occipital'	17	-68	20
60	135	Job02,04,07	'occipital'	39	-71	13

Ⅰ. 研 究 成 果 (2)

Ⅲ 1．職業適性関連脳ネットワークの同定

#	ROI numbers in 19 networks	ROI-belonging Job Network	Brain Region	MNI Coordinates		
				x	y	z
61	136	Job03	'occipital'	-9	-72	41
62	137	Job04	'occipital'	45	-72	29
63	138	Job07	'med cerebellum'	-11	-72	-14
64	139	Job11,16	'occipital'	29	-73	29
65	142	Job03	'occipital'	-29	-75	28
66	143	Job04,14	'med cerebellum'	5	-75	-11
67	146	Job01,06,10	'occipital'	-42	-76	26
68	152	Job12,16	'post occipital'	-5	-80	9
69	153	Job04,07,08,09,16	'post occipital'	29	-81	14
70	156	Job04,16	'post occipital'	-37	-83	-2
71	157	Job04	'post occipital'	-29	-88	8
72	160	Job07,09	'post occipital'	-4	-94	12
73	164		'Insular Cortex'	38	3	0
74	165	Job01,03,04,10	'Superior Frontal Gyrus'	-14	19	57
75	167	Job02,11,13,15	'Middle Frontal Gyrus'	-38	19	42
76	172	Job06	'Inferior Frontal Gyrus, pars opercularis'	52	15	16
77	176	Job08,09,12,14	'Temporal Pole'	41	13	-30
78	177	Job11	'Superior Temporal Gyrus, anterior division'	-56	-4	-8
79	179	Job19	'Superior Temporal Gyrus, posterior division'	-61	-27	2
80	180	Job08,09	'Superior Temporal Gyrus, posterior division'	60	-23	2
81	181	Job17,18	'Middle Temporal Gyrus, anterior division'	-58	-4	-22
82	184	Job03	'Middle Temporal Gyrus, posterior division'	61	-22	-13
83	186	Job06	'Middle Temporal Gyrus, temporooccipital part'	58	-49	2
84	187	Job10	'Inferior Temporal Gyrus, anterior division'	-48	-5	-39
85	189	Job04,07,15	'Inferior Temporal Gyrus, posterior division'	-54	-29	-26
86	192	Job19	'Inferior Temporal Gyrus, temporooccipital part'	54	-50	-17
87	196	Job16,19	'Superior Parietal Lobule'	29	-48	59
88	197	Job08,11,13	'Supramarginal Gyrus, anterior division'	-57	-33	37
89	198	Job11	'Supramarginal Gyrus, anterior division'	59	-27	38
90	201	Job07,13,14	'Angular Gyrus'	-50	-56	30

Ⅰ. 研 究 成 果 (2)

Ⅲ 1．職業適性関連脳ネットワークの同定

#	ROI numbers in 19 networks	ROI-belonging Job Network	Brain Region	MNI Coordinates		
				x	y	z
91	202	Job04,10	'Angular Gyrus'	52	-52	32
92	203	Job08	'Lateral Occipital Cortex, superior division'	-32	-73	38
93	205	Job11	'Lateral Occipital Cortex, inferior division'	-45	-76	-2
94	206	Job09,16	'Lateral Occipital Cortex, inferior division'	46	-74	-2
95	207	Job12,14	'Intracalcarine Cortex'	-10	-75	8
96	211	Job05,06	'Juxtapositional Lobule Cortex (formerly Supplementary Motor Cortex)'	-6	-3	56
97	212	Job05,06	'Juxtapositional Lobule Cortex (formerly Supplementary Motor Cortex)'	6	-3	58
98	215	Job15	'Paracingulate Gyrus'	-6	37	21
99	217	Job02	'Cingulate Gyrus, anterior division'	-5	18	25
100	221	Job13,15	'Precuneous Cortex'	-8	-60	37
101	222	Job02,11,13,15	'Precuneous Cortex'	9	-58	39
102	223	Job04,12,16	'Cuneal Cortex'	-8	-80	27
103	226	Job15	'Frontal Orbital Cortex'	29	23	-16
104	227	Job14	'Parahippocampal Gyrus, anterior division'	-22	-9	-30
105	228	Job03	'Parahippocampal Gyrus, anterior division'	22	-8	-30
106	230	Jon07	'Parahippocampal Gyrus, posterior division'	23	-30	-17
107	231	Job16	'Lingual Gyrus'	-13	-65	-5
108	236	Job03	'Temporal Fusiform Cortex, posterior division'	36	-24	-28
109	237	Job07	'Temporal Occipital Fusiform Cortex'	-34	-54	-16
110	241	Job02,05	'Frontal Operculum Cortex'	-40	18	5
111	242	Job02,06	'Frontal Operculum Cortex'	41	19	5
112	243	Job05	'Central Opercular Cortex'	-48	-8	12
113	244	Job05	'Central Opercular Cortex'	49	-6	11
114	246	Job19	'Parietal Operculum Cortex'	49	-27	21
115	247	Job07,08,14	'Planum Polare'	-47	-6	-7
116	251	Job19	'Planum Temporale'	-53	-30	11
117	253	Job12	'Supracalcarine Cortex'	-10	-72	15
118	257	Job07	'Brain-Stem'	-7	-31	-34
119	258	Job14	'Brain-Stem'	8	-31	-34
120	261	Job03	'Caudate'	-13	9	10
121	270	Job14	'Amygdala'	23	-4	-18

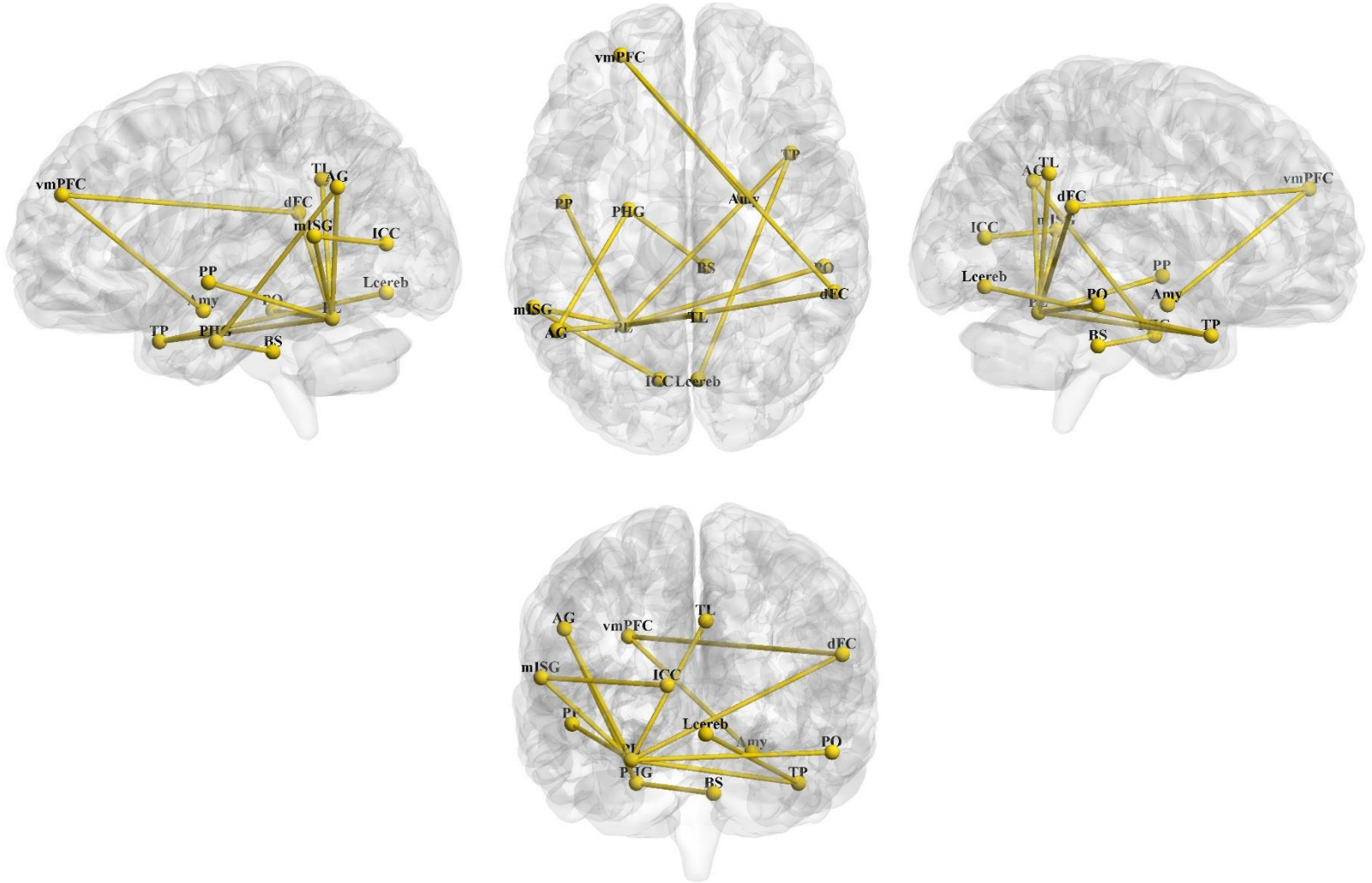
Ⅰ. 研 究 成 果 (2)

Ⅲ 1．職業適性関連脳ネットワークの同定

各職業に特異的な機能を表現する 個々のネットワーク （例）

Aptitude of Design & Visual Arts

Design & Arts network is composed of 14 nodes (ROI).
Among the nodes the middle occipital gyrus (MOG, M in the sagittal image), the fusiform gyrus (FG, F) and parahippocampal gyrus (PHG, P) are known to be involved in visual object and visuospatial contexture information processing, and also, the amygdala (Amy, A), brain stem (BS, B) and temporal pole (TP, T) are known to play some roles for social and emotional processing. These functional characteristics of each brain area in the network describe well the network's character for the vocational category.



Design & Visual Arts

Ⅲ. 研 究 成 果 (2)

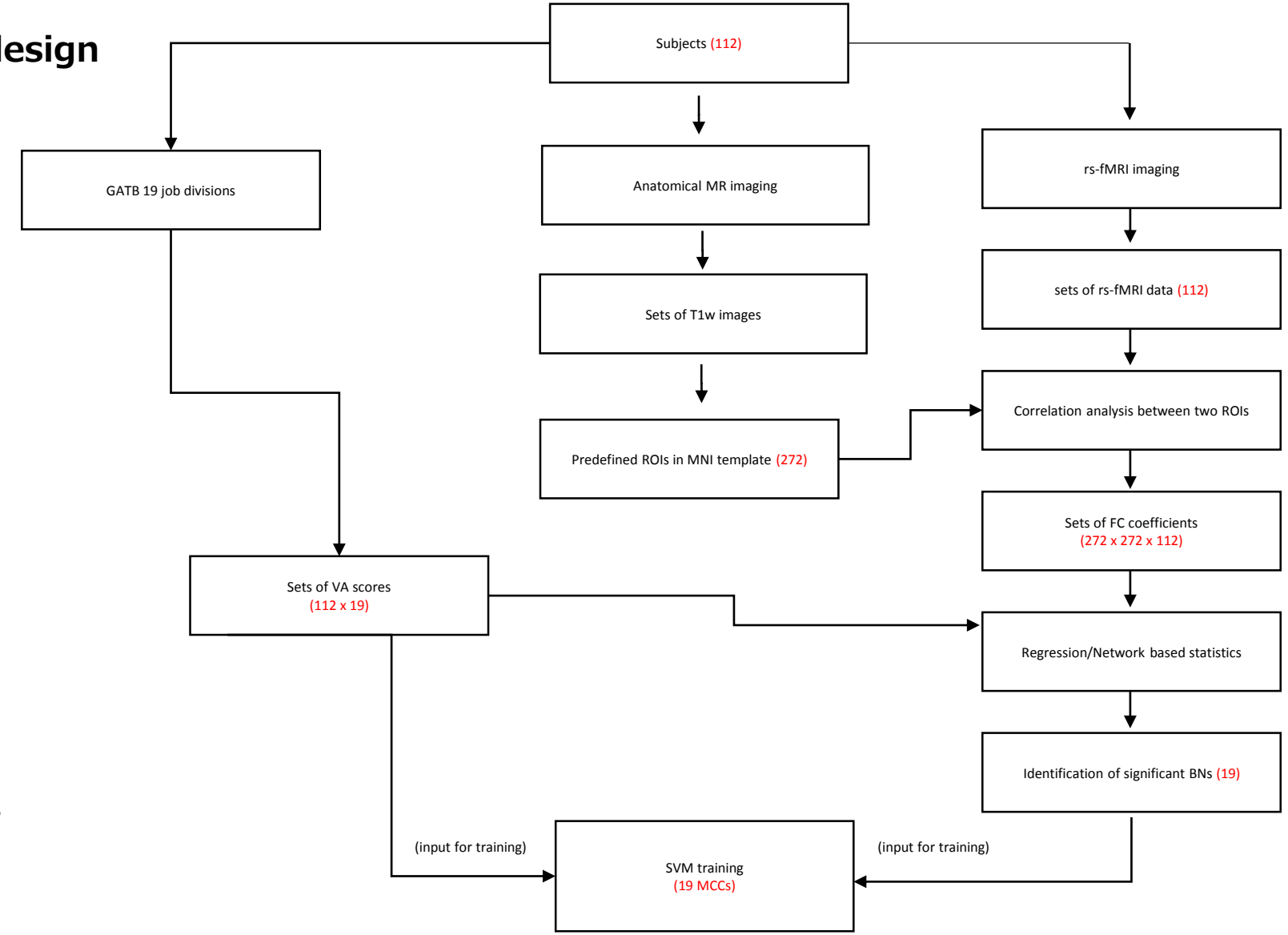
Ⅲ 2. 職業推定器の開発

- 職業適性をGATBの評価基準に従い、３段階にして
  ラーニングアルゴリズム(multi-class classifier)を設計。
- ラーニングアルゴリズムはmulti-class Support Vector Machine(SVM)を利用。
- 脳ネットワークごとに一つのmulti-class SVM classifierを設計。
- 脳ネットワークのセット(272個)から19個の脳ネットワークに対して
  significant accuracy(>33.3%)を有するclassifierが設計できた。
- 設計された１９個のSVM classifierで**職業適性19項目が推定可能**になった。

Ⅰ. 研 究 成 果 (2)

Training flow for SVM classifier design

Diagrams to illustrate the data flow for the primary data processing; identification of functional networks and derivation of multi-class classifiers (MCCs) using multi-class support vector machine (SVM). Step 1: resting-state functional MRI (rs-fMRI) signals are extracted from the predefined 272 ROIs, and functional connectivity (FC) matrices (correlation matrices) are constructed for the 112 training participants. Step 2: a simple regression and network-based statistics (NBS) analysis are performed for the FC matrices of the 112 participants, and functional brain networks (BNs) reflecting 19 job divisions are identified. Step 3: an input dataset (MRI data) to the MCCs—SVM classifiers—is constructed from the edges of the identified functional BNs in addition to another input dataset (vocational aptitude levels), which is constructed from the General Aptitude Test Battery (GATB). Step 4: the MCCs are trained by the input datasets. Step 5: the vocational aptitude (VA) levels of the job divisions estimated by the classifiers are compared with the VA levels determined by GATB to calculate accuracy.

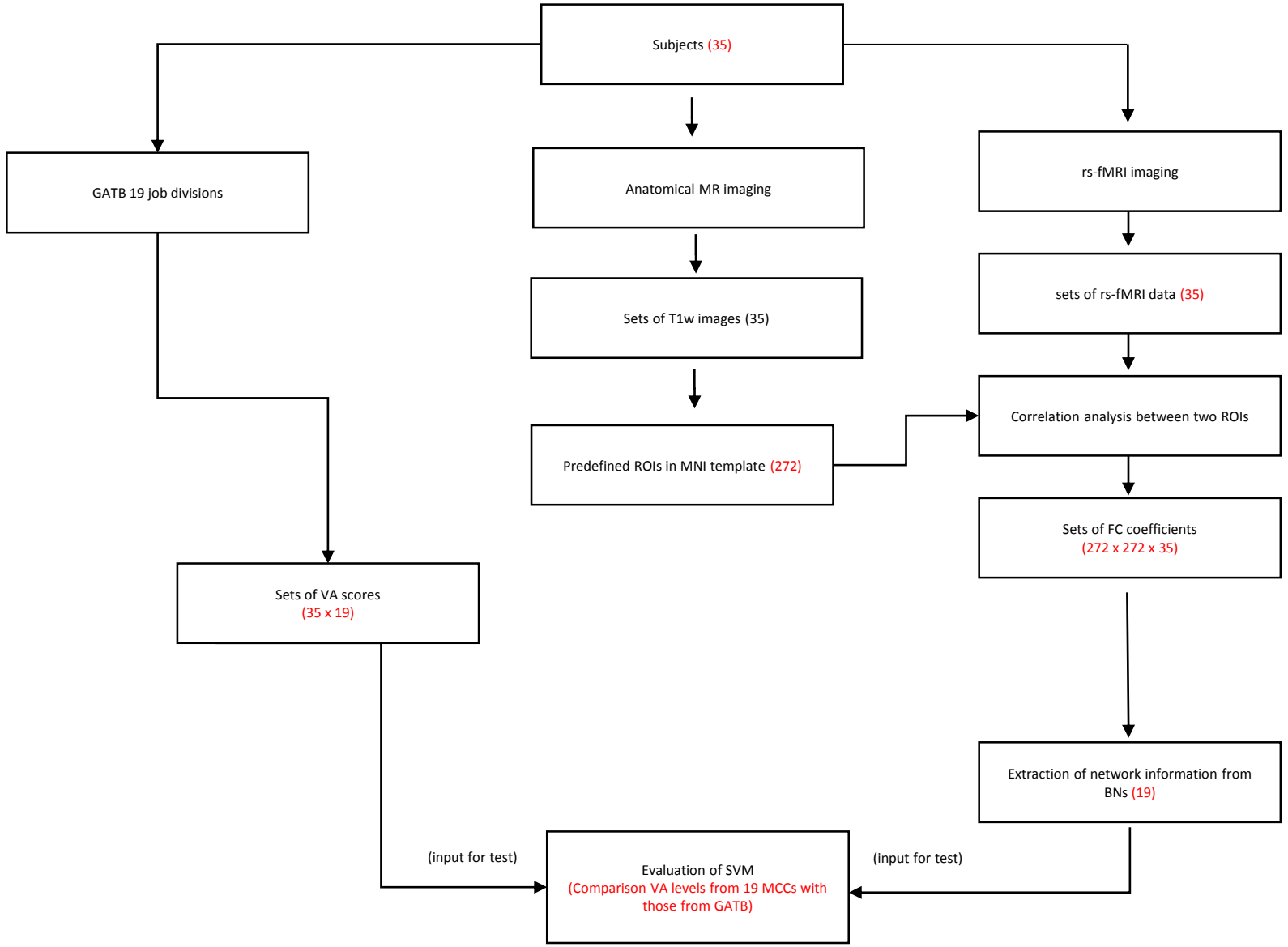


Ⅰ. 研 究 成 果 (2)

Ⅲ 2. 職業推定器の開発

Estimation flow from SVM classifier

Diagrams of data flow for the estimation. MCCs for the test group were verified: after making FC matrices for the 35 test participantsThe vocational aptitude (VA) levels of the job divisions are estimated by the MCCs. The VA levels estimated by the classifiers are compared with the VA levels determined by GATB to calculate accuracy.



Ⅰ. 研 究 成 果 (2) - Interim summary

Ⅲ

1．職業適性関連脳ネットワークの同定
2．職業推定器の開発

職業適性関連19個の脳ネットワークが同定できた。

職業適性が推定できる職業適性推定器（SVM classifier）を設計した。

働いている被験者のMRIデータから職業適性を推定し、
その職業に優位な適性を確認できた。

約36ヶ月間の大学生活の中で職業適性の変化を示したヒトの割合が
福祉関連が多かった。

Ⅰ. 研 究 成 果 (2)

Ⅳ　1．推定器の性能改善

ヒト特性推定器の**推定精度を改善**するための推定方法を考案した。

1）心理指標（SQ）のネットワーク：

ラーニングアルゴリズム（8 class-SVM）の教師データとしてMRIデータを使用。
各心理指標に対応するMRIデータを８グループにclusteringして得られる
8個のクラスターにラベルを与え、学習用教師データとして使用。

2）職業適性のネットワーク：

ラーニングアルゴリズム（3 class-SVM）の教師データとしてMRIデータを使用。
各職業適性に対応するMRIデータを3グループにclusteringして得られる
3個のクラスターにラベルを与え、学習用教師データとして使用。

Ⅰ. 研 究 成 果 (2) - Interim summary

Ⅳ　1．推定器の性能改善

MRIデータ分類後のSVMの設計では**高い推定精度**が得られた。

- **心理指標SQ：約80%**
- **職業適性：　約90%**

心理データとMRIデータの対応関係を活用した推定精度の高い分類器から脳機能の可塑的変化の**縦断的測定時の推定精度の改善が期待される。**

以上の知見を得た。

Ⅱ. ま と め

以下の研究成果より研究目標であるMRI測定による
個々人の社会的・職業的能力を推定するための情報基盤の策定
ができた。

1. **ヒト特性を現す心理データと脳MRIデータを統合したデータベース（TFU template）を構築できた。**
2. **データベースを用いたヒト特性推定器（SQ, IQ, EQ）を開発した。**
3. **データベースを用いた職業適性推定器を開発した。**
4. **データベースと推定器を用いて教育・訓練による脳機能の可塑的変化を検出できた。**

Ⅱ. まとめ

H26 年度
・大学生を対象とした縦断研究を行うための認知課題・MRI測定方法・データ分析法の選定・予備実験
・若年者・高齢者を対象とした横断研究への着手
・認知・脳機能測定パラダイムの向上と創出
完　了

H27 年度
・社会的・職業能力推定のための認知・脳機能の長期変化縦断データ収集への着手
・職業経験により発達する社会的職業能力固定の横断
・MRI測定・データ処理法の改良・開発
完　了

H28 年度
・中間的データマイニング
：教育・訓練課程、加齢・職業と相関する可塑性
・認知・脳機能モデルの推定
・測定方法・データ分析法の評価
完　了

H29 年度
・認知・脳計測による定量的指標の作成
・新たなデータ分析法の確立
・測定・分析過程のルーチン化
完　了

H30 年度
・研究全体のまとめ
・教育・職業による認知・脳機能変化に関する情報基盤(データベース)の策定
完　了

情報基盤の策定

1）心理・脳MRIデータベース作成

2）ヒト特性推定器・職業適性推定器の開発

3）可塑的変化の計測・検証

Ⅲ. 今 後 の 課 題

情報基盤の完成度を高めるために

① ヒト特性の推定精度の向上に向けた種々の評価

（1）今回の研究では心理測定によるデータを教師データとして脳機能ネットワークの同定を行った。しかし、個々人のヒト特性を表現する指標の妥当性・信頼性評価が必要である。

（2）ヒト特性が脳の機能部位または機能ネットワークにどのように顕現するか、また、脳に顕現するヒト特性に関するMRI測定限界などに対する評価が必要である。

（3）職業適性については多様な職業分野ごとに勤続年数の多いエキスパートをMRIで計測することにより職業と脳機能との相関を求める必要がある。

Ⅲ. 今後の課題

2 MRIによる計測と測定データ処理の精緻化

（1）測定精度の評価及び向上方法の考案

1：MRI装置由来の測定誤差の評価及び除去方法

2：被験者由来の測定誤差の評価及び除去方法

（2）推定精度の向上方法の考案

1：脳機能ネットワークの同定方法の改善・考案

2：マシンラーニングによる推定方法の改善・考案

3 学習効果の評価指標の明確化

（1）各教育カリキュラムの意図するゴールを明確に定義する必要がある。

（2）個々人によって異なるゴールにおける達成程度の評価指標が必要である。

(補足資料)

１．研究課題名：

『平成 26 年度採択私立大学戦略的研究基盤形成支援事業「社会的・職業能力育成プログラムに資する認知・脳科学エビデンス情報提供基盤の構築」』

２．背景：

昨今の教育現場では、経験豊かな教育者らの実践の妥当性や、学習者の行動について認知・脳科学研究の知見・エビデンスから検討しようとする動向がある。このような動向は教育現場に限らず、精神医学等の心を最たる問題とする医療現場や消費者の購買行動の正確な予測を目標とするビジネスの現場でも盛んである。本事業の取り組みは高まる関心をよそにほぼ手つかずの領域であった教育現場に焦点を合わせて、認知・脳科学的基盤技術の提供を目指す極めて重要な事業である。

従来の認知・脳科学研究の成果は、個々人に共通する法則性・全体的傾向に着目したものであり、ケース（個人）をいかに理解するかに着目しなければならない教育現場にその成果を還流することは困難であった。本事業はこうした状況を克服するべく、個々人の社会的・職業的能力の定量的な推定・理解・育成を志向した研究を展開する。

３．研究目的：

心の働きやそれを司る脳の機能は、教育や訓練、職業、成人までに形成されたパーソナリティ特性等に依存して、適応的に変化すると考えられる。この変化は認知・脳機能の最たる特徴（可塑性）である。近年の認知・脳科学研究は言語学習による可塑性に注目してきたが、長期にわたる教育効果や職業やパーソナリティの影響の検討には至っておらず、研究・計測環境の問題も大きく実現には至っていない。本研究では、教育・職業・パーソナリティ等の要因がいかにして認知・脳機能をダイナミックに変容させるかを、大学在籍期間の数年にわたって追跡する縦断研究と、年齢や職業経験の点で異なる集団間の変動を比較する横断研究を統合したマトリクス的アプローチにより明らかにする。得られた成果を大学等の教育機関・高齢者福祉施設・医療機関へ情報提供し、社会的・職業能力を育成する教育プログラムの改善支援へつなげていく。

４．研究戦略・方法：

(1) 研究戦略：

大学在籍期間の数年にわたって個人の変化を追跡する縦断研究と、職業経験や性格特性等の種々の点で異なる集団間の差異を比較検討する横断研究を統合したマトリクス的アプローチの採用

(2) 研究方法：

1) 心理・行動指標を用いたヒト心理・行動特性の計測

2) MRI によるヒト脳機能・構造の計測

3) 脳機能・構造情報からのヒト特性の推定方法の開発

５．研究過程：

(1) H26 年度での研究、MRI アップグレード、MRI 測定方法とパラメータの設定、予備実験、心理指標のための質問紙の準備などを計画通りに終えて、H27 年度から本実験を始めた。

(2) 教育・訓練による脳の可塑的変化を検出する上で必要な心理・脳データ基盤を作るための心理データと MRI データを収集した。

(3) MRI 解剖画像により、心理指標に関連する脳部位を同定し、心理指標を表現する脳部位のセットを作成した。

(4) MRI 機能画像により、心理指標（社会能力：SQ）に関連する脳機能ネットワークを同定した。H28 年度以後、その他の心理指標(IQ, EQ)をも含む脳機能ネットワークと脳部位のセットからデータベース（TFU template）を作製した。

(5) 脳の長期的な可塑的変化の測定を行った。

(6) H28 年度以後 MRI の縦断データの収集を継続するとともに、ヒト特性の可塑的変化の計測を行った。数十分間の認知トレーニングによる短期的可塑性と約 3 年間の大学生活による可塑的変化を心理測定により計測した。

(7) 心理測定によるデータと MRI による脳機能・構造データからなる TFU template とマシンラーニングを利用してヒト特性推定器（MRI データから各種心理指標を推定できるアルゴリズム）の設計を行った。

(8) MRI データが格納されている folder を指定した後、数ステップで SQ、IQ、EQ 等のヒト特性の推定結果が得られるヒト特性推定器の Stand Alone 版のユーザーインタフェースプログラムの作成を行った。

(9) 心理測定による職業適性データと MRI による脳機能・構造データ（TFU network と他機関が提供する脳構造データ）からなる Template とマシンラーニングを利用して職業適性推定器の設計を行った。

(10) ヒト特性推定器と職業適性推定器を用いて MRI データから各個人の約 3 年間の可塑的変化の推定を 12 名のデータを用いて行った。

６．研究結果・成果

(1) 参加協力者数（2019 年 2 月現在）

1) 心理測定参加者　331 名(男性 114 名、女性 217 名；平均年齢 18.9 ± 0.93)

2) MRI 測定参加者　心理測定参加者の中の 219 名（約 2 ヶ月ごとの縦断測定参加者の繰り返し測定を含める延べ測定数 811 名）

(2) 心理測定データと MRI データから 163 個の脳部位が同定できた。

(3) MRI データから同定された 163 個の脳部位をもとに各心理指標項目 130 個のうち 111 個を表す脳機能ネットワーク 111 個が同定できた。163 個の脳部位と 111 個の脳機能ネットワークにより東北福祉大学のデータベース（TFU template）を構築できた。

(4) 同定された脳機能ネットワークをもとに MRI データから 111 個の各心理指標が推定でき推定器が同定できた。また、MRI データから 111 個の心理指標を同定するヒト特性推定器をパソコン

上でユーザーインタフェースとして実現できた。

(5) 認知実験により、短期間の認知トレーニングによる認知機能の可塑的変化の検出ができ、physical training または長期的な学習訓練のみならず、短期間の認知トレーニングでも脳の可塑的変化が起きることを確認できた。

(6) 心理測定においても約 3 年間（30 ヶ月間以上）の大学生活により一部の心理指標において有意な変化があることが確認できた。

(7) ヒト特性推定器により約 3 年間約 2 ヶ月の間隔で縦断的測定を行ってきた 12 名の参加者の脳の可塑的な変化が検出できた。

(8) 職業適性・能力についてもヒト特性と同様に心理測定と MRI データから 19 職種の能力が評価できる職業適性推定器が開発できた。

(9) 5〜10 年の経験のある二つの職種群（看護関連職種と事務関連職種）に属する研究協力者に対して MRI データから職業適性推定器を利用し職業適性を推定した。その結果、職種の違いが脳機能ネットワークに反映されていることが確認できた。

(10) さらに縦断研究参加者 12 名のデータから看護関連職に関連する脳機能ネットワークでの可塑的変化が事務関連職に関連する脳機能ネットワークでの可塑的変化より多いことが確認でき、本学の教育課程による可塑的変化の可能性が示唆された。

7．まとめ

ヒトの各種心理・行動特性を総合的に評価した心理指標のセットとそれに対応する MRI データからなる中規模のデータベースの構築、さらに心理指標を表現する脳部位とネットワークからなるテンプレート（TFU template）の作成が完了した。さらに、それらを用いたヒト特性推定器・職業適性推定器の開発と、その推定器による縦断的可塑性の検出が可能になったことから、本研究事業の目標である“個々人に焦点を当てた社会的・職業的能力の定量的な推定・理解・育成を志向し、個々人を評価できる認知・脳科学的知見からの情報提供基盤の形成”が概ね達成できたと言える。

8．研究結果・成果における限界と課題

(1) 今回のデータベースの元となる 153 名のデータサンプルを用いて、統計的に有意な結果を得ることが出来た。しかし、このデータサンプルが日本全体のデータに対してどの程度の代表性を表すかについて検討を行う必要がある。また、最近の国内外の動向及び精度の向上の観点から、より規模の大きいデータベースへの拡張の必要性も検討する必要がある。さらに、心理指標同士の相関（独立性、重複機能）を検討して、各心理指標で構成されるヒト特性空間を総合的に現す新たな心理指標の作成についての検討も必要である。

(2) 縦断研究により可塑的変化が確認できたものの、測定のために使用したデータのサンプルサイズが小さいために大学の教育カリキュラムなどと可塑的変化の関連を解明するまでには至らなかった。10 回以上の繰り返し測定データについてのみ分析を行ったが、繰り返し測定の回数が少ないデータについても可塑的変化の検出が出来るように分析方法を検討する必要がある。また、この研究成果の発展を図る上で、今後新たな研究計画の策定をも検討する必要がある。

(3) 質問紙などの心理測定と resting-state fMRI により同定された脳機能ネットワークの機能的選

択性などの比較検討のために task fMRI またはメタ分析による検討が必要である。しかし、課題作成などの限界とメタ分析のための既存の task fMRI によるデータベースの不足などから、現段階での比較検討は困難であるため、今後、長期的な視野のもと検討方法などを計画していく必要がある。その一環として、現在、task-applied resting state fMRI パラダイムを考案して、通常の resting-state fMRI 測定と同様な条件で持続的に課題（パズル課題、実行機能課題など）を与えながら fMRI データを得ることにより task 時の脳機能ネットワークを同定する実験を遂行している。

(4) 脳機能ネットワークの同定で用いた 163 個の脳部位のセットにおける個々の脳部位は特定の心理特性を表現するものであり、同定されたネットワークの機能的特性を理解する上で有用である。しかし、その脳部位セットは脳全体を均一にカバーするものではなかった。より均一な脳部位セットを作成するために task fMRI データなどを追加して同定精度の比較を行う必要がある。

(5) 職業適性・能力の脳機能ネットワークの同定では、関連する心理・行動指標の数が少なかったことなどから、他の研究グループが作製した既存の脳部位のセットを組み合わせて構成した 272 個からなる脳部位のセットを用いた。TFU template の 163 個の脳部位セットと比較検討の上、二つを統合することをも検討する必要がある。

(6) 同定された各脳機能ネットワークは統計的に有意に関連する心理指標を表しているが、必ずしもそのネットワークが関連するヒト特性を処理するための核心的機能的活動に参加するとは限らない。この問題を解決するための方法の考案が要求される。

(7) ヒト特性推定器（８段階、約 30%の精度）と職業適性推定器(３段階、約 60%の精度)は現状でも応用方法を工夫することで実用的に使用可能である（グループデータの評価または個人データの場合は数回の反復測定などによる評価）が、より性能の向上が必要であり、そのための研究を継続している。MRI データだけで設計した推定器の精度は約 80%であり、追跡測定においては有効であると考えられるが、心理特性推定を含む精度の向上のためのさらなる努力が要求される。

(8) 心理測定と MRI 測定の両側面から測定誤差について検討が必要である。心理測定はより大規模なデータによってその妥当性・信頼性が評価されているので、今回のような中規模のデータでの測定の妥当性・信頼性については慎重に検討する必要がある。MRI 測定については、機械ノイズ、生理的変化などの測定誤差とともにデータ分析時の脳画像の標準化などの過程における誤差も含まれる。このデータ処理プロセスについては、他の方法、例えば、Human Connetome Project の一連のデータ処理パイプラインなどとの比較・検討を行う必要がある。また、脳ネットワークの定量化、グラフ理論で用いられる複数のネットワーク指標の比較検討も必要である。task fMRI データの追加とこのような誤差低減努力を通して推定精度の向上も期待できる。

８．今後の方針

今後は収集を終えた縦断データに基づいて、大学における社会的・職業能力の育成効果の抽出を行うとともに、一個人の受けた大学教育・大学生活の中での種々の経験の何が社会的・職業能力を育む糧となったのかの検討を行う形で本事業を纏め上げる。本事業において作製されたヒト特性推定器については、個々人のヒト特性を表現する指標の妥当性・信頼性の評価とヒト特性に関する MRI 測

定の限界についての評価、また職業適性推定器については、多様な職業分野ごとに勤務年数の多いエキスパートの脳機能測定データの活用を行っていくことで、推定精度のさらなる向上を目指す。

来年度は、本事業の成果を発展的に活用することを意識して、超高齢化する地域社会で生活する人々の認知機能に焦点を当てた研究を展開していく。とりわけ加齢に伴う通常の認知機能変化・軽度認知障害（Mild Cognitive Impairment: MCI）・認知症（主としてアルツハイマー型認知症）をターゲット分野として、多様な脳機能・構造指標および心理指標を用いて中高年の脳機能・構造画像および心理特性データベースを作成し、ヒト特性推定器の対象範囲の拡大を目指す。そのため、「介護老人保健施設せんだんの丘」との共同研究を中心とした研究体制の確立、半年または 1 年ごとの経時的変化の測定も含めたデータ計測・分析方法の選定、研究協力者の選定など研究フレームワークの構築を着実に進める。

９．同時並行で推進している研究課題のまとめ

(1) 各種認知実験（実行機能、メタ認知など）データ
(2) Diffusion Weighted Imaging による白質データ
(3) 脳活動に伴う fast signal の検出方法の検討
(4) 脳の可塑的変化と T1-value の関係
(5) resting state fMRI と brain metabolism の関係などについて得られている prelimenary なデータ・測定方法などをより発展させることにより、脳部位・脳ネットワークの機能特性の理解に活用できると期待できる。

１０．心理測定と MRI 測定の詳細

(1) 心理測定に使用された心理指標の一覧
(2) MRI 測定条件とデータ処理方法

（1）心理指標一覧

List of psychometric parameters. (**1-78**: Social ability/skill, **79-96**: IQ, **97-130**: EQ)

	Parameters
1	Cognitive competence
2	Extracurricular competence including physical competence
3	Social competence with friends of the same sex
4	Social competence with friends of opposite sex
5	General self-worth
6	**Perceived Competence Scale for Adolescence**
7	Inhibitory Control
8	Activation Control
9	Attentional Control
10	**Japanese version of Effortful Control (EC) scale for adults**
11	Trust vs. Mistrust

Autonomy vs. Shame/Doubt
Initiative vs. Guilt
Industry vs. Inferiority
Identity vs. Role Confusion
Intimacy vs. Isolation
Japanese version of Rasmussen’s Ego Identity Scale (REIS)
Behavioral Inhibition System (BIS)
BAS / Driver
BAS / Reward
BAS / Fun Seeking
Behavioral Inhibitory System(BIS)/Behavioral Activate System (BAS) Scale
Rosenberg Self Esteem Scale (RSES)
Anxiety regarding others' evaluation of oneself and perceived maladjustment to interpersonal situations
Emotional disturbance
Difficulty in expressing opinions
Japanese version of Jones and Russell's Social Reticence Scale for college students
Beginning social skills
Advanced social skills
Skills for dealing with feelings
Skill alternatives to aggression
Skills for dealing with stress
Planning skills
Kikuchi’s Scale of Social Skills (KiSS-18)
Public self-consciousness
Private self-consciousness
Self-consciousness scale for Japanese
Japanese Version of the Self-Concept Clarity (SCC) Scale
Self-Continuity Function Subscale
Directing-Behavior Function Subscale
Social-Bonding Function Subscale
Japanese version of the TALE (Thinking About Life Experiences) Scale
Japanese Version of the Ego-Resiliency Scale (ER89)
Positive Problem Orientation (PPO)
Negative Problem Orientation (NPO)
Problem Definition and Formulation (PDF)
Generation of Alternative Solution (GAS)
Decision Making (DM)
Solution Implementation and Verification (SIV)

Rational Problem Solving (RPS)
Impulsivity / Carelessness Style (ICS)
Avoidance Style (AS)
Japanese version of the Social Problem-Solving Inventory-Revised (SPSI-R)
Negative-Self (NS)
Positive-Self (PS)
Negative-Other (NO)
Positive-Other (PO)
Japanese version of the Brief Core Schema Scale (JBCSS)
Intentional behavior
Planfulness
Readiness for change
Using resource
Japanese version of the Personal Growth Initiative Scale-II (PGIS-II)
Subjective Happiness Scale (SHS)
The Satisfaction with Life Scale (SWLS)
State Anxiety (A-State)
Trait Anxiety (A-Trait)
Japanese edition of State-Trait Anxiety Inventory
Positive symptoms
Negative symptoms
Disorganization
Schizotypal Personality Questionnaire (SPQ)
Social skill
Attention switching
Attention to detail
Communication
Imagination
Autism-Spectrum Quotient

Verbal Intelligence Quotient (VIQ)
Performance Intelligence Quotient (PIQ)
Full scale Intelligence Quotient (FIQ)
Fluid intelligence
Crystallized intelligence
Verbal Comprehension
Perceptual Organization
Vocabulary
Similarities

88 Arithmetic
89 Digit Span
90 Information
91 Comprehension
92 Picture Completion
93 Digit Symbol
94 Block Design
95 Matrix Reasoning
96 Picture Arrangement

---

97 Emotional awareness
98 Self-efficacy
99 Perseverance
100 Enthusiasm
101 Self-decision
102 Impulse control
103 Patience
104 Sharing positive emotion
105 Sharing negative emotion
106 Personal consideration
107 Voluntary support
108 Personal management
109 Sociability
110 Cooperation
111 Decision making
112 Optimism
113 Group consideration
114 Influence
115 Risk management
116 Tactfulness
117 Adaptability
118 **Self-awareness**
119 **Self-motivation**
120 **Self-control**
121 **Empathy**
122 **Altruism**
123 **Interpersonal relationship**
124 **Situational awareness**
125 **Leadership**

126 **Flexibility**
127 **Intrapersonal Emotional Quotient Scale (EQS)**
128 **Interpersonal EQS**
129 **Situational EQS**
130 **EQS Total scale**

（2）MRI 測定条件とデータ処理法

1）MRI 測定条件

A 3-Tesla MRI scanner (Skyra-fit; Siemens Co., Erlangen, Germany) was used. All subjects were scanned in two sessions corresponding to a structural image (T1) measurement for VBM and a functional image measurement (resting-state fMRI). Structural images were acquired using the following parameters: repetition time = 1900 ms, echo time = 2.52 ms, matrix size = 256 × 256, in-plane resolution = 1 × 1 mm^2, slice thickness = 1 mm, and number of slices = 192. The imaging orientation was sagittal. Resting-state fMRI data were acquired using the following parameters: repetition time = 1000 ms, echo time = 24 ms, matrix size = 64 × 64, in-plane resolution = 3.4 × 3.4 mm^2, slice thickness = 3.4 mm, and number of volumes = 480. In the resting-state fMRI session, subjects were asked to lie on the bed and not to wander their mind with their eyes open and to gently focus their eyes on the center of the visual field. The lights in the room were turned off during all MRI scans.

2）MRI データ分析

VBM analysis. For identification of functional networks anatomical brain templates such as automated anatomical labeling (AAL) atlas have been used. To avoid partial volume effect and improve sensitivity, in this study, we tried to identify brain areas specific to psychometric parameters in each of gyri in AAL atlas. MRI data were analyzed using VBM8 implemented in the Statistical Parametric Mapping software (SPM 12), which was implemented via Matlab 2015a. The pre-processing by VBM8, with the default parameters used in each step, included segmentation with a bias-corrected option and spatial normalization with diffeomorphic anatomical registration using exponentiated Lie algebra (DARTEL), normalization to the Montreal Neurological Institute and Hospital (MNI) coordinate system with smoothing with an 8-mm full-width at half-maximum (FWHM) filter, and modulation by Jacobian determinants, which provided segmented, normalized, and modulated gray matter images. After preprocessing, a statistical test (simple regression analysis) was used to identify brain areas correlated with each psychometric parameter. In the regression analysis, total brain value (TBV) was used as a covariate. Our purpose was to find specific brain areas in AAL gyri we performed a small volume correction in each gyrus based on the AAL atlas to correct for multiple comparisons (Gur et al., 2000; Singh et al., 2014). The statistical threshold was set at an uncorrected $p = 0.001$ and at $p = 0.05$ for family-wise error (FWE) correction at the voxel level.

rs-fMRI analysis. For functional MRI data, we used the data processing assistant for resting-

state fMRI software (DPABI) (Chao-Gan and Yu-Feng, 2010; Yan et al., 2016) to pre-process the data of all 153 subjects. The pre-processing included slice-scan time correction, 3D motion correction (maximum head motion: 151 subjects passed the maximum threshold of 1.5 mm and 1.5 degrees, and other two subjects passed the maximum threshold of 3.0mm and 3 degrees), removal of head motion effects by the Friston 24-parameter model, bandpass temporal filtering (between 0.01 and 0.1 Hz), and artifact rejection based on the CSF signal. These functional images were smoothed with a 6-mm FWHM filter and co-registered with each corresponding structural image. All resting-state functional images were analyzed by ROI-based correlation analysis for the predefined 163 ROIs identified by VBM. In the analysis, for the time courses of the 163 ROIs, correlations were calculated, and correlation coefficient matrices (163 × 163 × 153) were created. A simple regression of the correlation coefficient matrices was performed with psychologically measured scores of the psychometric parameters, and then network-based statistics (NBS) were performed to identify sets of significant brain networks (i.e., a brain network for each psychometric parameter). (Zalesky et al., 2010) to identify sets of significant brain networks (mostly a brain networks for each psychometric parameter. In this step, randomly shuffled correlation matrices were generated for a permutation test. Then, correlational analyses were performed on the true correlation matrix with psychometric parameters, and a non-parametric permutation test was performed on random correlation matrices with 5000 iterations. Correction for multiple comparisons based on NBS statistics was performed at an initial threshold of $p < 0.005$, and the number of edges in the network was limited to as close to 15 as possible. Previous research has shown that a small number of brain connections can predict a psychiatric disorder(Yahata et al., 2016).

SVM analysis (*Classifier design*). SVMs are typically used to identify a hyperplane that distinguishes between 2 groups. But in this study we attempted to design 8-class SVM classifiers. Behavioral scores are measured on a scale of 1 to 100. Our purpose is ideally to measure psychometric parameters by MRI at the same scale. However, there are several limitations such as sensitivity and number of samples. So, we reduced it to a scale of 1 to 10, 10 levels. But in classification study such as the neural network, the number of levels should be a power of 2. Therefore we decided to use 8 (i.e., 2^3) classes. The 8-class SVM classifier can estimate the score of a psychometric parameter from rs-fMRI data into 8 levels. Although psychometric parameter scores are linear and some regression analyses such as support vector regression can be applied, we attempted to design the SVM classifiers because a discretization is generally stable to variations and some variations would exist in fMRI and psychometric measurements.

Multiple class classification with the one-against-all (OAA) method (Bishop, 2007) was performed using LIBSVM (Chang and Lin, 2011), which was implemented in Matlab 2015a (MathWorks, Sherborn, MA, USA). The OAA method involved two steps: training a single classifier per class with one positive sample of each class and all other negative samples of the remaining classes and repeating the procedure for the total number of classes. The classifier with the highest

classification score was selected as a final multi-class classifier.

SVM analysis (*Data preparation for training - Classification*). Data sets for the SVM classifier design were prepared from the results of the brain network analysis and the psychologically measured data. The input dataset consisted of data matrices of features and labels. A feature data matrix consisted of edges of a network (correlation coefficients of networks and a label matrix consisted of psychologically measured data. For classification label data (the label matrix), the scores of psychologically measured psychometric parameters were normalized and divided into eight classes by the equation {(x-min) / (max-min)} * 8, where x is the score of the psychologically measured psychometric parameter. In the calculation results, the number after the decimal point was rounded up. The dimensions of a feature matrix were the number of edges by the number of subjects, and the number of feature matrices was the number of functional networks. Therefore, the dimensions of the input data set for the SVM were the number of edges by the number of functional networks by the number of subjects. The dimensions of the label matrices were the number of functional networks (scores of psychologically measured psychometric parameters rated into one of eight classes) by the number of subjects.

(*Training of classifiers*) With the data sets of all psychometric parameters, a leave-one-out cross validation was run using a radial basis function (RBF) kernel defined as $K(x, y) = \exp(-\gamma \parallel x - y \parallel^2)$ for optimizing the C and gamma (γ) values. In parameter optimization, the grid-search method was performed with various ranges of C and γ values ($C = 2^{-5}, 2^{-4}, \ldots, 2^{15}$, $\gamma = 2^{-15}, 2^{-14}, \ldots, 2^{15}$). After cross validation, the multiple class classifiers of the psychometric parameters with the best C and γ values were varied and deemed significant.

評　価　票

記入日　　平成 31 年 4 月 15 日

評価委員氏名　松岡　和生

※下記項目について評価コメントをご記入のうえ、Ｓ～Ｃの４段階で下線部にご記入願います。

１．研究計画の達成状況　Ａ　（　Ｓ，Ａ，Ｂ，Ｃ　）

本研究プロジェクトの研究計画は概ね達成していると評価できる。

ヒトの各種心理・行動指標と脳機能データを対応づけるデータベースの構築と、それに基づくテンプレートからヒト特性を推定するための研究ツール（ヒト特性推定器）の開発に成功しており、この推定器を使って短期・中期・長期間に渡ってその可塑的変化を検出した研究成果も得られている。技術的な精度、信頼性、推定器ツールによる対象者の追跡調査等、残された課題はあるが、「教育現場に焦点を合わせて、認知・脳科学的基盤技術の提供を目指した」本事業の当初目標は十分に達成されている。

２．研究成果に対する評価　Ｓ　（　Ｓ，Ａ，Ｂ，Ｃ　）

①特に優れている点（成果の卓越性）

1) 心理測定と対応づけが可能な MRI 計測データの参加者は 200 名を超えており、縦断測定参加者の繰り返し測定を含むと延べ 811 名の MRI 計測データが収集されている。健常者の認知・行動特性との関係を検討した脳機能計測研究としては、類をみないデータ数といえる。また対象とされた心理・行動指標の数は 100 変数を超えており、その範囲も多様である。これらの諸変数と安静時脳機能結合データにもとづいて、脳機能ネットワークと関連づける大学生のデータベースが構築されたことは卓越した研究成果と思われる。

2) 認知特性および職業適性を推定するツール（推定器）の開発にある程度成功している。このツールは脳機能計測データを活用した画期的な手法であり、多方面への応用が考えられることから、本研究の中核的成果として高く評価される。

3) 本研究プロジェクトで蓄積された心理・行動指標と脳機能指標のデータベースとそれに基づいて作成された心理指標を表現する脳部位とネットワークのテンプレート(TFU template)は、広く心理―脳特性の個人差に関わる研究への応用・適応が可能であり、大学生の標準化データベースとしての利用価値も高い。日本におけるヒト脳機能研究の大きな財産となるものであり高く評価できる。

4) 本研究プロジェクトでは、従来検討されてこなかった a) 脳機能ネットワークによる「個々人」のヒト特性の同定、b) 縦断的な計測による脳の機能部位および機能ネットワークの「可塑的変化」の検出、という極めて挑戦的な研究課題に取り組んでいる。MRI テクノロジーを用いたヒト認知・脳特性研究に新たな道を開いた研究として高く評価できる。

5) MRI を用いた脳機能イメージ研究が教育・職業訓練の実践の場に具体的に応用可能であることを示した研究事業として重要な意義をもつ。

②伸長すべき点（今後の課題）

1) 本データベースを日本人の標準化データとしての活用可能なものしていくには、本研究で作成されたテンプレートを他の年代やグループへと拡張し適用していく必要がある。
2) 大学における教育カリキュラムの効果や社会的・職業能力の育成効果を推定するためには、卒業後の追跡調査が必要である。今後の課題として予定されているが、その研究成果が期待される。
3) ヒト特性推定器と職業適性推定器を用いた MRI データから、各個人の可塑的変化の推定が行なわれている。画期的な研究成果であるが、データ数はまだ十分ではなく今後のデータの蓄積が期待される。
4) 本研究では先端的な MRI 計測技術と解析技法が使われているが、将来的には、さらに多人数・多変量のビックデータの構築とその解析に対応するために、新たな MRI 計測解析技法の開発が望まれる。

③予想される波及効果

1) 本研究事業の成果は、いうまでもなく社会貢献に直接的に結びつくものになる。特に、個々人の知的能力や性格，資質あるいはそれらを変容させうる教育・訓練効果に対して、脳構造／機能レベルでエビデンスを与えるという重要な意義をもつ。したがって、本研究成果から得られた手法は，医学、心理学，認知科学，脳科学の分野だけでなく，大学教育，職業キャリア教育，科学や芸術における創造的能力の開発，本人に自覚されない隠された能力の発見，スポーツ，芸術，音楽におけるトレーニング効果への応用等，その波及効果は広範囲に及ぶことが予想される。
2) パーソナリティ等の心理学における査定研究の分野への波及効果も大きいと思われる。心理学における個人の性格や資質の研究は，その多くが心理検査や質問紙調査によって行われている。特に，社会的な心理・行動特性に関する研究は，質問紙尺度研究が一般的である。本研究において，脳構造／機能の量的データベースによって，生物学的なエビデンスを容易に提供できる道が開かれたことにより，従来の研究スタイルに大きな変化をもたらす可能性がある。
3) 知性の心理学・認知脳科学研究への波及効果も予想される。近年，多重知能理論，社会的知能やサクセスフルインテリジェンス，情動知能，心の理論など，人の知性を捉える枠組みが社会性や情動性にまで広がっている。人間の知的能力の本質的特徴とは何か，社会的・職業的な実践場面において真に必要とされる知的能力とは何か，という問いのもとで展開されてきた諸研究であるが，いずれもその実証的なエビデンスは心理・行動レベルにとどまっている。脳機能イメージング技法を用いた本研究の成果は、応用可能性の面で、人間の知性と感性の理解のための次世代の研究へと進む基盤ないし契機になると思われる。

３． 今後の展望（意見、助言、提案等） Ｓ （ Ｓ，Ａ，Ｂ，Ｃ ）

1) 本研究で得られた研究成果から、新たな研究への展開が期待される。特に、本研究で開発され「ヒト特性推定器」と名づけられた脳機能データから認知・職業能力を予測する研究ツールは医療、教育、AI などの分野へ広く適用が可能である。

2) エキスパート研究の重要性：本プロジェクトで開発された最新テクノロジーを用いて、様々な職業領域、分野において修練を積んだ人々あるいは特異な認知能力を持つ人々など、職業エキスパートおよび認知能力エキスパートを対象とした脳構造および脳機能ネットワークの検討は新たな研究展開をもたらす可能性がある。一部はこのあとの研究課題として挙げられているが、認知・脳機能科学分野においては優先的に取り組むべき重要課題と思われる。

3) ビックデータ化とＡＩ利用への展開：将来的には、ヒト認知能力の開発育成と変容に関するビックデータ化が構想されていくことになるだろう。現段階では中規模データベースの構築にとどまっているが、これをさらにビックデータ化しＡＩを用いた研究へとつなげていくために、さらに脳機能計測における先端的な技術開発とシステム構築が期待される。

4) 本研究では、個人の変化を追跡する縦断研究と異なる集団間の差異を比較検討する横断研究を統合したマトリクス的アプローチが採用されているが、今後は、このマトリクスに基づいた、認知・職業能力の可塑的変化に関わる「統合的な理論モデル」ないしは「グランドセオリ」の提案が必要になってくると思われる。

４．総評 Ｓ （ Ｓ，Ａ，Ｂ，Ｃ ）

心理測定と MRI 計測データからヒトの認知特性と職業適性能力を評価する試みは脳機能イメージング技術を使った次世代研究へとつながる研究課題として注目度の高いプロジェクトである。同一集団の多数の大学生を対象に、数年間にわたって心理測定と MRI 計測に基づく脳構造／機能の可塑的変化を追跡し、ヒトの能力・適性を推定する手法を開発していくことは容易な課題ではない。それを実現した本研究事業は学術的にも社会的にも大きな成果を残したものとして高く評価することができる。心理学と認知・脳科学の連携による社会的課題解決型の実践的な研究事業として、次のステージへの進展が期待される。

評　価　票

記入日　　平成 31 年 3 月 21 日

評価委員氏名　出江　紳一

※下記項目について評価コメントをご記入のうえ、Ｓ～Ｃの４段階で下線部にご記入願います。

１．研究計画の達成状況　Ｓ　（　Ｓ，Ａ，Ｂ，Ｃ　）

本事業の研究目標である「個々人に焦点を当てた社会的・職業的能力の定量的な推定・理解・育成を志向し，個々人を評価できる認知・脳科学的知見からの情報提供基盤の形成」が達成できたと考えられる．

２．研究成果に対する評価　Ｓ　（　Ｓ，Ａ，Ｂ，Ｃ　）

①特に優れている点（成果の卓越性）

第一に，心理測定参加者 331 名，MRI 測定参加者 219 名（延べ 811 名）のデータに基づいて 163 個の脳部位を同定し，心理指標項目を表す 111 個の脳機能ネットワークにより TFU template を構築した．第二に，短期間の認知トレーニングによる認知機能の可塑的変化を検出するとともに，３年間の大学生活による変化を確認した．第三に，ヒト特性推定器，職業推定器を開発し，その推定器による縦断的可塑性の検出に成功した．第四に，看護関連職と事務職のそれぞれの脳機能ネットワークの可塑的変化を比較し前者がより大きいことを示した．

②伸長すべき点（今後の課題）

第一に，今回の成果を日本全国に適用できるかどうかの検討，それに向けたより規模の大きなデータベースの構築が求められる．さらに心理指標間の関係の分析に基づいてデータベースを深化させることが課題である．第二に，縦断研究のサンプル数を増やすために繰り返し測定の回数が少ないデータについても可塑的変化を検出できる分析方法を検討する必要がある．第三に，MRI データのメタ分析を，脳全体をカバーして可能とする計測パラダイムを検討するとともに，今回同定された職業適性･能力の脳機能ネットワークについて TFU template を統合することを検討することが課題である．第四に，ヒト特性推定器と職業適性推定器の精度をさらに上げることが課題である．第五に，心理測定と MRI 測定についてさらなる誤差低減努力が求められる．

③予想される波及効果

第一に，大学における社会的・職業的能力の育成効果を，脳の可塑性を基盤とする学習的変化として定量的に評価することが可能となる．第二に，高齢者の認知機能低下を負の学習的変化と考えれば，本研究成果は，加齢に伴う認知機能の変化をターゲット分野として応用可能であり，脳機能・脳構造データと心理特性データからなるデータベースを作成し，推定器を拡張応用することが期待される．

３．　今後の展望（意見、助言、提案等）　Ｓ　（　Ｓ，Ａ，Ｂ，Ｃ　）

神経倫理学の観点から，本研究の精緻化は，遺伝学における優性思想と同様の危険を孕む可能性がある．研究成果の解釈を十分慎重に行うだけでなく，成果を適切に社会に公開することが大

切であると思われる．その上で，本研究によって開かれた学問領域は，人類の福祉に大きく貢献すると確信する．

４．**総評** Ｓ　（　Ｓ，Ａ，Ｂ，Ｃ　）

本研究事業は，脳科学の社会実装を大きく進めた．具体的には，「研究対象群ではなく個々人に焦点を当てた社会的・職業的能力の定量的な推定・理解・育成を志向し，個々人を評価できる認知・脳科学的知見からの情報提供基盤の形成」を十分に達成したと評価される．

評　価　票

記入日　　令和元年５月２０日

評価委員氏名　福永 雅喜

※下記項目について評価コメントをご記入のうえ、Ｓ～Ｃの４段階で下線部にご記入願います。

１．研究計画の達成状況　Ｓ　（　Ｓ，Ａ，Ｂ，Ｃ　）

本研究課題は、教育・職業・パーソナリティ等の要因がいかにして認知・脳機能をダイナミックに変容させるかを、大学在籍期間の数年にわたって追跡する縦断研究と、年齢や職業経験の点で異なる集団間を比較する横断研究を組み合わせ、種々の心理・行動指標とニューロイメージング手法で得られた知見から理解しようとするものである。５年の研究期間内に、計測法の確立、延べ1000名を超える心理指標や職業適性、同じく800名を超えるMRI計測を実施し、その関連解析、MRIデータを用いた判別器の確立などを実施した。年次計画で設定された個々の課題は、ほぼ実施されており、当初目標を達成したと考えられる。

２．研究成果に対する評価　Ａ　（　Ｓ，Ａ，Ｂ，Ｃ　）

①特に優れている点（成果の卓越性）

本研究課題にて収集したデータをもとに各種心理指標と関連する脳部位および脳ネットワークを同定し、TFU脳部位セットおよびTFU脳ネットワークセットとして脳画像テンプレートを独自に確立したこと、安静時脳機能MRIから得られる脳ネットワーク情報をもとに111項目にも及ぶ心理指標の推定器を確立したこと、同様に職業適性推定器を作成したこと等が成果として特に優れていると思われる。また、これらの成果の一部は論文発表として学術誌に発表されている。

②伸長すべき点（今後の課題）

心理･行動指標、職業適性とMRIデータの関連解析は、先端的技術が応用され、推定器の同定に成功するなど、高い次元で実施された。一方、MRIデータが心理･行動指標、職業適性のリプレイスとなるのではなく、両者を融合した形としての指標も検討すべきと思われた。また、研究プロジェクトの学術的な特色とされる ”縦断研究と横断研究を統合したマトリクス的アプローチ” に関しては、大学４年間に渡る縦断的な変化や、職業横断的な検討が実施されたが、サンプル数や職種が限定されていることなどから、データ収集を含め今後も継続した研究の実施が望まれる。

③予想される波及効果

本研究課題にて、心理･行動指標、職業適性とMRIデータからヒトの特性を理解し、判別する要素技術が確立された。これらの成果は、従来、科学的なエビデンスをもとに判断すること困難なであった能力育成プログラムの評価などに応用への道筋をつけるものと思われる。また、教育分野のみならず、加齢や発達など広く研究に応用できるものと考えられる。

３．今後の展望（意見、助言、提案等）　Ａ　（　Ｓ，Ａ，Ｂ，Ｃ　）

本研究でシステマティックに収集された心理・行動指標、職業適性およびニューロイメージングの膨大なデータは、多彩な指標を備える画像データとして、非常に価値の高いものである。また、心理・行動指標、職業適性と MRI データからヒト特性を分離・判別する要素技術の確立は、今後、教育養成分野以外への応用も期待される。高度なデータ処理技術を応用することで、安静時の脳ネットワーク動態から心理指標の個別項目の推定が可能となったことは特筆されるが、本研究課題で同定されたネットワークを個々に顧みると、その構成要素である複数の脳領域間結合は、各項目で広く重複している。また、これらが機械学習により同定されたことからも、本研究で同定されたネットワークが、心理バッテリーの神経基盤を直接的に表現すると結論するには早急すぎると思われる。心理バッテリーに神経科学的基盤を与えるためにも、両者の関連についてさらなる検討を進めて頂きたい。また、縦断+横断的データの収集は、本研究課題の大きな特徴の１つであるため、今回の優れた成果をより強固なものとするために、特に縦断データ、他職種のサンプル追加と、縦断+横断的データをもとにするマトリクス解析のさらなる推進を期待したい。

４．総評　Ａ　（　Ｓ，Ａ，Ｂ，Ｃ　）

本研究プロジェクトは、人材の育成という高等教育課程に期待される役割を、認知･脳科学的エビデンスに裏付けられた客観的な情報から評価し、その教育･育成の効果・価値を高めるための基盤構築を目指した挑戦的なプロジェクトである。個別に設定された研究計画はほぼ実施、展開され、その基盤・環境は整備されつつあり、当初の目標は、達成されたと考えられる。認知・脳科学的根拠にもとづいて教育・養成課程の評価、検証を行うことは、本研究の最終的な目標の１つであり、高い社会的還元性を持つ。今後、これらの実現のためにさらなる発展を期待したい。

Ⅳ 研究業績

（1）原著論文

1 Sung, Y., Kawachi, Y., Ogawa, S. (in press) Comparison of multichannel head array coils for fMRI experiments. Report of Kansei Fukushi Research Institute, 20, 153-157.

2 Otomo, Y., Kawachi, Y., Sung, Y., Ogawa S. (2019) A linear-mixed effect model analysis of the effect of schizotypal personality traits on confidence in reality monitoring. Tohoku Psychologica Folia, 77, 83-90.

3 阿部千裕・河地庸介 (2018) 実行機能を構成する要素に関する研究動向と課題. 感性福祉研究所年報, 19, 149-156.

4 小松紘 (2018) 理解とパーソナリティの研究－文章理解への性格特性の影響. 感性福祉研究所年報, 19, 115-127.

5 Nazari, Z., Inamine, M., Sugama, Y., Kang, D., Kawachi, Y., Sung, Y., Ogawa, S. (2018) Classification of Resting State fMRI Data by an Unsupervised Neural Network. Report of Kansei Fukushi Research Institute, 19, 135-139.

6 大友ゆき・河地庸介・阿部千裕・成烈完・小川誠二 (2018) 統合失調型パーソナリティ特性と自閉症スペクトラム特性のメタ認知における差異. 感性福祉研究所年報, 19, 157-165.

7 Sung, Y., Kang, D., Kawachi, Y., Ogawa, S. (2018) A Comparison of Resting State fMRI Signals Depending on Participant's Conditions under MRI Measurements. Report of Kansei Fukushi Research Institute, 19, 129-134.

8 Sung, Y., Kawachi, Y., Choi, U.-S., Kang, D., Abe, C., Otomo, Y., Ogawa, S. (2018) Estimation of vocational aptitudes using functional brain networks. Human Brain Mapping, 39(9), 3636-3651.

9 Sung, Y., Kawachi, Y., Choi, U.-S., Kang, D., Abe, C., Otomo, Y., Ogawa, S. (2018) A Set of Functional Brain Networks for the Comprehensive Evaluation of Human Characteristics. Front Neurosci, 12:149, doi: 10.3389/fnins.2018.00149

10 Nazari, Z., Inamine, M., Sugama, Y., Kang, D., Kawachi, Y., Sung, Y., Ogawa, S. (2017) Evaluation of characteristics of resting state fMRI data by Machine Learning. Report of Kansei Fukushi Research Institute, 18, 281-284.

11 Kang, D., Sung, Y., Ogawa, S. (2017) Realization of a Longitudinal Relaxation Time Measurement with High Spatial Resolution. Report of Kansei Fukushi Research Institute, 18, 285-292.

12 Sung, Y., Kang, D., Kawachi, Y., Ogawa, S. (2017) Detection of fast MRI signals by an EEG-like stimulus scheme and multi-voxel pattern analysis. Report of Kansei Fukushi Research Institute, 18, 275-280.

13 大友ゆき・河地庸介・阿部千裕・成烈完・小川誠二 (2017) メタ認知と自己成長主導性の関連性. 感性福祉研究所年報, 18, 293-299.
14 Abe, C., Kawachi, Y., Sung, Y., Ogawa, S. (2017). The effects of short-term practice on executive functions. Tohoku Psychologica Folia, 75, 15-21.
15 Sone, T., Kawachi, Y., Abe, C., Otomo, Y., Sung, Y., Ogawa, S. (2017) Attitude and Practice of Physical Activity and Social Problem-Solving Ability among University Students. Environmental Health and Preventive Medicine, 22:18, doi: 10.1186/s12199-017-0625-8
16 Choi, U.-S., Sung, Y., Ogawa, S. (2017) Steady-state and dynamic network modes for perceptual expectation. Scientific Reports 7, doi:10.1038/srep40626.
17 Kawachi, Y. (2016) Visual Mislocalization of Moving Objects in an Audiovisual Event. PLoS ONE 11(4): e0154147. doi:10.1371/journal.pone.0154147
18 河地庸介 (2016). 脳活動からみる芸術鑑賞・制作 臨床美術ジャーナル, 5(1), 75-81.
19 Sung, Y., Kawachi, Y, Choi, U.-S., Kang, D., Ogawa, S. (2016) Modality dependent sensitivity in evaluating brain plasticity. Report of Kansei Fukushi Research Institute, 17, 271-277.
20 Nazari, Z., Kang, .D, Kawachi, Y., Sung, Y., Ogawa, S. (2016) Hierarchical clustering of fMRI Data. Report of Kansei Fukushi Research Institute, 17, 279-285.
21 阿部千裕・河地庸介・成烈完・小川誠二 (2016) 一般知能と実行機能における共通性と差異性. 感性福祉研究所年報, 17, 287-293.
22 Choi, U.-S., Sung, Y., Hong Sujin, Chung, J.Y., Ogawa, S. (2015) Structural and functional plasticity specific to musical training with wind instruments. Front. Hum. Neurosci. 9: 597. doi: 10.3389/fnhum.2015.00597
23 Chung, J.Y., Sung, Y., Ogawa, S. (2015) Evaluation of the contribution of signals originating from large blood vessels to signals of functionally specific brain areas. Biomed Res Int., 2015; 2015: 234345.
24 Kang, D., Sung, Y., Kang, C.-K. (2015) Fast imaging techniques for fMRI: consecutive multi-shot echo planar imaging accelerated with GRAPPA technique. Biomed Res Int., 2015; 2015: 394213.
25 Sung, Y., Kawachi, Y., Kang, D., Ogawa, S. (2015) Evaluation of differences in brain plasticity with individual characteristics by MRI. Report of Kansei Fukushi Research Institute, 16, 35-242.
26 Sung, Y., Choi, U.-S., Ogawa, S. (2014) Invariance of functional characteristics to task difference at low-level and high-level areas in the ventral visual pathway. J. Behavioral and Brain Science, 4, 402-411.

原　著　論　文

Comparison of Multichannel Head Array Coils for fMRI Experiments

Yul-Wan SUNG, Yousuke KAWACHI, Seiji OGAWA
Kansei Fukushi Research Institute, Tohoku Fukushi University

Abstract

Magnetic resonance imaging (MRI) is realized by three components: a static field magnet/coil, gradient coil, and radio-frequency coil. To functional MRI (fMRI) users, this is often called the head array coil. Among these three components, the head coil is optional, whereas the other two coils are fixed by manufacturers. Several kinds of head coil are available, from single channel coils to multichannel head array coils. The most commonly used head coils for fMRI are 16ch, 32ch, and 52ch coils. In the planning stage of an fMRI study, researchers should choose one of the head coil types. However, there are no generalized criteria for coil selection as it depends on the study purpose and individual MRI system. In this study, we compared signal to noise ratio for three head coils, including 16ch, 32ch, and 52ch for an fMRI.

Keywords : multichannel head array coil, temporal signal-to-noise ratio (tSNR), functional MRI (fMRI)

Introduction

Magnetic resonance imaging (MRI) system is composed of largely three components of static field magnet/coil, gradient coil, and radio-frequency (RF) coil, which is often called as head coil by functional MMRI (fMRI) users. Characteristics of head coils in magnetic resonance imaging (MRI) systems are important to produce high quality images. There are two types of coil, single channel coil and multichannel array coil. In multichannel array coil, nowadays, mainly 4 coils (12, 16, 32, 52 channels) have been used for fMRI study.

There are two advantages in using multichannel coils (multichannel head array coil, especially for fMRI) : one is higher signal-to-noise ratio (SNR) and the other is reduction of imaging time by using parallel imaging technique. Factor of reduction of imaging time is proportional to the number of channels although the configuration of coils can affect to it. Generally, in a viewpoint of image quality, multichannel head array coils produce MRI images with higher SNR than single channel coils, and a multichannel head array coil with high number of channels produce higher SNR data than low number of channels up to a specific number of coils. However, as the number of channels increase, the size of each coil element decreases and the sensitivity of the coil to the signal from a signal source far from the subject decreases too. Therefore, the relation between the number of channels and SNR is dependent on locations of subjects to be imaged. Generally, surface areas of the brain show high SNR compared to deep brain areas. In fMRI studies, some require a high SNR at deep brain areas and some others in surface areas of the brain depending on study aims. Therefore, it is not a single way to choose the best head coil for fMRI study. There have been several studies compared two kinds of head

coil, such as, 12ch vs 32 [1-5], or 16ch vs 32 [6], 32ch vs 52ch [7]. However, we could not find any study compared three coils of 16ch, 32ch and 52ch with 1 ch head coil. In this short study, we compared the three types of multichannel head array coils in a viewpoint of temporal SNR for fMRI.

Methods.

MRI images were acquired from a 3 Tesla MRI system (SkyraFit, Siemans Co, Erlangen, Germany) with three multichannel head array coils of 16ch (20 matrix coil with 16ch array coils for the brain and 4 ch array coils for the neck), 32 ch, and 52ch (64 matrix coil with 52ch array coils for the brain and 12 for the neck), and 1 ch (Rx/Tx) head coil (Fig. 1 a, b). A phantom subject was used for measuring and evaluation. For fMRI study, temporal SNR (tSNR) was evaluated for the head coils. Gradient-echo Echo-Planar Imaging (GE EPI) sequence was used for acquiring MRI images, which is mostly used for fMRI study. Imaging parameters are as follows: matrix size of 96x96, slice thickness of 5 mm, number of slices of 1, TR of 2000s, TE of 52ms.



Figure 1 (a) Head coils: 1 ch, 16ch, 32ch and 52ch from the left.

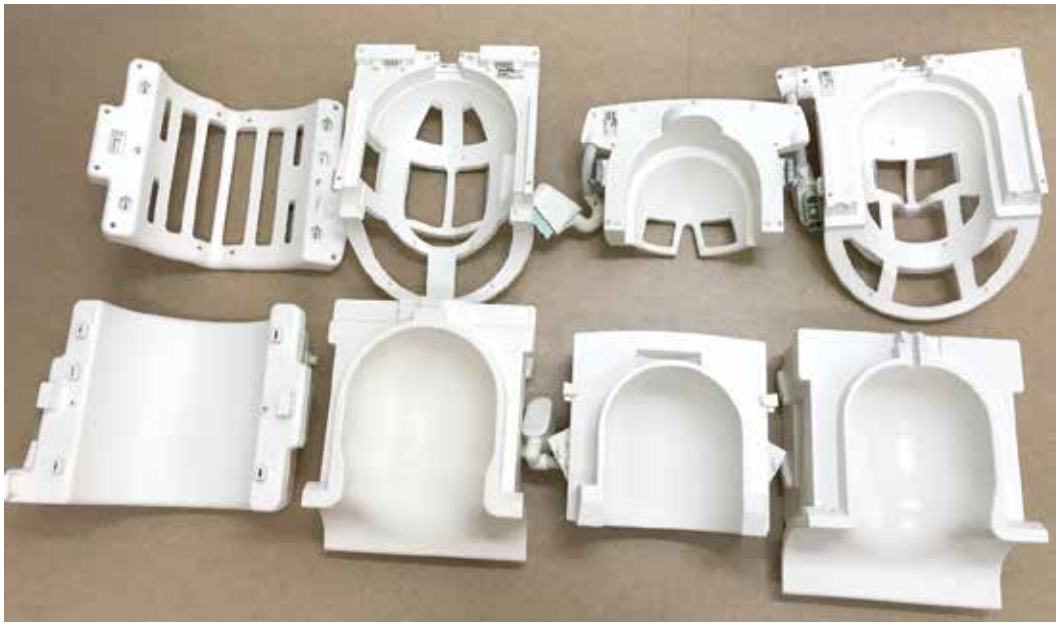


Figure 1 (b) Head coils (segments separated) : 1 ch, 16ch, 32ch and 52ch from the left

Results and Discussion

For four head coils, three multichannel array coils (16ch, 32ch, and 52ch) and single 1 ch coil, the evaluation was performed in a viewpoint of the temporal SNR at two locations on the phantom subject images: one was at the center and the other was at the surface of the image (Fig. 2). As we expected the tSNR of the three multichannel head array coils surpassed the tSNR of the single channel coil as seen in Figure 3 (a) and (b). Among the three head array coils, 32ch showed the best values of tSNR both at the center and the surface. For 52ch coil, the SNR at the center was not so much inferior to that for 32ch in spite that, generally, the size of each coil element in 52ch coil is smaller than in 32ch and that it was expected that reduction of SNR at the center was proportional to the number of the channels. Another interesting observation is the SNR of 52ch in the surface. The SNR of 52ch was slightly lower than that of 32ch at the surface although increase of the sensitivity was expected for 52ch at the surface.

The purposes using multichannel head array coils in fMRI study are to get high SNR and/or high imaging speed. According to our results of the comparison 16ch, 32ch and 52ch head coils in comparison with the 1 ch coil in a viewpoint of temporal SNR, all the multichannel head array coils give higher tSNR than 1 ch head coil and the increase of tSNR is not linear to the number of coil channels. From our observation, the suggestions for the choice of head array coils for fMRI study are as follows: (1) to use 32ch head array coil to acquire the highest SNR images both in the center and surface of the subject, (2) to use 52ch head array coil to achieve the highest speed of imaging while securing high SNR images comparable to 32ch, in this meaning, 52ch coil would be the best.

However, there is a case in which the coil size and shape are significant as resting state fMRI studies in which many subjects are required for a study purpose. In that case, the size of coil (inner space of the coil) may be an advantage to accommodate various sizes of heads of subjects. Figure 1 (b) shows shapes of four head coils. In that viewpoint 16ch coil may be the best because its size is larger than others although the tSNR is little bit inferior to the 32ch and 58ch coils.

In conclusion, the choice of the multichannel head array coil is depending on the study purpose and the population size of subjects. For traditional task fMRI study requiring a small population size of around 20-30, 52ch head array coil may be the best because it gives high tSNR and high imaging speed. Temporal SNR tends to vary among MRI systems, even in the case that the systems are from the same manufacturer with the same model specifications. Therefore, an evaluation of head coils by using the comparison data of different combinations of two out of three coils in the different systems as in the previous studies may produce inaccurate results. In this study, we made a reliable evaluation by direct comparison of tSNR for the three coils on the same MRI system and could provide some useful information for head coil selection.

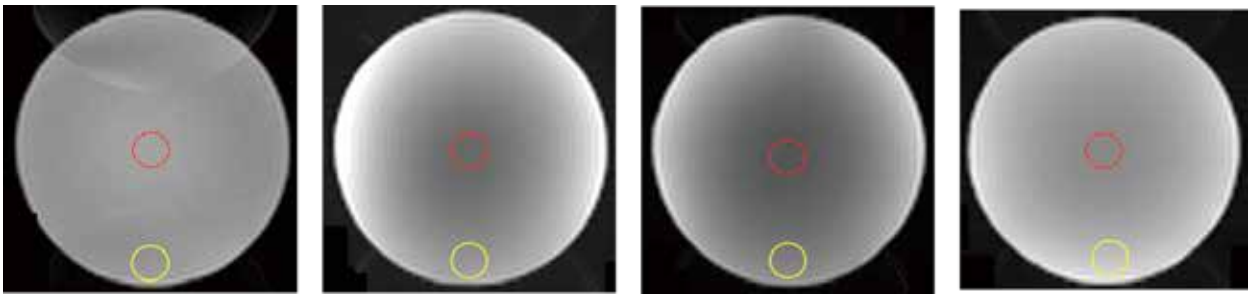


Figure 2. MRI images of the phantom subject with 1 ch, 16ch, 32ch, and 52ch from the left: red circle for the center and yellow circle for the surface.

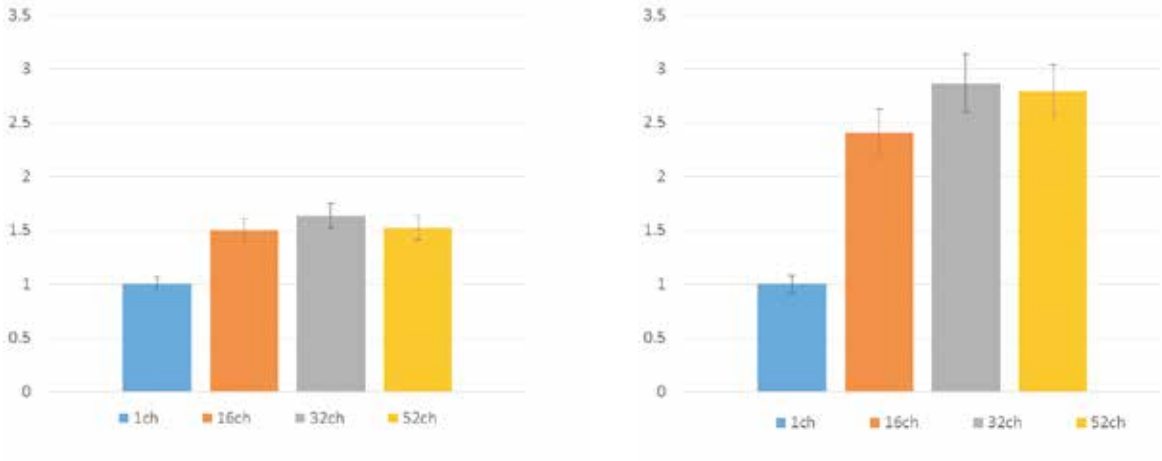


Figure 3. Normalized tSNR of the phantom subject at the center (a) and the surface (b). Error bars stand for standard deviation.

Acknowledgments

This study was supported by MEXT-Supported program for the Strategic Research Foundation at Private Universities, 2014-2018 and JSPS KAKENHI under Grant number 17K01993.

References

1) (12ch, 32ch) Ferré JC, Petr J, Bannier E, Barillot C, Gauvrit JY. (2012) Improving quality of arterial spin labeling MR imaging at 3 tesla with a 32 - channel coil and parallel imaging. J Magn Reson Imaging. 2012 May; 35 (5) : 1233-9. Do: 10.1002/jmri. 23586.

2) (12ch, 32ch) S. Arnold1, S. Whitfield-Gabrieli, S. Shannon, J. Gabrieli, and C. Triantafyllou. (2010) Improved BOLD Detection in the Working Memory Network using a 32 channel Phased Array Head Coil. Proc. Intl. Soc. Mag. Reson. Med. 18

3) (12ch, 32ch) Sheeba Arnold Anteraper, Susan Whitfield-Gabrieli, Boris Keil, Steven Shannon, John D. Gabrieli, and Christina Triantafyllou. (2013) Exploring Functional Connectivity Networks with Multichannel Brain Array Coils Brain Connect. 3 (3) :302-15. Do: 10.1089/brain. 2012.0113.

4) (12ch, 32ch) Triantafyllou C1, Polimeni JR, Wald LL. (2011) Physiological noise and signal-to-noise ratio in fMRI with multi-channel array coils. Neuroimage. 2011 Mar 15;55 (2) : 597-606. doi:

10.1016/j.neuroimage.2010.11.084.
5）(12ch, 32ch) Fellner C1, Doenitz C, Finkenzeller T, Jung EM, Rennert J, Schlaier J. (2009) Improving the spatial accuracy in functional magnetic resonance imaging (fMRI) based on the blood oxygenation level dependent (BOLD) effect: Benefits from parallel imaging and a 32-channel head array coil at 1.5 Tesla. Clin Hemorheol Microcirc. 43 (1-2) :71-82. doi: 10.3233/CH-2009-1222.
6）(16ch, 32ch) Sengupta S, Roebroeck A, Kemper VG, Poser BA, Zimmermann J, Goebel R, Adriany G. A Specialized Multi-Transmit Head Coil for High Resolution fMRI of the Human Visual Cortex at 7 T. PLoS One. 2016 Dec 2 ;11 (12) : e0165418. doi: 10.1371/journal.pone.0165418
7）(32ch vs 64ch) Boris Keil James N. Blau Stephan Biber Philipp Hoecht Veneta Tountcheva Kawin Setsompop Christina Triantafyllou Lawrence L. Wald
(2013) A 64 - channel 3 T array coil for accelerated brain MRI. Magn Reson Med. Jul; 70 (1) : 248-58. doi: 10.1002/mrm.24427

Tohoku Psychologica Folia
2018, 77, 83–90

A linear mixed-effect model analysis of the effect of schizotypal personality traits on confidence in reality monitoring

Yuki OTOMO (大友ゆき)[1*], Yousuke KAWACHI (河地庸介)[1,2],
Yul-wan SUNG (成　烈完)[1] and Seiji OGAWA (小川誠二)[1]

A number of previous studies have reported overconfidence in reality monitoring in patients with schizophrenia. Reality monitoring is defined as the ability to discriminate between internal and external sources of information. We consider that the research on reality monitoring confidence should be extended to healthy participants who have a predisposition toward schizophrenia (schizotypy) in order to elaborate the biological markers of risk for schizophrenia. In the present study, we precisely examined the effect of schizotypy on reality monitoring confidence using a linear mixed-effect model analysis, which can consider random variation across participants and stimuli (random participant and stimulus effects). The results showed that random participant and stimulus effects had significant effects on confidence ratings for reality monitoring, while the fixed effect of schizotypy had a marginally significant effect on the ratings. Our findings demonstrate the importance of considering random effects associated with stimuli and participants for evaluating the effects of schizotypy in reality monitoring confidence.

Key words: reality monitoring, linear mixed-effect model, confidence rating, schizotypal personality, schizotypy

Introduction

Reality monitoring refers to the ability to discriminate the information generated by one's own thoughts and actions from that generated by external events (Johnson & Raye, 1981). It is critical for adaptive behavior toward moment-to-moment changes in the surroundings. Patients with schizophrenia who have positive symptoms including hallucinations and delusions may show a lack of reality monitoring. They may not be able to recognize their own voice and perceive their own voice as other voices that are not actually present (Dunlosky & Metcalfe, 2010; Simons, Garrison, & Johnson, 2017).

However, a reality-monitoring deficit is not specific to schizophrenia and can be observed in patients with other psychiatric disorders (Moritz & Woodward, 2006). Therefore, recent research has focused on confidence in reality monitoring rather than on reality monitoring deficits (Moritz, Woodward, & Ruff, 2003) to discriminate schizophrenia from other psychiatric disorders. Importantly, overconfidence in erroneous reality monitoring has been specifically reported in patients with positive symptoms of schizophrenia (Moritz & Woodward, 2006; Moritz et al., 2003; Woodward, Menon, & Whitman, 2007).

Research on reality monitoring confidence in schizophrenia should be extended to healthy participants who have a predisposition toward schizophrenia, which is referred to

1. Kansei Fukushi Research Institute, Tohoku Fukushi University
2. Department of Psychology for Human Well-Being, Faculty of Comprehensive Welfare, Tohoku Fukushi University
*Correspondence concerning this article should be addressed to Yuki Otomo, 6-149-1, Kunimigaoka, Aoba-ward, Sendai 9893201, Japan. (Tel: +81-22-728-6085 E-mail: xxxxxyuk1@gmail.com)

as schizotypy (Claridge, 1997). Examining persons who exhibit schizotypy is a promising strategy for providing insights into the origins of schizophrenia (Raine, 2006), assessing behaviors without the confounding effects of studying chronically ill and medicated patients (Minas & Park, 2007), and elaborating the biological markers of risk for schizophrenia.

When examining reality monitoring confidence in healthy individuals with schizotypy, as in the present study, it is important to consider that the effect of random variation across experimental participants and stimuli (random participant and stimulus effects) could make it difficult to identify, among random effects, the effect of schizotypy on reality monitoring confidence as well as to interpret the present findings. Murayama (2018) raised an alarm over conventional statistical analyses using analysis of variance (ANOVA) in memory research. In general, to-be-remembered stimuli are considered as ideally randomly sampled from an infinite population of stimuli. Further, most studies assume that various properties of randomly sampled stimuli do not have a possible effect on dependent variables such as the confidence rating score. However, this possible effect is not completely zero, called as a random stimulus effect. Because conventional statistical analyses do not consider random stimulus effects, significant results may account for such effects and not fixed effects. In other words, these analyses could subsequently increase the Type-1 error rate. Therefore, we should interpret the significant fixed effects observed in these conventional analyses with caution. Thus, to address this issue, we newly examined reality monitoring confidence in a healthy population with high/low schizotypy using a linear mixed-effect model.

Method

Participants

Forty-one healthy graduate and undergraduate students (4 males and 37 females, with a mean age of 21.0 years and SD ±2.19 years) participated in this study. The experiment was approved by the Ethical Committee of Tohoku Fukushi University and conducted according to the principles of the Declaration of Helsinki. Written informed consent was obtained from all participants.

Materials and Procedure

Schizotypy: We used the Japanese version of the Schizotypal Personality Questionnaire Brief (SPQ-B) (Ito, Obu, Ota, Takao, & Sakamoto, 2008) to measure participants' schizotypy. The SPQ-B consists of 22 items, each answered as "Yes" or "No." Higher SPQ-B scores indicate high schizotypy. Participants were asked to answer the SPQ-B after completing the reality monitoring task. For the subsequent analysis of variance (ANOVA), the participants were divided into two groups based on the SPQ-B mean score: 22 participants into the high score group (mean score of 11.55, SD ±2.52) and 19 participants into the low score group (mean score of 6.00, SD ±1.83). A mean split allowed for classification of all participants, while a median split leads to the exclusion of the data for some participants with a SPQ-B score

corresponding to a median.

Reality monitoring task: We used 80 easy words including verbs or adjectives and had four different stimuli types: (1) which consisted of 20 words selected from Umemoto (1969) and Mizukami (2013; 2014), (2) which consisted of 10 words used as a synonym and 10 words used as an antonym of each word from (1), (3) which consisted of 20 words related to both (1) and (2) on the basis of a synonym and related word dictionary on the web (http://renso-ruigo.com/), and (4) which consisted of 20 words not related to both (1) and (2). All words from (1) and the first letter of the words from (2) in Japanese were recorded by an experimenter using a microphone (ATR1100 Unidirectional Dynamic Handheld Microphone, Audio-Technica U.S., Inc., Stow, Ohio, USA).

The experimental stimuli were created using E-prime 2.0 (Psychology Software Tools, Inc., Sharpsburg, PA, USA). These stimuli were generated and controlled on a PC (Endeavor MT7900, Epson, Nagano, Japan) and were presented on the monitor (ProLite E1902S PLE1902S-W1; resolution 1280×1024 pixels; refresh rate 60 Hz, iiyama, Tokyo, Japan). The experiment consisted of learning and test trials. In a learning trial (Figure 1), first, a fixation cross was presented on the center of the monitor for 1000 ms. Subsequently, the Chinese character cue "類" (synonymous) or "対" (antonymous) was presented for 2000 ms on the center of the monitor. A randomly selected word from (1) was presented through the speakers (ECLIPSE TD508II, Fujitsu Ten, Hyogo, Japan). The first letter of a synonymous (or antonymous) word selected from (2) was presented 1500 ms after the presentation. Participants were asked to speak a word that was synonymous (or antonymous) with the selected word from (1) when the "類" (or "対") cue was presented and that also includes the first letter. An experimenter checked whether the participant's answer matched a word from (2) for each trial. If the participant's answer did not match the word from (2) that was selected by the experimenters but was synonymous (or antonymous) and in the same word class, we used the participant's answer as a stimulus in a test trial.

In test trials, a word each from (1), (2), (3), and (4) were presented in random order. Simultaneously, the alternatives for "1: New" and "2: Old" were presented at the bottom of the monitor. Participants were asked to select "2: Old" if they listened to or spoke the presented word in the learning trials and to select "1: New" if not. Next, participants were asked to rate on a 6-point scale how confident their old-new judgement was. If they selected "2: Old," new alternatives for "1: Experimenter" and "2: Self" were presented at the bottom of the monitor. Subsequently, participants were asked to judge whether a presented word was heard or spoken in a learning trial: "1: Experimenter" was to be selected if participants had listened to the presented word and "2: Self" if they had spoken it in the learning trials. Participants were also asked to rate on a 6-point scale how confident the experimenter-self judgment was. All judgments in the experiment were self-paced.

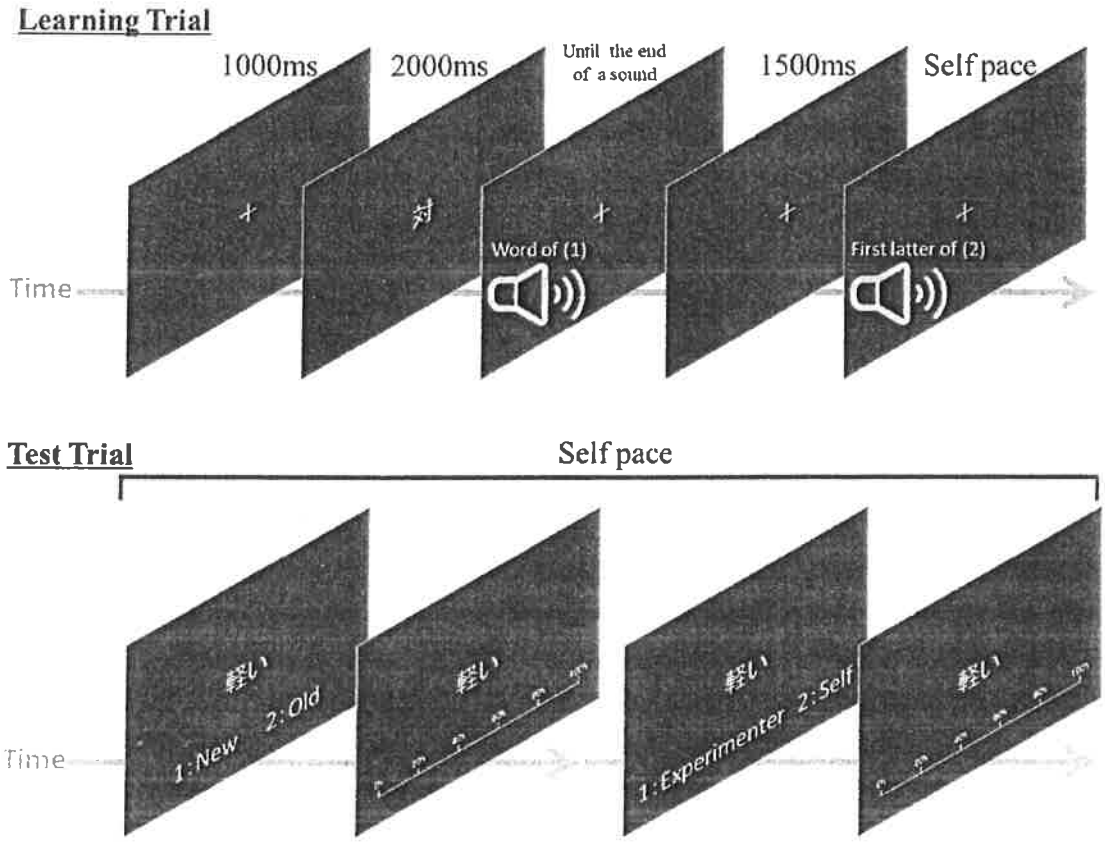


Figure 1. The stimulus sequence used in the reality monitoring task. (1) refers to the 20 words selected from Umemoto (1969) and Mizukami (2013; 2014). (2) refers to the 10 words used as a synonym and the 10 words used as an antonym of each word from (1). In this learning trial, participants were asked to speak a word that is antonymous with the word selected from (1) when the " 対 " cue was presented and that also includes the first letter of the antonymous word selected from (2). In this test trial, in which an alternative of "2: Old" was selected, the participants were also asked to select "1: Experimenter" or "2: Self." If an alternative of "1: New" was selected, the next test trial began.

Results

Analysis of Variance (ANOVA)

We first performed ANOVA with the factors of the SPQ-B total score, which have been used in previous studies on reality monitoring (Moritz & Woodward, 2006; Moritz, Woodward, Whitman, & Cuttler, 2005). Table 1 shows the mean reality monitoring accuracy for SPQ-B score group (high and low), and the mean reality monitoring confidence rating score for each reality monitoring response (correct and incorrect) and SPQ-B score group (high and low). We conducted a two-way mixed ANOVA for the confidence rating scores with reality monitoring response (correct or incorrect) as the within-participant variable and group (SPQ-B score high or low) as the between-participants variable. The main effects of both response and group were significant [response: $F(1, 39) = 60.16$, $p<.001$; group: $F(1, 39) = 9.32$, $p<.01$]. The interaction between response and group was not significant [$F(1, 39) = 1.47$, *n.s.*]. These results indicated that confidence rating scores were higher in correct than in incorrect reality monitoring

responses and participants with high schizotypy scores tended to rate their confidence higher than did those with low schizotypy scores.

Table 1. Mean reality monitoring accuracy and confidence rating scores.
Note. N: Number of participants, M: Mean, SD: Standard Deviation.

		Reality monitoring accuracy (%)			Confidence rating (%)		
					Reality monitoring response		Total
		N	M	SD	Correct	Incorrect	
SPQ-B score	High	22	67.78	3.74	88.71	78.39	83.55
	Low	19	66.45	3.89	75.71	68.18	71.94
Total		41	67.16	3.82	82.21	73.28	79.75

Linear Mixed-Effect Model

We used a linear mixed model to analyze the effects of reality monitoring response and the SPQ-B score on confidence ratings considering random variation across participants, stimulus items, and other factors that may have an effect on confidence ratings. The analysis was performed using the *R* package *lme4* (Bates, Mächler, Bolker, & Walker, 2015) and *lmerTest* (Kuznetsova, Brockhoff, & Christensen, 2017). We included reality monitoring response (correct or incorrect), the SPQ-B score groups (high or low), and the interaction between the two as fixed-effect factors. We included as random-effect factors of participants, gender, stimulus, trial number, answer type (New, Experimenter, or Self), stimuli type ((1), (2), (3), or (4)), and observed participants' responses (New, Experimenter, or Self) on the slope for confidence ratings and the fixed effect factors as well as the intercept. Table 2 shows the marginally significant fixed effects of the SPQ-B score groups on confidence ratings [β = .65, SE = .32, t = 2.06, p<.10]. Figure 2 shows the significant random effects of participants [p<.001], stimulus [p<.001], answer type [p<.001], and stimuli type [p<.01] on the intercept. The random participant effect [p<.001] was significant for the slope for confidence ratings and reality monitoring response (correct or incorrect). The random gender, trial number and observed participants' responses effects (New, Experimenter, or Self) were not significant for the intercept and slope for confidence ratings and the fixed effect factors. The results showed that the SPQ-B score groups had an effect on confidence ratings, as did random-effect factors such as participants and stimulus.

Table 2. Results of the linear mixed effect model analysis for fixed effects on reality monitoring confidence.

	β	SE	*t*	*p*
(Intercept)	4.11	.65	6.29	<.001
Reality monitoring response (Correct / Incorrect)	.33	.43	.77	*n.s.*
SPQ-B score group (High / Low)	.65	.32	2.06	<.10
Reality monitoring resoponse × SPQ-B score group	.06	.12	.50	*n.s.*

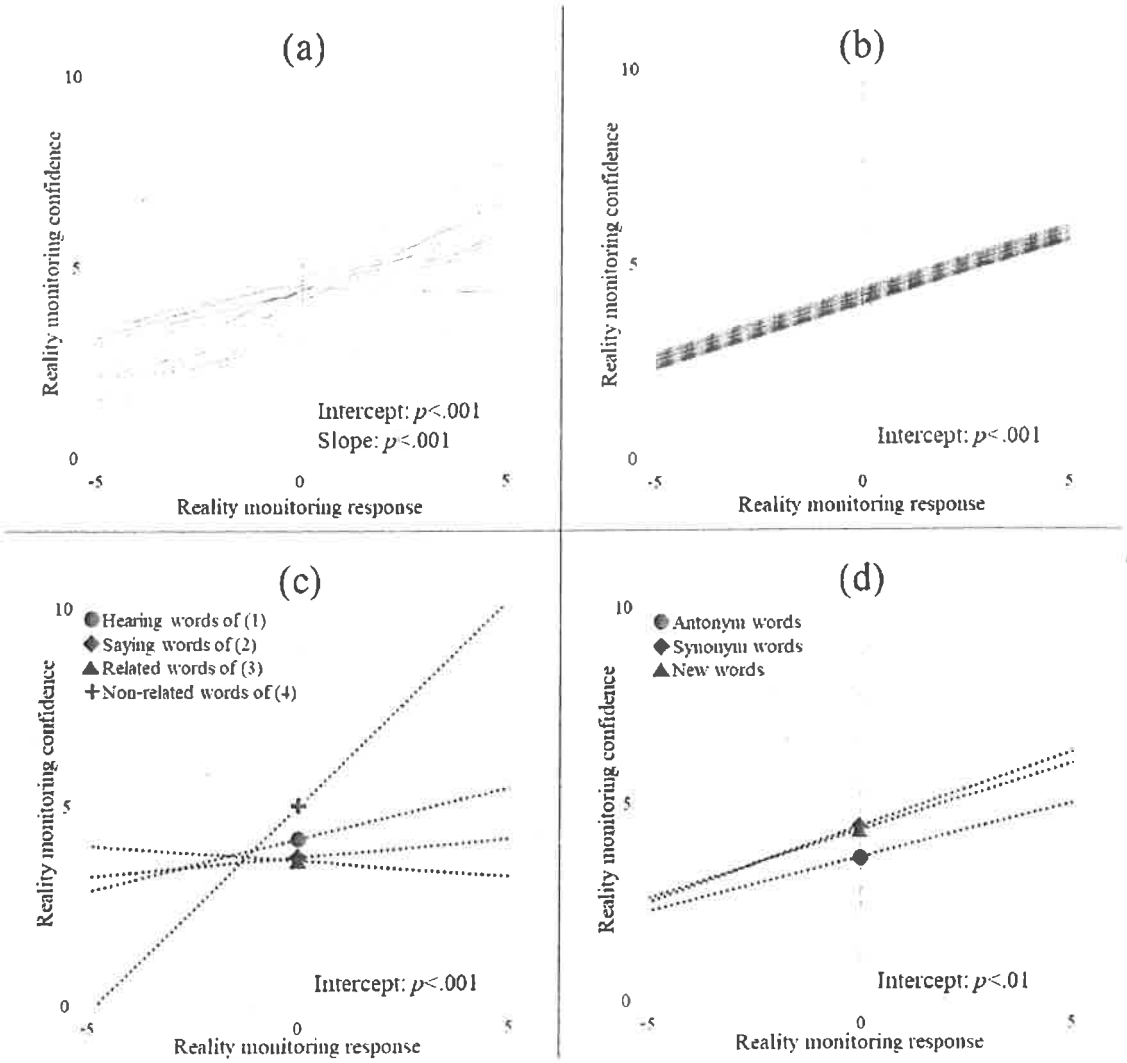


Figure 2. Results of the linear mixed effect model for reality monitoring confidence. (a) depicts random participant effects on the intercept and on the slope for confidence ratings and reality monitoring response (correct or incorrect). (b) depicts random stimulus effects on the intercept. (c) depicts random answer-type effects on the intercept. (d) depicts random stimuli-type effects on the intercept.

Discussion

We examined the effect of schizotypy on reality monitoring confidence using a linear mixed-effect model analysis as well as ANOVA. The result of ANOVA indicated that high schizotypy led to higher confidence in the reality monitoring task compared to low schizotypy. This result seems to be similar to previous studies on reality monitoring confidence in patients with schizophrenia (Moritz et al., 2003; Moritz & Woodward, 2006). However, the linear mixed-effect model analysis showed that the effect of schizotypy on reality monitoring confidence was marginally significant, while the random participant and stimulus effects were significant. In other words, the results of the linear mixed model analysis demonstrated that random variation across participants and stimulus (random participant and stimulus effects) increased the Type-1 error rate in the results as indicated by the ANOVA, which account for random participant but not random stimulus effects. Reality monitoring confidence for the word stimuli used in the present study cannot be necessarily equal to that in an infinite population of words that can be observed across schizotypy conditions (e.g., Murayama, Sasaki, Yan, & Smith, 2014). Conventional statistical analysis can detect significance in possible (small) differences in reality monitoring confidence between the sample and population. In other words, random variation in the random sampling of words may increase Type-1 errors and lead to erroneous results. Therefore, we need to be cautious about this possibility in conventional analyses that do not consider random stimulus effects.

In future research, similar findings might also be obtained in patients with schizophrenia. Therefore, it would be meaningful to elucidate the random stimulus effects on reality monitoring overconfidence in patients with schizophrenia for the quantitative and objective classification of schizophrenia and other psychiatric disorders and for devising a biological marker to predict proneness to schizophrenia.

Acknowledgments

This study was supported by a Grant-in-Aid of the Japan Society for the Promotion of Science (JSPS) for Scientific Research (no. 16K00212) and the Program of Finding Basic Research Center in Private Universities (MEXT) to the Kansei Fukushi Research Institute, Tohoku Fukushi University (2014-18).

References

Bates, D., Mächler, M., Bolker, B., & Walker, S. (2015). Fitting Linear Mixed-Effects Models using lme4. *Journal of Statistical Software, 67(1)*, 1-48.

Claridge, G. (Ed.). (1997). *Schizotypy: Implications for illness and health*. New York, US: Oxford University Press.

Dunlosky, J., & Metcalfe, J. (2010). *Metakioku kiso to ouyou [Metacogniton]*. Translated by Yukawa Y., Kinjo H., & Shimizu T., Kyoto, JP: kitaohjisyobo [Kitaooji Shobo Publishing]

Ito, S., Obu, S., Ota, M., Takao, T., & Sakamoto, S. (2008). Reliability and validity of Japanese version Schizotypal

personality questionnaire brief. *Japanese Bulletin of Social Psychiatry, 17(2)*, 168-176.

Johnson, M. K., & Raye, C. L. (1981). Reality Monitoring. *Psychological Review, 88(1)*, 67-85.

Kuznetsova, A., Brockhoff, P. B., & Christensen R.H.B. (2017). lmerTest Package: Tests in Linear Mixed Effects Models. *Journal of Statistical Software, 82(13)*

Minas, R. K. & Park, S. (2007). Attentional window in schizophrenia and schizotypal personality: Insight from negative priming studies. *Applied and Preventive Psychology, 12(3)*, 140-148.

Mizukami, Y. (2013). Compiling Synonym Lists (Verbs) Based on Practical Standards for Japanese Language Education. *Journal of Jissen Japanese Language and Literature, 84*, 186-159.

Mizukami, Y. (2014). Compiling Synonym Lists (Adjectives) Based on Practical Standards for Japanese Language Education. *Journal of Jissen Japanese Language and Literature, 85*, 90-71.

Moritz, S. & Woodward, T. S. (2006). The Contribution of Metamemory Deficits to Schizophrenia. *Journal of Abnormal Psychology, 15(1)*, 15-25.

Moritz, S., Woodward, T. S., & Ruff, C. C. (2003). Source monitoring and memory confidence in schizophrenia. *Psychological Medicine, 33*, 131-139.

Moritz, S., Woodward, T. S., Whitman, J. C. & Cuttler, C. (2005). Confidence in Errors as a Possible Basis for Delusions in Schizophrenia. *The Journal of Nervous and Mental Disease*, 193(1), 9-16.

Murayama, K., Sakaki, M., Yan, V. X., & Smith, G. (2014). Type-1 error inflation in the traditional by-participant analysis to metamemory accuracy: a generalized mixed-effects model perspective. *Journal of Experimental Psychology: Learning, Memory & Cognition, 40 (5)*, 1287-1306.

Murayama, K. (2018). Stimulus effect matters: The importance and cautionary notes of linear mixed-effects model with random stimulus effects. The Japanese Journal of Psychonomic Science, 36(2), 236-242

Raine, A. (2006). Schizotypal Personality: Neurodevelopmental and Psychosocial Trajectories. *Annual Review of Clinical Psychology, 2*, 291-326.

Simons, J. S., Garrison, J. R., & Johnson, M. K. (2017). Brain Mechanisms of Reality Monitoring. *Trends in Cognitive Sciences, 21(6)*, 462-473.

Umemoto, A. (1969). *Rensoukijunnhyou: Daigakusei 1000 nin no juyuurensou ni yoru [The standard association table: From free association by 1000 college students]*. Tokyo, JP: Tokyodaigakusyuppankai [University of Tokyo Press].

Woodward, T. S., Menon, M., & Whitman, J. C. (2007). Source monitoring biases and auditory hallucinations. *Cognitive Neuropsychiatry, 12(6)*, 477-494.

(Received December 21, 2018)
(Accepted January 18, 2019)

原　著　論　文

実行機能を構成する要素に関する研究動向と課題

阿部千裕、河地庸介
東北福祉大学

Research Trends and Issues Concerning the Components of Executive Functions

ABE Chihiro, KAWACHI Yousuke
Tohoku Fukushi University

Abstract

Executive functions (EF) are higher-level functions that regulate lower-level cognitive functions such as monitoring and adding information to memory to adaptively perform an individual's thoughts and actions. This article reviews recent studies to identify the core components of EF. In particular, we summarizes behavioral tasks corresponding to each component; the brain basis of each component; the relations between EF components and working memory; and the unity/diversity framework proposed to account for individual differences in EFs. On the basis of the review, we discuss two issues: the possibility of an interaction between the different EF components and the necessity of testing the predictive validity of EF components and their interactions for the adaptive behaviors in a daily life.

Keywords : executive functions, components, updating, shifting, inhibition

1．実行機能の定義

実行機能（executive functions）とは心理学のみならずリハビリテーションや精神医学等の分野においても近年注目されている心的機能のことである。様々な研究者が実行機能の定義をしているものの[1)2)3)]、その内容は概ね一致しており、中でも実証的に実行機能をモデル化し、定義したMiyakeとFriedmanらの定義が用いられることが多い。彼らによると、実行機能とは、記憶に関する情報の付加やモニタリング等をはじめとした低次の認知機能を制御し意思決定やプランニング等の社会的適応のための思考や行動を支えているとされる心的機能であるとされる。そしていくつかの構成要素から成ることを示している[4)5)]。ここでは、最も多く用いられ、一般性の高いと考えられる名称である「実行機能」を用いるが、実行機能が上述の通り種々の認知機能の幹部あるいは執行役のような立場であることから、「実行」のほかにも「執行」、「遂行」、「管理」、「制御」、「監督系」のような訳語を与えられることがあり、各研究領域に適した日本語訳を用いることが多い[5)6)]。種々の研究領域において、この実行機能は、類似の概念として取り上げられることの多い一般知能とは独立したものであり[7)]、前頭葉を損傷し実行機能の低下がみられた患者でも知能の低下はみられないことから、両者の独立性は示されている[8)]。

2．実行機能の構成要素

実行機能にはいくつかの構成要素が存在するという認識は一貫しているものの、構成要素に関する知見は研究者間で定まっておらず、その一貫性のなさが実行機能の概念を曖昧にしているという指摘もある[9)]。

現在最も支持されていると思われる知見は、Miyakeらの示す「更新（updating）」「切替（shifting）」「抑制（inhibition）」の3要素である（Fig.1）[5]。従来、前頭葉損傷により影響を受ける単一の機能として実行機能は考えられてきたが、彼らは実行機能課題とされてきたWisconsin Card Sorting Test（WCST）やTower of Hanoi（TOH）を用いて実行機能の個人差を検討する研究において、WCSTやTOHの課題成績の相関が統計的に有意でない、あるいは相関係数が低いことは、実行機能が単一の概念[7]ではない可能性を示唆していると考えた。そこで、プランニング等に比べて低次の機能であり、操作的定義がなされていること、十分な研究がなされた単純な測定課題があること、相対的により複雑な実行機能課題でのパフォーマンスに関係しうる機能であることを条件として3つの機能に着目した。その結果として提唱された構成要素が、暗算や電話の応対などに必要となるワーキングメモリ（working memory：一時的に保持した情報を保持し、状況に応じて操作できるような記憶）内の情報を必要に応じて追加したり削除したり保持する能力である「更新」、話しながら作業をするというような心的な構えの状態や課題ルールの切り替えを行う能力である「切替」、道路を横断する際に赤信号であるにも関わらず渡ってしまうというような適切ではない反応の抑制を行う能力である「抑制」の3要素である。

また、Smithらは前頭葉の働きによってなされるワーキングメモリ情報を扱う過程の制御について下位要素を提唱している[11]。注意を最新の情報に向けて最新ではない情報を抑制する「注意と抑制（attention and inhibition）」、複雑な課題において課題ごとの注意を切り替えることでスケジューリングする「課題の管理（task management）」、いくつかの目標を成し遂げるために課題の優劣を計画する「計画性（planning）」、優劣をつけた課題の中で次の段階を決めるために一時的に保持した情報を確認して更新する「モニタリング（monitoring）」、その場の状況に応じたワーキングメモリの表出を言語化する「符号化（coding）」が実行系の働きであるとしている。Diamondは、Miyakeらの示す構成要素を「ワーキングメモリ」「認知的柔軟性（cognitive flexibility）」「抑制制御（inhibitory control）」と称して実行機能の核としているものの、本来「切替」である「認知的柔軟性」には創造性（creativity）も含むとするように、従来実行機能が支えているとされる推論や問題解決、プランニング等のより高次の概念も実行機能の概念として含める必要があるとし、3つの核を改めて提唱している[12]。しかし、SmithらとDiamondの示す構成要素は実行機能が支える高次の認知機能を示す要素が多く全てが実行機能そのものの機能ではないとされ[9]、実験的に構成要素を示すことで実行機能の概念をより明確なものにしたMiyakeらの提唱が最も確実性の高いものであることから多くの研究者間で支持されている構成要素である。

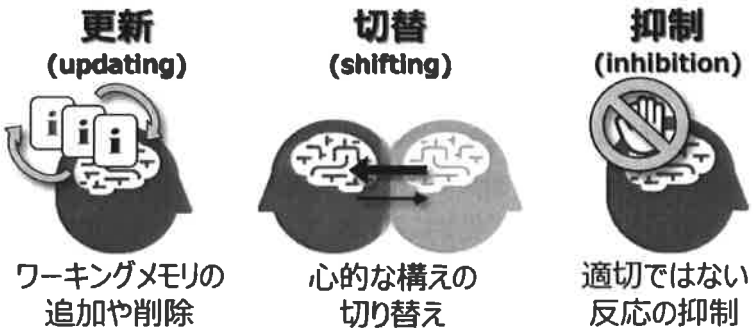


Fig. 1.　実行機能を構成する3つの構成要素のイメージ
Miyakeらの分類に従った実行機能の構成要素である[4]。

1）各構成要素の測定課題

3つの構成要素はそれぞれを反映する測定課題がいくつか存在する。Miyakeらは各構成要素につき3種、計9種の測定課題から、確証的因子分析により各構成要素について測定課題への回帰係数の大きさから最も妥当性のある測定課題を示しているが[4]、研究者間で各構成要素の測定課題の統一はなされておらず、研究テーマや用いる指標に適した測定課題を遂行する場合が多い。

「更新」は、主にワーキングメモリを要する課題を用いる。Miyakeらが示したのはletter memory課題、keep track課題、spatial 2-back課題である。いずれもワーキングメモリの情報を操作し、更新（追加）・保持・再生を行わなければならない課題で、正解率や反応時間が指標となる。「切替」は、注意や記憶を切り替えながら遂行する課題を用いる。Color Shape課題やnumber letter課題、category switch課題を遂行し、切り替えを要する試行のほうが切り替えのない試行よりも反応時間が長いと仮定してそれらの時間コストを指標とする。「抑制」はantisaccade課題やstroop課題、stop signal課題を用いて、適切ではない反応を抑制することで生じる反応時間の変化や反応の正答率を指標とする。

Miyakeらの示した課題の他にも実行機能を測定する認知課題はあり、DamasioらがいたWCSTは当時実行機能全体を測定する課題として認識されていたものの[8]、近年は「切替」が最も関連する課題であるとして捉えられることが多い。他にも、TOHは「抑制」を測定する課題として用いられ[4][12]、Behavioral Assessment of the Disexecutive Syndrome（BADS）は6つの下位検査により実行機能全体を測定する課題として、主に神経心理学分野において高次脳機能障害等の患者に対して用いることが多い[13]。

実行機能の測定は質問紙調査により主観的に評価することも可能である。例えば、エフォートフル・コントロール尺度は「行動始発の制御」「行動抑制の制御」「注意の制御」の下位尺度を実行機能の3要素に対応させる形で測定することが可能である[14]。実行機能の測定方法は上述したような認知課題を用いるのが主流であるため質問紙調査についてここではこれ以上取りあげないが、主観的な実行機能の評価は教育指導場面等で自己の適応的行動を意識する契機となる可能性も考えられる。

2）各構成要素の脳内基盤

実行機能は前頭葉領域と関連づけられて検討されることが多く、前頭葉に損傷のある患者は実行機能課題の成績が低下し、日常生活にも様々な支障が生じると報告されている[8]。3つの構成要素に関連する脳部位についても研究は進んでいるものの、全ての構成要素に関する脳部位について検討・言及している論文は少ないのが現状である。その理由の一つとして、実行機能の構成要素が定まっていないことに伴い、測定に用いる課題を絞り込むことができない等の理由から脳内基盤同定の困難さが指摘されている[15]。

しかし、「更新」「切替」「抑制」を支える脳内基盤に関する研究は数少ないものの、近年の研究動向をまとめて報告しているReinebergは、実行機能の個人差を最もよく反映している脳領域が前頭葉であるとした上で、各構成要素に関連する脳部位を示している[16]。「更新」は背外側前頭前皮質（dorsolateral prefrontal cortex :DLPFC）や前頭極（frontal pole :FP）、小脳（cerebellum）が関連しているとし、特に「更新」機能の個人差はワーキングメモリと密接に関連するDLPFCに依存することが報告されている。また、「切替」はDLPFCや小脳（cerebellum）、眼窩前頭皮質（orbitofrontal cortex :OFC）、腹外側部前頭前皮質（ventrolateral prefrontal cortex :VLPFC）が関連しているとされる。注意を切り替えるのに必要な情報を保持し、状況に応じて適切な判断に切り替えるためには注意と記憶が必要不可欠であり、DLPFCをはじめとした前頭前野の広範囲にわたって関与していると考えられている。「抑制」は、傍帯状回（paracingulate gyrus）やFPと関連し、学習や記憶、感情の処理に関わる部位に依存しているとされる。特にFPとの関連が強いとされ、FPが未来のことを予測し計画を立てて判断を行う能力に関する部位とされていることから、状況に応じた適切な判断をするために必要な能力を担っている可能性が示唆される。

3）実行機能とワーキングメモリ

実行機能の概念を整理する上で欠かせないのがBaddeleyの記憶貯蔵モデルである[10]。彼らは、目的達成に向けた情報の処理や行動の制御を支える認知的システムを中央実行系と称し、記憶の働きに着目した3つの下位機能を提唱した。音声情報の保持を行う音韻ループ、視空間情報の保持を行う視空間スケッチパッド、長期記憶の情報を扱うエピソディック・バッファにより注意の制御、長期記憶の活性化を行っているとした。例えば、初対面の人とあいさつする際に相手の名前や所属などの情報だけでなく、顔や声に注意が向き認識することで記憶する。全ての情報を一致させた上で、次に会った際には名前あるいは顔等の一部の手がかりだけで相手に関する情報を全てではなくともある程度引き出すことができる。これらを行うには視覚的・聴覚的な情報と長期記憶情報を駆使して記憶を更新、保持、再生する必要があり、Baddeleyの示す認知的な枠組みが日常的に機能しているのは容易に想像ができる。この10年以上後に提唱された実行機能はBaddeleyの記憶貯蔵モデルと同様の文脈で用いられることが多いが、両枠組みの関係性については現在も曖昧なままである。

実行機能の概念を提唱したMiyakeらは、目的を達成するためには記憶の認知的枠組みを超えた機能が必要不可欠であるとし、新たな構成要素（概念）を提唱している[4)9)]。この構成要素は2章で説明したとおりであるが、彼らは実行機能とワーキングメモリの関係性を相補的であるとしている（Fig. 2a）。目標や課題の情報を保持するという点において、実行機能を適切に働かせるにはワーキングメモリが必要であり、実行機能のパフォーマンスはワーキングメモリのパフォーマンスに依存すると考えられる。また、ワーキングメモリ内の情報を状況に適した形にしておくには実行機能によって情報の取捨選択をして制御する必要があるとも考えられる。一方で、これら二方向の考え方のうち一方向だけをとる立場の研究者もいて、Hofmannらのように実行機能はワーキングメモリの下位概念に属すると捉える研究もあれば（Fig. 2b）[17]、Diamondのように実行機能の概念はより広義であるべきとしてワーキングメモリを構成要素の1つに位置づける研究もある（Fig. 2c）[12]。しかし、齊藤らは実行機能が記憶にのみ依存するものではなく、「切替」や「抑制」といった行動の認知的制御を担う機能は、記憶以外の注意等にも依存しており、ワーキングメモリの枠組みを超える部分が存在すると考えているという点で一方向のみの捉え方については懐疑的であると考える[9)]。さらに実行機能の行動・思考制御を示す概念と記憶制御を示すワーキングメモリが互いに補い合うといった関係を仮定しない並列的概念であると考えるのにも無理があるとしている。齊藤らの主張する相補的関係性には根拠となる実験的な知見として、Friedmanらがワーキングメモリを要する一般知能と実行機能の関係性について検討している[7)]。実行機能の中でもワーキングメモリに関連する構成要素（「更新」）には強い相関があるものの、行動制御を捉える他の構成要素（「切替」と「抑制」）との間に相関はないことから、両概念は単純に並列的に存在しているわけでもなく、また必ずしも包含関係とは限らないことを示唆する有力な知見であると言える。そのため、現時点では実行機能とワーキングメモリが相補的に働いているという齊藤らの主張が両概念を比較的明確に説明すると考えられるが、各概念の整理を含め、今後より頑健な知見が必要であることに間違いはない。

4）実行機能の単一性と多様性

実行機能の構成要素を考慮した個人差に着目した研究が進む中で、Miyakeらは実行機能の個人差を捉えて評価するための理論的枠組み（単一性／多様性モデル）を提唱した[4)18)]。

従来、種々の実行機能課題成績を説明する潜在変数として「更新」「切替」「抑制」の3つの構成要素が同定されてきたが、これらの構成要素間には中程度の相関があり、MiyakeやFriedmanらは要素間に共通する成分の存在を示唆した[4)18)]。その共通する成分を「共通実行機能」（common EF）として、課題目標や目標に関する情報を保持し、それらの情報を低次の認知的処理に効果的に用いるための能力と考え

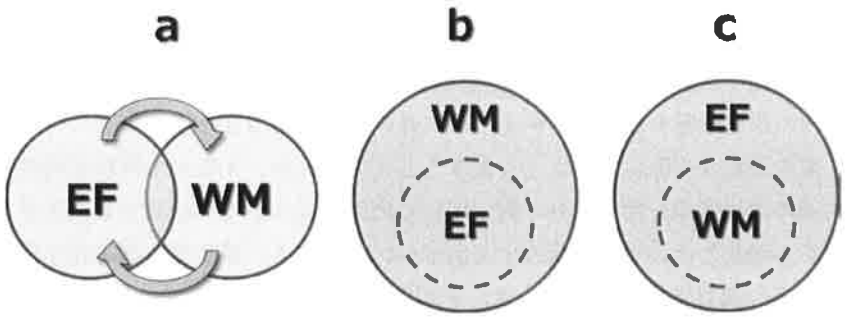


Fig. 2. 実行機能とワーキングメモリの関係
実行機能と中央実行系の核となるワーキングメモリの関係性を示した齊藤らの図を参照した[9]。a：相補的関係、b：実行機能がワーキングメモリの下位概念に属する関係、c：ワーキングメモリが実行機能の下位概念に属する関係、EF：実行機能、WM：ワーキングメモリ

た。その上で、「共通実行機能」と3つの各構成要素に固有の成分によって実行機能課題成績を説明するモデルを構築して確証的因子分析を行ったところ、「共通実行機能」に加えて、「更新」に固有の成分（updating-specific）と「切替」に固有の成分（shifting-specific）が同定された。「抑制」については、「共通実行機能」と非常に密接な関連があることから、この枠組みの中で「抑制」に固有の成分（inhibition-specific）は除外された[18]。実行機能研究の歴史的経緯の中で、前頭葉損傷により影響が生じる単一の機能としての実行機能、そして単一の機能だけでは説明できない個人差を反映する成分の存在について議論されてきたが、上述のFreidmanらの研究は、実行機能のあらゆる課題に共通して必要となる「共通実行機能」と、特定の実行機能課題に特化して必要となる「更新固有」実行機能と「切替固有」実行機能の存在を示すことで、実行機能課題の種類によって異なる成績という形で顕現する個人差を説明する枠組みを提唱できたと考えられている[18]。しかし、Miyakeらの提唱した3つの構成要素を軸に実行機能を捉える研究が多いのが昨今の研究動向である。今後前頭葉損傷による実行機能障害の個人差、さらには健常者における実行機能の個人差をより精緻に理解していくためには、単一性／多様性モデルと「更新」「切替」「抑制」の3つの構成要素からなるモデルのいずれのモデルの説明力が高いかについての詳細な検討の蓄積が期待される。

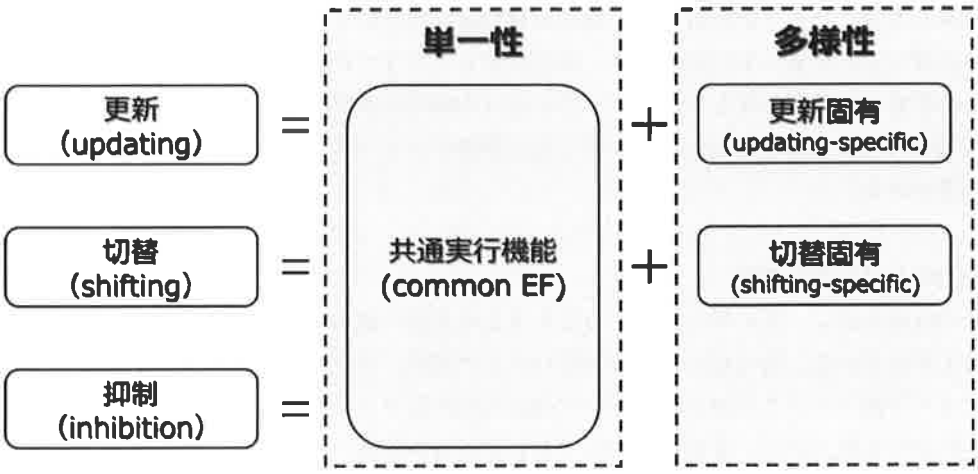


Fig. 3. 実行機能の単一性と多様性
Miyakeらと Friedmanらの提唱した実行機能の個人差を捉えるための理論的枠組みである[4][18]。独立であるとする「更新」「切替」「抑制」が単一性の要素と多様性の要素により成り立っていることを示す。

3．実行機能の構成要素に関する今後の課題

1）構成要素間の相互作用

これまで述べてきた通り、実行機能は「更新」「切替」「抑制」の3つの構成要素からなるとするモデルが有力で、それぞれの測定課題や脳部位の同定、個人差の説明に有意義な潜在変数についても研究が進んでいる。一方で、構成要素が実際にどのような働きをしているのか、すなわち同時並列的に、経時的に働いているのか、共通の認知資源が用いられて働いているのか等についての検討は未だなされていない。

構成要素を反映する課題とその成績に関連する脳部位についても、構成要素間の相互作用がネットワーク的に働いていること（実行機能ネットワーク）が仮定される知見が報告されている。Miyakeらは各構成要素を反映するいくつもの課題を示すとともに、それらの課題の一部が他の構成要素を反映する課題と相関することを示した[4]。例えば、「更新」を反映するletter memory課題は「切替」を反映するplus-minus課題と、「切替」を反映するtone monitoring課題は「抑制」を反映するantisaccade課題と有意な相関関係であることが示されている。この知見は、どれだけ実行機能を強力に反映していても他の機能による影響は排除しきれない「課題不純問題（task-impurity problem）」として広く認識されている[9]。近年の実行機能研究の動向を報告したDahlinも、Miyakeらの示す実験課題の関連性は構成要素が独立しているとは言い難いエビデンスであると言及しているように[19]、課題を遂行するためには各構成要素のみならず、他の構成要素の働きも要する可能性が考えられる。また、すでに述べたようにReinebergは各構成要素の指標である課題成績と関連する脳部位について知見を示すとともに、各構成要素の関連部位でFPや小脳が重複していることを報告している[16]。「共通実行機能」の存在とともに、構成要素は異なった脳内基盤により区別されるべきであるとした上で、これらの重複している脳部位あるいは脳ネットワークに対応する形で行動指標の知見が示されることを期待している。

これらの観点から、実行機能ネットワークが存在している可能性は十分にあると考えられる。例えば、社会的適応に必要不可欠であるとされる意思決定について実行機能の構成要素がどの程度の予測率を持つのか検討がなされているが結果に一貫性はなく、Schiebenerらは実行機能による意思決定の予測を示すためには、「更新」「切替」「抑制」の各構成要素から意思決定への直接的なパスを仮定するのではなく、構成要素間の相互作用の可能性も含め高次認知機能としての実行機能の役割を考慮すべきであると指摘している[20]。彼らは、意思決定プロセスにより近い高次の実行機能の概念として課題のルールや目標に従い情報を抑制したり切り替えたりしながら注意を向ける能力である「一般的制御（general control）」等の要素を用いることで、リスクがある状況における意思決定について実行機能が30％程度の従来の知見より高い予測率を持つことを示している。今後、実行機能ネットワークを実験的に検討することで、個々の要素の独立した影響、要素間の相互作用によって生まれる創発的な影響をも抽出することが可能になり、低次の認知機能から社会的適応行動を橋渡しする実行機能のメカニズムやその影響力を包括的かつ精緻に示すことが期待される。

2）日常生活における実行機能

実行機能の課題成績は一部の社会的適応行動を支える機能や能力における個人差の予測に有益であることがすでに示されている。例えば、注意の欠如やリスク選好、プランニングの欠如等は実行機能の課題成績の低下により予測できると示唆され、社会的適応行動の低下により特徴づけられる種々の障害との関連性も検討されている[21]。また、学習面においても計算能力や作文、読解の場面で実行機能を要すると示唆する研究もある[22]。学習面のみならず、幼児期から児童期にかけて発達する実行機能がその後の成長とともに日常生活に影響を及ぼしうる場面は大いにあるとされている[23]。しかし、いずれの研究も実行機能の構成要素の捉え方が一貫していない、あるいは一部の構成要素のみに着目していることから知見の不明瞭

さが指摘されている[9]。

様々な要因が影響しあう実生活において、社会的適応に実行機能が影響しているという頑健な知見は未だ示されていないものの、種々の従来研究による示唆や本論文で述べた実行機能概念の成り立ちから考えると、精神障害や脳機能障害等の不適応行動はもちろんのこと、健常者の日常的な社会的適応行動の個人差を実行機能という観点から説明できる可能性は高いと考えられる。さらに前項で述べた構成要素間の相互作用の検討は人々の適応行動をさらに詳細に説明する一助となると考える。実行機能の観点からの適応行動の理解や説明が可能となれば、将来的には実行機能の観点から適応的な行動の予測・制御が可能になり、また実行機能の訓練が不適応的な思考や行動を改善する一つのツールとなることも期待できる。

謝辞

本研究は、科学研究基盤研究C（16K00212）および東北福祉大学感性福祉研究所における文部科学省の私立大学戦略的研究基盤形成支援事業（平成26年度～30年度）による私学助成を得て行われ、感性福祉研究所の関係各位に感謝申し上げます。

引用文献

1）Jurado M. B., Rosselli M. "The Elusive Nature of Executive Functions: A Review of our Current Understanding" *Neuropsychological Review* **17**, 213-233, 2007

2）Diamond A. "Executive functions" *Annual Review of Psychology* **64**, 135-168, 2013

3）Duggan E. C., Garcia-Barrera M. A. "Executive Functioning and Intelligence" *S. Goldstein, Princiotta D., Neglieri J. A. (eds) Handbook of Intelligence: Evolutionary Theory, Historical Perspective, and Current Concepts. New York: Springer*, 435-458, 2015

4）Miyake A., Friedman N.P. Emerson M.J., Witzki A.H., Howerter A. "The Unity and Diversity of Executive Functions and Their Contributions to Complex Frontal Lobe Tasks: A Latent Variable Analysis" *Cognitive Psychology* **41**, 49-100, 2000

5）Friedman N.P., Miyake A. "Unity and Diversity of Executive Functions: Individual Differences as a Window on Cognitive Structure" *Cortex*, 2016

6）松吉大輔「実行機能」田中啓治, 御子柴克彦 編『脳科学辞典』, 2012

7）Friedman N.P., Miyake A., Corley R.P., Young S.E., De Fries J.C., Hewitt J.K. "Not All Executive Functions Are Related to Intelligence" *Psychological Science* **17** (**2**), 172-179, 2006

8）Damasio, A. R., "Descartes' error: Emotion, reason, and human brain" *New York: Grosset/Putnam*, 1994

9）齊藤智, 三宅昌「実行機能の概念と最近の研究動向」湯澤正通, 湯澤美紀 編『ワーキングメモリと教育』北大路書房, 27-45, 2014

10）Baddeley A.D. "The episodic buffer: a new component of working memory?" *Trends in Psychological Sciences* 4 (11), 417-423, 2000

11）Smith E. E., Jonides J. "Storage and Executive Processes in the Frontal Lobes" *Science* **283**, 1657-1661, 1999

12）Arnett P. A., Rao S. M., Grafman J., Bernardin L., Luchetta T., Binder J. R., Lobeck L. "Executive functions in multiple sclerosis: An analysis of temporal ordering, semantic encoding, and planning abilities" *Neuropsychology* **11** (**4**), 535-544, 1997

13）鹿島晴雄, 三村將, 田渕肇「BADS 遂行機能障害症候群の行動評価 日本版」新興医学出版社, 2003

14) 山形伸二, 高橋雄介, 繁桝算男, 大野裕, 木島伸彦「成人用エフォートフル・コントロール尺度日本語版の作成とその信頼性・妥当性の検討」『パーソナリティ研究』**14**（1）, 30-41, 2005
15) Banich M. T. "Executive function" *Current Directions In Psychological Science* **18**（2）, 89-94, 2009
16) Reineberg A. E. "On the Neural Basis of Individual Differences in Executive Function: a Series of Studies of the "Resting" Brain" *Psychology and Neuroscience*, 2016
17) Hofman W., Friese M., Schmeichel B. J., Baddeley A. D., "Working memory and self-regulation" *Handbook of self-regulation: Research, theory, and applications. 2nd ed.*, 204-225, 2010
18) Friedman N.P., Miyake A., Young S.E., De Fries J.C., Corley R.P., Hewitt J.K. "Individual Differences in Executive Functions Are Almost Entirely Genetic in Origin" *Journal of Experimental Psychology* **137**（2）, 201-225, 2008
19) Dahlin E. "Train your Brain Updating, Transfer, and Neural Changes"（Doctoral dissertation）*Umeå University Medical Dissertations, New Series* **1283**, 2009
20) Schiebener J., Wegmann E., Gathmann B., Laier C., Pawlikowski M., Brand M. "Among three different executive functions, general executive control ability is a key predictor of decision making under objective risk" *Frontiers in psychology* **5**, 1386, 2014
21) Young S. E., Friedman N. P., Miyake A., Willcutt E. G., Corlry R. P., Haberstick B. C., Hewitt J. K. "Behavioral disinhibition: Liability for externalizing spectrum disorders and its genetic and environmental relation to response inhibition across adolescence" *Jounal of Abnormal Psychology* **118**（1）, 2009
22) Yeniad N., Malda M., Mesman J., van IJzendoorn M. H., Pieper S. "Shifting ability predicts math and reading performance in children: A meta-analytical study" *Learning and Individual Differences* **23**, 2013
23) Moriguchi Y. "The early development of executive function and its relation to social interaction: a brief review" *Frontiers in psychology* **5**, 388, 2014

原 著 論 文

理解とパーソナリティの研究－文章理解への性格特性の影響

小松 紘
東北福祉大学

A study of comprehension and personality: The influence of personality traits on understanding sentences and passages.

KOMATSU Hiroshi
Tohoku Fukushi University

Abstract

The purpose of this study is to clarify the relationship between "comprehension" and "personality". This study's participants comprised of 55 female university students, out of which 28 of them were assigned to an experimental group and 27 to a control group. Four paragraphs were selected from essays and novels written by two writers. Each paragraph was composed of 5 sentences, and was arranged in a random order by the researcher. The participants were instructed to rearrange these sentences in the correct order. When the order of two successive sentences was correct, 1 point was awarded. The points awarded ranged from 0 to 4. In each pre- and post-session, two paragraphs were presented to the participants randomly to cancel the order effect. Consequently, the highest number of points that could possibly be awarded was 8 and the lowest number was 0. These points indicated comprehension scores for sentences and passages.

The influence of the personality traits on understanding sentences and passages was examined. The Big Five Personality Inventory was adopted. The "Big Five" refers to the following traits; extroversion (E), agreeableness (A), conscientiousness (C), emotional stability (N) and openness for experience (O). A Stroop task and a reverse-Stroop task were assigned to the participants of the experimental group (S group) as a cognitive conflict processing task between the pre- and post-session. The participants were instructed to carry out these task as quickly and accurately as possible. It was already known that about five minutes were required to complete them through a preliminary experiment. Therefore, a five minute break was also inserted between the pre- and post- session period for the control group (C group). The results were as follows.

1) As the experimental conditions were the same for the pre-session S group and the C group, the correlation coefficient was calculated for each combination of the comprehension scores and standard scores of personality traits. Consequently, a zero correlation coefficient was confirmed for the combinations of comprehension scores and standard scores of A, C and O personality traits. Conversely, a small positive correlation was found between the comprehension score and the E factor or N factor personality traits.
2) The middle degree of E factor contributed to the comprehension of context. Following the Stroop task the comprehension scores were lowered and standard deviations increased in the responses of the S group participants. We should be aware of the importance of the data variance as well as the central tendency. N factor demonstrated diverse effects. The time break may have substituted for rest time, while the Stroop task may have played a more complex role. The problems of cognitive conflict processing during the Stroop task were discussed, including social problems like "bullying".

Keywords : comprehension, personality, extroversion, emotional stability, Stroop effect

1．はじめに

本研究は、小川誠二を代用者とする研究プロジェクト「社会的・職業能力育成プログラムに資する認知・脳科学的エビデンス情報提供基盤の構築」の一環をなすものである。新入社員や職員、あるいは学校に入学したばかりの新入生にとって、新しい環境に適応できるためには、人的にも社会的にもその環境を支配している約束事と、自分の仕事そのものを理解しなければならなくなる。つまり「理解(comprehension)」は私たちの現実の生活における極めて重要な心的機能であるとともに、心理学にとっても、最重要課題の一つといえよう。しかしながら私たちの身の回りのいたるところに、相互の不理解にもとづくトラブルのいかに多いことか。国家間の争いも、とどのつまりは同じような原因によるところがあまりに多すぎるように思われる。認知科学の時代を迎え、「理解」についても膨大で質の高い研究成果が積み重ねられてきた。にもかかわらず、その貴重な知見がどれほど現実において生かされているか疑問である。

このようなときにあって、佐伯　胖[1]の「理解とは何か」は、1980年代の認知科学の研究事情を通覧するのに有役である。この書の中で取り上げられた話題は、「理解の文脈依存性」、「算数・数学における理解」、「理解におけるインターラクションとは何か」、「リテラシーの文化的起源」、「理解はどう研究されてきたか」の５題であった。この５題の中で本研究と関わりの深い話題は「理解の文脈依存性」である。この中で村上陽一郎[2]は「パラダイム論」を展開し、同じパラダイムに属するもの同士は、ジャーゴン（業界用語）のような共通の言語を持つ場合が多く、理解しやすい関係にあるが、異なるパラダイムに属する場合は、言語の問題も含め「共約不可能性」という問題に直面することが多くなることを指摘している。この問題は、実験などで必要とする被験者（参加者）集団構成員の性別のバランスが偏っている場合などにも問題になる。例えば、同性の多い集団内に少数の異性がいる場合、この少数の異性が異質な要素となり、それが無視できない効果として現れることがある。

もう一つの問題として、当事者のパーソナリティ(personality）の問題がある。「パーソナリティとは人の広い意味での行動（例えば具体的な振る舞い、言語表出、思考活動、認知や判断、感情表出、嫌悪判断など）に、時間的・空間的一貫性を与えているもの」と定義されている。また性格特性とは「性格特徴のなかで、一貫して出現する行動傾向やそのまとまりをいう」[3]。「パーソナリティ」と「性格」は語源的には前者が「仮面」を意味する “persona” で、個人の外界との適応の特徴を意味し、後者が「彫刻」または「刻みつけられたもの」を意味する “character” で、個人の情意面の特徴を意味するが、実際にはその区別はさほど明確ではない。しかし現実の問題として、パーソナリティや性格などの個人的、内的特徴によって、状況における個人の「理解」のあり方が様々な様相を呈することを私たちは経験的に知っている。この問題は情報を受け取る側に限らず、情報を送る側、例えば、教師や職場の上司にとっても面倒な問題であろう。つまり、いかに理解できる言葉で矛盾のない情報を送るかという情報の質や、知的面での混乱や情動的な不安を引き起こすことがないよう自分たちの態度や行動のあり方に配慮する必要がある。確かに、状況が理解できず、予測がことごとく裏切られたとき、その認知的葛藤のために私たちはパニックに陥るであろうし、その状態は簡単には回復できないかもしれない。このような状況要因が、「理解」にとって実際にどのような影響を及ぼすのか検討される必要があろう。本研究ではこの「理解」の主体である個人のパーソナリティの問題と、その個人の知的・情的状態に混乱や不安を引き起こす状況要因の影響を、認知的葛藤を引き起こす「ストループ課題」と、その効果の指標となる「不安」を捉える尺度を用いて検討する。

本研究は、実に多様な「理解」の問題の中から、「文章の理解」について取り上げる。「文章とは文よりも大きい言語単位で、通常は複数の文から構成されるものである。それ自身完結し、統一ある思想感情を伝達する[4]」と定義される。この「文章の理解」を「パーソナリティ」との関連で捉える方法には、大意

や要旨の把握問題、文脈（context）の理解問題などが考えられるが、本研究では、一つの文の前後の状況についての「推論」と「照応」から、正しい文のつながりを判断する文脈の理解問題に焦点を絞る。

注）川崎[5]によれば「推論とは、文章を読むことによってそこに直接書かれていない情報を読み手が自分の知識から引き出してくる過程を指している」、「照応とは、文中のある構成要素を他の構成要素と対応づける過程をいう」。

2．研究目的

個人のパーソナリティと文章理解、特に文脈の理解との関係を明らかにし、探索的ではあるが、文章の正しい理解のために個人のパーソナリティ特性のどのような側面が重要なのか、さらに、ストループ課題のような「認知的葛藤」が、文章理解という心的機能にどのような影響を及ぼすのかを検討する。

3．方法

1）被験者（参加者）

「理解」の課題に取り組む参加者の選出には、性別や年齢、人種など、感じ方、考え方、身につけた社会的慣習や価値観などをできる限り同質に近づける必要があった。これは上述したように、パラダイムの違いは、どうしても「共約不可能性」といわれる互いに相容れない要因を伴いやすく、参加者の質が多様になると、データの解釈が難しくなることが懸念されたためである。課題の違いによる影響も参加者集団が同質に近ければ、それだけ結果の変動要因を推測できることになり都合がよい。また、募集可能な参加者の母集団は女性が多かったので、本研究では性別は女子に統一された。具体的には、参加者の募集に伴う口頭と文書による説明に応じて同意書を提出した19～22歳の女子学生55名が選ばれた。参加者には相場に応じた謝金が支払われた。

2）群構成と負荷課題

本研究は、実験群（S群28名）と統制群（C群27名）の2群から構成される。本研究の目的は、「パーソナリティ」と「理解」との間の関係性を明らかにすることにあり、特に負荷の少ない条件と、何らかの心理的負荷がかかる条件とが用意され、それぞれの文章理解への影響が調べられた。実験デザインとしては、実験群では心理的負荷課題の前後において「文章理解」への影響が捉えられた。具体的にはストループ（Stroop）課題が導入された。例えば、赤、青、黄、緑の文字をそれぞれ文字が意味する色で示した場合と、文字の意味とは異なる色で示した場合では、後者の方のインクの色読みが困難となる。それは文字情報が色情報の認知を妨げた（干渉した）ためであり、この認知的葛藤を「ストループ効果」と呼ぶ。一方、後者のような色 - 文字不一致刺激の文字情報に合った色紙を選ばせた場合は、インクの色情報が文字の読みを妨げる結果が得られる。これを「逆ストループ効果」という。S群ではストループと逆ストループ2課題が課された。参加者はできる限り早く正確に、最後まで作業を行うよう求められ、所要時間とエラー数が記録された。ストループ課題が採用された理由は、「ストループ効果」が、言語中枢と考えられるブローカ野を含む、左半球下前頭回付近の活動性を高める（色の認知反応を抑え認知的葛藤を引き起こす）と考えられるからである[6]。一方C群には特に課題は与えられず、予備実験からストループ課題に要すると見なされた約5分間の自由時間が与えられた。

3）文章理解問題の作成

文章理解の課題として、大学生が読み慣れているジャンルと思われる小説とエッセイが選ばれた。具体的には、神谷克己[7]のエッセイと柴田 翔[8]の小説から、5つの文からなるパラグラフが各2つずつ、計4つ選ばれた。柴田の小説をA・C、神谷のエッセイをB・Dとした場合、4つの異なる文章課題は、実

験群、統制群の半数ずつ、Pre、Postの課題の提示順序を逆転することによって順序効果が相殺された。つまり、実験群の半数でPreにA・B、PostにC・Dが提示されたら、残りの半数ではPreにC・D、PostにA・Bが提示された。このA・BとC・Dのペアは実験を通して変えられることなく、統制群も同様な方式で課題が遂行された。理想的には4つのパラグラフの困難度がみな等しいことであるが、A・BとC・Dの課題得点の平均値の差は0.39と僅差であり、統計的にも有意ではなかったので、上記のような方法で課題の困難度や順序効果のカウンターバランスが図られた。(平均値：A・B＝4.62、C・D＝4.23、Fの確率値＝0.54>0.05、t (53) =0.84、P>0.05)。

被験者にはパラグラフを構成する文の順序がばらばらに示され、意味が通るように文末の□内に正しいと思われる順序に番号を記入し、全体を再構成するよう求められた。すでに述べたように、文脈の理解には文章の中に隠れている情報を「推論」によって引き出し、文中に述べられた事物からの表象を利用し、表象同士を「照応」させ、その関連性に注目することにより文章間の関係を見出し順序だてていく過程が想定される[5]。このことを考慮して次のような採点方式が採用された。即ち、1つの文とそれに続く文とが正しければ1点が与えられた。この方法を続けることによって、中間の2点、3点が与えられた。そして、つながりがすべて正しい場合に満点の4が与えられた。Pre、Postそれぞれで2課題提示されたので、Pre、Postともに8点が最高であった。

4）パーソナリティの検査と不安尺度検査

被験者のパーソナリティに関する基本情報を得るために、全被験者に対して村上亘寛・村上千恵子[9][10]による主要5因子性格検査が施行された。主要5因子とは、E外交性（Extroversion)、A協調性(Agreeableness)、C勤勉性（または良識性Conscientiousness)、N情緒安定性（Emotional Stability)、O知的好奇心（または知性Openness for Experience）である。以下の記述では、C因子は勤勉性、O因子は知的好奇心と表記を短縮する。さらに課題前後の不安の変化を調べるために、S群のストループ課題前後と、比較のためC群の自由時間の前後に、肥田野 直[11]らよる新版STAIの状態不安の検査が施行された。新版STAIは特性不安（Trait Anxiety）と状態不安（State Anxiety）からなっている。常日頃の不安状態を示す特性不安は、Big 5の情緒安定性因子によってある程度推定されるが、刺激効果などによるその時その状況での状態不安はSTAIの状態不安尺度によって測定された。

5）実験順序

(1) 実験群（S群)：主要五因子性格検査→STAI（状態不安）→文章理解課題（Pre）→ストループ課題→文章理解課題（Post）→STAI（状態不安）で終了。所要時間は50分～60分。

(2) 統制群（C群)：ストループ課題が導入されず、ストループ課題を遂行するのに要する平均時間とほぼ同じとみなされた5分間を、被験者控え室で自由に過ごす。他の実験手順は実験群と同じである。

6）実験期間と実験場所

実験機間：2015年12月～2016年2月。実験場所：東北福祉大学福祉心理学科ポリグラフ室②

4．結果

実験群のS群、統制群のC群に加え、文章理解課題の成績によって、高得点群（H群)、中得点群（M群)、低得点群（L群）が作られた。H群は8～6点、M群は5～3点、L群は2～0点であった。Big 5で調べられる性格特性の段階表示は、テストのマニュアルに従い、因子間の比較が可能な標準得点の値が

56以上を因子高群、44以下を因子低群とし、56未満から44を超える群を因子中群とした。標準得点が高いことは、外交性、協調性、勤勉性、情緒安定性、知的好奇心の程度が高いことを意味し、低い場合はこれらの特性が低いことを意味する。

1）文章理解度と性格特性との関係

実験群（S群）と統制群（C群）を込みにして、Preの文章理解度得点H、M、L群ごとに、主要5因子標準得点の平均値と標準偏差を表と図に示した（Table 1 ～ 3、Fig. 1 ～ 3）。以後S群とC群を込みにする場合はS+Cと表現する。

Table 1．H群/S+C（Pre）におけるBig 5標準得点

	E 外交性	A 協調性	C 勤勉性	N 情緒安定性	O 知的好奇心
平均値	43.5	52.1	48.3	45.6	43.5
標準偏差	7.2	11.3	9.6	7.7	8.5
人数	15	15	15	15	15

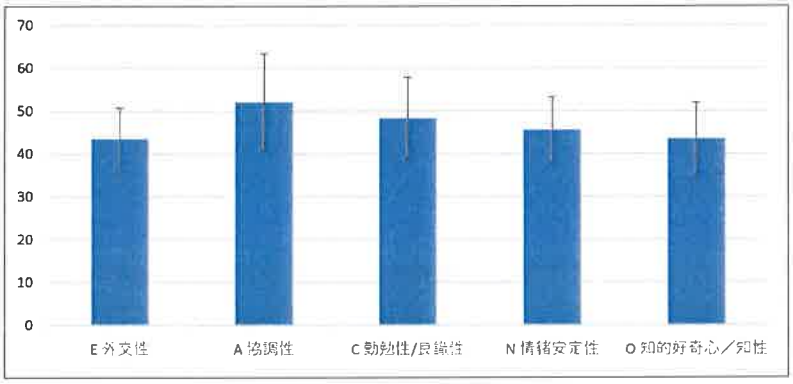


Fig. 1．H群／S+C（Pre）におけるBig 5標準得点（平均値と標準偏差）

Table 2．M群/S+C（Pre）におけるBig 5標準得点

	E 外交性	A 協調性	C 勤勉性	N 情緒安定性	O 知的好奇心
平均値	42.6	51.3	53.4	43.9	47.3
標準偏差	6.8	9.3	10.3	11.0	8.0
人数	32	32	32	32	32

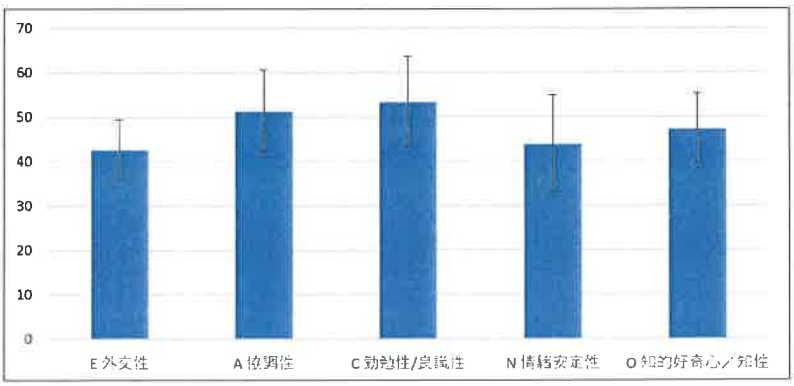


Fig. 2．M群／S+C（Pre）におけるBig 5標準得点（平均値と標準偏差）

Table 3．L群 /S+C（Pre）における Big 5 標準得点

	E 外交性	A 協調性	C 勤勉性	N 情緒安定性	O 知的好奇心
平均	39.9	55.1	48.9	43.1	43.1
標準偏差	7.8	15.5	8.0	8.7	6.1
人数	8	8	8	8	8

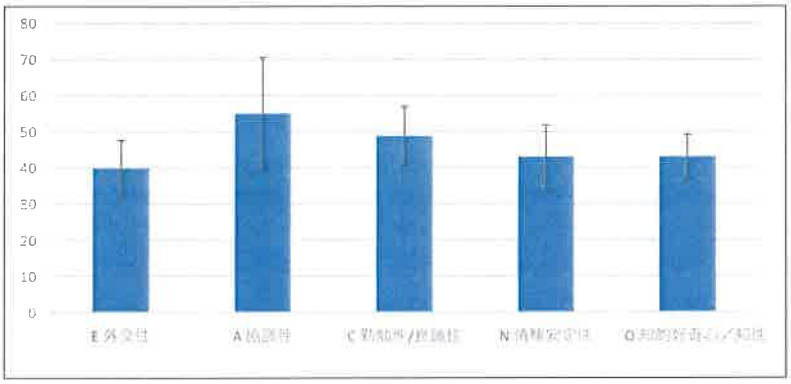


Fig. 3．L群／S+C（Pre）における Big 5 標準得点（平均値と標準偏差）

全体的傾向としては、5 因子のうち、A 協調性因子と C 勤勉性因子が他の因子に較べてやや高くなっているが、文章の理解度とどう関わるのかを調べるために、文章理解度得点と各性格特性因子の標準得点間の相関が調べられた（Table 4 の相関行列）。

Table 4．S+C（Pre）の文章理解課題得点および主要 5 因子標準得点間の相関行列

	文章理解課題	E 外交性	A 協調性	C 勤勉性	N 情緒安定性	O 知的好奇心
文章理解課題	1					
E 外交性	0.182124714	1				
A 協調性	-0.00726092	0.211955388	1			
C 勤勉性	-0.006715909	0.348128117	0.560872752	1		
N 情緒安定性	0.123338167	0.205087208	-0.09107761	0.027199812	1	
O 知的好奇心	0.007747916	0.243623324	0.179647596	0.523060181	0.221157607	1

Table 4 より、A 協調性因子と C 勤勉性因子は相関係数が0.561と高く、C 因子は O 知的好奇心因子とも相関係数0.523と関わりが深い。しかし、A、C、O の 3 因子は文章理解度とは無相関であった。これに対して、E 外交性因子は有意味なレベルではないが文章理解度と0.182の弱い正の相関が認められ（t（53）=1.347、p=0.184>0.05）。N 情緒安定性因子も、文章理解度と0.123の弱い相関が見られた（t（53）=0.902、p=0.371>0.05）。つまり、外交性と情緒安定性の因子は、文章理解に少しは関わりを持つ可能性を期待させる。そこで、文章理解度と性格特性との関係をさらに調べるために、E 外交性因子と N 情緒安定性因子が文章理解度とどのような関わりを持つかが検討された。

2）E外交性因子およびN情緒安定性因子の高低による文章理解度の違いと、ストループのような強い認知的葛藤を引き起こす課題の効果を検証する。

(1) E外交性因子：Table 5 と Fig.4の表・図は、E外交性因子中群の Pre-Post における文章理解度得点である。S群はストループ課題の前後の比較であり、C群は自由時間の前後の比較となる。両群ともに理解度得点は Pre から Post への低下傾向を示しているが、ともに対応のあるT検定では得点の平均値に有意な違いは見られなかった（S群：t (10)=0.89, p >0.05, C群：t (6)=0.92, p >0.05)。対応のある2条件でTテストを施行する場合、事前のF検定は省略されることが多いが、あえてF検定を施行した。その結果Fの確率値=0.015となり、S群の Pre-Post 間で Post における理解度得点の分散の増加が有意となった（p<0.05)。またC群においても、Post における理解度得点の分散の増加が有意傾向を見せた（Fの確率値=0.076, 0.10>p>0.05)。グラフからも分かるように、両群ともに Post の標準偏差が大きく、同様の傾向と見なすこともできるが、ストループ作業に従事するのと、自由時間を過ごすのとでは5分間の条件効果が異なることが考えられるので、改めて考察で検討する。

Table 5．S群E因子中群とC群E因子中群の Pre・Post 比較

	S・E因子中群		C・E因子中群	
	Pre	Post	Pre	Post
平均値	6.0	5.4	4.4	3.7
標準偏差	1.1	2.5	1.1	2.5
人数	11	11	7	7

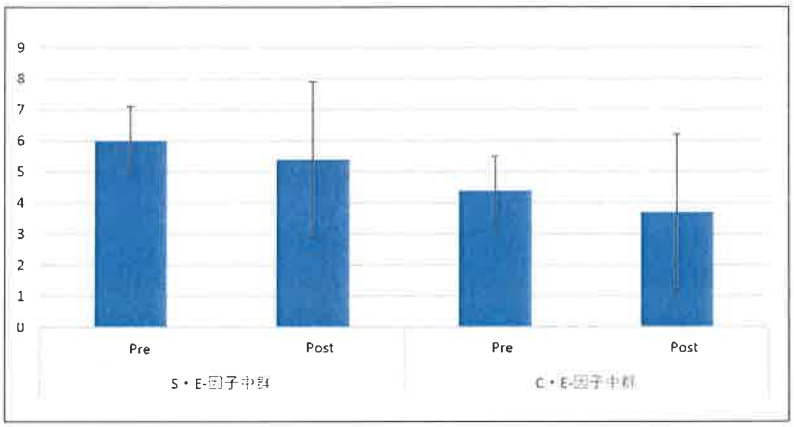


Fig. 4．E因子中群の理解度得点

Table 6. と Fig. 5. はE外交性因子低群の Pre-Post における文章理解度得点である。S群とC群の条件の違いは上記と同じである。S群、C群ともにF検定の結果は等分散が確認されたので、両群の Pre-Post 間の平均値の比較のために対応のあるT検定を行った。結果は両群ともに有意な違いは見られなかった（S群：t (16)=1.198, p>0.05、C群：t (17)=0.218, p>0.05)。表図から、S群、C群ともに Post での理解度得点のばらつきが大きくなり、個人差が増したように見えるが、平均値についてはS群とC群とで傾向に違いがあった。すなわち、S群ではE因子中群と同様、有意差は得られなかったが、理解度得点の低下傾向が見られたのに対して、C群では得点の平均値がほぼ同じになるという結果であった。

Table 6．S群E因子低群とC群E因子低群のPre・Post比較

	S・E因子低群		C・E因子中群	
	Pre	Post	Pre	Post
平均値	4.0	3.2	4	3.9
標準偏差	1.3	1.9	1.8	2
人数	17	17	18	18

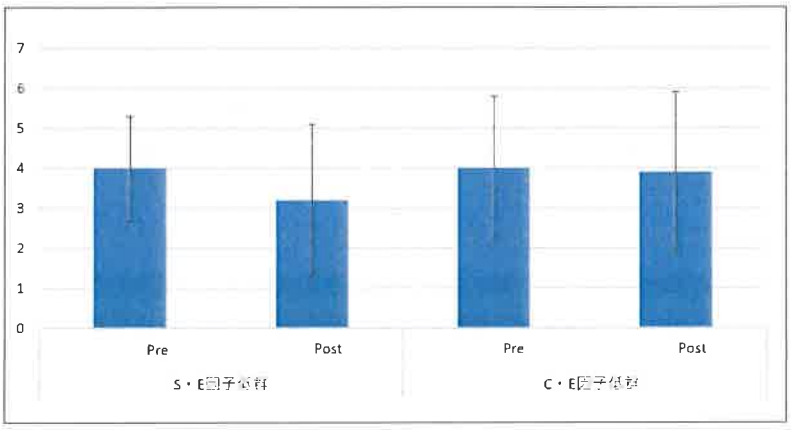


Fig. 5．E因子低群の理解度得点

次に、同じS群の中で、E因子中群（Table 5. とFig. 4.）とE因子低群（Table 6. とFig. 5.）のPreにおける理解度得点の平均値を較べて見ると、中群において理解度得点が高く、しかも1％レベルの優位性を示した（E因子中群の平均値＝6.0、E因子低群の平均値＝4.0、t（26）=3.522、p<0.01）。しかし、C群のPreにおけるE因子の中－低の比較では、傾向は同じであるが有意な差ではなかった（E因子中群の平均値=4.4、E因子低群の平均値＝4.0、t（23）=0.587、p>0.05）。上記の分散のことも含め、理解度に及ぼすE因子の効果については考察で検討を加える。

今回の実験では、E因子の高い被験者はS群には存在せず、C群においても2名しかいなかったため、分析の対象から除外された。

(2) N情緒安定性因子：Table 7とFig. 6.はS群N因子中群のPre・Postの理解度得点を表・図に表したものである。C群はデータ数が4と足らなかったのでPre-Postの統計的解析から除外された。表・図から推測される傾向は理解度の平均値はPostで低下し、ばらつきを示す標準偏差は大きくなるという点である。しかしいずれも統計的には有意な傾向ではなかった。

S群のN因子低群とC群N因子低群のPre・Postの理解度得点が、Table 8. とFig. 7. に示されてある。ストループ課題が課されるS・N因子低群は、これまでのPre-Postの傾向と同様に、統計的に有意な傾向ではなかったが、理解度の平均値の低下と標準偏差の増加を示した。これに対してC群では、理解度の標準偏差はS群と同様Postで増加しているが、平均値は同じ値を示した。

N因子の高群は、S群には2名しかおらず解析の対象から外され、C群の同因子の高群6名について検討された。Table 9. とFig. 8. によれば、統計的には有意ではないが標準偏差と理解度得点がPostで増加傾向を示した。

Table 7．S 群 N 因子中群の Pre・Post 比較

	S・N 因子中群	
	Pre	Post
平均値	4.6	3.9
標準偏差	1.8	2.5
人数	11	11

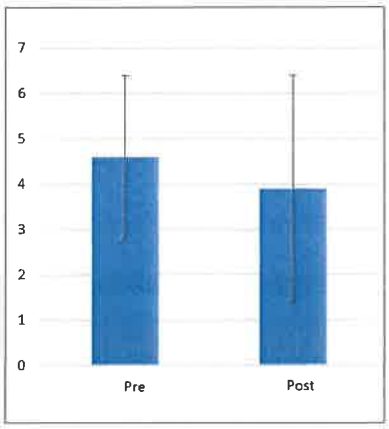


Fig. 6．S 群・N 因子中群の理解度得点

Table 8．S 群 N 因子低群と C 群 N 因子低群の Pre・Post 比較

	S・N 因子低群		C・N 因子低群	
	Pre	Post	Pre	Post
平均値	5.0	4.1	3.6	3.6
標準偏差	1.8	2.6	1.5	2.1
人数	15	15	17	17

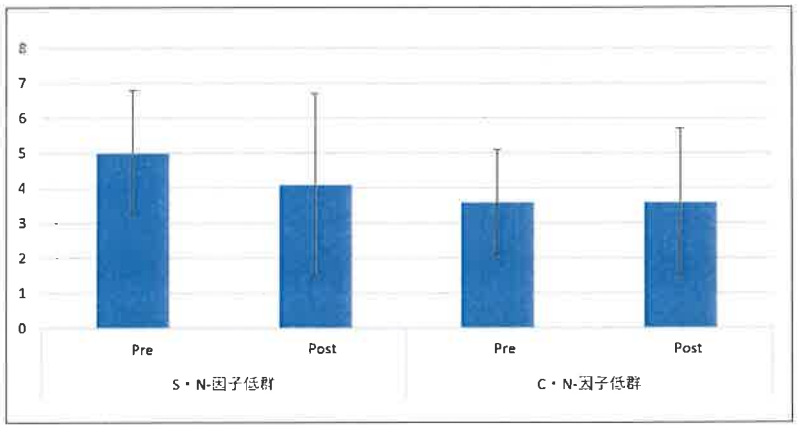


Fig. 7．N 因子低群の理解度得点

Table 9．C群N因子高群のPre・Post比較

	C・N因子高群	
	Pre	Post
平均値	4.5	5.0
標準偏差	2.0	2.5
人数	6	6

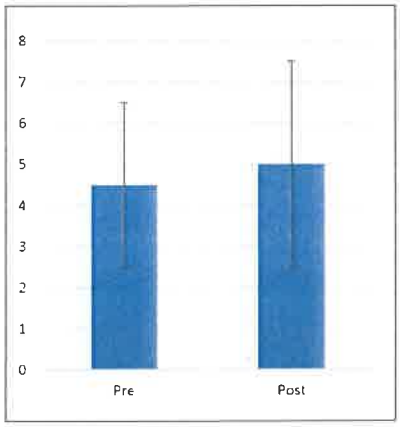


Fig. 8．C群N因子高群の理解度得点

3）ストループ課題の結果と課題前後のSTAI（状況不安）の結果

ストループ課題は実験群であるS群28名にのみ課された。S群におけるストループ課題の平均所要時間は137.3秒（標準偏差は26.7秒）、誤りは平均1回であった。逆ストループ課題の平均所要時間は156.3秒（標準偏差は18.1秒）、誤りは平均0.7回で、誤り数はストループ課題よりやや少ないが、時間は多くかかった。これは前の検査で形成された構えを改めなければならなかったためと推測される。かなりストレスフルな課題といえよう。STAI（状況不安）は、S群ではストループ課題の前後で、C群では自由時間の前後で実施された。S群のSTAI（状況不安）は、Pre平均42.4（SD=9.1）、Post平均39.1（SD=7.5）で、Postでの不安の低下は10％レベルで有意な傾向であった（t（27）＝2.008, 0.10>p>0.05）。C群の場合も、Preの平均45.4（SD=11.4）、Postの平均42.5（SD=8.2）で、Postでの不安の低下は10％レベルで優位な傾向であった（t（26）=1.850, 0.10> t >0.05）。この不安の低下の意味は考察で検討される。

5．考察

「パーソナリティ」の研究は、基礎学としては膨大な研究の積み重ねがあるが、実用を目指した研究では、種々のパーソナリティテストをベースとして、今必要とされる実践的能力や、将来力を発揮できる可能性など、いわゆる「適性」を調べる検査の類がよく知られている。しかしながら、雇用者側が適性検査を使用する場合、その目的の多くは採用試験の一部をなすものであったり、適正配置のためなど、雇用者側の要求にかなった者の選抜になる傾向がある。致し方のないことかもしれないが、被雇用者側にすれば、自分の希望がかなえられない不満が残ることもあろう。両者の希望がかなえられるためには、客観的な方法で被雇用者の得手不得手を明らかにし、不得手の部分が雇用者側の配慮や助言・援助によって改善され、仕事で十分能力を発揮できるようになることである。つまり、先輩や上司が本人の弱点を理解し、適切な対応をとることが必要となる。本研究では多様な理解領域の中から、実践的にも極めて重要な意味をもつ文章の理解を取り上げた。そして、文章理解テストとパーソナリティテストを実施することによって、

本人のパーソナリティのどの性格特性が「文章理解」と関係が深く、またどのような人的・社会的条件の影響を受けやすいかを明らかにすることが目指された。その上で、どうすればそれらの環境条件の効果を、よりプラスの効果へと転換できるか、その手がかりを得るためのアプローチが試みられた。

1）文章理解度得点とBig 5の5つの因子との関係性を調べたTable 4.の相関行列から、A協調性因子、C勤勉性因子、O知的好奇心因子が文章理解度得点と無相関であったのに対して、E外交性因子とN情緒安定性因子は0.1台の弱い正の相関を示した。この2因子を主たる対象として、文章理解度との関係性を捉えようとした試みは、相関係数が帰無仮説“無相関”を棄却できないレベルでは無理があるようにも思われる。しかしながらその後の条件分析的解析によって、以下のような興味ある知見が得られている。

2）E外交性因子とN情緒安定性因子の高低と文章理解度との関係は、E外交性因子において、いくつかの重要と思われる知見が得られた。先ず、E因子中群のS群とC群のPre-Postの比較で、どちらも文章理解度の平均値間にPostでの低下が見られたが、統計的には有意な違いではなかった。しかしながら、グラフでは縦バーの標準偏差で表されているデータの分散には、S群において5％水準でPostの分散が増す傾向が、Cでも10％水準のいわゆる有意な傾向が認められた。通常、統計的検定では、条件による代表値の変化が有意か否か問われる傾向にあるが、反応のばらつきも参加者の心理状態を反映する重要な指標であり、十分検討されなければならない。標準偏差の増加は、反応の個人差が拡大されたということになる。今回の実験に当てはめてみれば、ストループ課題の終了後は、負荷の大きな作業の効果と、作業からの解放効果とがミックスされた状態と推察される。一方、統制群の自由時間の過ごし方もまちまちで、両者とも個人差が拡大されていることが予想される。もしこれらの群がこのような状況のまま、職場で共同作業に当たった場合、めいめいの心身の状態にまとまりがなく、全体をまとめるための適切な指示や助言が必要になるかもしれない。

ここで、ストループ効果のような強い認知的葛藤が私たちの「理解」に及ぼす影響を、改めて考えてみる必要があろう。既に3.の「方法」で述べたように、ストループ課題は文字情報と色情報との認知的葛藤を引き起こす課題であり、Stroopによって開発された。ストループ効果は、言語中枢と考えられるブローカ野を含む、左半球下前頭回付近の活動性を高めるといわれるが[6]、その意味は単純ではなく、情報処理をかく乱する負の意味もある。このことを再び職場の問題に拡大して解釈すれば、上位と下位の者との間のコミュニケーションのあり方などが問われよう。コミュニケーションにトラブルが生じた場合、情報の送り手も受けても認知的葛藤に陥り、一時的にも状況を正しく理解できなくなる可能性があると考えられる。つまり「推論」と「照応」がうまくいかず、「理解」に至らなくなるわけである。この傾向は新人や下位の者ほど深刻かもしれない。上司や先輩によるメンタル面へのサポートが必要なところであろう。

これに対して、パーソナリティや性格特性面ではどうだろうか。S群のE外交性因子中群（Fig. 4）と低群（Fig. 5）のPreで確認された、E因子中群が低群より理解度が有意に高い傾向と（$p<0.01$）、有意ではなかったが、C群のE因子中・低群でも見られた同様の傾向は、適度な他者との交流を求める性格特性が、理解度を向上させる傾向のあることを示唆しているようにも思われる。これは新入生や新入社員にとって「適応」のためのヒントになるかもしれない。

N情緒安定性因子は、予測のつかない効果を持つ因子と思われる（Fig. 6～Fig. 8）。残念ながら情緒的に安定している人の条件効果については、S群N因子高群のデータ数が少なく解析にかからなかったが、C群N因子高群では、自由時間後の文章理解度が幾分増加し、回復傾向を示した。S群のN因子中群と低群では統計的に有意ではないが、文章理解度得点の平均値がPostにおいて低下傾向を示し、ストループ課題の文章理解に対する負の効果が見られている。その一方で、C群のN因子高群と低群のPostでの動きは、情緒安定性の高いN因子高群のPostで理解度得点が高くなり、一方、情緒安定性の低いN因子低群ではPreとPostの成績は同じであった。効果が一貫しておらず「自由時間」という曖昧な条件

の特徴とも考えられる。

3）ストループ課題の前後で行われた文章理解テストの成績と、STAIの状態不安検査の結果は、どちらの群もPostでの低下が認められた。本実験の負荷課題として選ばれたストループ検査は、強い認知的葛藤を起こすようである。その効果は言語機能に残留し、課題終了後すぐに消失するものではないのかもしれない。その点、STAIなどの不安検査によって検出されるもの、つまり、質問紙によって自分の内に感じ取るような不安とは異なる、なんらかの神経生理学的基礎をもつ効果のようにも思われる。その実態を明らかにするには脳科学や内分泌学を含めた、より精密な心理生理学的研究手法を導入しなければならないであろう。Champagne-Lavau,M.ら[12]やRapp,A.M.たち[13]は、schizophreniaの患者を対象として、ironyの理解に対する心理生理学的、認知科学的研究を行っている。Terrien,S.[14]らはERPを指標に、軽躁的なパーソナリティ特性との関連で、文脈における情動的意味を明らかにしようとしている。本研究のように健常な参加者を対象とした研究と、平衡して行われる必要がある研究といえよう。

6．結語

本研究で得られた知見は限られたものであったが、基礎研究と応用的研究の両者の性格を持つ研究の場合、データや理論の十分な積み重ねの結果として実践に移る慎重な研究だけではなく、必要に応じて双方の研究を続けながら情報のやり取りを行い、日々の前進を目指す姿勢も大切と考える。今回の研究で残された協調性因子（A）、良識性因子（C）、好奇心因子（O）についても、また男性のケースについても、今後継続して検討する予定である。

謝辞

・本研究は、東北福祉大学感性福祉研究所における文部科学省の私立大学戦略的研究基盤形成支援事業（平成26年度～平成30年度）による私学助成を得て行われた。
・本研究は、東北福祉大学研究倫理委員会への申請・承認を得た後に実施された（RS150607）。
・本研究への参加者の募集に当たって、東北福祉大学福祉心理学科渡部純夫教授、同・皆川州正教授、同・内藤裕子准教授のご協力を得ました。また、本論文の校正に当たって、東北福祉大学感性福祉研究所職員上野加奈さんのご協力を得ました。ここに深く感謝の意を表します。

引用文献と参考文献

1）佐伯　胖（編）『理解とは何か』（コレクション認知科学２），東京大学出版会，2015
2）村上陽一郎「理解の文脈依存性」，佐伯　胖（編）『理解とは何か』（コレクション認知科学２），東京大学出版会，9-36，2015
3）中島義明，安藤清志，子安増夫，坂野雄二，繁桝算男，立花政夫，箱田裕司（編）『心理学辞典』有斐閣，1999
4）新村　出『広辞苑』第六版，岩波書店，2008
5）川崎恵里子『文章理解の認知心理学』誠信書房　2014
6）福原理宏，三木光範，横内久猛，廣安知之「ストループテスト時における脳血流変化と課題成績の関係性の検討」『同志社大学理工学研究報告』**53**（4），185-190，2013
7）神谷克己『馬車の轍』東洋経済印刷株式会社，82，225，1990.（文章理解課題として引用）
8）柴田　翔『立ち盡す明日』新潮社，17-18，26，1971.（文章理解課題として引用）
9）村上宣寛，村上千恵子『臨床心理アセスメントハンドブック』北大路書房　2008
10）村上宣寛，村上千恵子「主要五因子性格検査の世代別標準化」『性格心理学研究』**8**（1），32-42，

1999
11) 肥田野　直・福原眞知子・岩脇三良・曽我祥子・Spielberger『新版 STAI』実務教育出版　2000.
12) Champagne-Lavau,M., Charest,A., Anselmo,K., Rodoriguez,J-P. and Blouin,G. " Theory of mind and context processing in schizophrenia:The role of cognitive flexibility" Psychiatry Research, **200 (2-3)**, 184-192, 2012.
13) Rapp,A.M., Langohr,K., Mutschler,D.E., Klingberg,S., Wild,B. and Erb,M., " Isn't it ironic? Neural correlates of irony comprehension in schizophrenia" PLoS One, **8 (9)**, ARTID:e74224, 2013.
14) Terrien,S., Gobin,P., Coutte,A., Thuaire,F., Iakimova,G., Mazzola-Pomietto,p., Besche-Richard,C., "Emotional meaning in context in relation to hypomanic personality traits : An ERP study" PLoS One, **10 (9)**, ARTID:e0138877, 2015.

原 著 論 文

Classification of Resting State fMRI Data by an Unsupervised Neural Network

Zahra NAZARI[1], Moriyuki INAMINE[1], Dongshik KANG[1], Yousuke KAWACHI[2], Yul-Wan SUNG[2], Seiji Ogawa[2]

[1]Department of Information Engineering, University of the Ryukyus, Okinawa, Japan

[2]Kansei Fukushi Research Institute, Tohoku Fukushi University, Sendai, Japan

Abstract

The self-organized map method is used to examine whether resting state fMRI data have intrinsic characteristics, based on which individual brain functions can be classified. We found that in spite of high variability, resting state fMRI data have common characteristics and can be classified on the basis of those characteristics. A self-organized map is an unsupervised neural network that further requires assignment of proper meaning or labeling to each classified data set. Here, we attempt to examine an assignment method for the classified data sets.

Keywords : resting state fMRI, self-organizing map, assignment

Introduction

Brain imaging studies by functional MRI (fMRI) with stimulus tasks usually have targeted a small number of several tens of subjects and limited number of brain areas. However, those by resting state fMRI target a large number of subjects, more than ten thousands in some cases. Therefore, the brain imaging study comes to require other analysis methods than the typical parametric methods that have been used so far. Artificial neural network (ANN) is one of the most well-known nonparametric machine learning methods [1, 2]. In the previous study we had applied self-organizing map (SOM), a type of artificial neural networks to know whether resting state fMRI (rs-fMRI) data can be classified by their intrinsic characteristics or not, and found that the rs-fMRI data are classifiable [3]. However, the SOM is an unsupervised neural network method and we could not know what meaning each classified data set had. In this study we examined an assignment method of the classified data sets after classification by the SOM.

Methods

(Self-organizing map: SOM)

The self-organizing map is a type of neural network proposed by Kohonen [4]. SOM consists of input and output layers and is useful especially for multi-dimensional data. The SOM algorithm is based on competitive learning. In the training stage, the input vectors pass through all units in the competitive layer and the network becomes self-organized by repeatedly comparing input vectors and those in each unit. The SOM does not use known information in the training process, so that it is known as an unsupervised neural network. SOM provides a topology preserving mapping from high dimensional space to map units. Map units, or neurons, usually form a two-dimensional lattice and thus

the mapping is a mapping from high dimensional space onto a plane (Fig. 1). The property of topology preserving means that the mapping preserves the relative distance between the points. Points that are near each other in the input space are mapped to nearby map units in the SOM. The SOM can thus serve as a cluster analyzing tool of high-dimensional data and it has the capability to generalize. Generalization capability means that the network can recognize or characterize inputs it has never encountered before. A new input is assimilated with the map unit it is mapped to [3, 4, 5]. After clustering, to make meaning for each cluster, we used an assignment method as a supportive method of the SOM where distribution of behavioral scores was referred after the classification. The largest bar of histogram plot was used to assign a label to a cluster.

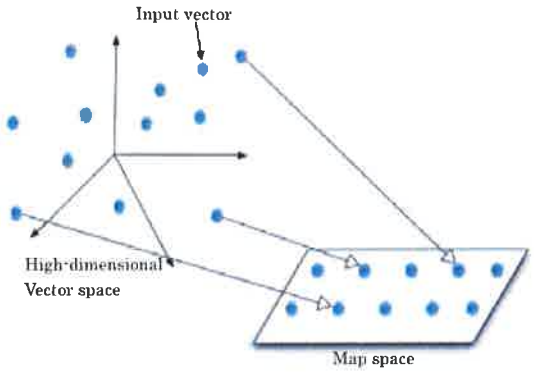


Figure 1. Network structure of the Self-organizing map.

(MRI data)

We used four sets of MRI data acquired in Tohoku Fukushi University (Sung et al.; accepted). The matrix size of the data was 123 x 15 x 4.

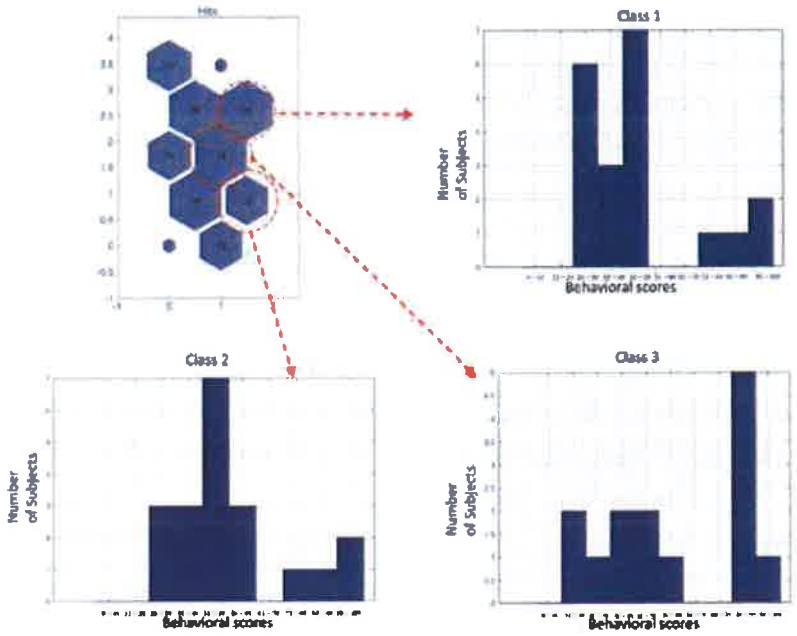


Figure 2. Clusters classified by SOM and distribution of elements in the clusters.

Results and discussion

For the given rs-fMRI data we could make 10 clusters by the SOM. The identified 10 clusters are able to be given labels such as class 1, class 2, ···, class 10. For the 10 classes having arbitrarily assigned labels, we examined distributions of the elements of the classes. Figure 2 shows the distribution of 3 classes as examples. Each histogram plot shows number of subjects belonging to each interval of behavioral scores. For example, 5 subjects belong to the behavioral-score-interval of 81-90 for the class 3. This histogram plots provide an information for assigning meaningful labels to the arbitrarily assigned clusters. By searching a behavioral-score-interval that has more elements than any other intervals we could assign the label corresponding to the interval to the cluster. In the case of the above class, the interval of 41-50 corresponds to "score 50" (as representing the interval 41-50). By the same way we can assign "score 50" to the class 2 and "score 9" to the class 3. However, this method gives a problem as we can see from the above examples. The class 1 and class 2 come to have the same labels. To solve the problem we devised a secondary measure in which the elements of the neighboring intervals are also counted. As the result the class 2 was assigned to "score 50" because the sum of elements including the left and right interval in class 2 are more than those in the class1. Through this kind of method we could assign labels based on the behavioral scores.

Figure 3 shows the clusters classified by SOM and then assigned the labels based on the behavioral scores through the propose method.

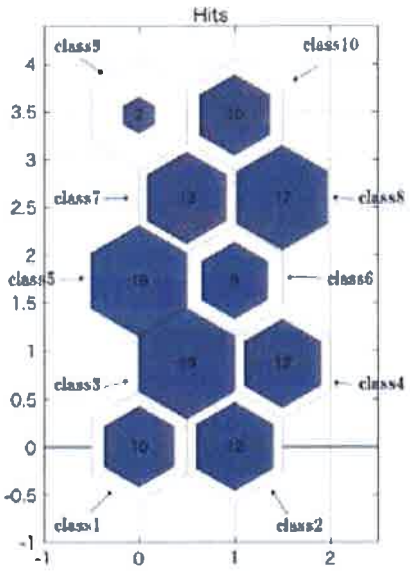
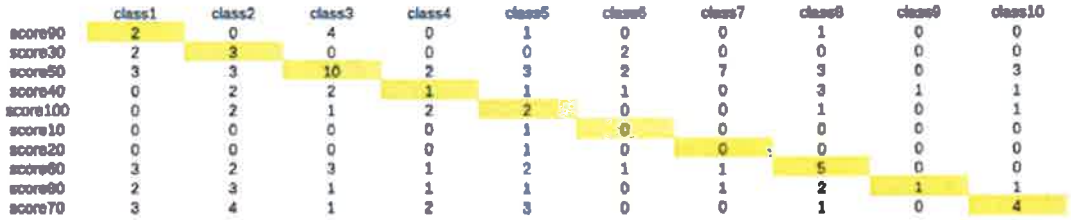


Figure 3. Clusters classified by SOM and then assigned label based on the behavioral scores.



	class1	class2	class3	class4	class5	class6	class7	class8	class9	class10
score90	2	0	4	0	1	0	0	1	0	0
score30	2	3	0	0	0	2	0	0	0	0
score50	3	3	10	2	3	2	7	3	0	3
score40	0	2	2	1	1	1	0	3	1	1
score100	0	2	1	2	2	0	0	1	0	1
score10	0	0	0	0	1	0	0	0	0	0
score20	0	0	0	0	1	0	0	0	0	0
score60	3	2	3	1	2	1	1	5	0	0
score80	2	3	1	1	1	0	1	2	1	1
score70	3	4	1	2	3	0	0	1	0	4

(a) Functional network 1

	class1	class2	class3	class4	class5	class6	class7	class8	class9	class10
score100	0	1	2	1	0	0	2	0	0	0
score70	0	2	1	2	1	0	2	1	2	0
score10	0	1	1	0	0	0	1	0	0	0
score40	0	1	3	5	1	1	4	2	1	0
score90	0	0	2	2	0	0	0	0	0	0
score80	0	1	0	1	0	0	0	1	1	0
score20	0	0	1	2	0	1	3	0	2	0
score50	3	5	3	6	4	0	4	9	4	2
score60	0	2	3	2	2	1	1	3	3	0
score30	0	2	1	2	2	0	1	3	0	0

(b) Functional network

	class1	class2	class3	class4	class5	class6	class7	class8	class9	class10
score60	5	1	1	1	0	2	3	3	1	2
score100	1	2	0	1	0	1	0	1	0	1
score90	1	0	3	1	0	1	1	3	0	3
score30	2	1	2	0	0	0	1	3	0	1
score20	0	0	1	0	0	0	0	2	0	0
score50	5	2	5	4	0	7	1	5	0	3
score40	0	0	1	1	0	0	2	1	0	3
score70	4	1	2	2	1	3	0	4	0	2
score10	0	0	0	0	0	0	0	0	0	0
score80	1	2	1	1	0	1	2	0	0	4

(c) Functional network 3

	class1	class2	class3	class4	class5	class6	class7	class8	class9	class10
score30	3	0	0	1	0	0	0	2	0	2
score100	1	0	0	0	0	0	0	1	0	1
score40	0	0	6	0	0	3	0	3	0	0
score90	0	1	1	2	0	0	0	0	0	1
score10	0	0	0	0	0	0	0	0	0	0
score50	9	2	1	1	0	10	4	7	1	6
score70	2	3	3	1	0	3	2	3	0	0
score60	3	2	1	1	1	2	2	3	1	3
score80	2	0	2	0	0	2	0	3	2	2
score20	0	0	0	0	0	1	2	0	0	2

(d) Functional network 4

Figure 4. Evaluation of assigned labels and behavioral-score intervals. Behavioral intervals were represented as a way such as score 10 for 0 to 10 interval and score 20 for 11 to 20,..., score 100 for 91 to 100.

The evaluation of the classification by SOM and the assignment method was made by the comparison of the labeled clusters and the behavioral scores, which gave the accuracy of 22.0 %, 17.9 %, 24.4 % and 30.0 % for the four functional networks 1, 2, 3, and 4, respectively. The accuracies are significant above chance level of 10 %.

These results suggest that the propose method can be used for supporting unsupervised classification methods such as SOM. This unsupervised method can be used in a classification method where a supervised method of SVM may be applied after the clustering by the SOM, which can give an independent training on behavioral data when the behavioral data are used as the output with MRI data as the input.

Acknowledgments

This study was supported by MEXT-Supported program for the Strategic Research Foundation at Private Universities, 2014-2018.

References

1. J. Mourão-Miranda, E. Reynaud, F. McGlone, G. Calvert and M. Brammera (2005) : "The impact of temporal compression and space selection on SVM analysis of single-subject and multi-subject fMRI data". Neuroimage **33**: 1055-1065.
2. M. Misaki, S. Miyauchi (2006) "Application of artificial neural network to fMRI regression analysis". Neuroimage **29**: 396-408.
3. N. Zahra (2017) "Evaluation of characteristics of resting state fMRI data by machine learning". Annual reports of Kansei Fukushi Research Institute 14: 281-284.
4. T. Kohonen (1982) "Self-Organized Formation of Topologically Correct Feature Maps". Biological Cybernetics. 43: 59–69.
5. T. Kohonen (1995) *"Self-Organizing Maps"*. Springer, Berlin, Heidelberg, 1995.

原 著 論 文

統合失調型パーソナリティ特性と自閉症スペクトラム特性のメタ認知における差異

大友ゆき、河地庸介、阿部千裕、成烈完、小川誠二
東北福祉大学

Differences in metacognition between schizotypal personality and autism-spectrum traits

OTOMO Yuki, KAWACHI Yousuke, ABE Chihiro,
SUNG Yul-wan, OGAWA Seiji
Tohoku Fukushi University

Abstract

It can be difficult to distinguish between schizophrenia and autism-spectrum disorders (ASD), because their symptoms are similar. However, separate previous studies of schizophrenia and ASD suggest that these disorders can be characterized differently, in terms of metacognition. Metacognition, or cognition about cognition, is the ability to report one's own mental state; it has the three aspects, namely metacognitive knowledge, metacognitive monitoring, and metacognitive control. To our knowledge, there has been no study investigating differences in metacognition between schizophrenia and ASD. This study examined the differences between schizophrenia and ASD in metacognition by recruiting a non-clinical sample, who were assessed for both the traits of schizotypal personality and those of ASD. The effects of schizotypal personality and ASD traits were measured in terms of the three components of metacognition with the use of three questionnaires: the Metacognitive Awareness Inventory, the Schizotypal Personality Questionnaire Brief (SPQ-B), and the Autism-spectrum Quotient (AQ). Multiple regression analyses showed the following results: metacognitive knowledge and metacognitive control were positively predicted by positive symptoms traits found on the SPQ-B and negatively predicted by several traits in the results of the AQ. Metacognitive monitoring was negatively predicted only by several traits in the AQ. We suggest that schizophrenia and ASD can be classified by the discriminative characteristics represented in the relationships between metacognition and these traits.

Keywords : metacognition, SPQ, AQ

背 景

1．統合失調型パーソナリティと自閉症スペクトラム

近年、社会的に「大人の発達障害」への関心が高まっている背景から、成人を過ぎてから発達障害の疑いを持って精神科を受診する患者が増加傾向にある[16)17)]。発達障害とは2004年に制定された発達障害者支援法において「自閉症、アスペルガー症候群その他の広汎性発達障害、学習障害、注意欠陥多動性障害などの脳機能の障害で、通常低年齢で発現する障害」とされているが[17)]、幼少期にはそれほど症状が目立たず大きな問題なく過ごし、青年期以降に社会生活上の問題や苦痛が大きくなり受診して診断を受けるケースもある[18)32)]。このような発達障害の１つである自閉症スペクトラム障害（ASD）は青年期以降に初めて

受診する場合、その症状の類似性から統合失調症との鑑別に困難が生じることが指摘されている[18)32)39)]。統合失調症の陽性症状は幻覚や妄想に代表されるような激しい症状であるが、ASDにおいても類似の状態を示すことが報告されている。ASD患者は過去の辛い経験が何らかのきっかけであたかも最近のように想起されパニックに陥るというフラッシュバック現象がみられるが、このきっかけは周囲の人には分かりにくく妄想や幻覚と誤認されることがある[26)32)]。また、聴覚が過敏であるために耳を塞ぐといった行為や「うるさい」と訴えること、好きなものに没頭すると独り言を繰り返すというような行動が幻聴や幻覚、妄想と誤認されることもある[32)33)]。感情の平板化や意欲の低下に代表される統合失調症の陰性症状については、ASD患者の表情の乏しさや興味・関心が狭く限定的といった特徴と外見的に類似しているために、誤認される場合があることを指摘されている[32)]。

統合失調症とASDの鑑別が十分に行われないことは、その後の治療方針に大きく影響する[18)]。統合失調症は一度発症してしまうと再発率が約80%と非常に高い精神疾患であるため[25)]、再発防止や予後の改善に効果的な早期発見・早期治療が重要視されている[21)34)]。しかし、ASDと誤って診断された場合には適切な治療を受けることができず、症状が慢性化し長期間苦しむことになりかねない。統合失調症の初期段階ではその特徴が顕著に表出されず、より両者の鑑別は困難を要することが推測できる。他方でASDが青年期以降に発覚する場合、それまでの日常生活には大きな問題がなかったことから、特徴的な症状があまり目立たない軽度のASDである可能性が高く、ASDの特性は心理的、環境的なストレスが加わったときに顕在化してくるとされているため[7)]、それ以外の場面での鑑別は困難を要すると推察できる。このような鑑別の困難さは、統合失調症の早期発見・早期治療やASDへの適切な対応を阻害する要因になると考えられる。

統合失調症では、発症の前駆段階として統合失調型パーソナリティとの連続性が仮定されており、症状の程度が大きくなることで疾患に発展することが示唆されている[3)]。すなわち、統合失調型パーソナリティを研究することは統合失調症の早期発見・早期治療に関する知見の提供につながると考えられる。一方、ASDにおいて、Baron-Cohen et al.[4)]はASDが健常者との連続体にあるという仮説に基づき、健常者のASD傾向を測定する代表的な質問紙であるAQを作成し、患者群のAQ得点が健常者群よりも顕著に高くなることから、AQが成人のASDを簡便に診断するツールとして有効であるとしている。すなわち、ASD傾向の強い健常者についての知見は、ASDに関する知見につながると考えられる。そこで本研究では、統合失調型パーソナリティ傾向とASD傾向を有する健常者を対象とする。先行研究において、健常者を対象にAQと、統合失調型パーソナリティ傾向を測定する代表的な質問紙であるSPQを用いて両者の関連を調査し、両者に多くの部分で相関がみられることが報告されており[7)13)]、症状が顕著でない段階で両者を鑑別できる可能性が示せれば、この問題に対応する知見を提供できるといえる。

2．メタ認知

メタ認知とは一般に「認知についての認知」と定義され[1)9)11)27)]、記憶や思考、知覚等の自己の認知機能を第三者的な立場から客観視するような、自分自身の内的状態についての認知であるといえる。このメタ認知は、主に「メタ認知的知識」、「メタ認知的モニタリング」、「メタ認知的コントロール」の3つの構成要素について研究が行われている[9)27)]。「メタ認知的知識」とは、認知についての信念やエピソードに基づいた知識である。「メタ認知的モニタリング」とは、ある特定の認知的活動の継続的な進捗状況や現在の状態を査定あるいは評価することである。「メタ認知的コントロール」とは、進行中の認知的活動について中断や変更などの調整を行うことである。我々は日常生活の中で何らかの認知的な活動を行うとき、メタ認知的モニタリングを用いて状況を査定し、その結果をもとにメタ認知的コントロールが実際の活動を調整する。その際にはメタ認知的知識として個人の「自分はこれが得意だ」というような信念や「前に

このやり方で行ったときに成功した」というようなエピソードの影響を受けるというように、これらの3つの要素はお互いに影響し合って我々の生活を円滑に送るために活用されている[9)27)]。

統合失調症のメタ認知については、多くの研究でソース・モニタリング機能に失調があることが報告されている[22)23)29)38)]。ソース・モニタリングとは、対象となる情報がどこに起因するのかというメタ認知的モニタリングの一つであり、この機能に問題があるために自分で発した言葉を自分の言葉として認識できずに幻聴として捉えるといったような陽性症状に発展すると考えられている[9)23)]。ASD患者では、メタ認知的モニタリングは健常者と同様に正確であることが報告されており[6)10)37)]、この点が統合失調症のメタ認知と異なっている。

若林[35)]はASDの特徴的な症状の一つである心の理論（他者の気持ちや心理を把握する能力）の欠如を統合失調症にも関連させて検討し、統合失調症患者では他者の気持ちを正確にモニタリングできないことが問題であり、ASDでは他者と自分の気持ちが異なるものであることを理解していない点が問題であると述べている。すなわち、ASDでは「他者と自分は同じだ」という誤ったメタ認知的知識があるために、心の理論の欠如が見られると考えられる。

Strauss & Gold[31)]は、統合失調症の陰性症状の一つで快楽を伴う感情の体験が低下するという失快楽症について次のように述べている。現在の情動体験については統合失調症患者でも健常者と同様に肯定的感情を報告するものの、過去のあるときにどのように感じたか、また、未来のある場面でどのように感じると予想できるかについては肯定的感情が減弱しているということから、統合失調症患者は情動体験をする能力が低下するというより、むしろ、これまでの経験の中で十分かつ多様な肯定的感情に関する信念を形成してこなかったことで、過去もしくは未来における自分の肯定的感情を推測する際に低く見積もる信念バイアスが生じている可能性を示唆している。それゆえ、信念に基づいた自分自身の知識であるメタ認知的知識と陰性症状が関連する可能性が考えられる。

以上から、統合失調症ではメタ認知的モニタリングとメタ認知的知識において、ASDではメタ認知的知識においてというように、両者は異なる側面のメタ認知機能と関連すると仮定できる。また、メタ認知的コントロールは、メタ認知的モニタリングの結果に基づいていることやメタ認知的知識の影響を受けることを考えると[8)26)]、両者のいずれにも関連すると仮定できる。しかし、これまでにメタ認知に着目して両者の類似性や相違性を検討した研究は見当たらず、さらに両者それぞれのメタ認知についての研究では、メタ認知のある一側面のみの検討に留まっている。そこで、本研究において、メタ認知を包括的に測定する質問紙を用いて、メタ認知の3つの側面ごとに両者の差異を明らかにすることができれば、統合失調症とASDを鑑別する手掛かりとして、より有益な情報を提供できると考える。

3．本研究の目的

統合失調型パーソナリティとASDには1．で述べたような類似性があるとされるものの、2．で述べたようにメタ認知についてはそれぞれ異なる特徴をもつように考えられる。具体的には、先行研究との関連から統合失調型パーソナリティ傾向はメタ認知的知識、メタ認知的モニタリング、メタ認知的コントロールと、ASD傾向はメタ認知的知識およびメタ認知的コントロールと関連すると考えられる。しかし、メタ認知に着目して両者の関連性を検討した研究はこれまでに見られない。本研究において、両者のメタ認知に関する差異が明らかになれば、統合失調型パーソナリティと連続性が仮定される統合失調症と自閉症スペクトラム障害の鑑別の一助となる知見を得られる可能性がある。また、健常者を対象とすることによって服薬等の影響を受けず、症状の程度が軽くより類似性が高いと考えられる段階での鑑別が可能になり、適切な早期治療につながることが期待できる。以上のことから、本研究では、統合失調型パーソナリティ傾向とASD傾向のメタ認知を詳細に検討し、その差異を明らかにすることを目的とする。

方　法

参加者

大学生および大学院生232人（男性44名、女性188名）で、平均年齢19.88歳（SD=1.86）であった。参加者には本研究について書面および口頭によるインフォームドコンセントを行った。なお、本研究は東北福祉大学研究倫理審査委員会の承認（RS150203およびRS150601）を得て実施した。

調査内容

(1) 成人用メタ認知尺度

Schraw & Sperilng[26] によって作成されたMetacognitive Awareness Inventory（MAI）を日本語訳した28項目からなる成人用メタ認知尺度を使用した[1]。質問紙は“過去に上手くいったやり方を試みている”等の質問項目からなる「メタ認知的知識」8項目、“学んだことを、どれくらい理解しているか、正確に判断できる”等の質問項目からなる「モニタリング」11項目、“理解できないときには、やり方を変えてみる”等の質問項目からなる「コントロール」9項目の3つの下位因子、合計28項目で、それらをまとめる高次の因子として「メタ認知」が仮定されている。回答は、“全くあてはまらない”“あまりあてはまらない”“ややあてはまらない”“ややあてはまる”“だいたいあてはまる”“とてもあてはまる”の6件法で行った。

(2) 短縮版統合失調型パーソナリティ尺度

Raine & Benishay[24] によって作成されたSchizotypal Personality Questionnaire Brief（SPQ-B）の日本語版である短縮版統合失調型パーソナリティ尺度を使用した[15]。質問紙は“姿は見えないが、私のまわりに人がいると感じたり、見えない力が存在すると感じたりしたことがある”等の質問項目からなる「認知・知覚（陽性症状）」8項目、“他の人とは親しくなれないと感じる”等の質問項目からなる「対人関係（陰性症状）」8項目、“言いたいことを人に明確に伝えるのは、私には難しい”等の質問項目からなる「解体」6項目の統合失調症の主要な症状である3つの下位因子、合計22項目で、得点が高いほど統合失調型パーソナリティ傾向が高いことを示す。回答は“はい”“いいえ”の2件法で行った。

(3) 自閉症スペクトラム指数

Baron-Cohen et al.[4] によって作成されたAutism-Spectrum Quotient（AQ）の日本語版である自閉症スペクトラム指数を使用した[36]。質問紙は“新しい友人を作ることは、難しい”等の質問項目からなる「社会的スキル」、“同じやりかたを何度もくりかえし用いることが好きだ”等の質問項目からなる「注意の切り替え」、“他の人が気づかないような小さな物音に気づくことがよくある”等の質問項目からなる「細部への注意」、“会話をどのように進めたらいいのか、分からなくなってしまうことがよくある”等の質問項目からなる「コミュニケーション」、“あること（もの）を、他の人がどのように感じるかを想像するのは苦手だ”等の質問項目からなる「想像力」のASDの症状を特徴づける5つの下位因子各10項目、合計50項目で構成されている。下位因子はいずれも得点が高いほど、「社会的スキル」が低いこと、「注意の切り替え」ができないこと、「細部への注意」が向くこと、「コミュニケーション」能力が低いこと、「想像力」に乏しいことを表し、得点が高いほどASD傾向が高いことを示す。回答は“あてはまる”“どちらかといえばあてはまる”“どちらかといえばあてなまらない”“あてはまらない”の4件法で行った。

(1)～(3) の質問紙について、それぞれ下位因子得点を算出した。

結　果

本研究では、まず、統合失調型パーソナリティ傾向とASD傾向における先行研究[8][14] と同様の結果が得られているかを調べるために、SPQ（Mean total score=9.44 , SD=3.84）、AQ（Mean total score=20.98,

SD=6.27）の下位因子における2変量の相関分析を行った（Table 1）。SPQとAQでは、「陽性症状」と「想像力」、「陰性症状」と「細部への注意」、「解体」と「細部への注意」以外のすべてで有意な正の相関が認められ、ほぼ先行研究と一致するものであったことから、正確に統合失調型パーソナリティ傾向およびASD傾向を測定できたと考える。

次に、統合失調型パーソナリティ傾向およびASD傾向がメタ認知に与える影響を検討するために、SPQおよびAQの下位因子を説明変数、MAIの「メタ認知的知識」（Mean score=36.37, SD=4.82）、「モニタリング」（Mean score=38.36, SD=8.67）、「コントロール」（Mean score=38.65, SD=6.07）をそれぞれ目的変数としたステップワイズ法による重回帰分析を行った（Table 2）。その結果、「メタ認知的知識」を目的変数とした場合には、SPQの「陰性症状」および「解体」とAQの「注意の切り替え」「細部への注意」「想像力」が除外され、「陽性症状」（β =.21, p<.01）と「社会スキル」（β =-.27, p<.001）、「コミュニケーション」（β =-.18, p<.05）から有意に予測され、その説明率は約17%であった（R^2=.17, p<.001）。「モニタリング」を目的変数とした場合には、すべてのSPQの下位因子とAQの「注意の切り替え」「コミュニケーション」「想像力」が除外され、「社会スキル」（β =-.31, p<.001）および「細部への注意」（β =.19, p<.01）から有意に予測され、その説明率は約13%であった（R^2=.13, p<.001）。「コントロール」を目的変数とした場合には、SPQの「陰性症状」および「解体」とAQの「注意の切り替え」「細部への注

Table 1 Correlations between the subscales of Schizotypal Personality Questionnaire Brief (SPQ) and Autism-Spectrum Quotient (AQ)

			mean	SD	1	2	3	4	5	6	7	8
SPQ	1	陽性症状	2.254	1.683	—							
	2	陰性症状	4.315	1.821	.278***	—						
	3	解体	2.875	1.622	.407***	.352***	—					
AQ	4	社会的スキル	3.896	2.543	.130*	.486***	.215**	—				
	5	注意の切り替え	5.267	1.796	.181**	.365***	.224**	.411***	—			
	6	細部への注意	4.991	2.275	.227**	.071	.009	-.032	.102	—		
	7	コミュニケーション	3.828	2.096	.156*	.376***	.405***	.470***	.412***	-.067	—	
	8	想像力	3.022	1.537	-.033	.170**	.212**	.353***	.242***	-.119	.380***	—

***p <.001 **p <.01 *p <.05

Table 2 Multiple regression analysis with the subscales of Metacognitive Awareness Inventory

		メタ認知的知識			モニタリング			コントロール		
		β	許容度	VIF	β	許容度	VIF	β	許容度	VIF
SPQ	陽性症状	.212**	.971	1.029				.171**	.983	1.017
	陰性症状									
	解体									
AQ	社会的スキル	-.274***	.772	1.295	-.305***	.999	1.001	-.200**	.983	1.017
	注意の切り替え									
	細部への注意				.189**	.999	1.001			
	コミュニケーション	-.175*	.769	1.300						
	想像力									
	R	.410			.365			.246		
	R^2	.168***			.133***			.061**		

Note : SPQ = Schizotypal Personality Questionnaire Brief AQ = Autism-Spectrum Quotient ***p <.001 **p <.01 *p <.05

意」「コミュニケーション」「想像力」が除外され、「陽性症状」（β =.17, p<.01）と「社会スキル」（β =-.20, p<.01）から有意に予測され、その説明率は約 6 %であった（R^2=.06, p<.01）。

なお、説明変数間に相関はあったものの著しく強い相関ではなく、許容度（.77～1.00）や VIF（1.00～1.30）の値から、多重共線性の問題はなく上記の偏回帰係数は適切に推定できたものとして判断した。

考　察

本研究の目的は、統合失調型パーソナリティ傾向と ASD 傾向におけるメタ認知の差異を詳細に明らかにすることによって、統合失調型パーソナリティと連続性が仮定される統合失調症と、統合失調症との弁別が困難であるとされる青年期以降の ASD について、鑑別を容易する知見を提供することであった。本研究の結果から、「メタ認知的知識」は SPQ の「陽性症状」と AQ の「社会スキル」「コミュニケーション」から、「モニタリング」は「社会スキル」「細部への注意」という AQ の下位因子のみから、「コントロール」は SPQ の「陽性症状」と AQ の「社会スキル」からそれぞれ影響を受けていることが示された。また、「メタ認知的知識」と「コントロール」では、SPQ の「陽性症状」における標準偏回帰係数はいずれも正の値である一方で、AQ に関しては関連が示されたいずれの下位因子も負の値であった。以上のことから、統合失調型パーソナリティ傾向と ASD 傾向はメタ認知に対してそれぞれ異なる影響を及ぼしている可能性が示唆された。

メタ認知的知識は、統合失調型パーソナリティ傾向と ASD 傾向の両者から影響を受けると予測された側面であり、仮説は支持されたといえる。さらに、メタ認知的知識は統合失調型パーソナリティ傾向の「陽性症状」からは正の方向、ASD 傾向からは負の方向というように異なる方向の影響を受けていた。統合失調症の陽性症状では周囲の状況に過剰な関心があり「自分に関係がある」と捉えるために、妄想に発展するとされる[32]。一方で、ASD では周囲の状況には無関心であり、自分のやりたいことが阻害されたことを被害的かつ短絡的に捉える様子が妄想のように見えるとされる[32]。このことから、統合失調症の陽性症状ではその認識が誤っているにしろ「自分に関係がある」と確信して捉えているために、メタ認知的知識が高くなる可能性が考えられる。ASD では、「社会スキル」の不足および「コミュニケーション」の困難さからメタ認知的知識のなさが予測されることから、他者や周囲とのエピソードを考慮することなく短絡的な思考に至ることが多く、メタ認知的知識が十分に蓄積されていかないことが推測される。すなわち、妄想様に見られる様子は、誤ったメタ認知的知識を用いたために見られるのか、メタ認知的知識を全く用いないために見られるのかという点において両者は異なるといえる。

メタ認知的コントロールは、統合失調型パーソナリティ傾向と ASD 傾向の両者から影響を受けると予測した側面であり仮説は支持されたといえる。また、メタ認知的知識と同様に統合失調型パーソナリティ傾向の「陽性症状」は正の方向、ASD 傾向からは負の方向に関連づけられていた。メタ認知的コントロールは、メタ認知的知識の影響を受けて行動を調整する側面であるため[9][27]、統合失調症の陽性症状では過剰な周囲への関心によって形成された誤ったメタ認知的知識に影響を受け、その行動が適応的かどうかに関わらず、自分の行動を調整しているに過ぎないのでメタ認知的コントロールは高くなる可能性がある。一方で、ASD 傾向では、そもそもメタ認知的知識が十分に蓄積されておらず、AQ の「社会的スキル」の不足がメタ認知的コントロールのなさを予測することから、ASD の行動的特徴である一人で活動することを好み人見知りや遠慮がないという社会的スキルに乏しい様子に見られるように[7]、他者や周囲の状況を調整しながら行動しようとはせずメタ認知的コントロールは十分に機能していないと考えらえる。

メタ認知的モニタリングは、統合失調型パーソナリティ傾向から影響を受けると予測した側面であったが、ASD 傾向のみから影響を受けることが示され、仮説は支持されなかった。AQ の「社会的スキル」の不足からメタ認知的モニタリングのなさが予測され、より「細部への注意」が向くことからメタ認知的

モニタリングの良さが予測されるように、ASDでは他者の感情を察して適切に反応することが苦手であり、自分の興味・関心があるものに対して異常にこだわり、その対象が変化することに敏感に気づき抵抗を示すことがある[7]。本研究の結果から、ASDでは自己のこだわりが強い内的な世界に関してはメタ認知的モニタリングが良い一方で、他者と関わる外的な世界の認知におけるメタ認知的モニタリングは低下している可能性が示された。また、統合失調型パーソナリティ傾向のいずれからも影響が示されなかったことについて、統合失調型パーソナリティにおけるメタ認知的モニタリングは統合失調症患者とは異なり一貫しておらず[12][13][19][20][29]、しかもそれほど多くの研究がない。本研究でメタ認知的モニタリングと統合失調型パーソナリティ傾向において関連性が見られなかったことは、メタ認知的モニタリングの低下が統合失調症と統合失調型パーソナリティで必ずしも連続しない可能性を示唆するものであり、統合失調型パーソナリティにおけるメタ認知的モニタリングの知見の蓄積という点で貢献できるものであるかもしれない。しかし、この点については今後さらなる検討の必要性があると考える。

本研究では数百名規模の参加者を対象としたため質問紙を用いたメタ認知の測定を行ったが、この測定については欠点もある。質問紙でのメタ認知の測定は過去の、あるいは普段のメタ認知を回顧的かつ自分自身で意識的に判断したものに限られる。しかし、実際に統合失調症やASDの症状によって表出される行動に関連するメタ認知は、意識できない部分を含めた遂行時のものであると考えられ、これは質問紙では測定できない側面であると考えられる。加えて、本研究の結果からは統合失調型パーソナリティ傾向の陽性症状以外でメタ認知への影響が示されなかった。そのため、本研究では陽性症状およびASD傾向とメタ認知の関連性の検討に留まっている。本研究で影響が示されなかった統合失調症の陰性症状や解体症状では、陰性症状とASDにおける抑うつ状態[2]、解体症状とASDにおける心の理論の欠如という点が類似していると考えられるため[5]、陽性症状とASDのみならず、これらの側面についても両者の鑑別の一助となる知見が求められる。したがって、今後は上記で述べたような質問紙調査での欠点を克服できるような行動指標を導入して、多角的に統合失調症とASDのメタ認知に着目した鑑別に関わる知見の検討が求められる。

謝辞

本研究は、東北福祉大学感性福祉研究所における文部科学省の私立大学戦略的研究基盤形成支援事業（平成26年度～30年度）およびJSPS科学研究費基盤研究C（16K00212）による助成を得て行われた。本研究にご協力いただいた研究協力者の皆様、感性福祉研究所の関係各位に心より感謝申し上げます。

引用文献

1）阿部真美子, 井田政則「成人用メタ認知尺度の作成の試み－Metacognitive Awareness Inventoryを用いて－」『立正大学心理学研究年報』1, pp.23-34, 2010

2）阿部隆明「横断面の症状から見た統合失調症と自閉スペクトラム症の鑑別」『児童青年精神医学とその近接領域』58（1), pp.54-60, 2017

3）浅井智久, 山内貴之, 杉森絵里子, 番頭奈緒子, 丹野義彦「統合失調型パーソナリティと統合失調症の連続性」『心理学評論』53（2), pp.240-261, 2010

4）Baron-Cohen S., Wheelwright S., Skinner R., Martin J., Clubley E. "The Autism-Spectrum Quotient（AQ）: Evidence from Asperger syndrome/ high-functioning autism, males and females, scientists and mathematicians" Journal of Autism and Developmental Disorders, 31（1), pp.5-17, 2001

5）Brüne M. ""Theory of Mind" in Schizophrenia: A Review of the Literature" Schizophrenia Bulletin, 31（1), pp.21-42, 2005

6）Cooper R. A., Plaisted-Grant K. C., Baron-Cohen S., Simons J. S. "Reality Monitoring and Metamemory in Adults with Autism Spectrum Conditions", Journal of Autism and Developmental Disorders, 46 (6), pp.2186-2198, 2016
7）傳田健三「自閉スペクトラム症（ASD）の特性理解」『心身医学』57 (1), pp.19-26, 2017
8）Dinsdale N. L., Hurd P. L., Wakabayashi A., Elliot M., Crespi B. J. "How Are Autism and Schizotypy Related? Evidence from a Non-Clinical Population" PLoS ONE, 8 (5), pp.1-10, 2013
9）Dunlosky J., Metcalfe J., 湯川良三, 金城光, 清水寛之 訳『メタ認知　基礎と応用』北大路出版, 2010
10）Farrant A., Boucher J., Blades M. "Metamemory in Children with Autism" Child Development, 70 (1), pp.107-131, 1999
11）Flavell J.H. "Metacognition and Cognitive Monitoring A New Area of Cognitive − Developmental Inquiry" American Psychologist, 34 (10), pp.906-911, 1979
12）Giráldez S.L., Caro M.I., Rodrigo A.M.L, Piñeiro M.P., Gonzále J.L.B. "Assessment of essential components of schizotypy using neurocognitive measures" Psychology in Spain, 4 (1), pp.183-194, 2000
13）Giráldez S.L., Piñeiro M.P., Caro M.I., Gonzále J.L.B. "A combined measure for detection of schizotaxia" Psicothema, 16 (2), pp.299-308, 2004
14）Hurst R. M., Nelson-Gray R. O., Mitchell J. T., Kwapil T. R. "The Relationship of Asperger's Characteristics and Schizotypal Personality Traits in a Non-clinical Adult Sample" Journal of Autism and Developmental Disorders, 37, pp.1711-1720, 2007
15）伊藤慎也, 大部聡子, 太田深秀, 高尾哲也, 坂本真士「日本語版 Schizotypal Personality Questionnaire Brief の信頼性・妥当性の検討」『日社精医誌』17, pp.168-179, 2008
16）加藤進昌「成人発達障害専門外来とリハビリテーション」『平成25年度東京都発達障害者支援体制整備推進事業シンポジウム報告書』, pp.1-20, 2014
17）厚生労働省「発達障害者支援関係報告会資料」, 2016
18）蔵下智子, 横田悠季, 君塚千恵, 富澤貴宏, 石原奈保子, 野口亜美梨「自閉症スペクトラム障害・統合失調症の鑑別における効果的な心理検査指標の探索」『研究助成論文集』51, pp.85-93, 2015
19）Lagioia A.C., Eliez S., Schneider M., Simons J.S. "Neural correlates of reality monitoring during adolescence" NeuroImage, 55, pp.1393-1400, 2011
20）Larøi F., Collignon O., Van der Linden M. "Source monitoring for actions in hallucination proneness" Cognitive Neuropsychiatry, 10 (2), pp.105-123, 2005
21）松本和紀, 宮越哲生, 伊藤文晃, 内田知宏, 鈴木健, 大野高司「統合失調症に対する早期介入」『精神医学』50 (3), pp.227-235, 2008
22）Moritz S., Woodward T.S., Chen E. "Investigation of metamemory dysfunctions in first-episode schizophrenia" Schizophrenia Research, 81, pp.247-252, 2006
23）Moritz S., Woodward T.S., Ruff C.C. "Source monitoring and memory confidence in schizophrenia" Psychological Medicine, 33, pp.131-139, 2003
24）Raine A., Benishay D. "The SPQ-B: A brief screening instrument for schizotypal personality disorder" Journal of Personality Disorder, 9, pp.346-355, 1995
25）Robinson D., Woerner M.G., Alvir J.M.J., Bilder R., Goldman R., Geisler S., Koreen A., Sheitman B., Chakos M., Mayerhoff D., Liebrman J.A. "Predictors of Relapse Following Response From a First Episode of Schizophrenia or Schizoaffective Disorder" Arch Gen Psychiatry, 56 (3), pp.241-247,

1999
26) 澤原光彦, 村上伸治, 青木省三「成人の精神医学的諸問題の背景にある発達障害特性」『心身医学』57 (1), pp.51-58, 2017
27) 三宮真智子『メタ認知　学習力を支える高次認知機能』北大路書房, 2008
28) Schraw G., Sperilng R.A. "Assessing metacognitive awareness" Contemporary Educational Psychology, 19, pp.460-475, 1994
29) Simons J.S., Garrison J.R., Johnson M.K. "Brain Mechanisms of Reality Monitoring" Trends in Cognitive Sciences, 21 (6), pp.462-473, 2017
30) Simons J.S., Henson R.N.A., Gilbert S.J., Fletcher P.C. "Separable Forms of Reality Monitoring Supported by Anterior Prefrontal Cortex", Journal of Cognitive Neuroscience, 20 (3), pp.447-457, 2008
31) Strauss G.P., Gold J.M. "A New Perspective on Anhedonia in Schizophrenia" The American Journal of Psychiatry, 169 (4), 364-373, 2012
32) 田中宏明, 立山清美, 谷口英治, 清水寿代, 吉田文「統合失調症と広汎性発達障害」『Journal of rehabilitation and health sciences』9, pp.1-6, 2011
33) 豊田佳子, 杉山登志郎「広汎性発達障害者への対応における留意点」『精神看護』8 (4), pp.46-52, 2005
34) 辻野尚久, 片桐直之, 小林啓之, 水野雅文「統合失調症の前駆期に対する精神科医の治療観」『精神神經學雑誌』111 (3), pp.293-297, 2009
35) 若林明雄「精神分裂病はメタ認知障害か？：心の理論仮説による理論的検討」『日本性格心理学会発表論文集』6, pp.31, 1997
36) 若林明雄, 東條吉邦, Baron-Cohen S., Wheelwright S.「自閉症スペクトラム指数（AQ）日本語版の標準化－高機能臨床群と健常成人による検討－」『心理学研究』75 (1), pp.78-84, 2004
37) Wojcik D.Z., Allen R.J., Brown C., Souchay C. "Memory for actions in autism spectrum disorder" Memory, 19 (6), pp.549-558, 2011
38) Woodward T.S., Menon M., Whitman J.C. "Source monitoring biases and auditory hallucinations" Cognitive Neuropsychiatry, 12 (6), pp.477-494, 2007
39) 吉川撤「若年発症の統合失調症と自閉スペクトラム症－併存例の診断と治療－」『児童青年精神医学とその近接領域』58 (1), pp.60-64, 2017

原 著 論 文

A Comparison of Resting State fMRI Signals Depending on Participants' Conditions under MRI Measurements

Yul-Wan SUNG, Daehun KANG, Yousuke KAWACHI, Seiji OGAWA
Kansei Fukushi Research Institute, Tohoku Fukushi University

Abstract

Resting state fMRI (rs-fMRI) is routinely used to identify brain networks related to cognition and diseases. However, no standardized measurement protocols are available. Moreover, no consensus has been defined on the participants' state in the MRI scanner during data acquisition. For example, there is no consideration on whether eye-open and eye-closed states produce different results when brain networks are measured by rs-fMRI in studies related to cognition and diseases. In our study on human traits, we have been measuring rs-fMRI signals. Before engaging in the detailed analysis of the rs-fMRI signals, we preliminarily examined whether the eye-open and eye-closed states would produce different profiles in rs-fMRI signals.

Keywords : resting state fMRI (rs-fMRI) , correlation, human traits, eye-open, eye-closed

Introduction

Task-based fMRI (tb-fMRI) has been used for mapping brain function. The tb-fMRI signal is measured while some tasks that are related to specific perception or cognition are provided. In comparison with tb-fMRI, resting state fMRI (rs-fMRI) is easy to apply because it does not need any task[1-6]. The rs-fMRI has been used to examine clinical studies such as Alzheimer's disease (AD) [7-9], Autism spectrum disorder (ASD) [10-12] and Schizophrenia[13-15] etc., mostly to find brain areas or networks reflecting the diseases. These studies usually compare patient and normal subjects groups to identify specific functional networks to the diseases. Recently some studies have showed functional areas/networks related to human traits by rs-fMRI[16-18]. Although there are a lot of studies related to rs-fMRI measurement, no unanimously agreed rs-fMRI protocols are reported. For example, as for conditions of subjects in the MRI scanner, a study measures rs-fMRI signals in the eye-open state and another does in the eye-closed state. For some studies differences in rs-fMRI signals resulting from two states may be not so serious if any but for some other studies such as cognitive studies related to human traits the differences may produce different results depending on the state.

We have been measuring rs-fMRI signals for examining human traits and come to be interested with the effect of eye-open and eye-closed states on rs-fMRI signals. Before detailed analysis of the rs-fMRI signals, in this study, we qualitatively examined whether two states of the eye-open and eye-closed produce different profiles in rs-fMRI signals.

Methods

Subjects

Thirteen subjects were participated. None of the subjects had a history of neurological disease or any medical conditions (i.e., pregnancy, use of a cardiac pacemaker, or claustrophobia). After subjects were given a complete description of the study, written informed consent was obtained in accordance with the Declaration of Helsinki. This study was approved by the Institutional Review Board of Tohoku Fukushi University.

MRI measurements

All subjects were scanned in two sessions that included structural (T1-weighted) and resting-state functional imaging (rs-fMRI). The rs-fMRI was performed in the eye-open and eye-closed states. Structural images were acquired using the following parameters: repetition time = 1900 ms, echo time = 2.52 ms, matrix size = 256 × 256, in-plane resolution = 1 × 1 mm^2, slice thickness = 1 mm, and number of slices = 192. Resting-state fMRI data were acquired using gradient-echo echo-planar imaging (EPI) sequence with the following parameters: repetition time = 2000 ms, echo time = 27 ms, matrix size = 64 × 64, in-plane resolution = 3.4 × 3.4 mm^2, slice thickness = 3.4 mm, and number of volumes = 240. In the rs-fMRI session, subjects were asked to lie on a bed in a dark room with their eyes opened or eyes closed and not moving and to try to think about nothing.

MRI data analysis

Statistical Parametric Mapping software (SPM 12B, Wellcome Department of Imaging Neuroscience, London, United Kingdom) was used. For resting state fMRI data, the images of 13 subjects were preprocessed using DPABI (rfmri.org/dpabi), which included slice scan time correction, 3 D motion correction, band pass temporal filtering (only signals with a frequency higher than 0.01 Hz and lower than 0.1 Hz), smoothing with 4-mm FWHM, and co-registration with each structural image. In the preprocessing, the time courses from 116 areas based on an anatomical brain template (AAL)[19] in which 116 brain areas are macroscopic brain structures as in Table 1. As one of measures to evaluate the difference between the eye-open and eye-closed states through brain networks by rs-fMRI signals, correlation maps were created between the 116 brain areas.

Results and Discussion

We made correlation maps to see the profiles of rs-fMRI signals in the eye-open and eye-closed states. Correlation maps between brain areas were made on the basis of the AAL template. The maps showed, as a whole, very similar correlation profiles of rs-fMRI signals between eye-open and eye-closed states. This is consistent with a previous study in which signal reliabilities were evaluated between the two states[20]. Even the partial correlation maps consisted of occipital areas were similar (red-dotted circles in Figure 1.). These results inform us that correlation profiles of functional dynamics related to some neuronal or cognitive changes can be reliably measured through rs-fMRI under both of the eye-open and eye-closed states. That means that we can get similar correlation profiles macroscopically whether participants of resting state MRI experiments are in eye-closed or eye-open states. On the other hand, when we examine the correlation in detail we can see small differences of

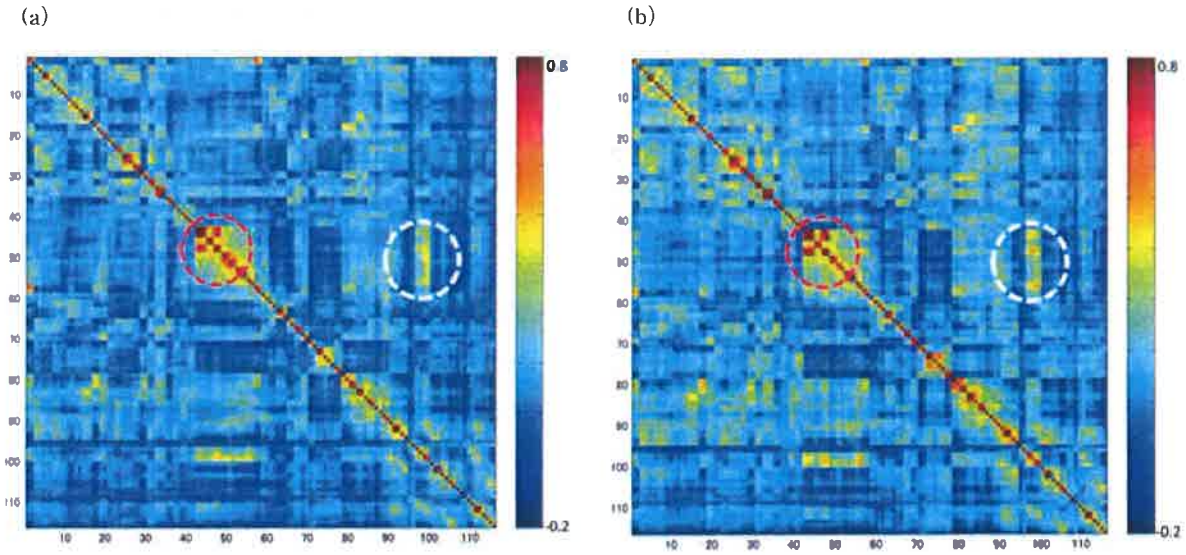


Figure 1. Correlation maps based on the AAL template: (a) Eye-open state (b) Eye-closed state.

correlation strength in a partial correlation map between the eye-open and eye-closed states (such as white dotted circles in Figure 1.).

These results suggest that participants' condition during acquisition of rs-fMRI data should be controlled to one of two states, the eye-open or eye-closed although two states elicit very similar profiles of correlation maps.

We can look upon functional dynamics as the same when we are interested in macroscopic activities of the resting brain. However, we have to consider the subtle differences in the correlation strength when we are interested in brain activities related to some cognitive functions such as the attention or arousal because brain activities can vary depending on the eye condition, as seen in the visual areas in which the alpha wave increases in the eye-closed state[21-22].

A future study is needed to examine which state is better to measure brain activities related to these kinds of cognitive functions and what aspects of the brain function the differences of the correlation strength in partial correlation maps reflect.

Acknowledgments

This study was supported by MEXT-Supported program for the Strategic Research Foundation at Private Universities, 2014-2018.

References

1. Fair D. A., Schlaggar B. L., Cohen A. L., Miezin F. M., Dosenbach N. U., Wenger K. K., Fox M. D., Snyder A. Z., Raichle M. E., Petersen S. E. (2007). A method for using blocked and event-related fMRI data to study "resting state" functional connectivity. Neuroimage 35, 396-40510.1016/j.neuroimage.2006.11.051
2. Fox M. D., Corbetta M., Snyder A. Z., Vincent J. L., Raichle M. E. (2006a). Spontaneous neuronal activity distinguishes human dorsal and ventral attention systems. Proc. Natl. Acad. Sci. U.S.A. 103, 10046-1005110.1073/pnas.0604187103

3. Fox M. D., Snyder A. Z., Vincent J. L., Raichle M. E. (2007b). Intrinsic fluctuations within cortical systems account for intertrial variability in human behavior. Neuron 56, 171–18410.1016/j.neuron.2007.08.023
4. Fox MD, Greicius M. (2010) Clinical applications of resting state functional connectivity. Front Syst Neurosci. 2010 Jun 17; 4 :19. doi: 10.3389/fnsys.2010.00019.
5. Gopinath K, Ringe W, Goyal A, Carter K, Dinse HR, Haley R, Briggs R. (2011) Striatal functional connectivity networks are modulated by fMRI resting state conditions. Neuroimage 54, 380-388.
6. Greicius MD, Supekar K, Menon V, Dougherty RF. (2009) Resting-state functional connectivity reflects structural connectivity in the default mode network. Cereb Cortex 19,72-78.
7. Göttler J, Preibisch C, Riederer I, Pasquini L, Alexopoulos P, Bohn KP, Yakushev I, Beller E, Kaczmarz S, Zimmer C, Grimmer T, Drzezga A, Sorg C. (2018) Reduced blood oxygenation level dependent connectivity is related to hypoperfusion in Alzheimer's disease. J Cereb Blood Flow Metab. 2018 Jan 1 :271678X18759182. doi: 10.1177/0271678X18759182.
8. Wang B, Niu Y, Miao L, Cao R, Yan P, Guo H, Li D, Guo Y, Yan T, Wu J, Xiang J, Zhang H. (2018) Decreased Complexity in Alzheimer's Disease: Resting-State fMRI Evidence of Brain Entropy Mapping. Front Aging Neurosci. 2017 Nov 20; 9 :378. doi: 10.3389/fnagi.2017.00378.
9. Zhang J, Guo Z, Liu X, Jia X, Li J, Li Y, Lv D, Chen W. (2017) Abnormal functional connectivity of the posterior cingulate cortex is associated with depressive symptoms in patients with Alzheimer's disease. Neuropsychiatr Dis Treat. 13, 2589-2598.
10. Jack A. (2018) Neuroimaging in neurodevelopmental disorders: focus on resting-state fMRI analysis of intrinsic functional brain connectivity. Curr Opin Neurol. doi: 10.1097/WCO.0000000000000536.
11. Duan X, Chen H, He C, Long Z, Guo X, Zhou Y, Uddin LQ, Chen H. (2017) Resting-state functional under-connectivity within and between large-scale cortical networks across three low-frequency bands in adolescents with autism. Prog Neuropsychopharmacol Biol Psychiatry 79, 434-441.
12. Hegarty JP 2 nd, Ferguson BJ, Zamzow RM, Rohowetz LJ, Johnson JD, Christ SE, Beversdorf DQ. (2017) Beta-adrenergic antagonism modulates functional connectivity in the default mode network of individuals with and without autism spectrum disorder. Brain Imaging Behav 11, 1278-1289.
13. Huang H, Shu C, Chen J, Zou J, Chen C, Wu S, Xiao L, Liu Z, Wang H, Zhou Y, Wang G, Jiang T. (2018) Altered corticostriatal pathway in first-episode paranoid schizophrenia: Resting-state functional and causal connectivity analyses. Psychiatry Res. 272, 38-45.
14. Wang S, Zhan Y, Zhang Y, Lyu L, Lyu H, Wang G, Wu R, Zhao J, Guo W. (2018) Abnormal long- and short-range functional connectivity in adolescent-onset schizophrenia patients: A resting-state fMRI study. Prog Neuropsychopharmacol Biol Psychiatry 81, 445-451.
15. Sharma A, Kumar A, Singh S, Bhatia T, Beniwal RP, Khushu S, Prasad KM, Deshpande SN. (2018) Altered resting state functional connectivity in early course schizophrenia. Psychiatry Res. 271,17-23.
16. Pezoulas VC, Zervakis M, Michelogiannis S, Klados MA. (2017) Resting-State Functional Connectivity and Network Analysis of Cerebellum with Respect to Crystallized IQ and Gender. Front Hum Neurosci. 2017 Apr 26;11:189. doi: 10.3389/fnhum.2017.00189.

17. Li T, Yan X, Li Y, Wang J, Li Q, Li H, Li J. (2017) Neuronal Correlates of Individual Differences in the Big Five Personality Traits: Evidences from Cortical Morphology and Functional Homogeneity. Front Neurosci. 2017 Jul 18;11:414. doi: 10.3389/fnins. 2017.00414.
18. Kong F, Liu L, Wang X, Hu S, Song Y, Liu J. (2015) Different neural pathways linking personality traits and eudaimonic well-being: a resting-state functional magnetic resonance imaging study. Cogn Affect Behav Neurosci. 15, 299-309.
19. Geerligs L, Cam-Can, Henson RN. (2016) Functional connectivity and structural covariance between regions of interest can be measured more accurately using multivariate distance correlation. Neuroimage 135, 16-31.
20. Patriat R, Molloy EK, Meier TB, Kirk GR, Nair VA, Meyerand ME, Prabhakaran V, Birn RM. (2013) The effect of resting condition on resting-state fMRI reliability and Cnsistency: a comparison between resting with eyes open, closed, and fixated. Neuroimage. 78, 463-73.
21. Janssens C, De Loof E, Boehler CN, Pourtois G, Verguts T. (2018) Occipital alpha power reveals fast attentional inhibition of incongruent distractors. Psychophysiology. 2018 Mar;55 (3). doi: 10.1111/psyp.13011.
22. Ben-Simon E, Podlipsky I, Okon-Singer H, Gruberger M, Cvetkovic D, Intrator N, Hendler T. (2013) The dark side of the alpha rhythm: fMRI evidence for induced alpha modulation during complete darkness. Eur J Neurosci. 37, 795-803.

Table 1. The 116 brain areas in the AAL template.

Number	Areas
ROI 1	'Precentral_L'
ROI 2	'Precentral_R'
ROI 3	'Frontal_Sup_L'
ROI 4	'Frontal_Sup_R'
ROI 5	'Frontal_Sup_Orb_L'
ROI 6	'Frontal_Sup_Orb_R'
ROI 7	'Frontal_Mid_L'
ROI 8	'Frontal_Mid_R'
ROI 9	'Frontal_Mid_Orb_L'
ROI10	'Frontal_Mid_Orb_R'
ROI11	'Frontal_Inf_Oper_L'
ROI12	'Frontal_Inf_Oper_R'
ROI13	'Frontal_Inf_Tri_L'
ROI14	'Frontal_Inf_Tri_R'
ROI15	'Frontal_Inf_Orb_L'
ROI16	'Frontal_Inf_Orb_R'
ROI17	'Rolandic_Oper_L'
ROI18	'Rolandic_Oper_R'
ROI19	'Supp_Motor_Area_L'
ROI20	'Supp_Motor_Area_R'
ROI21	'Olfactory_L'
ROI22	'Olfactory_R'
ROI23	'Frontal_Sup_Medial_L'
ROI24	'Frontal_Sup_Medial_R'
ROI25	'Frontal_Med_Orb_L'
ROI26	'Frontal_Med_Orb_R'
ROI27	'Rectus_L'
ROI28	'Rectus_R'
ROI29	'Insula_L'
ROI30	'Insula_R'
ROI31	'Cingulum_Ant_L'
ROI32	'Cingulum_Ant_R'
ROI33	'Cingulum_Mid_L'
ROI34	'Cingulum_Mid_R'
ROI35	'Cingulum_Post_L'
ROI36	'Cingulum_Post_R'
ROI37	'Hippocampus_L'
ROI38	'Hippocampus_R'
ROI39	'ParaHippocampal_L'
ROI40	'ParaHippocampal_R'
ROI41	'Amygdala_L'
ROI42	'Amygdala_R'
ROI43	'Calcarine_L'
ROI44	'Calcarine_R'
ROI45	'Cuneus_L'
ROI46	'Cuneus_R'
ROI47	'Lingual_L'
ROI48	'Lingual_R'
ROI49	'Occipital_Sup_L'
ROI50	'Occipital_Sup_R'
ROI51	'Occipital_Mid_L'
ROI52	'Occipital_Mid_R'
ROI53	'Occipital_Inf_L'
ROI54	'Occipital_Inf_R'
ROI55	'Fusiform_L'
ROI56	'Fusiform_R'
ROI57	'Postcentral_L'
ROI58	'Postcentral_R'
ROI59	'Parietal_Sup_L'
ROI60	'Parietal_Sup_R'
ROI61	'Parietal_Inf_L'
ROI62	'Paricta1_Inf_R'
ROI63	'SupraMarginal_L'
ROI64	'SupraMarginal_R'
ROI65	'Angular_L'
ROI66	'Angular_R'
ROI67	'Precuneus_L'
ROI68	'Precuneus_R'

ROI69	'Paracentral_Lobule_L'
ROI70	'Paracentral_Lobule_R'
ROI71	'Caudate_L'
ROI72	'Caudate_R'
ROI73	'Putamen_L'
ROI74	'Putamen_R'
ROI75	'Pallidum_L'
ROI76	'Pallidum_R'
ROI77	'Thalamus_L'
ROI78	'Thalamus_R'
ROI79	'Heschl_L'
ROI80	'Heschl_R'
ROI81	'Temporal_Sup_L'
ROI82	'Temporal_Sup_R'
ROI83	'Temporal_Pole_Sup_L'
ROI84	'Temporal_Pole_Sup_R'

ROI85	'Temporal_Mid_L'
ROI86	'Temporal_Mid_R'
ROI87	'Temporal_Pole_Mid_L'
ROI88	'Temporal_Pole_Mid_R'
ROI89	'Temporal_Inf_L'
ROI90	'Temporal_Inf_R'
ROI91	'Cerebelum_Crus 1_L'
ROI92	'Cerebelum_Crus 1_R'
ROI93	'Cerebelum_Crus 2_L'
ROI94	'Cerebelum_Crus 2_R'
ROI95	'Cerebelum_ 3_L'
ROI96	'Cerebelum_ 3_R'
ROI97	'Cerebelum_ 4_ 5_L'
ROI98	'Cerebelum_ 4_ 5_R'
ROI99	'Cerebelum_ 6_L'
ROI100	'Cerebelum_ 6_R'

ROI101	'Cerebelum_ 7b_L'
ROI102	'Cerebelum_ 7b_R'
ROI103	'Cerebelum_ 8_L'
ROI104	'Cerebelum_ 8_R'
ROI105	'Cerebelum_ 9_L'
ROI106	'Cerebelum_ 9_R'
ROI107	'Cerebelum_10_L'
ROI108	'Cerebelum_10_R'
ROI109	'Vermis_ 1_ 2'
ROI110	'Vermis_ 3'
ROI111	'Vermis_ 4_ 5'
ROI112	'Vermis_ 6'
ROI113	'Vermis_ 7'
ROI114	'Vermis_ 8'
ROI115	'Vermis_ 9'
ROI116	'Vermis_10'

Received: 11 September 2017 | Revised: 27 March 2018 | Accepted: 18 April 2018

DOI: 10.1002/hbm.24200

Check for updates

RESEARCH ARTICLE

WILEY

Estimation of vocational aptitudes using functional brain networks

Yul-Wan Sung[1] | Yousuke Kawachi[1] | Uk-Su Choi[2] | Daehun Kang[1] | Chihiro Abe[1] | Yuki Otomo[1] | Seiji Ogawa[1]

[1]Kansei Fukushi Research Institute, Tohoku Fukushi University, Sendai, Japan

[2]Neuroscience Research Institute, Gachon University, Incheon, Republic of Korea

Correspondence
Yul-Wan Sung, PhD, Kansei Fukushi Research Institute, Tohoku Fukushi University, Sendai, Japan.
Emails: sung@tfu-mail.tfu.ac.jp
or
sungstone@gmail.com

Abstract

The success of human life in modern society is highly dependent on occupation. Therefore, it is very important for people to identify and develop a career plan that best suits their aptitude. Traditional test batteries for vocational aptitudes are not oriented to measure developmental changes in job suitability because repeated measurements can introduce bias as the content of the test batteries is learned. In this study, we attempted to objectively assess vocational aptitudes by measuring functional brain networks and identified functional brain networks that intrinsically represented vocational aptitudes for 19 job divisions in a General Aptitude Test Battery. In addition, we derived classifiers based on these networks to predict the aptitudes of our test participants for each job division. Our results suggest that the measurement of brain function can indeed yield an objective evaluation of vocational aptitudes; this technique will enable a person to follow changes in one's job suitability with additional training or learning, paving a new way to advise people on career development.

KEYWORDS

brain function networks, vocational aptitudes, classifier, resting-state fMRI, multiclass, support vector machine

1 | INTRODUCTION

In modern society, the success of an individual is highly dependent on their occupation. Therefore, choosing and developing a career that takes advantage of one's aptitudes is of utmost importance.

The suitability for a job is typically assessed on the basis of psychometric properties, such as intellectual, clerical, perceptual, numerical, spatial performance, and so forth, and there is a battery of tests available to measure these abilities (Gottfredson, 1998; Gottfredson, 2003; Frey & Detterman, 2004). For example, the Minnesota Clerical Test (Andrew, Paterson, & Longstaff, 1979), the Differential Aptitude Test (Bennett, Seashore, & Wesman, 1974), the Wonderlic tests (Wonderlic, 1983), the General Aptitude Test Battery (GATB) (United States Department of Labor, 1970), and the Armed Services Vocational Aptitude Battery (United States Department of Defense, 1984) are used to evaluate vocational aptitude. These tests have been widely used for career guidance, selection, counseling, and so on (Hunter, 1986; Barrick, Mount, & Strauss, 1993; Lent, Brown, & Hackett, 1994; Legree, 1995; Kwallek, Lewis, Lin-Hsiao, & Woodson, 1996; Brown & Lent, 1996; Chan, 1997). However, these vocational aptitude tests are not oriented to evaluate the properties that affect suitability over time (i.e., progress or improvement of abilities), because repeating these tests can lead to biases in the results as participants become familiar with the questions.

The abilities evaluated in these tests are considered to be influenced by genetics, experiences, and environment (McGee, 1979; Plomin, Owen, & McGuffin, 1994; McCleam et al., 1997; Thompson et al., 2001; Turkheimer, Haley, Waldron, D'Onofrio, & Gottesman, 2003; Hackman & Farah, 2009), and these characteristics must be stored and represented in the brain. Therefore, we hypothesized that the vocational aptitudes measured by these tests could also be represented in the brain as intrinsic brain functions associated with job requirements. Conversely, by measuring brain function, we may be able to assess specific vocational aptitudes; hence, it will become possible to take repeated measurements, allowing us to evaluate changes in vocational aptitudes or to perform follow-up studies.

 © 2018 Wiley Periodicals, Inc.

TABLE 1 Vocational aptitudes: 19 divisions

Job 1	(M) Plant culture/animal breeding
Job 2	(GV) Animal training and service/aquaculture/gardening
Job 3	(KM) Physical works in mechanical/plants/animals
Job 4	(PM) Hand work
Job 5	(KFM) Industrial machine manipulation
Job 6	(PKM) Manufacture/assembly
Job 7	(SPM) Cutting/molding/construction/installation
Job 8	(SPF) Barber/beauty services
Job 9	(NSP) Drawing and architecture design/laboratory technology
Job 10	(GQM) Nursing/therapy/specialized teaching services/quality control/security management
Job 11	(GNS) Engineering technology/physical sciences/medical sciences
Job 12	(GVN) Social research/law/social service/mathematics and statistics
Job 13	(GVQ) General office work/educational and library services
Job 14	(SP) Design and visual arts
Job 15	(GQK) Clerical machine operation/communicator
Job 16	(GM) Nursing-care services
Job 17	(GNQ) General sales/accounting
Job 18	(GQ) Hospitality/security services
Job 19	(QK) Clerical handling

Note. Abbreviations: F = finger dexterity; G = general intelligence; K = motor coordination; M = manual dexterity; N = numerical aptitude; P = form perception; Q = clerical perception; S = spatial aptitude; V = verbal aptitude.

Only a few functional brain studies related to vocational aptitude have been reported, and these studies do not directly examine how specific vocational aptitudes are represented in the brain (Yurgelun-Todd, Killgore, & Cintron, 2003; Fan et al., 2013; Burgaleta et al., 2014; Jung et al., 2015). Technical difficulties in measuring brain function that specifically reflect vocational aptitudes may be the reason of this limitation.

Recently, numerous studies have shown that the effects of cognitive and physical training are reflected in morphological and functional brain changes (Golestani, Paus, & Zatorre, 2002; Dong & Greenough, 2004; Bermudez & Zatorre, 2005; Draganski et al., 2006; Maguire, Woollett, & Spiers, 2006; Pereira et al., 2007; Deng, Saxe, Gallina, & Gage, 2009; Voss & Schiff, 2009; Aimone, Wiles, & Gage, 2009; Tremblay, Lowery, & Majewska, 2010; Rhyu et al., 2010; Dosenbach et al., 2010; Teipel et al., 2010; Decety & Michalska, 2010; May, 2011), indicating the role of environment in neuroplasticity. Therefore, it is likely that changes in vocational aptitudes caused by the environment would also be reflected as functional and/or morphological changes in the brain and that measuring these changes would allow us to assess vocational aptitudes.

In this study, we attempted to assess vocational aptitudes by measuring brain function. We measured resting-state brain function using functional MRI and evaluated vocational aptitudes using the Japanese version of GATB (Employment Security Bureau, Ministry of Health, Labour & Welfare, 2013). To identify functional networks from the resting-state fMRI signals, we performed a region of interest (ROI)-based analysis, in which ROIs defined on the basis of previous studies (Desikan et al., 2006; Dosenbach et al., 2010) were used. Based on these functional networks, classifiers for vocational aptitude for 19 job divisions in GATB (Table 1) were derived using a multi-class (three levels) support vector machine (SVM).

2 | METHODS

2.1 | Participants

Two groups of participants were included in this study. The first group (for the training of classifiers) included 112 university students in their freshman and sophomore years (28 males, 84 females; mean age + standard deviation (*SD*): 20.14 ± 0.69 years). The second group (for the testing of classifiers) included 35 students also in their freshmen and sophomore years from the same university as the first group (5 males, 30 females; mean age + *SD*: 20.15 ± 0.75 years). The volunteers in these two groups participated in both the psychometric and MRI experiments. None of the participants had a history of neurological disease or any other medical conditions (e.g., pregnancy, arrhythmia, or claustrophobia). The participants were given a complete description of the study, and written informed consent was obtained in accordance with the Declaration of Helsinki. This study was approved by the Institutional Review Board of Tohoku Fukushi University in Japan.

2.2 | Psychometric measurements of vocational aptitudes

GATB was created by the US government based on a vast amount of occupational analyses (United States Department of Labor, 1970). In the analysis, the government classified more than 75,000 jobs into 20 job groups and then found nine aptitudes needed for each job group. In Japan, the Ministry of Health, Labour and Welfare created the Japanese version of GATB and has updated it over the years; it is still widely used today. The Japanese version of GATB, in the present day, has been recognized as having higher reliability and validity than any other test battery and has been through five revisions to track the development of Japanese lifestyle and culture (Muroyama, 2016).

The Japanese version of GATB classifies people into 40 subdivisions of jobs based on weighted combinations of the scores of the nine abilities. Additionally, 19 independent job divisions, which are larger categories than the 40 subdivisions, are derived from a linear combination of the nine ability scores without weighting and are linearly divided from low to high levels with even intervals of scores such as low, middle, and high, according to GATB (Employment Security Bureau, Ministry of Health, Labour & Welfare, 2013). The process of grouping into the 40 subdivisions is nonlinear but

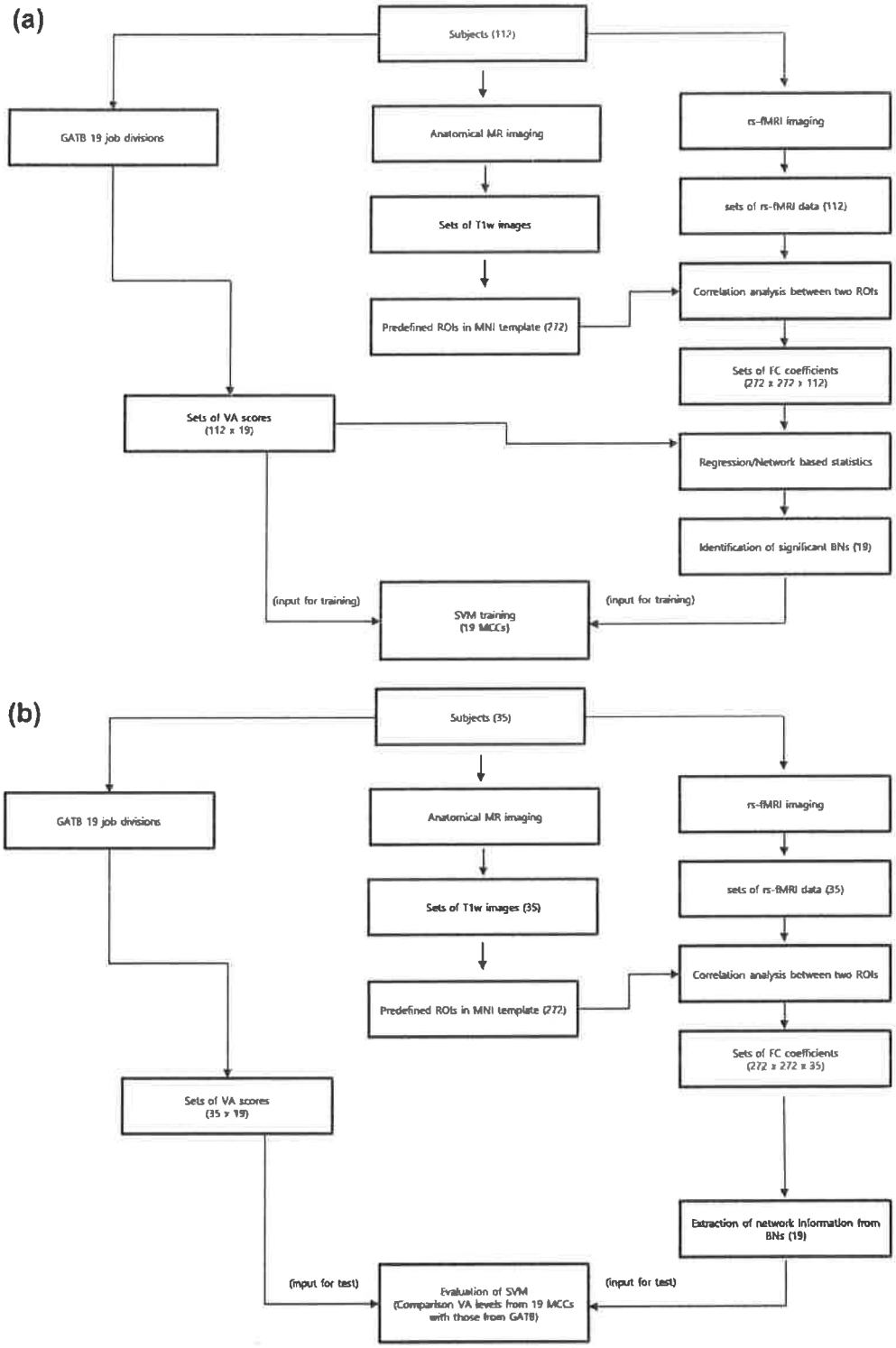


FIGURE 1 MRI data processing workflow. (a) Diagrams to illustrate the data flow for the primary data processing; identification of functional networks and derivation of multi-class classifiers (MCCs) using multi-class support vector machine (SVM). Step 1: resting-state functional MRI (rs-fMRI) signals are extracted from the predefined 272 ROIs, and functional connectivity (FC) matrices (correlation matrices) are constructed for the 112 training participants. Step 2: a simple regression and network-based statistics (NBS) analysis are performed for the FC matrices of the 112 participants, and functional brain networks (BNs) reflecting 19 job divisions are identified. Step 3: an input dataset (MRI data) to the MCCs—SVM classifiers—is constructed from the edges of the identified functional BNs in addition to another input dataset (vocational aptitude levels), which is constructed from the General Aptitude Test Battery (GATB). Step 4: the MCCs are trained by the input datasets. Step 5: the vocational aptitude (VA) levels of the job divisions estimated by the classifiers are compared with the VA levels determined by GATB to calculate accuracy. (b) Verification of MCCs for the test group: after making FC matrices for the 35 test participants, Steps 4 and 5 were carried out (see panel a). [Color figure can be viewed at wileyonlinelibrary.com]

grouping into the 19 divisions is linear. Therefore, we attempted to evaluate the 19 job divisions, because one of the purposes of this study is to directly provide information about the vocational aptitudes of individuals rather than just to provide information related to the nine abilities. The two student groups participated in psychometric measurements of vocational aptitudes for the 19 job divisions. The job divisions are listed in Table 1.

In the measurements of vocational aptitudes for the job divisions, there were no participants who reported any pre-experience or pre-knowledge about GATB until they underwent the testing. The measurements were administrated in the testing environment as follows: in a quiet, distraction-free, comfortable room and by well-trained testers according to the instructions (Shokugyo Tekisei Kenkyukai, 2011). Our testers cautiously checked whether participants were in a comfortable state before starting each subtest of GATB. All testers had experienced various other psychological tests before the GATB measurements. The measurements were mostly performed after MRI measurements, and the mean interval from the fMRI measurements to GATB was 3.27 months (SD = 1.67). For three of the participants, GATB was conducted before the MRI measurements.

2.3 | MRI measurements

We used a 3-Tesla MRI scanner (Skyra-fit; Siemens Co., Erlangen, Germany), and all participants were scanned in two sessions to obtain structural (T1) and functional image measurements (resting-state fMRI). Sagittal structural images were acquired using the following parameters: repetition time = 1,900 ms, echo time = 2.52 ms, matrix size = 256 × 256, in-plane resolution = 1 × 1 mm^2, slice thickness = 1 mm, and number of slices = 192. Resting-state fMRI data were acquired using the following parameters: repetition time = 1,000 ms, echo time = 24 ms, matrix size = 64 × 64, in-plane resolution = 3.4 × 3.4 mm^2, slice thickness = 3.4 mm, and number of volumes = 480. During the resting-state fMRI session, participants were asked to lie on the bed with their eyes open, to lightly focus on the center of their visual field, and to not think about anything as much as possible. The lights in the room were turned off for all MRI scans.

2.4 | Procedure for MRI data processing

The analysis of MRI data for the two groups was performed according to the processing pipeline described below.

2.5 | Preparation of ROIs for functional networks

We used ROIs based on the two templates from Dosenbach and Harvard (Desikan et al., 2006; Dosenbach et al., 2010) that were reported in the DPABI software (see below) (Chao-Gan & Yu-Feng, 2010; Yan, Wang, Zuo, & Zang, 2016) and defined brain areas of 272 ROIs (Supporting Information, Table 1) by removing redundant ROIs from the two templates. Each ROI was a sphere with a radius of 5 mm around the center coordinate. We used the Dosenbach template first and then added ROIs from the Harvard template, but only those that did not overlap with the Dosenbach ROIs. Originally, the Dosenbach template

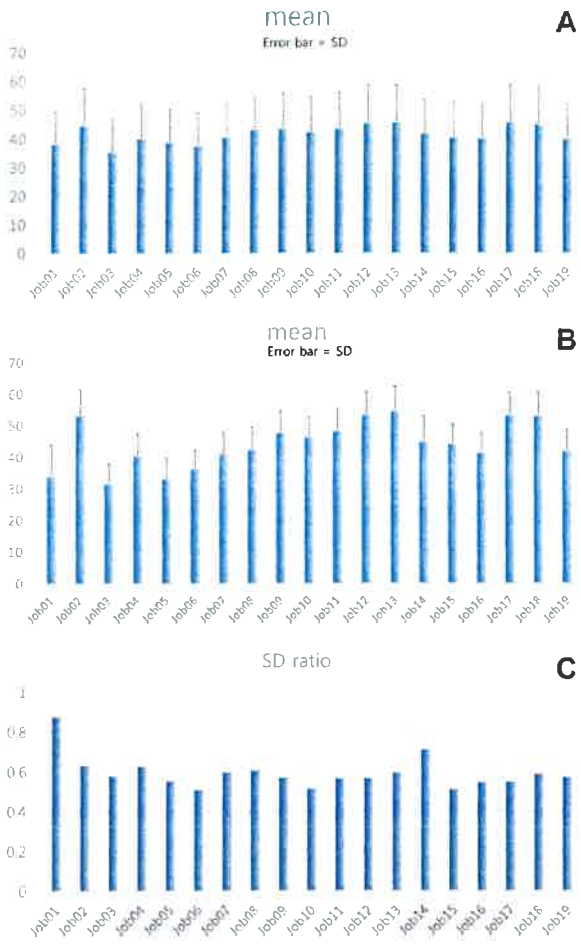


FIGURE 2 Data distribution of GABT scores as the mean value and standard deviation of vocational aptitude scores of 19 job divisions for the 112-participant training sample (a) and for the original (true) population of Japan (b), and the ratio of standard deviations of the two populations (c). [Color figure can be viewed at wileyonlinelibrary.com]

consisted of 160 ROIs, and the other 112 ROIs were added from the Harvard template to make our 272 ROIs.

2.6 | Preprocessing of fMRI data

To preprocess the resting-state fMRI data for the 112 training participants, we used the data processing assistant for a part of resting-state fMRI preprocessing software known as DPABI (Chao-Gan & Yu-Feng, 2010; Yan et al., 2016). The preprocessing included slice-scan time correction, 3D motion correction (maximum head motion: 111 participants passed the maximum threshold of 1.5 mm and 1.5°, and the remaining participant passed the maximum threshold of 3.0 mm and 3°), band-pass temporal filtering (between 0.01 and 0.1 Hz), and artifact rejection based on the CSF signal. To control for head motion confounds, the Friston 24-parameter model was used to regress out head motion effects. These functional images were co-registered with each corresponding structural image.

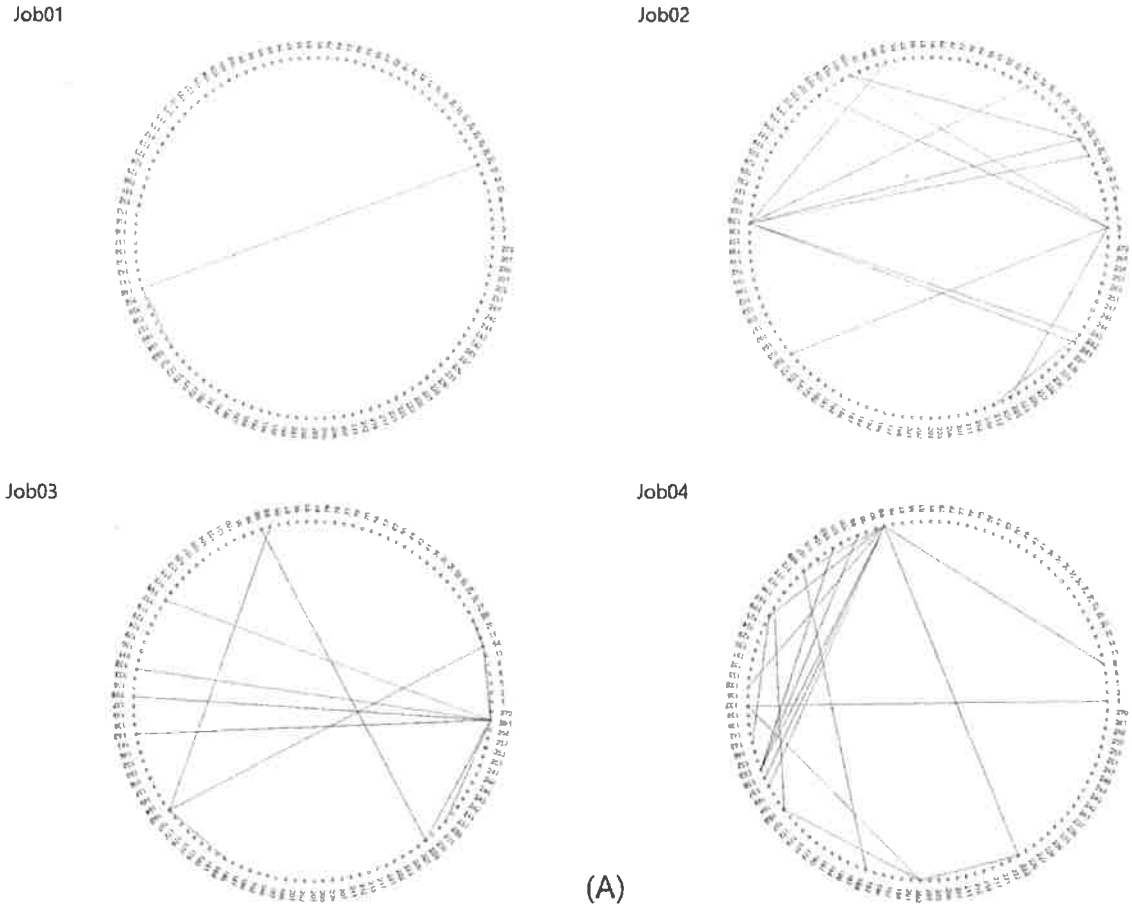


FIGURE 3 Functional networks identified for the 19 job divisions. Each functional network corresponds to a job division. The numbers assigned to each node (ROIs) of the networks appear in Table 2. (a) Functional networks for jobs 1, 2, 3, and 4. (b) Functional networks for jobs 5, 6, 7, and 8. (c) Functional networks for jobs 9, 10, 11, and 12. (d) Functional networks for jobs 13, 14, 15, and 16. (e) Functional networks for jobs 17, 18, and 19. [Color figure can be viewed at wileyonlinelibrary.com]

2.7 | Identification of functional networks

To identify functional networks for the job divisions, we performed a simple regression analysis with the vocational aptitude scores measured by GATB for each job division and the resting-state fMRI signals from the 272 predefined ROIs of the 112 training participants using network-based statistics (NBS) for multiple comparison correction (Zalesky, Fornito, & Bullmore, 2010) for each of the 19 job divisions (Figure 1a) as follows. (c) For the 272 time courses obtained from the 272 ROIs, the correlation was calculated between ROIs for each participant, which produced a coefficient matrix (272 × 272); (b) the process was performed for all 112 training participants, through which 112 correlation coefficient matrices (272 × 272) were created; (c) a simple regression analysis was performed with the 112 correlation matrices and a vector of vocational aptitude scores for the 112 training participants for each job division to identify functional brain networks in which randomly shuffled correlation matrices were generated for a permutation test, and then the regression analysis on the true correlation matrix with the vocational aptitude vector and a nonparametric permutation test on the random correlation matrices with more than 5,000 iterations were performed (Figure 1a); (4) NBS were used for multiple comparisons. For all 19 job divisions, the processing steps (a)–(d) were repeated. Correction for multiple comparisons based on NBS statistics was performed at an initial threshold of $p < .005$, and the number of edges in the network was limited to as close to 15 as possible, because a previous study has shown that a small number of brain connections can predict a psychiatric disorder (Yahata et al., 2016).

2.8 | Multiple SVM classifier design (training)

We attempted to design three-class multiple SVM classifiers to evaluate the vocational aptitudes, because the Japanese GATB classifies the job divisions into three classes as described in the previous section (Figure 1a). Datasets for the design were prepared from the results of the identified brain network analysis for the 112 training participants and the vocational aptitudes scores from GATB, which consisted of a data matrix with features and a label matrix

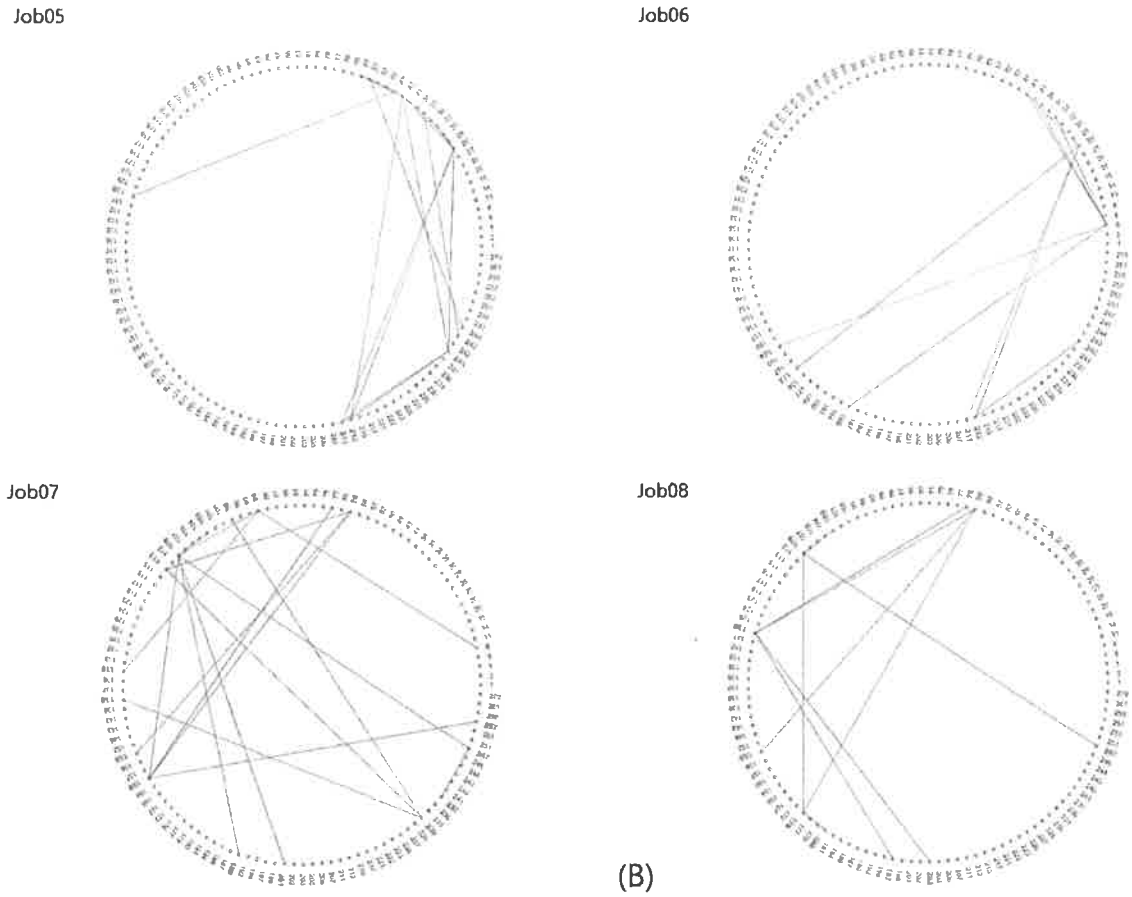


FIGURE 3 Continued

for each of the 19 job divisions. Data matrices were composed of correlation coefficients (features) of selected network edges. Label matrices were created based on the scores of the corresponding vocational aptitude of GATB, and the vocational aptitude scores were normalized and divided into three classes (levels) according to the GATB classification: "low," "middle," and "high," for which the GATB scores were divided into evenly with the same size intervals as those of the scores of vocational aptitudes from the minimum to the maximum; that is, the classes were defined using the equation $\{(x - \min)/(\max - \min)\} \times 3$, where x was the score of each vocational aptitude. In the calculation, the number after the decimal point was rounded up. With the datasets of network edges and all vocational aptitude scores grouped into three classes, multiclass (three classes) classifiers were designed using the "classification learner app" in MATLAB 2017b (Mathworks Co., USA), where a one-versus-one design method was used with 10-fold cross-validation, and the predictors were standardized in such a way that the software centered and scaled each column of the predictor data (network edges) by the weighted column mean and standard deviation. All support vector machine models for a job division were designed (using the "all SVM" option), among which an SVM model that showed the best performance was chosen as the classifier for the job division. This process was performed for all 19 job divisions.

2.9 | Verification of SVM classifiers (test)

The MRI data for the second student group of 35 participants were processed through the same pipeline as the data from the first student group except for the identification of functional networks, and the vocational aptitude levels of the 19 job divisions were also estimated for the second student group (Figure 1b).

3 | RESULTS

The measured vocational aptitude scores for the 19 job divisions in GATB for the 112 training participants were evaluated for normality, and the scores were revealed to have come from a normal distribution for all 19 job divisions (i.e., the hypothesis that aptitude scores of each job division came from other distributions than from a normal distribution was rejected with the minimum $p = .22$ and the maximum $p = .93$, chi-square test: goodness-of-fit). The histograms are summarized in Supporting Information, Figure 2. We compared the mean values of the vocational aptitude scores from our training

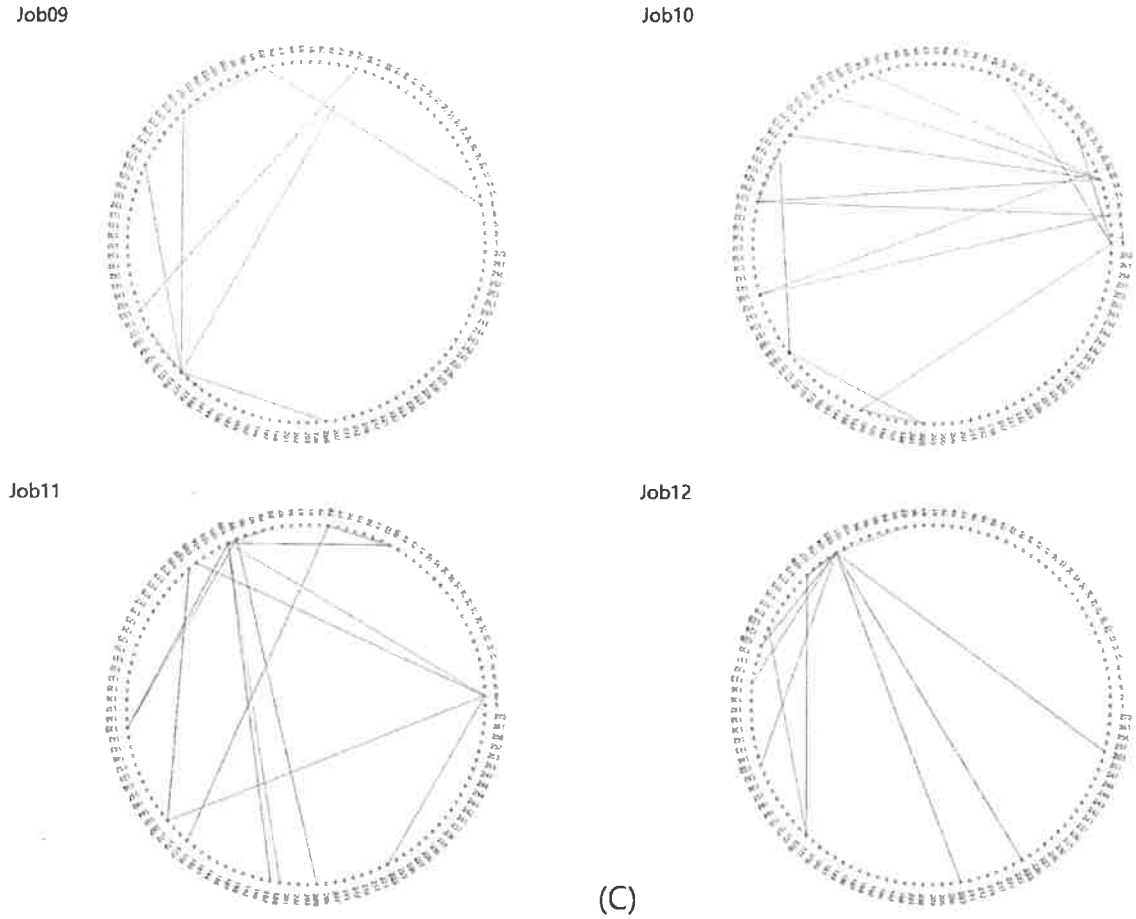


FIGURE 3 Continued

sample (112 participants) with those of the original (true) population of Japan (Employment Security Bureau, Ministry of Health, Labour and Welfare, 2013) to determine how they differed for each of the 19 vocational aptitudes. A two-sample *t* test was performed using mean values and standard deviations of the populations (Figure 2a, b), and six and eleven vocational aptitudes were found to be significantly different ($p = .01$ and .05, respectively). Comparison of the standard deviations of the 112-participant training sample and the original (true) population of Japan showed that the standard deviation of the sample data was more than 50% of the original population, with a maximum of 85.2% and a minimum of 50.7% (Figure 2c). For the 35-participant test sample, 17 job divisions revealed significant normal distribution (i.e., the hypothesis that the scores came from other distributions than from a normal distribution was rejected, with minimum $p = .09$ and the maximum $p = .89$; chi-square test: goodness-of-fit), and two job divisions were revealed not to have a normal distribution ($p = .03$). The histograms are summarized in Supporting Information, Figure 3.

A simple regression analysis of the resting-state connectivity and vocational aptitude scores measured by GATB gave 19 functional brain networks ($p = .005$, corrected by NBS); each network corresponded to one job division out of the 19 total GATB job divisions (Figure 3). The average number of edges of the networks was 11 ± 3.97. Each network had a different configuration from the others and showed that specific brain areas that were distinct in the network configuration were contributing to the aptitude required for that job division (Table 1 and Figure 3). Overall, 121 brain areas were involved in the 19 functional networks (Table 2 and Figure 3).

Classifiers corresponding to each of the functional networks were designed using multi-class (three classes: high, middle, and low) SVM, and the training accuracies of the classifiers for all the 19 job divisions were greater than chance (defined as 33.3%), as verified by cross-validation (Figure 4). The average accuracy of the 19 classifiers was $58.0\% \pm 8.6\%$, with a maximum of 70.5% and a minimum of 42.9%. The classifiers were then tested by applying them to the 35-participant test sample, whose data were not used for training the classifiers (multiclass SVM; see the Methods section). The prediction accuracy for the second student group was more than the level of chance for all classifiers in the 19 job divisions (Figure 5). The average accuracy of the 19 classifiers was $51.9\% \pm 8.1\%$, with a maximum accuracy of 68.5% and a minimum of 37.1%. The sensitivity and specificity of the classifiers were calculated and are summarized in Table 3. To evaluate the difference between the distribution of

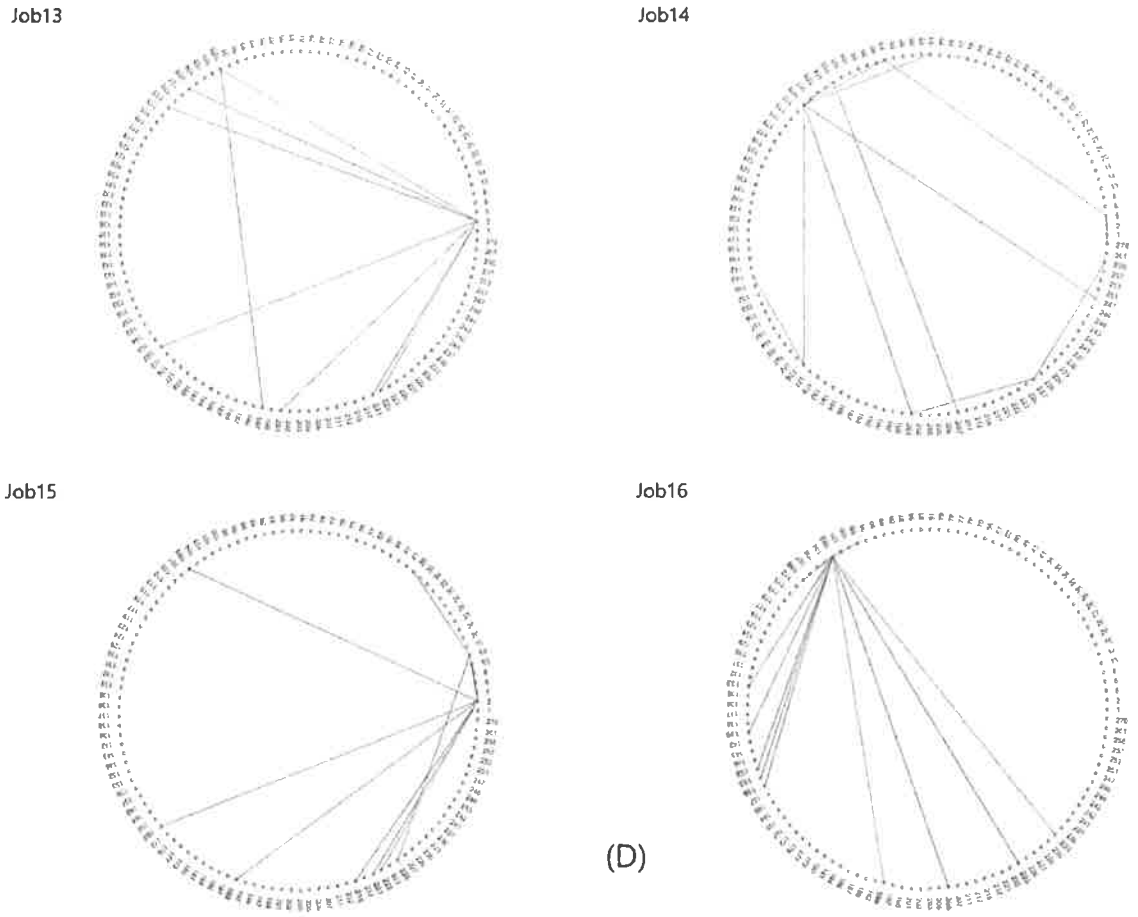


FIGURE 3 Continued

the GATB scores and that of the predicted scores of the 35-participant test sample, we compared the two data score sets for each vocational aptitude, which revealed no significant differences in any of the 19 job divisions (minimum $p = .17$; maximum $p = .99$; two-sample Kolmogorov–Smimov test). For additional classifier performance evaluation, we examined the classes which the mispredicted classes of a classifier belonged to, that is, the opposite or the neighboring class. For the classifiers of eight job divisions, all mispredicted classes were found to belong to the neighboring class, and for the other 11 classifiers, <8.5% of the mispredicted classes belonged to the opposite classes (Table 4).

4 | DISCUSSION

This study aimed to map brain functions that intrinsically represent vocational aptitudes and to determine the utility of this approach in assessing these aptitudes. We identified functional networks that reflected 19 distinct job divisions and used them to derive multiple SVM classifiers for each division. We validated that the SVM classifiers could significantly and accurately estimate the vocational aptitudes of the participants. The data indicated that functional networks intrinsically represent vocational aptitudes and that the measurement of these functional networks can assess these vocational aptitudes.

Measuring vocational aptitude in this manner can reveal what brain functions are involved in specific aptitudes, which may be used to develop methods to enhance an individual's career-specific abilities. Furthermore, the confounding effects of learning during repetition of psychometric aptitude tests prohibit the use of such tests for the evaluation of aptitude development over the course of an individual's training. Measuring brain functionality can circumvent this learned testing bias and allow for longitudinal evaluation over time.

Previous studies examining psychological scores and brain function or structural changes have identified brain areas associated with the intelligence quotient (Haier, Jung, Yeo, Head, & Alkire, 2004; Colom, Jung, & Haier, 2006; Royle et al., 2013; MacDonald, Ganjavi, Collins, Evans, & Karama, 2014). The assessment of vocational aptitudes by intelligence alone is limited because although it reflects a general cognitive ability, it only correlates with certain aspects of vocational abilities (Gottfredson, 2003). A previous study examined brain morphology and vocational aptitude by comparing subcortical brain regions and psychological test scores. However, it

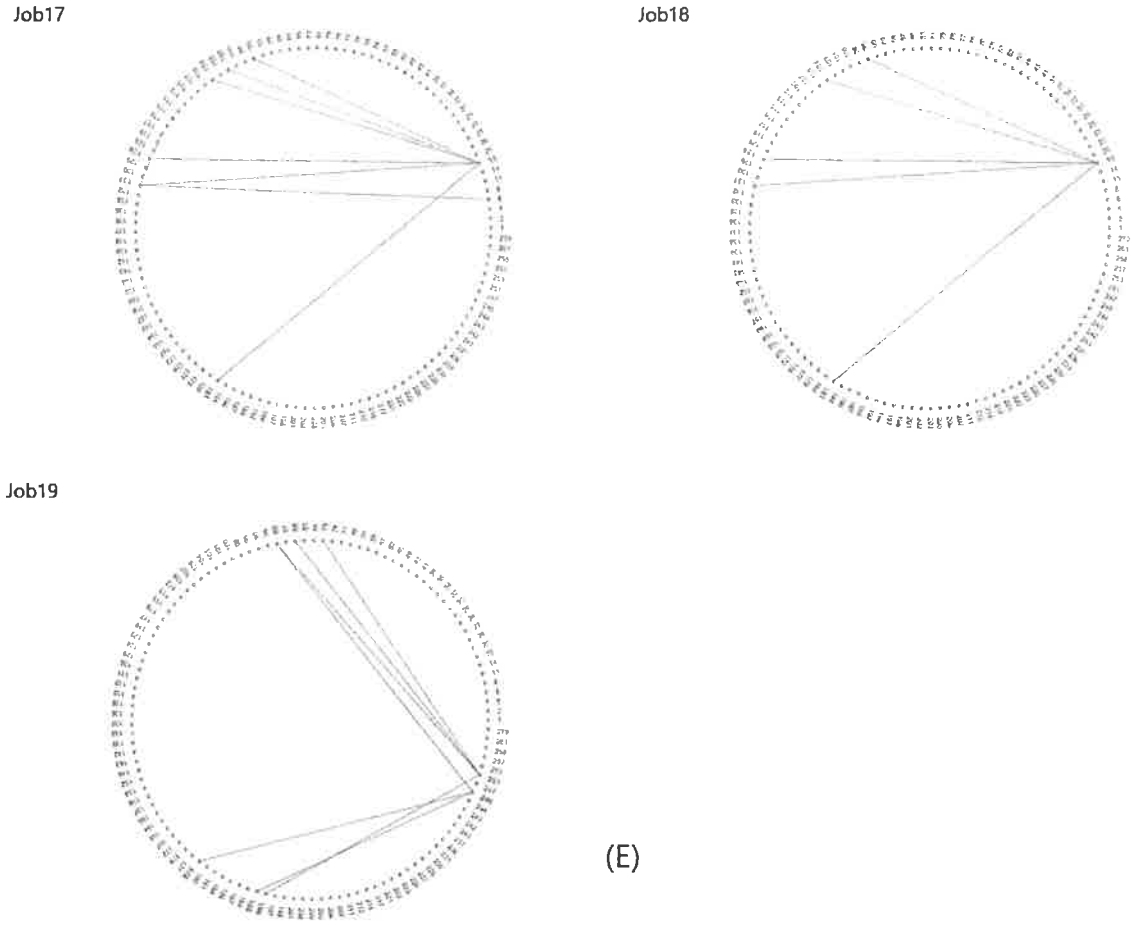


FIGURE 3 Continued

did not completely investigate all the traits required to assess aptitude (Burgaleta et al., 2014). To the best of our knowledge, this study is the first to use brain function to assess specific vocational aptitudes.

Task-based fMRI and resting-state fMRI studies have indicated that changes in functional networks are more sensitive than structural changes alone (Choi, Sung, Hong, Chung, & Ogawa, 2015; Ogawa, Lee, Kay, & Tank, 1990). Numerous fMRI studies have also demonstrated specific changes in functional networks associated with learning or training (Albert, Robertson, & Miall, 2009; Baldassarre et al., 2012; Guerra-Carrillo, Mackey, & Bunge, 2014; Dong et al., 2015; Sidarta, Vahdat, Bernardi, & Ostry, 2016; Yang et al., 2016; Wang et al., 2016; Nasrallah, To, Chen, Routtenberg, & Chuang, 2016; Rjosk et al., 2017). Consistent with the results of these studies, we found that we can evaluate and assess vocational aptitudes by measuring brain function that might occur during learning or training.

The accuracies of the classifiers were better than chance for the training and test groups for all job divisions, supporting the idea that functional networks can reliably reflect vocational aptitudes. There is some variation in this accuracy across the job divisions, and some characteristics of functional networks and vocational characteristics of GATB might contribute to this variation. Therefore, it may be difficult to determine why this accuracy varies across the job divisions, but classifiers with higher accuracy can be used to more reliably predict the corresponding job aptitudes.

The specificity of job aptitudes estimated by brain function is limited by the specificity of GATB, because the brain function networks were constructed based on the job divisions defined by GATB and covered several subdivisions. A major goal of this study is to make practically useful classifiers that can predict a job aptitude with a sufficiently high accuracy so that an individual's aptitudes can be evaluated by MRI. The performance of the classifiers in our study, 58.0% and 51.9% accuracy on average for the training and test, respectively, is not high enough for this purpose, although with this accuracy, we can still apply the classifiers to evaluate vocational aptitudes at the group level or even to individuals by performing repeated MRI measurements (e.g., three times for an individual by allowing the measurement time to be prolonged). Therefore, we need to improve the accuracy to increase the method's utility and practicality; future studies should aim to obtain more specific brain information or to engineer features to improve classifier performance.

TABLE 2 Brain areas involved in the functional networks associated with the job divisions shown in Figure 3 (121 regions of interest and the coordinates of the regions in MNI coordinates)

#	ROI numbers in 19 networks	ROI-belonging job network	Brain region	Brodmann	MNI coordinates		
					x	y	z
1	1	Job04,10	vmPFC_R	Brodmann area 10	6	64	3
2	2	Job02,11,13,15	mPFC	Brodmann area 6	29	57	18
3	5	Job06,14	vmPFC_L	Brodmann area 32	−25	51	27
4	6	Job10,17	vmPFC_L	Brodmann area 9	9	51	16
5	8	Job04,07,09	ACC_R	Brodmann area 32	27	49	26
6	13	Job15	Inf temporal_L	Brodmann area 21	8	42	−5
7	14	Job03,15	Post cingulate_R	Brodmann area 23	9	39	20
8	15	Job10,17,18	Fusiform_R	Brodmann area 36	46	39	−15
9	20	Job01,10	Post cingulate_L	Brodmann area 23	−16	29	54
10	26	Job02,03	Post cingulate_L	Brodmann area 30	38	21	−1
11	27	Job05	Angular gyrus_R	Brodmann area 39	9	20	34
12	28	Job02,05,06	Angular gyrus_L	Brodmann area 39	−36	18	2
13	29	Job10	Precuneus_R	Brodmann area 7	40	17	40
14	30	Job05	IPS_L	Brodmann area 19	−6	17	34
15	32	Job05	Occipital_R	Brodmann area 39	58	11	14
16	34	Job06	Occipital_L	Brodmann area 39	44	8	34
17	35	Job05	aPFC_R	Brodmann area 10	60	8	34
18	38	Job15	Vent aPFC_L	Brodmann area 46	−20	6	7
19	41	Job06	ACC_L	Brodmann area 32	10	5	51
20	43	Job02,05,06	vPFC_L	Brodmann area 45	0	−1	52
21	49	Job05	IPL_R	Brodmann area 40	−44	−6	49
22	50	Job11	Post parietal_L	Brodmann area 40	−26	−8	54
23	52	Job10	IPL_L	Brodmann area 40	−54	−9	23
24	57	Job05	vPFC_R	Brodmann area 13	−12	−12	6
25	58	Job05	ACC_L	Brodmann area 32	11	−12	6
26	70	Job07,08,09	Thalamus_L	Caudate Body	42	−24	17
27	76	Job08	Post insula_L	Brodmann area 13	−30	−28	9
28	77	Job07	Temporal_R	Brodmann area 41	−24	−30	64
29	78	Job11	Post cingulate_L	Pulvinar	51	−30	5
30	79	Job19	Fusiform_R	Brodmann area 20	−41	−31	48
31	81	Job14	Parietal_R	Brodmann area 13	54	−31	−18
32	83	Job19	Parietal_L	Brodmann area 40	−53	−37	13
33	86	Job19	Temporal_L	Brodmann area 21	34	−39	65
34	87	Job12	TPJ_L	Brodmann area 39	8	−40	50
35	88	Job11,19	Frontal_R	Brodmann area 44	−41	−40	42
36	89	Job02,03,04,07,09,14	dFC_R	Brodmann area 6	58	−41	20
37	90	Job03	vFC_L	Brodmann area 9	−8	−41	3

(Continues)

TABLE 2 (Continued)

#	ROI numbers in 19 networks	ROI-belonging job network	Brain region	Brodmann	MNI coordinates		
					x	y	z
38	96	Job10,17,18	Mid insula_L	Brodmann area 13	54	−44	43
39	98	Job04,07,11,16	Parietal_L	Brodmann area 6	−28	−44	−25
40	100	Job02,11,13	Precentral gyrus_L	Brodmann area 43	42	−46	21
41	101	Job17	Precentral gyrus_R	Brodmann area 4	−48	−47	49
42	103	Job04,07,08,12,14,16	Mid insula_R	*	−59	−47	11
43	104	Job10,17,18	Mid insula_L	Brodmann area 13	−53	−50	39
44	105	Job02,11,13,14,15	Temporal_R	Brodmann area 41	5	−50	33
45	107	Job11	Parietal_L	Brodmann area 2	44	−52	47
46	109	Job04,07,08,09, 12,14,16	Parietal_L	Brodmann area 2	−24	−54	−21
47	112	Job13	Parietal_R	Brodmann area 3	−6	−56	29
48	113	Job07	Post insula_R	Brodmann area 13	−34	−57	−24
49	115	Job10	Parietal_L	Brodmann area 3	−11	−58	17
50	116	Job03	Parietal_L	Brodmann area 40	32	−59	41
51	117	Job04,10,17	Post parietal_L	Brodmann area 40	51	−59	34
52	119	Job04	Temporal_L	Brodmann area 41	36	−60	−8
53	123	Job09,12	Occipital_R	*	46	−62	5
54	124	Job17,18	Temporal_R	Brodmann area 37	−48	−63	35
55	129	Job12	Occipital_R	Brodmann area 31	19	−66	−1
56	130	Job05,08	Occipital_L	Brodmann area 31	1	−66	−24
57	131	Job10,17,18	Occipital_L	Brodmann area 18	−34	−67	−29
58	132	Job03	Occipital_R	Brodmann area 23	11	−68	42
59	133	Job12,16	Occipital_R	Brodmann area 18	17	−68	20
60	135	Job02,04,07	Post occipital_L	Brodmann area 18	39	−71	13
61	136	Job03	Post occipital_R	Brodmann area 17	−9	−72	41
62	137	Job04	Post occipital_R	Brodmann area 18	45	−72	29
63	138	Job07	Post occipital_L	Brodmann area 19	−11	−72	−14
64	139	Job11,16	Post occipital	Brodmann area 18	29	−73	29
65	142	Job03	Post occipital	Brodmann area 17	−29	−75	28
66	143	Job04,14	Lat cerebellum_L	*	5	−75	−11
67	146	Job01,06,10	Lat cerebellum_L	*	−42	−76	26
68	152	Job12,16	Med cerebellum_R	*	−5	−80	9
69	153	Job04,07,08,09,16	Inf cerebellum_L	*	29	−81	14
70	156	Job04,16	Med cerebellum_R	*	−37	−83	−2
71	157	Job04	Med cerebellum_R	*	−29	−88	8
72	160	Job07,09	Inf cerebellum_R	*	−4	−94	12
73	164		Insular cortex_R		38	3	0
74	165	Job01,03,04,10	Superior frontal gyrus_L		−14	19	57

(Continues)

TABLE 2 (Continued)

#	ROI numbers in 19 networks	ROI-belonging job network	Brain region	Brodmann	MNI coordinates x	y	z
75	167	Job02,11,13,15	Middle frontal gyrus_L		−38	19	42
76	172	Job06	Inferior frontal gyrus, pars opercularis_R		52	15	16
77	176	Job08,09,12,14	Temporal pole_R		41	13	−30
78	177	Job11	Superior temporal gyrus, anterior division_L		−56	−4	−8
79	179	Job19	Superior temporal gyrus, posterior division_L		−61	−27	2
80	180	Job08,09	Superior temporal gyrus, posterior division_R		60	−23	2
81	181	Job17,18	Middle temporal gyrus, anterior division_L		−58	−4	−22
82	184	Job03	Middle temporal gyrus, posterior division_R		61	−22	−13
83	186	Job06	Middle temporal gyrus, temporooccipital part_R		58	−49	2
84	187	Job10	Inferior temporal gyrus, anterior division_L		−48	−5	−39
85	189	Job04,07,15	Inferior temporal gyrus, posterior division_L		−54	−29	−26
86	192	Job19	Inferior temporal gyrus, temporooccipital part_R		54	−50	−17
87	196	Job16,19	Superior parietal lobule_R		29	−48	59
88	197	Job08,11,13	Supramarginal gyrus, anterior division_L		−57	−33	37
89	198	Job11	Supramarginal gyrus, anterior division_R		59	−27	38
90	201	Job07,13,14	Angular gyrus_L		−50	−56	30
91	202	Job04,10	Angular gyrus_R		52	−52	32
92	203	Job08	Lateral occipital cortex, superior division_L		−32	−73	38
93	205	Job11	Lateral occipital cortex, inferior division_L		−45	−76	−2
94	206	Job09,16	Lateral occipital cortex, inferior division_R		46	−74	−2
95	207	Job12,14	Intracalcarine cortex_L		−10	−75	8
96	211	Job05,06	Juxtapositional lobule cortex (formerly supplementary motor cortex)_L		−6	−3	56
97	212	Job05,06	Juxtapositional lobule cortex (formerly supplementary motor cortex)_R		6	−3	58
98	215	Job15	Paracingulate gyrus_L		−6	37	21
99	217	Job02	Cingulate gyrus, anterior division_L		−5	18	25
100	221	Job13,15	Precuneous cortex_L		−8	−60	37
101	222	Job02,11,13,15	Precuneous cortex_R		9	−58	39

(Continues)

TABLE 2 (Continued)

#	ROI numbers in 19 networks	ROI-belonging job network	Brain region	Brodmann	MNI coordinates x	y	z
102	223	Job04,12,16	Cuneal cortex_L		−8	−80	27
103	226	Job15	Frontal orbital cortex_R		29	23	−16
104	227	Job14	Parahippocampal gyrus, anterior division_L		−22	−9	−30
105	228	Job03	Parahippocampal gyrus, anterior division_R		22	−8	−30
106	230	Jon07	Parahippocampal gyrus, posterior division_R		23	−30	−17
107	231	Job16	Lingual gyrus_L		−13	−65	−5
108	236	Job03	Temporal fusiform cortex, posterior division_R		36	−24	−28
109	237	Job07	Temporal occipital fusiform cortex_L		−34	−54	−16
110	241	Job02,05	Frontal operculum cortex_L		−40	18	5
111	242	Job02,06	Frontal operculum cortex_R		41	19	5
112	243	Job05	Central opercular cortex_L		−48	−8	12
113	244	Job05	Central opercular cortex_R		49	−6	11
114	246	Job19	Parietal operculum cortex_R		49	−27	21
115	247	Job07,08,14	Planum polare_L		−47	−6	−7
116	251	Job19	Planum temporale_L		−53	−30	11
117	253	Job12	Supracalcarine cortex_L		−10	−72	15
118	257	Job07	Brain stem		−7	−31	−34
119	258	Job14	Brain stem		8	−31	−34
120	261	Job03	Caudate		−13	9	10
121	270	Job14	Amygdala		23	−4	−18

In addition, the evaluation of professionals in each job division and measurements of longitudinal changes in vocational aptitudes on the way to becoming a professional will be needed for the further development of our approach.

Another thing we have to consider in relation to our results is the distribution of the population of the training data set, because the functional networks and classifiers for vocational aptitudes were constructed using information about the variance among the

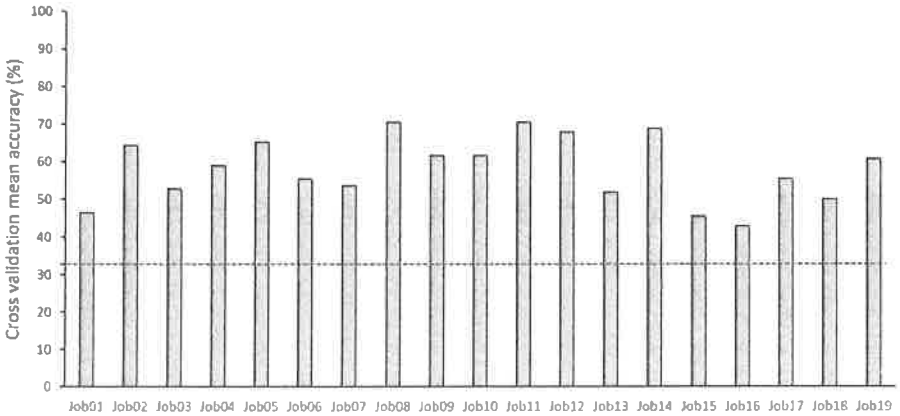


FIGURE 4 Training accuracies of the 19 multiclass classifiers. The training accuracies using 112 participants were acquired by the 10-fold cross-validation method. Accuracies for all 19 classifiers were better than chance (defined here as 33.3%)

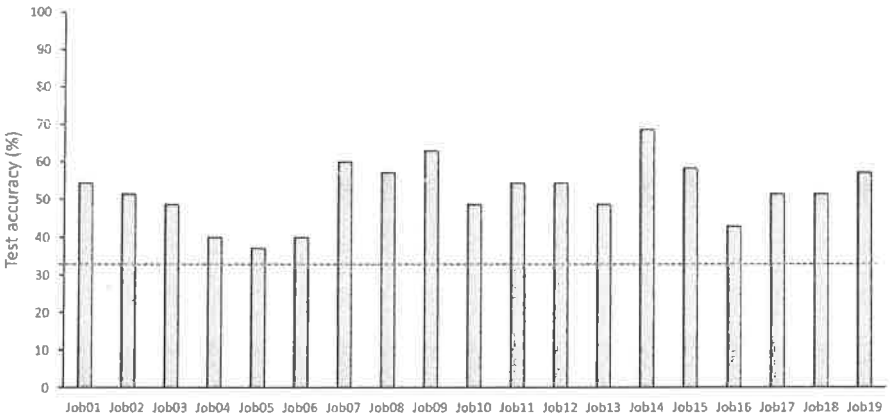


FIGURE 5 Test accuracies of the classifiers. The classifiers were tested for 35 participants whose data were not used in the training. Accuracy was determined by comparing the VA levels estimated by the classifiers and those measured by GATB. Accuracies for all 19 classifiers were better than chance

participants. For some job divisions, the distribution of the 112-participant training sample explains just over half of the distribution of the original population of Japan, as seen in Figure 1c, which may limit the external validity of our functional networks and classifiers. To devise a way to control data sets to have similar variance as the original population would be another aim for our future study, alongside the efforts for the improvement of classifier quality.

Taken together, our results demonstrate that vocational aptitudes are intrinsically represented in the brain and that we can assess them by measuring brain function. We were able to identify functional networks that reflected GATB job divisions and design classifiers that corresponded to these networks.

TABLE 3 Sensitivity (Sen) and specificity (Spe) of the classifiers of the 19 job divisions for the test group

Job divisions	Sen	Spe
Job01	35.10	69.30
Job02	35.20	63.20
Job03	32.00	65.60
Job04	32.00	65.50
Job05	32.10	65.70
Job06	30.00	65.20
Job07	34.30	71.40
Job08	42.00	75.00
Job09	33.30	66.70
Job10	41.00	75.30
Job11	33.50	67.30
Job12	32.40	63.30
Job13	37.70	74.20
Job14	31.00	64.40
Job15	35.50	73.40
Job16	60.70	76.40
Job17	31.40	67.00
Job18	28.90	70.60
Job19	41.20	71.10

TABLE 4 Ratio of mispredicted classes that actually belonged to the opposite classes (Opp) [%]

Job divisions	Opp
Job01	2.80
Job02	0.00
Job03	0.00
Job04	0.00
Job05	0.00
Job06	8.50
Job07	8.50
Job08	5.70
Job09	0.00
Job10	8.50
Job11	2.80
Job12	0.00
Job13	8.50
Job14	0.00
Job15	5.70
Job16	5.70
Job17	8.50
Job18	8.50
Job19	0.00

5 | CONCLUSIONS

We found that the vocational aptitudes are represented intrinsically in the brain and that they can be measured by fMRI. We also designed classifiers that can estimate vocational aptitudes. The evaluation of vocational aptitudes by brain function will allow us to make objective assessment of job aptitudes and follow the development of these aptitudes with training or learning, both of which will be useful in assisting with career development.

ACKNOWLEDGMENT

This study was supported by the MEXT-Supported program for the Strategic Research Foundation at Private Universities, 2014–2018.

ORCID

Uk-Su Choi http://orcid.org/0000-0001-6698-0898

REFERENCES

Aimone, J. B., Wiles, J., & Gage, F. H. (2009). Computational influence of adult neurogenesis on memory encoding. *Neuron*, *61*(2), 187–202.

Albert, N. B., Robertson, E. M., & Miall, R. C. (2009). The resting human brain and motor learning. *Current Biology*, *19*(12), 1023–1027.

Andrew, D. M., Paterson, D. G., & Longstaff, H. P. (1979). *Minnesota clerical test manual*, 2nd ed. San Antonio, TX: The Psychological Corporation.

Baldassarre, A., Lewis, C. M., Committeri, G., Snyder, A. Z., Romani, G. L., & Corbetta, M. (2012). Individual variability in functional connectivity predicts performance of a perceptual task. *Proceedings of the National Academy of Sciences of the United States of America*, *109*(9), 3516–3521.

Barrick, M. R., Mount, M. K., & Strauss, J. P. (1993). Conscientiousness and performance of sales representatives: Test of the mediating effects of goal setting. *Journal of Applied Psychology*, *78*(5), 715.

Bennett, G. K., Seashore, H. G., & Wesman, A. G. (1974). *Manual for the differential aptitude test*, 5th ed. New York, NY: Psychological Corporation.

Bermudez, P., & Zatorre, R. J. (2005). Differences in gray matter between musicians and nonmusicians. *Annals of the New York Academy of Sciences*, *1060*, 395–399.

Brown, S. D., & Lent, R. W. (1996). A social cognitive framework for career choice counseling. *Career Development Quarterly*, *44*(4), 354–366.

Burgaleta, M., MacDonald, P. A., Martínez, K., Roman, F. J., Álvarez-Linera, J., González, A. R., … Colom, R. (2014). Subcortical regional morphology correlates with fluid and spatial intelligence. *Human Brain Mapping*, *35*(5), 1957–1968.

Chan, D. (1997). Racial subgroup differences in predictive validity perceptions on personality and cognitive ability tests. *Journal of Applied Psychology*, *82*(2), 311.

Chao-Gan, Y., & Yu-Feng, Z. (2010). DPARSF: A MATLAB toolbox for "pipeline" data analysis of resting-state fMRI. *Frontiers in System Neuroscience*, *4*.

Choi, U.-S., Sung, Y.-W., Hong, S., Chung, J.-Y., & Ogawa, S. (2015). Structural and functional plasticity specific to musical training with wind instruments. *Frontiers in Human Neuroscience*, *9*.

Colom, R., Jung, R. E., & Haier, R. J. (2006). Distributed brain sites for the g-factor of intelligence. *NeuroImage*, *31*(3), 1359–1365.

Decety, J., & Michalska, K. J. (2010). Neurodevelopmental changes in the circuits underlying empathy and sympathy from childhood to adulthood. *Developmental Science*, *13*(6), 886–899.

Deng, W., Saxe, M. D., Gallina, I. S., & Gage, F. H. (2009). Adult-born hippocampal dentate granule cells undergoing maturation modulate learning and memory in the brain. *Journal of Neuroscience*, *29*(43), 13532–13542.

Desikan, R. S., Segonne, F., Fischl, B., Quinn, B. T., Dickerson, B. C., Blacker, D., … Killiany, R. J. (2006). An automated labeling system for subdividing the human cerebral cortex on MRI scans into gyral based regions of interest. *NeuroImage*, *31*(3), 968–980.

Dong, M., Li, J., Shi, X., Gao, S., Fu, S., Liu, Z., … Tian, J. (2015). Altered baseline brain activity in experts measured by amplitude of low frequency fluctuations (ALFF): A resting state fMRI study using expertise model of acupuncturists. *Frontiers in Human Neuroscience*, *9*,

Dong, W. K., & Greenough, W. T. (2004). Plasticity of nonneuronal brain tissue: Roles in developmental disorders. *Mental Retardation and Developmental Disabilities Research Reviews*, *10*(2), 85–90.

Dosenbach, N. U., Nardos, B., Cohen, A. L., Fair, D. A., Power, J. D., Church, J. A., … Lessov-Schlaggar, C. N. (2010). Prediction of individual brain maturity using fMRI. *Science (New York, N.Y.)*, *329*(5997), 1358–1361.

Draganski, B., Gaser, C., Kempermann, G., Kuhn, H. G., Winkler, J., Büchel, C., & May, A. (2006). Temporal and spatial dynamics of brain structure changes during extensive learning. *Journal of Neuroscience*, *26*(23), 6314–6317.

Employment Security Bureau, Ministry of Health, Labour and Welfare (2013). *Kousei Roudoushou Hen Ippan Shokugyou Tekisei Kensa Tebiki Shinro Shidou Syokugyou Shidou You Kaitei 2 Han* (The manual of Japanese version of general aptitude test battery revised 2nd edition). Tokyo: Employment Research Corporation.

Fan, F., Zhu, C., Chen, H., Qin, W., Ji, X., Wang, L., … Yu, C. (2013). Dynamic brain structural changes after left hemisphere subcortical stroke. *Human Brain Mapping*, *34*(8), 1872–1881.

Frey, M. C., & Detterman, D. K. (2004). Scholastic Assessment or g? The Relationship Between the Scholastic Assessment Test and General Cognitive Ability. *Psychological Science*, *15*(6), 373–378.

Golestani, N., Paus, T., & Zatorre, R. J. (2002). Anatomical correlates of learning novel speech sounds. *Neuron*, *35*(5), 997–1010.

Gottfredson, L. S. (1998). *The general intelligence factor*. Scientific American, Incorporated.

Gottfredson, L. S. (2003). The challenge and promise of cognitive career assessment. *Journal of Career Assessment*, *11*(2), 115–135.

Guerra-Carrillo, B., Mackey, A. P., & Bunge, S. A. (2014). Resting-state fMRI: A window into human brain plasticity. *Neuroscientist*, *20*(5), 522–533.

Hackman, D. A., & Farah, M. J. (2009). Socioeconomic status and the developing brain. *Trends in Cognitive Sciences*, *13*(2), 65–73.

Haier, R. J., Jung, R. E., Yeo, R. A., Head, K., & Alkire, M. T. (2004). Structural brain variation and general intelligence. *NeuroImage*, *23*(1), 425–433.

Hunter, J. E. (1986). Cognitive ability, cognitive aptitudes, job knowledge, and job performance. *Journal of Vocational Behavior*, *29*(3), 340–362.

Jung, R. E., Wertz, C. J., Meadows, C. A., Ryman, S. G., Vakhtin, A. A., & Flores, R. A. (2015). Quantity yields quality when it comes to creativity: A brain and behavioral test of the equal-odds rule. *Frontiers in Psychology*, *6*,

Kwallek, N., Lewis, C. M., Lin-Hsiao, J. W. D., & Woodson, H. (1996). Effects of nine monochromatic office interior colors on clerical tasks and worker mood. *Color Research & Application*, *21*(6), 448–458.

Legree, P. J. (1995). Evidence for an oblique social intelligence factor established with a Likert-based testing procedure. *Intelligence*, *21*(3), 247–266.

Lent, R. W., Brown, S. D., & Hackett, G. (1994). Toward a unifying social cognitive theory of career and academic interest, choice, and performance. *Journal of Vocational Behavior*, *45*(1), 79–122.

MacDonald, P. A., Ganjavi, H., Collins, D. L., Evans, A. C., & Karama, S. (2014). Investigating the relation between striatal volume and IQ. *Brain Imaging and Behavior*, *8*(1), 52–59.

Maguire, E. A., Woollett, K., & Spiers, H. J. (2006). London taxi drivers and bus drivers: A structural MRI and neuropsychological analysis. *Hippocampus*, *16*(12), 1091–1101.

May, A. (2011). Experience-dependent structural plasticity in the adult human brain. *Trends in Cognitive Sciences*, *15*(10), 475–482.

McClearn, G. E., Johansson, B., Berg, S., Pedersen, N. L., Ahern, F., Petrill, S. A., & Plomin, R. (1997). Substantial genetic influence on cognitive abilities in twins 80 or more years old. *Science (New York, N.Y.)*, *276* (5318), 1560–1563.

McGee, M. G. (1979). Human spatial abilities: Psychometric studies and environmental, genetic, hormonal, and neurological influences. *Psychological Bulletin*, *86*(5), 889.

Muroyama, H. (2016). *Shokugyo Nouryoku no Hyouka: GATB wo Mochiita 13 Nenkan no Data no Kentou. (The assessment of vocational aptitudes using the GATB date for 13 years. JILPT Reference (Shiryo) Series No.169.)* Tokyo: The Japan Institute for Labour Policy and Training.

Nasrallah, F. A., To, X. V., Chen, D.-Y., Routtenberg, A., & Chuang, K.-H. (2016). Functional connectivity MRI tracks memory networks after maze learning in rodents. *NeuroImage*, *127*, 196–202.

Ogawa, S., Lee, T.-M., Kay, A. R., & Tank, D. W. (1990). Brain magnetic resonance imaging with contrast dependent on blood oxygenation. *Proceedings of the National Academy of Sciences of the United States of America*, *87*(24), 9868–9872.

Pereira, A. C., Huddleston, D. E., Brickman, A. M., Sosunov, A. A., Hen, R., McKhann, G. M., … Small, S. A. (2007). An in vivo correlate of exercise-induced neurogenesis in the adult dentate gyrus. *Proceedings of the National Academy of Sciences*, *104*(13), 5638–5643.

Plomin, R., Owen, M. J., & McGuffin, P. (1994). The genetic basis of complex human behaviors. *Science (New York, N.Y.)*, *264*(5166), 1733.

Rhyu, I. J., Bytheway, J. A., Kohler, S. J., Lange, H., Lee, K. J., Boklewski, J., … Greenough, W. T. (2010). Effects of aerobic exercise training on cognitive function and cortical vascularity in monkeys. *Neuroscience*, *167*(4), 1239–1248.

Rjosk, V., Lepsien, J., Kaminski, E., Hoff, M., Sehm, B., Steele, C. J., … Ragert, P. (2017). Neural correlates of mirror visual feedback-induced performance improvements: A resting-state fMRI study. *Frontiers in Human Neuroscience*, *11*,

Royle, N. A., Booth, T., Hernández, M. C. V., Penke, L., Murray, C., Gow, A. J., … Deary, I. J. (2013). Estimated maximal and current brain volume predict cognitive ability in old age. *Neurobiology of Aging*, *34*(12), 2726–2733.

Sidarta, A., Vahdat, S., Bernardi, N. F., & Ostry, D. J. (2016). Somatic and reinforcement-based plasticity in the initial stages of human motor learning. *Journal of Neuroscience*, *36*(46), 11682–11692.

Shokugyou Tekisei Kensa Kenkyukai (Vocational aptitude test research corporation) (2011). *Kousei Roudoushou Hen Ippan Shokugyou Tekisei Kensa Tebiki Shinro Shidou Syokugyou Shidou You Q & A Syuu. (The Japanese version of general aptitude test battery for career and vocational guidance Q & A.)* Tokyo: Employment Research Corporation.

Teipel, S. J., Bokde, A. L., Meindl, T., Amaro, E., Soldner, J., Reiser, M. F., … Hampel, H. (2010). White matter microstructure underlying default mode network connectivity in the human brain. *NeuroImage*, *49*(3), 2021–2032.

Thompson, P. M., Cannon, T. D., Narr, K. L., Van Erp, T., Poutanen, V.-P., Huttunen, M., … Khaledy, M. (2001). Genetic influences on brain structure. *Nature Neuroscience*, *4*(12), 1253.

Tremblay, M.-È., Lowery, R. L., & Majewska, A. K. (2010). Microglial interactions with synapses are modulated by visual experience. *PLoS Biology*, *8*(11), e1000527.

Turkheimer, E., Haley, A., Waldron, M., D'Onofrio, B., & Gottesman, I. I. (2003). Socioeconomic status modifies heritability of IQ in young children. *Psychological Science*, *14*(6), 623–628.

United States Department of Defense (1984). *Test manual for the armed services vocational aptitude battery*. North Chicago, IL: U.S. Military Entrance Processing Command.

United States Department of Labor (1970). *Manual for the USES general aptitude test battery section III: Development*. Washington, DC: Government Printing Office.

Voss, H. U., & Schiff, N. D. (2009). MRI of neuronal network structure, function, and plasticity. *Progress in Brain Research*, *175*, 483–496.

Wang, S., Wang, G., Lv, H., Wu, R., Zhao, J., & Guo, W. (2016). Abnormal regional homogeneity as potential imaging biomarker for psychosis risk syndrome: A resting-state fMRI study and support vector machine analysis. *Scientific Reports*, *6*(1), http://www.ncbi.nlm.nih.gov/pmc/articles/PMC4897690/.

Wonderlic, E. F. (1983). *Wonderlic personnel test manual*. Northfield, IL: Wonderlic EF and Associates, INC.

Yahata, N., Morimoto, J., Hashimoto, R., Lisi, G., Shibata, K., Kawakubo, Y., … Kawato, M. (2016). A small number of abnormal brain connections predicts adult autism spectrum disorder. *Nature Communications*, *7*, 11254. https://doi.org/10.1038/ncomms11254.

Yan, C.-G., Wang, X.-D., Zuo, X.-N., & Zang, Y.-F. (2016). DPABI: Data processing & analysis for (resting-state) brain imaging. *Neuroinformatics*, *14*(3), 339–351.

Yang, C.-C., Barrós-Loscertales, A., Pinazo, D., Ventura-Campos, N., Borchardt, V., Bustamante, J.-C., … Ávila, C. (2016). State and training effects of mindfulness meditation on brain networks reflect neuronal mechanisms of its antidepressant effect. *Neural Plasticity*, *2016*, 1.

Yurgelun-Todd, D. A., Killgore, W. D., & Cintron, C. B. (2003). Cognitive correlates of medial temporal lobe development across adolescence: A magnetic resonance imaging study. *Perceptual and Motor Skills*, *96* (1), 3–17.

Zalesky, A., Fornito, A., & Bullmore, E. T. (2010). Network-based statistic: Identifying differences in brain networks. *NeuroImage*, *53*(4), 1197–1207.

SUPPORTING INFORMATION

Additional Supporting Information may be found online in the supporting information tab for this article.

How to cite this article: Sung Y-W, Kawachi Y, Choi U-S, et al. Estimation of vocational aptitudes using functional brain networks. *Hum Brain Mapp*. 2018;00:1–16. https://doi.org/10.1002/hbm.24200

frontiers in Neuroscience

ORIGINAL RESEARCH
published: 14 March 2018
doi: 10.3389/fnins.2018.00149

A Set of Functional Brain Networks for the Comprehensive Evaluation of Human Characteristics

Yul-Wan Sung[1], Yousuke Kawachi[1], Uk-Su Choi[2], Daehun Kang[1], Chihiro Abe[1], Yuki Otomo[1] and Seiji Ogawa[1]*

[1] *Kansei Fukushi Research Institute, Tohoku Fukushi University, Sendai, Japan,* [2] *Neuroscience Research Institute, Gachon University, Incheon, South Korea*

Many human characteristics must be evaluated to comprehensively understand an individual, and measurements of the corresponding cognition/behavior are required. Brain imaging by functional MRI (fMRI) has been widely used to examine brain function related to human cognition/behavior. However, few aspects of cognition/behavior of individuals or experimental groups can be examined through task-based fMRI. Recently, resting state fMRI (rs-fMRI) signals have been shown to represent functional infrastructure in the brain that is highly involved in processing information related to cognition/behavior. Using rs-fMRI may allow diverse information about the brain through a single MRI scan to be obtained, as rs-fMRI does not require stimulus tasks. In this study, we attempted to identify a set of functional networks representing cognition/behavior that are related to a wide variety of human characteristics and to evaluate these characteristics using rs-fMRI data. If possible, these findings would support the potential of rs-fMRI to provide diverse information about the brain. We used resting-state fMRI and a set of 130 psychometric parameters that cover most human characteristics, including those related to intelligence and emotional quotients and social ability/skill. We identified 163 brain regions by VBM analysis using regression analysis with 130 psychometric parameters. Next, using a 163 × 163 correlation matrix, we identified functional networks related to 111 of the 130 psychometric parameters. Finally, we made an 8-class support vector machine classifiers corresponding to these 111 functional networks. Our results demonstrate that rs-fMRI signals contain intrinsic information about brain function related to cognition/behaviors and that this set of 111 networks/classifiers can be used to comprehensively evaluate human characteristics.

Keywords: resting-state fMRI, functional network, neuronal plasticity, human characteristics, psychometric parameters

OPEN ACCESS

Edited by:
Bertrand Thirion,
Institut National de Recherche en Informatique et en Automatique (INRIA), France

Reviewed by:
Kaiming Li,
Sichuan University, China
Darya Chyzhyk,
Inria Saclay - Île-de-France Research Centre, France

****Correspondence:***
Yul-Wan Sung
sung@tfu-mail.tfu.ac.jp;
sungstone@gmail.com

Specialty section:
This article was submitted to Brain Imaging Methods, a section of the journal Frontiers in Neuroscience

Received: *04 September 2017*
Accepted: *26 February 2018*
Published: *14 March 2018*

Citation:
Sung Y-W, Kawachi Y, Choi U-S, Kang D, Abe C, Otomo Y and Ogawa S (2018) A Set of Functional Brain Networks for the Comprehensive Evaluation of Human Characteristics. Front. Neurosci. 12:149. doi: 10.3389/fnins.2018.00149

INTRODUCTION

Humans exhibit diverse characteristics of emotion, cognition, and behavior that describe individuals. Many different psychometric parameters from questionnaires or behavioral tasks have been developed to evaluate human characteristics of cognition/behavior (Diener et al., 1985; Raine, 1991; Carver and White, 1994; Yamauchi et al., 2009). Brain function underlies cognition/behaviors, and thus, it is possible that the characteristics of an individual can be evaluated by measuring brain function.

Functional MRI (fMRI) is the most widely used non-invasive method of measuring human brain function (Ogawa et al., 1992; Kim and Ugurbil, 1997). Measurements of human cognition/behavior by fMRI require psychometric parameters describing cognition/behavior that are embodied as tasks to induce neuronal processing in the brain (brain activation). Some psychometric parameters are easy to formalize, whereas others are not (Rupp and Zumbo, 2006). For the former type of parameters, a task can be established to evoke brain activation, and the corresponding fMRI signals of brain activation can be detected from the relevant brain areas.

Brain imaging by task-based fMRI (tb-fMRI) has provided information about the brain areas and brain networks that represent given tasks (Poldrack et al., 2013). However, most brain imaging studies have focused on specific psychometric parameters (Gauthier et al., 2000; Grill-Spector et al., 2004; Fernández-Alcántara et al., 2016; Krendl and Kensinger, 2016; Kogler et al., 2017) rather than considering a comprehensive set of psychometric parameters that can describe the diverse human characteristics of cognition/behavior. This is because it is very difficult to identify brain areas/networks responsible for the many diverse human characteristics due to limitations in task designs and time to perform tests.

In contrast to tb-fMRI, resting-state fMRI (rs-fMRI) signals come from intrinsic brain activities not designated to explicit tasks (Fransson, 2005; Fox and Raichle, 2007), and thus, there is no information to link a measured rs-fMRI signal with a specific brain function. However, functional networks produced from the correlation of rs-fMRI signals with certain brain areas, such as the default mode network, are known to represent various aspects of brain function (Greicius et al., 2004; Mason et al., 2007). Recent studies have further shown that task performance can be estimated by brain networks identified by rs-fMRI (Tavor et al., 2016; Craig et al., 2017; Song et al., 2017). In addition, some studies have proven that brain areas or functional connectivity in a rs-fMRI network are correlated with the scores of an explicit task used to identify functional areas by tb-fMRI (Finn et al., 2015; Meskaldji et al., 2016). These previous studies suggested that rs-fMRI signals can be used to identify brain networks that represent sensory and higher-order cognitive function or higher-order social function (Finn et al., 2015; Lei et al., 2017; Yang et al., 2017). That is, rs-fMRI signals may represent functional infrastructures for processing information in the brain that is highly involved in the brain function related to cognition/behavior. These characteristics of rs-fMRI may allow diverse information about the brain to be obtained from rs-fMRI signals acquired during a single MRI scan if appropriate supporting information is provided that can explain the characteristics of rs-fMRI signals or the correlation between brain areas based on the signals.

Using behavioral data about psychometric parameters as the supporting information, we attempted to test whether functional networks of the brain could be identified by rs-fMRI signals and psychological parameters (**Figure 1**). Recently some studies have shown that it is possible to decode brain states from fMRI responses using machine learning algorithms, such as a support

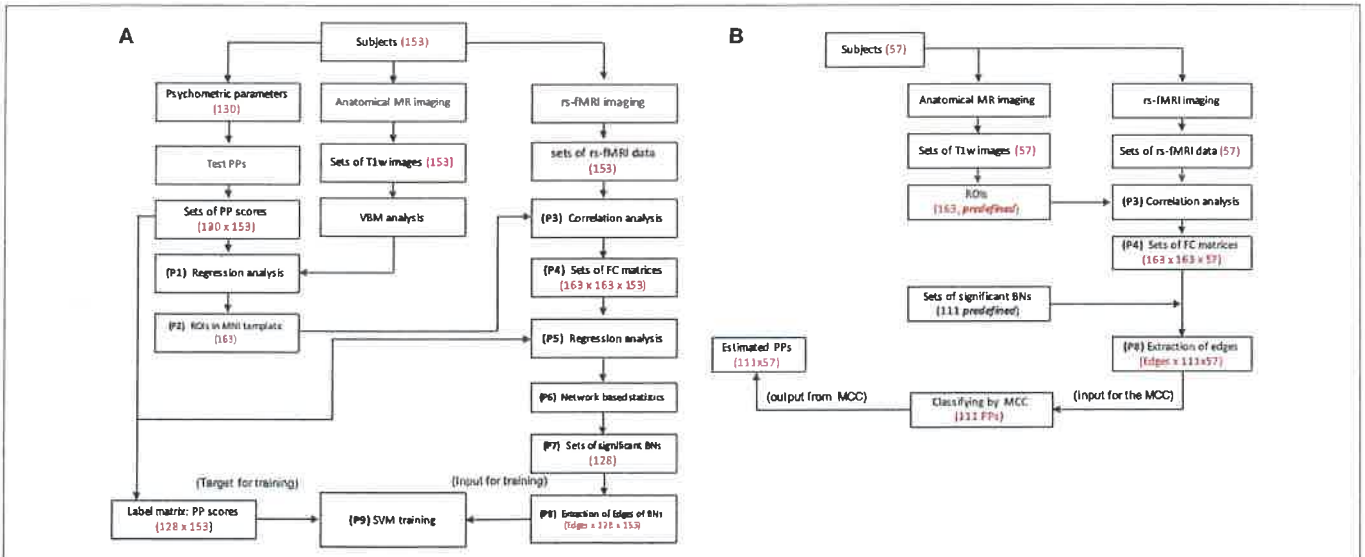


FIGURE 1 | Procedure for MRI data processing. P1, P2, etc., stand for processing steps. **(A)** Diagrams of data flow for the primary experiment. Brain areas are identified by psychometric parameters and MRI data by regression analysis (P1, P2). fMRI signals are extracted from the ROIs, and the correlation matrix is constructed (P3, P4). Regression analysis and network based statistics (NBS) analysis were performed for the correlation matrices of 153 subjects (134 for IQ and 123 for EQ), and significant brain networks are identified (P5, P6, P8). Inputs to the SVM classifiers are determined from the edges of the identified functional networks (P7, P8). Scores of psychometric parameters are estimated by classifiers and compared with psychologically measured scores to calculate accuracy. Numbers and letters in the parenthesis stand for specific information obtained after the processing at each step. PP, psychometric parameter; SVM, support vector machine; rs-Fmri, resting-state functional MRI; FC, functional connectivity; BN, brain network; MCC, multiple class classifiers; T1w, T1 weighted. **(B)** Diagrams of data flow for the supplementary experiment. Bypassing the regression analyses used during training, fMRI signals are extracted from the ROIs, and the edges of functional networks are calculated (P3, P4, P8) for input into the SVM classifiers (P9). Scores of psychometric parameters are estimated by the classifiers.

TABLE 1 | List of psychometric parameters.

	Parameters
1	Cognitive competence
2	Extracurricular competence including physical competence
3	Social competence with friends of the same sex
4	Social competence with friends of opposite sex
5	General self-worth
6	**Perceived competence scale for adolescence**
7	Inhibitory control
8	Activation control
9	Attentional control
10	**Japanese version of Effortful Control (EC) scale for adults**
11	Trust vs. mistrust
12	Autonomy vs. shame/doubt
13	Initiative vs. guilt
14	Industry vs. inferiority
15	Identity vs. role confusion
16	Intimacy vs. isolation
17	**Japanese version of Rasmussen's Ego Identity Scale (REIS)**
18	Behavioral inhibition system (BIS)
19	BAS/driver
20	BAS/reward
21	BAS/fun seeking
22	**Behavioral Inhibitory System (BIS)/Behavioral Activate System (BAS) scale**
23	**Rosenberg Self Esteem Scale (RSES)**
24	Anxiety regarding others' evaluation of oneself and perceived maladjustment to interpersonal situations
25	Emotional disturbance
26	Difficulty in expressing opinions
27	**Japanese version of Jones and Russell's social reticence scale for college students**
28	Beginning social skills
29	Advanced social skills
30	Skills for dealing with feelings
31	Skill alternatives to aggression
32	Skills for dealing with stress
33	Planning skills
34	**Kikuchi's Scale of Social Skills (KiSS-18)**
35	Public self-consciousness
36	Private self-consciousness
37	**Self-consciousness scale for Japanese**
38	**Japanese version of the Self-Concept Clarity (SCC) scale**
39	Self-continuity function subscale
40	Directing-behavior function subscale
41	Social-bonding function subscale
42	**Japanese version of the TALE (Thinking About Life Experiences) scale**
43	**Japanese version of the Ego-Resiliency Scale (ER89)**
44	Positive Problem Orientation (PPO)
45	Negative Problem Orientation (NPO)
46	Problem Definition and Formulation (PDF)
47	Generation of Alternative Solution (GAS)
48	Decision Making (DM)
49	Solution Implementation and Verification (SIV)
50	Rational Problem Solving (RPS)
51	Impulsivity/Carelessness Style (ICS)
52	Avoidance Style (AS)
53	**Japanese version of the Social Problem-Solving Inventory-Revised (SPSI-R)**
54	Negative-Self (NS)
55	Positive-Self (PS)
56	Negative-Other (NO)
57	Positive-Other (PO)
58	**Japanese version of the Brief Core Schema Scale (JBCSS)**
59	Intentional behavior
60	Planfulness
61	Readiness for change
62	Using resource
63	**Japanese version of the Personal Growth Initiative Scale-II (PGIS-II)**
64	**Subjective Happiness Scale (SHS)**
65	**The Satisfaction with Life Scale (SWLS)**
66	State Anxiety (A-State)
67	Trait Anxiety (A-Trait)
68	**Japanese edition of state-trait anxiety inventory**
69	Positive symptoms
70	Negative symptoms
71	Disorganization
72	**Schizotypal Personality Questionnaire (SPQ)**
73	Social skill
74	Attention switching
75	Attention to detail
76	Communication
77	Imagination
78	**Autism-spectrum quotient**
79	**Verbal Intelligence Quotient (VIQ)**
80	**Performance Intelligence Quotient (PIQ)**
81	**Full scale Intelligence Quotient (FIQ)**
82	**Fluid intelligence**
83	**Crystallized intelligence**
84	Verbal comprehension
85	Perceptual organization
86	Vocabulary
87	Similarities
88	Arithmetic
89	Digit span
90	Information
91	Comprehension
92	Picture completion
93	Digit symbol
94	Block design
95	Matrix reasoning
96	Picture arrangement

(Continued)

TABLE 1 | Continued

	Parameters
97	Emotional awareness
98	Self-efficacy
99	Perseverance
100	Enthusiasm
101	Self-decision
102	Impulse control
103	Patience
104	Sharing positive emotion
105	Sharing negative emotion
106	Personal consideration
107	Voluntary support
108	Personal management
109	Sociability
110	Cooperation
111	Decision making
112	Optimism
113	Group consideration
114	Influence
115	Risk management
116	Tactfulness
117	Adaptability
118	**Self-awareness**
119	**Self-motivation**
120	**Self-control**
121	**Empathy**
122	**Altruism**
123	**Interpersonal relationship**
124	**Situational awareness**
125	**Leadership**
126	**Flexibility**
127	**Intrapersonal Emotional Quotient Scale (EQS)**
128	**Interpersonal (EQS)**
129	**Situational (EQS)**
130	**EQS total scale**

Social ability/skill: 1-78, IQ: 79-96, EQ: 97-130.

vector machine (Guo et al., 2015; Altmann et al., 2016; Hu et al., 2017; Zafar et al., 2017). To verify that the functional networks identified represent the corresponding psychological parameters, and also to evaluate human characteristics from the rs-fMRI signals, we used a support vector machine (SVM).

We attempted to derive a specific SVM classifier related to each identified functional network. Second, we aimed to identify a set of functional networks of the brain to comprehensively evaluate human characteristics (**Figure 1**). For this purpose, we prepared a set of 130 psychometric parameters (**Table 1**; Supplementary References), including those related to intelligence quotient (IQ), emotional quotient (EQ), and social ability/skill that can explain the most conceivable aspects of human cognition/behavior by which an individual can be described.

MATERIALS AND METHODS

The experiments in this study comprised a primary experiment and a supplementary experiment. The primary experiment was designed to identify functional networks and to design the SVM classifiers. The supplementary experiment was performed to test the SVM classifiers developed in the primary experiment.

Measurements of Psychometric Parameters

In the primary experiment, psychometric parameters were measured on three separate days: one day for the Wechsler Adult Intelligence Scale (WAIS; a measure of IQ), one day for the Emotional Quotient Scale (EQS) (Uchiyama et al., 2001), and one day for the other psychometric parameters including those related to social ability/skill. The psychometric parameters related to IQ consisted of 11 subset scores, 5 IQ scores, and 2 sub-indices derived from the subset scores. The psychometric parameters related to EQS consisted of 21 sub-factors, 12 major factors derived from the sub-factors, and a total score. The other psychometric parameters consisted of 59 sub-factors and 19 major factors, some of which were derived from the sub-factors. The parameters are listed in **Table 1**. Major scores and factors appear in bold type. The total number of parameters including major parameters and sub-parameters was 130. To the best of our knowledge, the number of parameters in this study is greater than in any previous psychological study. This set of 130 parameters covers most conceivable human characteristics and is considered to provide sufficient information to complete a comprehensive evaluation of human characteristics, therefore, all 130 parameters were used for the identification of functional networks.

MRI Measurements

For both the primary experiment and the supplementary experiment, each subject underwent an MRI using a 3-Tesla MRI scanner (Skyra-fit; Siemens Co., Erlangen, Germany). All subjects were scanned in two sessions corresponding to a structural image (T1) measurement for VBM and a functional image measurement (resting-state fMRI). Structural images were acquired using the following parameters: repetition time = 1,900 ms, echo time = 2.52 ms, matrix size = 256 × 256, in-plane resolution = 1 × 1 mm^2, slice thickness = 1 mm, and number of slices = 192. The imaging orientation was sagittal. Resting-state fMRI data were acquired using the following parameters: repetition time = 1,000 ms, echo time = 24 ms, matrix size = 64 × 64, in-plane resolution = 3.4 × 3.4 mm^2, slice thickness = 3.4 mm, and number of volumes = 480. In the resting-state fMRI session, subjects were asked to lie on the bed and not to wander their mind with their eyes open and to gently focus their eyes on the center of the visual field. The lights in the room were turned off during all MRI scans.

Participants

Primary Experiment

A group of 162 participants consisting of university freshmen and sophomores [55 males, 107 females; mean age and standard deviation (SD) 20.10 ± 0.86 years; 26 left hand, 136 right hand]

TABLE 2 | Behavioral scores of 130 psychometric parameters (mean and standard deviation).

	N	Mean	*SD*
1	153	58.38	10.40
2	153	56.70	14.66
3	153	73.22	12.25
4	153	56.55	20.05
5	153	56.90	12.00
6	153	60.16	9.49
7	153	66.71	9.19
8	153	64.31	10.45
9	153	58.48	10.66
10	153	63.07	8.23
11	153	56.52	10.08
12	153	60.33	11.32
13	153	45.61	9.88
14	153	57.34	10.67
15	153	53.84	10.33
16	153	51.52	12.06
17	153	54.07	7.82
18	153	69.56	8.21
19	153	80.72	10.30
20	153	59.97	17.37
21	153	77.61	16.35
22	153	73.24	8.27
23	153	59.43	12.00
24	153	54.17	18.22
25	153	71.53	17.56
26	153	56.14	21.67
27	153	58.61	15.17
28	153	63.09	18.37
29	153	66.10	12.82
30	153	63.05	14.43
31	153	62.53	13.33
32	153	64.92	14.59
33	153	64.58	14.40
34	153	64.05	10.74
35	153	73.36	11.74
36	153	65.16	12.04
37	153	69.45	10.02
38	153	57.31	10.42
39	153	60.87	16.47
40	153	67.58	15.26
41	153	69.35	16.33
42	153	65.51	12.63
43	153	68.43	10.48
44	153	58.10	16.82
45	153	56.06	19.76
46	153	63.17	14.36
47	153	53.69	16.09
48	153	58.99	15.68
49	153	50.82	18.65
50	153	56.67	13.09
51	153	47.57	14.03
52	153	44.72	16.73
53	153	52.09	11.44
54	153	25.41	17.65
55	153	73.67	16.07
56	153	11.47	13.51
57	153	63.94	16.52
58	153	43.62	11.00
59	153	64.35	13.66
60	153	56.49	13.34
61	153	53.35	13.42
62	153	59.66	14.68
63	153	58.27	11.03
64	153	66.34	13.87
65	153	50.16	14.18
66	153	72.17	10.21
67	152	63.15	10.08
68	152	67.63	8.93
69	153	26.31	20.39
70	153	52.70	23.65
71	153	43.90	26.40
72	153	40.70	17.61
73	153	40.13	28.42
74	153	53.79	18.74
75	153	46.14	24.31
76	153	40.13	21.18
77	153	31.90	15.93
78	153	42.42	13.50
79	137	103.90	10.06
80	137	98.79	11.60
81	137	101.77	10.08
82	137	126.73	13.77
83	137	101.36	13.80
84	137	104.18	10.30
85	137	97.94	13.82
86	137	43.60	10.01
87	137	65.89	11.17
88	137	58.90	11.66
89	137	63.92	11.14
90	137	57.80	11.80
91	137	57.49	13.25
92	137	65.33	9.98
93	137	71.10	10.66
94	137	76.60	13.60
95	137	78.66	10.78
96	137	77.87	10.92
97	123	57.18	20.34
98	123	47.09	20.72
99	123	58.54	20.37
100	123	52.98	17.89
101	123	49.73	21.76

(Continued)

TABLE 2 | Continued

	N	Mean	SD
102	123	57.52	22.77
103	123	44.11	18.44
104	123	76.08	21.63
105	123	58.74	22.28
106	123	66.02	24.48
107	123	63.41	21.33
108	123	37.74	21.53
109	123	43.63	24.05
110	123	55.56	19.84
111	123	42.07	23.59
112	123	42.07	22.55
113	123	66.19	18.98
114	123	36.31	26.53
115	123	42.41	22.86
116	123	47.15	21.89
117	123	53.59	22.66
118	123	52.13	18.82
119	123	55.76	17.52
120	123	50.45	16.42
121	123	67.41	20.41
122	123	65.72	19.59
123	123	45.64	16.62
124	123	50.11	17.51
125	123	39.36	23.08
126	123	50.37	20.81
127	123	52.45	14.82
128	123	57.60	16.26
129	123	47.12	18.36
130	123	52.39	14.61

participated in both psychometric measurements and underwent MRI as part of the primary experiment. The aim of the primary experiment was to identify functional networks and to derive the classifiers.

Supplementary Experiment

In the supplementary experiment to test the networks and classifiers obtained in the primary experiment, a group of 57 participants (10 males, 47 females; mean age and *SD* 21.97 ± 1.47 years) participated in the psychometric measurements (parameters related to social ability/skill; refer to Measurements of Psychometric Parameters) and MRI measurements.

None of the participants had a history of neurological disease or any medical condition (i.e., pregnancy, use of a cardiac pacemaker, or claustrophobia). After the participants had been provided a complete description of the study, written informed consent was obtained in accordance with the Declaration of Helsinki. This study was approved by the Institutional Review Board Tohoku Fukushi University (Japan), and all experiments were performed with the relevant guidelines and regulations of the Institutional Review Board, which approved all the experimental protocols.

MRI Data Analysis: Primary Experiment

The analysis of the primary experiment was performed through several processing steps for 153 participants after the removal of participants with motion artifacts ($n = 9$) during MRI acquisition (**Figure 1A**).

VBM Analysis

For identification of functional networks anatomical brain templates such as automated anatomical labeling (AAL) atlas (Yahata et al., 2016) have been used. To avoid partial volume effect and improve sensitivity, in this study, we tried to identify brain areas specific to psychometric parameters in each of gyri in AAL atlas. MRI data were analyzed using VBM8 (http://dbm.neuro.uni-jena.de/vbm/) implemented in the Statistical Parametric Mapping software (SPM 12; Wellcome Department of Imaging Neuroscience, London, United Kingdom), which was implemented via Matlab 2015a (MathWorks, Sherborn, MA, USA). The pre-processing by VBM8, with the default parameters used in each step, included segmentation with a bias-corrected option and spatial normalization with diffeomorphic anatomical registration using exponentiated Lie algebra (DARTEL) (Ashburner, 2007), normalization to the Montreal Neurological Institute and Hospital (MNI) coordinate system with smoothing with an 8-mm full-width at half-maximum (FWHM) filter, and modulation by Jacobian determinants, which provided segmented, normalized, and modulated gray matter images. After preprocessing, a statistical test (simple regression analysis) was used to identify brain areas correlated with each psychometric parameter (P1 and P2 of **Figure 1A**). In the regression analysis, total brain value (TBV) was used as a covariate. Our purpose was to find specific brain areas in AAL gyri we performed a small volume correction in each gyrus based on the AAL atlas to correct for multiple comparisons (Gur et al., 2000; Singh et al., 2014). The statistical threshold was set at an uncorrected $p = 0.001$ and at $p = 0.05$ for family-wise error (FWE) correction at the voxel level.

rs-fMRI Analysis

For functional MRI data, we used the data processing assistant for resting-state fMRI software (DPABI) (Chao-Gan and Yu-Feng, 2010; Yan et al., 2016) to pre-process the data of all 153 subjects. The pre-processing included slice-scan time correction, 3D motion correction (maximum head motion: 151 subjects passed the maximum threshold of 1.5 mm and 1.5°, and other two subjects passed the maximum threshold of 3.0 mm and 3°), removal of head motion effects by the Friston 24-parameter model, bandpass temporal filtering (between 0.01 and 0.1 Hz), and artifact rejection based on the CSF signal. These functional images were smoothed with a 6-mm FWHM filter and co-registered with each corresponding structural image. All resting-state functional images were analyzed by ROI-based correlation analysis for the predefined 163 ROIs identified by VBM (P3 of **Figure 1A**). In the analysis, for the time courses of the 163 ROIs,

correlations were calculated, and correlation coefficient matrices (163 × 163 × 153) were created (P4 of **Figure 1A**). A simple regression of the correlation coefficient matrices was performed with psychologically measured scores of the psychometric parameters, and then network-based statistics (NBS) were performed to identify sets of significant brain networks (i.e., a brain network for each psychometric parameter). Zalesky et al. (2010) (P6 of **Figure 1A**) to identify sets of significant brain networks (mostly a brain networks for each psychometric parameter; P7 of **Figure 1A**). In this step, randomly shuffled correlation matrices were generated for a permutation test. Then, correlational analyses were performed on the true correlation matrix with psychometric parameters, and a non-parametric permutation test was performed on random correlation matrices with 5,000 iterations. Correction for multiple comparisons based on NBS statistics was performed at an initial threshold of $p < 0.005$, and the number of edges in the network was limited to as close to 15 as possible. Previous research has shown that a small number of brain connections can predict a psychiatric disorder (Yahata et al., 2016).

SVM Analysis

Classifier Design

SVMs are typically used to identify a hyperplane that distinguishes between 2 groups. But in this study we attempted to design 8-class SVM classifiers. Behavioral scores are measured on a scale of 1–100. Our purpose is ideally to measure psychometric parameters by MRI at the same scale. However, there are several limitations such as sensitivity and number of samples. So, we reduced it to a scale of 1–10, 10 levels. But in classification study such as the neural network, the number of levels should be a power of 2. Therefore we decided to use 8 (i.e., 2^3) classes. The 8-class SVM classifier can estimate the score of a psychometric parameter from rs-fMRI data into 8 levels. Although psychometric parameter scores are linear and some regression analyses such as support vector regression can be applied, we attempted to design the SVM classifiers because a discretization is generally stable to variations and some variations would exist in fMRI and psychometric measurements.

Multiple class classification with the one-against-all (OAA) method (Bishop, 2007) was performed using LIBSVM (Chang and Lin, 2011), which was implemented in Matlab 2015a (MathWorks, Sherborn, MA, USA). The OAA method involved two steps: training a single classifier per class with one positive sample of each class and all other negative samples of the remaining classes and repeating the procedure for the total number of classes. The classifier with the highest classification score was selected as a final multi-class classifier.

Data Preparation for Training—Classification

Data sets for the SVM classifier design were prepared from the results of the brain network analysis and the psychologically measured data. The input dataset consisted of data matrices of features (P8 of **Figure 1A**) and labels (P9 of **Figure 1A**). A feature data matrix consisted of edges of a network (correlation coefficients of networks at P8 of **Figure 1A**) and a label matrix consisted of psychologically measured data (P9 of **Figure 1A**). For classification label data (the label matrix), the scores

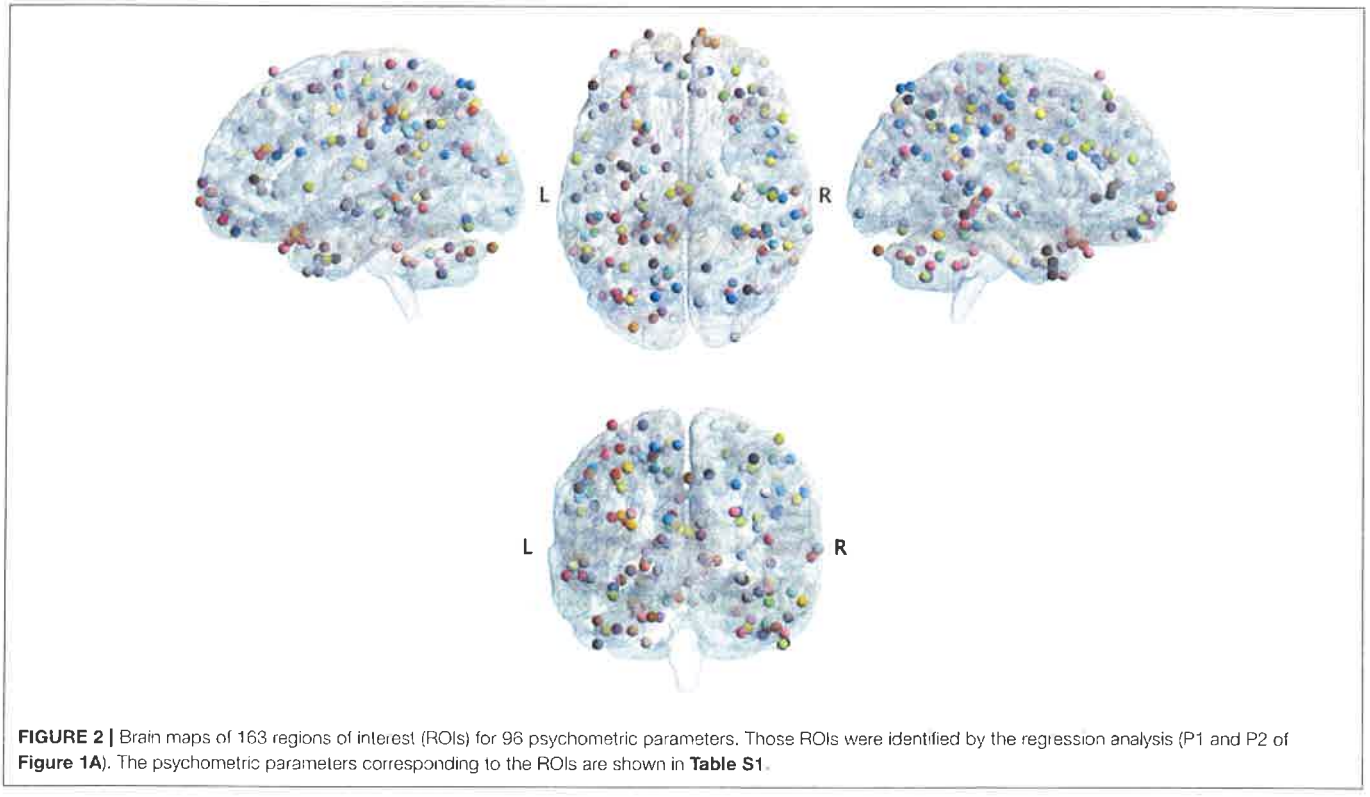


FIGURE 2 | Brain maps of 163 regions of interest (ROIs) for 96 psychometric parameters. Those ROIs were identified by the regression analysis (P1 and P2 of **Figure 1A**). The psychometric parameters corresponding to the ROIs are shown in **Table S1**.

of psychologically measured psychometric parameters were normalized and divided into eight classes by the equation {(x-min)/(max-min)} * 8, where × is the score of the psychologically measured psychometric parameter. In the calculation results, the number after the decimal point was rounded up. The dimensions of a feature matrix were the number of edges by the number of subjects, and the number of feature matrices was the number of functional networks. Therefore, the dimensions of the input data set for the SVM were the number of edges by the number of functional networks by the number of subjects (the number of edges were omitted in **Figure 1B** for simplification). The dimensions of the label matrices were the number of functional networks (scores of psychologically measured psychometric parameters rated into one of eight classes) by the number of subjects.

Training of Classifiers

With the data sets of all psychometric parameters, a leave-one-out cross validation was run using a radial basis function (RBF) kernel defined as $K(x, y) = \exp(-\gamma \| x - y \| 2)$ for optimizing the C and gamma (γ) values. In parameter optimization, the grid-search method was performed with various ranges of C and γ values ($C = 2^{-5}, 2^{-4}, \ldots, 2^{15}$, $\gamma = 2^{-15}, 2^{-14}, \ldots, 2^{15}$). After cross validation, the multiple class classifiers of the psychometric parameters with the best C and γ values were varied and deemed significant (P7 of **Figure 1A**).

Procedure for MRI Data: Supplementary Experiment

Test of Classifiers

In the supplementary experiment, the analyses were performed on 57 participants to test the classifiers. MRI data were preprocessed via the same procedures as in the primary experiment but bypassing the regression analyses in the training procedure. fMRI signals were extracted from the ROIs, the edges of the functional networks were calculated (P3, P4, P8), and inputs for the SVM classifiers were determined from the edges (P8). Scores of psychometric parameters were estimated by the trained classifiers (**Figure 1B**). The estimated scores were compared with the psychologically measured scores to calculate the accuracy.

Summary of the Data Processing Procedures

Training Procedure Figure 1A

Brain areas were identified by the psychometric parameters and the MRI data via a regressing analysis (P1, P2). From the ROIs, fMRI signals were extracted, and raw correlation matrices were constructed (P3, P4). A regression was performed and then a network-based statistics (NBS) analysis was performed, to identify significant brain networks (P5, P6, P7). The inputs for the SVM classifiers were from edges of the identified functional networks (P8). Scores for the psychometric parameters were estimated using a scale from 1 to 8 by the SVM classifiers and compared with psychologically measured scores, which were also rescaled to 8 levels, to calculate accuracy.

Test Procedure Figure 1B

Bypassing the regression analyses in the training, fMRI signals were extracted from the ROIs, and then the edges of functional networks were calculated (P3, P4, P7, P8). The extracted edges were used for the inputs for the SVM classifiers and the scores of psychometric parameters were estimated by the classifiers.

RESULTS

Psychological Data

Scores for the psychometric parameters were acquired for all 153 participants (153 for social ability, 134 for IQ, and 123 for EQ; as data were acquired over several days, IQ and EQ data could not be acquired for some participants) included in the primary experiment (see the Materials and Methods section) and are listed in the order of the MRI measurements performed. We used all 130 parameters for subsequent MRI processing to map each parameter to the brain, such that each functional network to be identified would have sufficient information to evaluate the psychometric parameters. The behavioral scores for all 130 parameters are listed in **Table 2** for the participants in the primary experiment.

Voxel-Based Morphometry

Brain areas that were significantly correlated with each psychometric parameter, reflecting a specific function of cognition/behavior related to the parameter, were identified by correlation analysis of the VBM data with the score of each psychometric parameter (P1 of **Figure 1A**). Brain areas for 96 parameters among 130 total psychometric parameters were identified by the analysis ($p = 0.05$, corrected; see section Materials and Methods for more details), which corresponded to a total of 187 brain areas, as some parameters were correlated with multiple brain areas. An ROI was defined as a 5-mm-diameter sphere around the voxel corresponding to the peak t-value in each of the 187 brain areas. Among the 187 ROIs, some ROIs overlapped with others. Therefore, the overlapping ROIs, except the first overlapping ROI in the parameter list, were removed, leaving a total of 163 remaining ROIs (P2 of **Figure 1A**). The locations of the ROIs in the brain are shown in **Figure 2**, and their coordinates are given in **Table 3**. The ROIs were distributed over the frontal, parietal, temporal, occipital, and cerebellar cortices and sub-cortices of the brain.

rs-fMRI

Functional networks were identified from the rs-fMRI time series. The rs-fMRI time series from the 163 ROIs were used to construct correlation matrices by correlation analysis (P3 of **Figure 1A**). After constructing of correlation matrices between ROIs (P4 of **Figure 1A**), a regression analysis was performed between the set of correlation matrices and the scores for the psychometric parameters to estimate statistically significant networks. Next, network-based statistics (NBS) were applied for network-based correction (P6 of **Figure 1A**). Networks were

TABLE 3 | Description of 163 regions of interest and the coordinates of the regions in MNI coordinates.

#	Region	MNI coordinates			Psychometric parameters
		x	*y*	*z*	
1	MFG_R	31	18	48	Cognitive competence
2	SFG_R	16	−7	69	Cognitive competence
3	MFG_ope_R	48	15	40	Cognitive competence
4	MFG_ope_L	−29	39	−16	Cognitive competence
5	MTG_L	−57	−37	−7	Cognitive competence
6	IPG_L	−49	−40	35	Social competence with friends of the same sex
7	PoCG_R	44	−16	56	Social competence with friends of the same sex
8	FG_R	44	−41	−21	Social competence with friends of the same sex
9	FG_L	−36	−74	−18	Social competence with friends of opposite sex
10	IPG_R	50	−46	36	General self-worth
11	PoCG_R	50	−17	49	Perceived competence scale for adolescence
12	IFG_orb_L	−38	58	−15	Inhibitory control
13	MFG_L	−29	38	20	Inhibitory control
14	MTG_R	44	−50	11	Inhibitory control
15	MTG_L	−52	−37	−8	Inhibitory control
16	MFG_L	−32	35	23	Activation control
17	MOG_L	−27	−92	18	Activation control
18	IFG_orb_L	−26	19	−22	Activation control
19	AG_L	−32	−59	37	Attentional control
20	SPG_L	−15	−66	47	Japanese version of Effortful Control (EC) scale for adults
21	MTG_R	69	−38	6	Japanese version of Effortful Control (EC) scale for adults
22	SPG_L	−15	−75	58	Trust vs. mistrust
23	SPG_L	−3	−70	59	Trust vs. mistrust
24	SMG_R	62	−30	35	Trust vs. mistrust
25	FG_R	33	−42	−19	Intimacy vs. isolation
26	Calc_L	−11	−83	11	Intimacy vs. Isolation
27	Calc_R	9	−78	13	Intimacy vs. isolation
28	MFG_L	−25	10	56	Intimacy vs. isolation
29	Hipp_L	−20	−35	−3	Japanese version of Rasmussen's Ego Identity Scale (REIS)
30	IFG_orb_R	10	70	−5	Japanese version of Rasmussen's Ego Identity Scale (REIS)
31	PrCG_R	48	−1	44	Behavioral Inhibition System (BIS)
32	SPG_L	−8	−63	45	BAS/driver
33	PrCG_R	30	−20	68	BAS/driver
34	Cu_L	−8	−61	21	BAS/reward
35	TP_Inf_R	41	6	−38	BAS/fun seeking
36	SPG_L	−21	−44	69	BAS/fun seeking
37	IPG_L	−51	−32	39	BAS/fun seeking
38	FG_R	39	−40	−16	BAS/fun seeking
39	SFG_orb_R	13	65	0	Rosenberg Self Esteem Scale (RSES)
40	Hipp_R	19	−31	0	Difficulty in expressing opinions
41	Cu_R	9	−77	19	Japanese version of Jones and Russell's social reticence scale for college students
42	PoCG_L	−37	−32	69	Beginning social skills
43	MOG_L	−37	−73	22	Beginning social skills
44	SFG_L	−21	−5	53	Advanced social skills
45	SMG_L	−54	−42	32	Advanced social skills
46	SFG_orb_R	17	64	0	Skills for dealing with feelings
47	IPG_L	−49	−33	44	Skills for dealing with feelings
48	PoCG_L	−32	31	71	Skill alternatives to aggression
49	PoCG_L	−47	−31	47	Skills for dealing with stress
50	PoCG_L	−39	−30	58	Planning skills
51	PrCG_L	−21	−20	70	Planning skills
52	Hipp_R	33	−16	−8	Planning skills
53	SMA_L	−7	−19	60	Kikuchi's Scale of Social Skills (KiSS-18)
54	IPG_R	46	−37	52	Public self-consciousness
55	SFG_L	−15	6	56	Private self-consciousness
56	TP_Mid_R	54	3	−29	Private self-consciousness
57	ACC_R	10	37	1	Private self-consciousness
58	MFG_R	31	37	48	Japanese Version of the Self-Concept Clarity (SCC) Scale
59	FG_R	44	−41	−15	Self-continuity function subscale
60	MTG_L	−60	−50	−8	Self-continuity function subscale
61	SPG_L	−12	−69	42	Directing-behavior function subscale
62	MOG_R	42	−71	35	Directing-behavior function subscale
63	SOG_L	−54	−54	37	Japanese version of the TALE (Thinking About Life Experiences) scale
64	FG_R	33	−15	−35	Decision Making (DM)
65	SPG_L	−29	−77	47	Decision Making (DM)
66	SMG_R	58	−47	31	Decision Making (DM)
67	MTG_R	66	−29	2	Impulsivity/Carelessness Style (ICS)
68	IFG_orb_R	28	22	−26	Impulsivity/Carelessness Style (ICS)
69	RectusG_L	−2	15	−19	Impulsivity/Carelessness Style (ICS)
70	IPG_L	−35	−76	44	Impulsivity/Carelessness Style (ICS)
71	IFG_orb_L	−22	16	−25	Impulsivity/Carelessness Style (ICS)
72	IFG_orb_L	−54	12	3	Avoidance Style (AS)
73	IFG_orb_L	−24	11	−27	Japanese version of the Social Problem-Solving Inventory-Revised (SPSI-R)
74	SOG_R	28	−67	25	Positive-Self (PS)

(Continued)

TABLE 3 | Continued

#	Region	MNI coordinates			Psychometric parameters
		x	*y*	*z*	
75	MFG_L	−44	29	20	Positive-Self (PS)
76	FG_L	−36	−73	−14	Positive-Self (PS)
77	Cerebellum_L	−44	−60	−43	Negative-Other (NO)
78	PCC_L	−6	−46	20	Positive-Other (PO)
79	ITG_R	61	−55	−21	Positive-Other (PO)
80	MFG_R	7	65	−7	Japanese version of the Brief Core Schema Scale (JBCSS)
81	Cerebellum_L	−21	−36	−29	Planfulness
82	Cerebellum_R	52	−59	−37	Planfulness
83	Cerebellum_R	30	−45	−37	Planfulness
84	SOG_R	26	−73	25	Planfulness
85	SOG_L	−27	−73	24	Planfulness
86	IPG_L	−40	−56	54	Planfulness
87	MFG_orb_R	44	54	−12	Readiness for change
88	MFG_R	38	39	22	Readiness for change
89	Cerebellum_R	51	−62	−43	Readiness for change
90	SFG_L	−20	18	52	Using resource
91	Cerebellum_L	−26	−41	−36	Japanese version of the Personal Growth Initiative Scale-II (PGIS-II)
92	Th_L	−2	−14	16	Subjective Happiness Scale (SHS)
93	Th_R	3	−17	14	Subjective Happiness Scale (SHS)
94	Cerebellum_R	48	−70	−34	The Satisfaction with Life Scale (SWLS)
95	Cerebellum_L	−44	−75	−31	The Satisfaction with Life Scale (SWLS)
96	Hipp_L	−32	−14	−10	The Satisfaction with Life Scale (SWLS)
97	IPG_L	−34	−39	41	State Anxiety (A-State)
98	IPG_R	35	−38	47	State Anxiety (A-State)
99	TP_Inf_L	−40	2	−36	Trait Anxiety (A-Trait)
100	Putamen_L	−27	−9	−5	Disorganization
101	MTG_L	−51	−51	−1	Disorganization
102	IFG_Med_R	3	56	−11	Disorganization
103	IFG_Tri_R	44	38	5	Disorganization
104	TP_Mid_L	−19	12	−42	Social skill
105	FG_R	31	−41	−10	Attention switching
106	IFG_Tri_L	−50	41	7	Attention switching
107	TP_Inf_R	43	6	−35	Attention switching
108	TP_Inf_R	52	6	−42	Attention switching
109	SFG_L	−19	69	5	Attention to detail
110	SFG_L	−9	−4	56	Attention to detail
111	Cerebellum_L	−12	−64	−29	Attention to detail
112	IFG_Tri_R	50	16	22	Communication
113	PrCG_R	49	3	26	Communication
114	Cerebellum_R	43	−54	−32	Imagination
115	SFG_Med	0	47	34	Imagination
116	PCC_L	−7	−44	17	Verbal IQ
117	PreCu_R	13	−59	44	Performance IQ
118	SFG_Med_R	11	48	−17	Full scale IQ
119	IFG_Med_R	5	40	−21	Full scale IQ
120	SFG_Med_L	−13	56	−5	Full scale IQ
121	PHG_L	−24	−24	−25	Full scale IQ
122	PCC_L	−7	−44	−16	Full scale IQ
123	PCC_L	−13	−43	9	Fluid intelligence
124	IFG_Tri_R	45	29	−1	Crystallized intelligence
125	SPG_L	−16	−57	53	Crystallized intelligence
126	PCC_L	−6	−38	23	Crystallized intelligence
127	TP_Sup_R	35	25	−30	Verbal comprehension
128	SFG_orb_L	−8	51	−21	Similarities
129	SFG_orb_R	14	49	−19	Similarities
130	Hipp_L	−22	−26	−11	Arithmetic
131	IFG_Tri_R	45	26	28	Arithmetic
132	PrCG_R	60	12	30	Arithmetic
133	SFG_R	22	35	54	Arithmetic
134	PrCG_L	−31	−4	64	Information
135	SMG_L	−59	−21	26	Information
136	PCC_L	−4	−42	18	Comprehension
137	SPG_L	−33	−44	57	Picture completion
138	Hipp_R	30	−39	3	Digit symbol
139	PoCG_R	55	−21	52	Digit symbol
140	SOG_R	27	−76	39	Digit symbol
141	PCC_L	−8	−43	9	Block design
142	IFG_Tri_L	−50	25	24	Matrix reasoning
143	IOG_R	29	−97	−9	Matrix reasoning
144	PoCG_R	49	−20	62	Picture arrangement
145	SMG_L	−53	−50	25	Emotional awareness
146	PoCG_R	62	−17	36	Self-efficacy
147	SMG_R	47	−40	24	Perseverance
148	Cerebellum_L	−16	−87	−29	Impulse control
149	PCC_M_L	−2	−17	32	Impulse control
150	PCC_M_R	3	−23	42	Impulse control
151	IFG_Tri_R	55	23	26	Patience
152	MFG_R	29	49	20	Patience
153	PrCG_L	−59	0	28	Patience
154	PrCG_L	−46	−5	28	Sharing positive emotion
155	ITG_R	56	−34	−16	Sharing negative emotion
156	MFG_R	38	32	17	Voluntary support
157	MTG_L	−48	−15	−9	Voluntary support
158	Th_R	10	−9	9	Decision making
159	MTG_L	−57	−46	−3	Decision making
160	ITG_L	−34	−3	−35	Optimism
161	MTG_L	−53	−8	−7	Group consideration
162	SPG_R	36	−71	52	Adaptability
163	MTG_L	−52	−16	−5	Situational awareness

(Continued)

identified for a fixed significance level of $p = 0.001$ (corrected), which had different numbers of edges ranging from a few edges to more than 50. To obtain a similar number of edges

for every identified network, two thresholds were used: one was at a significance level of $p = 0.005$ (corrected; see the Materials and Methods section for more details) and the other was the number of edges, namely, 15 per network (Termenon et al., 2016). Therefore, the number of edges in the identified networks were limited to as close to 15 as possible, except for those that had fewer than 15 edges even at the threshold of $p = 0.005$. For 116 of the 130 psychometric parameters, 128 significant functional networks were identified, of which 82 corresponded to social ability/skill parameters, 17 to IQ parameters and 29 to emotion quotient scale (EQS) parameters (P7 of **Figure 1A**). The functional networks corresponded to 116 psychometric parameters (74 for social ability/skill parameters, 15 for IQ parameters and 27 for EQS parameters), as 12 psychometric parameters corresponded to more than one functional network (8 for social ability/skill parameters, 2 for IQ parameters, and 2 for EQS parameters). The average number of edges of the 128 networks was 15.01 (mean) ± 4.72 (standard deviation). The set of all functional networks is shown in **Figure S1** and **Table S1**. Each network identified through these processes can be considered to be involved in a brain function responsible for the corresponding psychometric parameter. Ultimately, we identified 128 functional networks representing 116 psychometric parameters, from which we can evaluate a wide variety of human characteristics that the 116 psychometric parameters reflect.

As an example network, we show the network corresponding to the psychometric parameter "verbal intelligence quotient (VIQ)" (**Figure 3**) (Barona et al., 1984), as IQs are important in understanding human behavior and reflect diverse brain neurological differences (Deary et al., 2010). Among IQs, the VIQ reflects language ability, which is tightly associated with social function and is a basis of diverse human activities.

The ROIs constituting the functional network are shown in **Table 4**. The ROIs included in the brain areas of Brodmann area (BA) 47 and BA 22 are known to be associated with language-related function (Shaywitz et al., 1998).

SVM

To verify that the functional networks identified from the rs-fMRI signals and psychometric parameters can significantly represent cognition/behavior, we derived a multiclass SVM classifier for each functional network. A binary classifier was considered to be sufficient for verification, but we attempted to derive multiclass SVM classifiers because our future aim is to estimate scores of psychometric parameters using only rs-fMRI data. To determine if this was possible, an eight-class SVM classifier was chosen, although a multiclass SVM with more classes would have been ideal for estimating the scores. A multiclass (eight-class) SVM classifier for each psychometric parameter could be derived by using the edges of each network as the input (P8 of **Figure 1A**). All the classifiers were revealed to have significant accuracy upon cross-validation (one-sample t-test, $p = 0.05$) above the chance level, although the accuracy is low, except for five classifiers corresponding to five psychometric parameters (P9). That is, significant classifiers were derived for 123 of the 128 functional networks (78 for social ability/skill parameters, 17 for IQ parameters and 28 for EQS parameters). These 123 SVM classifiers were related to 111 psychometric parameters (70 for social ability/skill parameters, 15 for IQ parameters, and 26 for EQS parameters), as 12 psychometric parameters corresponded to more than one classifier (**Figure S2**, **Table S1**).

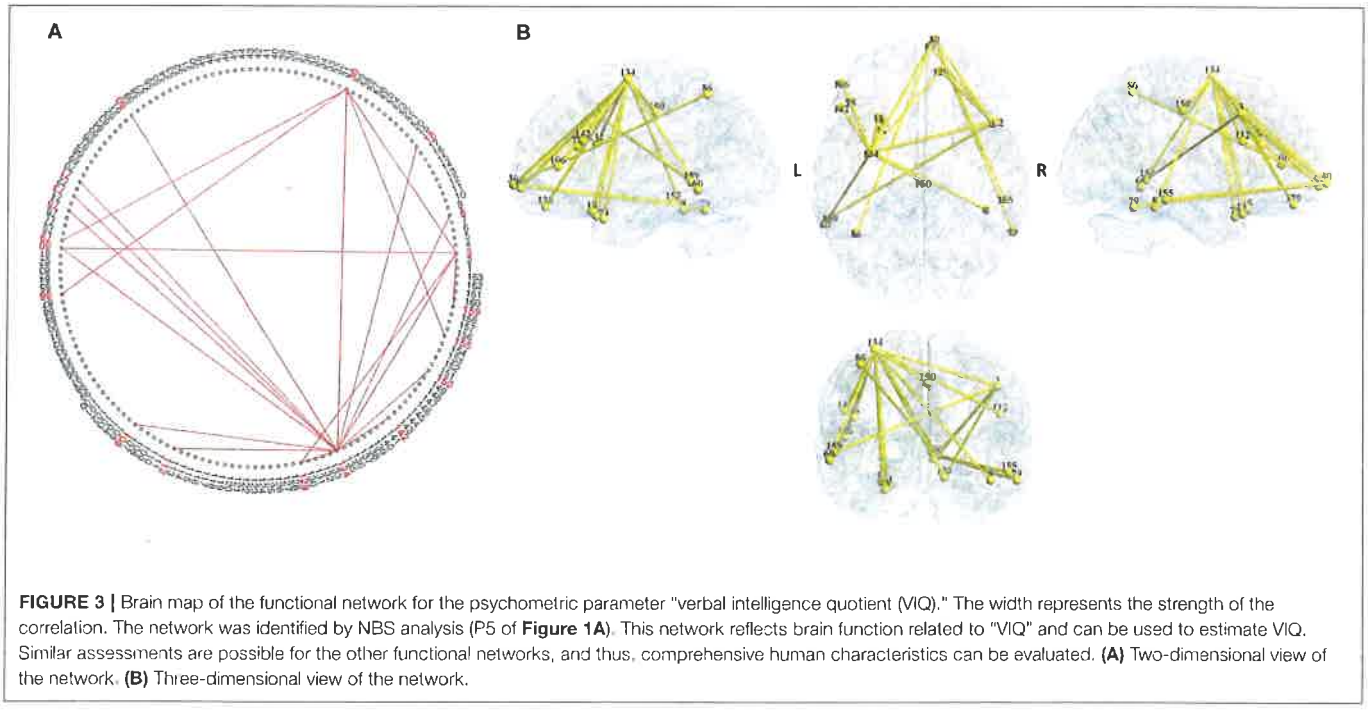


FIGURE 3 | Brain map of the functional network for the psychometric parameter "verbal intelligence quotient (VIQ)." The width represents the strength of the correlation. The network was identified by NBS analysis (P5 of **Figure 1A**). This network reflects brain function related to "VIQ" and can be used to estimate VIQ. Similar assessments are possible for the other functional networks, and thus, comprehensive human characteristics can be evaluated. **(A)** Two-dimensional view of the network. **(B)** Three-dimensional view of the network.

TABLE 4 | List of the ROIs included in the functional network corresponding to "Verbal IQ."

#	Region	MNI coordinates			Brodmann area	Psychometric parameters
		x	y	z		
7	PoCG_R	44	−16	56	BA 4	Social competence with friends of the same sex
38	FG_R	39	−40	−16	BA 37	BAS/fun seeking
50	PoCG_L	−39	−30	58	BA 40	Planning skills
52	Hipp_R	33	−16	−8	BA 28	Planning skills
68	IFG_orb_R	28	22	−26	BA 47	Impulsivity/Carelessness Style (ICS)
95	Cerebellum_L	−44	−75	−31	Pyramis_L	The Satisfaction with Life Scale (SWLS)
102	IFG_Med_R	3	56	−11	BA 10	Disorganization
107	TP_Inf_R	43	6	−35	BA 38	Attention switching
113	PrCG_R	49	3	26	BA 6	Communication
126	PCC_L	−6	−38	23	BA 23	Crystallized intelligence
132	PrCG_R	60	12	30	BA 9	Arithmetic
139	PoCG_R	55	−21	52	BA 2	Digit symbol
147	SMG_R	47	−40	24	BA 13	Perseverance
150	PCC_M_R	3	−23	42	BA 31	Impulse control
153	PrCG_L	−59	0	28	BA 6	Patience
154	PrCG_L	−46	−5	28	BA 6	Sharing positive emotion
155	ITG_R	56	−34	−16	BA 20	Sharing negative emotion
163	MTG_L	−52	−16	−5	BA 22	Situational awareness

Testing the SVM Classifiers in Different Populations

To test the performances of the SVM classifiers, we estimated the scores of the psychometric parameters from level 1 to 8 (related to social ability/skill) from MRI data using the 70 SVM classifiers (only one classifier was chosen for each psychometric parameter that corresponded to multiple classifiers) that corresponded to the 70 psychometric parameters related to social ability/skill. We compared the estimated scores with psychologically measured scores of the 70 psychometric parameters for 57 participants in the supplementary experiment. All 70 SVM classifiers exhibited an accuracy above chance level with low sensitivity of 14.1 ± 3.7% but high specificity of 87.8 ± 0.8% (**Table 5**), and the accuracy results found for this supplementary experiment were similar to those observed in the primary experiment (**Figure 4**).

DISCUSSION

The primary aims of this study were to prove that functional networks identified by rs-fMRI signals and psychometric parameters represent brain functions to which corresponding cognition/behavior are related and to determine whether the functional networks can be interpreted in a similar way to functional areas identified by tb-fMRI signals upon task stimulation. Another aim was to identify a set of functional networks for comprehensively evaluating human characteristics.

We found functional networks corresponding to 111 out of 130 psychometric parameters and derived a multiclass SVM classifier for each psychological parameter. These findings demonstrate that each rs-fMRI functional network can represent a corresponding cognition/behavior and that the set of functional networks reported here, which correspond to 111 psychometric parameters, can be used to comprehensively evaluate human characteristics.

Previous studies have attempted to identify functional networks from rs-fMRI signals. Some have identified functional networks by correlation between rs-fMRI signals and known ROIs (Wang et al., 2009; Tian et al., 2011), and others have derived functional networks by correlation between a known seed area or image voxel of the brain and other brain areas/voxels (Greicius et al., 2003; Fox et al., 2009) or by independent component analysis (ICA) in which a group of brain areas sharing a common component of an independent signal are identified to constitute a functional network (Damoiseaux et al., 2006; De Luca et al., 2006). However, the functional roles of the networks were interpreted based on various cognition/behavior related to the tasks in tb-fMRI (van den Heuvel and Hulshoff Pol, 2010), as a combination of functional areas previously identified by tb-fMRI and the tasks performed during tb-fMRI were used in the identification procedure of the functional networks. Therefore, it remains unclear whether functional networks can be identified by psychological indices (psychometric parameters consisting of self-reported questionnaire scores) and whether rs-fMRI signals can represent the corresponding cognition/behavior. By identifying brain networks related to psychometric parameters and the deriving multiclass SVM classifiers corresponding to those psychological parameters, our results demonstrate that rs-fMRI functional

TABLE 5 | Sensitivity and specificity of classifiers.

	Sensitivity	Specificity
Net_001	0.30	0.71
Net_002	0.25	0.62
Net_003	0.33	0.67
Net_004	0.27	0.62
Net_005	0.33	0.67
Net_006	0.32	0.64
Net_007	0.25	0.61
Net_008	0.29	0.65
Net_009	0.42	0.73
Net_010	0.33	0.67
Net_011	0.33	0.67
Net_012	0.33	0.68
Net_013	0.38	0.67
Net_014	0.33	0.67
Net_015	0.33	0.69
Net_016	0.30	0.64
Net_017	0.36	0.69
Net_019	0.29	0.66
Net_021	0.33	0.67
Net_022	0.32	0.66
Net_024	0.28	0.63
Net_025	0.24	0.63
Net_026	0.29	0.65
Net_027	0.29	0.67
Net_028	0.33	0.67
Net_029	0.36	0.72
Net_031	0.33	0.67
Net_034	0.33	0.67
Net_035	0.32	0.66
Net_037	0.28	0.62
Net_038	0.30	0.65
Net_039	0.33	0.67
Net_040	0.34	0.67
Net_041	0.30	0.65
Net_042	0.34	0.67
Net_043	0.34	0.68
Net_045	0.32	0.66
Net_046	0.39	0.71
Net_047	0.35	0.66
Net_048	0.33	0.67
Net_050	0.39	0.69
Net_051	0.32	0.67
Net_052	0.32	0.66
Net_053	0.28	0.62
Net_054	0.28	0.64
Net_056	0.33	0.67
Net_057	0.33	0.62
Net_058	0.35	0.68
Net_059	0.30	0.67
Net_061	0.31	0.65
Net_062	0.39	0.72
Net_063	0.39	0.70
Net_064	0.31	0.69
Net_065	0.45	0.66
Net_066	0.33	0.67
Net_067	0.31	0.65
Net_068	0.33	0.67
Net_069	0.28	0.64
Net_070	0.31	0.64
Net_071	0.33	0.66
Net_072	0.35	0.69
Net_073	0.40	0.69
Net_075	0.33	0.67
Net_076	0.31	0.64
Net_077	0.33	0.70
Net_078	0.33	0.67
Net_079	0.28	0.66
Net_080	0.32	0.66
Net_081	0.44	0.75
Net_082	0.33	0.65

networks can represent cognition/behavior. In tb-fMRI, SVM classifiers have been used to prove functional specificity of a brain area by testing whether the brain area can discriminate the related stimulus exemplar from other stimuli (MacEvoy and Epstein, 2009). Similarly, each of our identified classifiers could significantly discriminate the scores of the corresponding psychological parameter, showing that each functional network represented the corresponding cognition/behavior. The results indicate that the identified functional networks can be used in a similar way to the functional areas identified by tb-fMRI for brain imaging. Recent studies on rs-fMRI support our results that the functional brain networks identified by rs-fMRI signals contain intrinsic information of the brain system and have shown that similar brain maps obtained by tb-fMRI can also be acquired by rs-fMRI (Finn et al., 2015; Tavor et al., 2016).

The identification of 111 functional networks and the derivation of SVM classifiers for each of the 111 functional networks suggest that the variance of rs-fMRI signals between subjects reflects differences in cognition/behavior, which also indicates that variations in neural systems develop differently in each individual. Therefore, it is inferred that brain plasticity with different genetic and environmental conditions (Bouchard, 2004) varies among participants and that such variation in plasticity could appear in the functional network representation.

Several studies of brain plasticity at the systems level have been performed. Long-term plasticity has been shown in primary sensory areas, such as in visual areas of blind subjects and auditory areas of deaf subjects (Karni and Sagi, 1991; Gaser and Schlaug, 2003), which could be considered as modifications

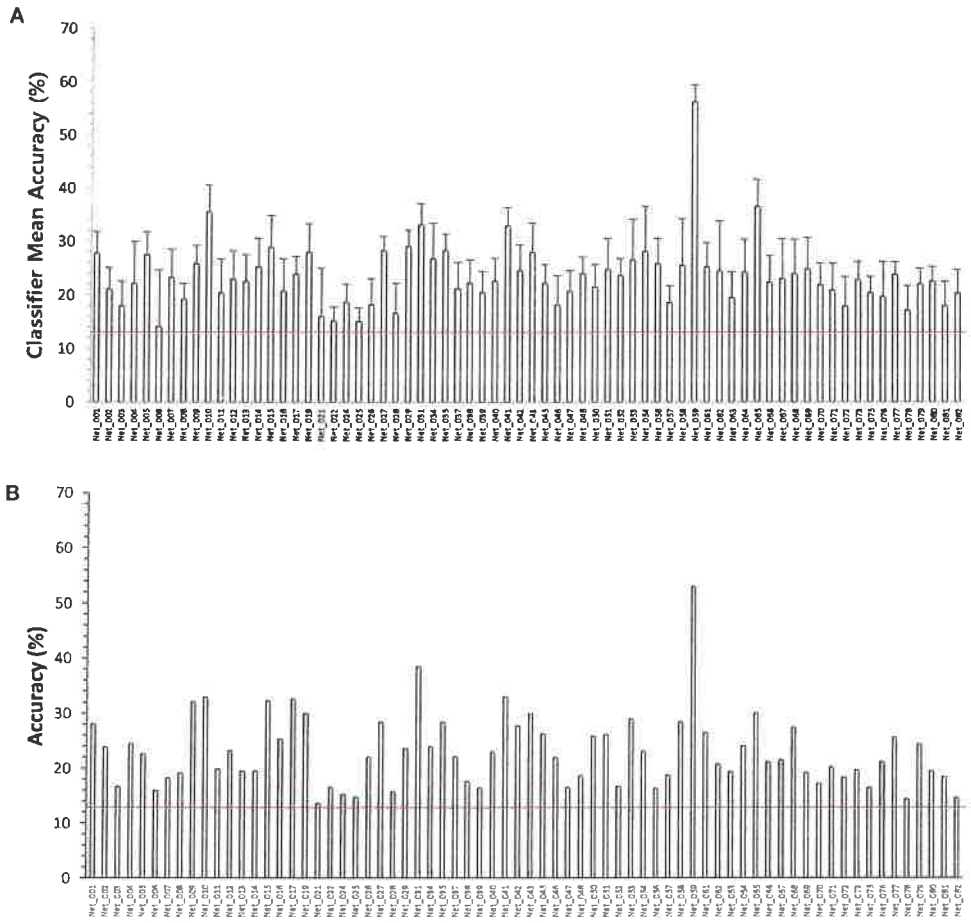


FIGURE 4 | (A) Accuracies of 70 SVM classifiers corresponding to the psychometric parameters related to social ability/skill in 153 participants. The error bar denotes the standard deviation. All classifiers are significant at $p = 0.05$. **(B)** Accuracies of same 70 SVM classifiers in another 57 participants. The accuracy results of test are similar to those observed during the training. This shows that the derived classifiers work properly. The redlines on the figures indicate the chance level 12.5%.

to brain "hardware." Mid-term plasticity was also shown in high-level areas like the hippocampus among people who have extensively trained for many years, such as in taxi drivers (Maguire et al., 2000). In addition, short-term plasticity was shown in high-level areas such as the hippocampus in those undergoing intense cognitive function training, such as in those studying for a difficult medical exam for a few months or during physical juggling training for a few weeks (Draganski et al., 2006). Such plastic changes have been observed by rs-fMRI and VBM. Considering the brain plasticity observed by rs-fMRI or VBM, we can infer that the 163 functional areas and 111 functional networks identified by the same modalities used in the previous studies also reflect brain plasticity.

We performed the leave-one-out cross validation in this study because we thought it gives less biased predictions. Recently a study has suggested conservative evaluation for reliability of cross-validation methods in applying machine learning algorithms for small sample sizes (Varoquaux, 2017). In this study, we completely separated data sets for the training and the test and could acquire similar results for the training and the test. In addition, the average accuracy 23.6% of the test data is still above a corrected chance level (about 17% for 150 samples), corrected by the number of samples, which was proposed by a previous study (Combrisson and Jerbi, 2015). These support that our classifiers are reliable.

In terms of the general use of classifiers, accuracy is an important factor. The accuracy of the SVM classifiers is low, although it is above the chance level. One reason is that the number of classes - 8 - could be too high. For 3-class SVM classifiers we could get about 53% accuracy; similarly, we can expect about 80% accuracy for a binary classifier. In this study, we used the same number of classes for all psychometric parameters when designing SVM classifiers, although there was an optimal number of clusters. We used the same algorithm and kernel for all psychometric parameters. However, other classification algorithms or kernels may be better for some psychometric parameters depending on their features and data structures. In future studies, it will be necessary to optimize the classification algorithm to each parameter and to optimize the

number of classes to suit the evaluation of human characteristics, especially transient changes in characteristics by brain plasticity resulting from education, training, or diseases. However, even with the 8-class SVM classifier we derived, we can significantly evaluate human characteristics. For example, in a supplementary experiment (not published), we obtained rs-fMRI data from one participant 8 times across 2 weeks. We found that 66 out of 70 SVM classifiers gave the same score (level) more than 4 times, which means that repeated measurements enable our 8-class SVM classifiers to be applied to estimate a wide variety of human characteristics with high specificity (more than 87%; **Table 5**).

For training, the SVM classifier that we used here only has information regarding the edges of the functional networks with which the correlations of the psychometric scores were comparatively low, 0.51 ± 0.07 (mean ± SD), as shown in **Figure S2**, which might be a limitation of the performance of the SVM classifiers. But other factors related to the topology of a functional network as a graph, such as centrality and mean path, can be used to improve the accuracy. Additional data from other modalities, such as fractional anisotropy or mean diffusivity from diffusion-weighted imaging, may also be useful for further improving the accuracy. In the future, we plan to use these types of data to further improve the accuracy for generalizing our classifiers.

The tb-fMRI signal is known to be induced by stimulation through neuro-vascular coupling, and the site at which an fMRI signal is measured is known to contain neurons that are processing the information related to a given stimulus. Therefore, tb-fMRI is known to be a direct method to identify functional areas. However, resting-state fMRI is considered to be indirect because additional supporting information is needed to characterize the connectivity, such as psychological parameters or behavioral information, and it remains unclear whether neurons in brain areas of a rs-fMRI functional network are directly related to the processing of the information required for the expected cognitive or behavioral brain function. Therefore, even in the case in which the data acquired by the two modalities can yield the same results in evaluating cognition/behavior, the functional mechanism represented by brain areas or networks may be different. This may explain why ROIs for a psychometric parameter were not identified but a functional network was identified. This type of problem related to intrinsic functional characteristics should be further examined to elucidate the mechanism of brain function.

To understand the details of the functional role of the functional network of each psychological parameter, tb-fMRI may be needed. However, in this study, the aim was to prove that functional networks can be identified from rs-fMRI signals and psychometric parameters and to identify biomarkers of cognition/behavior to evaluate a wide variety of human characteristics that can be used to describe individuals. Therefore, although the details of identified functional networks should be investigated further, we believe that our aim of identifying functional networks/classifiers that characterize most of the intended psychometric parameters has been achieved.

Regarding the size of the subject population for significantly obtaining brain information from rs-fMRI and psychological parameters, the population size of 153 subjects for this study is considered to be appropriate because a previous study suggested that more than 100 subjects can provide reliable variation for estimating brain plasticity (Termenon et al., 2016).

To the best of our knowledge, this study derived the largest number of functional networks/classifiers (or identified functional brain networks) reflecting cognition/behavior among fMRI studies performed to date. Although there are several large databases around the world that are represented by the "human connectome project" (www.humanconnectome.org), none of the databases include as many psychometric parameters as included in this study. This is the first study of its kind in the field of brain imaging that reveals the possibility to describe an individual based on a comprehensive set of diverse human characteristics. However, other psychometric parameters may need to be added to obtain more classifiers so that an individual can be described as completely as possible. In the present study, 19 psychological parameters were not significantly associated with a functional network, for which we may need to devise new tasks and use tb-fMRI to elucidate the corresponding functional networks. In addition, it may be possible that abilities or emotions related to the psychometric parameters are not reflected in resting state fMRI signals, which may be an interesting topic to investigate in a future study.

Taken together, our results demonstrate that; (i) rs-fMRI signals include intrinsic information of brain function related to cognition/behavior, (ii) functional networks identified by psychometric parameters can represent corresponding cognition/behavior, and (iii) the set of functional networks/classifiers identified here can be used to comprehensively evaluate human characteristics.

CONCLUSION

We identified a set of 128 functional networks of cognition/behavior by rs-fMRI that span a variety of human characteristics and psychometric parameters, and we derived 123 multiple-class SVM classifiers corresponding to 111 psychometric parameters. This demonstrates that we can identify functional areas or networks of the brain not only by tb-fMRI but also by rs-fMRI. It also demonstrates that we can evaluate cognition/behavior and develop biomarkers for a wide variety of human characteristics using the 111 dimensions of the data obtained from a single rs-fMRI scan. The data and classifiers may also be applied to longitudinal studies or studies evaluating educational, training, or career development programs.

AUTHOR CONTRIBUTIONS

Y-WS, YK, and SO designed this study. The psychological data for this study were acquired by YK, CA, and YO. The anatomical and functional magnetic resonance images (MRI) data were acquired by Y-WS and DK. The VBM analysis of anatomical data

was conducted by Y-WS and DK. Brain network analysis and SVM analysis of functional data was conducted by U-SC. Y-WS wrote the first draft of the manuscript with SO, YK, and U-SC contributed to revise this manuscript. All authors reviewed this manuscript.

ACKNOWLEDGMENTS

This study was supported by the MEXT-Supported program for the Strategic Research Foundation at Private Universities, 2014–2018.

SUPPLEMENTARY MATERIAL

The Supplementary Material for this article can be found online at: https://www.frontiersin.org/articles/10.3389/fnins.2018.00149/full#supplementary-material

Figure S1 | Set of all functional networks.

Figure S2 | Correlation between each functional network and its psychometric score for 70 functional networks with 153 subject data by a linear multiple regression based on the least square analysis. The average correlation value R is 0.51 ($S.D$ 0.07) and R^2 is 0.27 ($S.D$ 0.07), $p < 0.0001$.

Table S1 | Description of all functional networks.

Supplementary Datasheet 1 | Supplementary references.

REFERENCES

Altmann, A., Schröter, M. S., Spoormaker, V. I., Kiem, S. A., Jordan, D., Ilg, R., et al. (2016). Validation of non-REM sleep stage decoding from resting state fMRI using linear support vector machines. *NeuroImage* 125, 544–555. doi: 10.1016/j.neuroimage.2015.09.072

Ashburner, J. (2007). A fast diffeomorphic image registration algorithm. *NeuroImage* 38, 95–113. doi: 10.1016/j.neuroimage.2007.07.007

Barona, A., Reynolds, C. R., and Chastain, R. (1984). A demographically based index of premorbid intelligence for the WAIS—R. *J. Consult. Clin. Psychol.* 52, 885–887. doi: 10.1037/0022-006X.52.5.885

Bishop, C. (2007). *Pattern Recognition and Machine Learning (Information Science and Statistics), 1st Edn. 2006. Corr. 2nd Printing Edn.* New York, NY: Springer.

Bouchard, T. J. (2004). Genetic influence on human psychological traits a survey. *Curr. Dir. Psychol. Sci.* 13, 148–151. doi: 10.1111/j.0963-7214.2004.00295.x

Carver, C. S., and White, T. L. (1994). Behavioral inhibition, behavioral activation, and affective responses to impending reward and punishment: the BIS/BAS Scales. *J. Pers. Soc. Psychol.* 67, 319–333. doi: 10.1037/0022-3514.67.2.319

Chang, C.-C., and Lin, C.-J. (2011). LIBSVM: a library for support vector machines. *ACM Trans. Intell. Syst. Technol.* 2, 27:1–27:27. doi: 10.1145/1961189.1961199

Chao-Gan, Y., and Yu-Feng, Z. (2010). DPARSF: a MATLAB toolbox for "Pipeline" data analysis of resting-state fMRI. *Front. Syst. Neurosci.* 4:13. doi: 10.3389/fnsys.2010.00013

Combrisson, E., and Jerbi, K. (2015). Exceeding chance level by chance: the caveat of theoretical chance levels in brain signal classification and statistical assessment of decoding accuracy. *J. Neurosci. Methods* 250, 126–136. doi: 10.1016/j.jneumeth.2015.01.010

Craig, M. M., Manktelow, A. E., Sahakian, B. J., Menon, D. K., and Stamatakis, E. A. (2017). Spectral diversity in default mode network connectivity reflects behavioral state. *J. Cogn. Neurosci.* 30, 526–539. doi: 10.1162/jocn_a_01213

Damoiseaux, J. S., Rombouts, S. A., Barkhof, F., Scheltens, P., Stam, C. J., Smith, S. M., et al. (2006). Consistent resting-state networks across healthy subjects. *Proc. Natl. Acad. Sci. U.S.A.* 103, 13848–13853. doi: 10.1073/pnas.0601417103

Deary, I. J., Penke, L., and Johnson, W. (2010). The neuroscience of human intelligence differences. *Nat. Rev. Neurosci.* 11, 201–211. doi: 10.1038/nrn2793

De Luca, M., Beckmann, C. F., De Stefano, N., Matthews, P. M., and Smith, S. M. (2006). fMRI resting state networks define distinct modes of long-distance interactions in the human brain. *NeuroImage* 29, 1359–1367. doi: 10.1016/j.neuroimage.2005.08.035

Diener, E., Emmons, R. A., Larsen, R. J., and Griffin, S. (1985). The satisfaction with life scale. *J. Pers. Assess.* 49, 71–75. doi: 10.1207/s15327752jpa4901_13

Draganski, B., Gaser, C., Kempermann, G., Kuhn, H. G., Winkler, J., Büchel, C., et al. (2006). Temporal and spatial dynamics of brain structure changes during extensive learning. *J. Neurosci. Off. J. Soc. Neurosci.* 26, 6314–6317. doi: 10.1523/JNEUROSCI.4628-05.2006

Fernández-Alcántara, M., Cruz-Quintana, F., Pérez-Marfil, M. N., Catena-Martínez, A., Pérez-García, M., and Turnbull, O. H. (2016). Assessment of emotional experience and emotional recognition in complicated grief. *Front. Psychol.* 7:126. doi: 10.3389/fpsyg.2016.00126

Finn, E. S., Shen, X., Scheinost, D., Rosenberg, M. D., Huang, J., Chun, M. M., et al. (2015). Functional connectome fingerprinting: identifying individuals using patterns of brain connectivity. *Nat. Neurosci.* 18, 1664–1671. doi: 10.1038/nn.4135

Fox, M. D., and Raichle, M. E. (2007). Spontaneous fluctuations in brain activity observed with functional magnetic resonance imaging. *Nat. Rev. Neurosci.* 8, 700–711. doi: 10.1038/nrn2201

Fox, M. D., Zhang, D., Snyder, A. Z., and Raichle, M. E. (2009). The global signal and observed anticorrelated resting state brain networks. *J. Neurophysiol.* 101, 3270–3283. doi: 10.1152/jn.90777.2008

Fransson, P. (2005). Spontaneous low-frequency BOLD signal fluctuations: an fMRI investigation of the resting-state default mode of brain function hypothesis. *Hum. Brain Mapp.* 26, 15–29. doi: 10.1002/hbm.20113

Gaser, C., and Schlaug, G. (2003). Brain structures differ between musicians and non-musicians. *J. Neurosci.* 23, 9240–9245.

Gauthier, I., Skudlarski, P., Gore, J. C., and Anderson, A. W. (2000). Expertise for cars and birds recruits brain areas involved in face recognition. *Nat. Neurosci.* 3, 191–197. doi: 10.1038/72140

Greicius, M. D., Krasnow, B., Reiss, A. L., and Menon, V. (2003). Functional connectivity in the resting brain: a network analysis of the default mode hypothesis. *Proc. Natl. Acad. Sci. U.S.A.* 100, 253–258. doi: 10.1073/pnas.0135058100

Greicius, M. D., Srivastava, G., Reiss, A. L., and Menon, V. (2004). Default-mode network activity distinguishes Alzheimer's disease from healthy aging: evidence from functional MRI. *Proc. Natl. Acad. Sci. U.S.A.* 101, 4637–4642. doi: 10.1073/pnas.0308627101

Grill-Spector, K., Knouf, N., and Kanwisher, N. (2004). The fusiform face area subserves face perception, not generic within-category identification. *Nat. Neurosci.* 7, 555–562. doi: 10.1038/nn1224

Guo, B., Zheng, X., Lu, Z. G., Wang, X., Yin, Z., Hou, W. S., et al. (2015). Decoding brain responses to pixelized images in the primary visual cortex: implications for visual cortical prostheses. *Neural Regen. Res.* 10, 1622–1627. doi: 10.4103/1673-5374.167761

Gur, R. C., Alsop, D., Glahn, D., Petty, R., Swanson, C. L., Maldjian, J. A., et al. (2000). An fMRI study of sex differences in regional activation to a verbal and a spatial task. *Brain Lang.* 74, 157–170. doi: 10.1006/brln.2000.2325

Hu, X., Guo, L., Han, J., and Liu, T. (2017). Decoding power-spectral profiles from FMRI brain activities during naturalistic auditory experience. *Brain Imaging Behav.* 11, 253–263. doi: 10.1007/s11682-016-9515-8

Karni, A., and Sagi, D. (1991). Where practice makes perfect in texture discrimination: evidence for primary visual cortex plasticity. *Proc. Natl. Acad. Sci. U.S.A.* 88, 4966–4970. doi: 10.1073/pnas.88.11.4966

Kim, S. G., and Ugurbil, K. (1997). Functional magnetic resonance imaging of the human brain. *J. Neurosci. Methods* 74, 229–243. doi: 10.1016/S0165-0270(97)02252-8

Kogler, L., Seidel, E. M., Metzler, H., Thaler, H., Boubela, R. N., Pruessner, J. C., et al. (2017). Impact of self-esteem and sex on stress reactions. *Sci. Rep.* 7:17210. doi: 10.1038/s41598-017-17485-w

Krendl, A. C., and Kensinger, E. A. (2016). Does older adults' cognitive function disrupt the malleability of their attitudes toward outgroup members? an fMRI investigation. *PLoS ONE* 11:e0152698. doi: 10.1371/journal.pone.0152698

Lei, X., Zhong, M., Liu, Y., Jin, X., Zhou, Q., Xi, C., et al. (2017). A resting-state fMRI study in borderline personality disorder combining amplitude of low frequency fluctuation, regional homogeneity and seed based functional connectivity. *J. Affect. Disord.* 218, 299–305. doi: 10.1016/j.jad.2017.04.067

MacEvoy, S. P., and Epstein, R. A. (2009). Decoding the representation of multiple simultaneous objects in human occipitotemporal cortex. *Curr. Biol.* 19, 943–947. doi: 10.1016/j.cub.2009.04.020

Maguire, E. A., Gadian, D. G., Johnsrude, I. S., Good, C. D., Ashburner, J., Frackowiak, R. S., et al. (2000). Navigation-related structural change in the hippocampi of taxi drivers. *Proc. Natl. Acad. Sci. U.S.A.* 97, 4398–4403. doi: 10.1073/pnas.070039597

Mason, M. F., Norton, M. I., Van Horn, J. D., Wegner, D. M., Grafton, S. T., and Macrae, C. N. (2007). Wandering minds: the default network and stimulus-independent thought. *Science* 315, 393–395. doi: 10.1126/science.1131295

Meskaldji, D. E., Preti, M. G., Bolton, T. A., Montandon, M. L., Rodriguez, C., Morgenthaler, S., et al. (2016). Prediction of long-term memory scores in MCI based on resting-state fMRI. *NeuroImage Clin.* 12, 785–795. doi: 10.1016/j.nicl.2016.10.004

Ogawa, S., Tank, D. W., Menon, R., Ellermann, J. M., Kim, S. G., Merkle, H., et al. (1992). Intrinsic signal changes accompanying sensory stimulation: functional brain mapping with magnetic resonance imaging. *Proc. Natl. Acad. Sci. U.S.A.* 89, 5951–5955. doi: 10.1073/pnas.89.13.5951

Poldrack, R. A., Barch, D. M., Mitchell, J. P., Wager, T. D., Wagner, A. D., Devlin, J. T., et al. (2013). Toward open sharing of task-based fMRI data: the OpenfMRI project. *Front. Neuroinformatics* 7:12. doi: 10.3389/fninf.2013.00012

Raine, A. (1991). The SPQ: a scale for the assessment of schizotypal personality based on DSM-III-R criteria. *Schizophr. Bull.* 17, 555–564. doi: 10.1093/schbul/17.4.555

Rupp, A. A., and Zumbo, B. D. (2006). Understanding parameter invariance in unidimensional IRT models. *Educ. Psychol. Meas.* 66, 63–84. doi: 10.1177/0013164404273942

Shaywitz, S. E., Shaywitz, B. A., Pugh, K. R., Fulbright, R. K., Constable, R. T., Mencl, W. E., et al. (1998). Functional disruption in the organization of the brain for reading in dyslexia. *Proc. Natl. Acad. Sci. U.S.A.* 95, 2636–2641. doi: 10.1073/pnas.95.5.2636

Singh, M. K., Chang, K. D., Kelley, R. G., Saggar, M., Reiss, A. L., and Gotlib, I. H. (2014). Early signs of anomalous neural functional connectivity in healthy offspring of parents with bipolar disorder. *Bipolar Disord.* 16, 678–689. doi: 10.1111/bdi.12221

Song, X., Qian, S., Liu, K., Zhou, S., Zhu, H., Zou, Q., et al. (2017). Resting-state BOLD oscillation frequency predicts vigilance task performance at both normal and high environmental temperatures. *Brain Struct. Funct.* 222, 4065–4077. doi: 10.1007/s00429-017-1449-4

Tavor, I., Parker Jones, O., Mars, R. B., Smith, S. M., Behrens, T. E., and Jbabdi, S. (2016). Task-free MRI predicts individual differences in brain activity during task performance. *Science* 352, 216–220. doi: 10.1126/science.aad8127

Termenon, M., Jaillard, A., Delon-Martin, C., and Achard, S. (2016). Reliability of graph analysis of resting state fMRI using test-retest dataset from the Human Connectome Project. *NeuroImage* 142, 172–187. doi: 10.1016/j.neuroimage.2016.05.062

Tian, L., Wang, J., Yan, C., and He, Y. (2011). Hemisphere- and gender-related differences in small-world brain networks: a resting-state functional MRI study. *NeuroImage* 54, 191–202. doi: 10.1016/j.neuroimage.2010.07.066

Uchiyama, K., Shimai, T., Utsuki, N., and Otake, K. (2001). *EQS Manual*. Tokyo: Jitsumukyoiku Syuppan, Practical Education Press.

van den Heuvel, M. P., and Hulshoff Pol, H. E. (2010). Exploring the brain network: a review on resting-state fMRI functional connectivity. *Eur. Neuropsychopharmacol.* 20, 519–534. doi: 10.1016/j.euroneuro.2010.03.008

Varoquaux, G. (2017). Cross-validation failure: small sample sizes lead to large error bars. *Neuroimage*. doi: 10.1016/j.neuroimage.2017.06.061. [Epub ahead of print].

Wang, J., Wang, L., Zang, Y., Yang, H., Tang, H., Gong, Q., et al. (2009). Parcellation-dependent small-world brain functional networks: a resting-state fMRI study. *Hum. Brain Mapp.* 30, 1511–1523. doi: 10.1002/hbm.20623

Yahata, N., Morimoto, J., Hashimoto, R., Lisi, G., Shibata, K., Kawakubo, Y., et al. (2016). A small number of abnormal brain connections predicts adult autism spectrum disorder. *Nat. Commun.* 7:11254. doi: 10.1038/ncomms11254

Yamauchi, T., Sudo, A., Tanno, Y. (2009). [Reliability and validity of the Japanese version of the brief core schema scales]. *Shinrigaku Kenkyu* 79, 498–505. doi: 10.4992/jjpsy.79.498

Yan, C. G., Wang, X. D., Zuo, X. N., and Zang, Y. F. (2016). DPABI: data processing & analysis for (resting-state) brain imaging. *Neuroinformatics* 14, 339–351. doi: 10.1007/s12021-016-9299-4

Yang, X., Liu, J., Meng, Y., Xia, M., Cui, Z., Wu, X., et al. (2017). Network analysis reveals disrupted functional brain circuitry in drug-naive social anxiety disorder. *Neuroimage*. doi: 10.1016/j.neuroimage.2017.12.011. [Epub ahead of print].

Zafar, R., Kamel, N., Naufal, M., Malik, A. S., Dass, S. C., Ahmad, R. F., et al. (2017). Decoding of visual activity patterns from fMRI responses using multivariate pattern analyses and convolutional neural network. *J. Integr. Neurosci.* 16, 275–289. doi: 10.3233/JIN-170016

Zalesky, A., Fornito, A., and Bullmore, E. T. (2010). Network-based statistic: identifying differences in brain networks. *Neuroimage* 53, 1197–1207. doi: 10.1016/j.neuroimage.2010.06.041

Conflict of Interest Statement: The authors declare that the research was conducted in the absence of any commercial or financial relationships that could be construed as a potential conflict of interest.

Copyright © 2018 Sung, Kawachi, Choi, Kang, Abe, Otomo and Ogawa. This is an open-access article distributed under the terms of the Creative Commons Attribution License (CC BY). The use, distribution or reproduction in other forums is permitted, provided the original author(s) and the copyright owner are credited and that the original publication in this journal is cited, in accordance with accepted academic practice. No use, distribution or reproduction is permitted which does not comply with these terms.

原 著 論 文

Evaluation of Characteristics of Resting State fMRI Data by Machine Learning

Zahra NAZARI[1], Moriyuki INAMINE[1],Yuhei SUGAMA[1], Dongshik KANG[1], Yousuke KAWACHI[2], Yul-Wan SUNG[2], Seiji Ogawa[2]

[1] Department of Information Engineering, University of the Ryukyus, Okinawa, Japan

[2] Kansei Fukushi Research Institute, Tohoku Fukushi University, Sendai, Japan

Abstract

The Self-Organized Map (SOM) and K-means methods are used to examine whether the resting state fMRI data have some intrinsic characteristics by which individual brain function can be classified. The results show that individual brains have common characteristics in spite of high variability and why machine learning could have been successfully applied to the analysis of resting state fMRI data.

Keywords : resting state fMRI, Self-Organizing Map, K-means

Introduction

Brain imaging studies by functional MRI (fMRI) with stimulus tasks usually have targeted a small number of several tens of subjects and limited number of brain areas, but those by resting state fMRI target a large number of subjects more than ten thousands in some cases and the whole brain. Therefore, the brain imaging study comes to require other analysis methods than the typical methods using parametric analysis. Machine learning is a non-parametric method representing artificial intelligence such as neural network and pattern analysis [1, 2]. Recently, brain imaging studies have started to use machine learning for resting state fMRI data analysis, because of its advantages in analyzing high dimensional data. These studies have demonstrated that some significant information is contained in the resting state fMRI signals. One of them showed that a cognitive function could be estimated through only measuring resting state fMRI signals without using task stimuli [3]. However, it's not clear that what characteristics of the signals have made the estimation. Because in data analysis by machine learning techniques, we are interested on the output and often overlook the characteristics of the data. In this study we examined characteristics of the resting state fMRI signals for which we applied two clustering methods, SOM and K-means to data sets derived from brain networks made from resting state fMRI signals.

Methods

(SOM)

The SOM is a neural network proposed by Kohonen [4] which is especially useful for multi-dimensional data classification. A SOM consists of input and output layers and is trained by multi-dimensional input vectors. In the training stage the input vectors pass through all units in the competitive layer. The network becomes self-organized by repeatedly comparing input vectors and

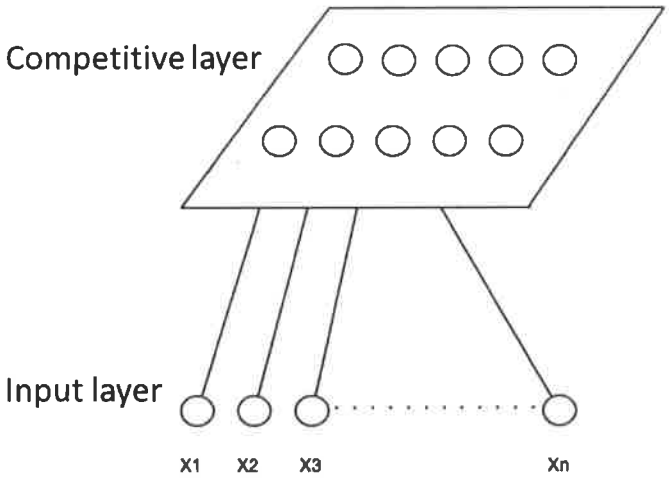


Figure 1. This figure demonstrates network structure of the SOM.

those in each unit. The SOM does not use known information in the training process, so that it is known to be an unsupervised neural network. The SOM algorithm is based on competitive learning. It provides a topology preserving mapping from the high dimensional space to map units. Map units, or neurons, usually form a two-dimensional lattice and thus the mapping is a mapping from high dimensional space onto a plane (Fig. 1). The property of topology preserving means that the mapping preserves the relative distance between the points. Points that are near each other in the input space are mapped to nearby map units in the SOM. The SOM can thus serve as a cluster analyzing tool of high-dimensional data. Also, the SOM has the capability to generalize. Generalization capability means that the network can recognize or characterize inputs it has never encountered before. A new input is assimilated with the map unit it is mapped to [5] (https://en.wikipedia.org/wiki/Self-organizing_map).

(K-means)

K-means is the simplest unsupervised learning algorithms that solve the well-known clustering problem [6]. The procedure follows a simple and easy way to classify a given data set through a certain number of clusters (assume k clusters) fixed in advance. The main idea is to define k centroids, one for each cluster. These centroids should be placed in a cunning way because of different location causes different result. So, the better choice is to place them as much as possible far away from each other. The next step is to take each point belonging to a given data set and associate it to the nearest centroid. When no point is pending, the first step is completed and an early groupage is done. At this point we need to re-calculate k new centroids as barycenters of the clusters resulting from the previous step. After we have these k new centroids, a new binding has to be done between the same data set points and the nearest new centroid. A loop has been generated. As a result of this loop we may notice that the k centroids change their location step by step until no more changes are done. In other words centroids do not move any more. Finally, this algorithm aims at minimizing an *objective function*, in this case a squared error function (https://home.deib.polimi.it/matteucc/Clustering/tutorial_html/kmeans.html).

The objective function

$$\phi = \sum_{x_j \in X}^{k} \min_{i \in k} \|x_j - c_i\|^2$$

where $\left\|x_i^{(j)} - c_j\right\|^2$, x_j, $j \in \{1, \ldots, n\}$ is a chosen distance measure between a data point $x_i^{(j)}$ and the cluster center c_j, is an indicator of the distance of the n data points from their respective cluster centers.

1. The algorithm is composed of the following steps:

Step 1

Place K points into the space represented by the objects that are being clustered. These points represent initial group centroids.

Step 2

Assign each object to the group that has the closest centroid.

$$c_i = \frac{1}{n} \sum_{x_j \in X}^{k} x_j$$

Step 3

When all objects have been assigned, recalculate the positions of the K centroids.

Step 4

Repeat Steps 2 and 3 until the centroids no longer move. This produces a separation of the objects into groups from which the metric to be minimized can be calculated.

(MRI data)

We used two sets of MRI data acquired in Tohoku Fukushi University (Sung et al.; submitted). The matrix size of the data was 153 by 2. The study was approved by the Institutional Review Board of Tohoku Fukushi University.

Results and Discussion

One input data set could be classified into eight classes by SOM (Fig. 2). The figure shows that each class is composed of several elements. The biggest class contained 28 elements and the smallest class has 9 elements. The classes are considered to have different characteristics at least in an aspect of the brain function. The elements included in the same class are considered to have similar characteristics. The specific characteristics represented by each class would be clarified by examining common traits of the

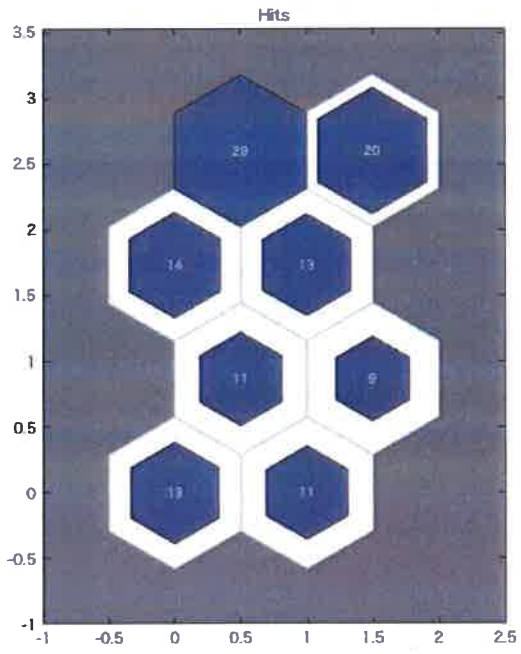


Figure 2. This figure shows the clustering results; the numbers in the hexagonal box represent number of elements.

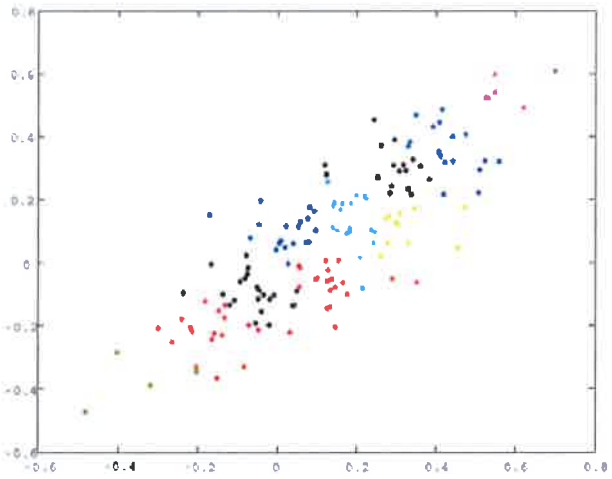


Figure 3. This figure shows clustering result by K-means. Classes are represented by different colors.

elements.

Another input data set could be classified into ten classes by K-means (Fig. 3). The figure shows that elements with the same color can be grouped into one class. This distribution of the elements in the figure demonstrates that linear classifiers would make incorrect classification.

The clustering of MRI data by SOM and K-means suggests that resting state fMRI data have some characteristics by which the elements can be classified. This demonstrates why machine learning algorithms have been successfully applied to resting state fMRI signal analysis.

Acknowledgments

This study was supported by MEXT-Supported program for the Strategic Research Foundation at Private Universities, 2014-2018.

References

1 JMourão-Miranda J., Reynaud E., McGlone F., Calvert G. and Brammera M. "The impact of temporal compression and space selection on SVM analysis of single-subject and multi-subject fMRI data" Neuroimage **33**: 1055-1065, 2005

2 Misaki M., Miyauchi S. "Application of artificial neural network to fMRI regression analysis" Neuroimage **29**: 396-408, 2006

3 Finn E. S., et al. "Functional connectome fingerprinting: identifying individuals using patterns of brain connectivity" Nat. Neurosci. **18**: 1664-1670, 2015

4 Kohonen T. "Self-Organized Formation of Topologically Correct Feature Maps" Biological Cybernetics. **43**: 59–69, 1982

5 Kohonen T. "Self-Organizing Maps". Springer, Berlin, Heidelberg, 1995

6 MacQueen J. B. "Some Methods for classification and Analysis of Multivariate Observations" Proceedings of 5-th Berkeley Symposium on Mathematical Statistics and Probability, Berkeley, University of California Press, **1**:281-297, 1967

原 著 論 文

Realization of a Longitudinal Relaxation Time Measurement with High Spatial Resolution

Daehun KANG, Yul-Wan SUNG, OGAWA Seiji

Kansei Fukushi Research Institute, Tohoku Fukushi University

Abstract

Structural information of the human cortex is related to its plasticity. For the evaluation of the structural information in a cortex, its volume and thickness that can be measured through a typical anatomical imaging of the cortical structure have been used in the previous studies. Among magnetic resonance (MR) properties, a longitudinal relaxation time (T_1) value could provide the information for the underlying neuronal densities in a straightforward way. However, the conventional imaging methods for measuring T_1 value are inappropriate for the clinical use because they need long scan time for acquiring the whole brain with high spatial resolution. A recently proposed alternative imaging method could reduce imaging time through the correction of the non-homogeneous field generated by RF coils causing an error in the calculation of T_1 value. In this study, we realized the imaging method to be performed in our 3-tesla MR imaging system in order to obtain the map of T_1 value with high spatial resolution of 1 mm^3 and developed a user-friendly program. By the realization of the imaging method into our system, we could measure T_1 values in white and gray matters, which were 889 ms and 1570 ms, respectively, consistent with those in the literatures.

Keywords : longitudinal relaxation time, gradient-recalled echo, actual-flip angle imaging, high spatial resolution

Introduction

Cortical structural information of the human brain is related to its plasticity [1]. The cortical volume and thickness has been used to assess the brain plasticity [2]. For evaluating the cortical volume or thickness, the analysis techniques such as voxel-based morphometry [3] or voxel-based cortical thickness [4] were developed, respectively. The magnetic resonance imaging (MRI) technique has supported the analyses by providing an anatomical brain image with high spatial resolution and high contrast, which enabled to discriminate the boundaries between gray matter and the neighboring tissues (white matter or cerebrospinal fluid (CSF)). For example, the magnetization-prepared radio-frequency pulses and rapid gradient-echo (MPRAGE) has been used widely, which provided a longitudinal relaxation time (T_1) weighted image with a high contrast. However, these analyses do not relate in a straightforward way to underlying neuronal densities and the intensity in T_1-weighted image is limited to be appropriate to reflect a change in intrinsic characteristics of cortical structure.

With the cortical volume and thickness, the T_1 value could be a potential index to assess the brain plasticity because any tissue property (e.g., cell density, cell size, myelination) is expected to affect the relaxation times which could be observed with voxel-based analysis [5, 6]. In contrast with T_1-weighted images, T_1 mapping could be derived by more than two images with different flip angles (FA). However, in practice, the B_1^- field which is an oscillating magnetic field at radiofrequency (RF)

generated by RF coils is not homogeneous spatially and results in error in T_1 value. Thus, it requires correction of the inhomogeneous fields by additional data acquisition and calculation. In this report, we introduce the MR pulse sequences and the data calculation which are realized to obtain T_1 map. For convenient use, the graphic user interfaces of the processes are developed.

Materials and methods

Imaging method

Two different imaging methods were used to measure apparent T_1 map and B_1^+ field map, respectively. All of scans were based on 3 D volume acquisition.

To obtain the apparent T_1 map, two sets of data were acquired by typical gradient-recalled-echo (GRE) pulse sequences with two different FAs [7, 8], as show in Figure 1 (a). The imaging parameters were as followings: TR_1 = 30 ms, TE=3.45 ms, a spatial resolution = 1.0 mm isotropic voxel, and a nominal FA θ_1 or θ_2 = 20 or 7°. The total scan time was about 12 min. (= 6 min. x 2 scans). To make complete spoiling of transverse magnetization, the user interface for the pulse sequence was modified to adjust a magnitude in a gradient crusher on x- and z-axes [9] and a phase increment in the RF pulses. A phase increment of the RF pulses was set into +160°.

To estimate B_1^+ field map, the Actual Flip-angle Imaging (AFI) was realized [10, 11]. It was performed by the interleaved different TRs (TR_2 and TR_3) in GRE pulse sequence as shown in Figure 1 (b). AFI produced two types of images obtained in two different TRs which were used to derive B_1^+ field map. The imaging parameters were as followings: TR_2/TR_3 = 20/100 ms, TE=3.45 ms, a spatial resolution = 3.5 mm isotropic voxel, and a nominal FA θ_3 = 60°. The scan time was about 6 min. To make complete spoiling of transverse magnetization, asymmetric gradient crushers were added and a phase increment of the RF pulses was adjusted to 129.3° [12, 13]

Calculation of maps

To calculate apparent T_1 map, i.e. $T_{1,app}$, we used the equation described below.

$$T_{1,app}=-2 \cdot TR \cdot (S_1/\theta_1 - S_2/\theta_2) / (S_1 \cdot \theta_1 - S_2 \cdot \theta_2) \quad (1)$$

, where S_n denotes the image intensity from the FA of θ_n. With the conditions of $\theta_n \ll 1$ and $TR \ll T_1$, $T_{1,app}$ can be obtained as a linear regression in a plot of $(S_n \cdot \theta_n)$ vs. (S_n/θ_n).

The B_1^+ field map is defined by two FAs of $\theta_{act.}/\theta_{nom.}$, where the subscripts of act. and nom. denote actual and nominal, respectively. To calculate $\theta_{act.}$ map, we used the equation described below.

$$\theta_{act.} \cong \arccos [(rn-1) / (n-r)], \text{ where } n=TR_3/TR_2 \ \& \ r=S_3/S_2 \quad (2)$$

, where S_2 and S_3 denote images with TR_2 and TR_3, respectively. Since $\theta_{nom.}=\theta_3$, B_1^+ field map is calculated by $\theta_{act.}/\theta_3$.

The correction of apparent T_1 map was performed by weighting the apparent T_1 map with a reciprocal of a square of the B_1^+ field map, as described below.

$$T_1 = T_{1,app} / (\theta_{act.}/\theta_3)^2 \quad (3)$$

Implementations and in-vivo test

The MR pulse sequences for GRE and AFI were modified to work on 3 T Skyra-fit system (Siemens Healthcare GmbH, Erlangen, Germany). Figure 2 showed the user interface with multiple inputs for two TRs in AFI pulse sequence. The imaging was performed with a standard 20-channel head matrix coil.

The calculations for maps were performed by a home-made code with DICOM data based on SPM 12 in MATLAB (SPM12; Functional Imaging Laboratory, London, England & MATLAB; MathWorks, Natick, MA, USA). For convenient use, the graphic user interface was realized as shown in Figure 3.

One healthy volunteer (female) participated in this test. After subject was provided a complete description of the study, informed and written consent was obtained in accordance with the Declaration of Helsinki. The study protocol was approved by the Institutional Review Board of Tohoku Fukushi University.

Results & discussions

The whole brain of the participant was scanned by using two GRE and AFI pulse sequences. The two images with high spatial resolution (isotropic voxel of 1 mm^3) were obtained by using GRE pulse sequences with two different FAs. The images with FA of 20° and 7° were weighted by T_1 value and proton density as shown in Figure 4 (a, b), respectively. By using the two images, the apparent T_1 map was calculated by using the Eq. 1 as shown in Figure 4 (d). The B_1^+ field map was calculated by AFI pulse sequence. In Figure 4 (c), the image intensity denoted a value in $\theta_{act}/\theta_{nom}$. By correcting the apparent T_1 with the B_1^+ field maps, the true T_1 map was obtained as Figure 4 (e).

To assess the effect of correction with B_1^+ field map, the apparent and true T_1 values were investigated by using a histogram, respectively. The region of interest was manually defined including two hemispheres except for areas of scalp and skull. The histograms of the apparent and true T_1 values were plotted in Figure 5 (a, b), respectively. To analyze the multiple components composing the histograms, three-term Gaussian model was used to fit the envelope of each histogram. The coefficients of Gaussian distributions were estimated and the two major Gaussian distributions were considered to be caused by a white matter and gray matter, respectively. The two major Gaussian distributions for the apparent T_1 values were individually reconstructed and displayed on Figure 5 (c). The means (standard deviations) of the normal distributions were 806 ms (72 ms) and 1159 ms (323 ms), respectively. Through the same process for the true T_1 values, the two major Gaussian distributions were plotted in Figure 5 (d). The means (standard deviations) of the Gaussian distributions were 889 ms (42 ms) and 1570 ms (268 ms), respectively. After the correction, the two distributions became sharp and the two peaks were separated with a larger margin.

Table 1 showed the comparison of T_1 values in white and gray matters with those in other studies [14–16]. In this study, the T_1 value for white matter was acceptable as a true value. The mean of T_1 value for gray matter was similar to the means in the previous studies. However, it had a relatively larger standard deviation comparing with the studies. It was considered to be caused by a partial volume effect. Since the gray matter was located on the surface of each hemisphere and in contact

with CSF having a long T_1 value (> 3 sec.), the Gaussian distribution of gray matter might become broad by a partial volume effect in a voxel including gray matter and CSF.

In this study, we used 3 D spoiled GRE imaging with short TR to achieve high spatial resolution (1 mm isotropic), geometrically less-distorted images and extensive coverage. However, the scan time of 18 min. was not enough for clinical use. It can be improved by parallel imaging techniques such as SENSE (Sensitivity Encoding) [17], GRAPPA (Generalized autocalibrating partially parallel acquisitions) [18], and CAIPIRINHA (Controlled Aliasing in Parallel Imaging Results in Higher Acceleration) [19] with phased array coils. Additionally, the use of shorter TR (<30ms) essentially reduce the scan time, which results in a low SNR of images and a problem for spoiling of residual transverse magnetization.

For improving the accuracy of T_1 value, the key requirement is the spoiling of transverse magnetization in this method. The residue of transverse magnetization causes a steady-state bias on signal intensity, which affects the results of both the FA deviation map and the apparent T_1 map and the error is accumulated. In order to a complete spoiling, the strong regime of gradient crusher and the optimized phase increment in the RF pulses were employed in this study [20].

The combination with the multiple-echo scheme can give additional advantages. By calculating T_1 value on multiple-echo times and averaging them, the SNR could be improved. Additionally, T_2^* map could be obtained because the signal intensity on multiple-echo times would decay with an exponential function with a time constant T_2^*.

In conclusion, we realized the MR pulse sequences and the calculation program to obtain T_1 map. The graphic user interfaces of the processes are developed for convenience. It is expected to use in a study of the brain plasticity in the future.

Acknowledgements

This study was supported by the MEXT-Supported program for the Strategic Research Foundation at Private Universities, 2014-2018.

References

[1] Bennett EL, Diamond MC, Krech D RM. Chemical and anatomical plasticity of brain. 1964 [classical article]. J Neuropsychiatry Clin Neurosci 8:459-70, 1996

[2] Hutton C, Draganski B, Ashburner J, Weiskopf N. A comparison between voxel-based cortical thickness and voxel-based morphometry in normal aging. Neuroimage 48:371-80, 2009

[3] Ashburner J, Friston KJ. Voxel-based morphometry -- the methods. Neuroimage 11:805-21, 2000

[4] Hutton C, De Vita E, Ashburner J, Deichmann R, Turner R. Voxel-based cortical thickness measurements in MRI. Neuroimage 40:1701-10, 2008

[5] Zatorre RJ, Fields RD, Johansen-Berg H. Plasticity in Gray and White. Nat Neurosci 15:528-36, 2012

[6] Okubo G, Okada T, Yamamoto A, Fushimi Y, Okada T, Murata K, et al. Relationship between aging and T 1 relaxation time in deep gray matter: A voxel-based analysis. J Magn Reson Imaging 2017

[7] Helms G, Dathe H, Dechent P. Quantitative FLASH MRI at 3 T using a rational approximation of the Ernst equation. Magn Reson Med 59:667–72, 2008

[8] Deoni SCL, Rutt BK, Peters TM. Rapid combinedT 1 andT 2 mapping using gradient recalled acquisition in the steady state. Magn Reson Med 49:515–26, 2003

[9] Yarnykh V. Improved accuracy of variable flip angle T 1 measurements using optimal radiofrequency and gradient spoiling. Proc. 16th Sci. Meet. Int. Soc. Magn. Reson. Med., p. 234, 2008

[10] Yarnykh VL. Actual flip-angle imaging in the pulsed steady state: A method for rapid three-dimensional mapping of the transmitted radiofrequency field. Magn Reson Med 57:192–200, 2007

[11] Yarnykh V, Yuan C. Actual flip angle imaging in the pulsed steady state. Proc Intl Soc Mag Reson Med 11:2004–2004, 2004

[12] Nehrke K. On the steady-state properties of actual flip angle imaging (AFI). Magn Reson Med 61:84–92, 2009

[13] Yarnykh V. Optimal spoiling of the transverse magnetization in the Actual Flip-angle Imaging (AFI) sequence for fast B 1 field mapping. Proc. 16th Sci. Meet. Int. Soc. Magn. Reson. Med., p. 3090, 2008

[14] Stanisz GJ, Odrobina EE, Pun J, Escaravage M, Graham SJ, Bronskill MJ, et al. T1, T 2 relaxation and magnetization transfer in tissue at 3 T. Magn Reson Med 54:507–12, 2005

[15] Zhu DC, Penn RD. Full-brain T 1 mapping through inversion recovery fast spin echo imaging with time-efficient slice ordering. Magn Reson Med 54:725–31, 2005

[16] Wansapura JP, Holland SK, Dunn RS, Ball WS. NMR relaxation times in the human brain at 3.0 tesla. J Magn Reson Imaging 9 :531–8, 1999

[17] Pruessmann KP, Weiger M, Scheidegger MB, Boesiger P. SENSE: Sensitivity encoding for fast MRI. Magn Reson Med 42:952–62, 1999

[18] Griswold MA, Jakob PM, Heidemann RM, Nittka M, Jellus V, Wang J, et al. Generalized autocalibrating partially parallel acquisitions (GRAPPA). Magn Reson Med 47:1202–10, 2002

[19] Breuer FA, Blaimer M, Heidemann RM, Mueller MF, Griswold MA, Jakob PM. Controlled aliasing in parallel imaging results in higher acceleration (CAIPIRINHA) for multi-slice imaging. Magn Reson Med 53:684–91, 2005

[20] Yarnykh VL. Optimal radiofrequency and gradient spoiling for improved accuracy of T 1 and B 1 measurements using fast steady-state techniques. Magn Reson Med 63:1610–26, 2010

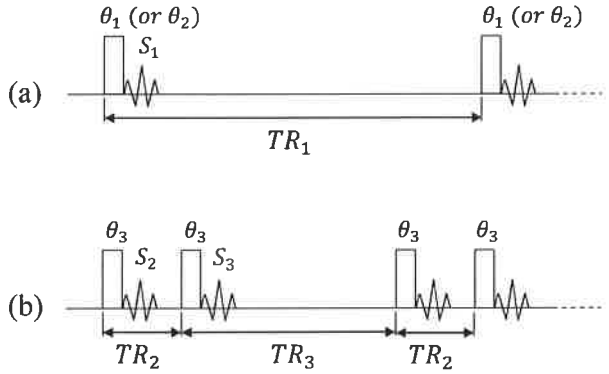


Figure 1. Pulse sequence diagrams for (a) the typical gradient-echo imaging and (b) the actual flip-angle imaging.

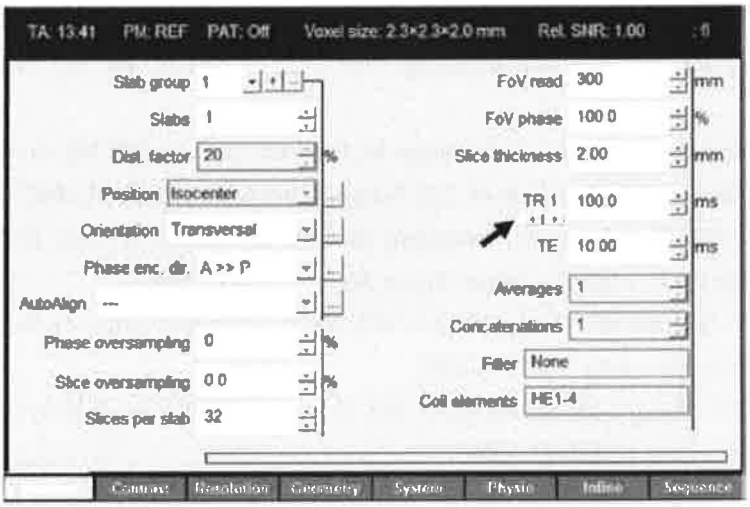


Figure 2. User interface for AFI pulse sequence. The two different TRs could be set (arrow).

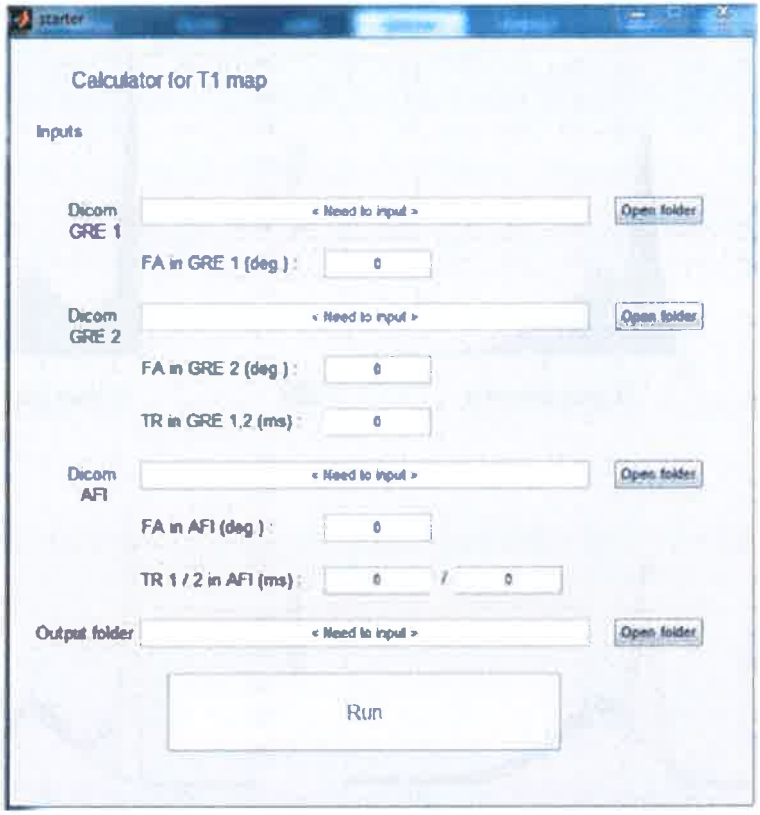


Figure 3. Graphic user interface of the program to calculate T 1 value, implemented on MATLAB.

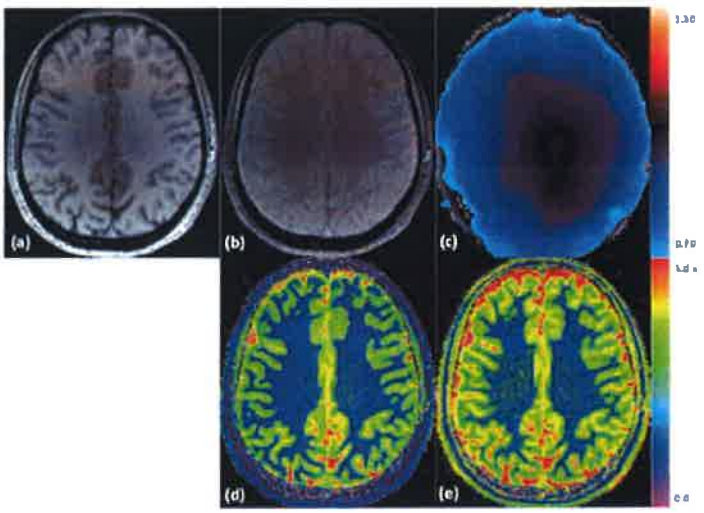


Figure 4. Images of human brain with (a)TR=30ms, θ=20°, (b)TR=30ms, θ= 7 °. Same brightness and contrast (500/600). (c) mis-calibration map of FA (1.0 means accurate FA), (d) apparent T 1 map, and (e) true T 1 map

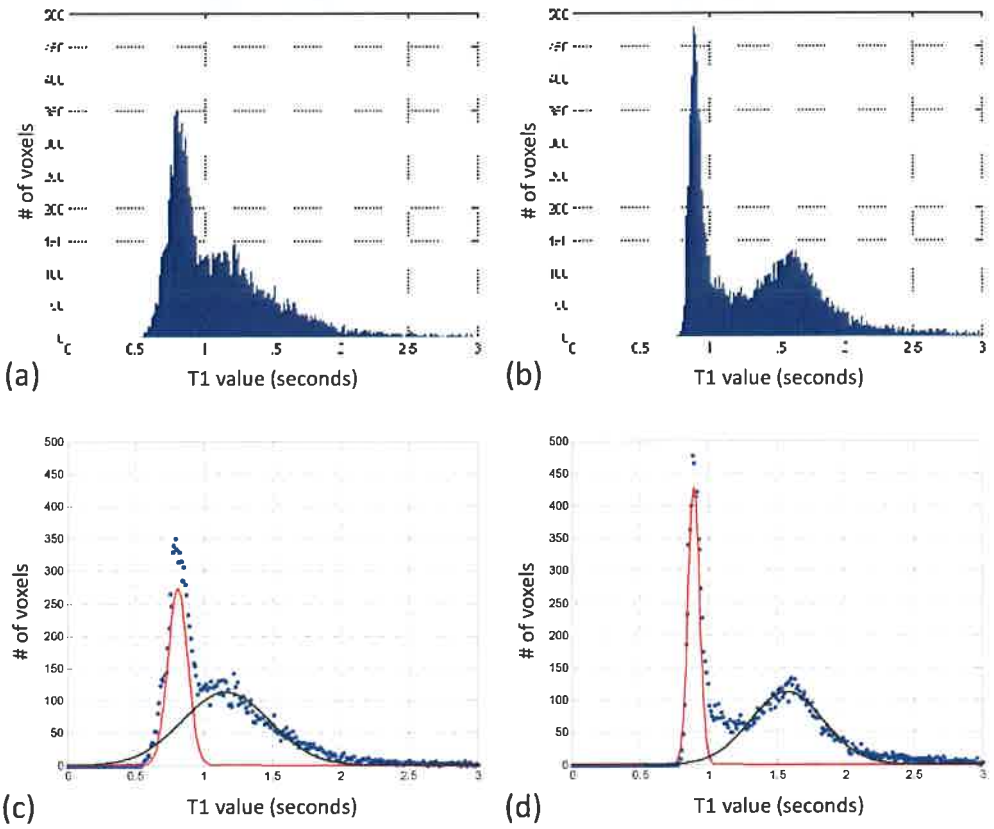


Figure 5. The histograms of (a) and (b) were evaluated from the apparent and the true T 1 maps (Figure 4), respectively. A three-term Gaussian model was used to estimate the peaks and the two major components of the model were plotted in the graphs of (c) and (d), respectively. The two peaks were at 806 ms and 1159 ms in (e) and at 889 ms and 1570 ms in (f), respectively. Each Gaussian distribution became sharper after correction.

Table 1. Comparison of T 1 values

Study	T1 in white matter (ms)	T1 in gray matter (ms)	References
1	750 ± 21 ms	1421 ± 43 ms	Zhu DC and Penn RD, 2005
2	832 ± 10 ms	1331 ± 13 ms	Wansapura JP et al., 1999
3	1084 ± 45 ms	1820 ± 114 ms	Stanisz GJ et al., 2005
4	889 ± 42 ms	1570 ± 268 ms	(Our data)

原 著 論 文

Detection of fast MRI signals by an EEG-like stimulus scheme and multi-voxel pattern analysis

Yul-Wan SUNG, Daehun KANG, Yousuke KAWACHI, Seiji OGAWA
Kansei Fukushi Research Institute, Tohoku Fukushi University

Abstract

Functional MRI (fMRI) has been the most useful tool for identifying the functional roles of brain areas. However, the temporal resolution of fMRI is too slow to measure fast neuronal activity directly. In this study, we propose an experimental scheme and analysis method for the detection of fast MRI signals. We show that fast MRI signals originating from neuronal activity can be measured by the proposed methods.

Keywords : Fast response MRI signals, neuronal activity, Classification, Multi-voxel pattern analysis

Introduction

The functional characteristics of brain areas have been determined due to advances in brain imaging technologies and analysis methods. However, to fully understand how the brain functions, it is necessary to understand the signaling processes between brain areas in addition to their functional characteristics. Although functional MRI (fMRI) has been the most useful tool for identifying the functional roles of brain areas[1], the temporal resolution of fMRI is too slow to measure fast neuronal activity directly. Measuring fast response MRI signals induced by neuronal activity has been a challenging problem. Changes in MRI signals due to neuronal activity are less than 1 nT[2, 3] and it is very difficult to directly detect neuronal activity using typical MRI sequences. Recently, in vivo studies have reported that MRI signals induced by neuronal activity could be detected[4, 5, 6]. However, those studies are rarely reproduced[7]. One recent study showed that changes in MRI signals were below the detectable level of a 0.1% change in signal magnitude[8].

In contrast to MRI experiments, which measure signals based on a single event or the average of several events, EEG experiments detect signals that are much smaller relative to noise by averaging hundreds of events.

To overcome the problem of a low signal to noise ratio in MRI measurements of neuronal activity and detect fast response MRI signals, we devised an EEG-like stimulation scheme to increase the signal to noise ratio by repeating the stimulation hundreds of times at a rate of 400 or 1000 ms. For the detection of fast signals, a fast MRI acquisition was performed using a repetition time (TR) of 50 or 100 ms. For data analysis, we used multi-voxel pattern analysis (MVPA). Pictures of objects and faces were used as visual stimuli. Object processing areas were selected as regions of interest (ROIs). Signals originating from neuronal activity have different values across image voxels (Fig. 1). Therefore, a stimulus can be represented as a pattern in specific brain areas and MRI signals from those object-processing areas can be analyzed using MVPA.

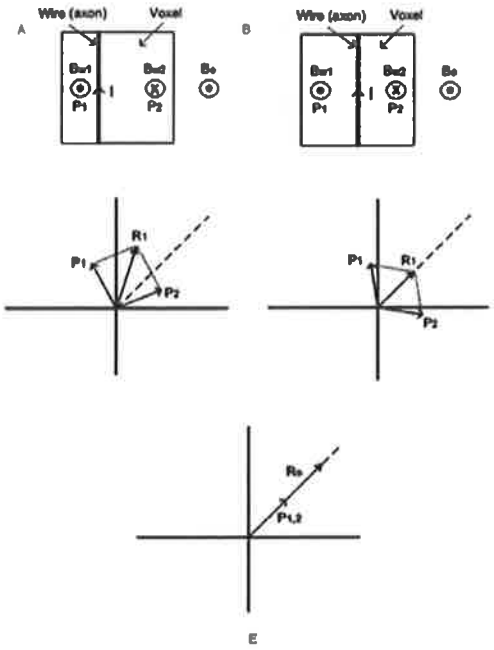


Figure 1. A model representing MRI signal changes induced by neuronal currents. Ro stands for the amplitude of MRI signals. R 1 represents the phase of MRI signals. P 1 and P 2 represent the set of spins in each compartment. Bw 1 and Bw 2 represent the magnetic fields in each compartment as determined by current flow[4].

Methods

MRI measurements

MRI experiments were performed using a Verio system (Siemens, Germany) with a standard, 12-channel head matrix coil operating at 3 Tesla. After the initial localization of images, functional imaging was obtained using single-shot gradient-echo echo planar imaging with a 220 mm field of view and a slice thickness of 5 mm. Two TR (50 and 100 ms) and two matrix sizes (64 x 64 and 128 x 128) were used. The orientation of image slices was approximately parallel to the inferior temporal sulcus.

Experimental procedures

Four experiments were conducted to evaluate signal detectability depending on sampling time, voxel size and stimulus duration. The stimulus events consisted of short and long periods. The long period stimulus event was for measuring BOLD (Blood Oxygenation Level Dependent) signals and the short period stimulus event was for measuring fast MRI signals. Short period events (fast events) were nested in long period events (slow events). Voxel resolution was varied to evaluate partial volume effects. To evaluate the probable effects of BOLD responses on the fast MRI signal, long period events were also varied.

(Exp. 1) This experiment used a TR of 50 ms, a matrix size of 64 x 64 and a stimulus duration of 200 ms (slow events were 12 s and fast events were 200 ms). The scan time was 120 s, during which long period object events and face events were repeated five times. Short period events were repeated 150 times during the five long period events of object or face stimulus (Fig. 2).

(Exp. 2) This experiment used a TR of 100 ms, a matrix size of 128 x 128 and a stimulus duration

of 500 ms (slow events were 12 s and fast events were 500 ms). The scan time was 120 s, during which long period object events and face events were repeated five times. Short period events were repeated 60 times during the five long period events of object or face stimulus (Fig. 3).

(Exp. 3) This experiment used a TR of 100 ms, a matrix size of 128 x 128 and a stimulus duration of 500 ms (slow events were 3 s and fast events were 500 ms). The scan time was 120 s, during which long period object events and face events were repeated 20 times. Short period events were repeated 60 times during the 20 long period events of object or face stimulus (Fig. 4).

(Exp. 4) This experiment used a TR of 50 ms, a matrix size of 64 x 64 and a stimulus duration of

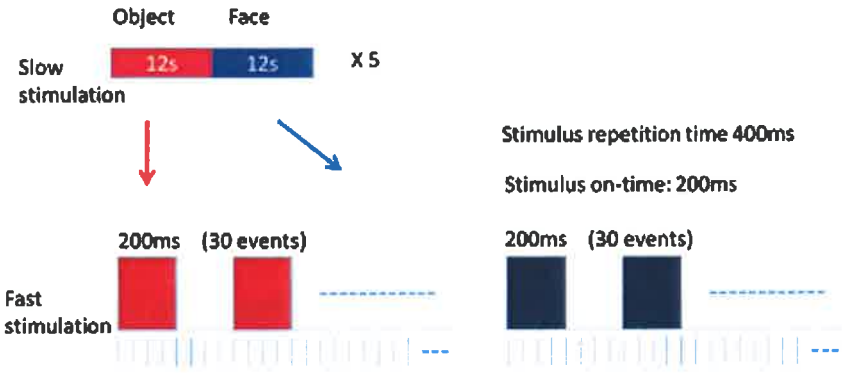


Figure 2. Stimulus scheme for Exp. 1

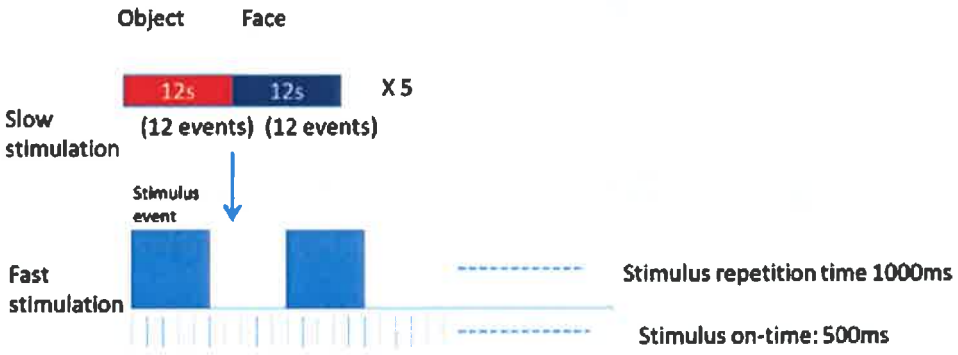


Figure 3. Stimulus scheme for Exp. 2

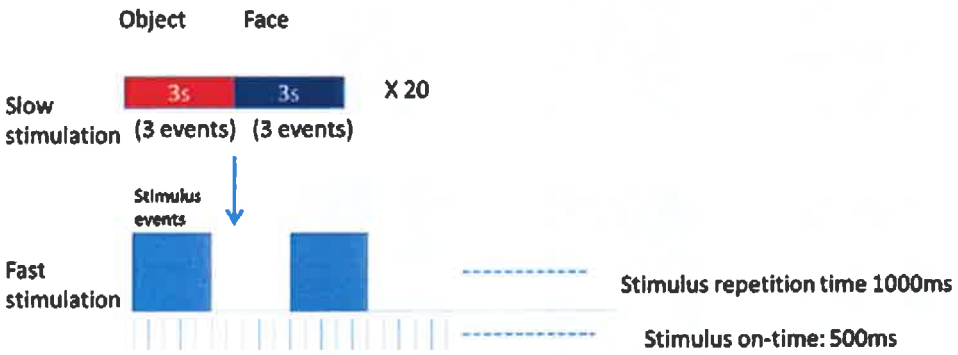


Figure 4. Stimulus scheme for Exp. 3

200 ms (slow events were 1200 ms and fast events were 200 ms). The scan time was 120 s, during which long period object events and face events were repeated 50 times. Short period events were repeated 150 times during the 50 long period events of object or face stimulus (Fig. 5).

Visual stimulation

Visual stimuli were presented on a mirror mounted on a head coil through a projector (spatial resolution, 1024 x 768 pixels; refresh rate 60 Hz; Panasonic, Japan). Pictures of faces and objects were used as stimuli. The pictures occupied 5° x 7° of the subject's visual field around the fovea. All pictures were grayscale images and novel stimuli developed by the investigators (Fig. 6).

Subjects

Four undergraduate students participated. None of the participants had a history of neurological disease or medical conditions that would prevent MRI screenings, such as pregnancy, the presence of a cardiac pacemaker or claustrophobia. Subjects provided written informed consent after a complete description of the study. The study was approved by the Institutional Review Board of Tohoku Fukushi University.

Each subject participated in one of four experiments, Exp. 1, Exp. 2, Exp. 3, or Exp. 4.

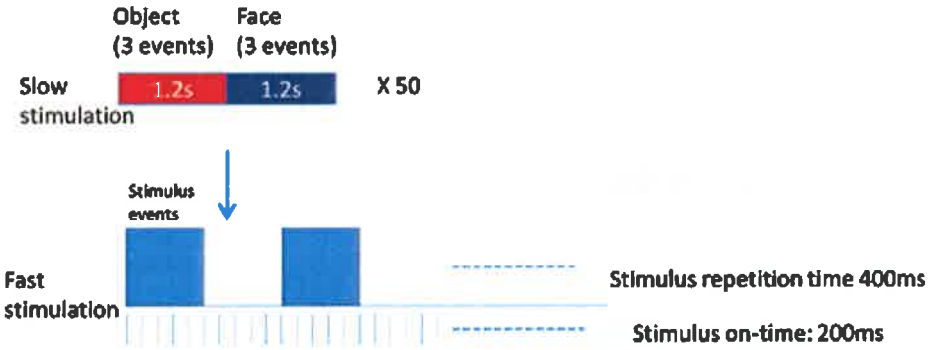


Figure 5. Stimulus scheme for Exp. 4

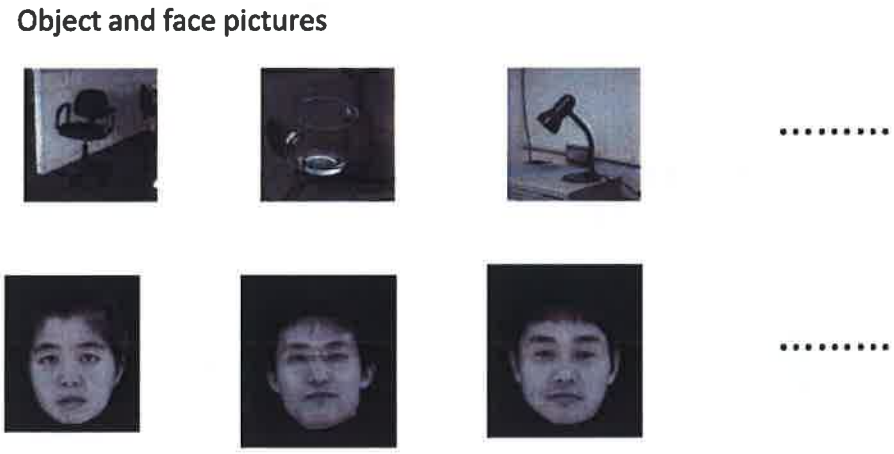


Figure 6. Object and face stimulus pictures

Image data analysis

The image data obtained from fMRI were processed using Brain Voyager QX software (Brain Innovation B.V., Postbus, Netherlands) then analyzed by MVPA using a support vector machine (SVM) for the detection of fast MRI signals (Fig. 7).

Results and discussion

All four experiments investigated the existence of fast MRI signals in four brain ROIs known as object processing areas: the right parahippocampal place area (PPA_R), the right lateral occipital cortex (LOC_R), the left lateral occipital cortex (LOC_L) and the left parahippocampal place area (PPA_L). In Exp. 1, the classification accuracy between the face and the object was 67% at PPA_R, 63% at LOC_R, 63% at LOC_L and 67% at PPA_L. They were all above 50%, the level of chance (Fig. 8). In Exp. 2, the classification accuracy between the face and the object was 70% at PPA_R, 70% at LOC_R, 65% at LOC_L and 80% at PPA_L. In Exp. 3, the classification accuracy between the

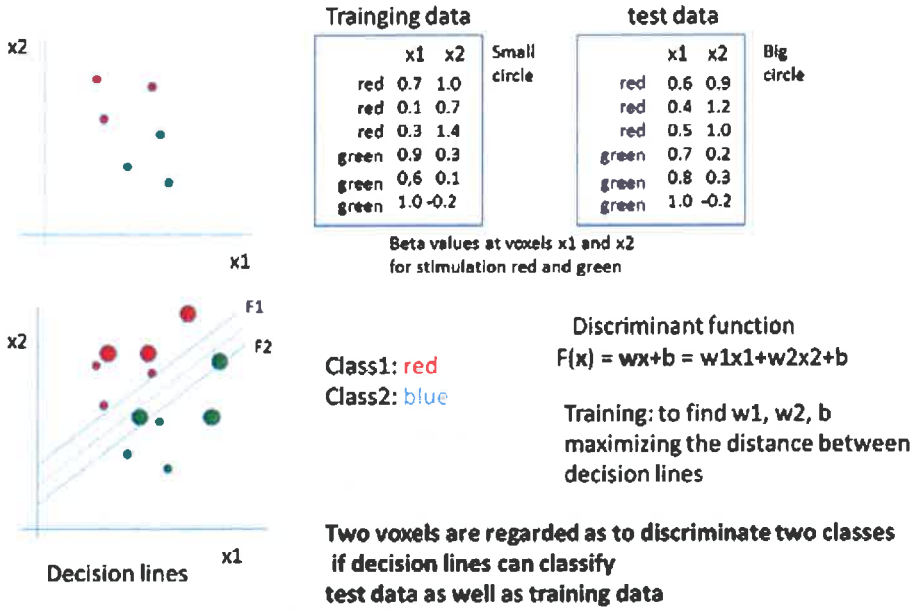


Figure 7. Description of support vector machine

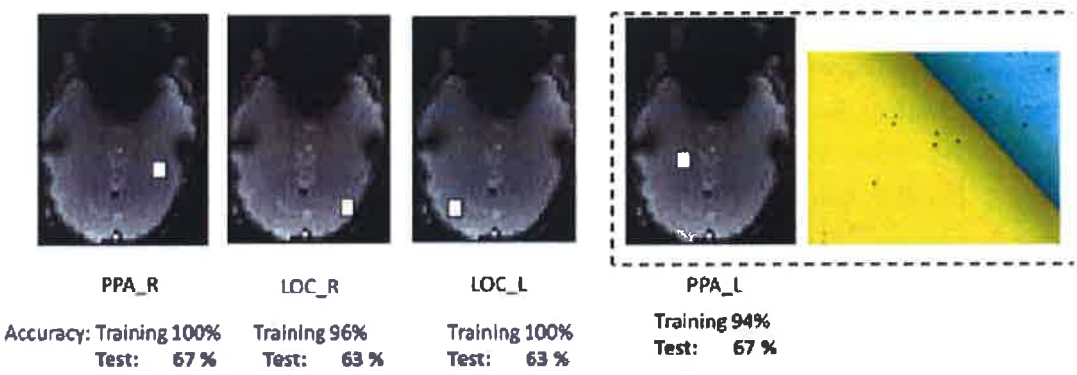


Figure 8. Accuracy at each area. The resulting SVM decision line is shown for PPA_L as an example.

face and the object was 60% at PPA_R, 80% at LOC_R, 70% at LOC_L and 60% at PPA_L. In Exp. 4, the classification accuracy between the face and the object was 63% at PPA_R, 63% at LOC_R, 67% at LOC_L and 77% at PPA_L. The object areas were used as ROIs because, compared with face areas, they are easy to localize using a single slice. The percent change in MRI signal for those areas was 0.1% to 0.2%.

The classification accuracy in these four experiments shows that the category-selective areas of the brain can discriminate between preferred and non-preferred stimuli based on fast MRI signals. This demonstrates that the fast response components were contained within MRI signals acquired via the fast MRI imaging used in this study. Varying imaging parameters and stimulation periods did not change the accuracy pattern, which suggests that the fast MRI signals detected by the fast MRI sequence originated from signal sources other than BOLD signals. The 0.1% ~ 0.2% signal change observed in this study is consistent with previous studies estimating that MRI signals originating from neuronal activity are approximately 0.1%[2,3]. Although this study was conducted with a small number of subjects, we observed a trend of test accuracy that was repeated in supplementary experiments with additional subjects.

In conclusion, our results show that some non-BOLD fast signals originating from neural activity can be detected by the EEG-like stimulation scheme and analysis method proposed in this study. This suggests that the direct measurement of neuronal activity by MRI is possible.

Acknowledgments

This study was supported by MEXT-Supported program for the Strategic Research Foundation at Private Universities, 2014-2018 and JSPS KAKENHI Grant Number 26350995.

References

1. Ogawa S., Lee T.M., Kay A.R., Tank D.W. "Brain magnetic resonance imaging with contrast dependent on blood oxygenation" *Proc Natl Acad Sci U S A.* **87**: 9868-9872, 1990.
2. Bodurka J., Bandettini P.A. "Toward direct mapping of neuronal activity: MRI detection of ultraweak, transient magnetic field changes" *Magn. Reson. Med.* **47**: 1052–1058, 2002.
3. Konn D., Leach S., Gowland P., Bowtell R. "Initial attempts at directly detecting alpha wave activity in the brain using MRI" *Magn. Reson. Imaging* **22**: 1413–1427, 2004.
4. Chow L.S., Cook G.G., Whitby E., Paley, M.N.J. "Investigating direct detection of axon firing in the adult human optic nerve using MRI" *NeuroImage* **30**: 835–846, 2006.
5. Kamei H., Iramina K., Yoshikawa K., Ueno S. "Neuronal current distribution imaging using MR" *IEEE Trans. Magn.* **35**: 4109–4111, 1999.
6. Xiong J., Fox P.T., Gao J.H. "Direct mapping magnetic field effects of neuronal activity by magnetic resonance imaging" *Hum. Brain Mapp.* **20**: 41–49, 2003.
7. Park T.S., Lee, S.Y. "Effects of neuronal magnetic fields on MRI: numerical analysis with axon and dendrite models" *NeuroImage* **35**: 531–538.
8. Luo Q.L., Lu H., Lu H., Senseman D., Worsley K., Yang Y. Gao J.-H. "Physioloically evoked neuronal current MRI in a bloodless turtle brain: Detectable or not?" *Neuroimage* **47**: 1268-1276, 2009.

原　著　論　文

メタ認知と自己成長主導性の関連性

大友ゆき、河地庸介、阿部千裕、成烈完、小川誠二
東北福祉大学

The Relationship between Metacognition and Personal Growth Initiatives

OTOMO Yuki, KAWACHI Yousuke, ABE Chihiro,
SUNG Yul-wan, OGAWA Seiji
Tohoku Fukushi University

Abstract

Metacognition, "cognition about cognition" is generally defined as the ability to report one's own mental state. In a related vein, personal growth initiatives (PGI) have been studied as a metacognitive construct. PGI is defined as developed cognitive and behavioral skills for self-improvement. PGI consists of the cognitive ("planfulness" and "readiness for change") and behavioral ("intentional behavior" and "using resources") components. It is suggested that these components are similar to the two aspects of metacognition, "metacognitive knowledge" and "metacognitive activity (monitoring and control)." However, no studies have quantitatively measured the comprehensive relationship between metacognition and PGI. Here we examined the effect of metacognitive aspects on PGI by using two questionnaires: PGIS- II and metacognitive awareness inventory. Multiple regression analyses showed that different aspects of metacognition have effects on four subcomponents of PGI: "metacognitive knowledge" affects "planfulness" and "intentional behavior"; "monitoring" affects "planfulness," "readiness for change," and "using resources"; and "control" affects "using resources." We suggest that PGI can be represented in terms of the effects of the three subcomponents of metacognition to some extent and imply that there is a possibility of enhancement of PGI by providing training for suitable behavioral metacognitive tasks.

Keywords : metacognition, personal growth initiative, PGI

背　景

1．メタ認知

メタ認知とは、一般に「認知についての認知」と定義される[1)5)6)11)]。認知とは、思考、記憶、学習、知覚などの外界の情報をもとに適応的行動を生み出すための心的活動であり、メタ認知は、それらの認知をしている自己の内的状態についての認知だといえる。

メタ認知の起源は、古代ギリシャのソクラテスが説いた「無知の知」にまで遡る[1)5)11)]。このようにメタ認知の概念は古くから存在していたが、1970年代になりようやく思考や記憶といった基本的な認知機能を対象とした実証的なメタ認知研究が始められ、近年は高次機能の１つと考えられる社会的認知を対象としたメタ認知というように急速な展開を見せている[1)]。

このメタ認知は、研究者によって分類の仕方は多少異なるが、主に「メタ認知的知識」と「メタ認知的活動」の２つの要素に分けられる[11)]。「メタ認知的知識」とは、認知についての信念やエピソードに基づいた知識である。例えば、テスト勉強をするときは書き取りした方が覚えるとか、勉強科目のうち自分が

苦手な科目を理解しているというようなことが挙げられる。もう1つの要素である「メタ認知的活動」は、さらに2つに分類されるのが一般的である[5)11)]。そのうちの1つの「メタ認知的モニタリング」は、ある特定の認知的活動の継続的な進捗状況や現在の状態を査定あるいは評価することである。先の例でいえば、テスト勉強をしていて、どこまでは完璧に学習できていて、どこからがまだ学習できていないのかということを客観的に評価することであるといえる。もう1つの「メタ認知的コントロール」は、進行中の認知的活動について、中断や変更などの調整を行うことである。先の例を用いると、完璧に学習できているというものについては勉強を中断し、まだ学習できていないというものについては、メタ認知的知識に基づいてより効率の良い勉強方法に変更するというように、自己の学習を調整することであるといえる。NelsonとNarens[9)]は、モニタリングに基づいて認知的活動をコントロールし、コントロール結果をまたモニタリングするというように、メタ認知的モニタリングとメタ認知的コントロールは循環的に働くとしたモデルを提唱している。

2．メタ認知と自己成長主導性

近年、メタ認知との関連が示唆される注目すべき心的特性として自己成長主導性がある。自己成長主導性とは、自分の人生をよりよいものにしようという、自己改善のための認知的・行動的スキルを発展させることと定義されており[10)17)]、自己成長がカウンセリングや認知行動療法においても重要視されている[2)8)]ことを考え合わせると、自己成長主導性の向上が心理的な問題解決の重要な役割を担う可能性が考えられる。

自己成長主導性には、「変化への準備」に関する認知、目標設定や計画に関する認知である「計画性」、自己成長のための「積極的な行動」、自分が利用可能な「資源の活用」という4つの因子がある。「変化への準備」と「計画性」は、自己成長のための方法や実現可能な目標の設定の仕方を知っているという認知的側面、「積極的な行動」と「資源の活用」は自己成長のために設定した目標を達成するためのことを利用可能なリソースを活用して率先して行うという行動的側面として2つの側面に大別されている[10)15)]。自己成長主導性は、自己成長に関する自己の内的状態を認知し、その認知に基づいて自己成長のために行動するという点で、メタ認知的なプロセスを使用すると考えられる。実際、自己成長主導性に関する多くの研究で自己成長主導性はメタ認知的な構成概念であるとされている[3)14)16)]。しかし、実際にメタ認知と自己成長主導性の関連性について検討した研究はまだなく、関連があるというのは理論上の話でしかない。また、1．で述べたようにメタ認知にはいくつかの構成要素が含まれるが、自己成長主導性がメタ認知的な構成概念であるか否かの検討やメタ認知の構成要素を考慮して、どの要素が自己成長主導性と関連しているのかという検討はまだなされていない。

メタ認知と自己成長主導性の関連性が未検討という問題は、自己成長主導性の向上を目指したアプローチを妨げている可能性がある。従来の研究では、自己成長主導性の測定は質問紙尺度のみで行われてきたため、具体的な作業や課題が提案されておらず、自己成長主導性そのものをトレーニングによって向上させることは困難であるといえる。一方で、自己成長主導性を基礎づける構成概念とされるメタ認知は記憶や注意等の一般的な心的機能と同様に行動指標によって測定することが可能であり、行動課題を繰り返すことでトレーニングできる可能性が高い。それゆえ、本研究によりメタ認知と自己成長主導性の関連を明らかにすることによって、自己成長主導性の向上のためにメタ認知をトレーニングするというアプローチの実現可能性につながると考えられ、意義深いと考えられる。

3．本研究の目的

メタ認知と自己成長主導性は、理論的には関連があるとされているが、実際にその関連性を検討した研

究や、メタ認知の各構成要素と自己成長主導性について検討している研究は見当たらない。そこで、本研究では両者を測定する質問紙を用いて、メタ認知と自己成長主導性が関連していることを直接的に検討し、メタ認知のどの構成要素がより自己成長主導性に影響を及ぼしているのかを詳細に検討する。近年、脳科学研究の発展に伴い、記憶や知覚などに関する認知機能およびメタ認知に関わる脳内基盤について多くの知見が得られるようになったが[5]、本研究では心的特性である自己成長主導性との関連性を検討することを踏まえ、心的機能としてのメタ認知に着目していく。

1．2．で述べたメタ認知の構成要素と自己成長主導性の認知的側面の特徴から、自己成長主導性の自己成長の方法や実現可能な目標の設定の仕方を知っているという認知的側面のうち、自己成長に関する方略を「知っている」という部分は「メタ認知的知識」が関連すると予測できる。また、実現可能な目標の設定には自己の置かれている状況を評価するという過程が必要となるため「メタ認知的モニタリング」が関連することが予測できる。他方で、自己成長主導性の行動的側面との特徴からは、自己成長主導の自己成長のために設定した目標を達成するためのことを利用可能なリソースを活用して率先して行うという行動的側面のうち、自己成長の達成度を把握するためには自己の状態を顧みる必要があるため「メタ認知的モニタリング」が関連し、自己成長の達成度に基づいて利用可能なリソースを調整しながら行動することを考えると「メタ認知的コントロール」が関連すると予測できると考える。

本研究により、メタ認知と自己成長主導性の関連性、メタ認知が自己成長主導性に及ぼす影響を明らかにすることで、自己成長主導性を向上させるアプローチとしてのメタ認知の可能性を見出せると考える。

方　法

参加者

大学生および大学院生105人（男性20名、女性85名）で、平均年齢20.63歳（SD=1.77）であった。参加者には本研究について書面および口頭によるインフォームドコンセントを行った。なお、本研究は東北福祉大学研究倫理審査委員会の承認（16K00212）を得て実施した。

調査内容

(1) 成人用メタ認知尺度[1]

Schraw と Dennison によって開発された Metacognitive Awareness Inventory[13] を日本語訳した28項目からなる成人用メタ認知尺度を使用した。質問紙は３つの下位因子からなっており、「モニタリング」11項目、「コントロール」９項目、「メタ認知的知識」８項目で構成され、それらをまとめる高次の因子として「メタ認知」が仮定されている。回答は、“全くあてはまらない”“あまりあてはまらない”“ややあてはまらない”“ややあてはまる”“だいたいあてはまる”“とてもあてはまる”の６件法とし、下位因子の得点と合計得点を算出した。

(2) 自己成長主導性尺度 II（PGIS-II）[17]

Robitschek らによって作成された Personal Growth Initiative Scale-II（PGIS-II）[10] を日本語訳した16項目からなる PGIS- II 日本語版を使用した。質問紙は「計画性」、「資源への活用」、「積極的な行動」、「変化への準備」の４つの下位因子、各４項目で構成されている。回答は、“全く当てはまらない”“当てはまらない”“あまり当てはまらない”“やや当てはまる”“当てはまる”“かなり当てはまる”の６件法とし、下位因子の得点と合計得点を算出した。

結　果

本研究では、まず、それぞれの尺度間の関連を調べるために、成人用メタ認知尺度の下位因子「モニタリング」「コントロール」「メタ認知的知識」と自己成長主導性尺度の下位因子「計画性」「変化への準備」「積極的な行動」「資源の活用」との2変量の相関分析を行った（Table 1）。成人用メタ認知尺度の3つの下位因子と「計画性」（モニタリング：r=.48, p<.001、コントロール：r=.23, p<.05、メタ認知的知識：r=.46, p<.001）「変化への準備」（モニタリング：r=.44, p<.001、コントロール：r=.21, p<.05、メタ認知的知識：r=.38, p<.001）「積極的な行動」（モニタリング：r=.31, p<.01、コントロール：r=.22, p<.05、メタ認知的知識：r=.44, p<.001）との間には、それぞれ有意な相関があった。成人用メタ認知尺度と「資源の活用」では、3つの下位因子のうち「コントロール」のみに有意な相関があった（r=.23, p<.05）。

Table 1　Correlations between subscales of the Personal Growth Initiative Scale-II and Metacognitive Awareness Inventory

	モニタリング	コントロール	メタ認知的知識	計画性	変化への準備	積極的な行動	資源の活用
モニタリング	1	.563***	.653***	.475***	.439***	.306**	-0.067
コントロール		1	.564***	.226*	.205*	.215*	.233*
メタ認知的知識			1	.456***	.380***	.439**	0.145
計画性				1	.730***	.670***	.194*
変化への準備					1	.438***	0.034
積極的な行動						1	.272**
資源の活用							1

***p<.001 **p<.01 *p<.05

次に、メタ認知が自己成長主導性に与える影響を詳細に検討するために、自己成長主導性尺度の4つの因子をそれぞれ目的変数とし、ステップワイズ法による重回帰分析を行った（Table 2）。その結果、「計画性」を目的変数とした場合には、「コントロール」が除外され、「モニタリング」（β=.31, p<.01）と「メタ認知的知識」（β =.25, p<.05）が有意に影響しており、説明率は約26%であることが示された（R^2=.26, p<.001）。「変化への準備」を目的変数とした場合には、「コントロール」と「メタ認知的知識」が除外され、「モニタリング」（β =.44, p<.001）が有意に影響しており、説明率は約19%であることが示された（R^2=.19, p<.001）。「積極的な行動」を目的変数とした場合は、「モニタリング」と「コントロール」が除外され、「メタ認知的知識」（β =.44, p<.001）が有意に影響しており、説明率は約19%であることが示された（R^2=.19, p<.001）。「資源の活用」を目的変数とした場合には、「メタ認知的知識」が除外され、「コントロール」（β =.40, p<.01）と「モニタリング」（β=-.29, p<.05）が有意に影響しており、説明率は約11%であることが示された（R^2=.11, p<.05）。

なお、説明変数間に相関はあったものの著しく強い相関ではなく、許容度（.57～1.00）やVIF（1.00～1.74）の値から、多重共線性の問題はなく上記の偏回帰係数は適切に推定できたものとして判断した。

考　察

本研究の結果から、メタ認知尺度と自己成長主導性尺度の各下位因子との間には有意な相関があることが示された。さらに重回帰分析の結果、「計画性」は「モニタリング」と「メタ認知的知識」から、「変化への準備」は「モニタリング」から、「積極的な行動」は「メタ認知的知識」から、「資源への準備」は「モニタリング」と「コントロール」から、それぞれ影響を受けていることが示された。また、メタ認知によ

Table 2　Multiple regression analysis with subscales of the Personal Growth Initiative Scale-II as a dependent

	計画性			変化への準備			積極的な行動			資源の活用		
	β	許容度	VIF	β	許容度	VIF	β	許容度	VIF	β	許容度	VIF
モニタリング	.309**	.574	1.744	.439***	1.000	1.000				-.291*	.683	1.464
コントロール										.397**	.683	1.464
メタ認知知識	.254*	.574	1.744				.439***	1.000	1.000			
R	.512			.439			.439			.335		
R^2	.263***			.193***			.193***			.112**		

***p<.001 **p<.01 *p<.05

る自己成長主導性の下位因子の分散に対する説明率が11～26%と有意であり、それぞれの偏回帰係数は.25～.44で有意であることからいずれのメタ認知の下位因子も自己成長主導性に影響していることが示された。以上から、自己成長主導性のそれぞれの側面は、異なるメタ認知の構成要素によって影響されると結論づけられる。

自己成長主導性の認知的側面である「計画性」と「変化への準備」は、関連すると予測した「メタ認知的知識」と「モニタリング」が影響することが示された。「計画性」は“どのような段階を踏めば自分自身が求められる変化を遂げられるか知っている”や“自分自身について変えたいと思う現実可能な目標を設定している”などの質問項目から測定され、自分自身への期待や置かれている現実について「モニタリング」を行い自分に見合った計画をこれまでの経験から培われた「メタ認知的知識」を活用して立てるという側面であるといえる。「変化への準備」では「モニタリング」のみが影響することが示された。「変化への準備」は“私は今、自分自身が何らかの変化をする態勢が整っているということができる”や“自分自身が変わるために何が必要かを理解している”などの質問項目からなり、自己の変化に対して「モニタリング」を行うことで結論づけられる側面であるといえる。

自己成長主導性の行動的側面である「積極的な行動」はメタ認知の構成要素のうち「メタ認知的知識」のみに影響されることが示された。メタ認知的知識は自己成長主導性の認知的側面と関連があると予測した要素であり、この結果は予想に反していた。しかし、Schraw と Moshman[12] は、自己成長主導性の行動的側面と関連があると予測したメタ認知的コントロールについて「年齢が上がるにつれ、多くのメタ認知的知識を所有し、課題に取り組む前に、課題への取り組みを調整するためにその知識を使う」と述べており、「積極的な行動」を測定する質問項目をみてみると“私は自分を向上させようと積極に取り組む”や“私は、絶えず人として成長しようとしている”などであり、自分が向上するためや成長するための知識を実際に行動する前に使用していると考えられることから「メタ認知的知識」が「積極的な行動」に影響する可能性は十分に考えられる。また、今回使用した「メタ認知的知識」を測定する質問項目は“過去に上手くいったやり方を試みている”や“重要なことがらに対して、意識的に注意を向けている”など、メタ認知的知識があることに加えて、それをどう活用しているのかという行動的な側面が含まれると考えられることも今回の結果を支持するものと思われる。もう1つの自己成長主導性の行動的側面である「資源の活用」では「モニタリング」は負の方向に影響していることが示された。つまり、自己を「モニタリング」しないことが、「資源の活用」を促す傾向があるということを表している。この結果に関して「資源の活用」を測定する質問項目をみてみると、“自分自身を変えようとするとき、積極的に支援を探し求める”や“成長しようと思うとき、資源を活用する”などであり、「モニタリング」した結果、どうすることにしたのかという「コントロール」の要素が強い質問項目になっているといえる。Nelson と Narens[9] の「コントロール」と「モニタリング」は循環的に働くというモデルに基づいて考えると、「資源を活用」しようとする段階は「モニタリング」に優先して「コントロール」が働いている段階であるた

めに、「モニタリング」を行うことは負の方向に影響することが推測される。この推測を支持するように、「モニタリング」とは反対に「コントロール」は正の方向により強い影響を「資源の活用」に及ぼしていることが示された。

本研究では、従来理論的に関連があるとされていたメタ認知と自己成長主導性の関連性を、質問紙を用いて詳細に検討を行った。その結果、先行研究で示唆されていた通り、メタ認知と自己成長主導性には関連があり、メタ認知の異なる構成要素が自己成長主導性の下位因子にそれぞれ影響していることが示された。

このことから、メタ認知の構成要素のうちのどの要素に焦点を当てたトレーニングをすることが、効率的な自己成長主導性の向上を促すことになるのかという知見を得られたといえる。Nelson と Dunlosky[8] はメタ認知的モニタリングに関する行動指標を用いた研究で、遅延学習判断効果という学習できたかどうかの判断は学習から時間をおいてからする方が、正確に判断できるようになるという効果を提唱している。この知見を応用すれば、メタ認知的モニタリングはある程度の時間をおいて行うようにトレーニングをすることで向上でき、関連する自己成長主導性の側面の向上も期待できる。将来的に自己成長主導性の向上を目指したメタ認知トレーニングを開発できる可能性は十分にあるといえる。

また、本研究の知見は自己成長主導性における認知的・行動的側面という区分に疑問を投げかけている。「メタ認知的知識」が自己成長主導性の行動的側面である「積極的な行動」と関連を示していたからである。この結果は、行動的側面とされてきた「積極的な行動」が、認知的側面を含む可能性を示唆している。このことは、従来の多くの先行研究[10)15)] でなされてきた自己成長主導性の 4 つの因子について認知的側面と行動的側面の 2 つの側面に区分することが適切かどうかという検討の必要性を提示しており、本研究のメタ認知との関連を検討する試みが自己成長主導性の概念の精緻化につながっていくものと期待できる。

本研究では100人規模の参加者を対象とするためにも質問紙を用いたメタ認知の測定を行ったが、この測定については欠点もある。質問紙で測定できるメタ認知は、過去の、あるいは普段のメタ認知を回顧的に自分自身で意識的に判断したものに限られている。しかしながら、日常生活の場面を考えると、意識することなくメタ認知的機能を用いている可能性はあると考えられる。このように、自分自身が意識できる部分、意識できない部分を含めて、実際の、遂行時のメタ認知を評価することは質問紙測定ではできない。加えて、質問紙測定では、参加者が社会的に望ましいとされる反応をしようとする反応バイアスが影響することが知られており、考慮が必要である[4)]。したがって、今後は、回顧的ではない遂行時のメタ認知を測定できる行動指標をも導入して、自己成長主導性の向上を目指したメタ認知的なトレーニングの具体的な開発を視野に入れたより詳細な検討が求められる。

謝辞

本研究は、東北福祉大学感性福祉研究所における文部科学省の私立大学戦略的研究基盤形成支援事業（平成26年度～30年度）による私学助成を得て行われた。本論文執筆に際してサポートして頂きました皆川州正教授、感性福祉研究所の関係各位に心より感謝申し上げます。

引用文献

1）阿部真美子, 井田政則「成人用メタ認知尺度の作成の試み－ Metacognitive Awareness Inventory を用いて－」『立正大学心理学研究年報』1, pp.23-34, 2010

2）Beck J. S. *Cognitive Behavior Therapy, Second Edition: Basics and Beyond*, Guilford Press, 2011

3）Büyükgöze H., "An Investigation of Pre-service Science and Mathematics Teachers' Personal Growth Initiative" *Acta Didactica Napocensia*, 8 (3), pp.47-53, 2005
4）Crowne D.P., Marlowe D. "A new scale of social desirability independent of psychopathology" *Journal of Consulting Psychology*, 24 (4), pp.349-354, 1960
5）Dunlosky J., Metcalfe J., 湯川良三, 金城光, 清水寛之 訳『メタ認知　基礎と応用』北大路出版, 2010
6）Flavell J.H. "Metacognition and Cognitive Monitoring A New Area of Cognitive – Developmental Inquiry" *American Psychologist*, 34 (10), pp.906-911, 1979
7）諸富祥彦『人生にいかすカウンセリング－自分を見つめる 人とつながる』有斐閣, 2011
8）Nelson T.O., Dunlosky J. "When People's Judgments of Learning (JOLs) are Extremely Accurate at Predicting Subsequent Recall: The "Delayed-JOL Effect"" *Psychological Science*, 2 (4), pp.267-270, 1991
9）Nelson T.O., Narens L. "Metamemory: A theoretical framework and new findings" *Psychology of Learning and Motivation*, 26, pp.125-173, 1990
10）Robitschek C., Ashton M.W., Spering C.C., Geiger N., Byers D., Schotts G.C., Thoen M.A. "Development and Psychometric Evaluation of the Personal Growth Initiative Scale-II" *Journal of Counseling Psychology*, 59 (2), pp.274-287, 2012
11）三宮真智子『メタ認知　学習力を支える高次認知機能』北大路書房, 2008
12）Schraw G., Moshman D. "Metacognitive Theories" *Educational Psychology Review*, 7 (4), pp.351-371, 1995
13）Schraw G., Sperilng R.A. "Assessing metacognitive awareness." *Contemporary Educational Psychology*, 19, pp.460-475, 1994
14）Shorey H.S., Little T.D., Snyder C.R., Kluck B., Robitschek C. "Hope and personal growth initiative: A comparison of positive, future-oriented constructs" *Personality and Individual Differences*, 43, pp.1917-1926, 2007
15）Shigemoto Y., Ashton M.W., Robitschek C. "Predictors of Growth in the Aftermath of Traumatic Events: The Role of Personal Growth Initiative" *Journal of Loss and Trauma*, 21 (5), pp.399-409, 2016
16）徳吉陽河, 岩崎祥一「自己成長主導性尺度 II (PGIS-II) 開発の試み：目標行動スキル・自動思考との関連」『日本パーソナリティ心理学会大会発表論文集』20, pp.82, 2011
17）徳吉陽河, 岩崎祥一「自己成長主導性尺度 II (PGIS-II) 日本語版の開発と心理的測定」『心理学研究』85 (2), pp.178-187, 2014

The effects of short-term practice on executive functions

著者	ABE CHIHIRO, KAWACHI YOUSUKE, SUNG YUL-WAN, OGAWA SEIJI
journal or publication title	Tohoku psychologica folia
volume	75
page range	15-21
year	2017-03-22
URL	http://hdl.handle.net/10097/00120348

Tohoku Psychologica Folia
2016, *75*, 15–21

The effects of short-term practice on executive functions

CHIHIRO ABE (阿部千裕)[1], YOUSUKE KAWACHI (河地庸介)[2],
YUL-WAN SUNG (成　烈完)[2] AND SEIJI OGAWA (小川誠二)[2]

Executive functions (EFs) are considered to be functions that adaptively control actions and thoughts in daily life, and consist of three components—updating, shifting, and goal-related processing. Previous studies reported that EF task performance is improved after practice over 1 month. Actually, improvement is often observed to begin earlier. Thus, we hypothesized that practice effects would occur even after short-term practice of approximately 30 minutes for each EF. In the present study, we measured the practice effect of EFs as a function of the number of blocks by using three behavioral tasks corresponding to the three components (Miyake et al., 2000). The results revealed that although the practice effect for the goal-related processing component task was marginally significant, even short-term practice of the updating and shifting components significantly improved performance. The findings suggest that an efficient practice schedule for EFs might exist, which can be linked to a possible resolution of psychological adjustment problems that individuals with EF deficits and maladaptive behavior have in daily life.

Key words: executive functions, practice effects, short-term practice

Introduction

General intelligence is conventionally known to be essential for humans to behave adaptively in various environments (e.g., Sternberg, 1994). However, recently, executive functions (EFs) are drawing attention in such adaptive daily life behaviors as planning, decision making, and controlling actions (Damasio, 1994; Friedman et al., 2006). EFs are defined as functions that control actions and thoughts (Baddeley & Hitch, 1974; Miyake et al., 2000). Though EFs may share similar roles with general intelligence, previous studies demonstrate that they are different. Some individuals with frontal lobe damage show EF deficits directly related to maladaptive behavior, but have intact general intelligence as measured by traditional intelligence tests (Damasio, 1994; Miyake et al., 2000). Thus, EFs are considered to be different from general intelligence and to be critical functions for adaptive social life.

Recent empirical studies reported that EFs are constructed from three functional components: updating, shifting, and goal-related processing (Miyake et al., 2000; Friedman et al., 2008; Friedman & Miyake, 2017). Updating is the ability to update and eliminate information content included in working memory. Shifting is the ability to flexibly switch

1. Course of Welfare Psychology, Graduate School of Synthetic Welfare, Tohoku Fukushi University
6-149-1, Kunimigaoka, Aoba-ward, Sendai 9893201, Japan
Tel: +81-22-728-6085 E-mail: apety22@gmail.com
2. Kansei Fukushi Research Institute, Tohoku Fukushi University

mental sets. Goal-related processing is the ability to maintain and manage goals, and use those goals to adjust ongoing processing. The goal-related processing component is also referred as "Common-EF" by Friedman and Miyake (2017) and had a modulatory effect on all the EF tasks used by Friedman et al. (2008).

An important related issue is the improvement of EFs after practice (Dahlin, 2009; Klingberg, 2010), because the effects of practice may be a measure of improved ability for individuals with EF deficits to adapt to their environment. The present study examined the effect of short-term practice on EFs. Most previous studies demonstrated that performance in EF tasks is significantly affected by practice for more than one month (Basso, Bornstein, & Lang, 1999; Benikos, Johnstone, & Roodenrys, 2013; Verbeken, Braet, Goossens, & Oord, 2013). It remains to be determined whether there is a possible limit to how long practice affects performance on EF tasks corresponding to all three components. Collie, Maruff, Darby, and McStephen (2003) showed improvement of performance on various tasks during the early phase of practice. Therefore, we hypothesized that practice effects would occur even in short-term practice of approximately 30 minutes for each EF task. We predicted that performance on EF tasks would improve (i.e., accuracy rate becomes higher and response time becomes shorter) as each trial for each EF task was repeated.

Method

Participants

Twenty-four healthy graduate and undergraduate students (age of 21.38 years, SD = ±1.96 years) participated in this study. All experiments were approved by the Ethical Committee of Tohoku Fukushi University and conducted according to principles of the Declaration of Helsinki. Written informed consent was obtained from all participants.

Materials, EF Tasks, and Procedure

All stimuli were made using MATLAB (The MathWorks, Inc., Natick, MA) and the Cogent Graphics package (http://www.vislab.ucl.ac.uk/cogent.php). Stimuli were controlled on a PC (Epson Endeavor MT7900, Epson, Nagano, Japan) and were presented on a CRT monitor (Mitsubishi Diamondtron Flat RDF225; resolution 1024 × 768 pixels; refresh rate 60 Hz, Mitsubishi, Tokyo, Japan). In the present study, three of the nine EF tasks used in Friedman et al. (2008)'s study were used; each of these corresponds to one of the three functional components. Completion of all tasks takes approximately two hours, including 10-minute rests after the completion of each task. The number of blocks for each task was decided so that each task could be completed within approximately 20-30 minutes, considering the experimental load imposed on participants. The order of tasks was counterbalanced for every participant.

Updating task: Keep track task. Figure 1 shows the stimulus sequence of the keep track task. Participants firstly were presented two, three, or four target categories of six possible categories (動物, 色, 国, 時, 金属, 家族) at the bottom of the display. Fifteen words, including two or three words from each category, were serially presented at the center of the display

in random order after participants pressed the space key. Each word was presented for 1500 milliseconds (ms). After the stimulus presentation, they wrote down the last presented word in each of the target categories on the answer sheet. When they finished answering, they pressed the space key to perform the next trial. The task was performed in a practice block of three trials and four blocks of 12 trials. In the practice block, they performed three trials in order from two to four target categories, and then performed four times for each of two to four target categories in random order in each block. Participants were asked to recall a total of 36 words. The dependent measure was the proportion of words recalled correctly on each trial.

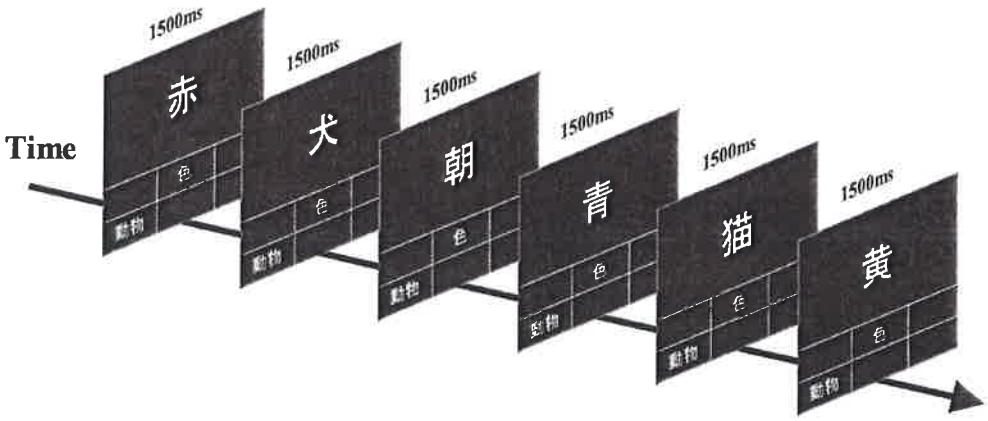


Figure 1. The stimulus sequence of the keep track task. The sequence shows the 2-category condition. In this case, the correct answers were "黄" for the "色" category and "猫" for the "動物" category.

Shifting task: Category switch task. Figure 2 shows the stimulus sequence of the category switch task. Participants were asked to categorize words at the center of the display as quickly and correctly as possible, depending on a cue in the upper part of the display in each trial. A word was randomly selected from words used by Mayr and Kliegl (2000) and translated into Japanese. A cue was a heart or a cross, which cued categorization in terms of whether the word described a living or nonliving thing, or whether it described a thing that is smaller or larger than a soccer ball. A word was presented 1500 ms after the onset of a cue. The word disappeared after they responded, and the next cue was presented after a blank of 350 ms. If participants did not respond during 1500 ms, the next trial was performed. A cue was randomly presented trial by trial with the constraint that no more than four switch trials could be performed. The right key was assigned to a living thing and a thing that is larger than a soccer ball, and the left arrow key to a nonliving thing and a thing that is smaller than a soccer ball. In the practice block, 24 trials were performed, including 12 switch trials and 12 no switch trials. In the test block, eight blocks of 54 trials were performed, including 27 switch trials and 27 no switch trials. The first six trials of each block were regarded as practice trials and excluded from the statistical analysis. The dependent measure was the switch cost, which is the median response time difference between the switch trials and no-switch trials.

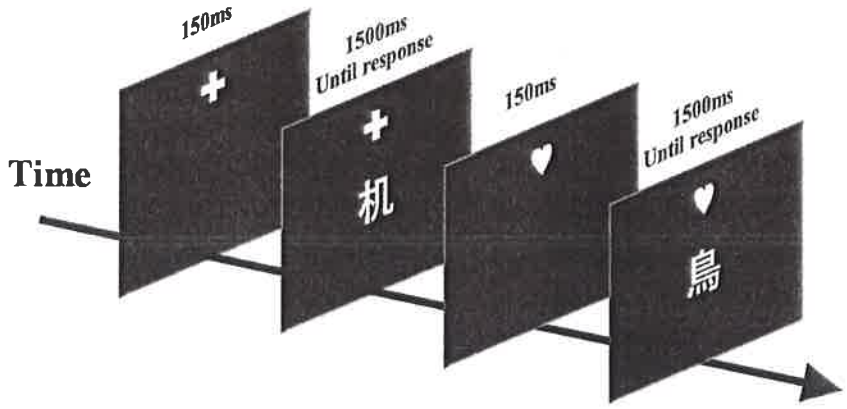


Figure 2. The stimulus sequence of the category switch task.

Goal-related processing task: Stop-signal task. Figure 3 shows the stimulus sequence of the stop-signal task. A square or a circle was randomly presented as the go signal at the center of the display for 1500 ms, following this a fixation cross was presented for 250 ms. The stop-signal (200 ms, 1800 Hz tone) was presented through headphones (DR-531, Elega Acous Co., Ltd., Tokyo, Japan) at a comfortable listening level. Participants were asked to judge a square or a circle as quickly and correctly as possible in the no-stop signal trial, and inhibit a response in the stop-signal trial. The stop-signal delay (SSD) was defined as the interval between the onset of the stop-signal and the go signal. The initial SSD was 250 ms; SSD was adjusted depending on participants' performance (Logan, Schachar, & Tannock, 1997). If a participant successfully inhibited (or failed to inhibit) a response on the stop-signal trial, then SSD increased (or decreased) by 50 ms. Participants were instructed to stop a response if they could when they heard the stop signal, but not to worry about failing to stop. They were also instructed that they should not wait for the stop-signal. There were eight practice trials, and six blocks of 72 trials were performed. In all blocks, stop-signals were presented on 25% of the trials in random order. The dependent measure was the median RT in the no-stop signal trials with correct response (go RT).

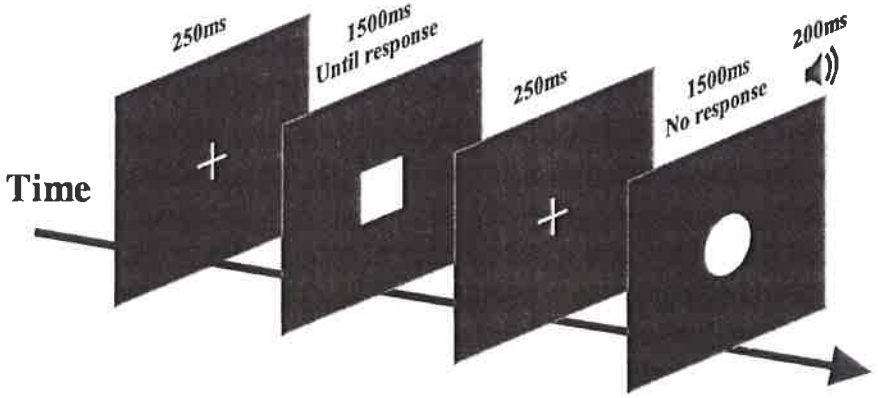


Figure 3. The stimulus sequence of the stop-signal task.

Results

Table 1 shows the mean accuracy (%) in the keep track task, the mean switch cost in the category switch task, and the mean median go RT in the stop-signal task across all participants as a function of the number of blocks. Repeated measures analysis of variance (ANOVA) for each dependent variable of each task was conducted on the variable of the number of blocks (and the number of target categories only in the keep track task).

In the keep track task, the main effects of both the number of target categories and the number of blocks were significant, $F(2, 46) = 72.24$, $p < .001$; $F(3, 69) = 8.30$, $p < .001$, respectively. The interaction was also significant, $F(6, 138) = 3.85$, $p = .001$. In the 3-target-categories condition, the simple main effect of the number of blocks was significant, $F(3, 207) = 3.21$, $p < .05$. In the 4-target-categories condition, the simple main effect of the number of blocks was significant, $F(3, 207) = 12.59$, $p < .001$. As the number of blocks increased, the proportion of correct recall became higher in the 3- and 4-target-categories condition. In the 2-target-categories condition, the proportion of correct recall was almost 100 % over all the blocks and there was no room for improvement in task performance.

In the category switch task, the main effect of the number of blocks was significant, $F(7, 161) = 3.90$, $p < .001$. As the number of blocks increased, the cost to switch categorization, the switch cost, became smaller.

In the stop-signal task, the data of one participant were excluded from the following analysis as an outlier for the percentage change score between the 1st and last blocks. The main effects of the number of blocks were marginally significant, $F(5, 100) = 2.20$, $p = .061$. As the number of blocks increased, the median go RT tended to become shorter.

Table 1. Descriptive and *F* statistics for the EF tasks. All data are presented as mean (±SD). Note: M = Mean; SD = Standard Deviation; ctgry (2) = 2-target category; ctgry (3) = 3-target category; ctgry (4) = 4-target category; RT = response time. %change was calculated by dividing the difference in values of the first and the last blocks by the value of the first block.
+p<.1; *p<.05; **p<.005; ***p<.001

EF tasks	Block 1 M (SD)	Block 2 M (SD)	Block 3 M (SD)	Block 4 M (SD)	Block 5 M (SD)	Block 6 M (SD)	Block 7 M (SD)	Block 8 M (SD)	%change	F statistic
Keep track task										
ctgry(2) accuracy (%)	98.44 (4.22)	96.35 (6.88)	98.96 (3.53)	96.88 (5.53)	-	-	-	-	-1.59	0.59
ctgry(3) accuracy (%)	90.28 (9.73)	93.4 (8.14)	95.49 (7.36)	96.88 (5.92)	-	-	-	-	7.31	3.21*
ctgry(4) accuracy (%)	73.7 (16.06)	79.43 (14.21)	83.33 (10.69)	86.98 (10.08)	-	-	-	-	18.02	12.59***
Category switch task										
switch cost (ms)	230.5 (163.82)	197.48 (148.38)	163.29 (122.63)	134.21 (110.54)	124.18 (114.63)	140.75 (151.96)	110.96 (138.89)	98.42 (86.34)	57.3	3.91***
Stop-signal task										
go RT (ms)	523.34 (112.25)	516.22 (137.42)	507.42 (94.02)	499.9 (81.58)	499.56 (89.64)	497.89 (99.02)	-	-	4.86	2.2+

Discussion

The results of this study indicated that the performance of EFs improved. Although the improvement by practice of the goal-related processing component was trending toward significance, generally improved performance of the updating and shifting components was

obtained by short-term practice of approximately 30 minutes for each task.

The long-term practice effects were examined for the updating (Dahlin, Neely, Larsson, Backman, & Nyberg, 2008) and shifting components (Basso et al., 1999). For the updating component, Dahlin et al. (2008) reported approximately 16 % performance improvement by long-term practice over five weeks. The present short-term practice produced improvement of 18.02 % for the updating component. Thus, both long- and short-term practice may have similar effects on the updating component. For the shifting component, Basso et al. (1999) reported that shifting performance improved 40.56 % (i.e., the number of perseverative errors decreased) by practice over 12 months. Even by very short-term practice in the present study, shifting performance displayed more improvement (57.3%) than in the previous study. Although it may be difficult to compare with different task performances for the percentage change scores (3-back task for Dahlin et al., 2008, and Wisconsin Card Sorting Test for Basso et al., 1999), it is possible that the maximal practice effect can be obtained with shorter practice time than previous studies indicated.

In this study, we did not examine transfer effects after short-term practice in other untrained EF tasks. Dahlin et al. (2008) reported transfer effects of updating practice (letter memory) over five weeks on the performance of the other updating task (n-back test). Considering that short- and long-term practice are suggested to have similar effects on the improvement of performance depending on the type of EF components involved, it is possible for the short-term practice effect to transfer to other untrained EF tasks. The findings of the present short-term practice effect and of possible transfer effects in future research could lead to efficient resolution of problems that individuals with EF deficits and maladaptive behavior have in daily life.

Acknowledgments

This study was supported by the Program of Finding Basic Research Center in Private Universities (MEXT) to the Kansei Fukushi Research Institute, Tohoku Fukushi University (2014-18) and a Grant-in-Aid of the Japan Society for the Promotion of Science (JSPS) for Scientific Research (no. 16K00212 and 26350995).

References

Baddeley, A.D., & Hitch G. (1974). Working Memory. *Psychology of Learning and Motivation, 8*, 47–89.

Basso, M. R., Bornstein, R. A., & Lang, J. M. (1999). Practice Effects on Commonly Used Measures of Executive Function Across Twelve Months. *The Clinical Neuropsychologist, 13 (3)*, 283–292.

Benikos, N., Johnstone, S. J., & Roodenrys, S. J. (2013). Short-term training in the Go/Nogo task: Behavioral and neural changes depend on task demands. *International Journal of Psychophysiology, 87 (3)*, 301–312.

Collie, A., Maruff, P., Darby, D. G., & McStephen, M. (2003). The effects of practice on the cognitive test performance of neurologically normal individuals assessed at brief test–retest intervals. *Journal of the International Neuropsychological Society, 9*, 419–428.

Dahlin, E., Neely, A. S., Larsson, A., Bäckman, L., & Nyberg, L. (2008). Transfer of Learning After Updating Training Mediated by the Striatum. *Science, 320,* 1510–1512.

Dahlin, E. (2009). Train your Brain: Updating, Transfer, and Neural Changes (Doctoral dissertation). *Umeå University Medical Dissertations, New Series, 1283*

Damasio, A. R. (1994). Descartes' error: Emotion, reason, and the human brain. *New York: Avon Books*

Klingberg, T. (2010). Training and plasticity of working memory. *Trends in Cognitive Sciences, 14 (7),* 317–324.

Friedman, N. P., Miyake, A., Corley, R. P., Young, S. E., DeFries, J. C., & Hewitt, J. K. (2006). Not All Executive Functions Are Related to Intelligence. *Psychological Science, 17 (2),* 172–179.

Friedman, N. P., Miyake, A., Young, S. E., DeFries, J. C., Corley, R. P., & Hewitt, J. K. (2008). Individual Differences in Executive Functions Are Almost Entirely Genetic in Origin. *Journal of Experimental Psychology: General, 137 (2),* 201–225.

Friedman, N. P., & Miyake, A. (2017). Unity and Diversity of Executive Functions: Individual Differences as a Window on Cognitive Structure. *Cortex, 86,* 186–204.

Logan, G. D., Schachar, R. J. & Tannock, R. (1997). Impulsivity and Inhibitory Control. *Psychological Science. 8 (1),* 60–64.

Mayr, U., & Kliegl, R. (2000). Task-Set Switching and Long-Term Memory Retrieval. *Journal of Experimental Psychology: Learning, Memory, and Cognition, 26 (5),* 1124–1140.

Miyake, A., Friedman, N. P. Emerson, M. J., Witzki, A. H., & Howerter, A., Wager, T. D. (2000). The Unity and Diversity of Executive Functions and Their Contributions to Complex Frontal Lobe Tasks: A Latent Variable Analysis. *Cognitive Psychology, 41,* 49–100.

Sternberg, R. J. (1994). A triarchic model for teaching and assessing students in general psychology. *General Psychologist, 30 (2),* 42–48.

Verbeken, S., Braet, C., Goossens, L., & Van der Ord, S. (2013). Executive function training with game elements for obese children: A novel treatment to enhance self-regulatory abilities for weight-control. *Behaviour Research and Therapy, 51 (6),* 290–299.

(Received December 21, 2016)
(Accepted January 21, 2017)

Sone et al. Environmental Health and Preventive Medicine (2017) 22:18
DOI 10.1186/s12199-017-0625-8

Environmental Health and Preventive Medicine

RESEARCH ARTICLE Open Access

Attitude and practice of physical activity and social problem-solving ability among university students

Toshimasa Sone[1*], Yousuke Kawachi[2], Chihiro Abe[3], Yuki Otomo[3], Yul-wan Sung[2] and Seiji Ogawa[2]

Abstract

Background: Effective social problem-solving abilities can contribute to decreased risk of poor mental health. In addition, physical activity has a favorable effect on mental health. These previous studies suggest that physical activity and social problem-solving ability can interact by helping to sustain mental health. The present study aimed to determine the association between attitude and practice of physical activity and social problem-solving ability among university students.

Methods: Information on physical activity and social problem-solving was collected using a self-administered questionnaire. We analyzed data from 185 students who participated in the questionnaire surveys and psychological tests. Social problem-solving as measured by the Social Problem-Solving Inventory-Revised (SPSI-R) (median score 10.85) was the dependent variable. Multiple logistic regression analysis was employed to calculate the odds ratios (ORs) and 95% confidence intervals (CIs) for higher SPSI-R according to physical activity categories.

Results: The multiple logistic regression analysis indicated that the ORs (95% CI) in reference to participants who said they never considered exercising were 2.08 (0.69–6.93), 1.62 (0.55–5.26), 2.78 (0.86–9.77), and 6.23 (1.81–23.97) for participants who did not exercise but intended to start, tried to exercise but did not, exercised but not regularly, and exercised regularly, respectively. This finding suggested that positive linear association between physical activity and social problem-solving ability (p value for linear trend < 0.01).

Conclusions: The present findings suggest that regular physical activity or intention to start physical activity may be an effective strategy to improve social problem-solving ability.

Keywords: Physical activity, Social problem-solving ability, University students, Exercise

Background

Social problem-solving ability involves the higher-level cognitive processes needed to cope appropriately with various stressful problems experienced in life [1, 2]. It can be described as encompassing two components: problem orientation and problem-solving skills. Problem orientation refers to an individual's awareness and perception of problems, and it performs a motivational function in the problem-solving process. Problem-solving skills are effective coping techniques for dealing with a particular problematic situation. They can be divided into four parts: (1) problem definition and formulation, (2) generation of alternative solutions, (3) decision making, and (4) solution implementation and verification [3]. Effective social problem-solving abilities can contribute to decreased risk of poor mental health, including depression [4–6]. Likewise, among university students, it has been reported that higher social problem-solving ability helps to prevent depression and psychological stress [7, 8].

People can also cope with various stresses related to social problems through the use of alternative coping techniques that regulate negative emotions. Physical activity is regarded as one of these emotion-focused coping techniques [9]. In addition, physical activity has a favorable effect on mental health [10, 11]. There are many studies that have reported on mental health issues in

* Correspondence: sone-t@umin.ac.jp
[1]Department of Rehabilitation, Faculty of Health Science, Tohoku Fukushi University, 1-8-1 Kunimi, Aoba-ku, Sendai 981-8522, Japan
Full list of author information is available at the end of the article

BioMed Central

© The Author(s). 2017 **Open Access** This article is distributed under the terms of the Creative Commons Attribution 4.0 International License (http://creativecommons.org/licenses/by/4.0/), which permits unrestricted use, distribution, and reproduction in any medium, provided you give appropriate credit to the original author(s) and the source, provide a link to the Creative Commons license, and indicate if changes were made. The Creative Commons Public Domain Dedication waiver (http://creativecommons.org/publicdomain/zero/1.0/) applies to the data made available in this article, unless otherwise stated.

students [12]. In addition, previous studies have reported that regular physical activity has been associated with a lower risk of poor mental health in student populations [13–16].

These previous studies suggest that physical activity and social problem-solving ability can interact by helping to sustain mental health. In addition, physical activity is known to be associated with various cognitive functions such as attention or memory [17–20]. Therefore, there could be a direct association between regular physical activity and social problem-solving.

In the present study, we aimed to determine the association between attitude and practice of physical activity and social problem-solving ability among university students. We hypothesized that engaging in regular physical activity enhances social problem-solving ability. We also sought to determine the linear association between these two characteristics.

Methods

Study design and participants

Questionnaire surveys and psychological tests were conducted between July and December 2015. The study population comprised students aged 18 years or older enrolled in Tohoku Fukushi University. We recruited 2750 first- and second-year students to participate in the study using email. A total of 186 students (6.8%) participated in the questionnaire surveys and psychological tests. One participant who did not answer questions about physical activity was excluded, leaving 185 participants (6.7%) for analysis. Tohoku Fukushi University has four faculties (including nine departments), in Welfare, Healthcare, Education, and Management. The mission of these faculties is to deeply inquire into the truth, develop widespread knowledge and specialized skills in their fields, and build meaningful relationships, with the ultimate aim of creating paths to the wellbeing for all mankind.

Measurements

The questionnaire requested the following information from each participant: age, sex, living situation, body weight, height, sleeping condition, dietary habits, physical activity, social activity, psychological distress, and life stressors. The printed questionnaires was administered to participant.

Attitude and practice of physical activity

Attitude and practice of physical activity was defined as "undertaking moderate physical activity such as walking, riding a bicycle, or doing household tasks while standing or walking for at least 60 min per day in daily life." This measure has been used in the National Health and Nutrition Survey, conducted by the Ministry of Health, Labour and Welfare of Japan [21]. The possible responses were as follows "I do not practice physical activity, and I never think about doing so," "I do not practice physical activity, but I intend to start doing so," "I try to do physical activity, but have not done it much yet," "Yes, I practice physical activity, but not regularly," and "Yes, I practice physical activity and regularly."

Social problem-solving ability

The Social Problem-Solving Inventory–Revised (SPSI-R) is a 52-item self-report questionnaire that assesses problem-solving skills [22]. The Japanese version of the SPSI-R, which has been validated previously, uses a 50-item self-report questionnaire [23, 24]. The questionnaire contains five subscales: positive problem orientation (PPO), negative problem orientation (NPO), rational problem solving (RPS) (which has four subcomponents: problem definition and formulation (PDF), generation of alternative solutions (GAS), decision making (DM), and solution implementation and verification (SIV)), impulsivity/carelessness style (ICS), and avoidance style (AS). The number of items on each subscale and a sample item are as follows: PPO, four items, e.g., "I believe I can solve a problem if I try hard enough"; NPO, 10 items, e.g., "I feel afraid when I have a problem to solve"; RPS, 20 items, e.g., "I approach problems from many angles"; ICS, 10 items, e.g., "I go with the first good idea that comes to mind"; AS, six items, e.g., "I avoid thinking about problems." Higher scores on the PPO and RPS (and its subcomponents) indicate more adaptive problem-solving capacity, whereas higher scores on the NPO, ICS, and AS reflect more a more maladaptive approach to problem solving. Each item is answered on a 5-point rating scale with anchors of 0 ("not at all true of me") and 4 ("extremely true of me"). Sato et al. indicated adequate internal consistency for the Japanese version of the SPSI-R (Cronbach's $\alpha = 0.89$) and all subscales (Cronbach's $\alpha = 0.72$ to 0.92). In addition, the test–retest reliability over 3 weeks for all subscales as indicated by Pearson's r was indicated from 0.38 to 0.61 [23]. In this study, Cronbach's α ranged from 0.61 to 0.90 (SPSI-R, 0.90; PPO, 0.61; NPO, 0.88; RPS, 0.86; PDF, 0.64; GAS, 0.61; DM, 0.62; SIV, 0.77; ICS, 0.77; and AS, 0.75).

Statistical analyses

First, comparisons between physical activity categories were performed via chi-squared analysis to assess differences in characteristics.

Previous studies did not report a well-accepted cut-point for the SPSI-R [22, 23]. Therefore, we conducted analysis of covariance using continuous variables and logistic regression analysis using median scores.

Second, an analysis of covariance was performed to investigate the significance of differences in the SPSI-R among respondents in the various physical activity categories.

Third, we conducted logistic regression analysis to evaluate the association between attitude and practice of physical activity and social problem-solving. Social problem-solving (median score 10.85) was the dependent variable, whereas the independent variable was physical activity, which was divided into five categories: "do not exercise, and never think about doing so ("I do not practice physical activity, and I never think about doing so")," "do not exercise but intend to start ("I do not practice physical activity, but I intend to start doing so")," "try to exercise but do not ("I try to do physical activity, but have not done it much yet")," "exercise but not regularly ("Yes, I practice physical activity, but not regularly,")," and "exercise regularly ("Yes, I practice physical activity and regularly")". Multiple logistic regression analysis was performed to calculate the odds ratios (ORs) and 95% confidence intervals (CIs) for higher social problem-solving according to these five physical activity categories. Furthermore, we repeated the logistic regression analysis after modifying the dependent variable to each subscale, including PPO, NPO, RPS (PDF, GAS, DM, and SIV taken individually), ICS, and AS. The median scores for each of these variables were as follows: PPO, 12; NPO, 23; RPS, 45; PDF, 13; GAS, 12; DM, 11; SIV, 10; ICS, 19; AS, 12.

Fourth, we estimated the p value for the linear trend using the five possible responses regarding physical activity level as a continuous variable ("do not exercise, and never think about doing," "do not exercise but intend to start," "try to exercise but do not," "exercise but not regularly," and "exercise regularly").

Fifth, we also conducted stratified analyses according to differences in sex, i.e., we queried whether sex significantly interfered with the association between physical activity and social problem-solving ability. Sex, as the interaction between physical activity and social problem-solving ability, was tested through the addition of cross-product terms to the multivariate-adjusted model.

Sixth, in a supplementary analysis, we conducted multiple Poisson regression analysis to evaluate the association between attitude and practice of physical activity and SPSI-R and subscales and to calculate the rate ratios (RRs) and 95% CIs for higher social problem-solving according to these five physical activity categories.

We considered the following variables to be potential confounders: age in years (continuous variable), sex (men or women), and living alone (yes or no). All statistical analyses were performed using SAS version 9.4 (SAS Inc., Cary, NC, USA). We considered differences at $p < 0.05$ to be statistically significant.

Results

Characteristics according to physical activity

As shown in Table 1, participants belonging to the categories of "try to exercise but do not," "exercise but not regularly," and "exercise regularly" were less likely to be women or living alone than those who said they never considered exercising. In contrast, the proportion of men and those living alone was similar with regards to those who responded that they never considered exercising, and those who did not exercise but intended to begin exercising.

Differences in SPSI-R and subscales among categories of physical activity

The mean score ± standard deviation (SD) on the SPSI-R was 10.4 ± 2.7 for participants who said they never considered exercising, 10.7 ± 2.0 for participants who did not exercise but intended to start, 10.6 ± 2.1 for participants who tried to exercise but did not, 10.8 ± 2.1 for participants who exercised but not regularly, and 12.3 ± 2.8 for participants who exercised regularly. We found significant differences between the five categories of physical activity with respect to the SPSI-R, at the $p < 0.01$ level. Subscale analyses showed the presence of significant differences in NPO means between the five categories of physical activity (NPO; $p = 0.03$) (Table 2).

Multivariate odds ratio and 95% confidence interval of higher SPSI-R and subscales according to physical activity

As shown in Table 3, the unadjusted analysis indicated that the ORs (95% CI) in reference to participants who answered "I do not practice physical activity, and I never think about doing so" were 2.03 (0.68–6.65), 1.68 (0.58–5.34), 3.11 (1.00–10.60), and 7.00 (2.11–26.13) for participants who did not exercise but intended to start, tried to exercise but did not, exercised but not regularly, and exercised regularly, respectively (p value for linear trend < 0.01). This finding remained basically unchanged, even after adjusting for age, sex, and living alone (p value for linear trend < 0.01). Thus, a greater frequency of higher SPSI-R scores was found among respondents stating that they tried or intended to exercise but did not, as well as those who exercised regularly or irregularly, when compared to those who had not even considered exercising. With regard to subscales and the subcomponents of RPS, linear associations were observed between physical activity and NPO, DM, and ICS. However, there were no significant linear associations between physical activity and PPO, RPS, PDF, GAS, SIV, or AS.

We further evaluated sex difference in the association between physical activity and social problem-solving ability (Table 4). There was no significant interaction between physical activity and social problem-solving ability (p value for interaction = 0.44).

Table 1 Characteristics according to physical activity

Characteristic	Total	Physical activity					*P* value
		Do not exercise			Exercise but not regularly	Exercise regularly	
		And never think about doing so	But intend to start	Try to exercise			
No. of subjects	185	20	43	55	35	32	
Age in years (%)							
18	34.6	30.0	23.3	34.5	48.6	37.5	0.44
19	42.2	50.0	53.5	38.2	31.4	40.6	
20	18.9	15.0	16.3	21.8	17.1	21.9	
21	3.2	5.0	2.3	5.5	2.9	0.0	
22	1.1	0.0	4.7	0.0	0.0	0.0	
Sex (%)							
Men	35.7	20.0	20.9	34.5	48.6	53.1	0.01
Women	64.3	80.0	79.1	65.5	51.4	46.9	
Living alone (%)							
Yes	43.2	50.0	48.8	40.0	40.0	40.6	0.85
No	56.8	50.0	51.2	60.0	60.0	59.4	

P values were calculated using a chi-square test

Multivariate rate ratio and 95% confidence interval of higher SPSI-R and subscales according to physical activity

The multiple adjusted analysis indicated that the RRs (95% CI) in reference to participants who answered "I do not practice physical activity, and I never think about doing so" were 1.57 (0.63–3.91), 1.36 (0.55–3.36), 1.78 (0.71–4.49), and 2.31 (0.93–5.74) for participants who did not exercise but intended to start, tried to exercise but did not, exercised but not regularly, and exercised regularly, respectively. Higher SPSI-R was more frequently observed among participants who exercised regularly than those who did not exercise. This linear association was marginally significant (p value for linear trend = 0.05). With regard to the subcomponents of RPS, linear associations were observed between physical activity and DM (p value for linear trend = 0.04) (Additional file 1: Table S1).

Table 2 Differences in SPSI-R and subscales among categories of physical activity

	Physical activity					*P* value
	Do not exercise			Exercise but not regularly	Exercise regularly	
	And never think about doing so	But intend to start	Try to exercise			
No. of subjects	20	43	55	35	32	
SPSI-R, mean ± SD	10.4 ± 2.7	10.7 ± 2.0	10.6 ± 2.1	10.8 ± 2.1	12.3 ± 2.8	<0.01
PPO, mean ± SD	11.4 ± 4.1	11.6 ± 2.8	11.7 ± 3.4	10.7 ± 3.1	12.9 ± 3.6	0.11
NPO, mean ± SD	23.3 ± 6.7	23.2 ± 6.9	24.0 ± 7.2	21.5 ± 8.2	18.2 ± 10.0	0.03
RPS, mean ± SD	43.9 ± 12.2	44.6 ± 8.6	45.0 ± 10.0	45.2 ± 8.4	49.8 ± 10.5	0.25
PDF, mean ± SD	12.1 ± 3.2	12.9 ± 2.8	12.4 ± 2.7	12.3 ± 2.5	13.4 ± 2.9	0.35
GAS, mean ± SD	11.2 ± 3.8	12.0 ± 2.9	11.5 ± 2.9	12.1 ± 2.8	13.0 ± 3.1	0.29
DM, mean ± SD	9.9 ± 3.0	10.5 ± 2.9	10.5 ± 2.9	11.0 ± 2.7	12.3 ± 3.7	0.08
SIV, mean ± SD	10.7 ± 4.2	9.3 ± 3.5	10.6 ± 3.7	9.8 ± 3.4	11.1 ± 3.6	0.23
ICS, mean ± SD	19.9 ± 6.6	19.3 ± 5.6	20.0 ± 5.6	19.3 ± 4.4	17.7 ± 6.1	0.42
AS, mean ± SD	14.1 ± 5.2	12.7 ± 3.7	13.1 ± 5.0	12.2 ± 4.1	10.8 ± 5.2	0.06

Abbreviations: *AS* avoidance style, *DM* decision making, *GAS* generation of alternative solutions, *ICS* impulsivity/carelessness style, *NPO* negative problem orientation, *PDF* problem definition and formulation, *PPO* positive problem orientation, *RPS* rational problem solving, *SD* standard deviation, *SIV* solution implementation and verification, and *SPSI-R* Social Problem-Solving Inventory–Revised

Analysis of covariance was adjusted for age in years (continuous variable), sex (men or women), and living alone (yes or no)

Table 3 Multivariate OR and 95% CI of higher SPSI-R and subscales according to physical activity

	Physical activity					*P* value for linear trend
	Do not exercise			Exercise but not regularly	Exercise regularly	
	And never think about doing so	But intend to start	Try to exercise			
No. of subjects	20	43	55	35	32	
SPSI-R						
No. of subjects with higher SPSI-R	6	20	23	20	24	
Crude OR (95% CI)	1.00 (Ref.)	2.03 (0.68–6.65)	1.68 (0.58–5.34)	3.11 (1.00–10.60)	7.00 (2.11–26.13)	< 0.01
Multivariate adjusted OR (95% CI)	1.00 (Ref.)	2.08 (0.69–6.93)	1.62 (0.55–5.26)	2.78 (0.86–9.77)	6.23 (1.81–23.97)	< 0.01
PPO						
Multivariate adjusted OR (95% CI)	1.00 (Ref.)	1.04 (0.35–3.02)	0.90 (0.32–2.53)	0.87 (0.28–2.68)	1.50 (0.47–4.81)	0.58
NPO						
Multivariate adjusted OR (95% CI)	1.00 (Ref.)	0.74 (0.22–2.28)	0.66 (0.20–1.94)	0.42 (0.12–1.34)	0.27 (0.07–0.88)	0.01
RPS						
Multivariate adjusted OR (95% CI)	1.00 (Ref.)	0.71 (0.24–2.08)	0.93 (0.33–2.64)	0.79 (0.25–2.45)	2.37 (0.73–8.00)	0.10
PDF						
Multivariate adjusted OR (95% CI)	1.00 (Ref.)	1.25 (0.43–3.66)	1.18 (0.42–3.33)	0.73 (0.23–2.26)	1.83 (0.57–5.97)	0.64
GAS						
Multivariate adjusted OR (95% CI)	1.00 (Ref.)	1.18 (0.40–3.49)	0.94 (0.33–2.70)	1.37 (0.44–4.35)	2.66 (0.80–9.16)	0.10
DM						
Multivariate adjusted OR (95% CI)	1.00 (Ref.)	1.01 (0.33–3.13)	1.00 (0.34–3.01)	3.34 (1.03–11.47)	3.67 (1.10–13.10)	< 0.01
SIV						
Multivariate adjusted OR (95% CI)	1.00 (Ref.)	0.46 (0.15–1.34)	0.74 (0.24–2.12)	0.82 (0.25–2.59)	1.61 (0.46–5.64)	0.12
ICS						
Multivariate adjusted OR (95% CI)	1.00 (Ref.)	1.38 (0.45–4.16)	0.94 (0.32–2.68)	0.58 (0.18–1.81)	0.48 (0.14–1.51)	0.04
AS						
Multivariate adjusted OR (95% CI)	1.00 (Ref.)	0.70 (0.22–2.08)	0.60 (0.20–1.70)	0.53 (0.16–1.66)	0.35 (0.10–1.11)	0.07

Abbreviations: *AS* avoidance style, *CI* confidence interval, *DM* decision making, *GAS* generation of alternative solutions, *ICS* impulsivity/carelessness style, *NPO* negative problem orientation, *OR* odds ratio, *PDF* problem definition and formulation, *PPO* positive problem orientation, *RPS* rational problem solving, *SIV* solution implementation and verification, and *SPSI-R* Social Problem-Solving Inventory–Revised

The outcomes were higher for SPSI-R, PPO, NPO, RPS, PDF, GAS, DM, SIV, ICS, and AS

Multivariate ORs were adjusted for age in years (continuous variable), sex (men or women), and living alone (yes or no)

The *p* value for the linear trend was estimated using the five categories of physical activity as a continuous variable

Discussion

This study, conducted with Japanese university students, indicated that higher SPSI-R was more frequently observed among participants who exercised regularly, compared to those who answered "I do not practice physical activity, and I never think about doing so". In addition, we found a statistically significant, positive linear association between physical activity and social problem-solving ability.

Our study indicated that higher SPSI-R was more frequently observed among participants who exercised regularly, as compared with those who answered "I do not practice physical activity, and I never think about doing so". There have been no reports on the reasons for higher SPSI-R scores in participants who exercised regularly. However, previous studies report that exercise may influence cognitive function by increasing brain

Table 4 Multivariate OR and 95% CI of higher SPSI-R according to physical activity stratified by sex

	Physical activity					*P* value for interaction
	Do not exercise			Exercise but not regularly	Exercise regularly	
	And never think about doing so	But intend to start	Try to exercise			
Men						0.44
No. of subjects	4	9	19	17	17	
No. of subjects with higher SPSI-R	1	5	10	10	15	
Crude OR (95% CI)	1.00 (Ref.)	3.75 (0.33–93.82)	3.33 (0.35–74.36)	4.29 (0.44–97.14)	22.50 (1.92–618.34)	
Multivariate adjusted OR (95% CI)	1.00 (Ref.)	3.85 (0.29–107.39)	3.13 (0.32–71.85)	3.58 (0.35–83.98)	20.60 (1.68–583.23)	
Women						
No. of subjects	16	34	36	18	15	
No. of subjects with higher SPSI-R	5	15	13	10	9	
Crude OR (95% CI)	1.00 (Ref.)	1.74 (0.51–6.52)	1.24 (0.36–4.67)	2.75 (0.69–11.99)	3.30 (0.78–15.54)	
Multivariate adjusted OR (95% CI)	1.00 (Ref.)	1.54 (0.44–5.91)	1.36 (0.39–5.23)	3.22 (0.79–14.62)	3.85 (0.88–18.85)	

Abbreviations: *CI* confidence interval, *OR* odds ratio, *SPSI-R* Social Problem-Solving Inventory–Revised
The outcomes were higher for SPSI-R
Multivariate ORs were adjusted for age in years (continuous variable), and living alone (yes or no)

blood flow [25, 26]. The possibility of a direct or indirect relationship between brain blood flow and higher cognitive function would require additional psychological and neuroscientific research.

Because social problem-solving ability consists of problem orientation and problem-solving skills [1, 2], we attempted to conduct analyses by subscale. We found significant linear associations between physical activity and NPO, DM, and ICS. The overall positive linear association between physical activity and SPSI-R was mainly attributable to the linear associations between physical activity and these three subscale or subcomponent scores. In addition, greater frequency of higher PPO and RPS (including all subcomponents) and lesser frequency of higher NPO, ICS, and AS were observed in participants who exercised regularly than in those who had not even considered exercising. Considering the findings with respect to the definition provided by D'Zurilla et al. [27], for NPO, higher motivation for physical activity is related to a lesser tendency to view a problem as a significant threat to one's well-being, to doubt one's own personal ability to solve problems successfully, or to easily become frustrated and upset when confronted with problems. For DM, greater motivation for physical activity is related to a stronger tendency to anticipate the consequences of different solutions, judge and compare them, and then choose the most effective solution. For ICS, greater motivation for physical activity is related to a weaker tendency to act impulsively on the first idea that comes to mind; to scan alternative solutions and consequences quickly, carelessly, and unsystematically; or to monitor solution outcomes carelessly and inadequately. Overall, we found that physical activity was associated with a positive result on the SPSI-R as well as on subscales of the SPSI-R.

Overall, 17.3% of the participants in this study indicated that they exercised regularly, and another 18.9% said that they exercised but not regularly. This means that only 36.2% did at least the relatively minimal amount of exercise defined as physical activity on this questionnaire. According to another study, the proportions of Japanese men and women age 20 to 29 engaging in regular exercise were 16.3% and 16.8%, respectively [28]. Because, in that Ministry of Health study, regular exercise was similarly defined as 30 min of physical activity at least twice a week in accordance with "Health Japan 21" [28, 29], it appears that our study participants were more likely to have regular physical activity than the average among all Japanese age 20 to 29. On the other hand, previous studies in the United States indicated that 39.1% of respondents engaged in at least moderate activity [30] and that 49.9% of students reported moderate to vigorous activity [31]. Therefore, our study participants were less likely to have a high level of physical activity than U.S. students.

The SPSI-R was developed to assess social problem-solving skills [22], and it has been translated in Spanish, Chinese, and Japanese [23, 32, 33]. Among our students, the mean on the SPSI-R was 10.9. Previous studies reported means of 12.0 [23], 11.9 [34], and 12.6 [35]. Thus, our average SPSI-R score was observed to be lower than that of students in previous studies. As our students

were recruited from one university without random sampling, our study may demonstrate selection bias. Participants in previous studies were selected from various U.S. universities using random sampling. Therefore, further study including a large sample size or a random sample is required to generalize our findings. Moreover, although we hypothesized that regular physical activity would enhance students' social problem-solving ability, our study was cross-sectional in design. A longitudinal study is required to confirm the assumed direction of the causal association studied here.

We found a statistically significant, positive linear association between physical activity and social problem-solving ability after adjusting for sex. Because participants who exercised were less likely to be women than those who did not exercise (Table 1), we conducted stratified analyses to examine whether the association between physical activity and social problem-solving ability was dependent on sex. In consequence, we found that higher SPSI-R was more frequently observed among participants who exercised regularly, irrespective of the sex.

The present study had the following limitations. First, we considered age in years, sex, and living alone as potential confounding factors. However, because the questionnaire did not include socioeconomic status, a family history of mental disorders, and having a part-time job, we did not control for these factors. A further study controlling for these factors will be required. Second, the present study may have information bias in regards to physical activity, because our questionnaire did not include metabolic equivalents (METs) or frequency per week as indicators of physical activity. We estimated the p value for the linear trend using the five possible responses regarding physical activity level as a continuous variable (the responses were: "do not exercise, and never think about doing," "do not exercise but intend to start," "try to exercise but do not," "exercise but not regularly," and "exercise regularly"). Therefore, further studies using METs or frequency per week as a proxy for the amount of physical activity undertaken will be required. Third, because the response rate was low (6.8%), the participants may not have been representative of the source population of Tohoku Fukushi University students. Our study participants were more likely to engage in regular physical activity than average among all Japanese aged 20 to 29. Therefore, this low response rate should be considered when interpreting the study results. Moreover, a form of selection bias may have occurred wherein participants who were interested in physical activity or a healthy lifestyle may have been more likely to participate in the study.

Conclusions

This study investigated the association between attitude and practice of physical activity and social problem-solving ability among Japanese university students. We found that higher SPSI-R could be more frequently observed among participants who exercised regularly, as compared to those who answered "I do not practice physical activity, and I never think about doing so". In addition, there was a positive linear association between physical activity and higher social problem-solving ability scores. The present findings suggest that regular physical activity, or an intention to start physical activity, may function as effective strategies for improving social problem-solving ability, which may subsequently help in improving university students' levels of mental health.

Additional file

Additional file 1: Table S1. Multivariate RR and 95% CI of higher SPSI-R and subscales according to physical activity. (DOCX 24 kb)

Abbreviations

AS: Avoidance style; CI: Confidence interval; DM: Decision making; GAS: Generation of alternative solutions; ICS: Impulsivity/carelessness style; MET: Metabolic equivalent; NPO: Negative problem orientation; OR: Odds ratio; PDF: Problem definition and formulation; PPO: Positive problem orientation; RPS: Rational problem solving; RR: Rate ratio; SD: Standard deviation; SIV: Solution implementation and verification; SPSI-R: Social Problem-Solving Inventory–Revised

Acknowledgments

This study was supported by the MEXT-Supported Program for the Strategic Research Foundation at Private Universities 2014–2018 (S1411001).

Funding

This study was supported by the MEXT-Supported Program for the Strategic Research Foundation at Private Universities 2014–2018 (S1411001).

Availability of data and materials

Please contact author for data requests.

Authors' contributions

TS participated in the design of the study, performed the statistical analysis, and wrote the first draft of the manuscript text. YK, CA, YO, and YS participated in its design, conducted research, and helped to draft the manuscript. SO participated in its design, and supervised and provided commentaries to the manuscript text. All authors read and approved the final manuscript.

Competing interests

The authors declare that they have no competing interests.

Consent for publication

Written informed consent was obtained from all participants.

Ethics approval and consent to participate

The study protocol was reviewed and approved by the Ethics Committee of Tohoku Fukushi University (RS150203). Written informed consent was obtained from all participants.

Publisher's Note

Springer Nature remains neutral with regard to jurisdictional claims in published maps and institutional affiliations.

Author details

[1]Department of Rehabilitation, Faculty of Health Science, Tohoku Fukushi University, 1-8-1 Kunimi, Aoba-ku, Sendai 981-8522, Japan. [2]Kansei Fukushi Research Institute, Tohoku Fukushi University, Sendai, Japan. [3]Department of

Welfare Psychology, Graduate School of General Welfare, Tohoku Fukushi University, Sendai, Japan.

Received: 31 October 2016 Accepted: 6 March 2017
Published online: 04 April 2017

References

1. D'Zurilla TJ, Goldfried MR. Problem solving and behavior modification. J Abnorm Psychol. 1971;78:107–26.
2. D'Zurilla TJ, Nezu AM. Social problem solving in adults. In: Kendall PC, editor. Advances in cognitive–behavioral research and therapy. 1. New York: Academic; 1982. p. 201–74.
3. D'Zurilla TJ, Nezu AM. Development and preliminary evaluation of the social problem-solving inventory. Psychol Assess. 1990;2:156–63.
4. Haaga DAF, Fine JA, Terrill DR, Stewart BL, Beck AT. Social problem-solving deficits, dependency, and depressive symptoms. Cognit Ther Res. 1995;19:147–58.
5. Heppner PP, Witty TE, Dixon WA. Problem-solving appraisal and human adjustment: A review of 20 years of research using the problem solving inventory. Couns Psychol. 2004;32:344–428.
6. Marx EM, Williams JM, Claridge GC. Depression and social problem solving. J Abnorm Psychol. 1992;101:78–86.
7. D'Zurilla TJ, Chang EC, Nottingham EJ 4th, Faccini L. Social problem-solving deficits and hopelessness, depression, and suicidal risk in college students and psychiatric inpatients. J Clin Psychol. 1998;54:1091–107.
8. D'Zurilla TJ, Sheedy CF. Relation between social problem-solving ability and subsequent level of psychological stress in college students. J Pers Soc Psychol. 1991;61:841–6.
9. Haskell WL, Blair SN. The physical activity component of health promotion in occupational settings. Public Health Rep. 1980;95:109–18.
10. Griffiths A, Kouvonen A, Pentti J, Oksanen T, Virtanen M, Salo P, Väänänen A, Kivimäki M, Vahtera J. Association of physical activity with future mental health in older, mid-life and younger women. Eur J Public Health. 2014;24:813–8.
11. Hamer M, Stamatakis E, Steptoe A. Dose-response relationship between physical activity and mental health: the Scottish Health Survey. Br J Sports Med. 2009;43:1111–4.
12. Storrie K, Ahern K, Tuckett A. A systematic review: students with mental health problems–a growing problem. Int J Nurs Pract. 2010;16:1–6.
13. Adams TB, Moore MT, Dye J. The relationship between physical activity and mental health in a national sample of college females. Women Health. 2007;45:69–85.
14. Ho FK, Louie LH, Chow CB, Wong WH, Ip P. Physical activity improves mental health through resilience in Hong Kong Chinese adolescents. BMC Pediatr. 2015;15:48. doi:10.1186/s12887-015-0365-0.
15. Hoegh Poulsen P, Biering K, Andersen JH. The association between leisure time physical activity in adolescence and poor mental health in early adulthood: a prospective cohort study. BMC Public Health. 2016;16:3. doi:10.1186/s12889-015-2658-5.
16. Tyson P, Wilson K, Crone D, Brailsford R, Laws K. Physical activity and mental health in a student population. J Ment Health. 2010;19:492–9.
17. Kamijo K, Pontifex MB, O'Leary KC, Scudder MR, Wu CT, Castelli DM, Hillman CH. The effects of an afterschool physical activity program on working memory in preadolescent children. Dev Sci. 2011;14:1046–58.
18. Lambourne K. The relationship between working memory capacity and physical activity rates in young adults. J Sports Sci Med. 2006;5:149–53.
19. Vanhelst J, Béghin L, Duhamel A, Manios Y, Molnar D, De Henauw S, Moreno LA, Ortega FB, Sjöström M, Widhalm K, Gottrand F, Healthy Lifestyle in Europe by Nutrition in Adolescence (HELENA) Study Group. Physical activity is associated with attention capacity in adolescents. J Pediatr. 2016;168:126–31.e2.
20. Sibley BA, Etnier JL. The relationship between physical activity and cognition in children: A meta-analysis. Pediatr Exerc Sci. 2003;15:243–56.
21. National Institute of Health and Nutrition. Summary Results of the National Health and Nutrition Survey Japan. http://www0.nih.go.jp/eiken/english/research/pdf/nhns2006_outline.pdf. Accessed 20 Oct 2016.
22. D'Zurilla TJ, Nezu AM, Maydeu-Olivares A. Social Problem-Solving Inventory-Revised. Technical Manual. New York: Multi-Health Systems Inc; 2002.
23. Sato H, Takahashi F, Matsuo M, Sakai M, Shimada H, Chen J, Kaiya H, Sakano Y. Development of the Japanese version of the Social Problem-Solving Inventory-Revised and examination of its reliability and validity. Jap J Behav Ther. 2006;32:15–30 (in Japanese).
24. Sumi K. Relations of social problem solving with interpersonal competence in Japanese students. Psychol Rep. 2011;109:976–82.
25. Hiura M, Nariai T, Ishii K, Sakata M, Oda K, Toyohara J, Ishiwata K. Changes in cerebral blood flow during steady-state cycling exercise: a study using oxygen-15-labeled water with PET. J Cereb Blood Flow Metab. 2014;34:389–96.
26. Querido JS, Sheel AW. Regulation of cerebral blood flow during exercise. Sports Med. 2007;37:765–82.
27. D'Zurilla TJ, Nezu AM, Maydeu-Olivares A. Social problem solving: Theory and assessment. In: Chang EC, D'Zurilla TJ, Sanna LJ, editors. Social problem solving: Theory, research, and training. Washington, DC: American Psychological Association; 2004. p. 11–27.
28. Ministry of Health, Labour and Welfare. The National Health and Nutrition Survey in Japan. http://www.mhlw.go.jp/bunya/kenkou/eiyou/dl/h25-houkoku-05.pdf. Accessed 20 Oct 2016 (in Japanese).
29. Ministry of Health, Labour and Welfare. A basic direction for comprehensive implementation of national health promotion. http://www.mhlw.go.jp/file/06-Seisakujouhou-10900000-Kenkoukyoku/0000047330.pdf. Accessed 20 Oct 2016.
30. Seo DC, Nehl E, Agley J, Ma SM. Relations between physical activity and behavioral and perceptual correlates among midwestern college students. J Am Coll Health. 2007;56:187–97.
31. Dinger MK, Brittain DR, Hutchinson SR. Associations between physical activity and health-related factors in a national sample of college students. J Am Coll Health. 2014;62:67–74.
32. Maydeu-Olivares A, Rodríguez-Fornells A, Gómez-Benito J, D'Zurilla TJ. Psychometric properties of the Spanish adaptation of the Social Problem-Solving Inventory-Revised (SPSI-R). Pers Individ Dif. 2000;29:699–708.
33. Siu AM, Shek DT. The Chinese version of the Social Problem-Solving Inventory: Some initial results on reliability and validity. J Clin Psychol. 2005; 61:347–60.
34. Trunzo JJ, Samter W, Morse C, McClure K, Kohn C, Volkman JE, O'Brien K. College students' use of energy drinks, social problem-solving, and academic performance. J Psychoactive Drugs. 2014;46:396–401.
35. Ranjbar M, Bayani AA, Bayani A. Social problem solving ability predicts mental health among undergraduate students. Int J Prev Med. 2013;4:1337–41.

Submit your next manuscript to BioMed Central and we will help you at every step:

- We accept pre-submission inquiries
- Our selector tool helps you to find the most relevant journal
- We provide round the clock customer support
- Convenient online submission
- Thorough peer review
- Inclusion in PubMed and all major indexing services
- Maximum visibility for your research

Submit your manuscript at
www.biomedcentral.com/submit

BioMed Central

SCIENTIFIC REPORTS

OPEN

Steady-state and dynamic network modes for perceptual expectation

Uk-Su Choi[1], Yul-Wan Sung[2] & Seiji Ogawa[1,2]

Received: 19 August 2016
Accepted: 08 December 2016
Published: 12 January 2017

Perceptual expectation can attenuate repetition suppression, the stimulus-induced neuronal response generated by repeated stimulation, suggesting that repetition suppression is a top-down modulatory phenomenon. However, it is still unclear which high-level brain areas are involved and how they interact with low-level brain areas. Further, the temporal range over which perceptual expectation can effectively attenuate repetition suppression effects remains unclear. To elucidate the details of this top-down modulatory process, we used two short and long inter-stimulus intervals for a perceptual expectation paradigm of paired stimulation. We found that top-down modulation enhanced the response to the unexpected stimulus when repetition suppression was weak and that the effect disappeared at 1,000 ms prior to stimulus exposure. The high-level areas involved in this process included the left inferior frontal gyrus (IFG_L) and left parietal lobule (IPL_L). We also found two systems providing modulatory input to the right fusiform face area (FFA_R): one from IFG_L and the other from IPL_L. Most importantly, we identified two states of networks through which perceptual expectation modulates sensory responses: one is a dynamic state and the other is a steady state. Our results provide the first functional magnetic resonance imaging (fMRI) evidence of temporally nested networks in brain processing.

Repetition suppression of brain responses observed using functional magnetic resonance imaging (fMRI) reflects short-term neuronal plasticity that results from sensitization or fatigue of neuronal circuits[1]. This process involves the adaptation of populations of neurons responding to the stimulus and occurs via a reduction in activation levels, number of neurons, or processing time[1]. The repetition suppression phenomenon has been used to resolve microscopic neuronal characteristics of brain areas at a resolution beyond the fMRI spatial resolution. This approach involves the use of a paired stimulus paradigm in which two stimuli are successively presented within a short time interval, leading to equivalent improvement in fMRI spatial resolution[2].

Several studies have suggested that this suppression phenomenon mostly occurs via passive processing of stimuli through a bottom-up (or feedforward) mechanism of signal processing. For example, repetition suppression of firing rates in the inferior temporal cortex (IT) has been observed in awake and anesthetized macaques[3,4]. Other studies have demonstrated that a period of 100–200 ms of repetition suppression in the visual ventral areas is too short to be mediated via top-down modulation because the mean population latency is approximately 150 ms in IT and below 75 ms in TE[4,5]. Furthermore, no repetition suppression effects of perceptual expectation have been observed in the lateral occipital complex (LOC) of human and monkey IT[6,7].

However, several previous studies have shown that repetition suppression is modulated by perceptual expectation in some category-specific areas such as the fusiform body area (FBA), fusiform face area (FFA), and parahippocampal place area (PPA)[8–10]. Repetition suppression occurring in these studies is caused by top-down (or feedback) signal processing because it is modulated by different expectation probabilities, showing increased repetition suppression during high expectation probability and decreased repetition suppression during low expectation probability[11,12]. However, these studies did not examine some systematic details of the suppression mechanism related to perceptual expectation, including the temporal range over which expectation probability can effectively suppress the neuronal response to the stimulus or the high-level areas involved in repetition suppression and how they interact with the low-level areas within the network (i.e., through functional or effective connectivity).

In this study, we examined the systematic details involved in the top-down modulation of perceptual expectation using the repetition suppression phenomenon. Some previous studies have shown that repetition suppression is attributable to bottom-up mechanisms[3,4] and the suppression disappears with intervals shorter than

[1]Neuroscience Research Institute, Gachon University of Medicine and Science, Incheon, Republic of Korea. [2]Kansei Fukushi Research Institute, Tohoku Fukushi University, Sendai, Japan. Correspondence and requests for materials should be addressed to Y.S. (email: sung@tfu-mail.tfu.ac.jp)

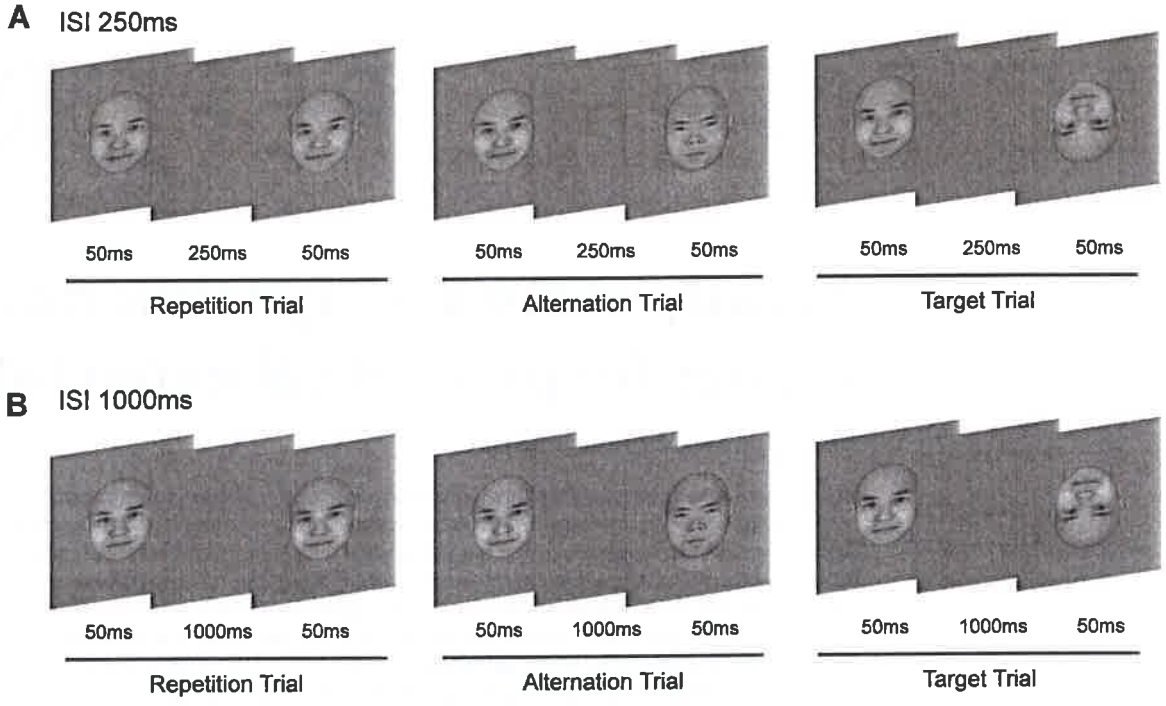


Figure 1. Experimental design. There were three types of trials: repetition, alternation, and target trials. Two different ISIs ((**A**) 250 ms and (**B**) 1,000 ms) were used for paired visual stimuli. The on time of the image was 50 ms.

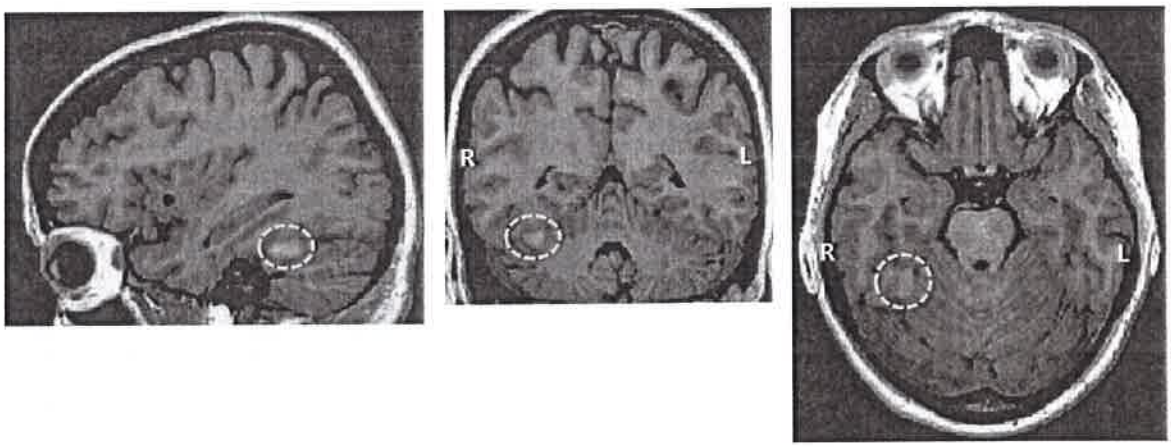


Figure 2. An example of an activation map for FFA_R. FFA ($x = 37.06 \pm 4.96$, $y = -49.76 \pm 9.86$, $z = -15.22 \pm 5.26$, Talairach coordinates) was identified in the right hemisphere by comparing responses to face versus scene stimuli ($p < 0.05$, FDR-corrected).

1,000 ms[13]. Therefore, we used short and long inter-stimulus intervals (ISIs) in a perceptual expectation paradigm of paired stimulation, as described previously[11], with the exception that we used ISIs of 250 and 1,000 ms and a short stimulus duration of 50 ms in the present study, in contrast to ISI of 500 ms and stimulus duration of 250 ms used previously (Fig. 1; Methods). In addition, we used effective functional connectivity analysis to investigate the causality between brain areas involved in repetition suppression.

Results

Right fusiform face area (FFA_R) was individually identified from all participants by contrasting the response to a face to that to a scene in the localization run ($x = 37.06 \pm 4.96$, $y = -49.76 \pm 9.86$, $z = -15.22 \pm 5.26$; $p < 0.05$, FDR-corrected) (Fig. 2).

For the main experimental runs, deconvolution analysis was performed because these runs involved the use of rapid event-related stimulation[14]. Estimated beta values were used for response comparison. The responses of

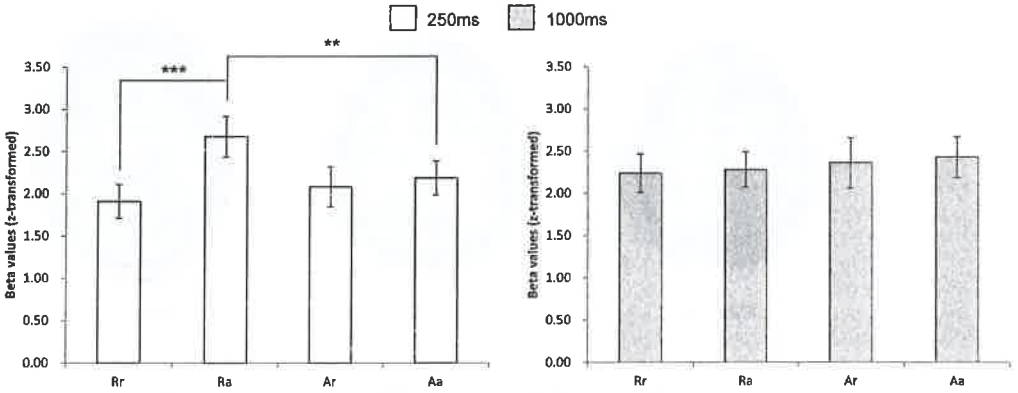


Figure 3. Responses during the four trial types (Rr, Ra, Ar, and Aa) in FFA_R for trials with 250 ms ISI and 1,000 ms ISI. ***$p < 0.001$, **$p < 0.01$. Error bars refer to standard error of the mean (SEM).

the identified FFA_R to four trial conditions [60% repetition trials (Rr), 20% alternation trials (Ra), 20% repetition trials (Ar), and 60% alternation trials (Aa); Methods] were acquired after deconvolution of the data for the trials with 250 ms or 1,000 ms ISI. For trials with 250 ms ISI, the responses to Rr, Ra, Ar, and Aa were evaluated using two-way repeated measured (RM) ANOVA with block and trial factors. There was a significant interaction between these two factors ($F_{(1, 10)} = 27.76$, $p < 0.001$). Simple effect analysis revealed that Ra was significantly larger than Rr (pairwise comparisons, $p < 0.001$). However, there was no significant difference between Aa and Ar (pairwise comparisons, $p = 0.50$) (Fig. 3). To examine whether this difference was from response suppression at Rr or response enhancement at Ra, we compared Ra and Aa (i.e., the condition with high probability and the pair consisting of two different stimuli, therefore, it can be used as a reference value for evaluating signal changes caused by the effects of probability or repetition). Ra was larger than Aa (pairwise comparisons, $p < 0.01$). In addition, we compared Aa and Rr by paired t-test to examine whether Rr was suppressed or not. The comparison between Rr (i.e., the condition with high probability and the pair consisting of two identical stimuli) and Aa revealed a trend toward repetition suppression at Rr (Rr < Aa; paired t-test, $p = 0.10$). This indicates that strong response enhancement occurred and that it was dependent on stimulus probability. For trials with 1,000 ms ISI, no significant interaction ($F_{(1, 10)} = 0.08$, $p = 0.78$) and no significant main effects of the block and of the trial were found ($F_{(1,10)} = 1.05$, $p = 0.33$ and $F_{(1, 10)} = 0.25$, $p = 0.63$, respectively) (Fig. 3). This indicates that enhancement or repetition suppression did not occur for the trials at 1,000 ms ISI; those had been recovered during the interval. Although left fusiform face area was identified from only 5 participants and was not further analyzed for the main experiment, but the response pattern was similar to that of FFA_R (see Supplementary Figs S2 and S3).

To find other brain areas showing significant responses to stimulus trial conditions, we performed whole brain analysis only for 250 ms ISI trials because there was no difference among trial conditions for 1,000 ms ISI. The analysis revealed several areas in the occipital, temporal, parietal, and frontal lobes ($p < 0.001$, FDR-corrected) (Fig. 4). For each of those areas, two-way RM ANOVA was performed with block and trial factors, and a significant interaction was found at three areas: the left inferior frontal gyrus (IFG_L) ($F_{(1,10)} = 21.44$, $p < 0.001$) (Fig. 5A), left parietal gyrus (IPL_L) ($F_{(1,10)} = 6.07$, $p < 0.05$) (Fig. 5B), and left fusiform gyrus (FG_L) ($F_{(1,10)} = 5.50$, $p < 0.05$) (Fig. 5C). Therefore, simple effect analyses were performed after the ANOVA. Rr was significantly smaller than Ra at IFG_L, IPL_L, and FG_L (pairwise comparisons; $p < 0.01$, $p < 0.001$, and $p < 0.05$, respectively), indicating the same block effect as that at FFA_R. In addition, at IFG_L, Ra was larger than Aa (pairwise comparisons, $p < 0.001$), with no significant difference between Rr and Aa (paired t-test, $p = 0.69$). This indicated that probability-dependent response enhancement occurred at this brain area. At IPL_L, Rr was smaller than Aa (paired t-test, $p < 0.05$), with no significant difference between Ra and Aa (pairwise comparisons, $p = 0.07$). This indicated that probability-dependent repetition suppression occurred at in this brain area. At FG_L, Ra was larger than Aa (pairwise comparisons, $p < 0.01$), with no significant difference between Rr and Aa (paired t-test, $p = 0.96$). This indicated that probability-dependent response enhancement occurred at this brain area.

Time courses for the four areas showing repetition suppression were also evaluated. Because the expectation of a stimulus precedes the physical stimulus, the expectation-related activation of neuronal circuits may occur at relevant brain areas prior to the presentation of the physical stimulus[15,16]. Therefore, responses occurring at the stimulus onset (averaged signal intensity at the first time point of the time course across the trial condition) were evaluated for four brain areas with 250 ms ISI and 1,000 ms ISI. For 250 ms ISI trials, the response at IPL_L was significantly larger than the baseline (beta value = 0) (one-sample t-test; $p < 0.001$), while those at other areas were not (one-sample t-test; $p = 0.33$, 0.63, and 0.20 at IFG_L, FFA_R, and FG_L, respectively). One-way RM ANOVA revealed that responses at stimulus onset were significantly different among the four areas ($F_{(3, 30)} = 4.53$, $p < 0.01$). The response at IPL_L at onset was significantly larger than the response at FFA_R ($p < 0.01$). Compared with IFG_L, and FG_L, IPL_L at onset also showed a trend toward a larger response ($p = 0.07$ and $p = 0.09$, respectively; multiple comparison by Tukey's test) (Fig. 6). The greater response at IPL_L preceding the stimulus indicates that the neuronal response at IPL_L precedes those at other areas and is not stimulus-induced but rather related to perceptual expectations. In addition, the effects of perceptual expectation

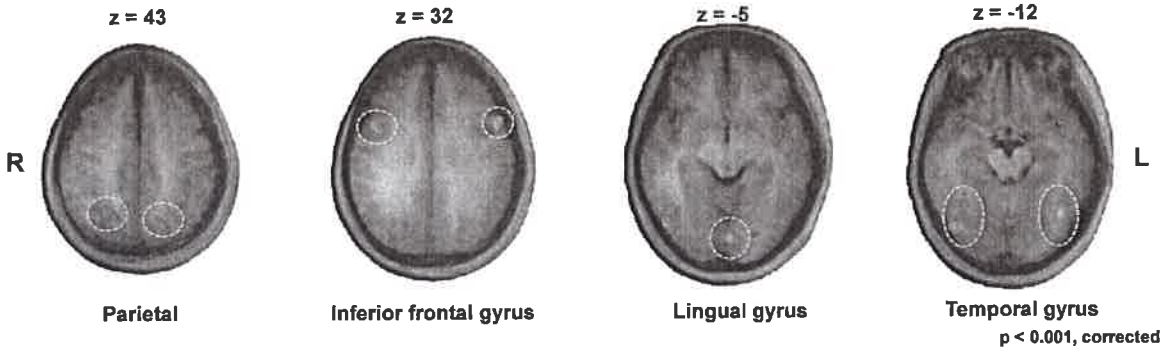


Figure 4. Activation areas of whole brain analysis based on estimated response using deconvolution analysis ($p < 0.001$, corrected). The location of these areas was represented by the following Talairach coordinates at peak statistical values: the right inferior frontal gyrus (39, 5, 31), left inferior frontal gyrus (IFG_L; −51, 8, 31), right parietal gyrus (27, −58, 43), left parietal gyrus (IPL_L; −12, −61, 46), lingual gyrus (−3, −79, −5), right temporal gyrus (42, −70, −11), and left temporal gyrus (FG_L; −39, −58, −11).

on response enhancement and repetition suppression were observed in the repetition block but not in the alternation block. Therefore, the earlier response at IPL_L may reflect the modulation of other areas, particularly FFA_R, by IPL_L, which may explain why response modulation occurs in the repetition block. For trials with 1,000 ms ISI, there was no significance difference ($F_{(3, 30)} = 1.77$, $p = 0.17$). These results indicate that only for 250 ms ISI, expectation-related neuronal processing for response enhancement and repetition suppression initiated at IPL_L before the start of neuronal stimulus processing at FFA_R, IFG_L, and FG_L. This reflects a temporal relationship among these four areas for the stimulus event and these areas are considered to constitute a dynamic network (Fig. 7).

It is considered that the brain has to maintain a steady state on the basis of previous information gathered in the experimental run; the brain has to continuously count previous events and memorize them in rest periods as well as stimulation periods. To show that these four areas constitute a network, we assessed whether there existed a network related to steady-state neuronal processing by examining the whole time series using GCM among the four brain areas (IFG_L, IPL_L, FFA_R, and FG_L) for the experimental runs with 250 ms ISI. There was a strong positive influence on IPL_L from IFG_L and FG_L, i.e., there was effective connectivity from IFG_L and FG_L to IPL_L ($p < 0.05$, corrected) (Fig. 7; Supplementary Fig. S1). In addition, there was a strong positive influence on FFA_R from IFG_L, i.e., there was effective connectivity from IFG_L to FFA_R ($p < 0.05$, corrected) (Fig. 7; Supplementary Fig. S1). These findings indicate that these four areas constitute a network with two types of network modes: a dynamic network mode and a steady-state network mode.

Comparison of the behavioral performance of target detection showed that there was no significant difference in detection times for target trials between the repetition block and the alternation block (t-test, $p = 0.28$ for 250 ms ISI; see Supplementary Fig. S4), which were consistent with the previous paper[11].

Discussion

This study examined the top-down modulatory effects of perceptual expectation. We found modulatory effects of response enhancement and repetition suppression and examined related systematic factors: the high-level areas involved in the modulation, the temporal window range over which the expectation probability is effective for the modulation, and the interplay between high-level and low-level areas. We observed response enhancement and repetition suppression in the experimental run with 250 ms ISI and identified four brain areas in the frontal, temporal, and parietal regions that are involved in the response modulation with dual network modes: steady-state and dynamic network modes. We observed that the temporal window for effective response modulation ends up, at best, at 1,000 ms.

Although the motivation for this study was to examine the top-down modulatory mechanism related to repetition suppression using a paradigm similar to that used in a previous study[11], we observed unexpectedly strong response enhancement at FFA_R with weak repetition suppression, strong response enhancement at IFG_L and strong repetition suppression at IPL_L.

For 250 ms ISI trials, the response enhancement and repetition suppression were observed only in the repetition block but not in the alternation block. This result is consistent with that of a previous study that had used the same probability-controlled paradigm and supported the top-down modulation hypothesis (perceptual expectation) for repetition suppression[11]. However, our results of the present study revealed response enhancement as well as repetition suppression.

In our results, the response enhancement may be explained as a top-down modulation similar to an odd-ball effect. FFA_R, IFG_L, and FG_L showed that the Aa response was smaller than the Ra response. Ra was an unexpected trial compared with Aa; therefore, an odd-ball-like effect may be observed in the Ra condition. In addition, alternation trials were not novel trials in the alternation block, which means that there was no chance for an odd-ball-like effect to occur. In the alternation block, an odd-ball-like effect could occur in repetition trials, but there may also be repetition suppression, which may lead to responses of similar magnitude during Ar and Aa.

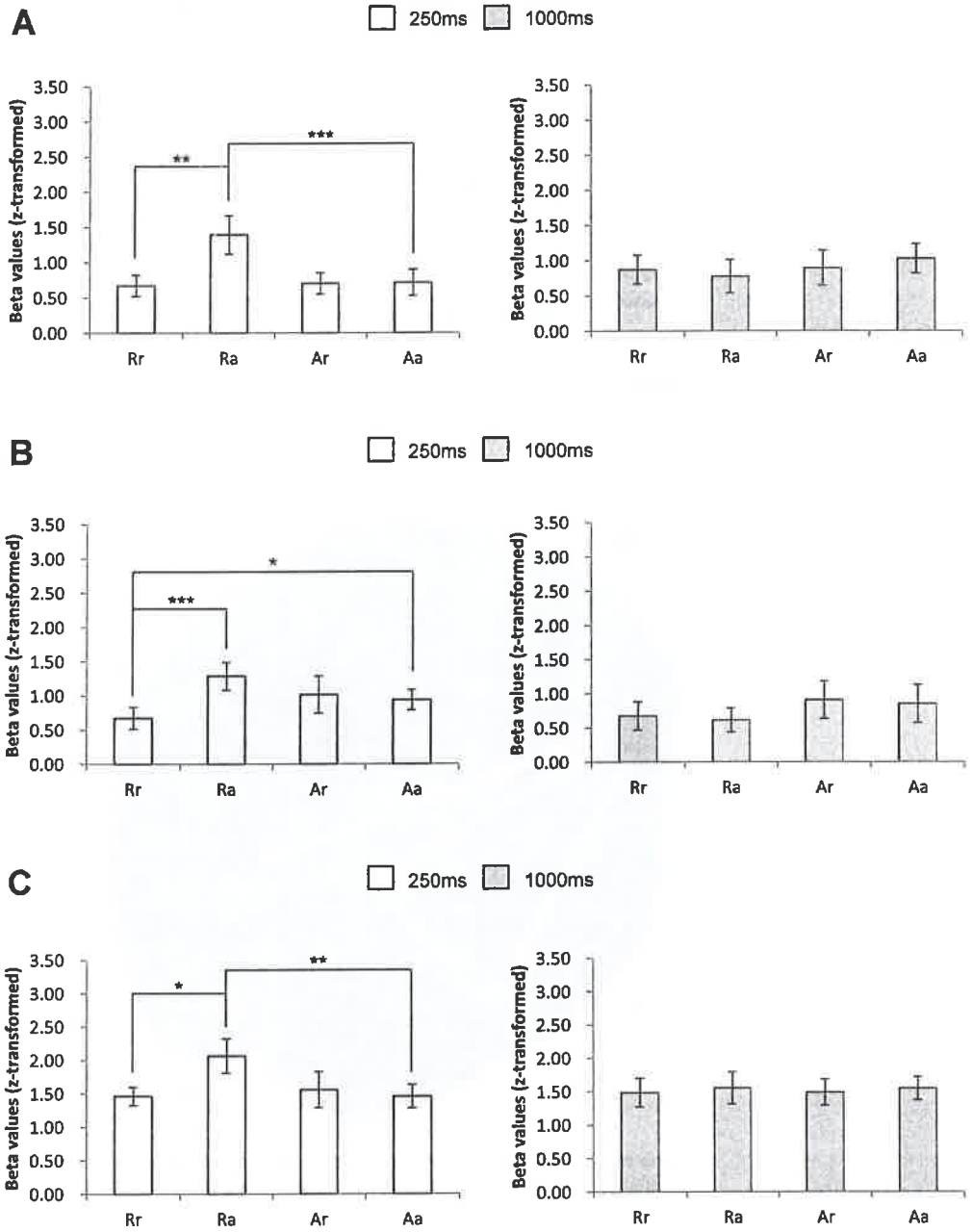


Figure 5. Responses during the four trial types (Rr, Ra, Ar, and Aa) in (**A**) IFG_L, (**B**) IPL_L and (**C**) FG_L for trials with 250 ms ISI and 1,000 ms ISI. ***$p < 0.001$, **$p < 0.01$, *$p < 0.05$. Error bars refer to standard error of the mean (SEM).

On the other hand, another previous study reported repetition suppression with 200 ms ISI using a passive experimental paradigm in which the stimuli were repeatedly presented for just short flashes (several tens of milliseconds); thus, the suppression was considered to be attributed to bottom-up modulation[17]. Together with results of previous studies, the response enhancement and repetition suppression observed in the present study demonstrate that response modulation at FFA_R can be partly attributed to both top-down and bottom-up modulation. This modulation should have occurred not only during the repetition block but also during the alternation block if the response enhancement and repetition suppression had exclusively resulted from bottom-up modulation[11,12]. In this response modulation, IFG_L and IPL_L appear to work differently, i.e., IFG_L is more related to response enhancement and IPL_L is more related to repetition suppression, as shown in the response patterns of those areas (Fig. 5). It has been reported that IPL_L is involved in a goal-directing function, which causes repetition suppression in human studies[18–20] or the prediction repetition priming phenomenon[21].

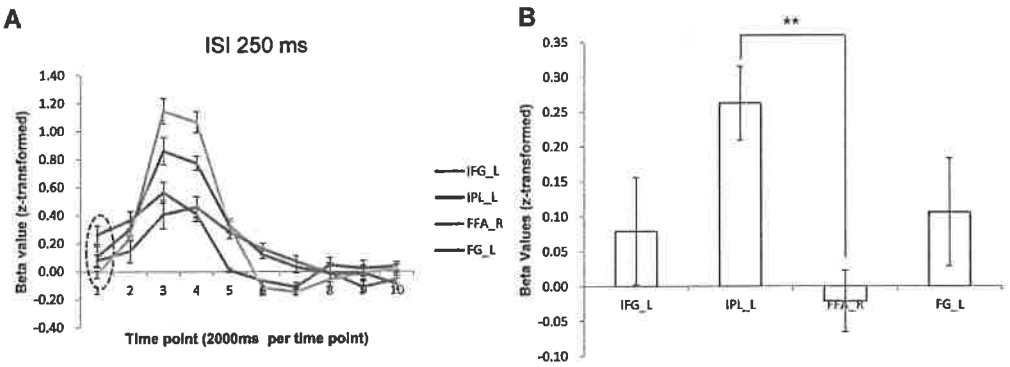


Figure 6. (A) Estimated time courses at FFA_R, IPL_L, IFG_L, and FG_R for trials with 250 ms ISI. (B) Responses at the stimulus onset in each area (IPL_L > FFA_R, $p < 0.03$; IPL > IFG_L, $p = 0.07$; IPL_L > FG_L, $p = 0.09$). **$p < 0.01$, Error bars refer to standard error of the mean (SEM).

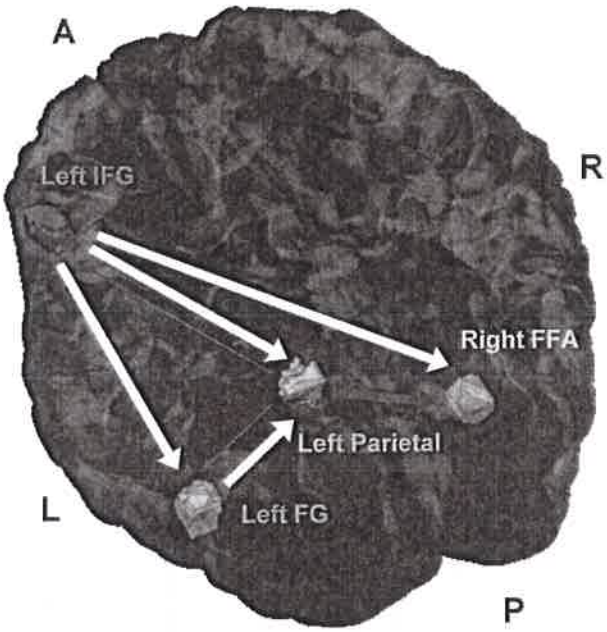


Figure 7. Three-dimensional view of dual network modes. White connections show the steady-state network mode, and red connections show the dynamic network mode.

Strong response enhancement and weak repetition suppression at FFA_R may be attributable to the stimulus parameter used. The current and previous study differ in terms of the stimulus duration of face pictures[11]. Although that difference could affect our results, it also demonstrates interplay of top-down and bottom-up processes in the response modulation.

For 1,000 ms ISI, unlike for 250 ms ISI, response enhancement and repetition suppression were not observed during repetition or alternation blocks. The finding that response modulation was observed with 250 ms ISI trials and not with 1,000 ms ISI trials suggests that, for our experimental conditions, the perceptual expectation effect on modulation faded when ISI lasted up to 1,000 ms, providing information regarding the temporal range over which this top-down modulation is effective. Previous studies[11,12] have reported the attenuation of repetition suppression at 500 ms ISI; the present study shows response modulation at 250 ms ISI and disappearance of the modulation at 1,000 ms ISI, indicating that the disappearance would have occurred between 500 ms and 1,000 ms. The use of three or more ISIs in a future study would give more precise temporal information.

IFG_L, IPL_L and FFA_R showed response enhancement or repetition suppression at 250 ms ISI during just the repetition block. This indicates that response modulation results from the interplay between FFA_R and these high-level areas. This type of interplay is supported by previous studies that demonstrated the inferior frontal and parietal cortices to be involved in probability-related processing[22–24]. Therefore, through the identification of the involvement of the high-level areas IFG_L and IPL_L, the present study indicates that response enhancement

and repetition suppression are attributable to top-down modulation more directly than previous studies did and suggests a brain network related to perceptual expectation[11,25]. Additional studies are needed to clarify whether the roles of the areas in this network are invariant regardless of the specific stimuli, tasks, or probabilities, which will give more information for understanding the interaction between low-level and high-level areas in this phenomenon.

Our results pertaining to the proposed brain network provide some information regarding the neuronal mechanism involved in top-down modulation signal processing. The earlier response at IPL_L in comparison with those at FFA_R, IFG_L, and FG_L indicates that top-down modulation is initiated first in the parietal area. Because response enhancement and repetition suppression are thought to be modulated by perceptual expectation, the early response at IPL_L may reflect a processing strategy in which stimulus probability information is updated first in the parietal area and is subsequently transferred to FFA_R, IFG_L, and/or FG_L for every stimulus input, constituting a dynamic network[26,27]. For this processing strategy to work, the parietal area has to maintain information regarding the frequency of previous trial occurrences or acquire this information from other areas.

Supporting that processing strategy is the steady-state network determined using GCM, which shows the directions of causality from IFG_L to IPL_L. This interaction between IFG_L and IPL_L in the steady-state network may be related to several cognitive functional processes such as attention, working memory, and predictive coding, and IFG_L seems to play some significant role in these processes. Many studies have shown that the frontal and parietal areas play a critical role in attention tasks, regardless of task types[28–30], and that they create a fronto–parietal network[31–33]. The fronto–parietal network is also reportedly involved in working memory processing[34,35]. Furthermore, there are some studies showing that the fronto–parietal network is involved in familiarity manipulation via a predictive coding model[26] as well as predictive modulation[36,37]. In addition to those previous reports, our result demonstrates that there was no significant difference in the response times for target trials between the repetition block and the alternation block in the ISI experiment (see Supplementary Fig. S4), which were consistent with the previous study[11]. These indicate that the responses in the higher areas cannot be explained by only a simple attentional effect and, therefore, suggest that IFG_L and IPL_L constitute a sub-network in the steady-state network and perform probability processing related to perceptual expectation.

Therefore, the results of previous studies and the present study suggest a mechanism for top-down modulation. In particular, the network composed of FFA_R, IFG_L, and IPL_L, operates in two modes: 1) The fronto–parietal interplay of IFG_L and IPL_L, working as a sub-network in the steady-state network mode, is involved in attending visual stimuli and sustaining information such as the probability variation in the task for the information for probability or expectation. 2) The information in the fronto-parietal sub-network is transferred to FFA_R from IPL_L in the dynamic network mode (Fig. 7).

Unlike other studies using explicit cues, the temporal relationship here is thought to result from an implicit processing mechanism of probability or expectation because we did not provide any explicit information to participants regarding expectation processing[38–41]. The similarity in behavioral data from trials with 250 ms ISI and 1,000 ms ISI also supports the implicit processing. This suggests that the paradigm used in the present study and in previous studies is useful to prove dynamic properties of brain networks[40–42].

For the response in the parietal area, which is locked to the stimulus input prior to other areas, a signal may be required to the parietal area from an area earlier than FFA_R. This could arise through a ventral to dorsal pathway that carries event information such as the stimulus-onset information that triggers expectation information. One of the candidate pathways is a major white-matter fascicle (vertical occipital fasciculus) connecting dorsal and ventral visual cortices[42]. However, further study is needed for elucidating the existence of such a pathway.

With regard to the specificity of top-down modulation, the response enhancement and suppression observed at FFA but not at the other areas in the temporal lobe indicates that this type of top-down modulation is spatially specific to stimulus contents. This is supported by previous studies focusing on repetition suppression modulated by perceptual expectation. In a study involving monkeys, there was no repetition suppression effect in LOC by repetition probability[7]; however, there was a significant effect in FBA[9], FFA, and PPA[8].

As for the lateralization for top-down modulation to the left hemisphere, previous several studies provide a possibility of the involvement of the left hemisphere (IFG_L and IPL_L) in temporal orienting (focusing to a specific moment in time)[43], disengaging temporally presented sequences of stimulus input[44] and categorization of stimulus inputs[45] although further study is required to clarify it.

From the physiological point of view, the activation of the parietal area at stimulus onset may not be consistent with the BOLD theory in which activation signals begin to rise at 2–4 s[46,47]. However, this type of response pattern is not unusual. In instances where prior information regarding a stimulus (such as a cue) had been given, a BOLD response was observed from stimulus-related areas before the responses to the physical stimuli appeared[38–41]. Although we did not provide any explicit cue in the present experiments, the expectation for probability variation may work as an implicit cue and activate the area prior to the activation by the physical stimulus.

Taken together, our results more directly verify that top-down modulation is involved in response enhancement and repetition suppression related to perceptual expectation and provide important systematic details for top-down modulation.

Methods

Participants. Eleven subjects (22.82 ± 0.55 years, four males and seven females) participated in the study. None of the subjects took medications that may affect brain function, and none of them had clinical or pathological neuropsychiatric disease. All subjects gave written informed consent. All experiments were performed in accordance with the relevant guidelines and regulations of the Gachon Gil Hospital's Institutional Review Board, which approved all the experimental protocols.

Experimental Procedure. A mixed block design, containing an event-related design in the stimulus block, was used (Fig. 1). There were three trial conditions: repetition, alternation, and target. Each trial consisted of facial images presented as paired stimuli separated by ISI. These images were generated using FaceGen (Singular Inversions, Toronto, Canada). The repetition trials used a pair of same images. The alternation trials used a pair of different facial images. The target trials used a pair of images in which the second facial image was an inverted version of the first image. The on-time for each image was 50 ms.

The study consisted of two task runs with different ISIs (250 ms and 1,000 ms) for each participant. Each task run was mixed block/event-related design. There were two kinds of blocks (repetition blocks and alternation blocks) and three kinds of trials (repetition trial, alternation trial and target trial). Repetition trial consisted of two same face images whereas alternation trial consisted of two different face images. In addition, target trial consisted of upright and inverted face images. Each block consisted of 20 trials including repetition, alternation and target trials. There were 12 repetition trials, 4 alternation trials and 4 target trials in each repetition block while 4 repetition trials, 12 alternation trials and 4 target trials in each alternation block. Repetition and alternation blocks were repeated thrice in each task at random order run and trials were separated by varying inter-trial intervals (2,000 ms–4,000 ms, mean = 3,000 ms). Three kinds of trial were presented randomly in both the repetition block and the alternation block. Each trial consisted of two stimuli with 50 ms duration and inter-stimulus interval of 250 ms, which made 350 ms for the 250 ms ISI experiment, and 1100 ms for the 1000ms ISI experiment. The stimulation was apparently event-related but implicitly grouped as the same way as the previous paper[11]. Each repetition and alternation block was 87 s.

To identify FFA, an additional experimental run was performed using a simple box-car design that included face and scene images. The run consisted of two types of stimulus blocks with either faces or scenes, which were interspersed with rest blocks. Each stimulus block was 12 s long and consisted of eight images. The duration of each image was 1500 ms. The rest block was 18 s long, during which a black crosshair was presented at the center of the screen on a gray background. Each stimulus block was repeated four times during the experimental run. The total scan time was 594s.

Data Acquisition. The experiment was conducted using a 3-Tesla MRI scanner (MAGNETOM VERIO, Siemens, Erlangen, Germany). Functional images were obtained using a Gradient Echo single-shot echo planar image sequence (repetition time = 2,000 ms; echo time = 30 ms; in-plane resolution = 3.4×3.4 mm^2; slice thickness = 3.4 mm; number of slices = 34 with no gap; slice orientation along AC-PC). Using a gradient echo, T1-weighted anatomical images were acquired with inversion recovery and magnetization-prepared rapid acquisition (repetition time = 1,900 ms; echo time = 2.93 ms; in-plane resolution = 1×1 mm^2; slice thickness = 1 mm). Functional images and T1-weighted images had the same orientation for better co-registration in 3D-space.

General Linear Model (GLM) Analysis. Functional image data were analyzed using Brainvoyager QX (Brain Innovation B.V., Maastricht, the Netherlands). Functional images were preprocessed by slice-timing correction, head motion correction, and temporal high-pass filtering (above 0.01 Hz) to remove physiological noise. These images were co-registered with each anatomical image. For analyzing our rapid event-related design, deconvolution analysis, which was implemented using Brainvoyager software, was performed. In deconvolution analysis, 10 shifted predictors per stimulus trial condition were used to define the respective BOLD responses. Each time point was 2,000 ms (one single volume), and a whole BOLD response (from the initial to final point) was considered to last for 20 s. GLM analysis was performed after deconvolution analysis. To acquire maximum estimated beta values, we used the third and fourth time points of the averaged estimated response (6 and 8 s after the stimulus onset) for random effect analysis in four trials (Rr, Ra, Ar, Aa)[48]. All beta values were corrected for serial correlation by autocorrelation and normalized by z-transformation.

Granger Causal Model (GCM) Analysis. We defined IFG_L, IPL_L and FG_L as reference ROIs. All time-series from those ROIs were used in GCM analysis. GCM analysis was conducted by a plugin in Brainvoyager QX. We firstly ran GCM analysis individually with those reference ROIs. A causality map of each reference ROI was computed. The causality map was difference GCM (dGCM) which showed effective connectivity from the reference ROI to other brain areas. The dGCM represented two types of causalities. One was the connectivity from a reference ROI to other areas and the other was the connectivity from the other areas to the reference ROI. All dGCM of four reference ROIs were analyzed individually and group dGCMs were estimated by using one-sample t-test. Group dGCMs were corrected for multiple comparisons at a cluster-level threshold of $p < 0.05$[49].

References

1. Grill-Spector, K., Henson, R. & Martin, A. Repetition and the brain: neural models of stimulus-specific effects. *Trends Cogn. Sci.* **10**, 14–23 (2006).
2. Krekelberg, B., Boynton, G. M. & van Wezel, R. J. A. Adaptation: from single cells to BOLD signals. *Trends Neurosci.* **29**, 250–256 (2006).
3. Sobotka, S. & Ringo, J. L. Stimulus specific adaptation in excited but not in inhibited cells in inferotemporal cortex of Macaque. *Brain Res.* **646**, 95–99 (1994).
4. Ringo, J. L. Stimulus specific adaptation in inferior temporal and medial temporal cortex of the monkey. *Behav. Brain Res.* **76**, 191–197 (1996).
5. Xiang, J.-Z. & Brown, M. W. Differential neuronal encoding of novelty, familiarity and recency in regions of the anterior temporal lobe. *Neuropharmacology* **37**, 657–676 (1998).
6. Kaliukhovich, D. A. & Vogels, R. Stimulus Repetition Probability Does Not Affect Repetition Suppression in Macaque Inferior Temporal Cortex. *Cereb. Cortex* **21**, 1547–1558 (2011).
7. Kovács, G., Kaiser, D., Kaliukhovich, D. A., Vidnyánszky, Z. & Vogels, R. Repetition Probability Does Not Affect fMRI Repetition Suppression for Objects. *J. Neurosci.* **33**, 9805–9812 (2013).

8. Egner, T., Monti, J. M. & Summerfield, C. Expectation and Surprise Determine Neural Population Responses in the Ventral Visual Stream. *J. Neurosci.* **30,** 16601–16608 (2010).
9. Ewbank, M. P. *et al.* Changes in 'top-down' connectivity underlie repetition suppression in the ventral visual pathway. *J. Neurosci. Off. J. Soc. Neurosci.* **31,** 5635–5642 (2011).
10. Larsson, J. & Smith, A. T. fMRI Repetition Suppression: Neuronal Adaptation or Stimulus Expectation? *Cereb. Cortex N. Y. NY* **22,** 567–576 (2012).
11. Summerfield, C., Trittschuh, E. H., Monti, J. M., Mesulam, M.-M. & Egner, T. Neural repetition suppression reflects fulfilled perceptual expectations. *Nat. Neurosci.* **11,** 1004–1006 (2008).
12. Mayrhauser, L., Bergmann, J., Crone, J. & Kronbichler, M. Neural repetition suppression: evidence for perceptual expectation in object-selective regions. *Front. Hum. Neurosci.* **8,** 225 (2014).
13. Sung, Y.-W. *et al.* An fMRI study of neuronal interactions in face-selective areas of the brain. *Brain Res.* **1366,** 54–59 (2010).
14. Serences, J. T. A comparison of methods for characterizing the event-related BOLD timeseries in rapid fMRI. *NeuroImage* **21,** 1690–1700 (2004).
15. Giesbrecht, B., Weissman, D. H., Woldorff, M. G. & Mangun, G. R. Pre-target activity in visual cortex predicts behavioral performance on spatial and feature attention tasks. *Brain Res.* **1080,** 63–72 (2006).
16. Molinaro, N. & Carreiras, M. Electrophysiological evidence of interaction between contextual expectation and semantic integration during the processing of collocations. *Biol. Psychol.* **83,** 176–190 (2010).
17. Ogawa, S. *et al.* An approach to probe some neural systems interaction by functional MRI at neural time scale down to milliseconds. *Proc. Natl. Acad. Sci.* **97,** 11026–11031 (2000).
18. Grafton, S. T. & de C. Hamilton, A. F. Evidence for a distributed hierarchy of action representation in the brain. *Hum. Mov. Sci.* **26,** 590–616 (2007).
19. Króliczak, G., McAdam, T. D., Quinlan, D. J. & Culham, J. C. The Human Dorsal Stream Adapts to Real Actions and 3D Shape Processing: A Functional Magnetic Resonance Imaging Study. *J. Neurophysiol.* **100,** 2627–2639 (2008).
20. Grabski, K., Lamalle, L. & Sato, M. Somatosensory-Motor Adaptation of Orofacial Actions in Posterior Parietal and Ventral Premotor Cortices. *PLOS ONE* **7,** e49117 (2012).
21. Ward, E. J., Chun, M. M. & Kuhl, B. A. Repetition Suppression and Multi-Voxel Pattern Similarity Differentially Track Implicit and Explicit Visual Memory. *J. Neurosci.* **33,** 14749–14757 (2013).
22. D'Arcy, R. C. N., Connolly, J. F., Service, E., Hawco, C. S. & Houlihan, M. E. Separating phonological and semantic processing in auditory sentence processing: A high-resolution event-related brain potential study. *Hum. Brain Mapp.* **22,** 40–51 (2004).
23. Zandbelt, B. B., Bloemendaal, M., Neggers, S. F. W., Kahn, R. S. & Vink, M. Expectations and violations: Delineating the neural network of proactive inhibitory control. *Hum. Brain Mapp.* **34,** 2015–2024 (2013).
24. Vink, M., Kaldewaij, R., Zandbelt, B. B., Pas, P. & du Plessis, S. The role of stop-signal probability and expectation in proactive inhibition. *Eur. J. Neurosci.* **41,** 1086–1094 (2015).
25. Ewbank, M. P., von dem Hagen, E. A. H., Powell, T. E., Henson, R. N. & Calder, A. J. The effect of perceptual expectation on repetition suppression to faces is not modulated by variation in autistic traits. *Cortex* **80,** 51–60 (2016).
26. Gardner, T., Goulden, N. & Cross, E. S. Dynamic Modulation of the Action Observation Network by Movement Familiarity. *J. Neurosci.* **35,** 1561–1572 (2015).
27. Leitão, J., Thielscher, A., Tünnerhoff, J. & Noppeney, U. Concurrent TMS-fMRI Reveals Interactions between Dorsal and Ventral Attentional Systems. *J. Neurosci.* **35,** 11445–11457 (2015).
28. Coull, J. T., Frith, C. D., Frackowiak, R. S. & Grasby, P. M. A fronto-parietal network for rapid visual information processing: a PET study of sustained attention and working memory. *Neuropsychologia* **34,** 1085–1095 (1996).
29. Pugh, K. R. *et al.* Auditory Selective Attention: An fMRI Investigation. *NeuroImage* **4,** 159–173 (1996).
30. Vanni, S. & Uutela, K. Foveal Attention Modulates Responses to Peripheral Stimuli. *J. Neurophysiol.* **83,** 2443–2452 (2000).
31. Linden, D. E. J. *et al.* Cortical capacity constraints for visual working memory: dissociation of fMRI load effects in a fronto-parietal network. *NeuroImage* **20,** 1518–1530 (2003).
32. Braga, R. M., Wilson, L. R., Sharp, D. J., Wise, R. J. S. & Leech, R. Separable networks for top-down attention to auditory non-spatial and visuospatial modalities. *Neuroimage* **74,** 77–86 (2013).
33. Mastroberardino, S., Santangelo, V. & Macaluso, E. Crossmodal semantic congruence can affect visuo-spatial processing and activity of the fronto-parietal attention networks. *Front. Integr. Neurosci.* **9,** 45 (2015).
34. Klingberg, T., O'Sullivan, B. T. & Roland, P. E. Bilateral activation of fronto-parietal networks by incrementing demand in a working memory task. *Cereb. Cortex N. Y. N 1991* **7,** 465–471 (1997).
35. Pessoa, L. & Ungerleider, L. G. Neural correlates of change detection and change blindness in a working memory task. *Cereb. Cortex N. Y. N 1991* **14,** 511–520 (2004).
36. Vossel, S., Thiel, C. M. & Fink, G. R. Cue validity modulates the neural correlates of covert endogenous orienting of attention in parietal and frontal cortex. *NeuroImage* **32,** 1257–1264 (2006).
37. Ahlheim, C., Stadler, W. & Schubotz, R. I. Dissociating dynamic probability and predictability in observed actions—an fMRI study. *Front. Hum. Neurosci.* **8,** 273 (2014).
38. Atlas, L. Y., Bolger, N., Lindquist, M. A. & Wager, T. D. Brain Mediators of Predictive Cue Effects on Perceived Pain. *J. Neurosci.* **30,** 12964–12977 (2010).
39. Hansen, K., Hillenbrand, S. & Ungerleider, L. Persistency of priors-induced bias in decision behavior and the fMRI signal. *Decis. Neurosci.* **5,** 29 (2011).
40. Li, C. & Wu, J. Activation of Right Ventral Prefrontal Cortex Using a Predictive Cue during Visual Spatial Orienting of Attentional Processes: An fMRI Study. *Neurol. Res. Int.* **2012,** e961342 (2012).
41. Bickel, S., Dias, E. C., Epstein, M. L. & Javitt, D. C. Expectancy-related modulations of neural oscillations in continuous performance tasks. *NeuroImage* **62,** 1867–1876 (2012).
42. Yeatman, J. D. *et al.* The vertical occipital fasciculus: a century of controversy resolved by *in vivo* measurements. *Proc. Natl. Acad. Sci. USA.* **111,** E5214–5223 (2014).
43. Correa, A., Lupiáñez, J., Milliken, B. & Tudela, P. Endogenous temporal orienting of attention in detection and discrimination tasks. *Percept. Psychophys.* **66,** 264–278 (2004).
44. Coull, J. T. & Nobre, A. C. Where and When to Pay Attention: The Neural Systems for Directing Attention to Spatial Locations and to Time Intervals as Revealed by Both PET and fMRI. *J. Neurosci.* **18,** 7426–7435 (1998).
45. Noesselt, T., Shah, N. J. & Jäncke, L. Top-down and bottom-up modulation of language related areas – An fMRI Study. *BMC Neurosci.* **4,** 13 (2003).
46. Ogawa, S. *et al.* Intrinsic signal changes accompanying sensory stimulation: functional brain mapping with magnetic resonance imaging. *Proc. Natl. Acad. Sci.* **89,** 5951–5955 (1992).
47. Aguirre, G. K., Zarahn, E. & D'Esposito, M. The Variability of Human, BOLD Hemodynamic Responses. *NeuroImage* **8,** 360–369 (1998).
48. Kohrs, C., Angenstein, N., Scheich, H. & Brechmann, A. Human striatum is differentially activated by delayed, omitted, and immediate registering feedback. *Front. Hum. Neurosci.* **6,** 243 (2012).
49. Forman, S. D. *et al.* Improved assessment of significant activation in functional magnetic resonance imaging (fMRI): use of a cluster-size threshold. *Magn. Reson. Med. Off. J. Soc. Magn. Reson. Med. Soc. Magn. Reson. Med.* **33,** 636–647 (1995).

Acknowledgements

This research was supported by MEXT-Supported Program for the Strategic Research Foundation at Private Universities, 2014–2018 and the National Research Foundation of Korea (NRF) Grant funded by Korea Government (MSIP) (no. NRF-2014M3C7033998).

Author Contributions

All authors, U.C., Y.S. and S.O., contributed equally to this work. All authors designed this study. U.C. collected the data. U.C. and Y.S. performed the data analysis. All authors discussed the results and implications, and wrote the manuscript at all stages.

Additional Information

Supplementary information accompanies this paper at http://www.nature.com/srep

Competing financial interests: The authors declare no competing financial interests.

How to cite this article: Choi, U.-S. *et al.* Steady-state and dynamic network modes for perceptual expectation. *Sci. Rep.* **7**, 40626; doi: 10.1038/srep40626 (2017).

Publisher's note: Springer Nature remains neutral with regard to jurisdictional claims in published maps and institutional affiliations.

This work is licensed under a Creative Commons Attribution 4.0 International License. The images or other third party material in this article are included in the article's Creative Commons license, unless indicated otherwise in the credit line; if the material is not included under the Creative Commons license, users will need to obtain permission from the license holder to reproduce the material. To view a copy of this license, visit http://creativecommons.org/licenses/by/4.0/

© The Author(s) 2017

PLOS | ONE

RESEARCH ARTICLE

Visual Mislocalization of Moving Objects in an Audiovisual Event

Yousuke Kawachi*

Kansei Fukushi Research Institute, Tohoku Fukushi University, Sendai, Japan

* kawachi@tfu-mail.tfu.ac.jp

CrossMark
click for updates

OPEN ACCESS

Citation: Kawachi Y (2016) Visual Mislocalization of Moving Objects in an Audiovisual Event. PLoS ONE 11(4): e0154147. doi:10.1371/journal.pone.0154147

Editor: Leonardo Chelazzi, University of Verona, ITALY

Received: July 10, 2015

Accepted: April 9, 2016

Published: April 25, 2016

Copyright: © 2016 Yousuke Kawachi. This is an open access article distributed under the terms of the Creative Commons Attribution License, which permits unrestricted use, distribution, and reproduction in any medium, provided the original author and source are credited.

Data Availability Statement: All datasets are available at https://dx.doi.org/10.6084/m9.figshare.3172696.v1 and https://sites.google.com/site/yousukekawachi/ovlprawdata.

Funding: This work was supported by a Grant-in-Aid of the Japan Society for the Promotion of Science (JSPS) for Scientific Research (no. 25530173 and 26350995) and MEXT-Supported program for the Strategic Research Foundation at Private Universities, 2014-2018. The funders had no role in study design, data collection and analysis, decision to publish, or preparation of the manuscript.

Competing Interests: The author has declared that no competing interests exist.

Abstract

The present study investigated the influence of an auditory tone on the localization of visual objects in the stream/bounce display (SBD). In this display, two identical visual objects move toward each other, overlap, and then return to their original positions. These objects can be perceived as either streaming through or bouncing off each other. In this study, the closest distance between object centers on opposing trajectories and tone presentation timing (none, 0 ms, ± 90 ms, and ± 390 ms relative to the instant for the closest distance) were manipulated. Observers were asked to judge whether the two objects overlapped with each other and whether the objects appeared to stream through, bounce off each other, or reverse their direction of motion. A tone presented at or around the instant of the objects' closest distance biased judgments toward "non-overlapping," and observers overestimated the physical distance between objects. A similar bias toward direction change judgments (bounce and reverse, not stream judgments) was also observed, which was always stronger than the non-overlapping bias. Thus, these two types of judgments were not always identical. Moreover, another experiment showed that it was unlikely that this observed mislocalization could be explained by other previously known mislocalization phenomena (i.e., representational momentum, the Fröhlich effect, and a turn-point shift). These findings indicate a new example of crossmodal mislocalization, which can be obtained without temporal offsets between audiovisual stimuli. The mislocalization effect is also specific to a more complex stimulus configuration of objects on opposing trajectories, with a tone that is presented simultaneously. The present study promotes an understanding of relatively complex audiovisual interactions beyond simple one-to-one audiovisual stimuli used in previous studies.

Introduction

The perceptual system estimates spatial positions, relationships, and trajectories of moving objects to understand causal relations [1], social interactions [2], and situations with obscured object locations. For a precise estimation, the system accumulates available sensory inputs to different modalities from events, across space and time. However, perceived positions and trajectories are not always veridical and are flexibly modulated by interactions between multisensory inputs.

Many previous multisensory studies have reported that vision provides precise spatial information to dominate a spatial percept, while audition provides precise temporal information. It has been assumed that multisensory interactions are subject to a "Modality Appropriateness" hypothesis [3], which postulates that a sensory modality more appropriate to a given task has a dominant effect on performance. A representative example is the spatial ventriloquism effect [4]. For this effect, the location of auditory stimuli (e.g., the ventriloquist's speech without lip movements) is mislocalized toward the location of the visual stimulus that is presented simultaneously with the auditory one (e.g., the puppet's lip movements). However, there are several reports suggesting that auditory information can affect visual spatial processing: spatial distortion mediated by auditory information attracting the perceived timing of a visual event [5–9]. An auditory tone presented before or after a visual flash can draw the perceived timing of the flash towards that of the auditory stimulus. This phenomenon is known as "temporal ventriloquism." In previous studies [5, 6], temporal ventriloquism has an effect on the performance of a visuospatial task in which observers judge the spatial position of a flash relative to that of a moving object (e.g., flash-lag effect paradigm). An auditory stimulus is presented temporally proximal to a flash and modulates perceived timing of the flash, which results in the modulation of the perceived spatial relationship between the flash and the moving object. Furthermore, Heron et al. [7] reported that a tone presented prior to the turn of a moving object causes the turn-point to be mislocalized in front of the physical turn-point. Non-simultaneity of audiovisual stimuli seems to be critical for such displacement phenomena. Teramoto, Hidaka, Gyoba and Suzuki [8] and Chien, Ono, and Watanabe [9] showed that auditory sustained or transient stimulation modulates the perceived disappearing point of a moving object. Auditory offset after or before the physical disappearance biases the perceived disappearing point in the forward or backward direction of visual motion, respectively. Thus, although visual mislocalization by an auditory stimulus is apparently inconsistent with visual dominance in the spatial domain, these studies [5–9] suggested that the auditory modulation of visual localization needs an auditory stimulus to attract the timing of a visual stimulus toward the auditory one.

The present study demonstrates a new type of audiovisual mislocalization in which it is unnecessary for an auditory stimulus to modulate perceived visual stimulus timing (see [10], for a related study). We used an audiovisual stream/bounce display. The stream/bounce display (SBD) includes two visually identical objects, which move toward each other, and then move apart in a two-dimensional display. Observers either perceive the objects as streaming through or bouncing off each other. Although the SBD is ambiguous, many observers tend to perceive the two objects as streaming through each other [11, 12]. However, Sekuler, Sekuler and Lau [13] reported that a brief tone presented at the moment the two objects completely overlap (or come closest to each other) predominantly induces the bouncing percept. Thus, in general, previous studies using the SBD focused on perceived motion trajectories affected by an auditory tone. Interestingly, in our previous studies [14, 15], observers informally reported that visual objects do not appear to be overlapping when an auditory tone is presented at the moment the objects physically overlap. Based on participants' introspective reports, we hypothesized that object overlap judgments would be affected by the auditory tone presented simultaneously with the overlapping of visual objects. This hypothesis is inconsistent with the modality appropriateness hypothesis. Given that the present task is not in the temporal domain, and audition does not have temporal information for attracting the perceived timing of a visual event, vision should dominate spatial localization performance. In the ambiguous stimulus configuration of the SBD, the perceptual system would have difficulty judging whether a sensory modality is appropriate and reliable for generating a veridical perception. Therefore, a visual dominance effect would not be sufficiently obtained. We expected that the perceptual system is able to

utilize such a salient stimulus as a sudden auditory tone in a cluttered surrounding environment, to resolve perceptual ambiguity in temporal proximity with the tone [16].

The present study assessed whether the spatial positions of overlapping visual objects in the SBD could be mislocalized due to simultaneous presentation of an auditory stimulus, so as to be perceived as non-overlapping (Experiment 1). Although previous studies reported that the non-simultaneity of audiovisual stimuli generates the mislocalization of an object [7–9], it is important to report that physically near-simultaneous stimuli can generate object mislocalization. Typically, multiple near-simultaneous sensory inputs should be considered as generated by a physical event in the environment. Simultaneous audiovisual stimuli exclude the possibility that an auditory tone dominates the perceived timing of a visual stimulus to modulate visuospatial localization. Thus, we can show a new type of audiovisual mislocalization without the auditory dominance effect in the temporal domain. For the present study, the closest distance between object centers, that is, the amount of overlap between objects in the SBD, and the tone presentation (presence or absence) were manipulated. Observers were asked to judge whether the two objects appeared to overlap with each other. We predicted that this crossmodal mislocalization would suggest that visual dominance is degraded in the SBD and object localization is flexibly modulated through multisensory interaction triggered by a sudden auditory tone.

We also tested whether mislocalization occurred through an auditory stimulus presentation before and after the instant when the object centers were closest (Experiment 2). If temporal offsets between an auditory stimulus and the overlap of visual objects are needed for any observed mislocalization, the degree of mislocalization in non-zero offset conditions may be larger than in the zero offset (simultaneity) condition, in line with studies of similar audiovisual effects [7–9]. This temporal profile is considered one of the main properties of visuospatial processing and crossmodal interaction. Object localization does not seem to be immediate and requires some time. The perceptual system accumulates evidence of multisensory inputs over a spatial and temporal window and determines momentary visual representations. When a sound is presented before the visual event (i.e., before overlap), the system makes a prediction in which it expects a certain visual event (e.g., non-overlap of objects) on the basis of prior information (auditory tone before the overlap). When a sound is presented after the visual event it may make a postdiction in which it interprets the event by incorporating information obtained after the events (auditory tone after the overlap) [17]. This test will reveal those predictive/postdictive properties involved in mislocalization and help relate the present findings to previous ones, which were obtained with non-simultaneous audiovisual stimuli. Moreover, to further understand mislocalization, the present study explored whether our observed mislocalization could be accounted for by the size and direction of other phenomena and the sensitivity to an auditory stimulus within other phenomena (i.e., representational momentum [18], the Fröhlich effect [19, 20], and a turn-point shift [10]) (Experiment 3).

In addition to the overlap judgment task as described above, we asked participants to judge whether the two objects appeared to be streaming through, bouncing off each other, or reversing their direction of motion in Experiments 1 and 2. We elucidated how directional change judgments are related to the object overlap judgments in order to show that both judgments are not always consistent with each other. Although the relationship between both judgments has yet to be sufficiently examined, object localization reflected in overlap judgments seems to be closely related to the directional change judgment. This is because the closest points between object centers are the points where objects are perceived as changing their motion trajectories.

We tried to show a new type of crossmodal mislocalization in the SBD. Crossmodal mislocalizations are induced by an auditory stimulus, near simultaneous with visual stimuli, different from a non-simultaneous stimulus in previous studies (Experiment 1 and Experiment 2). This

study also examined whether judgments regarding spatial positions (i.e., overlap judgments) and moving trajectories (i.e., directional change judgments) differ in terms of the SBD. Furthermore, crossmodal mislocalization is not predicted by previously reported mislocalization phenomena (Experiment 3). Our goal was to determine whether the present findings reveal a new crossmodal interaction inconsistent with the modality appropriateness hypothesis. During this interaction, vision does not dominate the visuospatial localization of objects, and a non-simultaneous auditory tone does not attract the timing of a visual event (auditory dominance effect in the temporal domain).

Experiment 1

Ethics statement

All experiments were approved by the Ethical Committee of Tohoku Fukushi University and conducted according to principles from the Declaration of Helsinki. Written informed consent was obtained from all participants.

Participants

Nineteen healthy adults (4 males and 15 females) participated in the experiment. Their average age was 21.94 years (age range, 19–32 years). Except for one author (YK), all participants were naive as to the purpose of the experiment. All were right-handed, had either normal or corrected-to-normal vision, and reported no hearing anomalies.

Stimuli

All stimuli were generated on a PC (Dell Precision T5500; Dell: Austin, TX) running Matlab 2007a (The MathWorks, Inc.: Natick, MA) using the Cogent Graphics package (http://www.vislab.ucl.ac.uk/cogent.php). Visual stimuli were presented on a CRT monitor (Sony GDM-F520, Sony: Tokyo, Japan; refresh rate 100 Hz; resolution 1024×768 pixels). As shown in Fig 1, a red fixation dot was presented at the center of the monitor (13.19 cd/m2, 20.46 arc min of visual angle) on a gray background (52.99 cd/m2). Each one of the two objects subtended 36.37 arcmin of visual angle (13.33 cd/m2). The objects, presented 182.40 arcmin above the fixation point, moved from opposite sides toward each other. The monitor refresh rate was 100 Hz, but the actual frame rate of the animation was 33 frames per second (1 frame = 30 ms). Object positions were displaced every 30 ms. This displacement, combined with the frame rate, resulted in an object speed of 3.79 deg/s. After 630 ms of motion, objects started to reverse their direction with some degree of object overlap and returned to their original positions. The closest distance between object centers, that is, the amount of overlap between objects, was manipulated by increasing the inter-object distances: 0 (complete overlap), 13.64, 20.46, 27.28, 34.10, 40.92, and 54.56 arcmin between the object centers. Moreover, the spatial positions where the objects change motion trajectories fluctuated by the objects' starting point jittering in the range of ± 61.38 arcmin on a trial-by-trial basis. In half of the trials, a brief tone (800 Hz, 10 ms, 68 dB SPL; background noise level: 40 dB) was introduced through headphones (HDA 200; Sennheiser: Wedemark, Germany), only at the instant for the closest distance. The physical simultaneity of auditory and visual stimuli was assessed with an oscilloscope (TBS 1102; Tektronix, Pittsfield, MA). Deviations from simultaneity did not exceed 5 ms.

Procedure

Each participant sat approximately 57 cm away from the display and used a chin rest to stabilize the visual field. Observers judged whether two moving objects appeared to overlap

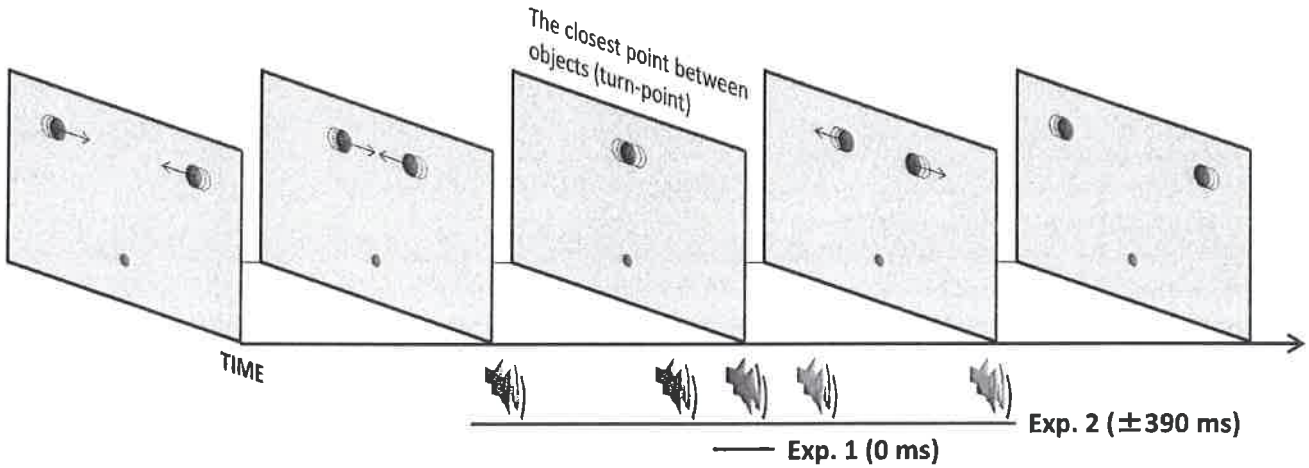


Fig 1. Schematic illustration of stimuli for Experiment 1. The objects moved from opposite sides toward each other. After 630 ms of motion, objects started to reverse their direction with some degree of overlap and returned to their original positions. The starting points for either object (dashed-line circle) were displaced to manipulate the distance between the object centers, that is, the degree of object overlap in a trial-by-trial manner.

doi:10.1371/journal.pone.0154147.g001

and then judged whether the objects appeared to stream through, bounce off each other, or reverse their motion direction. Experimental conditions included the presentation of a brief tone (tone/no-tone) and the degree of maximal overlap between the objects (0, 13.64, 20.46, 27.28, 34.10, 40.92, or 54.56 arcmin). Each condition combination was repeated over 20 trials.

Results

For the motion direction (stream/bounce/reverse) judgment task, we combined bounce and reverse judgments into directional change judgments. Then, a cumulative Gaussian function was fitted to each proportion of overlap judgments and directional change judgments (Fig 2a and 2b). We calculated the point of subjective equality (hereafter referred to as PSE) corresponding to 50% in the function (Fig 2c and 2d). In other words, the PSE indicates the closest distance between object centers (the degree of object overlap) at which point the participant is equally likely to report the objects as overlapping or not (for the overlap judgment task) or to report the objects as changing directions or not (for the motion direction judgment task) [21, 22]. For example, smaller (larger) PSEs mean that although objects overlap to a larger (smaller) extent, observers tend to perceive them as non-overlapping. A two-way repeated measures ANOVA for PSE was conducted with *judgment type* (2: overlap judgment task/motion direction judgment task) and *tone presentation* (2: tone/no tone) as factors. The main effects of judgment type and tone conditions were significant, $F(1, 18) = 19.18$, $p < .001$, and $F(1, 18) = 79.44$, $p < .001$. The interaction was also significant, $F(1,18) = 9.23$, $p < .01$. A post hoc analysis (Ryan's method) revealed that the PSEs in the tone conditions were smaller than those in the no-tone condition, indicating that the tone influenced participants to underestimate the amount of overlap (i.e., overestimate the closest distance between object centers) and promoted directional change responses, $F(1, 36) = 12.67$, $< .005$, and $F(1,36) = 66.31$, $< .001$. Moreover, the PSE for the motion direction judgment task was smaller than for the overlap judgment task in the tone condition, $F(1, 36) = 27.60$, $p < .001$. Additionally, when objects completely overlapped, the direction change judgment rate was lower than what had been observed in several previous studies [13]. This low rate may be due to the relatively slow velocity of the object.

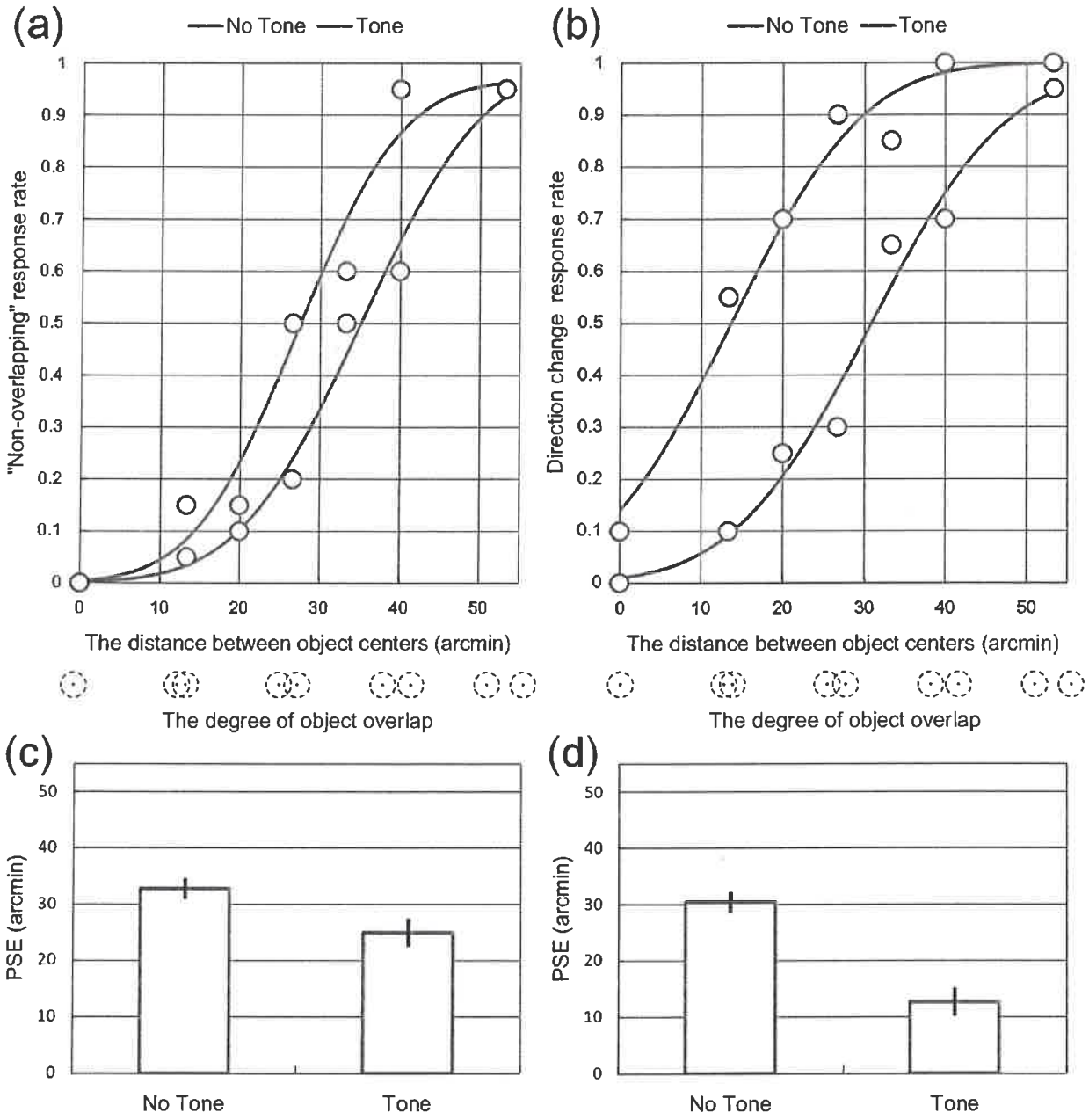


Fig 2. Results of Experiment 1. The psychometric functions fitted to "non-overlapping" judgment data (a) and directional change judgment data (b) from Subject 8. Below the abscissae, the degree of object overlap corresponds to the distance between object centers. Group mean PSEs for tone conditions in the (c) overlap and (d) directional change judgment tasks. Error bars denote standard errors of the mean (n = 19).

doi:10.1371/journal.pone.0154147.g002

Compared to the 6 deg/s velocity in Sekuler's study, a 3.79 deg/s velocity is relatively slow. As object velocity increases, the bouncing response rate (i.e., direction change response rate) increases, irrespective of sound presentation [23]. Thus, our low direction change response rate may be due to a slower object velocity.

Finally, we conducted a one-sample *t*-test to examine whether there was a significant difference from 36.37 arcmin in terms of physical contact distances between objects (this value corresponds to object size) for the PSE during the overlap judgment task in the tone-present condition. Results showed that the PSE was smaller than the 36.37 arcmin of the physical contact distances, $t(18) = -5.77$, $p < 0.001$, indicating that participants illusorily overestimated the physical distance between the object centers.

We conducted a supplementary experiment with 13 healthy participants (9 new participants; 2 males and 11 females; average age of 21.92) in reversed task order. This was done in order to test the effect of motion direction judgment on the preceding overlap judgment task, as organized in the main experiment. Even in reversed task order (i.e., the motion direction judgment task after the overlap judgment task), almost identical results as those described above were obtained (PSEs for the overlap judgment: 34.77 arcmin in the no-tone condition, 27.74 arcmin in the tone condition; PSEs for the motion direction judgment: 30.43 arcmin in the no-tone condition, 15.50 arcmin in the tone condition). These results indicated that task order did not affect audiovisual mislocalization of objects.

Experiment 2: Temporal Properties

Experiment 1 demonstrated an audiovisual mislocalization and a directional change bias induced by an auditory stimulus simultaneous with a visual event, with maximal object overlap. Meanwhile, several previous audiovisual mislocalization studies showed a maximal mislocalization at approximately ± 100 ms temporal offset between audiovisual signals [7–9]. Thus, we sought to demonstrate commonalities and differences between the present and previous studies by using non-simultaneous audiovisual stimuli. Moreover, this experiment explored whether the present audiovisual mislocalization could be predictively/postdictively obtained.

Participants

Eleven healthy adults (3 males and 8 females) participated. Ten participants were from Experiment 1, and one of the authors (YK) participated. Average age was 22.27 years (age range, 19–32 years). Except for YK, all participants were naive as to the purpose of the experiment. All were right-handed, had either normal or corrected-to-normal vision, and reported no hearing anomalies.

Stimuli and Procedure

The stimuli were identical to those in Experiment 1, except that sound conditions (no tone, ± 390 ms, ± 90 ms, and 0 ms offset relative to the maximal overlap point of the SBD) were used. The procedure for Experiment 2 was identical to that of Experiment 1.

Results

For the motion direction (stream/bounce/reverse) judgment task, we combined bounce and reverse judgments into directional change judgments. Then, a cumulative Gaussian function was fitted to each proportion of overlap and directional change judgments. We calculated the PSE corresponding to 50% in the function (Fig 3a and 3b). A two-way repeated measures ANOVA for PSE was conducted with *judgment type* (2: overlap judgment task/motion direction judgment task) and *tone presentation* (6: no tone, ± 390 ms, ± 90 ms, and 0 ms offset) as factors. The main effects of judgment type and sound conditions were significant, $F(1, 50) = 5.50$, $p < .05$, and $F(5, 50) = 15.81$, $p < .001$, respectively. The interaction was also significant, $F(5, 50) = 4.66$, $p < .005$. A post hoc analysis (Ryan's method) revealed that in the overlap

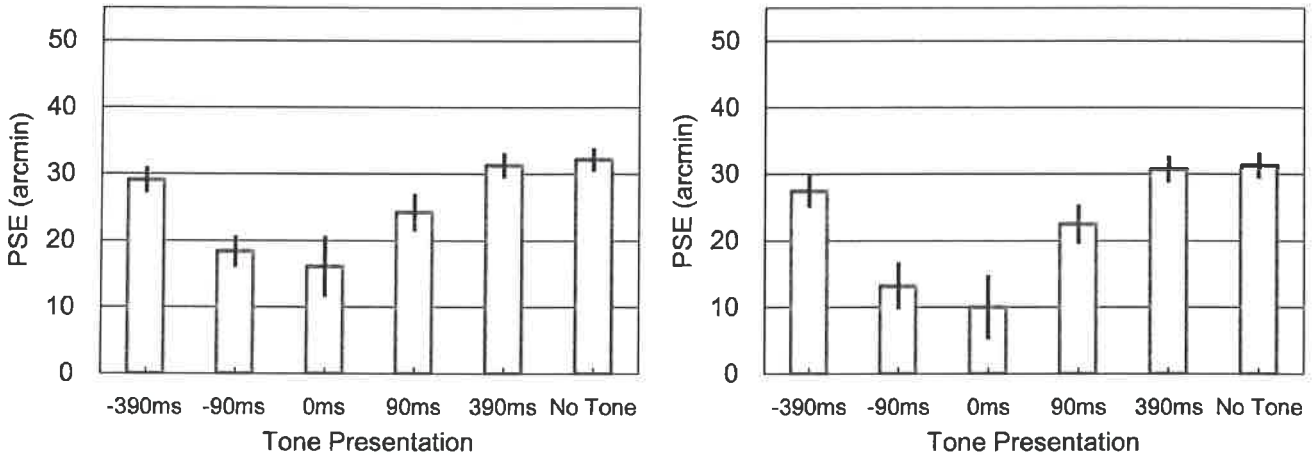


Fig 3. Results of Experiment 2. Group mean PSEs for tone conditions in the (a) overlap and (b) directional change judgment tasks. Error bars denote standard errors of the mean ($n = 11$).

doi:10.1371/journal.pone.0154147.g003

judgment task, tone presentation significantly lessened the PSE in the −90 ms and 0 ms offset conditions compared to the no tone condition, $ps < .05$, indicating that a tone caused participants to underestimate the overlap amount. In the motion direction judgment task, tone presentation significantly lessened the PSE in the ± 90 ms and 0 ms offset conditions, $ps < .05$, indicating that a tone promoted the directional change response. Additionally, the PSEs were smaller in the −90 ms and 0 ms conditions compared to the 90 ms condition. Although the PSE in the ± 90 ms and 0 ms offset conditions was smaller than in the + 390 ms offset condition, only the PSE in the −90 ms and 0ms offset conditions was smaller than in the −390 ms offset condition. Moreover, compared to the overlap judgment task, PSEs at −90-ms and 0-ms offsets were smaller in the motion direction judgment task, $F(1,60) = 11.65, < .005$ and $F(1,60) = 16.22, p < .001$.

Finally, PSEs in the −90 ms, 0 ms, and 90 ms offset conditions were smaller than the 36.37 arcmin of the distances of physical contact, $t(10) = -7.27, p < 0.001$; $t(10) = -6.36, p < 0.001$; $t(10) = -4.11, p < 0.005$, with Bonferroni-corrections, indicating that participants illusorily overestimated the physical distance between the object centers (or underestimated the physical overlap). Meanwhile, in the ± 390 ms offset and no-tone conditions, there was no significant overestimation. Audiovisual mislocalization was obtained in the 0 and ± 90 ms offset conditions. However, the degree of mislocalization was not larger for certain temporal offsets between audiovisual stimuli compared to a zero offset, which was different from previous studies [7–9].

Experiment 3: Crossmodal Modulation for Other Mislocalization Types

Experiments 1 and 2 demonstrated that a tone before and at the instant for the closest distance between object centers promoted the perception of "non-overlapping." A tone also induced overestimation of the physical object distance for the 0 ms and ± 90 ms offset conditions. Experiment 3 explored the relationship between the observed audiovisual mislocalization and other mislocalization phenomena (i.e., representational momentum, RM; the Fröhlich effect, FE; onset repulsion, OR; or a turn-point shift, TPS). RM is where the vanishing point of a moving object is mislocalized further ahead in the motion direction [18]. FE (OR) refers to when

the starting point of a moving object is mislocalized forward or backward in the motion trajectory [19, 20]. For the TPS, when a moving object moves diagonally and then suddenly turns 90 degrees, observers mislocalize the turn-point [10]. Observers tend to estimate the turn-point backward relative to the post-turn trajectory. In Experiment 3, we measured endpoint mislocalization of the pre-turn motion trajectory (RM), the starting point of the post-turn motion trajectory (FE), or the turn-point of the full motion trajectory (TPS) used in Experiments 1 and 2 (Fig 4). This was done in order to explore whether the present mislocalization could be associated with the endpoints and turn-point of the partial and full trajectory.

Participants

Twelve healthy adults (2 males and 10 females) participated. Six participants were from Experiment 1, and one of the authors (YK) participated. Their average age was 21.84 years (age range, 20–35 years). Except for YK, all participants were naive as to the purpose of the experiment. All were right-handed, had either normal or corrected-to-normal vision, and reported no hearing anomalies.

Stimuli and Procedure

The stimuli were identical to those from Experiment 1, except for the following: only one moving object was used, and an experimental block was conducted for each of the 3 motion trajectory conditions: (1) a pre-turn motion trajectory condition, in which the object moved to the left or right in proximity to the fixation point at 3.79 deg/s for 690 ms and then disappeared without a trajectory turn; (2) a post-turn motion trajectory condition, in which the object appeared proximal to the fixation point, moved away for 690 ms, and then disappeared; (3) a full motion trajectory condition, in which the object moved to the left or right in proximity to the fixation point for 690 ms. The object then reversed its motion and returned to its original position. In half of the trials, a brief tone was introduced through headphones and simultaneous with the endpoint (vanishing point) in the pre-turn motion trajectory condition, the starting point in the post-turn motion trajectory condition, and the turn-point in the full motion trajectory condition. Five hundred ms after observing the stimulus sequence, a probe object (identical to the moving object) was presented at ±36.38, ±9.09, and 0 arcmin relative to the endpoint in the pre-turn motion trajectory condition, the starting point in the post-turn motion trajectory condition, and the turn-point in the full motion trajectory condition. Positive (negative) values indicated forward (backward) positions of the vanishing point for the pre-turn trajectory. Observers judged whether the probe was located to the left or right, relative to the vanishing point, the starting point, and the turn-point. Each combination of tone presentation (tone/no-tone) and probe position (± 36.38, ± 9.09, or 0 arcmin) was repeated over 28 trials for each trajectory condition. Each block of 280 trials, which consisted of a block for each trajectory condition, was counterbalanced across participants.

Results

A cumulative Gaussian function was fitted to each proportion of probe "right" judgments. The PSE was 50% in the function for the probe position to be perceived as being at a position equal to the vanishing point, the starting point, or turn-point (Fig 5). A two-way repeated measures ANOVA for PSE was conducted with *trajectory* (3: full, pre-turn, and post-turn motion trajectory conditions) and *tone presentation* (2: tone/no-tone) as factors. The main effect of trajectory condition was significant, $F(2, 22) = 6.55$, $p < .01$. The interaction was not significant, $F(2, 22) = 1.26$, $p = .029$. A post hoc analysis (Ryan's method) revealed that mislocalization of the turn-point backward in the pre-turn trajectory was larger in the full motion trajectory

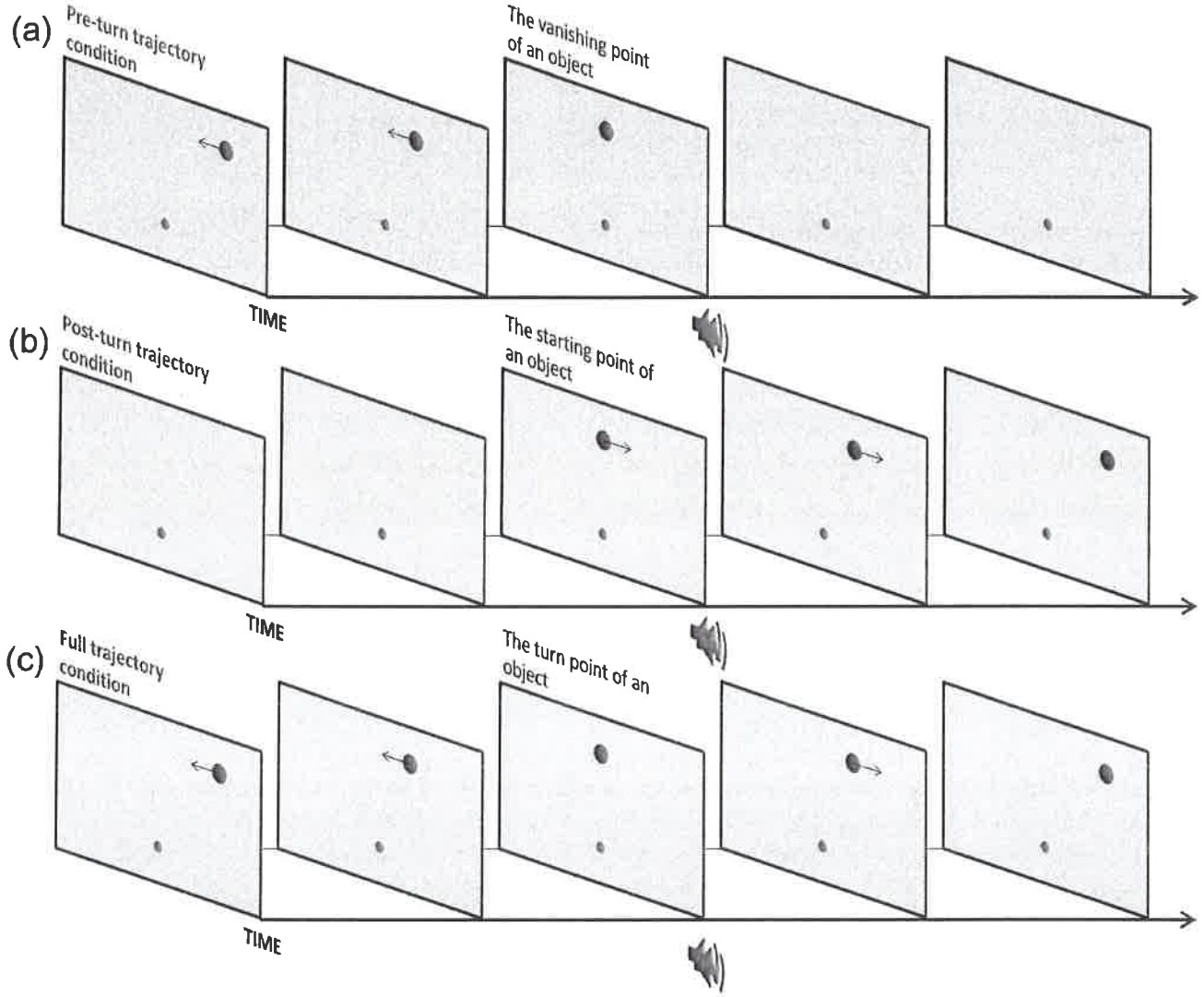


Fig 4. Schematic illustration of stimuli used in Experiment 3. (a) Pre-turn motion trajectory condition: the object moved proximal to the fixation point for 690 ms and then disappeared without the object turning. (b) Post-turn motion trajectory condition: the object appeared proximal to the fixation point, moved away from this location for 690 ms, and then disappeared. (c) Full motion trajectory condition: the object moved proximal to the fixation point for 690 ms, reversed its motion, and returned to the original position.

doi:10.1371/journal.pone.0154147.g004

condition than in the pre-turn trajectory condition ($p < .05$). Finally, we conducted one-sample *t*-tests with Bonferroni-corrections to examine whether the PSE was significantly different from the physical vanishing point, starting point, or turn-point. Results revealed no significant differences. These findings indicated that only a turning motion trajectory (full motion trajectory condition) promoted mislocalization of the turn-point backward (forward) in the pre-turn (post-turn) motion trajectory. Considering the turn-point as the starting point for the post-turn trajectory, mislocalization in the full trajectory condition is similar to the FE. However, the sizes of these mislocalizations were not significantly different from the physical zero (no mislocalization). Moreover, tone presentation did not modulate this mislocalization

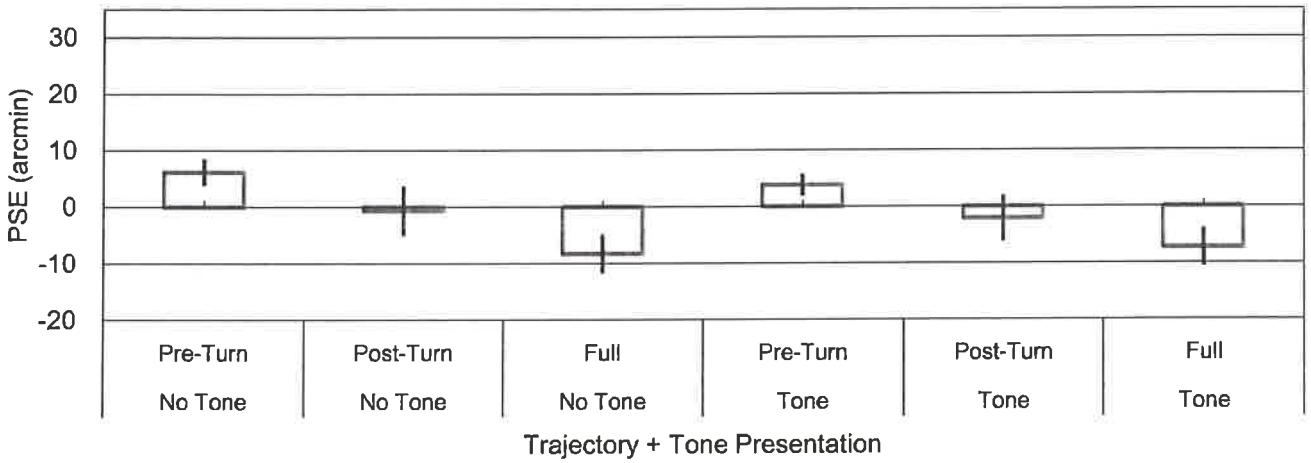


Fig 5. Results of Experiment 3. Group mean PSEs for tone conditions in combination with the 3 trajectory conditions. Positive (negative) PSEs indicate that the vanishing point, starting point, or turn-point was localized forward (backward) within the pre-turn trajectory, respectively. Error bars denote standard errors of the mean ($n = 12$).

doi:10.1371/journal.pone.0154147.g005

phenomenon. Accordingly, observed audiovisual mislocalization in the SBD was unlikely accounted for by other mislocalization phenomena.

Discussion

The present study examined the influence of an auditory tone on the localization of visual objects embedded in the SBD. In Experiment 1, we demonstrated that a tone presented at the instant of a maximal overlap (i.e., the closest distance between objects) promoted perceptual non-overlap in the SBD. The degree of a perceived non-overlap was larger in the tone-present condition than in the no-tone condition, and it was also larger than that of the physical non-overlap. In other words, a tone that is simultaneous with a visual event (maximal overlap) induces spatial mislocalization of objects to repel each other. Previous studies showed that a tone presented before or after a visual event is necessary for the occurrence of mislocalization [7–9]. In these previous studies, the timing of a visual event may be attracted toward the timing of a tone, resulting in mislocalization of a visual event in the spatial domain. In those studies, audiovisual simultaneity generates little or no mislocalization. Thus, mislocalization observed in the current study provides a new example of crossmodal mislocalization that is not mediated by a tone attracting the timing of a visual event. The present mislocalization can now be added to the list of crossmodal phenomena that is clearly inconsistent with a "Modality Appropriateness" hypothesis. This hypothesis states that the sensory modality that provides more accurate information for a given task dominates performance. According to this hypothesis, vision should have dominated the overlap judgment (spatial localization judgment) in the present study. Audition also provided no temporal information for attracting the timing of a visual event toward that of the auditory stimulus. Moreover, several studies assessing crossmodal interactions have indicated that a concurrent auditory stimulus enhances perceived visual stimulus intensity [24, 25]. Nevertheless, the present findings can be interpreted such that a concurrent auditory stimulus interferes with the perception of visual objects at the closest distance, resulting in significant mislocalization of visual objects.

The present results also show commonalities and differences within the temporal domain, for the present and previous studies through Experiment 2, by using non-simultaneous

audiovisual stimuli. Although only a tone in the 0 and −90 ms offset conditions induced a bias toward non-overlapping judgments compared to the no-tone condition, our observed audiovisual mislocalization was persistent across ± 90 ms temporal offsets between a tone and a to-be-modulated visual event (i.e., maximal overlap or the closest points between objects in the SBD). A tone presented before or after a to-be-modulated visual event predictively and postdictively modulates object localization [26]. Thus, our observed audiovisual mislocalization in the SBD had similar temporal characteristics to those of previous audiovisual mislocalizations. However, some temporal offset conditions did not generate a larger degree of mislocalization than a zero temporal offset (0 ms condition) in the present study. This differed from previous studies [7–9]. Therefore, the results of Experiment 2 more clearly support the notion that a tone that attracts the timing of a visual event is not necessary for mislocalization. A tone will directly affect the localization of visual moving objects. The results also suggest a temporal window in which the mislocalization effect is largest near the synchrony between audiovisual stimuli and becomes smaller as a temporal offset between audiovisual stimuli increases.

Here we will consider what occurs when moving objects overlap along crossing trajectories. Goldberg and Pomerantz [27] and Qian, Andersen, and Adelson [28] have stated that the motion system averages signals in opposite directions within a small region (similar to the overlapping of objects), yielding a zero resultant (null vector), which is assigned to the objects. Moreover, we have limited capacities for attentively tracking objects when they overlap or are very close to each other. At a maximal overlap, or the closest (non-overlapping) points of objects, participants may have difficulty distinguishing those objects. This loss of discriminability makes the attentive tracking of objects difficult [29]. The perceptual system has the complex task of gathering motion signals and/or tracking objects. Meanwhile, these weaker motion signals and/or object representations around the closest points are interpolated by motion signals integrated along with previous motion trajectories [23, 30]. As a result, the decision reached by the perceptual system may result in an overlap percept by default.

For the tone-present condition in this study, we need to consider the possible role of an auditory transient on weaker motion signals and/or object representations at the closest points of objects. If attention toward moving objects is distracted (i.e., attentional resources are captured) by a sudden tone when the objects were at the closest point, visual information processing may be temporally delayed [31]. Concretely, interpolating motion signals at the closest point may be delayed and interrupted for some time by shifting attention toward the auditory modality. Then, motion signals (around the closest point) that are re-processed and collected some time after an abrupt tone presentation may not be strong enough to be perceptible. This may generate a non-overlap percept in the SBD [15, 32]. Thus, the observed mislocalization suggests that weaker motion signals and/or object representations within a complex stimulus are paid less attention to. This is because presentation of an auditory transient distracts attention toward the auditory domain.

Interestingly, in Experiments 1 and 2, the PSEs in the tone-present condition for the overlap judgment task were significantly larger than for the motion direction judgment task. Moreover, PSEs for the overlap and motion direction judgment tasks are characterized by different temporal properties: for the motion direction judgment task, tone presentation at and before the instant of the closest distance has a stronger effect than a tone after the timing. Kawachi et al. [15] suggested that if a tone occurs before complete object overlap in the SBD, the observer can deploy attention toward the tone with some time left over for determining how the tone relates to the complete overlap. Alternatively, if the tone is presented too long after the complete overlap, by the time attention has been deployed toward the sound, the objects are too far apart to be interpreted as changing their motion direction (e.g., bouncing). Thus, the present study shows that whereas tone presentation induces participants to overestimate the closest distance

(i.e., underestimate the degree of overlap), the overlap and motion direction judgments had different susceptibilities to the tone presentation. The motion direction judgment task (stream/bounce judgments in the conventional SBD study) is mainly influenced by response biases in the terminology referential to signal detection theory (SDT) [33]. Based on SDT, an overlap detection task is assumed to be affected by perceptual sensitivity and response biases [34]. Considered together, part of the stronger tone effect may be accounted for by a relatively strong response bias in the motion direction judgment task. These findings suggest that although both judgments may be partially supported by common perceptual processes, the overlap judgments are likely less susceptible to response biases compared to the direction change judgments. However, it should be noted that although a few studies indicated the effect of perceptual sensitivity/response biases on the SBD [33, 34], the detailed contents of each process remains to be elucidated. Recently, Witt, Raylor, Sugovic, and Wixted [35] pointed out that signal detection measures could not distinguish "perceptual" biases from response biases.

To further explore the observed mislocalization effects, Experiment 3 was conducted to relate the present findings to other mislocalization phenomena (i.e., FE, RM and TPS) and to explore a possible account for audiovisual mislocalization in the SBD. However, mislocalization of the endpoint of the pre-turn trajectory (RM), the starting point of the post-turn trajectory (FE), or the turn-point of the full trajectory (TPS) does not seem to contribute to the present phenomenon. Critically, we found that these mislocalizations were not modulated by tone presentation. Moreover, although the sizes and direction of these mislocalizations were significantly different from each other, the sizes of these mislocalizations were not significantly dissociable from the physical zero (no mislocalization). Therefore, it may be difficult to account for our mislocalizations by those associated with an endpoint and a turn-point within the partial and full trajectories. Thus, the results may point to a new type of mislocalization obtained from a relatively complex stimulus configuration: visual objects moving in opposite directions.

The present study clearly indicates that the spatial positions of moving objects on opposing trajectories are mislocalized by an auditory stimulus that is presented slightly before, at, or after the instant of their closest distance. However, slight temporal offsets between visual and auditory events do not promote the present mislocalization, as observed in previous studies. Larger temporal offsets do not have an effect on object localization. The present crossmodal mislocalization is inconsistent with the modality appropriateness hypothesis whereby vision dominates audition in the spatial domain [3]. This is an example of crossmodal mislocalization, which is not mediated by an auditory stimulus attracting the perceived timing of a visual stimulus. Even during a visuospatial task (i.e., overlap judgment task), the perceptual system may construct perceptual content that is strongly dependent on more reliable and salient sensory information. Moreover, auditory stimulation may not affect possible mislocalizations observed at the endpoint of the pre-turn trajectory (RM), the starting point of the post-turn trajectory (FE), or the turn-point of the full trajectory (TPS). Therefore, mislocalizations in the present study are unlikely to be accounted for by other mislocalization phenomena. We suggest that the present audiovisual mislocalization is specific to our complex stimulus configuration, which involves objects on opposing motion trajectories. The present study contributes to a better understanding of audiovisual interactions in cluttered multisensory environments, beyond simple one-to-one interactions between auditory and visual signals.

Author Contributions

Conceived and designed the experiments: YK. Performed the experiments: YK. Analyzed the data: YK. Contributed reagents/materials/analysis tools: YK. Wrote the paper: YK.

References

1. Michotte A (1963) In Miles T, Miles Trans E (Eds), The perception of causality. New York, NY: Basic Books. Original work published 1946.
2. Heider F, Simmel M (1944) An experimental study of apparent behavior. Am J Psychol, 57: 243–249.
3. Welch RB, Warren D H (1980) Immediate perceptual response to intersensory discrepancy. *Psychol Bull*, 88: 638–667. PMID: 7003641
4. Bertelson P. (1999) Ventriloquism: A case of crossmodal perceptual grouping. In: Aschersleben G, Bachmann T, Musseler J, Eds. Cognitive Contributions to the Perception of Spatial and Temporal Events. North-Holland: Elsevier. pp. 347–63.
5. Fendrich R, Corballis PM (2001) The temporal cross-capture of audition and vision. Percept Psychophys 63: 719–725. PMID: 11436740
6. Vroomen J, de Gelder B (2004) Temporal ventriloquism: Sound modulates the flash-lag effect. J Exp Psychol: Hum Percept Perform 30: 513–518.
7. Heron J, Whitaker D, McGraw PV (2004) Sensory uncertainty governs the extent of audio-visual interaction. Vision Res, 44: 2875–2884. PMID: 15380993
8. Teramoto W, Hidaka S, Gyoba J, Suzuki Y (2010) Auditory temporal cues can modulate visual representational momentum. Atten Percept Psychophys, 72: 2215–2226. doi: 10.3758/APP.72.8.2215 PMID: 21097864
9. Chien S, Ono F, Watanabe K (2013) A transient auditory signal shifts the perceived offset position of a moving visual object. Front Psychol, 4(70): 1–10. doi: 10.3389/fpsyg.2013.00070
10. Nieman D, Sheth BR., Shimojo S (2010) Perceiving a discontinuity in motion. *Journal of Vision*, 10 (6):9, 1–23. http://www.journalofvision.org/content/10/6/9, doi: 10.1167/10.6.9 PMID: 20884558
11. Bertenthal BI, Banton T, Bradbury A (1993) Directional bias in the perception of translating patterns. Perception, 22: 193–207. PMID: 8474844
12. Sekuler AB, Sekuler R (1999) Collisions between moving visual targets: What controls alternative ways of seeing an ambiguous display? Perception, 28: 415–432. PMID: 10664783
13. Sekuler R, Sekuler AB, Lau R (1997). Sound alters visual motion perception. Nature, 385: 308. PMID: 9002513
14. Kawachi Y, Gyoba G (2006) Presentation of a visual nearby moving object alters stream/bounce event perception. Perception, 35: 1289–1294. PMID: 17120846
15. Kawachi Y, Grove PM, Sakurai K (2014) A single auditory tone alters the perception of multiple visual events. J Vis, 14(8):16, 1–13. http://www.journalofvision.org/content/14/8/16, doi: 10.1167/14.8.16 PMID: 25052696
16. Watanabe K, and Shimojo S. (2001). When sound affects vision: Effects of auditory grouping on visual motion perception. Psychol Sci, 12(2), 109–116. PMID: 11340918
17. Yamada Y, Kawabe T, Miyazaki M (2015) Awareness shaping or shaped by prediction and postdiction: Editorial. Front Psychol, doi: 10.3389/fpsyg.2015.00166
18. Freyd J J, Finke RA (1984) Representational momentum. J Exp Psychol: Learn Mem Cogn, 10: 126–132.
19. Frohlich FW (1923) Uber die Messung der Empfindungszeit [Measuring the time of sensation]. Zeitschrift fur Sinnesphysiologie, 54: 58–78.
20. Thornton IM (2002) The onset repulsion effect. Spat Vis, 15: 219–243. PMID: 11991576
21. Rolfs M, Dambacher M, Cavanagh P (2013) Visual adaptation of the perception of causality. Curr Biol, 23: 1–5.
22. Zhou F, Wong V, Sekuler R (2007) Multi-sensory integration of spatio-temporal segmentation cues: one plus one does not always equal two. Exp Brain Res, 180: 641–654. PMID: 17333010
23. Kawachi Y, Kawabe T, Gyoba J (2011) Stream/bounce event perception reveals a temporal limit of motion correspondence based on surface feature across space and time. i-Perception, 2: 428–439. doi: 10.1068/i0399 PMID: 23145236
24. Stein BE, London N, Wilkinson LK, Price DD (1996) Enhancement of perceived visual intensity by auditory stimuli: A psychophysical analysis. J Cog Neurosci, 8: 497–506.
25. Vroomen J, de Gelder B (2000) Sound enhances visual perception. J Exp Psychol: Hum Percept Perform, 26: 1583–1590.
26. Choi H, Scholl BJ (2006) Perceiving causality after the fact: Postdiction in the temporal dynamics of causal perception. Perception, 35: 385–399. PMID: 16619953

27. Goldberg DM, Pomerantz JR (1982) Models of illusory pausing and sticking. J Exp Psychol: Hum Percept Perform, 8: 547–547.

28. Qian N, Andersen RA, Adelson EH (1994) Transparent motion perception as detection of unbalanced motion signals. I. Psychophysics. J Neurosci, 14: 7357–7366. PMID: 7996181

29. Makovski T, Jiang YV (2009) Feature binding in attentive tracking of distinct objects. Vis Cogn, 17: 180–194. PMID: 19492017

30. Kanai R, Sheth BR., Shimojo S (2007) Dynamical evolution of motion perception. Vis Res, 27: 937–945.

31. Koelewijn T, Bronkhorst A, Theeuwes J (2010) Attention and the multiple stages of multisensory integration: A review of audiovisual studies. Acta Psychol, 134: 372–384.

32. Watanabe K (2001) Crossmodal interaction in humans (Doctoral dissertation, California Institute of Technology). Retrieved from http://resolver.caltech.edu/CaltechTHESIS:10122010-090303102

33. Grove PM, Ashton J, Kawachi Y, Sakurai K (2013) Auditory transients do not affect visual sensitivity in discriminating between objective streaming and bouncing events. J Vis, 12(8):5, 1–11. http://www.journalofvision.org/content/12/8/5, doi: 10.1167/12.8.5

34. Grassi M, Casco C (2012) Revealing the Origin of the Audiovisual Bounce-Inducing Effect. *Seeing Perceiving*, 25: 223–233. doi: 10.1163/187847612X626372 PMID: 22370960

35. Witt JK, Taylor JET, Sugovic M, Wixted JT (2015) Signal detection measures cannot distinguish perceptual biases from response biases. Perception, 44: 289–300. doi: 10.1068/p7908 PMID: 26562253

臨床美術ジャーナル　5巻　第1号　(2016年度)　75-81

総説

脳活動からみる芸術鑑賞・制作

Appreciation and Production of Art from functional brain imaging

河地　庸介
(東北福祉大学感性福祉研究所)

【要旨】 非侵襲的脳機能計測法の急速な進展は，基本的な心的機能（知覚・注意・記憶・言語など）のみならず，人間の社会性等の高次機能をも脳活動を通して理解しようとする試みを盛んにしている．本稿では芸術行動，なかでも芸術鑑賞と制作の２つの側面に関してfMRIを用いた脳機能計測研究を中心に概観しながら今後の課題について述べる．さらに，今後特定の心的機能に関する脳機能計測研究が意義あるものとしてより一層発展していくために留意すべき事項について考察する

Ⅰ．はじめに

1990年代初頭に脳の局所的な血流変化情報から脳の活動状態を計測できることが示されて以来[1]，基本的な心的機能（知覚・注意・記憶・言語など）とともに活動する脳部位・脳部位間ネットワークについての検討が盛んに行われている．この計測技術は脳が担う機能を測定できることから，機能的MRI（fMRI: functional Magnetic Resonance Imaging）と呼ばれる．fMRIは身体に有害な放射能等を用いずに非侵襲的かつ正確に局所的な脳活動の計測ができるため，多くの研究者が用いるようになり，現在の脳神経科学への高い関心を生み出す契機となった．

近年脳神経科学の研究者の関心は，基本的な心的機能だけではなく，より我々の生活にとって身近な問題として存在する社会性，政治的態度，消費行動といったより高次の心的機能へと広がりをみせ，社会脳（social brain），ニューロポリティクス（neuropolitics），ニューロマーケティング（neuromarketing），といった言葉や研究領域をそれぞれ生んでいる．そして本稿で取り上げる芸術行動については神経美学（neuroaesthetics）[4]という分野が作られた[2]．Zekiは，あらゆる芸術は脳を介して表現されるものだとし，制作や鑑賞等のあらゆる活動は脳の法則に従っているはずであり，芸術を深く理解するには脳を踏まえる必要があると考えた[2]．

人は，芸術作品はもちろんのこと，様々な対象の姿・形等の外的特徴のみならず，心的特徴や利他的行為・道徳的判断など人間生活の様々な場面で「美」を体験し，心動かされる．そして“Beauty is good”というステレオタイプ（美しく魅力的な人は性格がよく，能力も高いと感じる傾向）に代表されるように[3]，体験される「美」は情動的・価値的判断や行動選択に強い影響を与える．それだけにこの「美」という体験が脳内でいかにして生まれるのかという問いは，人の心の理解に深く関連する問いであり，研究者のみならず多くの人々が関心を抱くことは想像に難くないだろう．

神経美学，なかでも芸術にかかわる脳機能イメージング研究の目的は，芸術を体験しているときの脳活動を計測し，芸術体験の脳内基盤を調べることにある．なかでも，芸術作品を鑑賞し，美しさを体験しているときの脳活動に焦点があてられることが多い．本稿でも審美判断時の脳活動の研究を中心に概観する．しかし，芸術作品により喚起される主観的体験は「美」に限定されない．そして，芸術体験には，対象によって生み出される情動・価値判断・行動だけではなく，解釈や制作を基礎づける過程をも含むと考えられる[1]．したが

って本稿では，芸術，なかでも視覚芸術に焦点をしぼりながら，様々な主観的体験を伴う美術鑑賞と美術制作の2つに大別して神経美学研究を概観するとともに，今後期待される研究の方向性や留意事項について考察する。

Ⅱ．美術鑑賞と脳

芸術鑑賞，特に作品の美しさといった審美判断にかかわる脳機能イメージングが現在のように展開される端緒となったのは2004年に発表されたKawabata & Zeki (2004)，Cela-Conde et al. (2004)，Vertanian & Goel (2004) による3件の論文である[5-7]。Kawabata & Zekiの研究[5] では，様々な絵画刺激（抽象画・静物画・風景画・人物画）がMRI装置内にて被験者に呈示され，被験者は呈示された絵画の美しさの程度をボタン押しにより回答した。その結果，異なる視覚属性によって特徴づけられる絵画の種類によって活動が顕著となる脳部位が異なることが示されるとともに，醜いと判断したときに比べて美しいと判断しているときの内側眼窩前頭皮質（medial orbitofrontal cortex: mOFC）の活動が有意に高いことが示された。さらに，その後の研究ではmOFCの活動強度は美の主観的な強さと相関することもわかっている[8]。このmOFCは様々な報酬に対応して神経伝達物質ドーパミンを放出する細胞群からなる報酬系の一部とされており，美しさを感じることが脳内で報酬として扱われている可能性が示唆される

近年では，従来の研究が視覚芸術に特化していたことを踏まえて感覚モダリティに依存しない審美判断の脳内基盤の研究も行われており，視覚芸術か音楽かにかかわらず美しさを感じるときにはそうでないときに比べてOFCの活動が有意に高まることが報告されている[9]。またtDCS (transcranial direct current stimulation) によって磁気刺激を脳に与えてOFCの活動を一時的に抑制することで絵画作品に対する「美しさ」の評定値が低下することも報告されている[9]。このことからもOFCが「美しさ」判断に決定的な影響をもつことがわかる。

しかし，これらの研究は芸術作品から喚起される美しいという主観的体験がmOFCのみで反映されることを示しているわけではない。事実，Cela-Conde et al.[6] は背外側前頭前野（dorsolateral prefrontal cortex），Vertanian & Goel[7] は前部帯状回（anterior cingulate gyrus）や尾状核（caudate nucleus）の関与を報告している。いずれの研究も用いられている絵画刺激のカテゴリなどに違いがあり，また被験者の課題も同じではないために活動部位の違いが生じたのかもしれない。同時に，得られた脳活動部位は芸術鑑賞の異なる側面を反映している可能性も示唆されており[10]，芸術鑑賞にかかわるであろう複数の心的機能（例えば，知覚，注意，記憶，感情，意思決定等）についてより詳細な仮説を立てた上で脳部位間のネットワークの検討が今後必要となるだろう。

上述のように，芸術鑑賞の脳科学では主として審美的な選好・判断を対象としているが[11]，人は芸術鑑賞の際には美的判断のみならず様々な感性印象を抱く[12]。Kawachiらの研究[12] ではMRI装置内で提示された線画刺激について，様々な形容詞対尺度（'醜い－美しい'，'不快な－快い'，'にごった－澄んだ'，'静かな－にぎやかな'，'地味な－派手な'，'静的な－動的な'，'柔らかい－硬い'，'なめらかな－とげとげした'，'ゆるんだ－緊張した'）を用いて評価させる実験を行った。その結果，醜い－美しい'，'不快な－快い'，'にごった－澄んだ'で評価する場合にはKawabata & Zekiの研究[5] と同様にOFCの活動が他の尺度で評価するときよりも高くなることが示された。加えて，'にごった－澄んだ'，'静かな－にぎやかな'，'地味な－派手な'で評価したときには上側頭回（superior temporal gyrus），'柔らかい－硬い'，'なめらかな－とげとげした'，'ゆるんだ－緊張した'で評価したときには上前頭回（superior frontal gyrus）の活動が高まることが明らかとなった。このことは，芸術作品により誘発される多様な感情状態は複数の脳部位に分散する形で表現されていることを示唆する。審美判断は芸術鑑賞における極致であり，最も優先的に検討される心的過程であるのは間違いないが，芸術鑑賞に伴う多様な側面，さらには作品の種類に依存して生じる異なる感情状

態をもとらえる詳細な検討も期待される。

概観してきた芸術鑑賞に伴う脳活動イメージング研究の大半は，一般人（多くは大学生）を対象としたものである。キュレーターや芸術評論家等の専門家，さらには芸術に関する教育を受けている，または頻繁に美術館に出向く等のように芸術に接する機会が多い人々が鑑賞する際の脳活動イメージング研究は十分になされているとはいえない。様々な芸術に接し，鑑賞し，感性豊かに生活することが脳機能の発達に及ぼす影響，そして種々の心的機能や心理状態に及ぼす影響を検討することは，感性の涵養を目指す教育法の開発につながりうるという点で意義深いと考える。

Ⅲ．芸術制作と脳

脳機能イメージングを用いた神経美学の主流である鑑賞者側の脳機能研究が進展している一方で，アーティストをはじめとした制作側の脳機能の検討は，様々な技術的な問題もあり，鑑賞側の脳活動ほど脳機能イメージングによる検討は十分になされていない

従来芸術制作にかかわる脳神経科学研究の多くは，アーティストの作品を脳の情報処理と結びつけて考察する記述的な神経美学（descriptive neuroaesthetics）によるものが大半であった　そしてZeki[2]やCavanagh[13]など視覚科学の研究者が，アーティストの描画アプローチはあたかも脳内における視覚情報処理の特性が反映されているかのようだと指摘している。例えば，色や形，そして運動などの個々の視覚情報が個別の脳部位において処理されるという脳機能局在を反映するかのように，Henri Matisseを代表とするフォービスト（fauvist）が色に着目し，Pablo Picassoが代表するキュビスト（Cubist）が形に，Alexander Calderが運動に着目して，鑑賞者の脳の特定の情報処理を刺激するような作品を制作していた。この意味で優れた芸術家はその作品を通して脳にかかわる実験を行う神経科学者という側面をもつと指摘されている[13]。

他方で，特定の脳部位に損傷・病変によって生じる患者やアーティストの芸術制作の変化の諸相を検査や実験的手法を用いて把握し，芸術制作を支える脳内基盤を明らかにする実証的な神経美学研究も行われてきた。Chatterjee, Bromberger, Smith, Sternschein & Widick[11]は，脳卒中により左右半球いずれか一方を損傷した3名のアーティストの作品を対象に，損傷前後で生じた変化を60名の被験者に質問紙を用いて評価させた。その結果，損傷した半球の左右にかかわらず，損傷後の彼らの作品は損傷前の作品に比べて抽象的になり，事物の描写は歪められ，より現実感のないものになったことが報告されている。それと同時に，損傷後の彼らの作品は批評家らに高く評価され，アーティスト本人はより創造的になることができ，感情表現をよりうまく表現できるようになったと感じていると報告されている。このように脳損傷により，表現方法が変化するだけではなく，芸術制作への意欲や表現が促進される事例が報告されている。さらに前頭側頭型認知症（Frontotemporal dementia: FTD）により脳に病変が生じたケースについても報告がなされており，半球損傷のケースと類似して，一部のFTD患者において前頭側頭葉の病変による機能低下が芸術制作への意欲を低下させるのではなく，むしろ意欲を生み出している[15，16]　これらの研究が示唆しているのは，芸術制作の脳内基盤は片側半球や前頭側頭葉等や特定の部位に局在しているのではなく，脳内に広く分布する形で存在している可能性，そして病変により機能低下した脳部位と連絡していた脳内ネットワークが可塑的に変化し，再体制化が行われ，芸術制作を促進させる，表現方法を変化させるといった行動の変容を生み出している可能性であろう[17，18]。

しかしながら，脳損傷患者を対象とした研究では，損傷部位が障害された心的機能に必要な脳部位だといえるものの，実際には損傷部位がかなり広範な場合が多いために脳と心的機能について精査することが困難な場合も多い。一方で，脳機能イメージング研究では，芸術制作という複数の心的機能から生み出されるであろう行動について仮説を立てて実験課題を工夫できれば，芸術制作に関連した脳部位をかなり限定することができる。近年はfMRIを用いて，被験者に実際に絵を描い

てもらっている最中の脳活動を撮像する研究が報告されている．Ellamil, Dobson, Beeman, & Christoff[19]は，創造的な絵画表現は新しくて独自性のあるアイデアの生成と当該アイデアの適切さや意味の評価という2つの要素から構成されていると仮説を立て，MRI装置内で利用できるペンタブレットを用いて，ある書籍に関する説明を読んだ後にブックカバーのデザインをし，その後そのデザインを評価するというサイクルを複数回繰り返すという課題を行った．その結果，アイデア生成については海馬や海馬傍回といった中側頭葉（medial temporal lobe; MTL）が関与していることが示された．このMTLの活動は，課題に関連する情報の記憶を想起し，想起した内容を互いに関連づけて，これまでにない新たな情報の組み合わせを作り上げることによると推測された．他方でアイデア評価については，背外側前頭前野（dorsolateral prefrontal cortex）や背側前帯状皮質（dorsal anterior cingulate cortex）を含む脳内ネットワークである実行制御ネットワーク（executive network）が関与していることが示された．このネットワークの関与は，生成した絵画表現を分析的に判断する際に必要となる認知的制御を意識的に行うことによるとされる．さらにアイデア評価については，不随意的に生じる感情的評価に関連するデフォルトモードネットワーク（default-mode network）も関与することが示唆された．このようにEllamilら[19]は芸術制作を構成すると考えられる2つの心的機能に対応して異なる脳内基盤が存在しうることを示した．Ellamilら[19]の研究により芸術制作の脳内基盤のfMRIを用いた検討が本格的に始まったが，追随するfMRI研究は現時点で皆無に等しく，結果の妥当性の確認はもとより，芸術制作を支えるメカニズムの解明は今後の課題となる．また，Ellamilら[19]の実験課題では，被験者はブックカバーのデザインと評価を要求されているのみであり，デザインによって鑑賞者に伝えるメッセージや感情情報・情緒的意味についての要求や評価の基準は示されていなかった．しかし，作品制作時のアイデア生成・評価の検討をさらに発展させるためには，制作者が制作時に意識するであろう鑑賞者が作品から感じ取るもの，鑑賞者が主観的に体験するものという視点を導入することが必要となるだろう．

上述までの芸術作品の制作に伴う研究は，記述的神経美学，脳損傷患者を対象とした研究，そしてEllamilら[19]の研究を含めて，ほぼ全てがアーティストや芸術教育を受けている学生を対象としていた．しかし，絵を描くという芸術行動は現代の人間活動として一般的かつ基本的なものである．また，言語表現の難しい心理状態を表現できるコミュニケーション手段として絵画表現を用いるメンタルヘルスケアの取り組みもなされている．神経美学研究がより日常生活に即した有意義な研究領域となるためにも，人々が日常的に行う創造的な取り組みとしての芸術制作の理解，また芸術制作への取り組みがもつ治療的効果の理解が期待される

Ⅳ．脳機能イメージングによって得られるもの

ここまで芸術行動と脳との関係について概観してきたが，ここでは芸術行動にかかわる脳活動を検討する意義と留意点について述べる．Zeki[2]も述べているように，脳神経科学や実験心理学では，あらゆる心理現象や行動は脳活動に関連づけられる，依拠していると考えられている．したがって脳機能イメージングを通して芸術鑑賞や制作という行動と特定の脳部位の活動を関係づける，特に計測された脳活動によって行動がいかにして生み出されるのかを説明しうる形で関係づけることができれば，脳機能イメージングは芸術行動をより包括的に理解する非常に有効な手段となりうる

ここで留意すべきは，ある心理課題の遂行と相関して働く脳部位をみつけただけでは，脳がどのように働いて行動を生み出すに至ったかについて理解したことにはならないということである．もう一歩踏み込んで，行動を計測された脳活動の観点から説明するには，実験心理学的な知識・行動データと脳神経科学的知識に基づいて測定対象となる行動・心理現象を生起させる情報処理過程に関する仮説を立て，計測時に行う行動課題を作成

し，脳機能計測実験を通して仮説検証することが重要となる[20]

また，脳機能イメージングは必ずしも自覚を伴わない心的状態のマーカーとなりうるといわれている[21, 22]　従来的なアンケートや内省報告等の被験者の主観的判断に依存する測定方法は主として被験者が意識可能な心的状態のみが測定対象となる　そのため，被験者から集められる種々のデータのうち被験者が意識できない心的状態に関するデータを収集することができない　ここで脳機能イメージングを用いれば，客観的な方法で被験者が意識できない心的状態を定量的データとして収集することができる　例えば，芸術療法（art therapy）や臨床美術（clinical art）等のメンタルヘルスケアの効果を評価する際に，被験者の主観的判断は重要であるものの，どの程度信頼できるデータであるかは疑問もあり，ケア効果のすべてを被験者が意識化できるとも限らない　このとき脳機能イメージングを用いてケア効果を定量的に表すことができれば非常に有意義なものだといえるだろう．しかしながら，実際のところ脳機能イメージングによる客観的データをケア効果等の心的状態のマーカーとして用いるには様々なハードルがある　1 測定対象である心的状態を基礎づける心的な情報処理過程がある程度わかっている　2 対象となる心的な情報処理過程と相関する特定脳部位・ネットワークの活動がすでに見つかっている　3 当該脳部位・ネットワークが特定の刺激や行為にのみ反応するというように選択性をもっている　等が必要になり[21–23]，脳機能イメージングによって心的状態を推定するにはそれ相応の準備や確認をしなければならない

V．まとめ

本稿では近年の脳機能イメージングの発展に伴って盛んとなった神経美学，中でも視覚芸術の鑑賞と制作を扱っている脳機能計測研究に焦点をあてて概観した　その中で今後の展開として，芸術鑑賞により喚起される「美」を含む多様な主観的体験，そして鑑賞者の主観的体験を想定した制作活動等，鑑賞者や制作者の多種多様な心的状態を踏まえた研究が期待された　また，本稿で概観した芸術鑑賞と制作に焦点を当てた研究では，前者は一般人，後者はアーティストや専門家といったように対象者に偏りがみられた．このような芸術鑑賞・制作における経験の個人差は脳機能イメージングにおいてノイズとなる側面もあるが，むしろ個人差を考慮に入れた研究がなされれば，芸術教育・学習・芸術表現を用いたメンタルヘルスケアによって得られる効果について有益な示唆ができると思われる　これらの芸術行動にかかわる心的状態の脳機能イメージング研究を有意義なものにするには，事前に測定対象となる行動を生み出すメカニズムについて実験心理学的知識と脳神経科学的知識を組み合わせて検証可能な仮説を立てて脳機能イメージング実験に取り組んでいくことが必要であろう

【脚注】

1．美学というと「美」について問う学問という印象を抱かせるが，「美学」という訳は18世紀半ばのドイツの哲学者バウムガルテンのepisteme aisthetikeという言葉に由来するとされる[24]　Epistemeは「知」「科学」，aisthetikeは「様々な感覚や感情」を意味する　後者は日本語でいう感性という言葉に似ていると考えられる　したがって「美学」は本来「様々な感覚や感情を含む感性に関する学問」と理解したほうがよいと思われる[25]

【謝辞】

本研究は，JSPS科学研究費基盤研究C（16K00212, 26350995）および東北福祉大学感性福祉研究所における文部科学省私立大学戦略的研究基盤形成支援事業（平成26年度～30年度）による援助を得て行われた

【引用文献】

1）Ogawa, S. Lee, T.M., Kay, A.R., & Tank, D.W. (1990). Brain magnetic resonance imaging with contrast dependent on blood oxygenation. Proc Natl Acad Sci U S A, 87, 9868-9872.

2）Zeki, S. (1999). Inner Vision: An Exploration of Art and the Brain. New York: Oxford

University Press.

3) Dion, K., Berscheid, E., & Walster, E. (1972). What is beautiful is good. J Pers Soc Psychol, 24 (3), 285-290.

4) Chatterjee, A. & Vartanian, O. (2014). Neuroaesthetics. Trends Cogn Sci, 18 (7), 370-375.

5) Kawabata, H., & Zeki, S. (2004). Neural correlates of beauty. J Neurophysiol, 91, 1699-1705.

6) Cela-Conde, C.J., Marty, G., Maestú, F., Ortiz, T., Munar, E., Fernández, A., Roca, M., Rosselló, J., & Quesney, F. (2004). Activation of the prefrontal cortex in the human visual aesthetic perception. Proc Natl Acad Sci U S A, 101, 6321-6325.

7) Vertanian, O., & Goel, V. (2004). Neuroanatomical correlates of aesthetic preference for paintings. Neuroreport, 15 (5), 893-897.

8) Ishizu, T. & Zeki, S. (2011). Toward a brain-based theory of beauty. PLoS ONE 6 (7): e21852. doi:10.1371/journal.pone.0021852

9) Nakamura, K., & Kawabata, H. (2015). Transcranial Direct Current Stimulation over the Medial Prefrontal Cortex and Left Primary Motor Cortex (mPFC-lPMC) Affects Subjective Beauty but Not Ugliness. Front Hum Neurosci. 2015; 9: 654. doi: 10.3389/fnhum.2015.00654

10) Nadal, M. (2013). The experience of art: Insights from neuroimaging. Prog Brain Res, 2013;204: 135-158. doi: 10.1016/B978-0-444-63287-6.00007-5.

11) Zaidel, D.W. (2010). Art and brain: insights from neuropsychology, biology and evolution. J Anat, 216, 177-183.

12) Kawachi, Y., Kitamura, M.S., Kawabata, H., Shibata, M., Imaizumi, O., & Gyoba, J. (2011). Topographic distribution of brain activities corresponding ot psychological structures underlying affective meanings: An fMRI study. Jpn Psychol Res, 53 (4), 361-371.

13) Cavanagh, P. (2005). The artist as neuroscientist. Nature, 434, 301-307.

14) Chatterjee, A., Bromberger, B., Smith, W. B., Sternschein, R., & Widick, P. (2011). Artistic Production Following Brain Damage: A Study of Three Artists. Leonardo, 44 (5), 405-410. http://dx.doi.org/10.1162/LEON_a_00240

15) Miller, B.L., Cummings, J., Mishkin, F., Boone, K., Prince, F., Ponton, M., & Cotman, C. (1998). Emergence of artistic talent in frontotemporal dementia. Neurology, 51 (4), 978-982.

16) Midorikawa, A., Fukutake, T., & Kawamura, M. (2008). Dementia and painting in patients from different cultural backgrounds. Eur Neurol, 60 (5), 224-9. doi: 10.1159/000151697. Epub 2008 Aug 29.

17) Moss, H., Donnellan, C., & O'Neill, D. (2012). A review of qualitative methodologies used to explore patient perceptions of arts and healthcare. Med Humanit, 38 (2), 106-9. doi: 10.1136/medhum-2012-010196.

18) Chatterjee, A., & Vartanian, O. (2016). Neuroscience of aesthetics. Ann N Y Acad Sci, 1369, 172-194.

19) Ellamil, M., Dobson, C., Beeman, M., & Christoff, K. (2012). Evauative and generative modes of thought during the creative process. Neuroimage, 59, 1783-1794.

20) 宮内哲 (2013). 脳を測る：改訂 人の脳既往の非侵襲的測定. 心理学評論, 56 (3), 414-454.

21) Mather, M., Cacioppo, J.T., & Kanwisher, N. (2013). How fMRI can inform cognitive theories. Perspect Psychol Sci, 8 (1), 109-113.

22) Pearce, M.T., Zaidel, D.W., Vartanian, O., Skov, M., Lederm H., Chatterjee, A., & Nadal, M. (2016). Neuroaesthetics: The cognitive neuroscience of aesthetic experience. Perspect Psychol Sci, 11 (2), 265-279.

23) Wilkinson, D., & Halligan, P. (2004). The relevance of behavioural measures for functional-imaging studies of cognition. Nature

Rev Neurosci, 5, 68-73.
24）三浦佳世（2007）．知覚と感性の心理学．東京：岩波書店．
25）川畑秀明（2012）．脳は美をどう感じるか―アートの脳科学．東京：筑摩書房．

原 著 論 文

Modality dependent sensitivity in evaluating brain plasticity

Yul-Wan SUNG, Kawachi YOUSUKE, Uk-Su CHOI,
Daehun KANG, Ogawa SEIJI

Kansei Fukushi Research Institute, Tohoku Fukushi University

Abstract

As part of our research project for developing an evaluation system for brain plasticity for learning or training, we will use two MRI modalities to compare the effects of different academic majors. To prepare for this future study, here we determine whether brain differences exist at the outset of academic careers. Specifically, we examined the brains of freshmen and sophomores specializing in three different majors and evaluated the sensitivity of two MRI modalities, voxel-based morphometry (VBM) and resting state fMRI (rs-fMRI). There were no differences detected using VBM across the subject groups. However, a brain network was detected using rs-fMRI that showed differences across the subject groups. The brain network had several edges that had significantly different connectivity values between subject groups. The brain network also included ventral prefrontal cortex, which is known to play important roles in social function, such as decision-making and regulation of responses to emotion. These results suggest that rs-fMRI is more sensitive to plasticity changes than VBM, and that brain development for students who choose different majors differs prior to college entrance.

Keywords : Plasticity, rs-fMRI, Voxel-based morphometry, Brain networks

Introduction

We are running a research project to develop an evaluation system for the effects of academic, social, and vocational training programs. In this program we are using MRI to measure brain plasticity and brain function for identification of brain areas and networks related to specific human traits and behaviors.

Currently, two changes are trending in MRI-based brain research. One is the use of anatomical imaging to study brain function, and the other is the use of functional MRI (fMRI)[1] to study brain structure (functional brain structure). Although anatomical MRI imaging modalities have long been used as tools for disease diagnosis, recently, they have also been used for examining functional differences or changes in the brain because of learning or training. One such anatomical MRI modality is voxel-based morphometry (VBM)[2]. Some studies using VBM have reported that brain areas can show structural differences following different specific training of the subject[3-9]. Similarly, although fMRI has long been used to study brain function following stimulation, recently, fMRI without stimulation (resting state fMRI or rs-fMRI)[10-12] has also been used to identify brain networks. Some studies have used brain networks identified using rs-fMRI for diagnostic purposes in certain diseases[13-17].

Plasticity changes seen in anatomical images are understood to reflect changes in neuronal characteristics in a particular brain region that are related to development of a particular function that brought about the structural change[18-22]. On the other hand, plasticity changes observed in brain

networks using rs-fMRI are understood to reflect that signaling affects connectivity between brain regions with different functional roles but are related by development towards a particular brain function[23-25].

Data from the two different MRI measurement modalities (VBM and rs-fMRI) are likely to represent different functional characteristics and provide different sensitivities. To measure a change in neuronal properties using anatomical imaging, the change would have to affect the longitudinal relaxation time, T1, or the transverse relaxation time, T2. On the other hand, rs-fMRI is based on the BOLD signal and can reflect certain changes in neuronal processing that do not accompany changes in T1 or T2. Therefore, rs-fMRI could be more sensitive to neuronal changes than VBM.

Within the framework of our project, we plan to develop an objective method to compare the effects of learning or training among students specializing in different academic majors. To do so, we need to first to examine whether these students already show initial brain differences upon their entrance to academia, because such differences could interfere with any differential effects that their educational programs might have on their brains.

In this study, as a preliminary step for developing an MRI-based method to evaluate the effects of different educational programs, we used two MRI measurement modalities to examine initial differences between students planning to specialize in different majors, and we compared the sensitivities of the two modalities.

Methods

Subjects

Forty-five subjects specializing in different majors (M1, M2, and M3), with 15 subjects for each major, participated in this study. The subject groups M1 and M2 were freshmen, and M3 was sophomores from the same college. None of the subjects had a history of neurological disease or any medical conditions (i.e., pregnancy, use of a cardiac pacemaker, or claustrophobia). After subjects were given a complete description of the study, written informed consent was obtained in accordance with the Declaration of Helsinki. This study was approved by the Institutional Review Board of Tohoku Fukushi University.

MRI measurements

All subjects were scanned in two sessions that included structural (T1-weighted) and resting-state functional imaging (rs-fMRI). Structural images were acquired using the following parameters: repetition time = 1900 ms, echo time = 2.52 ms, matrix size = 256 × 256, in-plane resolution = 1 × 1 mm^2, slice thickness = 1 mm, and number of slices = 192. Resting-state fMRI data were acquired using a multi-band EPI sequence with a multi-band factor of 2 (Minnesota University, USA) and the following parameters: repetition time = 1000 ms, echo time = 25 ms, matrix size = 64 × 64, in-plane resolution = 3.4 × 3.4 mm^2, slice thickness = 3.4 mm, and number of volumes = 480. In the rs-fMRI session, subjects were asked to lie on a bed in a dark room with their eyes opened and not moving and to try to think about nothing.

MRI data analysis

The structural imaging data were analyzed using VBM implemented in the Statistical Parametric Mapping software (SPM 12B, Wellcome Department of Imaging Neuroscience, London, United Kingdom). The preprocessing and statistical tests (two-sample *t*-test and multiple regression) were performed according to a tutorial described in detail at the website http://www.nemotos.net and included segmentation, image registration (Dartel), normalization (modulation), and smoothing (Gaussian FWHM $8 \times 8 \times 8$ mm^3).

For resting state fMRI data, the images of 45 subjects were preprocessed using DPABI (rfmri.org/dpabi), which included slice scan time correction, 3 D motion correction, band pass temporal filtering (only signals with a frequency higher than 0.01 Hz and lower than 0.1 Hz), smoothing with 4-mm FWHM, and coregistration with each structural image. In the preprocessing, the time courses from 160 ROIs selected based on a previous study[26] were correlated, and correlation maps were created for brain networks. Brain networks were analyzed for the three groups using GraphVar (www.fmri.org/GraphVar).

Results

Structural images (VBM) were compared using one-way ANOVA and showed no significantly different areas among the three majors (M1, M2, and M 3) at a significance level of $p = 0.05$.

Brain networks determined using rs- fMRI were analyzed using a three-way ANOVA and one network showed significant differences among the three majors ($p = 0.001$) (corrected by NBS multiple comparison). The network consisted of seven brain areas (nodes) and six connections (edges) (Fig. 1); the left ventromedial prefrontal cortex (vmPFC_L), the left dorsal frontal cortex (dFC_L), the right prefrontal cortex (vPFC_R), the left anterior cingulate cortex (ACC_L), the left basal ganglia (basal_ganglia_L), the left precentral gyrus (precentral_gyrus_L), and the posterior occipital cortex.

In the network, the node area vmPFC_L was a hub and connected to nodes dFC_L, vPFC_R, ACC_L,

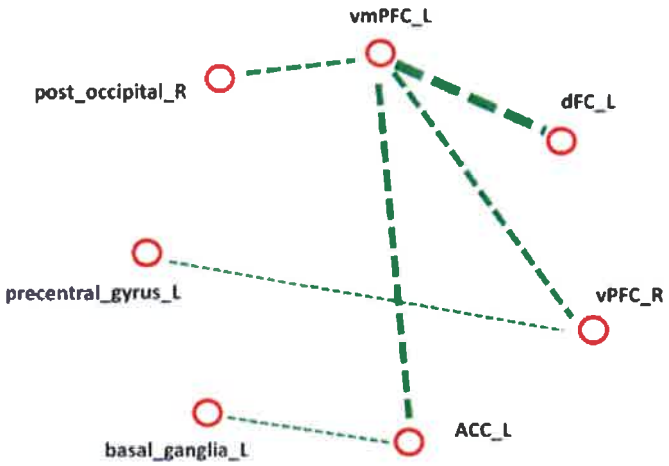
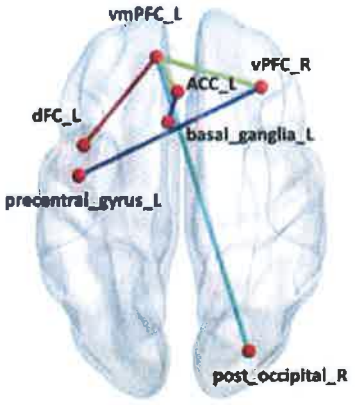
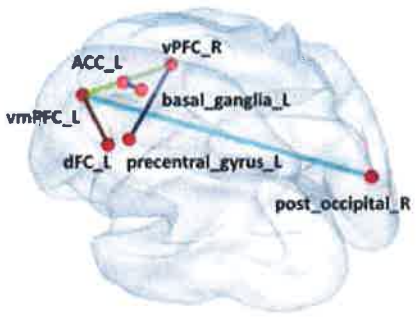


Figure 1 A brain network that showed significant differences among three majors, M1, M2, and M3.
(a) The brain network shown by nodes of brain areas and connectivity edges between them. Dotted green lines are edges, and red circles are nodes. The width of edges stands for connectivity with a value between 0 and 1.



(b) The brain network overlaid on a grass brain, as viewed from below.



(c) The brain network overlaid on a grass brain, as viewed from left-back

and post_occipiatal_L. The two nodes vPFC_R and ACC_L were connected to the nodes basal_ganglia_L and precentral_gyrus_L, respectively, in addition to the hub node.

Among edges of the network, the edge between the hub node vmPFC_L and vPFC_R was larger in M 1 than in M 2 (Fig. 2), and the edges between the hub node vmPFC_L and two other nodes, dFC_L and ACC_L, were larger in M 1 than in M 3 (Fig. 3). There was no significant edge difference between M 2 and M3. The hub node of a network is known to have an important role, and it was the hub node, vmPFC, in the network that showed significant difference between M1, M2, and M3. The functional roles of vmPFC are related to personal and social decision-making and to the regulation/inhibition of responses to emotions, which are considered to be crucial for developing social abilities[27-30]. Therefore, the differences in this network between subjects specializing in different majors likely reflect the different social experiences the subjects in each group have had up to entrance to college.

Discussion

As expected differences in the brain network were detected using rs-fMRI, but no differences were detected using VBM. This observation supports our hypothesis that rs-fMRI is more sensitive to neuronal changes than VBM.

The differences in the brain network from different majors, as detected by rs-fMRI, can be understood to originate from software-like changes rather than hardware-like changes because VBM, which mainly originates from structural changes of neurons, did not show any differences. For example, although the number of neurons in a brain area and nerve fibers between two brain areas may be the same, the numbers of neurons in a brain area activating together or communicating between two brain areas for a period of time during a processing function may be different between different subjects. This type of difference may result from the different traits in subjects.

The participants of this study, M 1 and M2, were freshmen, and, thus, the differences between their rs-fMRI brain networks developed prior to their entrance into academia and do not reflect effects of academic educational programs or training.

In our previous study[31], we had found some brain areas with different VBM values between subjects groups specializing in different majors, which differs from the result presented here. One reason for

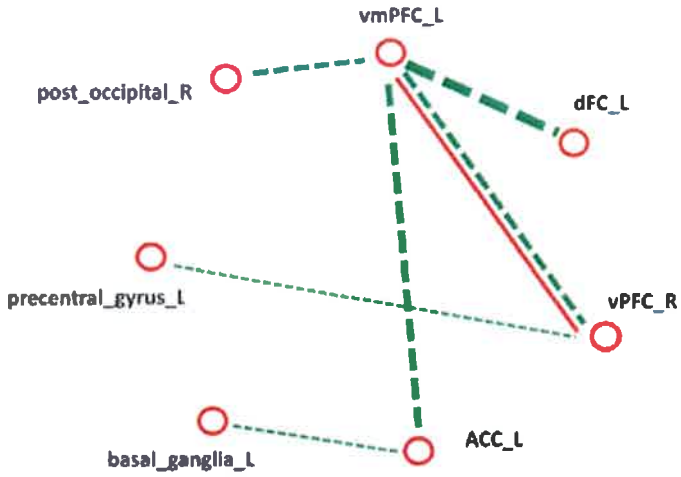


Figure 2 An edge of the brain network between vmPFC_L and vPFC_R (red color) that showed a larger connectivity value in M 1 than in M2.

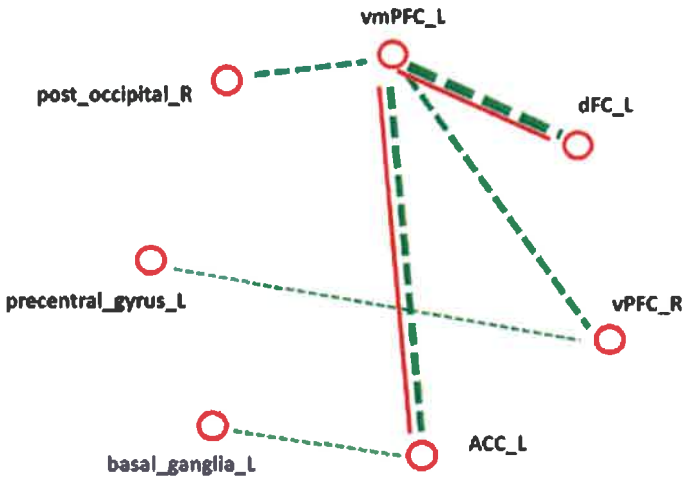


Figure 3 Two network edges (red color) of the brain network that showed larger connectivity value in M 1 than in M3. One runs between vmPFC_L and dFC_L and the other runs between vmPFC_L and ACC_L.

this discrepancy may be variability within the subject groups. In the previous study we did not consider the academic years of the subjects, but the present study included only students who were just initiating their majors. Therefore, the brain areas found in the previous study might reflect some plasticity changes due to participation in the different academic programs of their majors.

There are two limitations of this study. First, the exact psychological/behavioral factors reflected by the observed differences in the brain network are not examined. Another is that the exact function of the brain network found by group comparison is not determined. To examine these components, task-related fMRI should be performed. Further, as our project progresses, a future study will examine the extent that the initial differences between brain networks affects educational programs for each major and the aptitudes of students to theirs majors reflected by this initial difference.

Conclusions

The sensitivity of rs-fMRI in measuring differences in the brain across subject groups is higher than that of VBM. There are differences in brain networks developed prior to initiation of academic study between student groups specializing in different majors, and these initial differences should be considered when evaluating the effects of educational programs.

Acknowledgments

This study was supported by MEXT-Supported program for the Strategic Research Foundation at Private Universities, 2014-2018.

References

1. Ogawa S., Lee T.M., Kay A.R., Tank D.W. "Brain magnetic resonance imaging with contrast dependent on blood oxygenation" *Proc Natl Acad Sci U S A.* **87**: 9868-9872, 1990
2. Ashburner J., Friston K.J. "Voxel-based morphometry - The methods" Neuroimage 11: 805-821, 2000
3. Bermudez P., Zatorre R.J. "Differences in gray matter between musicians and nonmusicians" *Ann N Y Acad Sci* **1060**: 395-399, 2005
4. Deng, W., Saxe, M.D., Gallina, I.S. Gage, F.H. "Adult-born hippocampal dentate granule cells undergoing maturation modulate learning and memory in the brain" *J Neurosci* **29**: 13532–13542, 2009
5. Draganski B., Gaser C., Busch V., Schuierer G., Bogdahn U., May A. "Neuroplasticity: changes in grey matter induced by training" *Nature* **427**: 311-312, 2004
6. Draganski B., Gaser C., Kempermann G., Kuhn H.G., Winkler J., Büchel C., May A. "Temporal and spatial dynamics of brain structure changes during extensive learning" *J Neurosci* **26**: 6314-6317, 2006
7. Golestani N., Paus T., Zatorre R.J. "Anatomical correlates of learning novel speech sounds" *Neuron* **35**: 997-1010, 2002
8. Maguire E.A., Woollett K., Spiers, H. "London taxi drivers and bus drivers: a structural MRI and neuropsycholocical analysis" *Hippocampus* **16**: 1091-1101, 2006
9. May A. " Experience-dependent structural plasticity in the adult human brain" *Trends Cogn Sci* **15**: 475-482, 2011
10. Biswal B.B., VanKylen J., Hyde J.S. "Simultaneous assessment of flow and BOLD signals in resting-state functional connectivity maps". Nmr in Biomedicine, **10**: 165-170, 1997
11. Fox M.D., Snyder A.Z., Vincent J.L., Corbetta M., Van Essen D.C. Raichle M. E. "The human brain is intrinsically organized into dynamic, anticorrelated functional networks" *Proc Natl Acad Sci U S A.* **102**: 9673-9678, 2005
12. Fox M.D., Snyder A.Z., Zacks J.M., Raichle M.E. "Coherent spontaneous activity accounts for trial-to-trial variability in human evoked brain responses" *Nat Neurosci* **9**: 23-25, 2006
13. Rosazza C., Minati L. "Resting-state brain networks: literature review and clinical applications" Neurol Sci **32**: 773-785, 2011
14. Hafkemeijer A., Moller C., Dopper E.G.P., et al. "Resting state functional connectivity differences

between behavioral variant frontotemporal dementia and Alzheimer's disease", Front Hum Neurosci **9**: 474, 2015

15. Agosta F., Sala S., Valsasina P. et al. "Brain network connectivity assessed using graph theory in frontotemporal dementia" Neurology **81**: 134-143, 2013
16. Allen G., Barnard H., McColl R. et al. "Reduced hippocampal functional connectivity in Alzheimer disease" Arch. Neurol. **64**: 1482-1487, 2007
17. Zhou B., Yao H., Wang P., Zhang Z. et al. "Aberrant functional connectivity architecture in Alzheimer's disease and mild cognitive impairment: a whole-brain, data-driven analysis" Biomed. Res. Int. **2015**: 495375, 2005.
18. Tremblay, M.È., Lowery, R.L., Majewska, A.K. "Microglial interactions with synapses are modulated by visual experience" *PLoS Biol* **8**: e1000527, 2010.
19. Aimone, J.B., Wiles, J. Gage, F.H. "Computational influence of adult neurogenesis on memory encoding" *Neuron* **61**: 187–202, 2009
20. Dong, W.K., Greenough, W.T. "Plasticity of nonneuronal brain tissue: roles in developmental disorders" *Ment Retard Dev Disabil Res Rev* **10**, 85–90, 2004
21. Rhyu, I.J. et al. "Effects of aerobic exercise training on cognitive function and cortical vascularity in monkeys" *Neuroscience* **167**: 1239–1248, 2010
22. Pereira, A.C. et al. "An in vivo correlate of exercise-induced neurogenesis in the adult dentate gyrus" *Proc Natl Acad Sci USA* **104**: 5638–5643, 2007
23. Voss H.U., Schiff N.D. "MRI of neuronal network structure, function, and plasticity" Prog Brain Res **175**: 483-496, 2009
24. Van del Heuvel M.P., Mandl R.C., Kahn R.S., Hulshoff Pol H.E. "Functionally linked resting-state networks reflect the underlying structural connectivity architecture of the human brain" Hum Brain Mapp **30**: 3127-3141, 2009
25. Teipel S.J., Bokde A.L., Amaro E.Jr. et al. "White matter microstructure underlying default mode network connectivity in the human brain" Neuroimage **49**: 2021-2032, 2010
26. Dosenbach N.U.F., Nardos B., Cohen A.L. et al. "Prediction of individual brain maturity using fMRI" Science **329**: 1358-1361, 2010
27. Decety J., Michalska K. "Neurodevelopmental changes in the circuits underlying empathy and sympathy from childhood to adulthood" Developmental Science **13**: 886–899, 2010
28. Aaron D.B. et al. "Behavioral effects of congenital ventromedial prefrontal cortex malformation" BMC Neurology **11**: 151, 2011
29. Bechara A., Tranel D., Damasio H. "Characterization of the decision-making deficit of patients with ventromedial prefrontal cortex lesions" Brain **123**: 2189–2202, 2000
30. Fellows L.K., Farah M.J. "The Role of Ventromedial Prefrontal Cortex in Decision Making: Judgment under Uncertainty or Judgment Per Se?" Cerebral Cortex **17**: 2669–2674, 2007
31. Sung Y., Kawachi Y., Kang D., Ogawa S. "Evaluation of differences in brain plasticity with individual characteristics by MRI" Report of Kannsei Fukushi Research Institute **16**: 235-242, 2015

原 著 論 文

Hierarchical Clustering of fMRI Data

Zahra NAZARI [1], Dongshik KANG [1], Kawachi YOUSUKE [2], Yul-Wan SUNG [2] and Ogawa SEIJI [2]

[1] Department of Information Engineering, University of the Ryukyus, Okinawa, Japan

[2] Kansei Fukushi Research Institute, Tohoku Fukushi University, Sendai, Japan

Abstract

The purpose of a data clustering algorithm is to form clusters of data points with high intra-cluster and low inter-cluster similarity. There are different types of clustering methods such as hierarchical, partitioning, gird, density-based and hierarchical agglomerative clustering ones. Each of these uses a different induction principle. In the present study we use the hierarchical agglomerative clustering method to examine whether similarities between high dimensional functional Magnetic Resonance Imaging (fMRI) data can be estimated by the method.

Keywords : data clustering algorithm, fMRI, hierarchical agglomerative clustering

Introduction

Clustering is a fundamental problem that has been the focus of considerable researches in machine learning, pattern recognition and statistics. Clustering is an example of unsupervised learning which means there are no training samples from which to learn. Clustering automatically forms clusters of samples which of all are closely related. Therefore, the similarities between those samples assigned to the same cluster tend to be bigger than those in different clusters. It is also called unsupervised classification, because it produces the same result as classification algorithms, but without having predefined classes. In a simple form, the goal of clustering algorithms is to take a dataset and find the distinct clusters that exist within it. Clustering is widely used algorithm in different areas such as psychology, business and retail, computational biology, social media network analysis, and etc. There are many types of clustering methods such as hierarchical, partitioning, grid and density based, each of which uses a different induction principle. Briefly, the hierarchical method produces a sequence of clusterings in which each clustering is nested into the next clustering in the sequence. The partitioning method splits the dataset into k partitions, where each partition represents a cluster. The density based clustering finds clusters of data which are dense regions of dataset. These clusters are separated by low density regions from each other. The grid based clustering method is the fastest processing time that typically depends on the size of the grid instead of the dataset. This method uses the single uniform grid mesh to partition the entire problem domain into cells. However, according to Farley and Rafery (1998) clustering methods are mainly divided only into two groups of hierarchical and partitioning [1-3]. In this study we applied a hierarchical clustering method, hierarchical agglomerative clustering, to a high dimensional data set of functional MRI signals.

Methods

Hierarchical clustering is a well known clustering method that can be thought of as a set of flat clustering methods organized in a tree structure. These methods construct the clusters by recursively partitioning the data in either a top-down or bottom-up fashion, applicable to different domain regions. Hierarchical methods are commonly used for clustering in Data Mining problems. Among hierarchical algorithms, bottom-up approaches tend to be more accurate, but have higher computational cost than top-down approaches. However, this increased computational complexity does not coincide with increased conceptual or algorithmic complexity, since the process of cluster hierarchy formation can be organized as a sequence of basic cluster merging or partitioning operations [4-6]. Hierarchical method can be subdivided as following:

(Hierarchical agglomerative clustering)

A bottom-up approach which each object initially represents a cluster of its own, then clusters are iteratively merged until the desired cluster structure is obtained. This algorithm for N samples begins with N clusters and each cluster contains a single sample. Afterwards two clusters with the closest similarity will merge until the number of clusters becomes one or as specified by the user. The criterion which is used in this algorithm is min distance, max distance, average distance, and center distance [1,5].

(Divisive hierarchical clustering)

A top-down approach that all objects initially belongs to a single root cluster and iteratively partitions existing clusters into sub-clusters. This method is introduced in Kaufmann and Rousseeuw (1990) and is inverse of agglomerative method [1].

Hierarchical algorithms are of great interest for a number of application domains. Embedded flexibility with regard to the level of granularity, ease of handling any forms of similarity and distance and applicability to any attributes type are some of the advantages of hierarchical clustering methods. Meanwhile there are two disadvantages for these methods: most of hierarchical algorithms do not revisit once constructed clusters with the purpose of improvement; vagueness of termination criteria. While most of hierarchical clustering algorithms involve joining two sub-clusters or splitting a cluster into two sub-clusters in one step, some hierarchical algorithms join more than two sub-clusters or split a cluster into more than two sub-clusters. In hierarchical clustering, one can represent the clustering of objects as a tree called a dendrogram, in which the nodes represent subsets of the input dataset. The leaf nodes correspond to the individual elements of the dataset, and the root corresponds to the entire dataset. Each edge in the dendrogram represents an inclusion relationship (see Figure 1 for illustration) [2,7].

(M 1) Process of clustering

(A)Dimensionality Reduction

Principal Component Analysis, or PCA, is a very popular technique for dimensionality reduction and feature extraction. PCA constructs a low-dimensional representation of the data that describes as much of the variance in the data as possible. This is done by finding a linear basis of reduced dimensionality

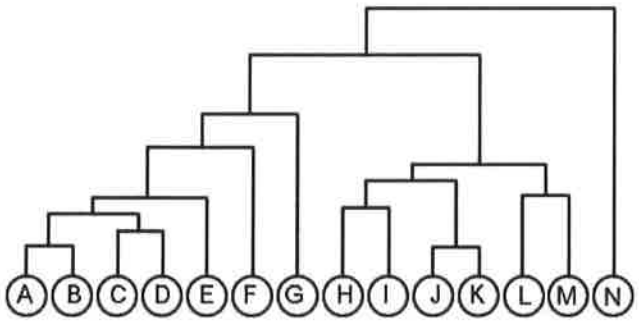


Figure 1 This figure illustrates the dendrogram for an agglomerative hierarchical clustering (bottom-up)

for the data, in which the amount of variance in the data is maximal. Kernel PCA is the nonlinear form of PCA, which better exploits the complicated spatial structure of high dimensional features [8].

Kernel PCA (KPCA) is the reformulation of traditional linear PCA in a high-dimensional space that is constructed using a kernel function. Kernel PCA computes the principal eigenvectors of the kernel matrix, rather than those of the covariance matrix. The reformulation of traditional PCA in kernel space is straightforward, since a kernel matrix is similar to the in product of the data points in the high-dimensional space that is constructed using the kernel function. The application of PCA in kernel space provides Kernel PCA the property of constructing nonlinear mappings. Since Kernel PCA is a kernel-based method, the mapping performed by Kernel PCA highly relies on the choice of the kernel function. Possible choices for the kernel function include the linear kernel (making Kernel PCA equal to traditional PCA), the polynomial kernel, and the Gaussian kernel. Kernel PCA has been successfully applied to, e.g., face recognition, speech recognition, and novelty detection. In the present study, KPCA with Gaussian kernel is used to reduce the dimensionality of functional MRI (fMRI) data [8].

(B) Hierarchical Clustering

Hierarchical clustering algorithm maintains an "active set" of clusters and at each stage decides which two clusters to merge. When two clusters are merged, they are each removed from the active set and their union is added to the active set. This iterates until there is only one cluster in the active set. The tree is formed by keeping track of which clusters were merged. The clustering found by hierarchical agglomerative clustering can be examined in several different ways. Of particular interest is the dendrogram, which is a visualization that highlights the kind of exploration enabled by hierarchical clustering over flat approaches such as K-Means. A dendrogram shows data items along one axis and distances along the other axis. A dendrogram shows a collection of $\prod$ shaped paths, where the legs show the groups that have been joined together. These groups may be the base of another $\prod$ or may be singleton groups represented as the data along the axis. A key property of the dendrogram is that vertical base of the $\prod$ is located along the x-axis according to the distance between the two groups that are being merged. For this to result in a sensible clustering – and a valid dendrogram – these distances must be monotonically increasing. That is, the distance between two merged groups G and G′ must always be greater than or equal to the distance between any of the previously-merged subgroups that formed G and G′ [4].

Steps of clustering:

1. Find the similarity of dissimilarity between every pairs of objects in the dataset. In this step, we calculate the distance between objects using pdist() in MATLAB. This function supports many different ways to compute this measurement (Euclidean distance is used).

2. Group the objects into a binary hierarchical cluster tree. In this step we link pairs of objects that are in close proximity using the linkage() in MATLAB. This function uses the distance information generated in step 1 to determine the proximity of objects to each other. As objects are paired into binary clusters, the newly formed clusters are grouped into larger clusters until a hierarchical tree is formed. (the length of a branch shows the difference between clusters/points. When length of branches are short, the similarity is very high and vice versa, so the point with longer branch can be an outlier.)

- Complete linkage: Maximum or complete linkage minimized the maximum distance between observations of pairs of clusters.

- Ward linkage: Ward's linkage uses the incremental sum of squares; that is, the increase in the total within-cluster sum of squares as a result of joining two clusters. The within-cluster sum of squares is defined as the sum of the squares of the distances between all objects in the cluster and the centroid of the cluster. The sum of squares measure is equivalent to the following distance measure $d(r, s)$, which is the formula linkage uses:

$$d(r,s)=\sqrt{\frac{2n_r n_s}{(n_r+n_s)}}\|\bar{x}_r-\bar{x}_s\|_2$$

3. Determine when to cut the hierarchical tree into clusters. In this step we use the cluster() in MATLAB to prune branches of the bottom of the hierarchical tree, and assign all the objects below each cut to a single cluster. This creates a partition of the data. The cluster function can create these clusters by detecting natural groupings in the hierarchical tree or by cutting off the hierarchical tree at an arbitrary point.

(M 2) Clustering of Functional MRI Data

(Subjects)

One hundred and twenty undergraduate students participated in this study. None of the subjects had a history of neurological disease or any medical conditions (i.e., pregnancy, use of a cardiac pacemaker, or claustrophobia). After subjects were given a complete description of the study, written informed consent was obtained in accordance with the Declaration of Helsinki. This study was approved by the Institutional Review Board of Tohoku Fukushi University.

(MRI measurements)

All subjects were scanned in two sessions that included structural (T1-weighted) and resting-state functional imaging (rs-fMRI). Structural images were acquired using the following parameters: repetition time = 1900 ms, echo time = 2.52 ms, matrix size = 256 × 256, in-plane resolution = 1 × 1 mm^2, slice thickness = 1 mm, and number of slices = 192. Resting-state fMRI data were acquired using the following parameters: repetition time = 2000 ms, echo time = 25 ms, matrix size = 64 × 64, in-plane resolution = 3.4 × 3.4 mm^2, slice thickness = 3.4 mm, and number of volumes = 250. In the rs-fMRI

session, subjects were asked to lie on a bed in a dark room with their eyes closed and not moving and to try to think about nothing.

(MRI data analysis)

For resting state fMRI data, the images of 120 subjects were preprocessed using DPABI (rfmri.org/dpabi), which included slice scan time correction, 3 D motion correction, band pass temporal filtering (only signals with a frequency higher than 0.01 Hz and lower than 0.1 Hz), smoothing with 4-mm FWHM, and coregistration with each structural image. After the preprocessing, the time courses from the 160 ROIs selected based on a previous study[9] were extracted and a mean fractional amplitude of low-frequency fluctuations (mfALFF) was calculated for each ROI.

Results and Discussion

The mfALFF data were used for clustering. The original dimension of the data was 160 which was reduced to 10. After reducing the dimension of data by KPCA, we used hierarchical agglomerative clustering method with ward linkage to cluster the data and we used dendrogram to show clusters. There was no termination criteria for this clustering method, so we selected 4 arbitrary numbers of clusters and performed clustering according to them. Afterwards we calculated the distance of each point to the mean of its cluster and summed up all distances for each clusters as total distance (d). Finally we summed up all total distances as D. By comparing the D values that was calculated for each number of clusters we chose that number of clusters with smallest D. An example of dendrogram and clustering result are shown in the following (see Figure 2).

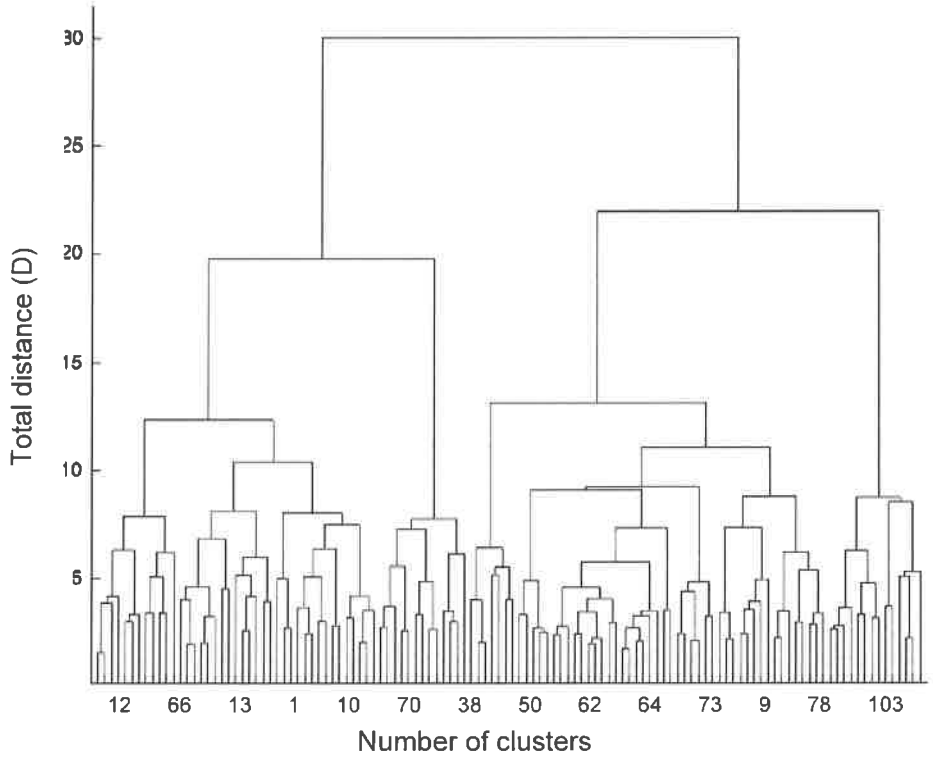


Figure 2 This dendrogram shows the clustering result of 120 subjects.

Number of clusters	Total distance (D)
3	40.5
6	40.4
10	36
14	33

c 1 =[17, 54, 103, 112]

c 2 =[4, 8, 33, 40, 42, 60, 67, 92, 93, 101]

c 3 =[51, 62, 78, 94, 97]

c 4 =[20, 36, 48, 34, 41, 49, 56, 72]

c 5 =[19, 23, 28, 34, 41, 49, 56, 72]

c 6 =[2, 5, 10, 21, 39, 45, 61, 75, 81, 91, 98, 100, 116, 119]

c 7 =[9, 11, 25, 26, 53, 55, 58, 77, 83, 84, 85, 88]

c 8 =[35, 57, 70, 80, 104, 111]

c 9 =[12, 16, 30, 47, 73, 76, 95, 113, 115]

c10=[1, 13, 27, 50, 65, 106, 117, 120]

c11=[15, 22, 38, 46, 52, 59, 64, 68, 71, 79, 86, 89, 90, 102, 105]

c12=[3, 24, 29, 32, 37, 96, 108, 109, 110, 114]

c13=[43, 44]

c14=[6, 7, 14, 18, 31, 63, 66, 69, 74, 82, 107, 118]

According to the distance calculation, 14 was selected as a number of clusters, because the total distance (D) was smaller in case of 14. The above dendrogram and clustering result are illustrating data clustering using hierarchical agglomerative clustering method. In this experiment there was no predefined label for data points, therefore we needed to perform clustering with different number of clusters and methods and compared their results to obtain the appropriate clustering result.

The clustering is based on a specific frequency band of the fMRI signal which is known to reflect functional characteristics of brain areas. Therefore, it can be considered that each cluster reflects a common attribute related with a specific brain function to the cluster which all members of the cluster share. Although what exact function a cluster reflects should be estimated through a function of each ROI and component loadings in our future study, the clustering method based on only fMRI data, which is different from other methods such as a correlation analysis based on subjective psychological data, will give objective information of functional characteristics of brain areas.

Conclusions

We examined whether the hierarchical agglomerative clustering method, which did not use predefined label, could classify high dimensional data such as functional Magnetic Resonance Imaging (fMRI) data and demonstrated its possibility. The future work to be done is to change the termination criteria as well as using other clustering methods and make a comparison between them.

Acknowledgments

This study was supported by MEXT-Supported program for the Strategic Research Foundation at Private Universities, 2014-2018.

References

1) P. Cichosz, Data Mining Algorithms Explained Using R, pp.349-362, John Wiley & Sons, Ltd. 2015.
2) A. K. Mann & N. Kuar, "Review paper on clustering techniques" Global Journal of Computer Science and Technology Software & Data Engineering, pp. 43-46, vol. 13, issue. 5, version. 1.0, 2013.
3) M. Kaur & U. Kaur, "Comparison between k-means and hierarchical algorithm using query redirection", International Journal of Advanced Research in Computer Science and Software Engineering, pp. 1454-1455, vol. 3, issue. 7, July 2013.
4) Y. Zhao & G. Karypis, "Hierarchical clustering algorithm for document datasets", pp. 141-142, Data Mining and Knowledge Discovery, 10, 141-168, 2005 Springer Science + Business Media, Inc.
5) O. Maimon & L. Rokach, The Data Mining and Knowledge Discovery Handbook, pp. 321-340, Springer Science+ Business Media, Inc 2005.
6) E. Alpydin, Introduction to Machine Learning, pp. 143-158, The MIT Press 2010.
7) E. Masciari, G. M. Mazzeo & C. Zaniolo, "A new, fast and accurate algorithm for hierarchical clustering on euclidean distance", pp. 111-114, Springer-Verlag Berlin Heidelberg 2013, Part II, LNAI 7819.
8) L. J. P. Van der Maaten, "An Introduction to dimensionality reduction using MATLAB", pp. 5-8, July N.U.F.2007.
9) Dosenbach, B. Nardos, A.L. Cohen et al., "Prediction of individual brain maturity using fMRI" Science, pp. 1358-136, vol. 329, 2010

原　著　論　文

一般知能と主観的実行機能の関連性

阿部千裕、河地庸介、坪川　宏、成　烈完、小川誠二
東北福祉大学

Relationship between Intelligence and Subjective Executive Functions

ABE Chihiro, KAWACHI Yousuke, TSUBOKAWA Hiroshi,
SUNG Yul-wan, OGAWA Seiji
Tohoku Fukushi University

Abstract

Many studies have provided evidence that general intelligence is positively correlated with various cognitive functions. However, one study (Friedman & Miyake, 2006) indicated that all three components of executive functions (EFs) are not related to intelligence measures. EFs, which are defined as processes that effectively control thought and action, have been attracting the interest of psychology/brain science researchers in recent times. Friedman and Miyake's (2006) study measured EFs by using only objective performance data such as response time and accuracy rate. Therefore, the relationship between intelligence measures and self-report measures of EF remains to be scrutinized. We examined the relationship between intelligence and EFs, using the Wechsler Adult Intelligence Scale (WAIS) and an EF questionnaire. Correlation analysis and structural equation modeling showed that three subordinate measures of the EF questionnaire were differently related to intelligence measures. The pattern of results was similar to that found by Friedman and Miyake (2006). Considering their results in conjunction with those of the present study, we suggest that although intelligence measures are partially related to performance-based/self-report EF measures, intelligence measures cannot assess all the components of EFs necessary for possible adaptive behaviors.

Keywords : intelligence, executive function, effortful controls

背　景

1．知能の定義と理論の発展

知能の定義は現在に至るまで一貫していないが、様々な理論家や研究者によって数多くの定義が提唱されてきた[1]。これまでの知能の定義では、あらゆる課題に対応できる一般的な能力、もしくは個々別々の課題に対応するために必要となる特定の機能に注目したものが多かった。今から1世紀以上前、そして現在も知能研究に影響を与えているSpearmanの知能の2要因説（Two-factor theory of intelligence）では、様々な個別の課題遂行能力（特殊因子, s因子）を基礎づける一般的な能力（g因子）の存在が仮定され、自らが考案した因子分析によりg因子の下位にs因子が存在すると提唱された[2]。またBinet and Simonは知能を「優れた感覚や日常場面における実際的な感覚、自発的な力、自分自身の置かれている状況に適した能力」と定義し、優れた判断をするため、または十分に物事を理解するため、論理的に考えるためには知能の働きが必要であるとした[3]。

Wechslerは、知能を「個人が環境に対して目的的に行動するためや理性的に考えるため、効果的に対

応するための包括的な能力、あるいはその集合体」と定義した[4]。Wechslerはその定義に基づいて Wechsler Adult Intelligence Scale（WAIS）を開発した。この知能検査はこれまでに信頼性の高い検査として認識され、現在までに2回の改訂を経て一般的な知能検査として多く用いられている。WAISを開発するにあたり、彼は知能とは言語性と動作性の課題によって測られるものであり、両課題を合わせて測定することで一般的な知能を測ることができると考えていた。言語性知能とは学歴や教育的水準、社会的階層などにより影響を受け蓄積された知能のことであり、動作性知能は生得的な要因に強い影響を受けた状況対応的な能力としての知能である。WAISでは様々な認知検査を行い、言語性知能（Verbal intelligence quotient）・動作性知能（Performance intelligence quotient）・全体性知能（Full scale intelligence quotient）の3つの知能を測ることができる。しかし、知能研究の進展とともに、WAISにはSpearmanの因子分析を用いた研究等のように[5]統計的な裏付けがないこと、新規な課題を遂行する際に必要となる能力（流動性推理能力）に関する検査が欠けていること等が指摘され、WAISは改良を余儀なくされた。このWAISの改良に関連して大きな影響を与えた理論の一つにCattell-Horn理論が挙げられる[6]。流動性－結晶性理論（Fluid Intelligence-Crystalized Intelligence Theory: Gf-Gc Theory）とも呼ばれる、一般的な知能を流動性知能と結晶性知能などの複数の因子に分けた理論である。流動性知能とは思考や推論を含む包括的能力のことであり、結晶性知能とは学校教育などの環境の中で学んだ知識や理解のことである[7]。従来のWAISには流動性知能に必要な検査が十分に含まれていないという批判から、改訂版には新たな下位検査を加えてより幅広い知能を測れるものへと改良された。以上、全体性知能も含めたこれら5つの因子は、知能を取り上げるには欠かすことのできない因子であると考えられている。

WAISのように一般的には普及していないために本研究ではこれ以上扱わないが、近年は学業成績のようなアカデミックな場面だけではなく、より日常場面との関わりを重視した知能の定義と心理検査が提案されている。Sternbergは知能には3つの側面があるとし、推論や判断する能力である分析的な知能と、新しいアイディアを生み出したり、新奇の問題に対処する中で独創的になる能力である創造的な知能、人々が日常の生活の中で出くわすような問題に対して効果的に対処する能力である実際的な知能とに区別した[8]。特に実際的な知能には、環境に対して何が効果的に働くのかということの潜在的知識を習得するという重要な部分があるとし、Sternbergはその知能を測定するためのテストを作成している。また、Gardnerは、人はそれぞれ一組の多重知能を持っており、いくつかの知的活動の特定の分野で才能を伸ばすことができるという考えのもと、多重知能理論（Theory of Multiple Intelligence）を提唱した[9]。従来の知能検査では学校の成績しか予測することはできないとし、自分に合った職業や趣味を選択するための知能として、「音楽的知能」や「身体運動的知能」等10の知能を提唱し、ゲームや活動またはそれに取り組む姿勢から知能を評価するプロジェクト・スペクトラム（The Spectrum Approach）という方法を作成した。

2．実行機能の定義

実行機能は、自分自身の思考や行動を制御する心的機能を総称したものとして近年注目を集めている[10), 11)]。特に、日常生活におけるプランニング、意思決定、行動の制御を担うとされている。実行機能には大きく分けて2つのモデルがある[12)]。Baddeleyによるモデルでは、音声情報を保持する音韻ループ、視空間情報を保持する視空間スケッチパッド、長期記憶からの情報を扱うエピソディック・バッファという3つの記憶貯蔵庫を制御し、注意の焦点化と分割、スイッチング、長期記憶の活性化を行い、目標達成的行動を支える機能として考えられている。一方、Miyakeらが示した実行機能は3つの要素で構成されているというものである[13)]。ワーキングメモリの情報の追加や削除を行う能力であるupdating、心的な構えの状態や課題の切り替えを行う能力であるshifting、反応の抑制を行う能力であるinhibitionの3要素である

注1。近年は複合モデルを実行機能の基本モデルとして扱う研究が多く、3要素に対応した課題で実行機能のメカニズムや働きが検証されている[14]。本研究でも3要素の観点から実行機能を捉えていく。

3．知能と実行機能の関連性

実行機能は前頭葉領域と関連づけられて検討されることが多く、事実前頭葉に損傷のある被験者は実行機能課題の成績が低下し、日常生活にも様々な支障が生じる[15]。しかし、それにも関わらず知能指数は健常被験者と差異がないことが報告されている。この知見は実行機能と知能が独立であることを示唆している。

他方で、Friedman and Miyakeは、実行機能の3つの構成要素それぞれに対応する認知課題とWAISで測定した知能との関連を検討した[14]。その結果、知能とupdatingとの間に相関が確認された。その一方で、他の2つの要素とは相関がないことを示した。UpdatingはWAISの下位検査に含まれているワーキングメモリを要するものであるため、知能との相関が高いことは当然の結果であるといえるだろう。以上の結果を踏まえて、Friedman and Miyakeは、知能指数は実行機能と一部関連するものの基本的に異なるものであるとした[14]。

4．実行機能の測定

実行機能は主に行動実験を通じて測定される。実行機能全体を測定する課題の他に、実行機能の3要素それぞれに対応した課題もある。課題の妥当性についてもすでに検証され、実行機能全体で10程度の課題が提唱されている[13), 11)]。Updatingについてはkeep track課題やletter memory課題、shiftingについてはnumber-letter課題やcategory switch課題、inhibitionについてはstop signal課題やantisaccade課題などが挙げられている。

質問紙による実行機能の測定も可能である。山形らは成人用エフォートフル・コントロール（Effortful Control: EC）尺度日本語版を作成し、実行機能を測定する課題の1つであるストループ課題の成績を質問紙得点によって予測できるかを検証している[17]。その結果、EC得点の高い人あるいは下位項目である「注意の制御」得点が高い人はストループ課題の成績がよいことが示された。このようにEC尺度は実験課題の成績を予測するものとなっており、基準関連妥当性が確認された尺度とされている。さらに、Ruedaや関口もECを実行機能と同様の概念を表すものとして使用している[18), 19)]。

5．本研究の目的

実行機能の測定方法は大きく分けて2通りの方法があるが、実行機能と知能の関連性について検討した先行研究では行動実験データのみが用いられてきた。そこで本研究ではEC尺度という質問紙による実行機能得点を用いて、実行機能の主観的評価の観点から一般知能との関連性を検討することを目的とした。すなわち、主観的評価という観点からも実行機能と一般知能は独立のものとして捉えられるのかを検討する。特定の認知機能は主として実験により測定されることが多いことに加えて、Goldenbergらが指摘しているように、行動実験により客観的に測定されたデータと質問紙等により主観的に測定されたデータは必ずしも相関しないことがある[20]。それゆえ、実行機能の主観的評価は実際の課題遂行能力と同様の内容を測定・反映しているのかについては検討が必要である。本研究で用いるEC尺度の下位項目はFriedman and Miyakeの実行機能の3要素の測定[14]と完全に対応するものではないために直接比較は難しいが、一般知能との関連性の検討は可能であると考える。Friedman and Miyakeと同様に、EC尺度の3つの下位項目の一部で一般知能と関連性が示されるという結果が得られるという仮説のもと[14]、質問紙による実行機能の測定結果と知能との関連性を検討する。

方　法

参加者

大学生113人（男性40名、女性73名）で、平均年齢19.4歳（SD=0.76）であった。参加者には本研究について書面および口頭によるインフォームドコンセントを行った。なお、本研究は東北福祉大学研究倫理審査委員会の承認を得て実施した。

調査内容

(1) 成人用エフォートフル・コントロール（EC）尺度日本語版[17]

Rothbart らの作成した Adult Temperament Questionnaire を日本語訳した EC 尺度 35項目を使用した[21]。質問紙は３つの下位尺度からなっており、「行動抑制の制御（Inhibitory Control）」11項目、「行動始発の制御（Activation Control）」12項目、「注意の制御（Attentional Control）」12項目で構成されている。回答は、“あてはまらない”“あまりあてはまらない”“少しあてはまる”“あてはまる”の４件法とした。下位尺度の得点の他に、合計得点を EC 得点として算出した。

(2) 日本版 Wechsler Adult Intelligence Scale（WAIS）- Ⅲ

Wechsler が開発した成人用の知能検査を使用し、11種の下位検査を対面式で実施した。下位検査の粗点に加え、５因子それぞれの知能指数（Intelligence Quotient: IQ）を日本版 WAIS- Ⅲ換算アシスタントにより算出した。

結　果

本研究では、Friedman and Miyake の研究と同様の相関分析と SEM（Structural Equation Modeling, 構造方程式モデリング）を行うこととした[14]。

EC 尺度の下位項目「行動抑制の制御」「行動始発の制御」「注意の制御」の３得点と WAIS- Ⅲの５つの知能指数（全体性、言語性、動作性、結晶性、流動性）で２変量の相関分析を行った（Table 1）。その結果、弱いながらも有意な正の相関が見られたのは、「注意の制御」と言語性 IQ（$r = .20, p < .05$）、「注意の制御」と全体性 IQ（$r = .19, p < .05$）、「行動抑制の制御」と流動性 IQ（$r = .19, p < .05$）であった。その他の項目には有意な相関は見られなかった。

次に、Friedman and Miyake の研究とのより詳細な比較のために、EC 尺度の下位項目と流動性 IQ・結晶性 IQ との関係性について SEM を用いて検討を行った（Figure 1）[14]。本研究で用いたモデルは、Friedman and Miyake のモデルのうち行動指標によって測定された updating, inhibition, shifting という変数[14] を EC 尺度の３つの下位項目「注意の制御」、「行動抑制の制御」、「行動始発の制御」に置き換えたものであった。ただし「行動始発の制御」については流動性・結晶性 IQ との有意な相関が得られないことから両 IQ へのパスは仮定しなかった。分析の結果、適合度指標は χ^2 (2) = .509, $p < .775$, RMSEA = .000, GFI=.998, AGFI=.986となり、十分に高い適合度が得られている。SEM ではモデル適合度がパスの有意性に優先するものの[22]、Friedman and Miyake 同様にパスの有意性を概観する[14]。全体として有意なパスは示されなかったが、「注意の制御」から結晶性 IQ へのパスは有意傾向であった（.19, $p < .10$）。その他の尺度については有意なパスは見られなかった。

考　察

本研究の結果から、主観的実行機能を反映する EC 尺度の下位項目のうち「行動抑制の制御」が流動性 IQ と、「注意の制御」が言語性 IQ との間に弱いが有意な相関があることが示された。他方で「行動始発の制御」はいずれの IQ とも有意な相関は見られなかった。SEM の結果、相関分析の結果を反映する適合度の高いモデルを構成することができた。しかし、有意傾向であるのは「注意の制御」から言語性 IQ

Table 1　Correlations between five intelligence quotients and subscales of the effortful control questionnaire.

	行動抑制の制御	行動始発の制御	注意の制御	全体性IQ	言語性IQ	動作性IQ	結晶性IQ	流動性IQ
行動抑制の制御	−	.524**	.579**	.133	.088	.140	.054	.195*
行動始発の制御		−	.492**	.100	.057	.127	.056	.166
注意の制御			−	.196*	.200*	.125	.159	.173
全体性 IQ				−	.847**	.820**	.769**	.779**
言語性 IQ					−	.393**	.906**	.511**
動作性 IQ						−	.360**	.802**
結晶性 IQ							−	.434**
流動性IQ								−

*p<.05.　**p<.01.

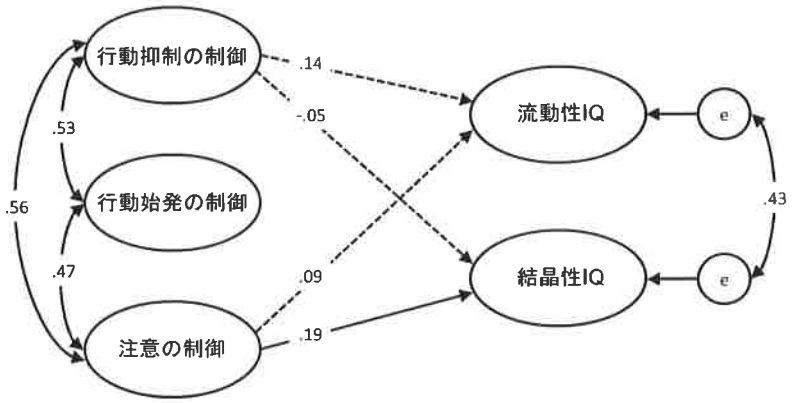


Figure 1. Structural equation model predicting the relationship between fluid/crystallized intelligence quotients and subscales of the effortful control questionnaire. A solid-line arrow indicates a marginally significant path at the .05 level. Dashed-line arrows indicate non-significant paths. Curved arrows indicate significant correlations at the .05 level. The two small circles are the residual variances of fluid and crystalized IQ.

へのパスのみであった。これらの結果を踏まえると、主観的に評価された実行機能も客観的に評価された実行機能[14]と同じく、一般知能と実行機能は一部関連しているが、実行機能によって一般知能を説明しきることはできないと結論づけることができる。

Friedman and Miyake の研究では、inhibition に対応する各実験課題と流動性 IQ との間に一部に有意な相関が出ているが、SEM の結果、inhibition から流動性 IQ へのパスは有意ではなかった[14]。本研究においては inhibition に対応する下位項目として「行動抑制の制御」が挙げられる。山形らが、「行動抑制の制御」に優れている人は不適切な反応が生じやすい時にその抑制が容易であると述べており[17]、「行動抑制の制御」は inhibition の概念に近いことが考えられる。実際に本研究でも Friedman and Miyake と同様に「行動抑制の制御」は流動性 IQ との間に有意な相関が見られている[14]。しかし、SEM の結果、「行動抑制の制御」から流動性 IQ へのパスは有意ではなかった。したがって、両者は関連しているものの「行動抑制の制御」が流動性 IQ を予測する変数にはなりえないといえる。

また Friedman and Miyake は、ワーキングメモリを要する updating が結晶性 IQ と有意に相関し、SEM の結果、updating から結晶性 IQ への有意なパスを報告している[14]。本研究における類似の結果として、「注意の制御」と言語性 IQ の間に有意な相関が得られた。SEM では「注意の制御」から言語性 IQ と似た概念を持つと考えられる結晶性 IQ へのパスが有意傾向であった。「注意の制御」は Miyake らの分類でいうと updating に関連していると考えられ[16]、ワーキングメモリ容量は次々に提示される情報への

注意の制御を反映しているという知見も報告されている[23), 24)]。以上から、updating についても Friedman and Miyake の研究と類似した結果がいえるだろう[14)]。

「行動始発の制御」に関しては、本研究では相関のある変数は見つからなかった。また報告はしていないが、「行動始発の制御」から流動性 IQ と結晶性 IQ へのパスを仮定したモデルは適合度がかなり低かった。このことは「行動始発の制御」が両 IQ から独立した機能であることを示唆する。山形らは「行動始発の制御」は実行機能測定課題の１つであるストループ課題の遂行成績と無相関であることから、実行機能を反映していない可能性を指摘している[17)]。ただしストループ課題は実行機能の中でも inhibition や「行動抑制の制御」にかかわる課題とされているため、「行動始発の制御」と相関がないことは想像に難くない。本研究から結論を出すことはできないが、「行動始発の制御」に限らず、EC 尺度の各下位項目が updating, shifting, inhibition のいずれに対応しているのか否かについては今後さらなる精査が必要かと思われる。

本研究では、EC 尺度を用いて一般知能と主観評価された実行機能との関連性を検討した。その結果、客観的に評価された実行機能と同様に、実行機能の一部のみが一般知能と関連しているという結果が得られた。本研究は、質問紙による主観的実行機能得点が行動実験データと同様の心理的特性をもつ可能性を示した。従来、知能は将来の社会的成功や学業成績を最もよく予測できるとされてきたが、今後は適応的な日常生活にかかせない実行機能[15)] を自分自身で意識し、主観的に評価・制御していける認知機能として、教育指導場面での配慮事項となりうるか等、社会的適応との関連を視野に入れて詳細に検討することが求められる。

謝辞

本研究は、東北福祉大学感性福祉研究所における文部科学省の私立大学戦略的研究基盤形成支援事業（平成26年度～30年度）による私学助成を得て行われ、感性福祉研究所の関係各位、また統計的分析に協力してくださった大友ゆき氏に感謝申し上げます。

注１：Friedman らの研究では unity/diversity framework 理論に基づいた研究により、updating と shifting の他に common EF という要素があると提唱されている[13)]。Common EF とは課題の目標や情報を維持する機能であり、全ての課題に影響を与える要素である。Inhibition は common EF を介して行われるものとされている。

引用文献

1）Wagner R.K. "Practical Intelligence" *Encyclopedia of psychology* 6, 266-270, 2000

2）Spearman C. "General Intelligence, Objectively Determined and Measured" *American Journal of Psychology* 15, 201-293, 1904

3）Binet A., Simon T. "New Methods for the Diagnosis of the Intellectual Level of Subnormals" *L' Annee Psychologique* 11, 191-244, 1905

4）Wechsler D. "The Measurement and Appraisal of Adult Intelligence（4th ed.)" *Journal of Medical Education* 33, 709, 1958

5）藤田和弘，前川久男，大六一志，山中克夫『日本版 WAIS-Ⅲの解釈事例と臨床研究』日本文化科学社，2011

6）Horn J.L. "Cognitive Diversity: A Framework of Learning" *Learning and individual differences*, 61-116, 1989

frontiers in Human Neuroscience

Front Hum Neurosci. 2015; 9: 597.
Published online 2015 Oct 29. doi: 10.3389/fnhum.2015.00597

PMCID: PMC4624850

Structural and functional plasticity specific to musical training with wind instruments

Uk-Su Choi,[1] Yul-Wan Sung,[2,*] Sujin Hong,[3] Jun-Young Chung,[1] and Seiji Ogawa[2]

[1]Neuroscience Research Institute, Gachon University of Medicine and Science, Incheon, South Korea
[2]Kansei Fukushi Research Institute, Tohoku Fukushi University, Sendai, Japan
[3]Reid School of Music, Edinburgh College of Art, Institute for Music and Human Society Development, University of Edinburgh, Edinburgh, UK

Edited by: Yong He, Beijing Normal University, China
Reviewed by: Jürgen Hänggi, University of Zurich, Switzerland; Xin Di, New Jersey Institute of Technology, USA

*Correspondence: Yul-Wan Sung ; Email: sung@tfu-mail.tfu.ac.jp; Email: sungstone@gmail.com

Received 2015 Jul 7; Accepted 2015 Oct 14.

Copyright © 2015 Choi, Sung, Hong, Chung and Ogawa.

This is an open-access article distributed under the terms of the Creative Commons Attribution License (CC BY). The use, distribution or reproduction in other forums is permitted, provided the original author(s) or licensor are credited and that the original publication in this journal is cited, in accordance with accepted academic practice. No use, distribution or reproduction is permitted which does not comply with these terms.

Abstract

Go to:

Numerous neuroimaging studies have shown structural and functional changes resulting from musical training. Among these studies, changes in primary sensory areas are mostly related to motor functions. In this study, we looked for some similar functional and structural changes in other functional modalities, such as somatosensory function, by examining the effects of musical training with wind instruments. We found significant changes in two aspects of neuroplasticity, cortical thickness, and resting-state neuronal networks. A group of subjects with several years of continuous musical training and who are currently playing in university wind ensembles showed differences in cortical thickness in lip- and tongue-related brain areas vs. non-music playing subjects. Cortical thickness in lip-related brain areas was significantly thicker and that in tongue-related areas was significantly thinner in the music playing group compared with that in the non-music playing group. Association analysis of lip-related areas in the music playing group showed that the increase in cortical thickness was caused by musical training. In addition, seed-based correlation analysis showed differential activation in the precentral gyrus and supplementary motor areas (SMA) between the music and non-music playing groups. These results suggest that high-intensity training with specific musical instruments could induce structural changes in related anatomical areas and could also generate a new functional neuronal network in the brain.

Keywords: cortical thickness, resting-state network, wind instruments, musical training, neuronal plasticity

Introduction

Go to:

Structural and functional changes in the human brain resulting from musical training have been noninvasively studied using various imaging modalities, including magnetic resonance imaging (MRI; Schlaug, 2001; Münte et al., 2002; Schmithorst and Wilke, 2002; Schlaug et al., 2005, 2009; Hyde et al., 2009; Penhune, 2011; Steele et al., 2013). Two main approaches have been used in MRI studies: structural and functional. For structural approaches, diffusion tensor imaging (DTI), cortical thickness analysis, and voxel-based morphometry (VBM) have been widely used.

Changes in the white matter (WM) of musicians have been demonstrated by DTI (Schlaug et al., 1995; Rüber et al., 2015). Musicians often show different fractional anisotropy (FA) maps in several brain areas compared with non-musicians (Schmithorst and Wilke, 2002; Bengtsson et al., 2005; Halwani et al., 2011; Engel et al., 2014; Moore et al., 2014). For example, they showed lower FA maps compared with non-musicians in the corticospinal tract, corona radiate, and internal capsules bilaterally (Schmithorst and Wilke, 2002; Imfeld et al., 2009), but higher FA maps in the right posterior limb of the internal capsule (Han et al., 2009) and corpus callosum (Schmithorst and Wilke, 2002; Steele et al., 2013). FA values are often used to study the strength of the WM fiber tract. Low FA values mean weak connectivity of the fiber tract, and high FA values mean strong connectivity of the fiber tract

(Schmithorst and Wilke, 2002). Even within some groups of musicians, different FA maps can be found depending on whether or not they have absolute pitch (AP), which is the ability to detect a pitch without any tonal reference (Oechslin et al., 2010). Musicians with AP showed significantly higher FA maps compared with those without it in the subgyral WM of the right temporal lobe, particularly within the path of the inferior fronto-occipital and inferior longitudinal fasciculus (Dohn et al., 2015).

Changes in the gray matter (GM) have been demonstrated by cortical thickness analysis and VBM. It has been reported that musicians have greater cortical thickness in the superior temporal and dorsolateral frontal regions as a result of their training (Bermudez et al., 2009). Musicians who were trained at a younger age showed greater cortical thickness in the ventral premotor cortex compared with those who were trained at an older age (Bailey et al., 2014). Among the other brain areas that showed different cortical thickness, Heschl's and bilateral intraparietal sulci strongly correlated with musical performances in relative pitch tasks (Foster and Zatorre, 2010). Along with cortical thickness analysis, VBM is also a very useful tool for finding structural changes. Musicians have been shown to have a significant increase in the volume of GM in the right fusiform (James et al., 2014), right posterior and middle cingulate, right and left superior temporal (Schneider et al., 2002; Bermudez and Zatorre, 2005), and right inferior orbitofrontal gyri as well as in the Broca's area in the left inferior frontal gyrus (IFG) that is associated with music-related abilities (Sluming et al., 2002; Fauvel et al., 2014), premotor cortex (Gaser and Schlaug, 2003), cerebellum (Hutchinson et al., 2003), and hippocampus (Groussard et al., 2010). Musicians who were trained before the age of seven showed an increased volume of the vPMC compared with musicians who were trained at an older age (Bailey et al., 2014).

For functional studies, activation of brain areas and functional connectivity among them have been measured to examine neuronal differences between the musicians and non-musicians. A representative functional difference between the musicians and non-musicians in functional MRI (fMRI) studies showed strong activation in auditory and motor areas, which are known to play crucial roles in musical activities (Baumann et al., 2005). Other studies have reported that non-musicians show a significant decrease in the brain activation in the right superior temporal gyrus when listening to trained melodies (Chen et al., 2012). Among musicians, enhancement of functional activity was found in the left middle and superior temporal gyri, left IFG, and right ventromedial prefrontal cortex in response to pattern deviation (Habermeyer et al., 2009). While performing musical tasks, musicians showed increased audiovisual asynchrony responses and effective connectivities in their superior temporal sulcus-premotor-cerebellar circuitry (Lee and Noppeney, 2011). Musicians also showed different functional connectivities not only during the task but also at rest. Furthermore, musicians also showed strong functional connectivity among the cingulate, right prefrontal cortex, and left temporal pole (Fauvel et al., 2014).

Most previous studies investigating either structural or functional changes in the brain have focused on musicians who play keyboard (Jäncke et al., 2000; Krings et al., 2000; Itoh et al., 2001; Haslinger et al., 2004; Meister et al., 2004; Parsons et al., 2005; Bengtsson et al., 2005; Baumann et al., 2007; Han et al., 2009; Gärtner et al., 2013; Engel et al., 2014; Alves-Pinto et al., 2015) or string instruments (Kim et al., 2004; Norton et al., 2005; Bangert and Schlaug, 2006; Vaalto et al., 2013; Verrel et al., 2013; Vollmann et al., 2014; Rüber et al., 2015). The instruments in those studies require the use of hands, and brain areas that showed specific functional and structural changes in those studies were related to motor activities. These functional studies reported different brain activation associated with motor practice (Jäncke et al., 2000; Haslinger et al., 2004) and functional connectivity between auditory and motor areas (Krings et al., 2000). Structural changes were also shown in both WM (Bengtsson et al., 2005) and GM (Han et al., 2009).

While many previous music-related studies have been conducted, none has examined neuroplasticity relating to wind instruments, which mainly require the mouth (lips and tongue) to play, in contrast to instruments described above, which mainly use other body parts, such as hands. Although the mouth is also used for singing (Sundberg, 1975; Ladefoged, 1978; Sundberg and Rossing, 1990), mouth usage while singing is different from playing wind instruments because the mouth interacts with objects when playing the latter (Gallivan and Eitnier, 2006; Wolfe et al., 2009).

In the current study, we hypothesized that similar structural and functional changes would occur in other brain modalities, such as the somatosensory, and examined the effects of musical training with the subjects who play wind instruments ("music playing group") compared with the subjects who do not play music ("non-music playing group"). Wind instrument players are expected to develop their lips and tongue touches. Therefore, we assumed that the structures of somatosensory areas of the brain that are associated with the lips and tongue would differ

between the music and non-music playing groups. In addition, we performed a resting-state fMRI analysis to investigate the possibility of functional connectivity modifications due to musical training.

Materials and methods

Go to:

Participants

Fourteen music playing [all female; mean age ± standard deviation (SD), 20.35 ± 1.21 years] and 14 non-music playing subjects (all female; mean age ± SD, 20.14 ± 1.23 years) participated in this study. Those included in the music playing group played wind instruments (woodwinds and brass) for more than 7 years (mean ± SD, 7.93 ± 1.21 years) as members of junior and senior high school and university wind ensembles. In contrast, non-music playing subjects did not have any extra musical experience except for regular music classes in school.

None of the subjects had a history of neurological disease or any medical conditions (i.e., pregnancy, use of a cardiac pacemaker, or claustrophobia). After subjects were given a complete description of the study, written informed consent was obtained in accordance with the Declaration of Helsinki. This study was approved by the Institutional Review Board of Tohoku Fukushi University (Japan).

MRI data acquisition

All subjects were scanned in two sessions that included structural (T1) and functional imaging (resting-state fMRI). Structural images were acquired using the following parameters: repetition time = 1900 ms, echo time = 2.52 ms, matrix size = 256 × 256, in-plane resolution = 1 × 1 mm^2, slice thickness = 1 mm, and number of slices = 192. Resting-state fMRI data were acquired using the following parameters: repetition time = 2000 ms, echo time = 30 ms, matrix size = 64 × 64, in-plane resolution = 3.4 × 3.4 mm^2, slice thickness = 3.4 mm, and number of volumes = 150. In the resting-state fMRI session, subjects were asked to lie on a bed and try to think about nothing about nothing with closed eyes.

Data analysis

All data were analyzed with Brainvoyager QX software (Brain Innovation B.V., Maastricht, Netherlands). Structural images were spatially normalized through Talairach transformation with Brainvoyager QX. In the first part of the transformation, we detected the anterior and posterior commissure as landmarks for the y-axis of the Talairach coordinate system. In the anterior commissure, the x-axis runs from the left to the right hemisphere, while the z-axis runs from the inferior to the superior part of the brain. All boundaries were decided manually. After the anterior-posterior commissure transformation, the brain was separated by 12 sub-cuboids. These 12 sub-cuboids were expanded or shrunken linearly to correspond to the size standard Talairach brain sub-cuboids. These normalized T1 images were corrected by an intensity inhomogeneity correction (Sled et al., 1997; Hou et al., 2006). After this correction, non-cortical structures [other than GM, WM, and cerebral spinal fluid (CSF)] were removed by a brain extraction process. The extracted T1 images were segmented by several types of brain tissues (i.e., GM, WM, and CSF) with different ranges of intensities.

For cortical thickness measurements, we first defined boundary voxels, one at the WM–GM boundary and one at the GM–CSF boundary. The values of those boundary voxels were kept, and the intensities between the GM voxels were smoothed by Laplace's equation (Jones et al., 2000). From the smoothed values, the gradient value of each voxel was calculated and then streamlines with those values were made. To calculate cortical thickness, we checked the gradient and evaluated along the gradient direction. This process was repeated until we could approach other boundaries, such as WM or CSF. The sum of the process provides the cortical thickness. Cortical thickness measures were calculated by processes within Brainvoyager QX. Individual cortical thickness measures were aligned to each normalized cortex mesh for group analysis. Cortical thickness maps were calculated for all subjects.

Region of interest (ROI)-based analysis is known to be very useful in studies of specific brain areas (Gur et al., 2000; Singh et al., 2014; Kauttonen et al., 2015). Therefore, we performed a ROI-based analysis wherein the postcentral gyrus was defined as a ROI containing somatosensory areas (Biswal et al., 1995; Stippich et al., 1999; Ruben et al., 2001; Nguyen et al., 2004; Miyamoto et al., 2006). Cortical thickness maps of the two groups were analyzed by a two sample *t*-test in the ROI, and the result was corrected for multiple comparison at a cluster-level threshold of $p < 0.005$ by Brainvoyager QX (Forman et al., 1995; Goebel et al., 2006).

One subject in the non-music playing group was excluded from the analysis of resting-state functional images

because of large head motion. The images of 25 subjects were preprocessed by slice scan time correction, 3D motion correction, and high pass temporal filtering (only signals with relatively high frequency >0.01 Hz). These functional images were smoothed with 6-mm FWHM and coregistered with each structural image. All resting-state functional images were analyzed by seed-based correlation analysis using Brainvoyager QX. In the analysis, the time course of seed ROIs were correlated with whole brain and correlation maps were created. Seed ROIs were those brain regions that showed different cortical thickness between the music and non-music playing groups. Individual correlation maps were made from seed ROIs. Correlation maps were analyzed by two sample *t*-test for two groups, and the resultant map was corrected for multiple comparison at a cluster-level threshold of $p < 0.05$.

Results

Go to:

Cortical thickness analysis

Cortical thickness difference maps for music and non-music playing groups were evaluated using a two sample *t*-test ($p < 0.005$, corrected). Two brain areas, which showed significant differences between the two groups, were found in the postcentral gyrus of the right hemisphere (Figure 1). The music playing group showed a thicker cortex in an area of the anterior part of the postcentral gyrus corresponding to the lips (Breshears et al., 2015) [*t*-value = 3.41; *p*-value = 0.003; cluster size = 9.71 mm^2; Brodmann's area (BA) 3; Talairach coordinates: x = 58, y = −14, z = 44] but a thinner cortex in an area of the posterior part of the postcentral gyrus corresponding to the tongue (Breshears et al., 2015) [*t*-value = − 3.51; *p*-value = 0.002; cluster size = 10.93 mm^2; BA2; Talairach coordinates: x = 64, y = −14, z = 35] compared with the non-music playing group. Areas with significantly different cortical thickness were subjected to ROI-based correlation analysis of thickness and years of musical training (association analysis). In the lip-related area of the postcentral gyrus, three participants of the music playing group were found as outliers at the 99% confidence interval (Figure 2A). Therefore, these three data points were excluded, and the remaining 11 subjects' data were used for the correlation analysis, which revealed significant and positive high correlations between the thickness and years of musical training ($r = 0.761$, $p = 0.006$ by Pearson correlation; Figure 3A). This means that changes in cortical thickness resulted from musical training. In the same way, in the tongue-related area, three participants in the music playing group were also found as outliers at 99% confidence interval (Figure 2B). Therefore, these three data points were excluded, and the remaining 11 subjects' data were used for the correlation analysis. However, there was no significant correlation between the thickness and years of musical training in this area ($r = 0.262$, $p = 0.437$ by Pearson correlation; Figure 3B).



Figure 1

A surface atlas showing of the postcentral gyrus and a cortical thickness difference map. The orange represents the area in which the music playing group had greater cortical thickness than the non-music playing group. The blue represents the area in ...



Figure 2

Confidence interval (CI) for cortical thickness and musical training years in lip- (A) and tongue-related (B) brain areas.



Figure 3

Correlation between cortical thickness and musical training years in lip- (A) and tongue-related (B) brain areas.

Resting-state fMRI analysis

Seed-based correlation analysis of tongue-related areas of the brain did not show any significantly different maps between the music and non-music playing groups. Correlation analysis of lip-related areas revealed some significantly different maps between the two groups (higher correlation in the music playing group) ($p < 0.05$, corrected) in the precentral gyrus and supplementary motor areas (SMA) bilaterally (BA6; Figure 4). The correlation map located in the lower part of the precentral gyrus of the left hemisphere (BA6) was in the motor-related mouth region and corresponded to the somatosensory mouth region. Correlation maps located in the middle part of the precentral gyrus (BA4) of both hemispheres were in motor-related hand regions (the middle part was clearly separated from upper and lower parts in the left hemisphere but not separated from those in the right

hemisphere). These results indicate that cortical thickness changes in somatosensory areas were related to new neuronal network developments in primary and supplemental motor areas.

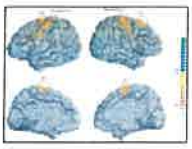


Figure 4

Correlation map differences between music and non-music playing groups from lip-related brain areas (higher correlation in the music playing group); left column, left hemisphere; right column, right hemisphere. Both brain hemispheres showed differences ...

Discussion

Go to:

The aim of our study was to determine how musical training with wind instruments causes structural and functional changes in the brain that could be attributed to specific ways of playing instruments. We mostly focused on somatosensory areas. Participants in this fMRI study were university students who received several years of training on wind instruments in junior and senior high school and are now members of reputable university wind ensembles. Participants chosen as non-music playing were university students with no special musical training. Cortical thickness analysis of structural plasticity in the brain showed significant differences in two areas of the postcentral gyrus associated with the lips and tongue according to previous reports (Pulvermüller et al., 2006; Meister et al., 2007; Brown et al., 2008; Venezia et al., 2012). In addition, correlation analysis in the lip-related area revealed a significant positive correlation between the thickness and years of musical training demonstrating that cortical thickness changes were longitudinal. In addition, seed-based correlation analysis by resting-state fMRI also revealed some areas that significantly differed between the music and non-music playing groups in the correlation map of lip-related areas, including those within the precentral gyrus and SMA, which are known to be related to learning mouth and motor skills and musical activity (Chen et al., 2012; Grabski et al., 2012; Gebel et al., 2013; Kim and Shin, 2014).

Along with changes in lip- and tongue-related brain areas, some reports suggest that playing wind instruments could result in physical changes to related body parts (i.e., the tongue and lips). For example, the muscles of the lips and tongue may change while playing a wind instrument (Methfessel, 1990). Also, lips are crucial to musicians who use only a single reed that physically produces sound on a wind instrument (Fuhrimann et al., 1987; Benade, 1990; Chen and Weinreich, 1996). Therefore, training with wind instruments can physically alter the lips and tongue, leading to changes in corresponding somatosensory brain areas (Draganski et al., 2006) as found in the current study. The positive correlation between the cortical thickness and training period in lip-related brain areas strongly suggests that changes in these areas were caused by musical training over several years.

The thickening of lip-associated brain areas can be explained in the same way as increased GM volume in certain areas associated with other types of training, such as juggling and piano playing. In contrast, the cause of cortical thinning in tongue-related brain areas is not easy to explain. Explanations for the cortical thickness decrease can be found in several previous studies. One explanation stems from previous studies showing sharpening in populations of neurons frequently recruited for a specific function (Desimone, 1996; Wiggs and Martin, 1998; Grill-Spector et al., 2006). Another possible explanation is that an increase in WM may cause a decrease in the ratio of GM in an imaging voxel as shown from some reports in which WM increased with musical training (Bengtsson et al., 2005; Zatorre, 2013). However, further study is needed to clarify the cause of this decrease as it relates to wind instrument training.

By resting-state fMRI, the music playing group showed stronger correlations with some areas in the precentral gyrus and SMA, and the relationship between precentral areas and SMAs with music has been found in previous studies. The precentral gyrus has been shown to be involved in musical instrument playing (Schieber, 1990; Amunts et al., 1997), musical training (Lin et al., 2002), and musical ability (Schlaug, 2001), while SMAs have been shown to be involved in musical training, especially in brain networks associated with rhythmic motor movements (Zatorre et al., 2007). In addition, the precentral gyrus and SMA are also known to interact closely for learning of musical instruments (Kim and Shin, 2014).

Unfortunately, the current study is limited in its design. Because the present study was designed to be cross-sectional, we cannot exclude the possibility that the music playing group members' abilities come from certain anatomical advantages over those of the non-music playing group rather than functional changes resulting from musical training. However, the positive correlation between the cortical thickness and years of musical training in

lip-related brain areas suggests otherwise. This longitudinal evidence and the appearance of the new functional neuronal network in the music playing group support our interpretation that cortical thickness changes reflect changes in neuronal plasticity by musical training.

In conclusion, we found structural and functional changes in lip- and tongue-related areas in the postcentral gyrus related to longitudinal musical training with wind instruments. These results indicate that high-intensity musical training can change the structure and function of the brain. Furthermore, the current findings support the idea of altered neuroplasticity by musical training.

Conflict of interest statement

The authors declare that the research was conducted in the absence of any commercial or financial relationships that could be construed as a potential conflict of interest.

Acknowledgments

Go to:

This study was supported by MEXT-Supported Program for the Strategic Research Foundation at Private Universities 2014–2018 and the National Research Foundation of Korea (NRF) Grant funded by Korea Government (MSIP) (no. NRF-2014M3C7033998).

References

Go to:

1. Alves-Pinto A., Turova V., Blumenstein T., Thienel A., Wohlschläger A., Lampe R. (2015). fMRI assessment of neuroplasticity in youths with neurodevelopmental-associated motor disorders after piano training. Eur. J. Paediatr. Neurol. 19, 15–28. 10.1016/j.ejpn.2014.09.002 [PubMed] [Cross Ref]
2. Amunts K., Schlaug G., Jäncke L., Steinmetz H., Schleicher A., Dabringhaus A., et al. . (1997). Motor cortex and hand motor skills: structural compliance in the human brain. Hum. Brain Mapp. 5, 206–215. [PubMed]
3. Bailey J. A., Zatorre R. J., Penhune V. B. (2014). Early musical training is linked to gray matter structure in the ventral premotor cortex and auditory-motor rhythm synchronization performance. J. Cogn. Neurosci. 26, 755–767. 10.1162/jocn_a_00527 [PubMed] [Cross Ref]
4. Bangert M., Schlaug G. (2006). Specialization of the specialized in features of external human brain morphology. Eur. J. Neurosci. 24, 1832–1834. 10.1111/j.1460-9568.2006.05031.x [PubMed] [Cross Ref]
5. Baumann S., Koeneke S., Meyer M., Lutz K., Jäncke L. (2005). A network for sensory-motor integration. Ann. N.Y. Acad. Sci. 1060, 186–188. 10.1196/annals.1360.038 [PubMed] [Cross Ref]
6. Baumann S., Koeneke S., Schmidt C. F., Meyer M., Lutz K., Jancke L. (2007). A network for audio–motor coordination in skilled pianists and non-musicians. Brain Res. 1161, 65–78. 10.1016/j.brainres.2007.05.045 [PubMed] [Cross Ref]
7. Benade A. H. (1990). Fundamentals of Musical Acoustics: Second, Revised Edition, 2nd Edn, Revised Edition. New York, NY: Dover Publications.
8. Bengtsson S. L., Nagy Z., Skare S., Forsman L., Forssberg H., Ullén F. (2005). Extensive piano practicing has regionally specific effects on white matter development. Nat. Neurosci. 8, 1148–1150. 10.1038/nn1516 [PubMed] [Cross Ref]
9. Bermudez P., Lerch J. P., Evans A. C., Zatorre R. J. (2009). Neuroanatomical correlates of musicianship as revealed by cortical thickness and voxel-based morphometry. Cereb. Cortex 19, 1583–1596. 10.1093/cercor/bhn196 [PubMed] [Cross Ref]
10. Bermudez P., Zatorre R. J. (2005). Differences in gray matter between musicians and nonmusicians. Ann. N.Y. Acad. Sci. 1060, 395–399. 10.1196/annals.1360.057 [PubMed] [Cross Ref]
11. Biswal B., Yetkin F. Z., Haughton V. M., Hyde J. S. (1995). Functional connectivity in the motor cortex of resting human brain using echo-planar MRI. Magn. Reson. Med. 34, 537–541. 10.1002/mrm.1910340409 [PubMed] [Cross Ref]
12. Breshears J. D., Molinaro A. M., Chang E. F. (2015). A probabilistic map of the human ventral sensorimotor cortex using electrical stimulation. J. Neurosurg. 123, 340–349. 10.3171/2014.11.JNS14889 [PubMed] [Cross Ref]
13. Brown S., Ngan E., Liotti M. (2008). A larynx area in the human motor cortex. Cereb. Cortex 18, 837–845. 10.1093/cercor/bhm131 [PubMed] [Cross Ref]
14. Chen F.-C., Weinreich G. (1996). Nature of the lip reed. J. Acoust. Soc. Am. 99, 1227–1233.

10.1121/1.414604 [PubMed] [Cross Ref]
15. Chen J. L., Rae C., Watkins K. E. (2012). Learning to play a melody: an fMRI study examining the formation of auditory-motor associations. Neuroimage 59, 1200–1208. 10.1016/j.neuroimage.2011.08.012 [PubMed] [Cross Ref]
16. Desimone R. (1996). Neural mechanisms for visual memory and their role in attention. Proc. Natl. Acad. Sci. U.S.A. 93, 13494–13499. 10.1073/pnas.93.24.13494 [PMC free article] [PubMed] [Cross Ref]
17. Dohn A., Garza-Villarreal E. A., Chakravarty M. M., Hansen M., Lerch J. P., Vuust P. (2015). Gray- and White-matter anatomy of absolute pitch possessors. Cereb. Cortex 25, 1379–1388. 10.1093/cercor/bht334 [PubMed] [Cross Ref]
18. Draganski B., Gaser C., Kempermann G., Kuhn H. G., Winkler J., Büchel C., et al. . (2006). Temporal and spatial dynamics of brain structure changes during extensive learning. J. Neurosci. Off. J. Soc. Neurosci. 26, 6314–6317. 10.1523/JNEUROSCI.4628-05.2006 [PubMed] [Cross Ref]
19. Engel A., Hijmans B. S., Cerliani L., Bangert M., Nanetti L., Keller P. E., et al. . (2014). Inter-individual differences in audio-motor learning of piano melodies and white matter fiber tract architecture. Hum. Brain Mapp. 35, 2483–2497. 10.1002/hbm.22343 [PubMed] [Cross Ref]
20. Fauvel B., Groussard M., Chételat G., Fouquet M., Landeau B., Eustache F., et al. . (2014). Morphological brain plasticity induced by musical expertise is accompanied by modulation of functional connectivity at rest. Neuroimage 90, 179–188. 10.1016/j.neuroimage.2013.12.065 [PubMed] [Cross Ref]
21. Forman S. D., Cohen J. D., Fitzgerald M., Eddy W. F., Mintun M. A., Noll D. C. (1995). Improved assessment of significant activation in functional magnetic resonance imaging (fMRI): use of a cluster-size threshold. Magn. Reson. Med. Off. J. Soc. Magn. Reson. Med. Soc. Magn. Reson. Med. 33, 636–647. 10.1002/mrm.1910330508 [PubMed] [Cross Ref]
22. Foster N. E. V., Zatorre R. J. (2010). Cortical structure predicts success in performing musical transformation judgments. Neuroimage 53, 26–36. 10.1016/j.neuroimage.2010.06.042 [PubMed] [Cross Ref]
23. Fuhrimann S., Schüpbach A., Thüer U., Ingervall B. (1987). Natural lip function in wind instrument players. Eur. J. Orthod. 9, 216–223. 10.1093/ejo/9.1.216 [PubMed] [Cross Ref]
24. Gallivan G. J., Eitnier C. M. (2006). Vocal fold polyp in a professional brass/wind instrumentalist and singer. J. Voice 20, 157–164. 10.1016/j.jvoice.2004.11.006 [PubMed] [Cross Ref]
25. Gärtner H., Minnerop M., Pieperhoff P., Schleicher A., Zilles K., Altenmüller E., et al. . (2013). Brain morphometry shows effects of long-term musical practice in middle-aged keyboard players. Audit. Cogn. Neurosci. 4:636. 10.3389/fpsyg.2013.00636 [PMC free article] [PubMed] [Cross Ref]
26. Gaser C., Schlaug G. (2003). Gray matter differences between musicians and nonmusicians. Ann. N. Y. Acad. Sci. 999, 514–517. 10.1196/annals.1284.062 [PubMed] [Cross Ref]
27. Gebel B., Braun C., Kaza E., Altenmüller E., Lotze M. (2013). Instrument specific brain activation in sensorimotor and auditory representation in musicians. Neuroimage 74, 37–44. 10.1016/j.neuroimage.2013.02.021 [PubMed] [Cross Ref]
28. Goebel R., Esposito F., Formisano E. (2006). Analysis of functional image analysis contest (FIAC) data with brainvoyager QX: from single-subject to cortically aligned group general linear model analysis and self-organizing group independent component analysis. Hum. Brain Mapp. 27, 392–401. 10.1002/hbm.20249 [PubMed] [Cross Ref]
29. Grabski K., Lamalle L., Vilain C., Schwartz J.-L., Vallée N., Tropres I., et al. . (2012). Functional MRI assessment of orofacial articulators: neural correlates of lip, jaw, larynx, and tongue movements. Hum. Brain Mapp. 33, 2306–2321. 10.1002/hbm.21363 [PubMed] [Cross Ref]
30. Grill-Spector K., Henson R., Martin A. (2006). Repetition and the brain: neural models of stimulus-specific effects. Trends Cogn. Sci. 10, 14–23. 10.1016/j.tics.2005.11.006 [PubMed] [Cross Ref]
31. Groussard M., La Joie R., Rauchs G., Landeau B., Chételat G., Viader F., et al. . (2010). When music and long-term memory interact: effects of musical expertise on functional and structural plasticity in the hippocampus. PLoS ONE 5:e13225. 10.1371/journal.pone.0013225 [PMC free article] [PubMed] [Cross Ref]
32. Gur R. C., Alsop D., Glahn D., Petty R., Swanson C. L., Maldjian J. A., et al. . (2000). An fMRI study of sex differences in regional activation to a verbal and a spatial task. Brain Lang. 74, 157–170. 10.1006/brln.2000.2325 [PubMed] [Cross Ref]
33. Habermeyer B., Herdener M., Esposito F., Hilti C. C., Klarhöfer M., di Salle F., et al. . (2009). Neural correlates of pre-attentive processing of pattern deviance in professional musicians. Hum. Brain Mapp. 30, 3736–3747. 10.1002/hbm.20802 [PubMed] [Cross Ref]

34. Halwani G. F., Loui P., Rüber T., Schlaug G. (2011). Effects of practice and experience on the arcuate fasciculus: comparing singers, instrumentalists, and non-musicians. Front. Psychol. 2:156. 10.3389/fpsyg.2011.00156 [PMC free article] [PubMed] [Cross Ref]
35. Han Y., Yang H., Lv Y.-T., Zhu C.-Z., He Y., Tang H.-H., et al. . (2009). Gray matter density and white matter integrity in pianists' brain: a combined structural and diffusion tensor MRI study. Neurosci. Lett. 459, 3–6. 10.1016/j.neulet.2008.07.056 [PubMed] [Cross Ref]
36. Haslinger B., Erhard P., Altenmüller E., Hennenlotter A., Schwaiger M., Gräfin von Einsiedel H., et al. . (2004). Reduced recruitment of motor association areas during bimanual coordination in concert pianists. Hum. Brain Mapp. 22, 206–215. 10.1002/hbm.20028 [PubMed] [Cross Ref]
37. Hou Z., Huang S., Hu Q., Nowinski W. L. (2006). A fast and automatic method to correct intensity inhomogeneity in MR brain images, in Medical Image Computing and Computer-Assisted Intervention – MICCAI 2006 Lecture Notes in Computer Science, eds Larsen R., Nielsen M., Sporring J., editors. (Berlin; Heidelberg: Springer;), 324–331. Available online at: http://link.springer.com/chapter/10.1007/11866763_40 (Accessed December 1, 2014).
38. Hutchinson S., Lee L. H.-L., Gaab N., Schlaug G. (2003). Cerebellar volume of musicians. Cereb. Cortex 13, 943–949. 10.1093/cercor/13.9.943 [PubMed] [Cross Ref]
39. Hyde K. L., Lerch J., Norton A., Forgeard M., Winner E., Evans A. C., et al. . (2009). Musical training shapes structural brain development. J. Neurosci. 29, 3019–3025. 10.1523/JNEUROSCI.5118-08.2009 [PMC free article] [PubMed] [Cross Ref]
40. Imfeld A., Oechslin M. S., Meyer M., Loenneker T., Jancke L. (2009). White matter plasticity in the corticospinal tract of musicians: a diffusion tensor imaging study. Neuroimage 46, 600–607. 10.1016/j.neuroimage.2009.02.025 [PubMed] [Cross Ref]
41. Itoh K., Fujii Y., Suzuki K., Nakada T. (2001). Asymmetry of parietal lobe activation during piano performance: a high field functional magnetic resonance imaging study. Neurosci. Lett. 309, 41–44. 10.1016/S0304-3940(01)02024-9 [PubMed] [Cross Ref]
42. James C. E., Oechslin M. S., Van De Ville D., Hauert C.-A., Descloux C., Lazeyras F. (2014). Musical training intensity yields opposite effects on grey matter density in cognitive versus sensorimotor networks. Brain Struct. Funct. 219, 353–366. 10.1007/s00429-013-0504-z [PubMed] [Cross Ref]
43. Jäncke L., Shah N. J., Peters M. (2000). Cortical activations in primary and secondary motor areas for complex bimanual movements in professional pianists. Cogn. Brain Res. 10, 177–183. 10.1016/S0926-6410(00)00028-8 [PubMed] [Cross Ref]
44. Jones S. E., Buchbinder B. R., Aharon I. (2000). Three-dimensional mapping of cortical thickness using Laplace's Equation. Hum. Brain Mapp. 11, 12–32. 10.1002/1097-0193(200009)11:1<12::AID-HBM20>3.0.CO;2-K [PubMed] [Cross Ref]
45. Kauttonen J., Hlushchuk Y., Tikka P. (2015). Optimizing methods for linking cinematic features to fMRI data. Neuroimage 110, 136–148. 10.1016/j.neuroimage.2015.01.063 [PubMed] [Cross Ref]
46. Kim D.-E., Shin M.-J., Lee K.-M., Chu K., Woo S. H., Kim Y. R., et al. . (2004). Musical training-induced functional reorganization of the adult brain: functional magnetic resonance imaging and transcranial magnetic stimulation study on amateur string players. Hum. Brain Mapp. 23, 188–199. 10.1002/hbm.20058 [PubMed] [Cross Ref]
47. Kim Y. K., Shin S. H. (2014). Comparison of effects of transcranial magnetic stimulation on primary motor cortex and supplementary motor area in motor skill learning (randomized, cross over study). Front. Hum. Neurosci. 8:937. 10.3389/fnhum.2014.00937 [PMC free article] [PubMed] [Cross Ref]
48. Krings T., Töpper R., Foltys H., Erberich S., Sparing R., Willmes K., et al. . (2000). Cortical activation patterns during complex motor tasks in piano players and control subjects. A functional magnetic resonance imaging study. Neurosci. Lett. 278, 189–193. 10.1016/S0304-3940(99)00930-1 [PubMed] [Cross Ref]
49. Ladefoged P. (1978). Physiology of speech production: an introduction for speech scientists by W. J. Hardcastle (review). Language 54, 757–758. 10.1353/lan.1978.0013 [Cross Ref]
50. Lee H., Noppeney U. (2011). Long-term music training tunes how the brain temporally binds signals from multiple senses. Proc. Natl. Acad. Sci. U.S.A. 108, E1441–E1450. 10.1073/pnas.1115267108 [PMC free article] [PubMed] [Cross Ref]
51. Lin K.-L., Kobayashi M., Pascual-Leone A. (2002). Effects of musical training on speech-induced modulation in corticospinal excitability. Neuroreport 13, 899–902. 10.1097/00001756-200205070-00033 [PubMed] [Cross Ref]
52. Meister I. G., Krings T., Foltys H., Boroojerdi B., Müller M., Töpper R., et al. . (2004). Playing piano in the

mind—an fMRI study on music imagery and performance in pianists. Cogn. Brain Res. 19, 219–228. 10.1016/j.cogbrainres.2003.12.005 [PubMed] [Cross Ref]
53. Meister I. G., Wilson S. M., Deblieck C., Wu A. D., Iacoboni M. (2007). The essential role of premotor cortex in speech perception. Curr. Biol. 17, 1692–1696. 10.1016/j.cub.2007.08.064 [PubMed] [Cross Ref]
54. Methfessel G. (1990). [Myofunction in players of wind instruments]. Dtsch. Zahnärztl. Z. 45, S48–50. [PubMed]
55. Miyamoto J. J., Honda M., Saito D. N., Okada T., Ono T., Ohyama K., et al. . (2006). The representation of the human oral area in the somatosensory cortex: a functional MRI study. Cereb. Cortex 16, 669–675. 10.1093/cercor/bhj012 [PubMed] [Cross Ref]
56. Moore E., Schaefer R. S., Bastin M. E., Roberts N., Overy K. (2014). Can musical training influence brain connectivity? Evidence from diffusion tensor MRI. Brain Sci. 4, 405–427. 10.3390/brainsci4020405 [PMC free article] [PubMed] [Cross Ref]
57. Münte T. F., Altenmüller E., Jäncke L. (2002). The musician's brain as a model of neuroplasticity. Nat. Rev. Neurosci. 3, 473–478. 10.1038/nrn843 [PubMed] [Cross Ref]
58. Nguyen B. T., Tran T. D., Hoshiyama M., Inui K., Kakigi R. (2004). Face representation in the human primary somatosensory cortex. Neurosci. Res. 50, 227–232. 10.1016/j.neures.2004.07.004 [PubMed] [Cross Ref]
59. Norton A., Winner E., Cronin K., Overy K., Lee D. J., Schlaug G. (2005). Are there pre-existing neural, cognitive, or motoric markers for musical ability? Brain Cogn. 59, 124–134. 10.1016/j.bandc.2005.05.009 [PubMed] [Cross Ref]
60. Oechslin M. S., Imfeld A., Loenneker T., Meyer M., Jäncke L., Oechslin M. S., et al. . (2010). The plasticity of the superior longitudinal fasciculus as a function of musical expertise: a diffusion tensor imaging study. Front. Hum. Neurosci. 3:76. 10.3389/neuro.09.076.2009 [PMC free article] [PubMed] [Cross Ref]
61. Parsons L. M., Sergent J., Hodges D. A., Fox P. T. (2005). The brain basis of piano performance. Neuropsychologia 43, 199–215. 10.1016/j.neuropsychologia.2004.11.007 [PubMed] [Cross Ref]
62. Penhune V. B. (2011). Sensitive periods in human development: evidence from musical training. Cortex 47, 1126–1137. 10.1016/j.cortex.2011.05.010 [PubMed] [Cross Ref]
63. Pulvermüller F., Huss M., Kherif F., Martin F. M. del P., Hauk O., Shtyrov Y. (2006). Motor cortex maps articulatory features of speech sounds. Proc. Natl. Acad. Sci. U.S.A. 103, 7865–7870. 10.1073/pnas.0509989103 [PMC free article] [PubMed] [Cross Ref]
64. Ruben J., Schwiemann J., Deuchert M., Meyer R., Krause T., Curio G., et al. . (2001). Somatotopic organization of human secondary somatosensory cortex. Cereb. Cortex 11, 463–473. 10.1093/cercor/11.5.463 [PubMed] [Cross Ref]
65. Rüber T., Lindenberg R., Schlaug G. (2015). Differential adaptation of descending motor tracts in musicians. Cereb. Cortex 25, 1490–1498. 10.1093/cercor/bht331 [PMC free article] [PubMed] [Cross Ref]
66. Schieber M. H. (1990). How might the motor cortex individuate movements? Trends Neurosci. 13, 440–445. 10.1016/0166-2236(90)90093-P [PubMed] [Cross Ref]
67. Schlaug G. (2001). The brain of musicians. Ann. N.Y. Acad. Sci. 930, 281–299. 10.1111/j.1749-6632.2001.tb05739.x [PubMed] [Cross Ref]
68. Schlaug G., Forgeard M., Zhu L., Norton A., Norton A., Winner E. (2009). Training-induced neuroplasticity in young children. Ann. N.Y. Acad. Sci. 1169, 205–208. 10.1111/j.1749-6632.2009.04842.x [PMC free article] [PubMed] [Cross Ref]
69. Schlaug G., Jäncke L., Huang Y., Staiger J. F., Steinmetz H. (1995). Increased corpus callosum size in musicians. Neuropsychologia 33, 1047–1055. 10.1016/0028-3932(95)00045-5 [PubMed] [Cross Ref]
70. Schlaug G., Norton A., Overy K., Winner E. (2005). Effects of music training on the child's brain and cognitive development. Ann. N.Y. Acad. Sci. 1060, 219–230. 10.1196/annals.1360.015 [PubMed] [Cross Ref]
71. Schmithorst V. J., Wilke M. (2002). Differences in white matter architecture between musicians and non-musicians: a diffusion tensor imaging study. Neurosci. Lett. 321, 57–60. 10.1016/S0304-3940(02)00054-X [PubMed] [Cross Ref]
72. Schneider P., Scherg M., Dosch H. G., Specht H. J., Gutschalk A., Rupp A. (2002). Morphology of Heschl's gyrus reflects enhanced activation in the auditory cortex of musicians. Nat. Neurosci. 5, 688–694. 10.1038/nn871 [PubMed] [Cross Ref]
73. Singh M. K., Chang K. D., Kelley R. G., Saggar M., Reiss A. L., Gotlib I. H. (2014). Early signs of anomalous neural functional connectivity in healthy offspring of parents with bipolar disorder. Bipolar

Disord. 16, 678–689. 10.1111/bdi.12221 [PMC free article] [PubMed] [Cross Ref]
74. Sled J. G., Zijdenbos A. P., Evans A. C. (1997). A comparison of retrospective intensity non-uniformity correction methods for MRI, in Information Processing in Medical Imaging Lecture Notes in Computer Science, eds Duncan J., Gindi G., editors. (Berlin; Heidelberg: Springer;), 459–464. Available online at: http://link.springer.com/chapter/10.1007/3-540-63046-5_43 (Accessed December 1, 2014).
75. Sluming V., Barrick T., Howard M., Cezayirli E., Mayes A., Roberts N. (2002). Voxel-based morphometry reveals increased gray matter density in broca's area in male symphony orchestra musicians. Neuroimage 17, 1613–1622. 10.1006/nimg.2002.1288 [PubMed] [Cross Ref]
76. Steele C. J., Bailey J. A., Zatorre R. J., Penhune V. B. (2013). Early musical training and white-matter plasticity in the corpus callosum: evidence for a sensitive period. J. Neurosci. 33, 1282–1290. 10.1523/JNEUROSCI.3578-12.2013 [PubMed] [Cross Ref]
77. Stippich C., Hofmann R., Kapfer D., Hempel E., Heiland S., Jansen O., et al. . (1999). Somatotopic mapping of the human primary somatosensory cortex by fully automated tactile stimulation using functional magnetic resonance imaging. Neurosci. Lett. 277, 25–28. 10.1016/S0304-3940(99)00835-6 [PubMed] [Cross Ref]
78. Sundberg J. (1975). Formant technique in a professional female singer. Acta Acust. United Acust. 32, 89–96.
79. Sundberg J., Rossing T. (1990). The Science of singing voice. J. Acoust. Soc. Am. 87, 462–463. 10.1121/1.399243 [Cross Ref]
80. Vaalto S., Julkunen P., Säisänen L., Könönen M., Määttä S., Karhu J. (2013). Long-term plasticity may be manifested as reduction or expansion of cortical representations of actively used muscles in motor skill specialists: Neuroreport 24, 596–600. 10.1097/WNR.0b013e3283628636 [PubMed] [Cross Ref]
81. Venezia J. H., Saberi K., Chubb C., Hickock G. (2012). Response bias modulates the speech motor system during syllable discrimination. Audit. Cogn. Neurosci. 3:157. 10.3389/fpsyg.2012.00157 [PMC free article] [PubMed] [Cross Ref]
82. Verrel J., Pologe S., Manselle W., Lindenberger U., Woollacott M. (2013). Coordination of degrees of freedom and stabilization of task variables in a complex motor skill: expertise-related differences in cello bowing. Exp. Brain Res. 224, 323–334. 10.1007/s00221-012-3314-2 [PubMed] [Cross Ref]
83. Vollmann H., Ragert P., Conde V., Villringer A., Classen J., Witte O. W., et al. . (2014). Instrument specific use-dependent plasticity shapes the anatomical properties of the corpus callosum: a comparison between musicians and non-musicians. Front. Behav. Neurosci. 8:245. 10.3389/fnbeh.2014.00245 [PMC free article] [PubMed] [Cross Ref]
84. Wiggs C. L., Martin A. (1998). Properties and mechanisms of perceptual priming. Curr. Opin. Neurobiol. 8, 227–233. 10.1016/S0959-4388(98)80144-X [PubMed] [Cross Ref]
85. Wolfe J., Garnier M., Smith J. (2009). Vocal tract resonances in speech, singing, and playing musical instruments. HFSP J. 3, 6–23. 10.2976/1.2998482 [PMC free article] [PubMed] [Cross Ref]
86. Zatorre R. J. (2013). Predispositions and plasticity in music and speech learning: neural correlates and implications. Science 342, 585–589. 10.1126/science.1238414 [PubMed] [Cross Ref]
87. Zatorre R. J., Chen J. L., Penhune V. B. (2007). When the brain plays music: auditory–motor interactions in music perception and production. Nat. Rev. Neurosci. 8, 547–558. 10.1038/nrn2152 [PubMed] [Cross Ref]

Articles from Frontiers in Human Neuroscience are provided here courtesy of **Frontiers Media SA**

Hindawi Publishing Corporation
BioMed Research International
Volume 2015, Article ID 234345, 6 pages
http://dx.doi.org/10.1155/2015/234345

Hindawi

Research Article

Evaluation of the Contribution of Signals Originating from Large Blood Vessels to Signals of Functionally Specific Brain Areas

Jun-Young Chung,[1,2] Yul-Wan Sung,[2,3] and Seiji Ogawa[2,3]

[1]*Department of Biomedical Engineering, College of Health Sciences, Gachon University, 191 Hambakmoero, Yeonsu-gu, Incheon 406-799, Republic of Korea*
[2]*Neuroscience Research Institute, Gachon University, 774 Namdong-daero, Namdong-gu, Incheon 405-835, Republic of Korea*
[3]*Kansei Fukushi Research Institute, Tohoku Fukushi University, 6-149-1 Kunimigaoka, Aoba, Sendai 989-3201, Japan*

Correspondence should be addressed to Yul-Wan Sung; sung@tfu-mail.tfu.ac.jp

Received 14 July 2014; Revised 5 September 2014; Accepted 19 September 2014

Academic Editor: Zhengchao Dong

Copyright © 2015 Jun-Young Chung et al. This is an open access article distributed under the Creative Commons Attribution License, which permits unrestricted use, distribution, and reproduction in any medium, provided the original work is properly cited.

The fusiform face area (FFA) is known to play a pivotal role in face processing. The FFA is located in the ventral region, at the base of the brain, through which large blood vessels run. The location of the FFA via functional MRI (fMRI) may be influenced by these large blood vessels. Responses of large blood vessels may not exactly correspond to neuronal activity in a target area, because they may be diluted and influenced by inflow effects. In this study, we investigated the effects of large blood vessels in the FFA, that is, whether the FFA includes large blood vessels and/or whether inflow signals contribute to fMRI signals of the FFA. For this purpose, we used susceptibility-weighted imaging (SWI) sequences to visualize large blood vessels and dual-echo gradient-echo echo-planar imaging (GE-EPI) to measure inflow effects. These results showed that the location and response signals of the FFA were not influenced by large blood vessels or inflow effects, although large blood vessels were located near the FFA. Therefore, the data from the FFA obtained by individual analysis were robust to large blood vessels but leaving a warning that the data obtained by group analysis may be prone to large blood vessels.

1. Introduction

Brain imaging via functional MRI is used to identify the functional sites that play specific roles in information processing in the brain. For an identified functional site, we expect that the site is as specific as possible to a function without exhibiting an overlap with other functional sites.

In BOLD imaging, on which most fMRI studies are based, the paramagnetic property of blood produces a bulk susceptibility difference between a blood vessel and the surrounding brain tissue, thus producing resonance frequency shifts in extravessel molecules. Thus, signals from oxygenation modulation can be expected in the tissues and for some distance into the venous side of the capillary bed [1]. This is, in itself, a short-range phenomenon located within a few tens of microns.

However, two factors make an undesirable contribution to BOLD-based fMRI signals, leading to an exaggeration of the spatial specificity and signal amplitude compared with those expected. One factor is the propagation of the bolus of oxygen-enriched blood by neuronal activation to the larger draining venous structures, which leads to the appearance of BOLD contrast in remote regions downstream of the actual site of neuronal activation [1, 2]. Another factor is the inflow effect. Neuronal activation alters vascular physiology, leading to increased flow both in the resistance pial arteries that feed the activated capillary beds and in the venules that drain these beds. MRI signals are inherently sensitive to inflowing fully magnetized spins; therefore, hemodynamic changes, particularly in larger blood vessels, can create signal fluctuations that are coincident with neuronal activation due to the inflow effect [3, 4].

Face recognition is important for social communication. The fusiform face area (FFA) is known to play a pivotal role in face processing [5, 6]. The measurement of responses of the FFA can provide crucial information regarding face recognition. The FFA is located in the ventral region [5, 6], at the base of the brain, through which large vessels, such as the inferior temporooccipital vein, middle temporal vein, vein of Labbé, middle temporobasal vein, and posterior temporobasal vein, run. The location of the FFA via fMRI varies across subjects, although the average location is almost invariant across groups of subjects. If the variation in location is dependent on large blood vessels, then the signal of the FFA can be under- or overestimated. However, this issue has not been examined. Although other functional sites also rely on individual brain structures and show variation in their location, the FFA is a special area in that it is surrounded by many large blood vessels.

In this study, we investigated the effects of large blood vessels in the FFA, that is, whether the FFA includes large blood vessels and/or whether inflow signals contribute to fMRI signals of the FFA. For this purpose, we used susceptibility-weighted imaging (SWI) sequences to visualize large blood vessels [7, 8] and dual-echo gradient-echo echo-planar imaging (GE-EPI) sequences to measure inflow signals [9, 10].

2. Materials and Methods

2.1. Subjects. Ten healthy volunteers participated in this study. After subjects were given a complete description of the study, written informed consent was obtained. This study was approved by the Institutional Review Board of Tohoku Fukushi University.

2.2. Measurements. All MRI experiments were performed using a Verio system (Siemens, Germany) with a standard 12-channel head matrix coil operating at 3 Tesla.

2.2.1. Dual-Echo EPI. The dual-echo EPI sequence was modified from the default single-shot GE-EPI of the Siemens apparatus to acquire images at the two echo times of 13 and 38 ms, which were determined as the shortest echo times possible. For functional imaging, the dual-echo GE-EPI sequence was used with a 2000 ms repetition time (TR), 90° flip angle (FA), 220 mm field of view (FOV), 64 × 64 mm matrix size, and 3.4 mm slice thickness with 0.5 mm gaps. Twenty slices parallel to the AC-PC were acquired for each volume.

2.2.2. SWI Imaging. An SWI 3D sequence was used with the parameters of TR of 28 ms, TE of 20 ms, FA of 15°, 294 × 320 matrix size, 220 mm FOV, and 1.13 mm thickness with 0.23 mm gaps. The orientation and center of slice positions were the same as those used in EPI. SWI image processing was performed using the Siemens default program.

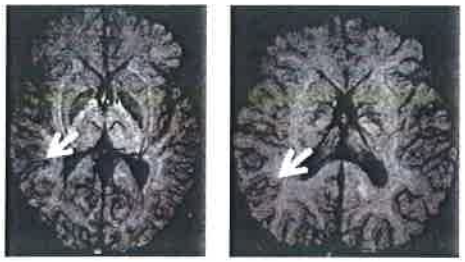


FIGURE 1: SWI-MIP images (across eight slices in sliding window mode). Image slices were from two subjects. The dark lines in the slices represent large blood vessels. The white arrows indicate some of the large blood vessels.

2.3. Derivation of an Image for Inflow Effects. The MRI signal evolution is, after a single RF excitation, as follows [3, 11]:

$$S(TE) = S0(T1) \cdot \exp\left(-\frac{TE}{T2^*}\right), \quad (1)$$

where S0 is the initial intensity, which is dependent on the $T1$ of a voxel and is responsible for inflow effects; TE is the effective echo time; and $T2^*$ is the apparent transverse relaxation time. As reported in a previous study S0 is calculated directly using the MRI signals S(TE1) and S(TE2) corresponding to TE1 and TE2. The equation that yields S0 for the corresponding voxel is as follows [4]:

$$S0 = \exp\left[\frac{\{\log(S(TE1)) - (TE1/TE2)\log(S(TE2))\}}{(1 - ET1/TE2)}\right]. \quad (2)$$

2.4. Stimulation Procedure. Visual stimuli were images presented in the center of the visual field. An experimental run consisted of 12 event blocks of four stimulation conditions, three blocks of single stimulation for face images (SF) and scene images (SS), and three paired stimulations for face images (PF) and scene images (PS). The SF, SS, PF, and PS condition blocks were randomized at intrasubject and intersubject levels. Single stimulation blocks (SF and SS) consisted of eight different face or scene images that were presented for 50 ms, with a 1.5-s repetition period interspersed with the control state. The paired stimulation blocks (PF and PS) consisted of eight pairs of faces or scenes, with a 1.5-s repetition period between pairs and a 150 ms interstimulus interval.

2.5. Visual Stimulation. Visual stimuli were grayscale images presented using a projector and displayed on a mirror mounted on the head coil (spatial resolution, 1024 × 768 pixels; refresh rate, 60 Hz; Panasonic, Japan). The images occupied 3.5°× 4°, and the crosshair occupied 0.34°× 0.34°.

2.6. Imaging Data Analysis. The imaging data acquired from the functional session were preprocessed using BrainVoyager QX (Brain Innovation B.V., Postbus, The Netherlands) for motion correction, scan time correction, and high-pass filtering, with a cutoff frequency of 0.005 Hz. In each functional

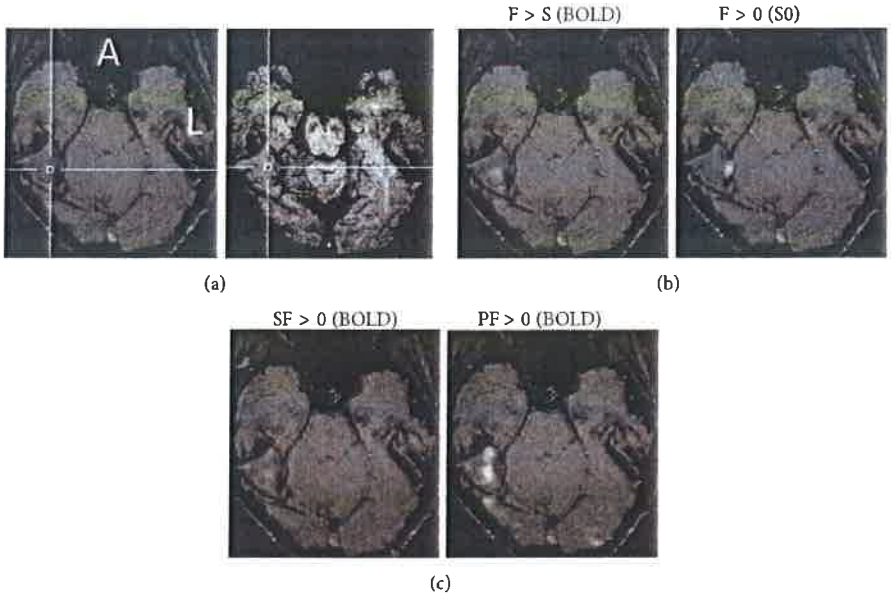


FIGURE 2: SWI images and activation maps for one subject in whom activation of BOLD and inflow signals appeared in the same image slice. The crossing of the two white lines indicates the center of the FFA. (a) SWI-noMIP (left) and SWI-MIP (right) images. (b) Activation maps on the SWI-noMIP of the FFA by BOLD signals using the contrast of the face and scene conditions (F > S) (left) and an activation site caused by inflow (S0) signals using the contrast of the face and control conditions (F > 0) (right). (c) Activation maps on the SWI image using SF > 0 (left) and PF > 0 (right). A: anterior; L: left. $P < 0.005$ (uncorrected).

run, the prestimulus was discarded from the estimation. The 2D data from the functional session were converted into the 3D data via trilinear interpolation using BrainVoyager QX. For the multisubject analysis, 3D Gaussian spatial smoothing (full width at half-maximum, 5 mm) was applied to the data. Statistical analysis was performed using BrainVoyager QX with a procedure based on general linear modeling. Each experimental condition (with the exception of the control) was defined as a separate predictor. The default hemodynamic response function of BrainVoyager QX was the reference time course used as the predictor. This analysis was performed independently for the time course of each voxel for each subject. To complete this analysis, time series of the images obtained from each subject were converted into the native space and Z-normalized.

3. Results

SWI images were acquired with minimum intensity projection (MIP) reconstruction across eight images (SWI-MIP) and without MIP. Activation maps were overlaid on SWI images without MIP (SWI-noMIP). SWI-MIP images were used to show large blood vessels more clearly. The SWI-MIP images showed blood vessels as a dark contrast, which was similar to previous reports that proposed the SWI method (Figure 1) [7, 8].

S0 images were acquired from images of two TEs of a dual-echo sequence. The activation map of S0 was acquired by contrasting the face conditions (SF and PF) to the control condition (this contrast included the contrast of the face versus scene conditions). Five of 10 subjects exhibited activation maps of S0 in the visual ventral region, which reflects inflow effects, while another five subjects did not. Among the data from the five subjects that showed inflow effects, variation was found in the location of activation sites (Figures 2 and 3; see Supplementary Figures 1–3 of the Supplementary Material available online at http://dx.doi.org/10.1155/2014/234345).

The FFA was identified from images with a TE of 38 ms (BOLD signals) of the dual-echo sequence by contrasting the face conditions (SF and PF) with the scene conditions (SS and PS). The data from some subjects showed that the FFA was located near the sites that reflected inflow signals. Other data showed that the FFA was located a little bit more remotely from those sites (Figures 2 and 3; Supplementary Figures 1–3). The images acquired from other subjects are shown in the supplementary figures (Supplementary Figures 4–8).

The images presented in Figure 2 are from one of ten subjects. The FFA was located at a cortical site that did not contain large blood vessels or strong susceptibility (Figure 2(a), right, and Figure 2(b), left). The activation site that reflected inflow signals was located on the right of the FFA in the same image slice (Figure 2(b), right). However, these areas did not overlap. The activation map obtained by PF was broader and stronger compared with that obtained by single stimulation (SF) (Figure 2(c), left and right).

The images presented in Figure 3 are for another subject and show the FFA and large blood vessels or susceptibility around the FFA where sites activated by inflow signals

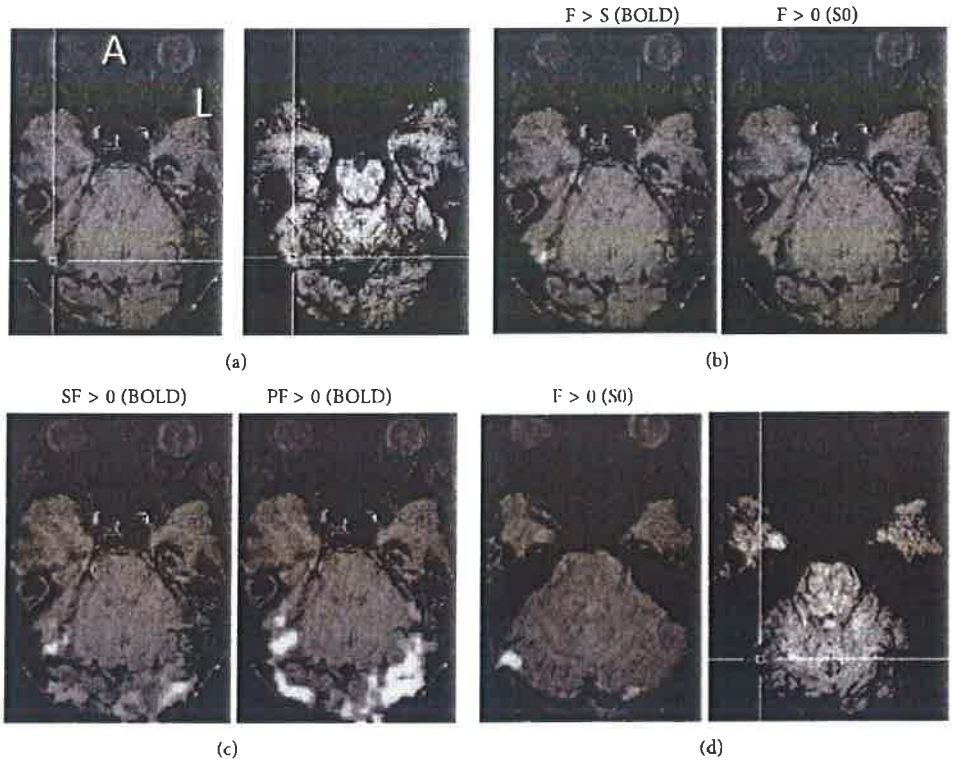


FIGURE 3: SWI images and activation maps for one subject in whom activations of BOLD and inflow signals appeared in different image slices. The crossing of the two white lines indicates the center of the FFA for (a) and the center of the S0 activation map for (d). (a) SWI-noMIP (left) and SWI-MIP (right) images. (b) Activation maps on the SWI image of the FFA were obtained by BOLD signals using the contrast of the face and scene conditions (F > S) (left), but not by inflow (S0) signals using the contrast of the face and control conditions (F > 0) (right). (c) Activation maps on the SWI image using SF > 0 (left) and PF > 0 (right). (d) Activation maps by S0 signals in a different image slice obtained by BOLD signals. A: anterior; L: left. $P < 0.005$ (uncorrected).

are located in different image slices. The FFA appeared to be located near large blood vessels (Figure 3(a), right, and Figure 3(b), left). Activation reflecting inflow signals was not found on the same image slice as that including the FFA (Figure 3(b), right). The activation map obtained by PF was much larger than that obtained by single SF (Figure 3(c), left and right). An activation map reflecting inflow signals was found at a lower region than the FFA (Figure 3(d), right). An activation site reflecting inflow signals appeared at large blood vessels (Figure 3(d), left and right).

To assess the effect of large surrounding blood vessels in the FFA, we processed the FFA data at individual and group levels. The results of the comparison of the SF and PF conditions were different between these two analyses (Figure 4). SF and PF were not significantly different ($P = 0.39$; paired t-test) but PF was larger than SF ($P = 0.01$; paired t-test).

4. Discussion

Our aim was to examine the contribution of large blood vessels to the fMRI response of the FFA. The data demonstrated, based on the presence of separate locations of activation sites of BOLD and S0, that fMRI responses of the FFA were not affected by inflow signals. The data also showed that no large blood vessels were present in the FFA. This means that the FFA was not affected directly by inflow signals and that its location was not biased by large blood vessel signals.

However, the presence of large blood vessels and the activation by inflow effects around the FFA represent a warning that the evaluation of FFA responses via intersubject averaging may lead to a wrong direction, because a representative location of the FFA acquired by averaging activated sites across subjects can pick up signals that originate from large blood vessels that surround the FFA. In fact, the comparison between an averaged signal from the locations of individual subjects and a signal from a common location based on the group-averaged data yielded different results; that is, the difference between the SF and PF conditions was larger in the group analysis than in the individual subjects' analysis (Figure 4). It is considered that broader activation maps of paired stimulation reached large blood vessels and that signals from the common area contained responses originating from large blood vessels.

The contribution of signals originating from large blood vessels to BOLD activation has been reported, and several previous studies attempted to remove this contribution or identify the location of large blood vessels [12–15]. One of

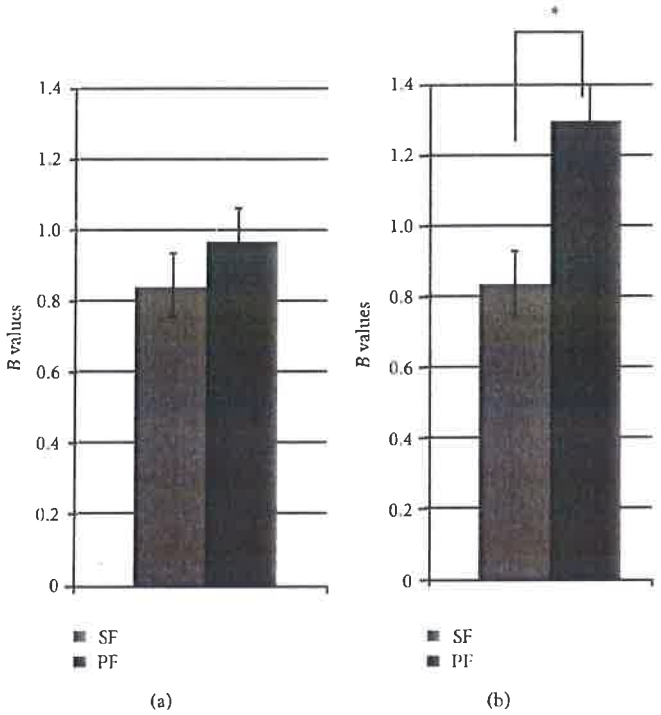


FIGURE 4: Averaged responses of the FFA in 10 subjects and estimated beta values based on BOLD signals using individual and group analyses. (a) Individual data; no significant difference was observed between SF and PF ($P = 0.39$, paired t-test). (b) Group data; PF was larger than SF ($P = 0.01$, paired t-test). Errors represent standard errors of the mean.

the ways to achieve this is to use a spin-echo (SE) EPI sequence and compare SE-EPI with GE-EPI sequences. An SE-EPI sequence with an additional gradient can remove the contribution of large blood vessels to BOLD signal, because diffusion effects are small around large blood vessels, and the velocity in the vessels is high [13, 16]. However, the disadvantages of using these methods include small signal changes, which preclude their routine use in fMRI studies of perception and cognition, although it is helpful to determine the exact components of BOLD signals. Another reason for not using these methods is that many fMRI studies are based on low spatial resolution images.

In the present study, we used SWI sequences to acquire blood vasculature information and dual-echo EPI sequences to measure inflow effects. Imaging using SWI sequences represents anatomical scanning, whereas imaging using dual-echo sequences represents functional scanning. Therefore, there was no penalty regarding scanning time for function or regarding signal intensity, because the second echo signal can be used for typical BOLD.

Signals originating from large blood vessels may lead to misinterpretation of the functional characteristics of brain areas examined using typical fMRI, particularly in high spatial resolution studies or high functional resolution studies (which deal with subtle differences between responses to similar stimuli). Therefore, the consideration of the contribution of large blood vessels in parallel with the typical functional analysis would be needed for ensuring reliability. The present study revealed that large blood vessels do not run through the FFA and that inflow effects did not affect fMRI signals of the FFA. This assures that the fMRI data from the FFA do not include functional artifacts resulting from large blood vessels, such as the variation in the location of the FFA between subjects or the modulation of signal intensity. Conversely, information on the large vessels that surrounded the FFA provided a warning regarding group analyses. The results obtained for the FFA can also be applied to other functional areas. Therefore, it may be advisable to use SWI and dual-echo EPI sequences for high spatial resolution studies or for perception or cognitive studies that deal with subtle differences in signals [11, 17].

Our study has some limitations. Although SWI images provided a strong contrast to large blood vessels, cerebral spinal fluid (CSF) also provided a contrast of a similar level. Some additional efforts may be needed to delineate vessels if greater detail regarding the blood vasculature is required. The method used in the present study consisted of the observation of the effects of large blood vessels rather than the removal of the effects. Therefore, other methods may be used in combination with the present approach if the proposed method shows that some target areas are influenced by large blood vessels.

Taken together, the results of the present study demonstrated that the location or response signals of the FFA were not influenced by large blood vessels or inflow effects, despite large blood vessels being located near the FFA and the

variation in the location of the FFA across subjects. However, a group analysis of multiple subjects may be affected by large blood vessels. This suggests that the data from the FFA obtained by individual analysis would be robust to large blood vessels, whereas the data obtained by group analysis may be prone to large blood vessels.

5. Conclusions

The data from the FFA obtained by individual analysis were robust to large blood vessels but leaving a warning that the data obtained by group analysis may be prone to large blood vessels. This shows that SWI sequences and dual-echo GE-EPI sequences can be used to probe functional characteristics of brain areas.

Conflict of Interests

The authors declare that there is no conflict of interests regarding the publication of this paper.

Acknowledgments

This study was partly supported by MEXT-Supported Program for the Strategic Research Foundation at Private Universities (2014–2018) and the National Research Foundation of Korea (NRF) Grant funded by Korea Government (MSIP) (no. NRF-2014M3C7033998).

References

[1] S. Ogawa, R. S. Menon, D. W. Tank et al., "Ugurbil , Functional brain mapping by blood oxygenation level-dependent contrast magnetic resonance imaging," *Biophysical Journal*, vol. 44, no. 3, pp. 803–812, 1993.

[2] J. S. Gati, R. S. Menon, K. Uğurbil, and B. K. Rutt, "Experimental determination of the BOLD field strength dependence in vessels and tissue," *Magnetic Resonance in Medicine*, vol. 38, no. 2, pp. 296–302, 1997.

[3] J.-H. Gao, I. Miller, S. Lai, J. Xiong, and P. T. Fox, "Quantitative assessment of blood inflow effects in functional MRI signals," *Magnetic Resonance in Medicine*, vol. 36, no. 2, pp. 314–319, 1996.

[4] J.-H. Gao and H.-L. Liu, "Inflow effects on functional MRI," *NeuroImage*, vol. 62, no. 2, pp. 1035–1039, 2012.

[5] R. Epstein and N. Kanwisher, "A cortical representation of the local visual environment," *Nature*, vol. 392, no. 6676, pp. 598–601, 1998.

[6] N. Kanwisher, J. McDermott, and M. M. Chun, "The fusiform face area: a module in human extrastriate cortex specialized for face perception," *The Journal of Neuroscience*, vol. 17, no. 11, pp. 4302–4311, 1997.

[7] E. M. Haacke, Y. Xu, Y.-C. N. Cheng, and J. R. Reichenbach, "Susceptibility weighted imaging (SWI)," *Magnetic Resonance in Medicine*, vol. 52, no. 3, pp. 612–618, 2004.

[8] E. M. Haacke and Y. Yongquan, "The role of susceptibility weighted imaging in functional MRI," *NeuroImage*, vol. 62, no. 2, pp. 923–929, 2012.

[9] G. H. Glover, S. K. Lemieux, M. Drangova, and J. M. Pauly, "Decomposition of inflow and blood oxygen level-dependent (BOLD) effects with dual-echo spiral gradient-recalled echo (GRE) fMRI," *Magnetic Resonance in Medicine*, vol. 35, no. 3, pp. 299–308, 1996.

[10] F. Beissner, S. Baudrexel, S. Volz, and R. Deichmann, "Dual-echo EPI for non-equilibrium fMRI—implications of different echo combinations and masking procedures," *NeuroImage*, vol. 52, no. 2, pp. 524–531, 2010.

[11] K. Grill-Spector, R. Sayres, and D. Ress, "High-resolution imaging reveals highly selective nonface clusters in the fusiform face area," *Nature Neuroscience*, vol. 9, no. 9, pp. 1177–1185, 2006.

[12] T. E. Conturo, R. C. McKinstry, J. A. Aronovitz, and J. J. Neil, "Diffusion MRI: precision, accuracy and flow effects," *NMR in biomedicine*, vol. 8, no. 7-8, pp. 307–332, 1995.

[13] T. Q. Duong, E. Yacoub, G. Adriany, X. Hu, K. Uğurbil, and S.-G. Kim, "Microvascular BOLD contribution at 4 and 7 T in the human brain: gradient-echo and spin-echo fMRI with suppression of blood effects," *Magnetic Resonance in Medicine*, vol. 49, no. 6, pp. 1019–1027, 2003.

[14] O. Speck and J. Hennig, "Functional imaging by I0- and T2*-parameter mapping using multi-image EPI," *Magnetic Resonance in Medicine*, vol. 40, no. 2, pp. 243–248, 1998.

[15] J. Zhong, R. P. Kennan, R. K. Fulbright, and J. C. Gore, "Quantification of intravascular and extravascular contributions to BOLD effects induced by alteration in oxygenation or intravascular contrast agents," *Magnetic Resonance in Medicine*, vol. 40, no. 4, pp. 526–536, 1998.

[16] A. W. Song, H. Fichtenholtz, and M. Woldorff, "Bold signal compartmentalization based on the apparent diffusion coefficient," *Magnetic Resonance Imaging*, vol. 20, no. 7, pp. 521–525, 2002.

[17] U.-S. Choi, Y.-W. Sung, S.-H. Choi et al., "Intermixed structure of voxels with different hemispheric characteristics in the fusiform face area," *NeuroReport*, vol. 24, no. 2, pp. 53–57, 2013.


The Scientific World Journal
Gastroenterology Research and Practice
MEDIATORS INFLAMMATION
Journal of Diabetes Research
Disease Markers
Journal of Immunology Research
International Journal of Endocrinology
Hindawi
Submit your manuscripts at
http://www.hindawi.com
PPAR Research
BioMed Research International
Journal of Ophthalmology
Stem Cells International
eCAM
Evidence-Based Complementary and Alternative Medicine
Journal of Obesity
Journal of Oncology
Computational and Mathematical Methods in Medicine
Behavioural Neurology
Parkinson's Disease
AIDS Research and Treatment
Oxidative Medicine and Cellular Longevity

Hindawi Publishing Corporation
BioMed Research International
Volume 2015, Article ID 394213, 7 pages
http://dx.doi.org/10.1155/2015/394213

Hindawi

Research Article

Fast Imaging Technique for fMRI: Consecutive Multishot Echo Planar Imaging Accelerated with GRAPPA Technique

Daehun Kang,[1,2] Yul-Wan Sung,[1] and Chang-Ki Kang[3]

[1] *Kansei Fukushi Research Institute, Tohoku Fukushi University, Sendai 989-3201, Japan*
[2] *Graduate School of Information Science, Tohoku University, Sendai 980-8579, Japan*
[3] *Neuroscience Research Institute and Department of Radiological Science, Gachon University, 1198 Kuwol-dong, Namdong-gu, Incheon 405-760, Republic of Korea*

Correspondence should be addressed to Chang-Ki Kang; changkik@gmail.com

Received 18 August 2014; Revised 13 October 2014; Accepted 3 November 2014

Academic Editor: Trevor Andrews

Copyright © 2015 Daehun Kang et al. This is an open access article distributed under the Creative Commons Attribution License, which permits unrestricted use, distribution, and reproduction in any medium, provided the original work is properly cited.

This study was to evaluate the proposed consecutive multishot echo planar imaging (cmsEPI) combined with a parallel imaging technique in terms of signal-to-noise ratio (SNR) and acceleration for a functional imaging study. We developed cmsEPI sequence using both consecutively acquired multishot EPI segments and variable flip angles to minimize the delay between segments and to maximize the SNR, respectively. We also combined cmsEPI with the generalized autocalibrating partially parallel acquisitions (GRAPPA) method. Temporal SNRs were measured at different acceleration factors and number of segments for functional sensitivity evaluation. We also examined the geometric distortions, which inherently occurred in EPI sequence. The practical acceleration factors, $R = 2$ or $R = 3$, of the proposed technique improved the temporal SNR by maximally 18% in phantom test and by averagely 8.2% in in vivo experiment, compared to cmsEPI without parallel imaging. The data collection time was decreased in inverse proportion to the acceleration factor as well. The improved temporal SNR resulted in better statistical power when evaluated on the functional response of the brain. In this study, we demonstrated that the combination of cmsEPI with the parallel imaging technique could provide the improved functional sensitivity for functional imaging study, compensating for the lower SNR by cmsEPI.

1. Introduction

In functional magnetic resonance imaging (fMRI) studies, echo planar imaging (EPI) technique has been widely used for investigating brain functions in which the signal is based on blood-oxygen-level-dependent (BOLD) contrast, reflecting the relationship between neuronal activity and concentration of deoxyhemoglobin in a blood vessel [1, 2]. Since EPI is one of the fastest imaging techniques, it has been suitable for observing functional dynamic changes of the brain. For high-resolution functional imaging, a segmented EPI, that is, multishot EPI (msEPI), has been employed as an alternative to a typical single-shot EPI (ssEPI) [2–5], because ssEPI image showed severe geometrical distortion and signal loss caused by accumulated magnetic susceptibility or field inhomogeneity. Also, the effective spatial resolution became worse by T_2^* filter effect of a tissue, as a readout period in ssEPI increases [3, 6, 7].

In the previous study [4], the authors suggested msEPI to be performed by the acquisition of all the segments in a single slice before continuing on to the next slices in turn. The study demonstrated that optimum contrast sensitivity in BOLD-based fMRI experiments using msEPI could be achieved by using the short repetition time (TR) values between segments and the long echo train length. The short TR between segments was achievable with minimized intersegment delay. The other studies suggested variable flip angles (VFA) to maximize signal-to-noise ratio (SNR) for a short duration of a segment, rather than the Ernst angle [5, 8]. Thus, both the minimum intersegment delay and VFA were employed to optimize msEPI for functional imaging. This technique was named as interleaved or snapshot EPI in the previous

studies [5, 8]. To avoid confusing with other multishot EPI techniques, we called it as consecutive multishot EPI (cmsEPI).

In the meantime, the advance of RF multicoil arrays and their encoding capability has made the parallel imaging acquisition possible, which was associated with the significant scan time reduction in many clinical applications. Many parallel imaging reconstruction methods such as sensitivity encoding (SENSE) [9], simultaneous acquisition of spatial harmonics (SMASH) [10], and generalized autocalibrating partially parallel acquisitions (GRAPPA) [11] have been suggested. However, they also come with a nonuniform noise enhancement and then with a nonuniform loss in SNR compared to nonaccelerated images as presented in the previous studies [9, 12, 13]. Nevertheless, the utilization of the parallel imaging acquisitions became essential due to the enhancement of imaging speed and sensitivity, especially at high field MRI above 3T [14].

The combined technique, however, of cmsEPI with a parallel imaging has not been reported in ultrahigh field 7T MRI. In this study, therefore, we investigated cmsEPI with GRAPPA technique to improve SNR and evaluated the functional sensitivity of the proposed technique.

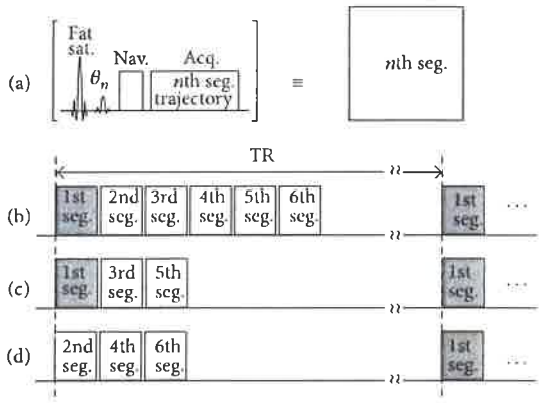


FIGURE 1: Simplified pulse sequence diagram. (a) The definition of a segment in multishot EPI, which consists of a fat-saturating RF pulse, a slice-selective RF pulse, navigators, and a data acquisition. Timing diagrams of (b) cmsEPI for 6 segments and (c) accelerated cmsEPI with reduction factor of $R = 2$ for 6 segments. For the reference data of $R = 2$, all six segments need to be acquired but in two sets: one includes 1st, 3rd, and 5th segments and the other 2nd, 4th, and 6th segments as described in (d). Fat Sat.: fat saturation; FA: flip angle; Nav.: navigation echo; Seg.: segment; TR: repetition time or time for acquisition of one slice.

2. Materials and Methods

2.1. Sequence Design. Each segment of cmsEPI pulse sequence consisted of a fat-saturating RF pulse, a slice-selective RF pulse, navigators, and a data acquisition as plotted in Figure 1(a). The minimized interval between the segments required VFA for the slice-selective RF pulses, which allowed the segments to have an equivalent transverse magnetization theoretically. A typical Cartesian k-space was filled with k-space trajectories as many as the number of segments without overlapping. The relative size of a blip along a phase-encoding direction of each segment was also the same as the number of segments.

For the accelerated acquisition, the number of segments to be measured was reduced by the factor of $1/R$, in which R denoted the reduction or acceleration factor. The corresponding modified VFA were also adjusted to the reduced number of segments, which was defined as the following:

$$\theta_n = \sin^{-1}\left(\frac{1}{\sqrt{N/R - n + 1}}\right), \quad (1)$$

where θ_n, N, and n denote the nth flip angle, the number of segments, and an integer in range between 1 and N/R, respectively.

For 6 segments, for example, a sequence of flip angles was 24°, 26°, 30°, 35°, 45°, and 90° in order, as shown in Figure 1(b). In a reduction factor of 2 ($R = 2$), only three flip angles were required, that is, 35°, 45°, and 90°, in order. In a k-space with a reduction factor of 2, three segments were chosen to make a trajectory with a constant interval along phase-encoding direction. Two measurements were conducted for the reference lines, each of which had 3 segments (1st, 3rd, and 5th segments or 2nd, 4th, and 6th segments) as described in Figures 1(c) and 1(d). Parallel imaging reconstruction was conducted with the autocalibration of a GRAPPA reconstruction kernel [11, 15].

At the same time, the navigator echoes following the excitation pulse were used for correcting not only the misalignment between alternating echoes along readout direction but also the intersegment amplitude discontinuities along phase-encoding direction [5]. A varying timing gap, namely, echo time shifting, was also inserted prior to data acquisition for preventing phase discontinuities of intersegment [16, 17].

2.2. Data Acquisition. For investigating the effect of parallel imaging on cmsEPI, we obtained images with different segments and acceleration factors, that is, 8 segments with $R = 1$, 2, and 4 or 6 segments with $R = 1$, 2, and 3. The acquisitions were performed three times on different days for reproducibility. The data with $R = 8$ in 8 segments and $R = 6$ in 6 segments were excluded, because the image reconstruction failed. Each dataset consisted of 50 volumes with which the temporal SNR (tSNR) was calculated. This experiment was performed with a spherical phantom filled with water.

Functional in vivo experiments consisted of two protocols: one was performed without any stimulus in order to analyze tSNR with the acquired 50 volumes during a resting state and the other was performed with visual stimulus, in which a flickering checker board of 8 Hz was utilized. A dummy period of 18 seconds was given prior to the initial session. A stimulus session of 18 seconds and a resting session of 18 seconds were repeated 4 times. Hence, each functional experiment was conducted for 162 seconds and 54 volumes were acquired. In functional in vivo experiment, only two conditions of 6 segments with $R = 1$ and $R = 3$ were acquired for comparison. The functional data were preprocessed and

analyzed with SPM8 (The Wellcome Department of Imaging Neuroscience, London, UK).

All imaging was performed in 7T MRI (MAGNETOM, SIEMENS, Erlangen). Data acquisition parameters were as follows: field of view (FOV) 220 × 220 mm^2, in-plane resolution 1.0 × 1.0 mm^2, partial Fourier factor 6/8, slice thickness 1.0 mm, TE 30 ms, TR 3000 ms, 5 slices, and 3.0 mm interslice gap. Note that TR 3000 ms means the time interval between subsequent volumes. The actual TR between segments was about 55 ms per segment per slice. For the acceleration factor $R = 3$, only 2 segments were acquired with an additional temporal gap of 220 ms between slices, which corresponds to the duration of 4 segments.

2.3. Image Reconstruction. Based on the reference data, the images were reconstructed by using multicolumn multiline interpolation (MCMLI) with a kernel of 5 × 4 ($k_x \times k_y$), resulting in nonaliased images. Both nearest acquired line (k_y) and column (k_x) neighboring points were interpolated to reconstruct each missing data in the k-spaces from multiple channels [15].

To compensate for the error of intersegment, the acquired navigators were used to determine the amplitude gains of segments, in which each navigator's energy, that is, sum of square of navigator, was calculated. Then, the intersegment amplitude discontinuity was corrected by the gains. The accelerated data were recovered by GRAPPA algorithm implemented on MATLAB program (The MathWorks, Inc., Natick, Massachusetts, USA).

2.4. Data Analysis. Datasets for tSNR analysis were handled with a voxel-based analysis by the following equation [18, 19]:

$$\mathrm{tSNR}(r) = \frac{\mathrm{mean}_{k=1\cdots K}\left(S_N(r,k)\right)}{\mathrm{stdev}_{k=1\cdots K}\left(S_N(r,k)\right)}, \quad (2)$$

where S_N, r, and K denoted a noised (measured) signal, a voxel position, and the number of measurements.

For in vivo dataset, region-of-interest (ROI) was determined within the gray matters chosen by threshold of the magnitude of a mean image. The threshold was selected to determine a midrange between representative intensities of CSF and white matter, which played a role in making a mask. The ROI was divided to three regions along a phase-encoding direction in order to evaluate the nonuniform loss in tSNR, and the mean and the standard deviation of voxels of each ROI or all the ROIs were evaluated.

3. Results

Figure 2 showed the normalized tSNRs at different acceleration factors of cmsEPI in a phantom test. Comparing with $R = 1$, the mean tSNR in $R = 2$ increased by 18% and 12% in 6 and 8 segments, respectively. After that, with the acceleration factors of 3 and 4, the tSNR was decreased as acceleration factor increased. The mean tSNR with 6 segments and $R = 3$ was similar to that of $R = 1$.

In in vivo experiment, Figures 3(a) and 3(b) showed the tSNR maps of cmsEPI with $R = 3$ and $R = 1$, respectively.

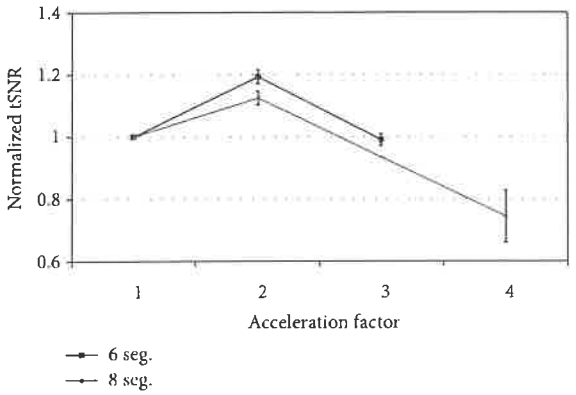


FIGURE 2: Comparison of temporal SNR at different conditions in phantom test. All of data were normalized to $R = 1$.

TABLE 1: Comparison of averaged tSNRs on ROIs selected from the gray matter compartment.

	$R = 1$	$R = 3$	Gain (%)
ROI 1	33.7 ± 7.6	38.5 ± 9.0	+14.2
ROI 2	34.1 ± 7.9	34.3 ± 7.9	+0.6
ROI 3	30.4 ± 6.9	32.2 ± 7.5	+6.0
Whole ROIs	33.1 ± 7.7	35.8 ± 8.7	+8.2

Basically, voxels including CSF tended to have a relatively high tSNR and voxels around brain ventricle had the highest tSNR. The tSNR difference between reduction factors was plotted in Figure 3(c). The most brain area of cmsEPI with $R = 3$ had a higher tSNR than that with $R = 1$ in in vivo experiment, although only the small portion of the image, especially at the midline of an image, had a decreased tSNR. For quantitatively evaluating the gain in tSNR, a mean and a standard deviation of voxels at ROIs were calculated from the tSNR difference map, and the result was presented in Table 1. The tSNR of each ROI of cmsEPI with $R = 3$ was equal to or larger than $R = 1$, and an average gain of the tSNR was about 8.2% up to 14.2%.

In functional experiments, the visual stimulus was utilized in order to observe the activations on the primary visual area of the brain. As a result, Figures 4(a) and 4(b) showed the activation maps obtained by cmsEPI with $R = 3$ and $R = 1$, respectively. To compare the two statistical values, they were displayed in the same range of t-value. The result of cmsEPI with $R = 3$ had larger activated areas and higher t-values than that of $R = 1$. Figure 4(c) showed activation profiles in white lines on Figures 4(a) and 4(b), which showed similar patterns to each other. The profile of $R = 3$, however, provided better statistical power for activation than that of $R = 1$.

Figure 5 showed the distortion comparison between cmsEPI and ssEPI. Images in cmsEPI had almost the same degree of distortion, regardless of acceleration factors, while ssEPI showed explicit geometric distortion.

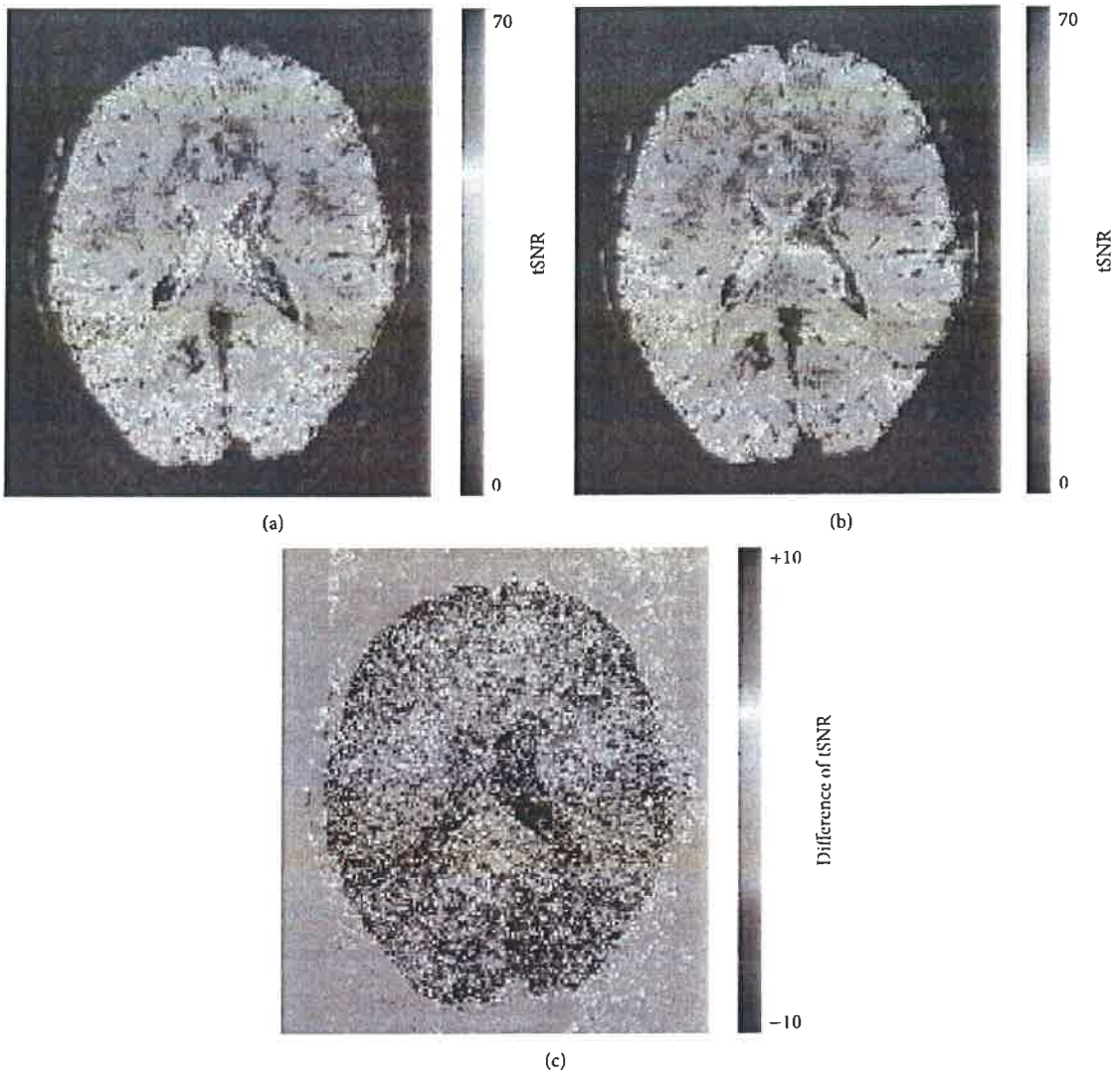


FIGURE 3: tSNR maps with/without parallel acquisition. (a) tSNR map with parallel acquisition. (b) tSNR map without parallel acquisition. (c) Difference of temporal SNR. In (c), the difference map was derived by subtraction of both maps ($tSNR_{R=3} - tSNR_{R=1}$).

4. Discussion

In this study, we demonstrated that cmsEPI combined with GRAPPA reconstruction provided increased tSNR compared to cmsEPI without acceleration. The image quality of the accelerated image such as signal deformation and geometrical distortion was preserved similarly to or better than the nonaccelerated image. The functional experiment to prove the functional effectiveness showed the increased functional sensitivity, in which the activated area was much broader and t-values were higher than in the nonaccelerated cmsEPI.

According to the previous study [20], better tSNR resulted from improved static SNR within some boundaries. Similarly, the static SNR mainly improved by the modified VFA in the parallel imaging acquisition could lead to increased tSNR. With employing acceleration acquisition, VFA were increased, leading to gain of a magnitude of transverse magnetization for each segment. When a longitudinal magnetization of M_0 was given, the transverse magnetization of $M_0/\sqrt{n/R}$ will be applied to each segment of cmsEPI by the modified VFA. For instance, 6 segments with $R = 1$ or $R = 3$, would lead to the applied transverse magnetization of $0.4 \cdot M_0$ ($\approx M_0/\sqrt{6}$) or $0.7 \cdot M_0$ ($\approx M_0/\sqrt{6/3}$), respectively. Hence, the modified VFA by parallel imaging acquisition could produce higher strength of signal.

It should be noted that the improved tSNR seems to mitigate the disadvantage of parallel imaging reconstruction such as noise enhancement. Typically, parallel imaging such as GRAPPA resulted in a loss in tSNR by a factor of $g\sqrt{R}$, where g denoted nonuniform loss in tSNR based on coil geometry. With considering the transverse magnetization

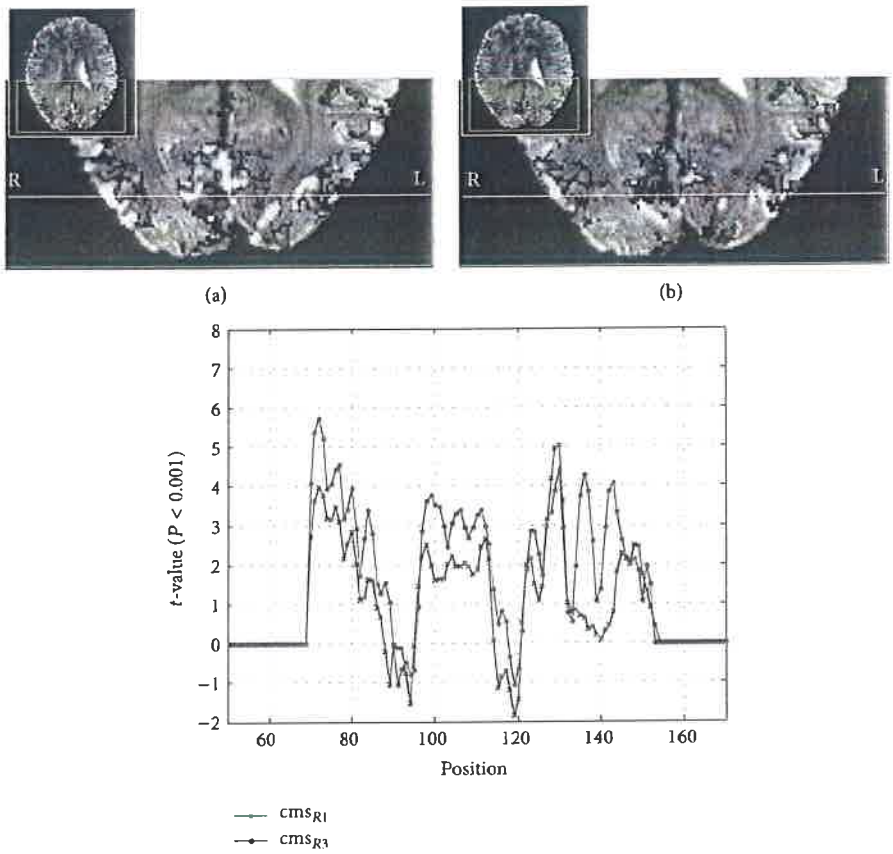


FIGURE 4: fMRI activation maps with/without parallel acquisition. (a) fMRI activation map with parallel acquisition. (b) fMRI activation map without parallel acquisition. (c) Comparison of t-values with/without parallel acquisition, in which t-values came from the white lines of (a) and (b). The improved tSNR led to entirely increased t-value (statistical power) to functional responses.

and the effect of parallel imaging, the tSNRs can be estimated as follows:

$$\begin{aligned} \mathrm{tSNR}^{\mathrm{non}} &\propto \left(\frac{M_0}{\sqrt{n}}\right)^2 = \frac{M_0^2}{n}, \\ \mathrm{tSNR}^{\mathrm{acc}} &\propto \left(\frac{M_0}{\sqrt{n/R}}\right)^2 \cdot \frac{1}{g\sqrt{R}} = \frac{\sqrt{R}}{g} \cdot \frac{M_0^2}{n}. \end{aligned} \tag{3}$$

In (3), the superscripts of "non" and "acc" denoted a nonaccelerated and an accelerated cmsEPI, respectively. According to the equations, the tSNR of the accelerated cmsEPI entirely increased by a square root of a reduction factor but still could be decreased locally and nonuniformly by g-factor. Here, the variable of $\sqrt{R}$ at the equation led to improvement of the tSNR, when implemented with modified VFA described in (1). It was a contrast from the original VFA consistently decreasing the tSNR as shown in the supplementary figure, in Supplementary Material available online at http://dx.doi.org/10.1155/2015/394213, where the original VFA was in a condition without taking account of the acceleration factor of R in (1). Therefore, the modified VFA could essentially increase the tSNR in accelerated acquisitions.

In functional study, acceleration factor $R = 3$ was selected instead of $R = 2$, although $R = 2$ provided higher tSNR than $R = 3$. Since tSNR of $R = 3$ was similar to $R = 1$ in phantom test, the physiological effect of $R = 3$ could be investigated and compared with $R = 1$ in vivo test. And the acceleration factor of $R = 3$ or 4 has been used in most of functional experiments as well as $R = 2$ in ssEPI. In comparison of $R = 1$ and $R = 3$, tSNR difference between phantom and in vivo tests was observed due to the possible existence of physiological noise. It showed that images in $R = 3$ were less affected by physiological noise due to the shorter acquisition time so that tSNR in $R = 3$ might be better than expected in in vivo test.

It was not performed to directly compare the tSNR of the proposed method with the tSNR of ssEPI. The tSNR in ssEPI has been known to decrease with the acceleration factor, which is typically proportional to $M_0^2/g\sqrt{R}$. However, the accelerated acquisition in ssEPI could additionally provide the shorter TE due to the reduced echo train length.

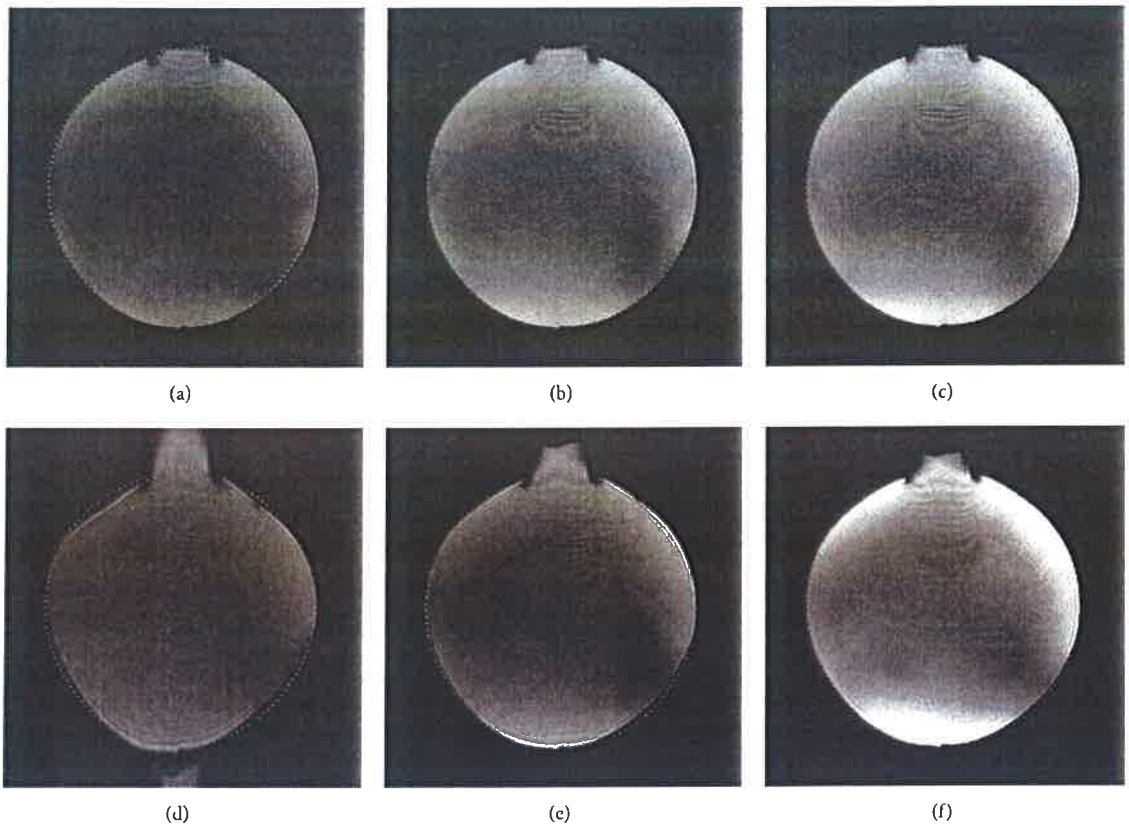


FIGURE 5: Comparison with single-shot EPI. Images were acquired by cmsEPI with 6 segments and (a, b, and c) $R = 1, 2$, and 3 and single-shot EPI with (d, e, and f) $R = 1, 2$, and 3, respectively. The yellow dotted line was drawn from the outline of (a).

The reduced TE would have more influence on tSNR than the acceleration factor and the g-factor. In practical cases, possibly minimal TEs of ssEPI having the in-plain resolution of 1.0 mm^2 were 68 ms and 29 ms in $R = 1$ and $R = 3$, respectively. Considering a voxel with T_2^* of 60 ms, the signal intensity in TE of 29 ms would apparently be about 1.9 times higher than in TE of 68 ms. Thus, since the tSNR was determined by imaging parameters, the direct comparison of the tSNR would not be necessary. As the same TE was given, the proposed method would provide lower tSNR than ssEPI.

Artifacts on the image could occur by intersegment modulations arising from VFA, which would occur in both magnitude and phase. The magnitude modulation would be caused by a nonideal shape in a slice-selective RF profile and different sensitivities of a RF coil to various flip angles, but it could be almost compensated by the comparison of navigators of segments. The intersegment phase modulation would be also caused by B1 field differences of various flip angles, that is, signal phase difference between practical excitation RF pulses with 45° and 90°. In contrast to the magnitude modulation described above, the level of the artifact by the phase modulation could be changed in the region where B1 significantly deviates from the nominal one. Further study will be needed for handling these artifacts.

The proposed method has the similar image contrast with conventional ssEPI, because cmsEPI with parallel imaging can preserve the image contrast given by the same TR and TE as ssEPI. The image contrast of a typical msEPI, however, includes the different T1 recovery effect as well as the T_2^* relaxation effect due to a time interval between excitation RF pulses, compared with ssEPI.

In addition, the proposed method with the shorter echo time and the echo train length could function as an alternative and controllable geometrical distortion correction technique, leading to reduction in the geometrical distortion inherently and preventing of the signal loss by field inhomogeneity. Though the postprocessing distortion correction techniques such as PSF-mapping can produce a distortion-corrected image similar to the distortion-free gradient-recalled echo image (GRE) [21], the information loss by a fast T_2^* decay is hard to be recovered completely. Therefore, the proposed method is possible to be easily implemented with other postprocessing correction techniques.

The proposed method also has the potential capability of further improving the imaging coverage. The future extension of the proposed method for imaging coverage can be achieved by multiband (MB) or simultaneous multislice (SMS) techniques based on 2D imaging [22]. However, direct

3D approach using multiple excitations should be carefully applied to the proposed method, because minimum intersegment can be conflicted by multiple excitations with constant interval or too many segments can cause the decrease in static SNR of an image.

5. Conclusions

This study proposed an advanced technique of cmsEPI for functional study. We demonstrated that the combination of cmsEPI with parallel imaging acquisition could provide a synergic effect to improve functional sensitivity.

Conflict of Interests

The authors declare that there is no conflict of interests regarding the publication of this paper.

Acknowledgments

The authors acknowledge JSPS KAKENHI Grant nos. 26350995 and 25330173 and MEXT-Supported Program for the Strategic Research Foundation at Private Universities, 2014–2018.

References

[1] S. Ogawa, T. M. Lee, A. R. Kay, and D. W. Tank, "Brain magnetic resonance imaging with contrast dependent on blood oxygenation," *Proceedings of the National Academy of Sciences of the United States of America*, vol. 87, no. 24, pp. 9868–9872, 1990.

[2] N. K. Logothetis, J. Pauls, M. Augath, T. Trinath, and A. Oeltermann, "Neurophysiological investigation of the basis of the fMRI signal," *Nature*, vol. 412, no. 6843, pp. 150–157, 2001.

[3] F. G. C. Hoogenraad, P. J. W. Pouwels, M. B. M. Hofman et al., "High-resolution segmented EPI in a motor task fMRI study," *Magnetic Resonance Imaging*, vol. 18, no. 4, pp. 405–409, 2000.

[4] R. S. Menon, C. G. Thomas, and J. S. Gati, "Investigation of BOLD contrast in fMRI using multi-shot EPI," *NMR in Biomedicine*, vol. 10, no. 4-5, pp. 179–182, 1997.

[5] S.-G. Kim, X. Hu, G. Adriany, and K. Uğurbil, "Fast interleaved echo-planar imaging with navigator: high resolution anatomic and functional images at 4 tesla," *Magnetic Resonance in Medicine*, vol. 35, no. 6, pp. 895–902, 1996.

[6] F. Farzaneh, S. J. Riederer, and N. J. Pelc, "Analysis of T_2 limitations and off-resonance effects on spatial resolution and artifacts in echo-planar imaging," *Magnetic Resonance in Medicine*, vol. 14, no. 1, pp. 123–139, 1990.

[7] A. Jesmanowicz, P. A. Bandettini, and J. S. Hyde, "Single-shot half k-space high-resolution gradient-recalled EPI for fMRI at 3 Tesla," *Magnetic Resonance in Medicine*, vol. 40, no. 5, pp. 754–762, 1998.

[8] D. N. Guilfoyle and J. Hrabe, "Interleaved snapshot echo planar imaging of mouse brain at 7.0 T," *NMR in Biomedicine*, vol. 19, no. 1, pp. 108–115, 2006.

[9] K. P. Pruessmann, M. Weiger, M. B. Scheidegger, and P. Boesiger, "SENSE: sensitivity encoding for fast MRI," *Magnetic Resonance in Medicine*, vol. 42, pp. 952–962, 1999.

[10] D. K. Sodickson and W. J. Manning, "Simultaneous acquisition of spatial harmonics (SMASH): fast imaging with radiofrequency coil arrays," *Magnetic Resonance in Medicine*, vol. 38, no. 4, pp. 591–603, 1997.

[11] M. A. Griswold, P. M. Jakob, R. M. Heidemann et al., "Generalized autocalibrating partially parallel acquisitions (GRAPPA)," *Magnetic Resonance in Medicine*, vol. 47, no. 6, pp. 1202–1210, 2002.

[12] D. K. Sodickson, M. A. Griswold, P. M. Jakob, R. R. Edelman, and W. J. Manning, "Signal-to-noise ratio and signal-to-noise efficiency in SMASH imaging," *Magnetic Resonance in Medicine*, vol. 41, pp. 1009–1022, 1999.

[13] F. A. Breuer, S. A. R. Kannengiesser, M. Blaimer, N. Seiberlich, P. M. Jakob, and M. A. Griswold, "General formulation for quantitative G-factor calculation in GRAPPA reconstructions," *Magnetic Resonance in Medicine*, vol. 62, no. 3, pp. 739–746, 2009.

[14] K. P. Pruessmann, "Parallel imaging at high field strength: synergies and joint potential," *Topics in Magnetic Resonance Imaging*, vol. 15, no. 4, pp. 237–244, 2004.

[15] Z. Wang, J. Wang, and J. A. Detre, "Improved data reconstruction method for GRAPPA," *Magnetic Resonance in Medicine*, vol. 54, no. 3, pp. 738–742, 2005.

[16] F. Hennel, "Multiple-shot echo-planar imaging," *Concepts in Magnetic Resonance*, vol. 9, no. 1, pp. 43–57, 1997.

[17] D. A. Feinberg and K. Oshio, "Phase errors in multi-shot echo planar imaging," *Magnetic Resonance in Medicine*, vol. 32, no. 4, pp. 535–539, 1994.

[18] O. Dietrich, J. G. Raya, S. B. Reeder, M. F. Reiser, and S. O. Schoenberg, "Measurement of signal-to-noise ratios in MR images: influence of multichannel coils, parallel imaging, and reconstruction filters," *Journal of Magnetic Resonance Imaging*, vol. 26, no. 2, pp. 375–385, 2007.

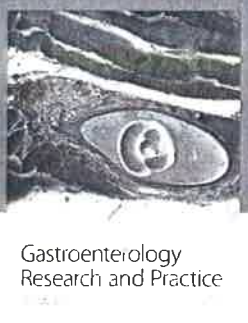
[19] C. Triantafyllou, R. D. Hoge, G. Krueger et al., "Comparison of physiological noise at 1.5 T, 3 T and 7 T and optimization of fMRI acquisition parameters," *NeuroImage*, vol. 26, no. 1, pp. 243–250, 2005.

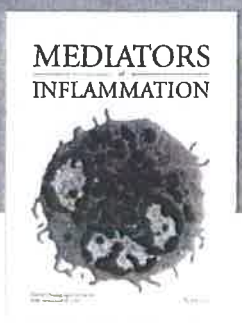
[20] C. Triantafyllou, R. D. Hoge, G. Krueger et al., "Comparison of physiological noise at 1.5 T, 3 T and 7 T and optimization of fMRI acquisition parameters," *NeuroImage*, vol. 26, no. 1, pp. 243–250, 2005.

[21] M.-H. In and O. Speck, "Highly accelerated PSF-mapping for EPI distortion correction with improved fidelity," *Magnetic Resonance Materials in Physics, Biology and Medicine*, vol. 25, no. 3, pp. 183–192, 2012.

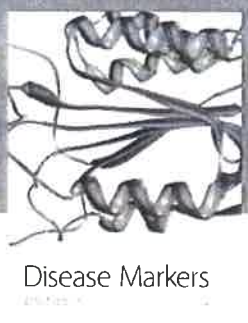
[22] S. Moeller, E. Yacoub, C. A. Olman et al., "Multiband multislice GE-EPI at 7 tesla, with 16-fold acceleration using partial parallel imaging with application to high spatial and temporal whole-brain FMRI," *Magnetic Resonance in Medicine*, vol. 63, no. 5, pp. 1144–1153, 2010.

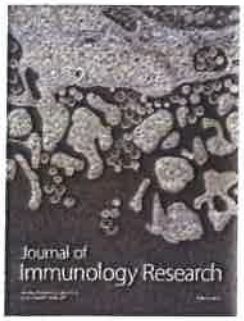

The Scientific World Journal

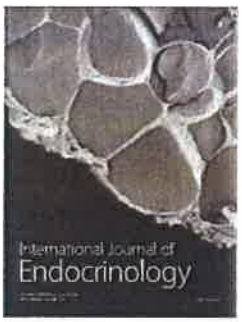

Gastroenterology Research and Practice




Journal of Diabetes Research


Disease Markers





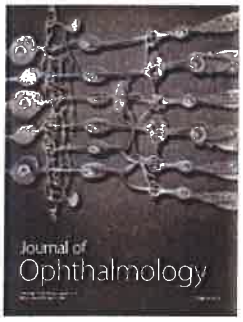


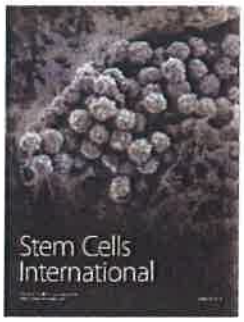
Hindawi

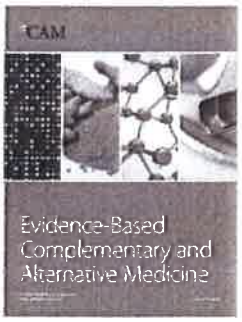
Submit your manuscripts at
http://www.hindawi.com

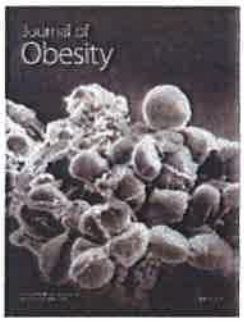


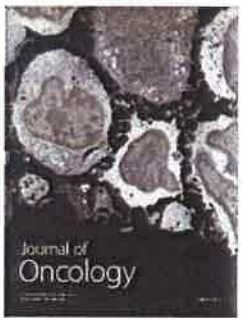


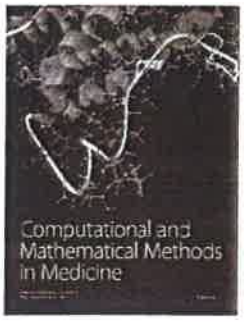


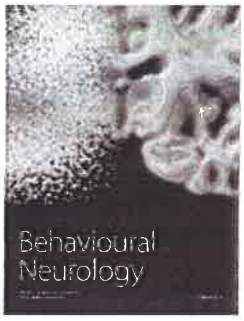


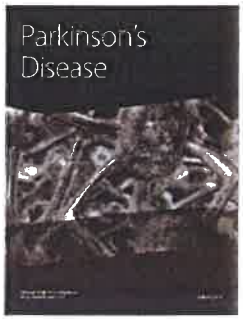


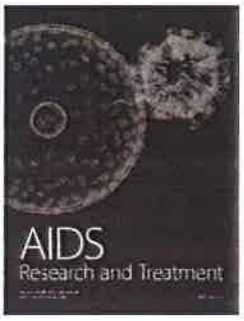


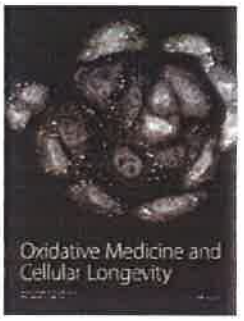












原 著 論 文

Evaluation of differences in brain plasticity with individual characteristics by MRI

Yul-Wan SUNG, Yousuke, KAWACHI, Deahun KANG, Seiji OGAWA
Kansei Fukushi Research Institute, Tohoku Fukushi University

Abstract

To let our research capability in brain function studies contribute to society, we plan to develop an evaluation system for brain plasticity. Prior to the project, we have collected some of our own evidence for brain plasticity through our previous brain anatomical data. We revisited our previous MRI data by voxel-based morphometry (VBM) analysis. We found gray-matter volume changes in the brain corresponding to individual characteristics such as satisfaction levels of majors and different hobbies as well as to the duration of their college enrolment. This demonstrates the possibility to evaluate plasticity changes in the brain through MRI measurements in cross-sectional and longitudinal ways.

Keywords : Voxel-based morphometry (VBM), plasticity, MRI

Introduction

Measurement and evaluation of the effects of academic, social and vocational skill training programs in educational institutions, such as universities, are very effective in ensuring the quality of teaching and training. Feedback of the evaluation of the effects on students or trainees would be also effective for improving the motivation of learning and training of students. The changes in mind and behavior through learning and training are reflected as plasticity changes in the brain; therefore, it is expected that the effects of those educational programs can be evaluated through brain function measurements.

Plasticity change has been one of the main themes in system neuroscience; however, long-term plasticity under the influence of individual or social environmental factors, such as education, vocation, social relationships, and personality, has not yet been investigated much. Therefore, we have launched a project aiming to develop new objective criteria for an evaluation system of the effects of teaching and training programs through the measurement of cognitive and brain functions. To realize this challenge, we will perform a longitudinal study tracking students over several years during their enrolment in college and a cross-sectional study comparing the young and elderly. For this purpose a cognitive task or questionnaire and functional and anatomical brain imaging by MRI will be used.

Since the development of the Blood Oxygenation Level-Dependent (BOLD) method[1)] in the early 1990s, functional MRI (fMRI) on the human brain has been actively conducted and has elucidated functional roles of brain areas in higher cognitive function as well as in primary sensory functions. In addition, resting-state fMRI[2)], which emerged in the middle 2000s, has been used for functional network studies of the brain. At present, the fMRI method (including resting-state fMRI) has been applied even in clinical use. In parallel with the advances in fMRI, brain imaging methods by anatomical MRI, such

as voxel-based morphometry (VBM)[3,4], cortical thickness measurement[5], and fractional anisotropy (FA)[6], have been used to examine plasticity changes of the brain at the system level. VBM is easy to apply than the other MRI modalities and it has generated data proving its usefulness for brain plasticity measurement[7-10]; therefore, in this study we performed VBM to obtain some of our own evidence for brain plasticity as a preliminary study for our project.

We already had a lot of anatomical data from our previous fMRI experiments; therefore, we planned to reanalyze them through VBM to evaluate brain plasticity. By revisiting participants' questionnaires, we gathered some information related to individuals' characteristics such as majors, hobbies, and satisfaction levels with their majors. Anatomical brain data were classified and analyzed in correlation with this information.

Material and methods

(Subjects)

One hundred and fifty undergraduate students and two graduate students participated. No participant had a history of neurological disease or a medical condition that would prevent MRI screenings, such as pregnancy, presence of a cardiac pacemaker, or claustrophobia. Subjects provided written informed consent after they were given a complete description of the study. This study was approved by the Institutional Review Board of Tohoku Fukushi University.

(Measurements)

MRI experiments were performed using a Verio system (Siemens, Germany) with a standard, 12-channel head matrix coil operating at 3 Tesla. After the initial localization of images, T1-weighted anatomical images were obtained with an inversion recovery and magnetization-prepared rapid acquisition using a gradient echo with a matrix size of 256 × 256 mm over a 256-mm field of view, 192 sagittal partitions, and a 1-mm slice thickness.

(MRI Data)

MRI data were analyzed using VBM implemented in the Statistical Parametric Mapping software (SPM 12B, Wellcome Department of Imaging Neuroscience, London, United Kingdom). The preprocessing and statistical tests (two-sample *t*-test and multiple regression) were performed according to a tutorial described in detail at the website http://www.nemotos.net and included segmentation, image registration (Dartel), normalization (modulation), and smoothing (Gaussian FWHM $8 \times 8 \times 8\,mm^3$).

Psychological data such as their majors, degree of satisfaction with their majors, and hobbies were voluntarily provided by the participants. The degree of satisfaction had five levels (5 to 1) from very satisfactory to very unsatisfactory.

Based on these psychological data, subject groups were classified. For majors, major A and B groups were classified with 16 and 20 participants each. For hobbies, four groups were classified: the no-hobby group of 11 participants, the reading group (READ) of 19 participants, the sports group (SPORT) of 46 participants, and the mixture group (MIX) of 19 participants who reported hobbies other than music,

reading, or sports. Three participants had participated more than six times over 22 to 34 months, and their data were longitudinally analyzed.

Results

Image data were analyzed in relation to the degree of satisfaction of students with their majors, hobbies, and students' majors from a cross-sectional point of view and in relation to the number of college years from a longitudinal point of view.

The regression of gray-matter volume with the level of satisfaction did not highlight any particular brain area. The questionnaire showed only two participants each for level 5 and level 1. Therefore, we performed a two-sample *t*-test by regrouping the participants into a high and a low level with 18 participants each. The contrast between the high- and the low-level groups identified brain areas of the bilateral hippocampi and the left temporal pole (Fig. 1 a, b), which showed larger gray-matter volume for the high level [high > low, two-sample *t*-test, p = 0.001 (uncorrected), cluster threshold 400]. As an example, gray-matter volume at the left hippocampus is shown in Figure 2.

For the hobby, the group of participants who reported no hobby was used as the control group (CON). Target groups were the music or video appreciation group (APP), the reading group (READ), the sports group (SPORT), and the mixture group (MIX). A comparison of the appreciation group with the control group showed larger gray-matter volume in the right inferior frontal gyrus [APP > CON, two-sample *t*-test, p = 0.001 (uncorrected), cluster threshold 100] (Fig. 3). A comparison of the reading group with the control group showed larger gray-matter volume in the left middle frontal gyrus and the left precentral gyrus [READ > CON, two-sample *t*-test, p = 0.001 (uncorrected), cluster threshold 200] (Fig. 4). A comparison of the sports group to the control group showed larger gray-matter volume in the right supramarginal gyrus and left medial superior frontal gyrus [SPORT > CON, two-sample *t*-test, p = 0.001 (uncorrected), cluster threshold 400] (Fig. 5). Although the occipital gyrus, including the calcarine sulcus and the right postcentral gyrus, showed a larger gray-matter volume in all three target groups of APP, READ, and SPORT than in the control group, the gray-matter volume of these areas was also larger even in the mixture group than in the control group [MIX > CON, two-sample *t*-test, p = 0.001 (uncorrected), cluster threshold 100]. Therefore, this predominant gray-matter volume

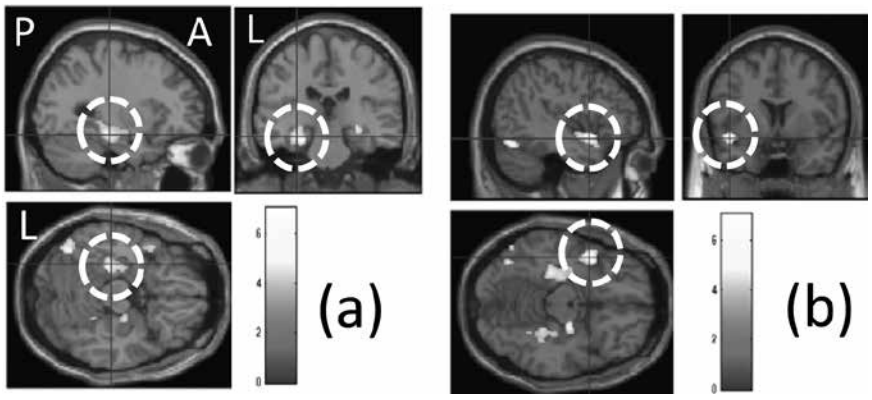


Figure 1
Maps of the left hippocampus (-29, -25, -17) and temporal pole (-44, 7, -13) for the satisfaction level [high > low, two-sample *t*-test, p = 0.001 (uncorrected), cluster threshold 400]. Locations are based on MNI coordinates.

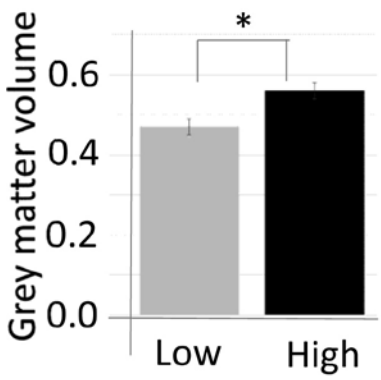


Figure 2
Difference in gray-matter volume for high and low satisfaction levels. * $p < 0.0001$. SEM, given by error bars

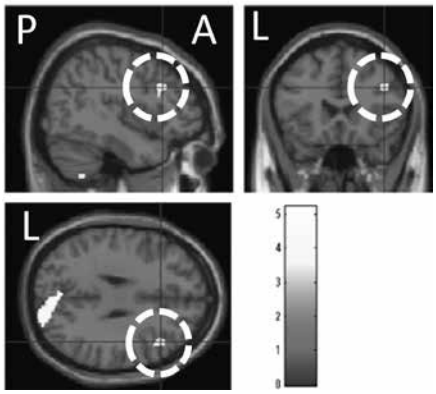


Figure 3
Maps of the right inferior frontal gyrus (43, 22, 29) for the hobby appreciation [APP > CON, two-sample *t*-test, $p = 0.001$ (uncorrected), cluster threshold 100]. Locations are based on MNI coordinates.

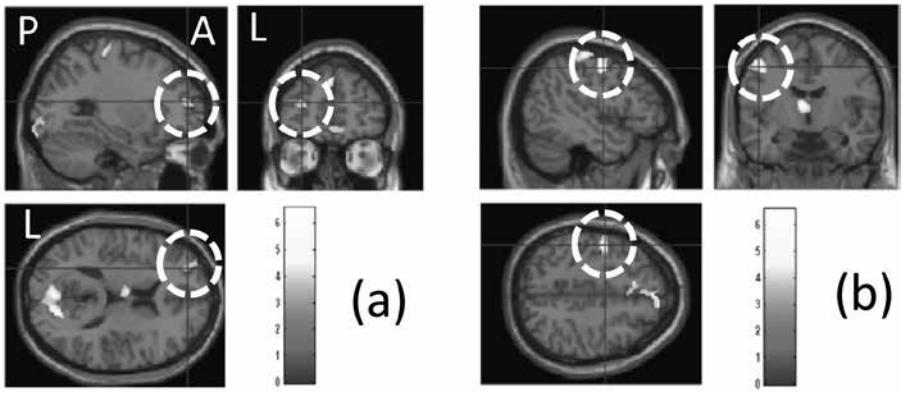


Figure 4
Maps of the left middle frontal gyrus (-28, 50, 14) (a) and the left precentral gyrus (-47, -6, 47) (b) for the hobby reading [READ > CON, two-sample *t*-test, $p = 0.001$ (uncorrected), cluster threshold 200]. Locations are based on MNI coordinates.

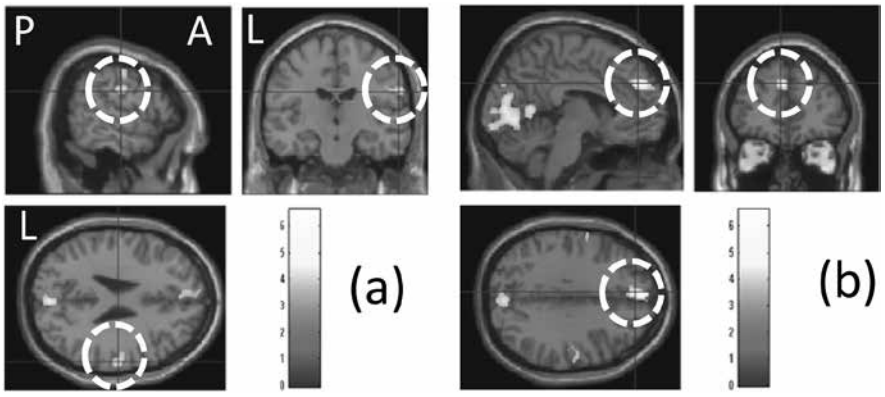


Figure 5
Maps of the right supramarginal gyrus (61, -16, 27) (a) and the left medial superior frontal gyrus (-5, 44, 33) (b) for the hobby sports [SPORT > CON, two-sample *t*-test, $p = 0.001$ (uncorrected), cluster threshold 400]. Locations are based on MNI coordinates.

of the right postcentral gyrus and the occipital gyrus was thought to result from some intrinsic anatomical differences between the control group and the other groups than to be related to a hobby.

With respect to the different majors, the major A group showed a larger gray-matter volume than the major B group in the right posterior orbital gyrus [A > B, two-sample *t*-test, p = 0.001 (uncorrected), cluster threshold 50] (Fig. 6 a). On the other hand, the major B group showed a larger gray-matter volume than the A group in the left precentral gyrus [A < B, two-sample *t*-test, p = 0.001 (uncorrected), cluster threshold 50] (Fig. 6 b).

For the longitudinal analysis of three participants, among the three participants, two (participant X and participant Y) showed gray-matter volume changes that correlated with an increase in length of stay at the college (number of months). Participant X whose data were sampled over 34 months showed a decrease in the right middle temporal gyrus [multiple regression, p = 0.001 (uncorrected), cluster threshold 0] (Fig. 7). Participant Y whose data were sampled over 24 months showed a

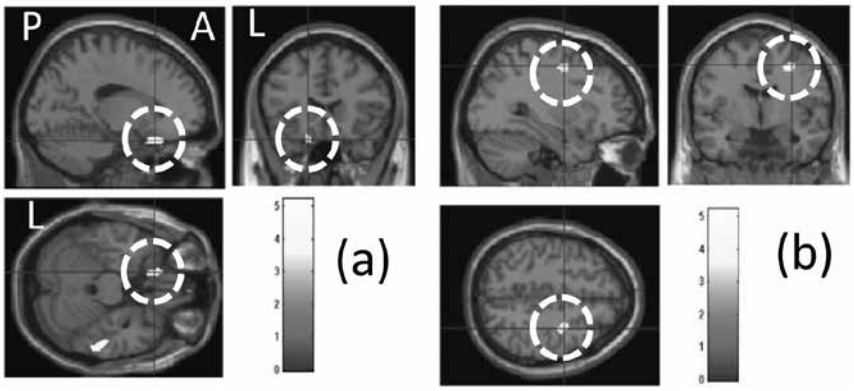


Figure 6
Maps of the right posterior orbital gyrus (61, -16, 27) (a) and the left precentral gyrus (-5, 44, 33) (b) shown the difference between majors A and B, A > B and A < B respectively [two-sample *t*-test, p = 0.001 (uncorrected), cluster threshold 50]. Locations are based on MNI coordinates.

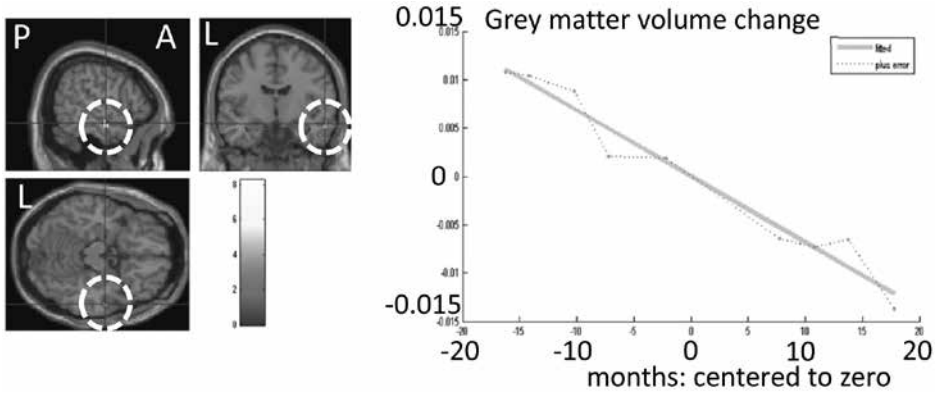


Figure 7
Maps of the right middle temporal gyrus (55, -9, -16) showing a negative correlation of volume with time at college (in months) and a plot of volume changes [multiple regression, p = 0.001 (uncorrected), cluster threshold 0]. The red dots indicate volumes at the measurement months. The gray solid line is the best-fitting line. Locations are based on MNI coordinates.

decrease in the left hippocampus and the lingual gyrus, but showed an increase in the left superior parietal lobule [multiple regression, $p = 0.001$ (uncorrected), cluster threshold 0] (Fig. 8).

Discussion

Questionnaire and MRI data enables cross-sectional and longitudinal analyses. The questionnaire enabled a classification of participants into the categories of major, hobby, and level of satisfaction with the major. MRI data for these groups were analyzed and evaluated by VBM. The brain imaging data and questionnaire demonstrated plasticity changes in the brain. Longitudinal MRI data also demonstrated plasticity changes in some brain areas in which the gray-matter volume increased or decreased. Therefore, in this study our own data also show that VBM can be used to measure plasticity.

Although VBM proved to be a useful tool for plasticity measurement, there are two points we should consider. One is what aspects of characteristics of participants are reflected by the plasticity change in those brain areas. The other is which neuronal sources induce the plasticity observed in VBM. For the former, psychological information may provide some clues. For example, the hippocampus of participants with a high satisfaction level had a larger gray-matter volume than that of those with a low satisfaction level. However, the hippocampus is known for memory processing, and memory processing does not directly explain the relation with the satisfaction level. On the contrary, the famous VBM study that examined a London taxi driver and bus driver could clearly derive a relationship between VBM data and hippocampus function; this study showed that taxi drivers developed a greater capacity for navigating a large complex city[4]. This study and the present work differ by the larger amount of psychological data and the higher number of controlled participants in the former study. This indicates that for our project to be successful, considerable psychological data and a thorough experimental design are necessary.

Several candidates, such as neurogenesis[11, 12], gliogenesis[13, 14] and angiogenesis[15, 16] exist as neuronal sources for plasticity. Some of these changes may be detected more easily by other MRI imaging modalities; therefore, using other existing or developing new imaging technologies would be helpful. In addition, the brain areas that show plasticity changes differ depending on the classification obtained from the questionnaire and those areas usually have multiple functions. Therefore, on the basis of these preliminary data, we also need to clarify the roles of brain function in relation to the plasticity for which resting-state fMRI and task fMRI would be needed.

Conclusions

We found gray-matter volume changes in the brain corresponding to individual characteristics such as satisfaction levels to majors, different hobbies, and the duration of their college enrolment. Although the present study is a preliminary one, our results show the possibility of evaluating plasticity changes through MRI measurements both cross-sectionally and longitudinally.

Acknowledgements

This study was supported by MEXT-Supported program for the Strategic Research Foundation at Private Universities, 2014-2018.

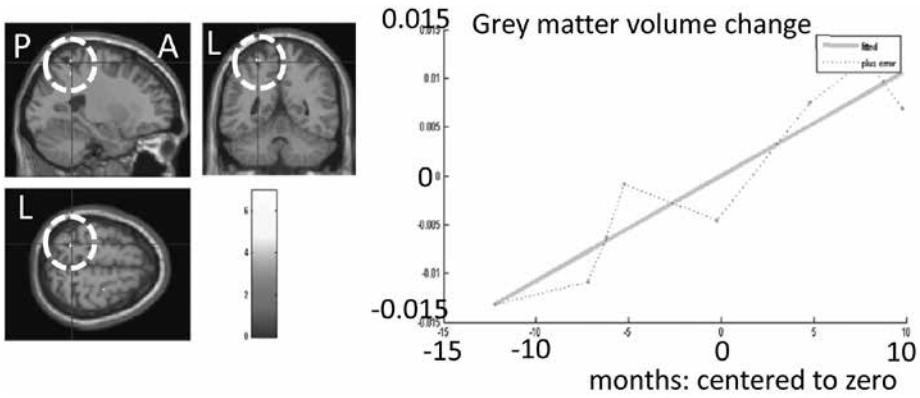


Figure 8
Maps of the left superior parietal lobule (-24, -48, 61) showing a positive correlation of volume with time at college (in months) and a plot of volume changes [multiple regression, p = 0.001 (uncorrected), cluster threshold 0]. The red dots indicate volumes at the measurement months. The gray solid line is the best-fitting line. Locations are based on MNI coordinates.

References

1. Ogawa S., Lee T.M., Kay A.R., Tank D.W. "Brain magnetic resonance imaging with contrast dependent on blood oxygenation" *Proc Natl Acad Sci U S A*. **87**: 9868-9872, 1990
2. Fox M.D., Snyder A.Z., Zacks J.M., Raichle M.E. "Coherent spontaneous activity accounts for trial-to-trial variability in human evoked brain responses" *Nat Neurosci* **9** : 23-25, 2006
3. Golestani N., Paus T., Zatorre R.J. "Anatomical correlates of learning novel speech sounds" *Neuron* **35**: 997-1010, 2002
4. Maguire E.A., Woollett K., Spiers, H. "London taxi drivers and bus drivers: a structural MRI and neuropsycholocical analysis" *Hippocampus* **16**: 1091-1101, 2006
5. Fischl B., Dale A.M. "Measuring the thickness of the human cerebral cortex from magnetic resonance images" *Proc Natl Acad Sci U S A*. **97**: 11050-11055, 2000
6. Basser, P.J., Pierpaoli, C. "Microstructural and physiological features of tissues elucidated by quantitative-diffusion-tensor MRI" *J of Magn Reson* **111**: 209-219, 1996
7. Draganski B., Gaser C., Busch V., Schuierer G., Bogdahn U., May A. "Neuroplasticity: changes in grey matter induced by training" *Nature* **427**: 311-312, 2004
8. Draganski B., Gaser C., Kempermann G., Kuhn H.G., Winkler J., Büchel C., May A. "Temporal and spatial dynamics of brain structure changes during extensive learning" *J Neurosci* **26**: 6314-6317, 2006
9. Bermudez P., Zatorre R.J. "Differences in gray matter between musicians and nonmusicians" *Ann N Y Acad Sci* **1060**: 395-399, 2005.
10. May A. " Experience-dependent structural plasticity in the adult human brain" *Trends Cogn Sci* **15**:475-482, 2011
11. Deng, W., Saxe, M.D., Gallina, I.S. Gage, F.H. "Adult-born hippocampal dentate granule cells undergoing maturation modulate learning and memory in the brain" *J Neurosci* **29**: 13532–13542, 2009
12. Aimone, J.B., Wiles, J. Gage, F.H. "Computational influence of adult neurogenesis on memory encoding" *Neuron* **61**: 187–202, 2009

13. Dong, W.K., Greenough, W.T. "Plasticity of nonneuronal brain tissue: roles in developmental disorders" *Ment Retard Dev Disabil Res Rev* **10**, 85–90, 2004
14. Tremblay, M.È., Lowery, R.L., Majewska, A.K. "Microglial interactions with synapses are modulated by visual experience" *PLoS Biol* **8** : e1000527, 2010.
15. Rhyu, I.J. et al. "Effects of aerobic exercise training on cognitive function and cortical vascularity in monkeys" *Neuroscience* **167**: 1239–1248, 2010.
16. Pereira, A.C. et al. "An in vivo correlate of exercise-induced neurogenesis in the adult dentate gyrus" *Proc Natl Acad Sci USA* **104**: 5638–5643, 2007

Journal of Behavioral and Brain Science, 2014, 4, 402-411
Published Online September 2014 in SciRes. http://www.scirp.org/journal/jbbs
http://dx.doi.org/10.4236/jbbs.2014.49039

Scientific Research

Invariance of Functional Characteristics to Task Difference at Low-Level and High-Level Areas in the Ventral Visual Pathway

Yul-Wan Sung[1,2], Uk-Su Choi[2], Seiji Ogawa[1,2]

[1]Kansei Fukushi Research Institute, Tohoku Fukushi University, Sendai, Japan
[2]Neuroscience Research Institute, Gachon University, Incheon, Korea
Email: sung@tfu-mail.tfu.ac.jp

Received 4 July 2014; revised 21 August 2014; accepted 3 September 2014

Copyright © 2014 by authors and Scientific Research Publishing Inc.
This work is licensed under the Creative Commons Attribution International License (CC BY).
http://creativecommons.org/licenses/by/4.0/
Open Access

Abstract

Tasks with stimuli are often used for the examination of stimulus-related functional characteristics of brain areas. However, the task can affect the response to a stimulus. Repetition suppression is a phenomenon that can be used to probe neuronal properties using macroscale functional magnetic resonance imaging (fMRI). The use of repetition suppression as an investigative tool to assess functional characteristics warrants the investigation of the invariance of repetition suppression to a given task. In this study, we examined repetition suppression using images of faces during different tasks. We found that the task difference did not change the response patterns related to repetition suppression in high-level areas and the primary visual area while it changed amplitudes of fMRI response to the visual stimuli. The result suggests that the repetition-suppression phenomenon is robust compared with the amplitude of fMRI response, and functional characteristics can be examined using the repetition-suppression phenomenon even under the condition that fMRI response is varied by task difference.

Keywords

Task Difference, Repetition Suppression, FFA, Central Stimulation, Peripheral Stimulation, fMRI, Face Images

1. Introduction

The repetition suppression observed in functional MRI (fMRI), which is also known as refractory suppression or fMRI adaptation, is a phenomenon in which the response to the second presentation of a visual stimulus de-

How to cite this paper: Sung, Y.-W., Choi, U.-S. and Ogawa, S. (2014) Invariance of Functional Characteristics to Task Difference at Low-Level and High-Level Areas in the Ventral Visual Pathway. *Journal of Behavioral and Brain Science*, **4**, 402-411. http://dx.doi.org/10.4236/jbbs.2014.49039

creases when the stimulus is presented repeatedly at short intervals. Refractory suppression is a suppression phenomenon that occurs between two input signals that arise successively within a short interval (<1000 ms). The response of a pair of identical stimuli is ideally twice that of one of the stimuli in the pair. The response to a pair of identical stimuli is about 20% larger than that to one of the stimuli in the pair with a short interval of 200 ms. However, the suppression recovers almost completely at 1000 ms, *i.e.*, the response to paired stimulation becomes twice as large as that of one of the two stimuli in the pair [1] [2]. fMRI adaptation is a reduction in the response to a stimulus that is presented repeatedly with a relatively long interval, even up to several tens of seconds, *i.e.*, the recovery in response takes longer in the case of fMRI adaptation than in the case of refractory suppression [3] [4]. Therefore, the latter can be used to assess the temporal characteristics of fast neuronal processing. However, in the case of two different stimuli in a pair, pair suppression can be weak, even with a very short interval (less than hundreds of milliseconds), when the common components of the two stimuli in the pair are small. Therefore, the phenomenon can also be used to assess the spatial characteristics of the distribution of different neuronal populations in a given brain area. This phenomenon has been used to examine neuronal properties via macroscale measurements using fMRI. In the context of refractory suppression, it is understood that the input signals to an area stem in a feed-forward manner from the lower area, and that signal suppression occurs via an interaction between the signals that arise successively.

Signal processing in the feed-forward manner has been found in the ventral visual pathway oriented for object processing which has a set of interconnected cortical regions from primary visual cortex (V1) to the temporal end. However, the processing in visual object areas in the ventral visual pathway is not solely dependent on feed-forward inputs. Many previous studies have reported that neuronal responses at V1 and high-order areas for object processing are enhanced in the presence of spatial attention [6]-[12] and that the response enhancement differs depending on visual field on which stimuli are presented [13]. Among those, Reddy *et al.* also reported that higher-order areas such as fusiform face area (FFA) show that an fMRI response to a task-relevant stimulus is enhanced compared with task-irrelevant stimuli [10]. They interpreted the task-relevant effect as top-down attention in that top-down attention is non-spatial and bottom-up is spatial. The response modulations by spatial and non-spatial (or bottom-up and top-down) attention give a possibility that an area in the ventral visual pathway get modulatory inputs from lateral areas or higher-order areas and the inputs affect refractory suppression for the area, that is, if an fMRI response to some stimulus is modulated by attention or an assigned task and the modulation of response reflects some changes of neuronal activity then the change of neuronal activity may lead to some modulation in refractory suppression. Although direct evidence of modulation about refractory suppression by attention does not exist, one of the characteristics of refractory suppression supports the possibility. It is that refractory suppression is strong in case that two stimuli in a stimulus pair elicit strong responses but week in case that both stimuli elicit weak responses or the second stimulus of two successive stimuli in the pair is weak [14].

In this study, we tested whether fMRI response modulation by task difference accompanies with refractory suppression in relation with visual field differences (visual eccentricity).

For the purpose, we used task-irrelevant and task-relevant conditions. Under the task-irrelevant condition, participants performed color discrimination of a cross-hair at the center of the visual field while target face images are given at the central or peripheral visual fields. Under the task-relevant condition, participants performed an associative task composed of the color discrimination of the cross-hair and a gender discrimination of faces (**Figure 1**).

2. Materials and Methods

2.1. Subjects

Twenty-six healthy volunteers participated in this study. Thirteen subjects participated in the low-load and high-load tasks, respectively. The participants were interviewed and their health was evaluated on the basis of physical examinations performed in the last 6 months of the experiment. All participants had normal or corrected-to-normal vision with 20/20 acuity, no history of neurological disease, and no medical conditions that would prevent MRI screenings, such as pregnancy, presence of a cardiac pacemaker, or claustrophobia. Subjects provided written informed consent after they were given a complete description of the study. This study was approved by the Institutional Review Board of Tohoku Fukushi University.

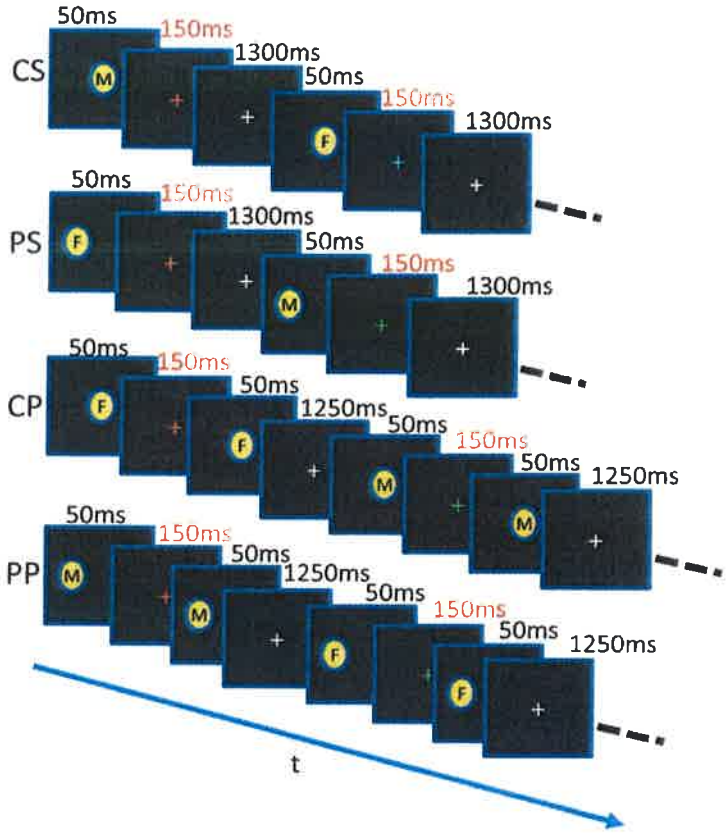


Figure 1. Stimulation conditions. There were 3 conditions for the central and peripheral stimulation. CS: Single central stimulation, CP: paired central stimulation, PS: single peripheral stimulation, PP: paired peripheral stimulation. F: female, M: male. Within the paired stimulation, faces were the same (SP) or different (DP). Each block included 8 stimuli with images female and male presented randomly. Color for the fixation task was changed randomly. The presentation time was 50 ms for each image and 150 ms for each colored crosshair. The same stimulation conditions were used for the low- and high-load tasks. Under the task-irrelevant condition participants were required to detect color change of the crosshair by pressing button 1 for green and 2 for red. Under the task-relevant condition participants were required to identify the gender of the face presented in an image, in addition to the color change of the crosshair. Responses required participants to press button 1 for the combinations of gender and color, such as male and green or female and red, and button 2 for the other combinations.

2.2. Stimulation Procedure

The visual stimuli were images presented in the center of the visual field (central stimulation) or unilaterally in the left visual field (peripheral stimulation; **Figure 1**). There were 24 event blocks, with each block lasting 12 s. The 24 event blocks each consisted of 12 blocks of central and peripheral stimulation, respectively. The 12 blocks of central or peripheral stimulation comprised four blocks of single stimulation (S), paired stimulation with the same face (SP), and paired stimulation with different faces (DP) of the same but and different identities. The S, SP, and DP blocks were randomized at the intrasubject and intersubject levels. Therefore, there were three stimulus conditions for central and peripheral stimulation: S, SP, and DP (**Figure 1**). The experimental run started with a 12 s prestimulus state (for the removal of transient effects), and each stimulus block was followed by a 12 s control block; the total scan time was 600 s. The S block consisted of eight images of different faces that were presented for 50 ms and a 1.5 s repetition period interspersed with the control state. Each paired block

(SP or DP) consisted of eight pairs of faces, with a 1.5 s interval between pairs. The interstimulus interval (ISI) of the SP and DP blocks was 150 ms. Images presented in the paired stimulation blocks were different between pairs, even in the SP block (**Figure 1**). During the scan, the colored crosshair was presented for 150 ms and the color was changed randomly to green or red with a 1.5 s interval. The onset of the colored crosshair occurred after the offset of the stimulus in the S block, and after that of the first stimulus in the SP and DP blocks. A gray crosshair was presented at the left period. The control block was the same as the stimulus block with the exception that there was no image presentation, *i.e.*, the colored crosshair was presented for 150 ms and the gray crosshair period became longer, to match the period of face stimulation. The tasks in the stimulation state had two levels: task-irrelevant (T-I) and task-relevant (T-R). In the task-irrelevant condition, subjects were required to press buttons 1 or 2 according to the color of the crosshair (green or red, respectively). In the task-relevant condition, subjects were required to detect simultaneously the color changes of the crosshair and the gender of the individuals portrayed in the images, *i.e.*, they had to press button 1 when the crosshair was green and the image showed a man, or when the crosshair was red and the image showed a woman, and press button 2 in any other case. The tasks in the control state were the same for both the T-I and T-R conditions and required detection of only a color change of the crosshair.

After this main experimental scan (refractory experiment), a localization scan (localization experiment) was performed to localize V1 and FFA in each subject. The localization scan included eight blocks. The duration of each block was 12 s. Out of these eight blocks, four blocks included images of faces, whereas four blocks included images of buildings that were interspersed with the 16-s control states and the 16 s poststimulus intervals. During the control state, a black crosshair was presented in the center of a gray background. Each event block consisted of eight different images. Each image in each block was presented for 1 s in the center of the visual field, and the same black crosshair was presented at an interimage interval of 0.5 s. The subjects performed a one-back task during the scan, in which they pressed button 1 when an image was repeated and pressed button 2 in all other scenarios.

2.3. Measurements

MRI experiments were performed using a Verio system (Siemens, Germany) with a standard, 12-channel head matrix coil operating at 3 Tesla. After the initial localization of images, T1-weighted anatomical images were obtained with an inverted recovery- and magnetization-prepared rapid acquisition using a gradient echo with a matrix size of 256 × 256 mm over a 256-mm field of view and a 1-mm slice thickness. For functional imaging, single-shot, gradient echo, planar imaging was performed using the following parameters: repetition time = 1000 ms, echo time = 25 ms, flip angle = 80°, field of view = 220 mm, matrix size = 64 × 64 mm, and slice thickness = 3.4 mm, with no gap. Eighteen slices parallel to the anterior–posterior commissure line were acquired for each volume. The slice acquisition order was interleaved.

2.4. Visual Stimulation

The visual stimuli were grayscale images presented using a projector and displayed on a mirror mounted on the head coil (spatial resolution, 1024 × 768 pixels; refresh rate, 60 Hz; Panasonic, Japan). The images occupied 3.5° × 4° for the SP experiment, and the black crosshair was 0.34° × 0.34°. The center of the images used for the peripheral stimulation was shifted 2° to the subject's left. The reason parafovea was used for peripheral stimulation was to allow the discrimination of faces and facilitate fixation. The images were novel stimuli that were developed by the investigators. The images used for localization occupied 5° × 7° at the center of the visual field.

3. Results

The primary visual area V1 were identified near the posterior tip of the calcarine sulcus on activation map by a conjunction analysis of face and building stimulation in the localization experiments (**Figure 2(a)**). FFA was identified as a cluster of >200 voxels with a p-value of <0.001 around the fusiform gyrus by contrasting fMRI responses for the face and building stimulation in the localization experiment (**Figure 2(b)** and **Figure 2(c)**).

For analysis at each ROI, data (beta values) regarding fMRI signal changes were extracted from each V1 and FFA. FMRI signal time-courses at FFA were plotted for each task-irrelevant condition and task-relevant condition to see response profiles on the temporal axis (**Figure 3**). To examine the task effects on the stimulus, a

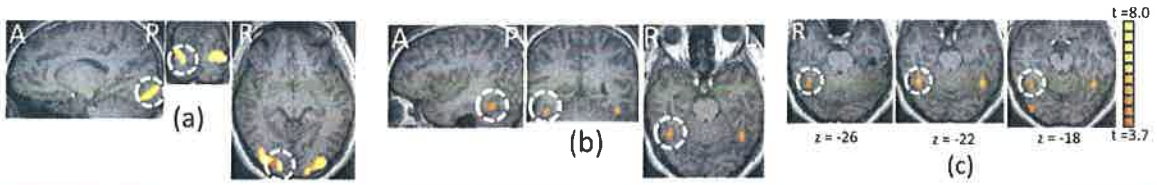


Figure 2. Activation maps by the localization experiment. (a) V1 (15, −95, −8) was identified by a conjunction analysis of the face and building conditions; (b) FFA (40, −49, −22) was identified by a contrast analysis of the face and building conditions; (c) FFA activation maps were seen at the z-direction to display the shape of activation site. The locations are based on Talairach coordinates. A, anterior; P, posterior; R, right; L, left. $p < 0.001$ (uncorrected).

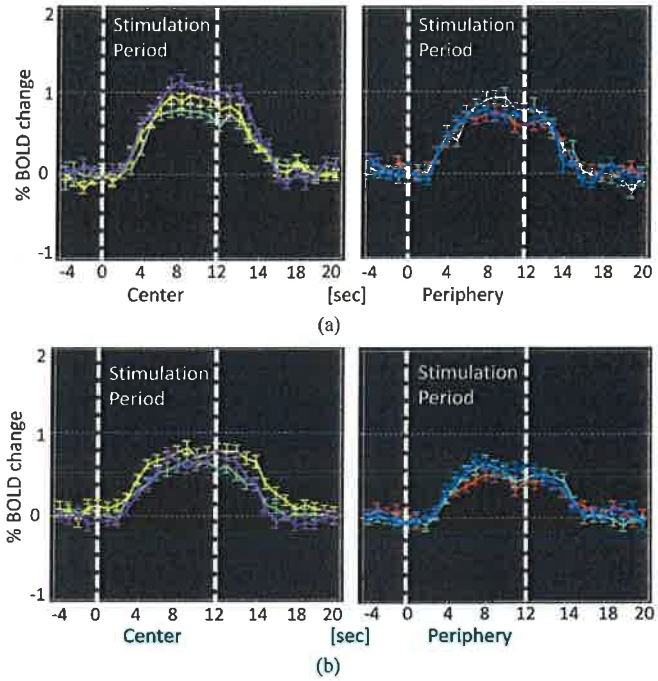


Figure 3. FMRI time-courses at FFA. (a) Task-irrelevant condition; (b) Task-relevant condition. The left panel of each figure is for "Central" stimulation and the right panel is for "Peripheral" stimulation. Green is for S, yellow is for SP and purple is for DP for "Central" stimulation, and red is for S, cyan is for SP and light purple is for DP for "Peripheral" stimulation.

four-way ANOVA was performed for the central stimulation using the factors of ROI (V1 and FFA), task (T-I and T-R), visual eccentricity (central and peripheral) and stimulus (S, SP, and DP) and the signal change as the dependent variable. This analysis revealed significant interactions between three factors of ROI, visual eccentricity and task [$F(3, 228) = 11.33$, $p = 0.022$], and significant main effect for the stimulus factor [$F(2, 188) = 5.315$, $p = 0.001$] (**Figure 4**). Therefore, two-way ANOVA was performed for each area (V1, FFA) with the factors of eccentricity and task.

The analysis at V1 revealed significant interaction between the eccentricity and task factors [$F(1, 152) = 7.67$, $p = 0.006$]. Further analysis regard to the task were not significant for the central stimulation [$F(76) = 2.48$, $p = 0.119$] but significant for the peripheral stimulation, that is, task-irrelevant (T-I) < task-relevant (T-R) [$F(76) = 5.36$, $p = 0.023$] (**Figure 5**). The analysis at FFA revealed no significant interaction between the visual eccentricity and task factors [$F(1, 152) = 1.66$, $p = 0.200$]. The main effect of the task factor was significantly different between T-I and T-R (T-I < T-R) [$F(1, 152) = 10.11$, $p = 0.002$] and the main effect of the visual eccentricity factor was significantly different between the central and peripheral stimulation (central stimulation > peripheral stimulation) [$F(1, 152) = 22.35$, $p = 0.001$] (**Figure 6**).

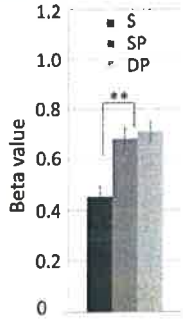


Figure 4. Averaged responses of three stimulus conditions of S, SP and DP. **: $p < 0.001$. The error bars represent S.E.M.

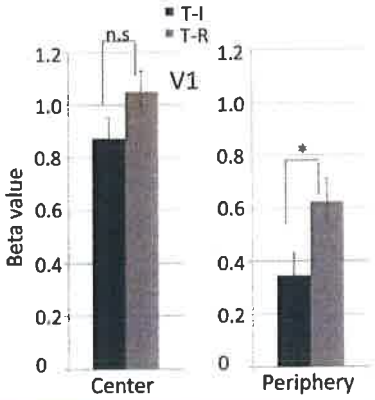


Figure 5. Responses of task-irrelevant and task-relevant conditions for central and peripheral stimulation (visual eccentricity factor) respectively. (a) Central stimulation; (b) Peripheral stimulation. *: $p < 0.03$. n.s.: not significant. The error bars represent S.E.M.

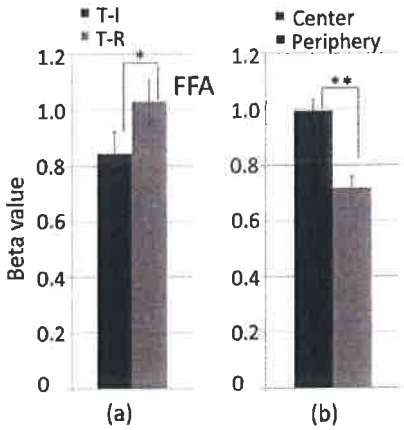


Figure 6. Responses for task-difference and visual eccentricity factors (a) task-irrelevant and task-relevant conditions (b) central and peripheral stimulation. *: $p < 0.002$, **: $p < 0.001$. The error bars represent S.E.M.

4. Discussion

The results that task difference was not reflected at V1 and FFA whether the stimuli were presented at the center

or the periphery of the visual field, while task difference modulates fMRI response to the peripheral stimulation at V1 and to both central and peripheral stimulation at FFA, indicate that refractory suppression is more robust phenomenon than fMRI signal. Under the conditions of the present experiment, the results reject the hypothesis that fMRI response modulation by task difference accompanies with refractory suppression.

The larger response to task-relevant stimulation presented at peripheral visual field of V1 can be explained in relation with the distance from the fixation point to the location of target stimulus images. Amplitude of fMRI signal to unattended target stimulus images is known to decrease as the distance of the location of the stimulus images from the fixation point increases when attention is given to the fixation point [11]. This response decrease in task-irrelevant condition and a response increase in task-relevant condition by spatial attention might make significant difference between task-irrelevant and task-relevant conditions.

Enhancement in fMRI response at FFA for the task-relevant condition is consistent with the previous studies [6] [10]. The response enhancement at FFA can also be explained in relation with the studies of spatial attention because there would be partial increase in attention to the target stimulus face images in the task-relevant condition [7]-[9] [15] [16]. The response difference at FFA between the central and peripheral stimulation is consistent with the preference of the central vision of FFA [17].

Object processing varies depending on not only stimulus-driven selection but also other factors such as visual eccentricity (or positon) and top-down selection [5] [18]-[20]. However, it is unclear yet to what extent those factors contribute to visual object processing. The present study may give some information about the effect of those factors on visual object processing; the effect by those factors to neuronal activity underlying the refractory suppression is not much as to affect an average activity in brain areas even if it exists.

In regard to signal processing modality, we used univariate analysis. Our results derived from evaluation of an average activity in a brain area rejected the hypothesis that refractory suppression would be modulated by task difference but it does not deny the possibility of acceptance of the hypothesis in case that multivariate analysis is applied [21]-[25]. However, most of the studies on repetition suppression is based on an average activity in brain areas and our objective in this study is also to examine whether the modulation occurs at the level of the average activity [1] [26]-[31]. Moreover, the experimental design in this study was not oriented to multivariate analysis, so that data processing by multivariate analysis is not appropriate. To examine refractory suppression by multivariate analysis will be our future study.

These, all together, suggest that the refractory suppression is robust to the task difference compared to the amplitude of fMRI signal.

Ideally it may be best to measure refractory suppression under a passive condition in which participants focus on the center of the visual field while stimulus images are given at some locations of the visual field because refractory suppression is known to reflect an interaction between feed-forward inputs. However, under the passive condition participants tends to lose their attention or fall asleep in the MRI scanner. Therefore, a task is needed to keep participants' arousal state or attention constant, and the task should be exclusively independent on target stimulus. However, the task, even if it is independent, the response to the target stimulus can be affected [8] [10] [11]. Therefore, the finding in this study that the refractory suppression is robust to the task difference would be useful information in applying the refractory suppression to studies of functional characteristics of brain areas.

In regard to the refractory suppression, one hypothesis is that the response to a paired stimulus is ideally twice the response to one stimulus (single) in the pair when ISI is sufficiently long, *i.e.*, around 1000 ms. According to this hypothesis, a response to a paired stimulus is regarded as suppressed if the response is less than twice of response to a single stimulus. Another hypothesis for refractory suppression is that the recovery from suppression (that is, for response to a pair to reach twice the response to a single stimulus) is faster for a paired stimulus when the paired stimulus consists of different types of stimuli. Previous studies on refractory suppression have not described explicitly the "twice" value in the evaluation of response suppression as the criterion for suppression. However, it remains uncertain whether the criterion can be affected by experimental conditions and the fully recovered response does not reach twice the value of the response to a single stimulus. In this context, a previous study showed that the refractory suppression at V1 by checker pattern stimulation had almost completely recovered after a 1000 ms interval [1]; moreover, in our supplementary experiment using face images, we observed that the refractory suppression at FFA had recovered by >80% (*i.e.*, a factor of 1.8 relative to the single stimulus), even with a short interval of 532 ms, whereas the recovery was about 40% for an interval of 132 ms when different faces were used in a pair. Therefore, it is reasonable to regard the double of the value of the single stimulus as the criterion for suppression. Those provide the validity to the implicit criterion for re-

fractory suppression. Thus, it is reasonable to think that the responses to SP and DP at V1 and FFA, in which responses to SP or DP are less than twice that to the corresponding S, are regarded as suppressed. In the present study, the suppression for SP was weak compared with those reported by other studies that were conducted using similar ISIs [32]. One of the reasons for this discrepancy may be the switching of the location of stimulation between the center and the periphery in the same stimulus run, although the interval between the stimulus blocks was long [33].

Next, we will describe the expected criticism regarding the intersubject design of and ROI identification in this study. One explanation for the use of the intersubject design to examine the effect of task condition was to avoid any possible interaction between task-irrelevant and task-relevant conditions when participants perform two tasks in the same experimental session, one of considered is that participants may perform the task under task-relevant condition implicitly while they are performing under task-irrelevant conditon explicitly. Another is that the scan time (600 s) and the performance of two tasks in one session can yield data with a worse quality. In fact, in our preliminary experiment in which two 600 s scans were performed, the data for the second scan contained much more physiological fluctuation and variation in response amplitudes than did the first scan.

For the localization of an ROI for FFA, the possibility that the ROI of FFA was shifted to an area preferring central stimulation should be considered, because face images were presented at the central visual field in the localization experiment. Even if there was a bias in FFA localization, which was shifted in the direction of the fovea due to the presentation of images at the center it does not defy the results because the effects of task condition and repetition suppression at FFA were evaluated separately for the central and periphery condition. Therefore, the definition of ROI based on the central presentation of images does not have an impact on our results.

5. Conclusion

The task difference did not affect the suppression phenomenon although fMRI response amplitudes are modulated by the task difference. This suggests that the refractory suppression is robust to the task difference than fMRI signal. This also suggests that task difference does not have to be considered, as long as univariate analysis is applied, when examining the suppression phenomenon, regardless of the presentation of the stimulation in the center or the periphery of the visual fields, and that the suppression phenomenon can be used as a tool for probing functional characteristics at both high-level and low-level areas.

Acknowledgements

This work was supported by JSPS KAKEN Grant Number 26350995 and 25330173, and MEXT-Supported program for the Strategic Research Foundation at Private Universtities, 2014-2018.

References

[1] Ogawa, S., Lee, T.-M., Stepnoski, R., Chen, W., Zhu, X.-H. and Ugurbil, K. (2000) An Approach to Probe Some Neural Systems Interaction by Functional MRI at Neural Time Scale down to Milliseconds. *Proceedings of the National Academy of Sciences*, **97**, 11026-11031. http://dx.doi.org/10.1073/pnas.97.20.11026

[2] Waldeck, R., Pereda, A. and Faber, D.S. (2000) Properties and Plasticity of Paired-Pulse Depression at a Central Synapse. *The Journal of Neuroscience*, **20**, 5321-5320.

[3] Henson, R.N. and Rugg, M.D. (2003) Neural Response Suppression, Haemodynamic Repetition Effects, and Behavioral Priming. *Neuropsychologia*, **41**, 263-270. http://dx.doi.org/10.1016/S0028-3932(02)00159-8

[4] Grill-Spector, K., Henson, R. and Martin, A. (2006) Repetition and the Brain: Neural Models of Stimulus-Specific Effects. *Trends in Cognitive Sciences*, **10**, 14-23. http://dx.doi.org/10.1016/j.tics.2005.11.006

[5] Kravitz, D.J., Vinson L.D. and Baker C.I. (2008) How Position Dependent Is Visual Object Recognition? *Trends in Cognitive Sciences*, **12**, 114-122. http://dx.doi.org/10.1016/j.tics.2007.12.006

[6] Harel, A., Kravitz D.J. and Baker C.I. (2014) Task Context Impacts Visual Object Processing Differentially across the Cortex. *Proceedings of the National Academy of Sciences*, in press.

[7] Kanwisher N. and Wojciulik E. (2000) Visual Attention: Insights from Brain Imaging. *Nature Reviews Neuroscience*, **1**, 91-100. http://dx.doi.org/10.1038/35039043

[8] O'Conner, D.H., Fukui, M.M., Pinsk, M.A. and Kastner, S. (2002) Attention Modulates Responses in the Human Lat-

eral Geniculate Nucleus. *Nature Neuroscience*, **5**, 1203-1209. http://dx.doi.org/10.1038/nn957

[9] O'Craven, K.M., Downing P.E. and Kanwisher N. (1999) fMRI Evidences for Objects as the Units of Attentional Selection. *Nature*, **401**, 584-587. http://dx.doi.org/10.1038/44134

[10] Reddy, L., Moradi, F. and Koch C. (2007) Top-Down Biases Win against Focal Attention in the Fusiform Face Area. *Neuroimage*, **28**, 730-739. http://dx.doi.org/10.1016/j.neuroimage.2007.08.006

[11] Sprague, T.C. and Serences, J.T. (2013) Attention Modulates Spatial Priority Maps in the Human Occipital, Parietal and Frontal Cortices. *Nature Neuroscience*, **16**, 1879-1887. http://dx.doi.org/10.1038/nn.3574

[12] Yantis, S. (2008) The Neural Basis of Selective Attention. *Current Directions in Psychological Science*, **17**, 86-90. http://dx.doi.org/10.1111/j.1467-8721.2008.00554.x

[13] Davidesco, I., Harel, M., Ramot, M., Kramer, U., Kipervasser, S., *et al.* (2013) Spatial and Object-Based Attention Modulates Broadband High-Frequency Responses across the Human Visual Cortical Hierarchy. *The Journal of Neuroscience*, **16**, 1228-1240. http://dx.doi.org/10.1523/JNEUROSCI.3181-12.2013

[14] Ogawa, S., Sung, Y., Kamba, M. and Nagaoka, T. (2003) Probing the Temporal Dynamics of the Functional System Interaction in the Brain by Functional MRI. *Advances in Neurological Sciences*, **47**, 902-908.

[15] Bressler, D., Fortenbaugh, F., Robertson, L. and Silver, M. (2013) Visual Spatial Attention Enhances the Amplitude of Positive and Negative fMRI Responses to Visual Stimulation in an Eccentricity-Dependent Manner. *Vision Research*, **85**, 104-112. http://dx.doi.org/10.1016/j.visres.2013.03.009

[16] Bressler, D. and Silver, M. (2010) Spatial Attention Improves Reliability of fMRI Retinotopic Mapping Signals in Occipital and Parietal Cortex. *Neuroimage*, **53**, 526-533. http://dx.doi.org/10.1016/j.neuroimage.2010.06.063

[17] Levy, I., Hasson, U., Avidan, G., Hendler, T. and Malach, R. (2001) Center-Periphery Organization of Human Object Areas. *Nature Neuroscience*, **4**, 533-539.

[18] Hemond, C., Kanwisher, N. and Op de Beeck, H. (2007) A Preference for Contralateral Stimuli in Human Object-and Face-Selective Cortex. *PLoS ONE*, **2**, e574. http://dx.doi.org/10.1371/journal.pone.0000574

[19] Pernet, C., Schyns, P. and Demonet, J.-F. (2007) Specific, Selective or Preferential: Comments on Category Specificity in Neuroimaging. *Neuroimage*, **35**, 991-997. http://dx.doi.org/10.1016/j.neuroimage.2007.01.017

[20] Sowden, P.T. and Schynes, P.G. (2006) Channel Surfing in the Visual Brain. *Trends in Cognitive Sciences*, **10**, 538-545. http://dx.doi.org/10.1016/j.tics.2006.10.007

[21] Haynes, J.D. and Rees, G. (2006) Decoding Mental States from Brain Activity in Humans. *Nature Reviews Neuroscience*, **7**, 523-534. http://dx.doi.org/10.1038/nrn1931

[22] Mourao-Miranda, J., Bokde, A.L.W. and Born, C. (2005) Classifying Brain States and Determining the Discriminating Activation Patterns: Support Vector Machine on Functional MRI Data. *Neuroimage*, **28**, 980-995. http://dx.doi.org/10.1016/j.neuroimage.2005.06.070

[23] Norman, K.A., Polyn, S.M., Detre, G.J. and Haxby, J.V. (2006) Beyond Mind-Reading: Multi-Voxel Pattern Analysis of fMRI Data. *Trends in Cognitive Sciences*, **10**, 424-430. http://dx.doi.org/10.1016/j.tics.2006.07.005

[24] Johnson, J.D., McDuff, S.G.R., Rugg, M.D. and Norman, K.A. (2009) Recollection, Familiarity and Cortical Reinstatement: A Multivoxel Pattern Analysis. *Neuron*, **63**, 697-708. http://dx.doi.org/10.1016/j.neuron.2009.08.011

[25] Schyns, P.G., Gosselin, F. and Smith, M.L. (2008) Information Processing Algorithms in the Brain. *Trends in Cognitive Sciences*, **13**, 20-26. http://dx.doi.org/10.1016/j.tics.2008.09.008

[26] Eger, E., Henson, R.N., Driver, J. and Doaln, R.J. (2004) BOLD Repetition Decreases in Object-Responsive Ventral Visual Areas Depend on Spatial Attention. *Journal of Neurophysiology*, **92**, 1241-1247. http://dx.doi.org/10.1152/jn.00206.2004

[27] Grill-Spector, K. and Malach, R. (2001) fMR-Adaptation: A Tool for Studying the Functional Properties of Human Cortical Neurons. *Acta Psychologica*, **107**, 293-321. http://dx.doi.org/10.1016/S0001-6918(01)00019-1

[28] Henson, R.N., Shallice, T., Gorno-Tempini, M.L. and Dolan, R.J. (2002) Face Repetition Effects in Implicit and Explicit Memory Tests as Measured by fMRI. *Cerebral Cortex*, **12**, 178-186. http://dx.doi.org/10.1093/cercor/12.2.178

[29] James, T.W. and Gauthier, I. (2007) Repetition-Induced Changes in BOLD Response Reflect Accumulation of Neural Activity. *Human Brain Mapping*, **27**, 37-46. http://dx.doi.org/10.1002/hbm.20165

[30] Schweinberger, S.R., Huddy, V. and Burton, A.M. (2004) N250r: A Face-Selective Brain Response to Stimulus Repetitions. *Neuroreport*, **15**, 1501-1505. http://dx.doi.org/10.1097/01.wnr.0000131675.00319.42

[31] Winston, J.S., Henson, R.N., Fine-Goulden, M.R. and Dolan, R.J. (2004) fMRI-Adaptation Reveals Dissociable Neural Representations of Identity and Expression in Face Perception. *Journal of Neurophysiology*, **92**, 1830-1839. http://dx.doi.org/10.1152/jn.00155.2004

[32] Sung, Y., Someya, Y., Eriko, Y., Choi, S.-H., Cho, Z.-H., and Ogawa, S. (2011) Involvement of Low-Level Visual

Areas in Hemispheric Superiority for Face Processing. *Brain Research*, **1366**, 54-59. http://dx.doi.org/10.1016/j.brainres.2010.10.020

[33] Rauss, K., Pourtois, G., Vuilleumier, P. and Schwartz, S. (2009) Attentional Load Modifies Early Activity in Human Primary Visual Cortex. *Human Brain Mapping*, **30**, 1723-1733. http://dx.doi.org/10.1002/hbm.20636

Scientific Research Publishing (SCIRP) is one of the largest Open Access journal publishers. It is currently publishing more than 200 open access, online, peer-reviewed journals covering a wide range of academic disciplines. SCIRP serves the worldwide academic communities and contributes to the progress and application of science with its publication.

Other selected journals from SCIRP are listed as below. Submit your manuscript to us via either submit@scirp.org or Online Submission Portal.

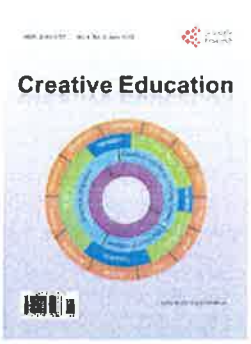


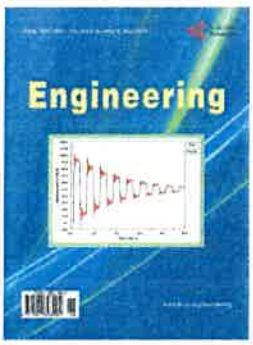










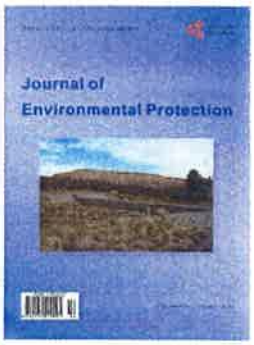






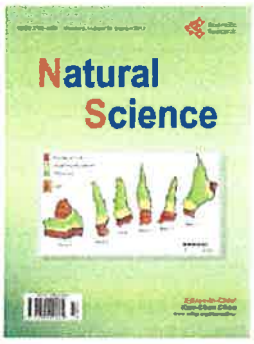


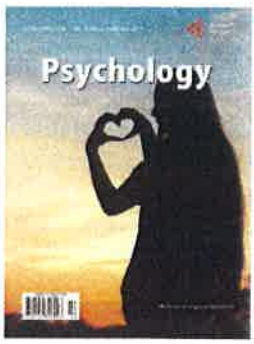












（2）学会報告等

（国際学会）

1 Kang, D., Sung, Y., Shioiri, S. Estimation of physiological sources of nonlinearity in bold signals. The 26th annual meeting of International Society for Magnetic Resonance Imaging, Paris, France, July 17-21, 2018

2 Sung, Y., Kawachi, Y., Ogawa, S. Functional specificity of resting-state fMRI signals. The 22th annual meeting of the Organization for Human Brain Mapping, Singapore, July 17-21, 2018

3 Sung, Y., Ogawa, S. Modality-dependent functional specificity in resting-state fMRI signals. The 46th annual meeting of the Japanese Society for Magnetic Resonance In Medicine, Kanazawa, Japan, Sep 18-20, 2018

4 Sung, Y., Kawachi, Y., Otomo, Y., Ogawa, S. Occupational abilities and function networks estimated through resting state fMRI. The 45th annual meeting of the Society for Neuroscience, San Diego, USA, Nov 3-7, 2018

5 Sung Y., Brain profile seen by functional networks and human traits. The 2nd International Neuroscience Symposium, Incheon, Korea, May 24, 2017.

6 Sung, Y., Kang, D., Ogawa, S. Measurement of task-induced high frequency band signals by ultrahigh temporal resolution imaging. The 25th annual meeting of International Society for Magnetic Resonance Imaging, Hawaii, USA, April 22-27, 2017

7 Sung, Y., Kang, D., Kawachi, Y., Ogawa, S. Brian maps reflected in different imaging modalities. The 22st annual meeting of the Organization for Human Brain Mapping, Vancouver, Canada, June 25-27, 2017

8 Sung, Y., Kang, D., Kawachi, Y., Kang, D., Abe, C., Otomo, Y., Ogawa S. Functional brain networks reflecting human characteristics. The 45th annual meeting of the Society for Neuroscience, Washington DC, USA, Oct. 11-15, 2017

9 Niwano, K., Ito, A., Tanabe, M., Sato, Y., Fujii, T. An fMRI study of the relationship between neuroticism and neural responses to infant emotional faces. 15th European Congress of Psychology, Amsterdam, Netherlands, July 12-14, 2017

10 Ito, A., Kawachi, Y., Kawasaki, I., Fujii, T. Age-related reduction of cognitive dissonance. 31st International Congress of Psychology (ICP2016) July 24-29, 2016, Yokohama, Japan

11 Ito, A., Niwano, K., Tanabe, M., Sato, Y., Fujii, T. The effect of childcare

training on the perception of infant's emotional facial expression. 31st International Congress of Psychology (ICP2016), Yokohama, Japan, July 24-29, 2016

12 Niwano, K., Ito, A., Tanabe, M., Sato, Y., Fujii, T. Relationship between regional brain responses to infant faces and personality traits in young female adults. 31st International Congress of Psychology (ICP2016), Yokohama, Japan, July 24-29, 2016

13 Niwano, K., Ito, A., Tanabe, M., Sato, Y., Fujii, T. Behavioral inhibition system relates to the responses of the dorsal anterior cingulate cortex and the orbitofrontal cortex to infant emotional faces. The 39th Annual Meeting of JNS, Yokohama, Japan, July 20-22, 2016

14 Tanabe, M., Niwano, K., Ito, A., Sato, Y., Fujii, T. Correlations between the brain responses of nulliparous females when viewing infants' facial expressions and their personality. 31st International Congress of Psychology (ICP2016), Yokohama, Japan, July 24-29, 2016

15 Fujii, T., Ito, A., Jenkins, R., Sanders, J., Yoshida, K., Murakami, Y., Sakai, S., Tanabe, M. The effect of wearing a medical mask and sunglasses on perceiver's impression. 31st International Congress of Psychology (ICP2016), Yokohama, Japan, July 24-29, 2016

16 Sung, Y., Choi, U.-S., Ogawa, S., Interaction between high and low level areas and the temporal window for repetition suppression. The 22st annual meeting of the Organization for Human Brain Mapping, Geneva, Switzerland, Jun 26-30, 2016.

17 Sung, Y., Kang, D., Ogawa, S., A challenge for sub‐millisecond fMRI. The 44th annual meeting of the Japanese Society for Magnetic Resonance In Medicine, Omiya, Japan, Sep 9-11, 2016.

18 Kang, D., Sung, Y., Ogawa, S., Comparison of voxel-based morphometry and T1 absolute value. The 44th annual meeting of the Japanese Society for Magnetic Resonance In Medicine, Omiya, Japan, Sep 9-11, 2016.

19 Sung, Y., Kang, D., Kawachi, Y., Ogawa, S., Brain plasticity changes by playing wind instruments and piano. The 46th annual meeting of the Society for Neuroscience, SanDiego, USA, Oct 12-16, 2016.

20 Sung, Y., Microscopic functional structures seen through fMRI signals. BIT's 6th annual world congress of neurotalk-2015, Hanzhou, China, May 22-

24, 2015.

21 Choi, U.-S., Sung, Y., Chung J.Y., Ogawa, S. Brain plasticity seen in musicians of wind instruments. 21st annual meeting of the Organization for Human Brain Mapping, Hawaii, USA, Jun 14-18, 2015.

22 Kang, D., Sung, Y., Shioiri, S., Ogawa, S. Investigation of microscopic functional specificity for attention in peripheral visual field. 21st annual meeting of the Organization for Human Brain Mapping, Hawaii, USA, Jun 14-18, 2015.

23 Sung, Y., Kang, D., Ogawa, S., Robustness of microscopic functional structures estimated by dynamic magnetic susceptibility change. The 21st annual meeting of the Organization for Human Brain Mapping, Hawaii, USA, Jun 14-18, 2015.

24 Sung, Y., Yoon, H., Choi, U.-K., Ogawa, S. Regional difference in characteristics for top-down modulation in the ventral visual stream. The 45th annual meeting of the Society for Neuroscience, Chicago, USA, Oct 17-21, 2015

25 Sung, Y., Kang, D., Ogawa, S. Morphological changes in cortical microstructure of the brain by short-term training. The 45th annual meeting of the Society for Neuroscience, Chicago, USA, Oct 17-21, 2015

26 Ogawa S., Macro-scale structure and function of the brain visualized by MRI, Gachon Univ. NRI Symposium, Incheon, Korea, Feb 24, 2016

27 Kang, D., Sung, Y., Shioiri, S., Ogawa, S., Estimation of functional specificity of visual areas by a transverse relaxation profile. The 10th Asia-Pacific conference on Vision, Takamatsu, Japan, July 19-22, 2014.

28 Sung, Y., Chung, J.Y., Ogawa, S. Effects of signals originating from large blood vessels on BOLD signals of the fusiform face area. The 44th society for neuroscience meeting, Washington DC, USA, November 15-19, 2014

29 Choi, U.-S., Sung, Y., Kim ,Y.-B., Cho, Z.-H., Yoon, H., Ogawa, S., Functional differences in processing preferred and non-preferred stimuli at object selective areas. The 44th society for neuroscience meeting, Washington DC, USA, November 15-19, 2014

(国内学会)

30 成烈完・河地庸介・小川誠二 脳機能ネットワークによるヒト特性変化の推定. 第21回日本ヒト脳機能マッピング学会, 東京, 2019年3月.

31 Sung Y, Kawachi Y, Ogawa S. Estimation of specific functional brain areas reflecting individual characteristics. The 21st Congress of Japan Human Brain

Mapping Society, Tokyo, Japan, Mar 15-16, 2019

32 Kikuchi Y, Sung Y, Ogawa S. Quantification method of functional brain networks and estimation of network measure. The 21st Congress of Japan Human Brain Mapping Society, Tokyo, Japan, Mar 15-16, 2019

33 阿部千裕・河地庸介 実行機能ネットワークの同定. 日本心理学会第 82 回大会, 宮城, 2018 年 9 月

34 阿部千裕・河地庸介 実行機能ネットワークテストの考案. 日本認知心理学会第 16 回大会, 大阪, 2018 年 9 月

35 大友ゆき・河地庸介　線形混合モデルでみるメタ記憶. 日本感性福祉学会第 18 回大会, 宮城, 2018 年 11 月

36 大友ゆき・河地庸介 パーソナリティ特性が既学習判断(Judgment of Learning: JOL)に及ぼす影響. 東北心理学会第 72 回大会, 岩手, 2018 年 11 月

37 阿部千裕・河地庸介 短期的訓練が実行機能に及ぼす影響. 日本感性福祉学会第 17 回大会, 宮城, 2017 年 10 月

38 大友ゆき・阿部千裕・河地庸介 メタ認知と自己成長主導性の関連性. 日本感性福祉学会第 17 回大会, 宮城, 2017 年 10 月

39 阿部千裕・河地庸介・北村康宏・成烈完・小川誠二 報酬を導く意思決定方略への依存－アイオワギャンブリング課題を用いた検討. 日本基礎心理学会第 36 回大会, 大阪, 2017 年 12 月

40 河地庸介・阿部千裕・成烈完・松江克彦・小川誠二 統合失調型パーソナリティの個人差が注意の下位機能間の相互作用に及ぼす影響. 第 46 回日本臨床神経生理学会学術大会, 福島, 2016 年 10 月.

41 阿部千裕・河地庸介・成烈完・松江克彦・小川誠二 実行機能と統合失調型パーソナリティの関係. 第 46 回日本臨床神経生理学会学術大会, 福島, 2016 年 10 月.

42 大友ゆき・阿部千裕・河地庸介・成烈完・松江克彦・小川誠二 統合失調型パーソナリティ傾向におけるメタ記憶の特徴. 第 46 回日本臨床神経生理学会学術大会, 福島, 2016 年 10 月.

ISMRM 2018
#2385

ESTIMATION OF PHYSIOLOGICAL SOURCES OF NONLINEARITY IN BOLD SIGNALS

Daehun Kang[1], Yul-Wan Sung[1], and Satoshi Shioiri[2]

[1]Kansei Fukushi Research Institute, Tohoku Fukushi University, Sendai, Japan, [2]Graduate School of Information Sciences, Tohoku University, Sendai, Japan

Purpose

- The **nonlinearity in BOLD** signals, showing nonlinear aspects with echo time [1–3].
- **Two-compartment model**
  - BOLD signals can be modeled originating from both **intravascular (IV)** and **extravascular (EV)** spaces [4].
  - The TE-dependent nonlinearity in BOLD signals attributable to IV component [9].
  - Including **a chemical exchange** between plasma and deoxy-Hb [7]
- Activity-evoked pH change on the brain has been demonstrated [5].
  - Since the chemical exchange is often pH-dependent [6], the chemical exchange time, τ_{ex}, would change.
- The two-compartment model that incorporates the change, $\Delta\tau_{ex}$, would be more accurate for estimation of parameters

Methods

- **Two-compartment model**

$$S = (V+\Delta V)\cdot\exp\left(-R'_{2,IV}\cdot \mathrm{TE}\right) + (1-V-\Delta V)\cdot\lambda\cdot\exp\left(-(R'_{2,EV,0}+\Delta R'_{2,EV})\cdot \mathrm{TE}\right), \quad (1)$$

$$R'_{2,IV}(\mathrm{TE}) = R'_{2,IV,0} + R'_{2,IV,Hb}\cdot\left|1-(Y+\Delta Y)\right|^2\cdot(1+\Delta\tau_{cx}/\tau_{ex})\cdot\left\{1-2(\tau_{cx}+\Delta\tau_{ex})/\mathrm{TE}\cdot\tanh\left[\mathrm{TE}/2(\tau_{cx}+\Delta\tau_{ex})\right]\right\} \quad (2)$$

$\%S = (S-S_0)/S_0 \times 100\ (\%)$, where S_0 was a signal when stimulus-dependent parameters were zero.
The two-compartment model was used with **time-varying $\Delta\tau_{ex}$ (TV-model)** or **$\Delta\tau_{ex} = 0$ (zero-model)**.

Table 1 Parameters used in two-compartment model

Components	Parameters	Constant -valued	Location -dependent	Stimulus -dependent
Intra-vascular	Transverse relaxation			
	Intrinsic transverse relaxation in blood	$R'_{2,IV,0}$	-	-
	Additional transverse relaxation by deoxy-Hb	$R'_{2,IV,Hb}$	-	-
	Blood oxygen level	Y	-	ΔY
	Chemical exchange time	τ_{ex}	-	$\Delta\tau_{ex}$
Extra-vascular	Spin density ratio	λ	-	-
	Transverse relaxation	$R'_{2,EV}$	-	$\Delta R'_{2,EV}$
-	Blood volume fraction of venous blood	-	V	ΔV

- **Parameter simulation**

Table 2 Preparation of parameters for estimation

Parameters	Unit	Min. value (or single)	Increment	Max. value
λ	n/a	1.03	-	-
$R'_{2,IV,0}$	[s^{-1}]	13	-	-
$R'_{2,IV,Hb}$	[s^{-1}]	181	-	-
$R'_{2,EV,0}$	[s^{-1}]	21	-	-
Y	[%]	60	-	-
τ_{cx}[a]	[ms]	1	1	10
V	[%]	1	1	15
$\Delta R'_{2,EV}$	[s^{-1}]	-2.0	0.02	0.5
ΔY	[%]	-5.0	0.2	20.0
ΔV	[%]	-0.2	0.01	1.0
$\Delta\tau_{ex}$[b]	[ms]	$-\tau_{cx}$	0.2	$10-\tau_{cx}$

[a] Since there was no clear representative value of this parameter in the exchange model, all possible cases within the range were tested.
[b] The range of this parameter was used in the two compartment model with time-varying $\Delta\tau_{ex}$.

- **Data acquisition**
- 3T Skyra-fit system (Siemens, Erlangen, Germany) with a standard, 16-channel head matrix coil.
- 9 healthy volunteers (3 females) with the consent written.
- Imaging parameters
  - 6-echo-time GRE EPI sequence
  - TR / TEs = 2000 / 11, 26, 41, 56, 71 & 86 ms
  - FA:90°, FOV:220 mm.
  - Resolution: 3.44 mm (in-plane), 3.4 mm (thickness)
  - PE Acc. Factor 2.
  - 15 slices including the calcarine sulcus of the brain.
- Visual stimulation : 8 blocks of 16 / 36 sec. on / off with 8Hz flickering checkerboard

- **Error evaluation between measured and simulated signals**

$$\mathrm{Error}\ (s^{-1}) = \frac{1}{N\cdot 100(\%)}\sum_{t\in\mathrm{TE}}\left|\%S_{m,t} - \%S_{c,t}\right|/t \quad (5)$$

$\%S_{m,t}$ and $\%S_{c,t}$ denote measured and simulated signal changes at echo time t, respectively.

- The corrected **Akaike information criterion (AICc)**:
  - to validate a goodness of fit with the complexity of the model [8]

Acknowledgements

- This study was supported by JSPS KAKENHI under Grant number 17K01993 and Supported program for the Strategic Research Foundation at Private Universities, 2014-2018.
- References [1] Duong TQ et al., MRM 2003. [2] Jin T et al., MRM 2006. [3] Kang D et al., MRI 2014. [4] Ogawa S et al., Biophys J 1993. [5] Magnotta V a et al., PNAS 2012. [6] Matthew JB et al., J Biol Chem 1983. [7] Luz Z, Meiboom S, J Chem Phys 1963. [8] Burnham KP et al., Springer; 2002. [9] Donahue MJ et al., NMR Biomed 2011.

Results

- **Non-linearity in multiple-echo BOLD signals**

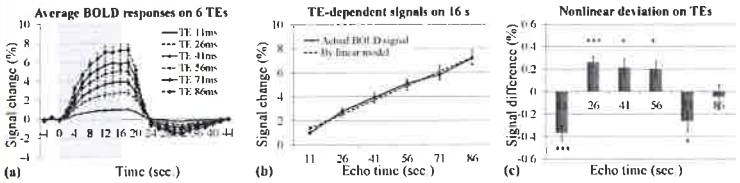


Figure 1. (a) Average BOLD responses on six echo times of 11–86 ms. A transparent gray-filled box denotes the visual stimulation period. (b) To show the nonlinearity in BOLD signals, the actual TE-dependent signals on 16 s (solid line) were compared with the signals (dotted line) estimated by a linear model. (c) The differences between the actual BOLD signals and the signals generated by a linear model were plotted. The nonlinear deviation was dominant at TEs of 11 ms to 41 ms (*:p<0.05, ***:p<0.001, paired Student's t-test). The error bar denotes the standard error (N=18).

- **Comparison between TV-model and zero-model**

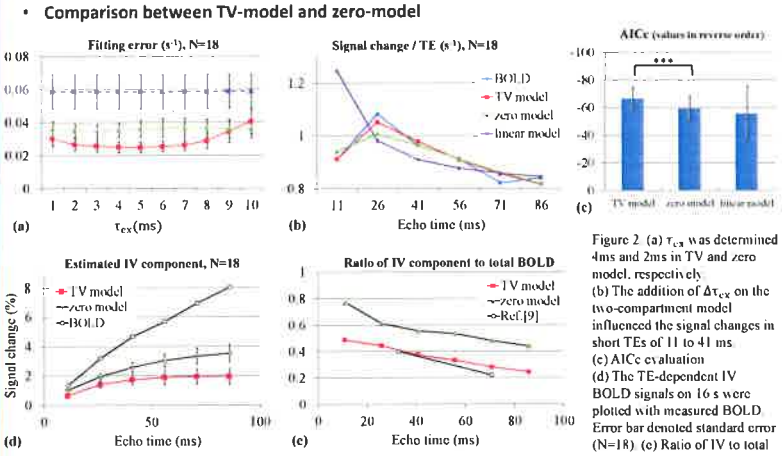


Figure 2. (a) τ_{cx} was determined 4ms and 2ms in TV and zero model, respectively. (b) The addition of $\Delta\tau_{cx}$ on the two-compartment model influenced the signal changes in short TEs of 11 to 41 ms. (c) AICc evaluation. (d) The TE-dependent IV BOLD signals on 16 s were plotted with measured BOLD. Error bar denoted standard error (N=18). (e) Ratio of IV to total BOLD.

- **Responses of stimulus-dependent parameters**

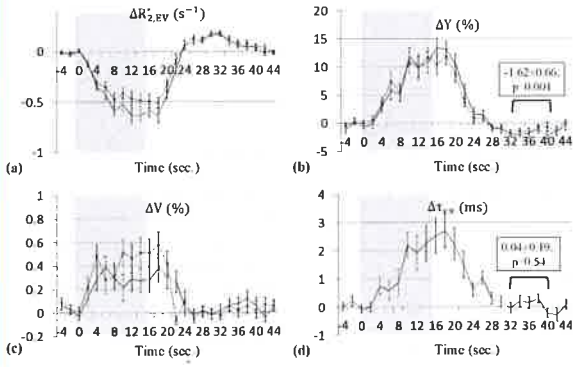


Figure 3. They are based on the **TV $\Delta\tau_{ex}$ model (solid line) and the zero $\Delta\tau_{ex}$ model (dotted line)** and averaged across ROIs (N=18).

In the post-stimulus undershoot, $\Delta\tau_{ex}$ was almost zero while ΔY was non-zero. These implied that the source of $\Delta\tau_{ex}$ might be different from that of ΔY.

Discussion & conclusion

- The nonlinearity in TE-dependent BOLD signals was analyzed with the two-compartment model. The existence of $\Delta\tau_{ex}$ in the model produced better fitting results and IV/EV separation comparable for results of the previous study. $\Delta\tau_{ex}$ was considered to be influenced by a stimulus-related non-BOLD factor differing from ΔY.
- The proposed method is appropriate for simultaneous observations of several physiological sources that contribute to BOLD signals by using a single measurement modality.

E-mail : sung@tfu-mail.tfu.ac.jp

Functional specificity of resting-state fMRI signals

Yul-Wan Sung, Yousuke Kawachi, Seiji Ogawa

Kansei Fukushi Research Institute, Tohoku Fukushi University, Sendai, Japan

Introduction

1. Task-fMRI has been used to localize brain regions specifically reflecting a task-related function.
2. Resting-state fMRI is known to reflect some intrinsic brain function such as the default mode network but not to reflect a specific function.
3. Resting-state fMRI measurement is comparatively easy because it does not need tasks.
4. Some studies reported that similar functional areas were identified as those in task-fMRI but by using indirect methods such as machine learning.
5. In this study we examined functional specificity of resting-state fMRI signals by direct measurements of a task-related resting state fMRI and the typical resting-state fMRI.

Method

(*Subjects*) Ten college students were participated. (*Data measurements*) Structural images and functional images were measured. Parameters for structural images were matrix size= 256 × 256, voxel size=1mm3, and number of slices=192. Parameters for functional fMRI measurements were repetition time = 1000 ms, echo time = 24 ms, matrix size = 64 × 64, in-plane resolution = 3.4 × 3.4 mm2, slice thickness = 3.4 mm, and number of volumes = 480. 3T MRI scanner (Skyra-fit, Siemens) was used. The imaging orientation was axial for the fMRI (Acquisition) In the typical resting-state fMRI session, subjects were asked to lie on the bed and not to wander their mind with their eyes open and to gently focus their eyes on the center of the visual field. In the following task-related resting state fMRI session where subjects performed finger tapping by both hands continually during the 8 min scan with their eyes open. The lights in the room were turned off during MRI scans.

Results

There were several fMRI signal features by which we could compare the task-related resting-state fMRI and the typical resting-state fMRI. We used in this study fractional amplitude of low frequency fluctuations (fALFF). By comparing fALFF values of the task-related resting-state fMRI signals and the typical resting-state fMRI signals:

1. The primary motor areas were identified in the both hemispheres in which the fALFF of the typical resting-state fMRI was larger than that of the task-related resting-state fMRI.
2. Any brain regions other than the primary motor areas showing the difference between the task-related fMRI and the typical resting-state fMRI were not found.

Results

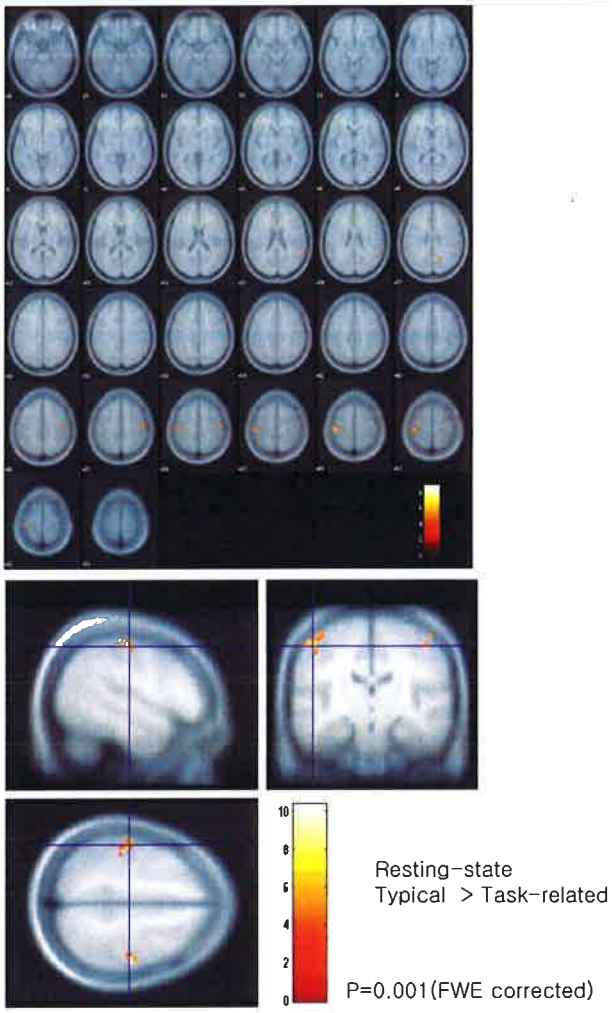


Fig.1 Primary motor area identified by the task-related resting state fMRI

Discussion/Conclusion

1. The result shows that low frequency coherent neuronal activities at a resting state is disturbed by the external stimulation input and that the disturbance of coherent low frequency signals in a functional area by stimulation is highly specific to the brain function.
2. This supports previous observations that resting-state fMRI signals contain information related to the functional specificity as measured by the task-fMRI.
3. Although the primary motor area was clearly identified in a task-related resting-state fMRI, further study will be made to see whether other primary areas such as the primary visual area can be identified with the same approach.

Acknowledgements

This research was supported by MEXT-Supported Program for the Strategic Research Foundation at Private Universities, 2014–2018.

JSMRM 2018
PDF-006

Modality-dependent functional specificity in resting-state fMRI signals

Yul-Wan Sung[1] and Seiji Ogawa[1]
[1]*Kansei Fukushi Research Institute, Tohoku Fukushi University, Sendai, Japan*

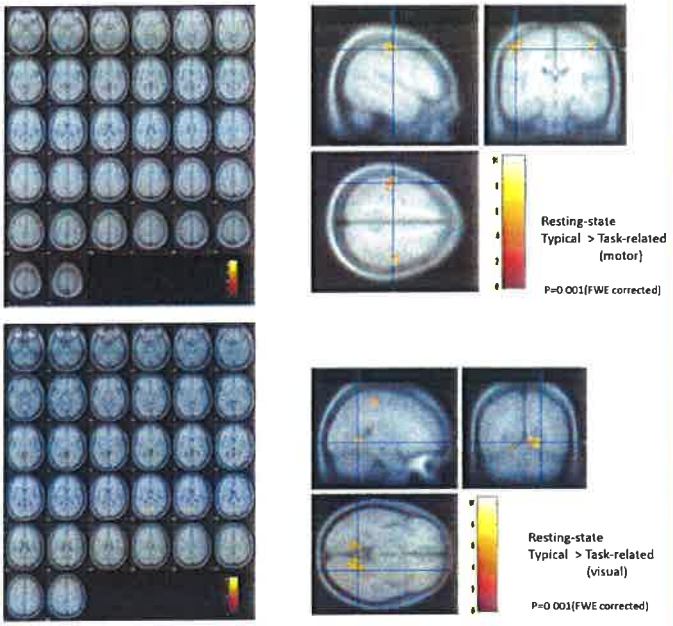
Introduction

1. Task-fMRI has been used to localize brain regions specifically reflecting a task-related function.
2. Resting-state fMRI is known to reflect some intrinsic brain function such as the default mode network but not to reflect a specific function.
3. Resting-state fMRI measurement is comparatively easy because it does not need tasks.
4. Some studies reported that similar functional areas were identified as those in task-fMRI but by using indirect methods such as machine learning.
5. In this study we examined functional specificity of resting-state fMRI signals depending on modality by direct measurements of a task-related resting state fMRI and the typical resting-state fMRI.

Methods

(*Subjects*) Twenty college students were participated. (*Data measurements*) Structural images and functional images were measured. Parameters for structural images were matrix size= 256 × 256, voxel size=1mm3, and number of slices=192. Parameters for functional fMRI measurements were repetition time = 1000 ms, echo time = 24 ms, matrix size = 64 × 64, in-plane resolution = 3.4 × 3.4 mm2, slice thickness = 3.4 mm, and number of volumes = 480. 3T MRI scanner (Skyra-fit, Siemens) was used. The imaging orientation was axial for the fMRI (Acquisition) In the typical resting-state fMRI session, subjects were asked to lie on the bed and not to wander their mind with their eyes open and to gently focus their eyes on the center of the visual field. In the following task-related resting state fMRI session where subjects performed finger tapping by both hands continually during the 8 min scan for motor function and were presented face pictures for visual function with their eyes open. The lights in the room were turned off during MRI scans.

Results



There were several fMRI signal features by which we could compare the task-related resting-state fMRI and the typical resting-state fMRI. We used in this study fractional amplitude of low frequency fluctuations (fALFF). By comparing fALFF values of the task-related resting-state fMRI signals and the typical resting-state fMRI signals:

1. The primary motor areas were identified in the both hemispheres in which the fALFF of the typical resting-state fMRI was larger than that of the task-related resting-state fMRI.
2. Any brain regions other than the primary motor areas showing the difference between the task-related fMRI and the typical resting-state fMRI were not found.
3. The primary visual area was not identified although several brain areas were identified.

Discussion and Conclusion

1. The result shows that low frequency coherent neuronal activities at a resting state is disturbed by the external stimulation input and that the disturbance of coherent low frequency signals in a functional area by stimulation is highly specific to the brain function but it is depending on stimulus modality.
2. This supports previous observations that resting-state fMRI signals contain information related to the functional specificity as measured by the task-fMRI.
3. Although the primary motor area was clearly identified in a task-related resting-state fMRI, the primary visual was not identified. Other modalities such as auditory will be examined in our future study for further elucidation of the characteristics of resting state signals.

Acknowledgements: This study was supported by MEXT-Supported program for the Strategic Research Foundation at Private Universities, 2014-2018, and JSPS KAKENHI Grant Number 17K01993

Occupational abilities and functional networks estimated through resting state fMRI

Yul-Wan Sung, Yousuke Kawachi, Yuki Otomo & Seiji Ogawa

Kansei Fukushi Research Institute, Tohoku Fukushi University, Sendai, Japan

795.17

Background

The successful human life in modern society requires proper choice of occupation. Therefore, it is very important for people to know their abilities and develop career plans that best suit their abilities. Traditional test batteries have been used for evaluating occupational abilities but it is not known about what brain functions are related to the evaluated abilities by the test batteries. In this study, we attempted to identify functional networks related to occupational abilities by resting state fMRI.

Methods

[Subjects]

112 college students

[Behavioral tests]

General Aptitude Test Battery (GATB) was used for 19 occupational abilities.

[MRI measurements]

Siemens 3T, Skyra-fit

1. Anatomical Image

T1 MPRAGE, 1x1x1 mm^3

2. Resting state fMRI

TR 1s, Sices 34, FA 70, Matrix 64x64, 3.4x3.4x3.4mm^3

Number of volumes 480, MB-EPI sequence

[Data analysis]

(Functional network identification for Occupational abilities)

(1) ROI-based network analysis

1) 272 ROIs based on two templates from Dosenbach and Harvard (Desikan et al., 2006; Dosenbach et al., 2010)

2) Simple regression analysis for each psychometric variable (p = 0.005, corrected), (GraphVar)

(2) Multiple class Support Vector Machine

Design of 3classes SVM

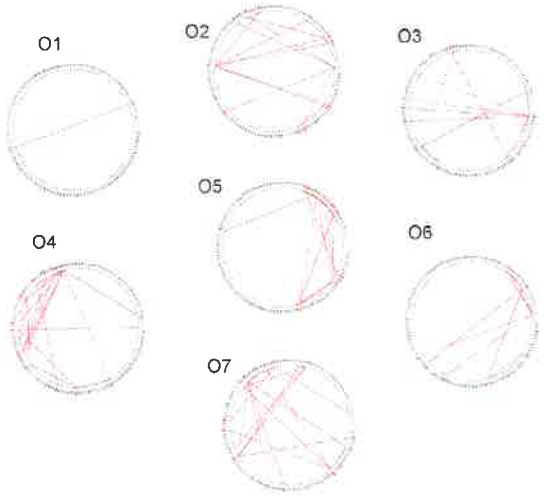
Methods

[19 occupational abilities]

O1 (M) Plant culture/animal breeding; **O2** (GV) Animal training and service/aquaculture/gardening; **O3** (KM) Physical works in mechanical/plants/animals; **O4** (PM) Hand work; **O5** (KFM) Industrial machine manipulation; **O6** (PKM) Manufacture/ assembly; **O7** (SPM) Cutting/molding/ construction/installation; **O8** (SPF) Barber/beauty services; **O9** (NSP) Drawing and architecture design/laboratory technology; **O10** (GQM) Nursing/therapy/specialized teaching services/quality control/ security management; **O11** (GNS) Engineering technology/ physical sciences/medical sciences; **O12** (GVN) Social research/law/social service/mathematics and statistics; **O13** (GVQ) General office work/educational and library services; **O14** (SP) Design and visual arts; **O15** (GQK) Clerical machine operation/communicator; **O16** (GM) Nursing-care services; **O17** (GNQ) General sales/accounting; **O18** (GQ) Hospitality/security services; **O19** (QK) Clerical handling. *[F:finger dexterity; G:general intelligence; K:motor coordination; M:manualdexterity; N:numerical aptitude; P:form perception; Q:clerical perception; S5spatial aptitude; V:verbal aptitude]*

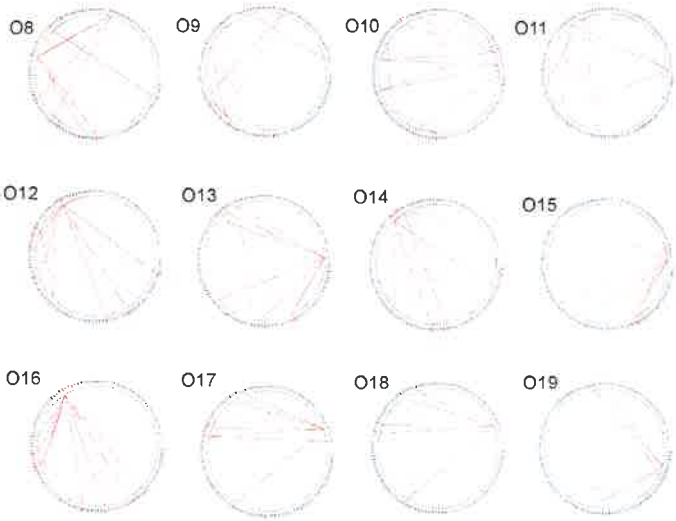
Results

1. Functional networks identified for 19 occupational abilities



Results

2. There were functional networks with and without a rich hub.



Discussion and Conclusion

1. We could identify functional networks reflecting 19 occupational abilities.
2. These functional networks can be used for objective evaluation of occupational abilities.
3. These functional networks also can be used to examine how the brain is organized for realizing each occupational abilities or to know what brain function is needed to develop for an occupation ability.
4. In addition, the measurement of the occupational abilities by fMRI takes only less than 15 minutes including acquisition times of anatomical and functional images.
5. These show a possibility that we can effectively evaluate occupational abilities and develop some programs for development of occupational abilities through brain function measurements.

Acknowledgements

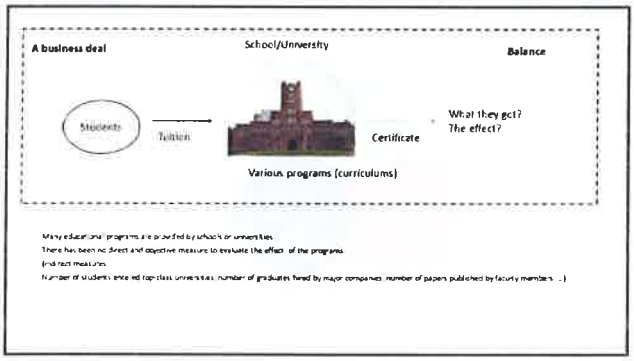
Supported by MEXT-Supported Program for the Strategic Research Foundation at Private Universities, 2014-2018

Brain profile seen by functional networks and human traits

Yul-Wan Sung
Kansei Fukushi Research Institute, Tohoku Fukushi University
Neuroscience Research Institute, Gachon University

Contents

1. Background
2. Mapping human characteristics into the Brain
   (Identification of functional brain networks)
3. Creation of an evaluation system of human characteristics
4. Application examples.



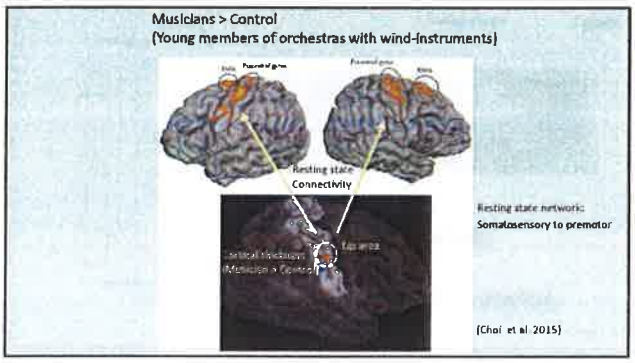
(Study goal)

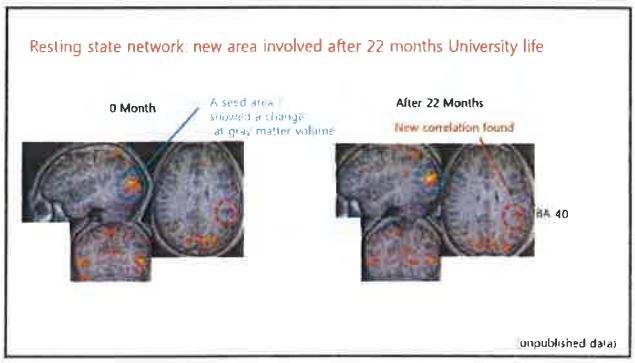
To develop an evaluation system by which we can objectively evaluate the effects of academic, social and vocational skill training programs in educational institutions through measuring human characteristics by MRI.

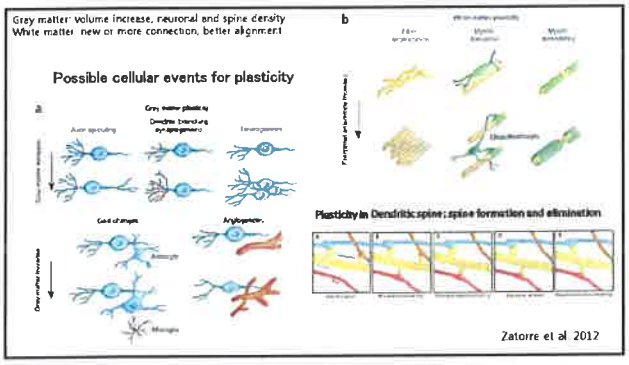
(Hypothesis)

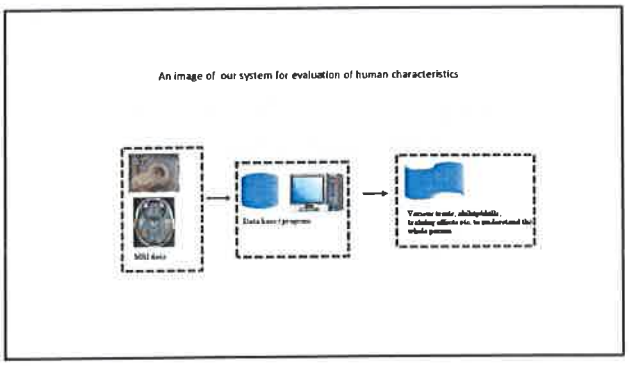
(1) Academic, social and vocational skill training programs can affect various human characteristics.

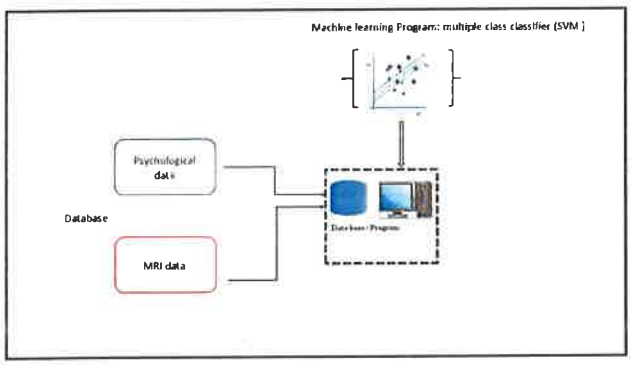
(2) The changes in the human characteristics through learning or training would be reflected as plasticity changes in the brain; it is expected that the effects of those educational programs can be evaluated through brain function measurements.

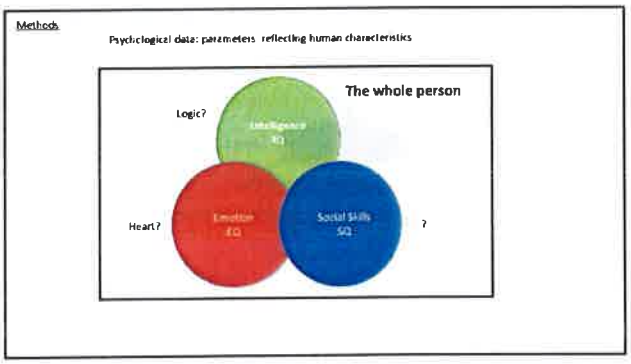


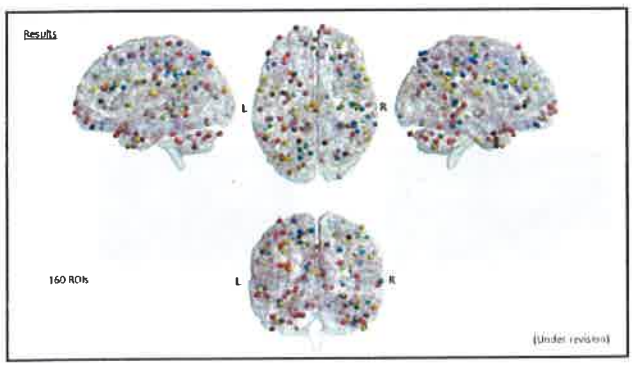


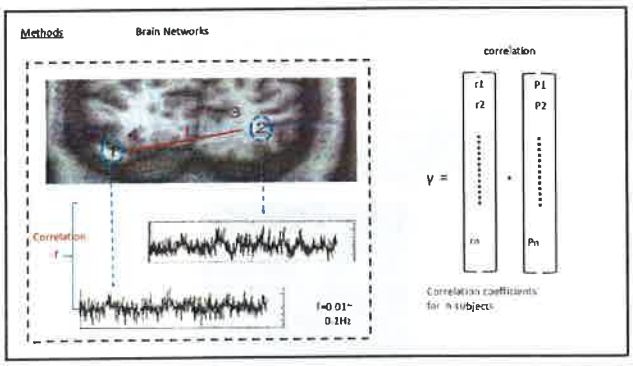

Grey matter volume increase, neuronal and spine density
White matter new or more connection, better alignment
Possible cellular events for plasticity
Plasticity in Dendritic spine : spine formation and elimination
Zatorre et al 2012

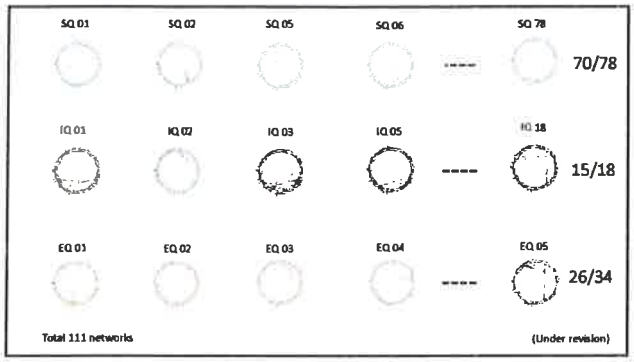

An image of our system for evaluation of human characteristics


Machine learning Program: multiple class classifier (SVM)
Psychological data
Database
MRI data


Methods
Psychological data: parameters reflecting human characteristics
The whole person
Logic?
Heart?
?


Results
160 ROIs
(Under revision)


Methods
Brain Networks
correlation
Correlation r
f=0.01~0.1Hz
Correlation coefficients for n subjects



Conclusions

1. Functional networks representing various human characteristics (111) were identified by rs-fMRI.
2. Classifiers (111) were made.
3. Prototype of a system for evaluation of the whole person were made (Just 13 minutes MRI measurement is sufficient to evaluate).
4. The effectiveness of the system were seen through three examples.

→ Comprehensive human characteristics can be evaluated by MRI, and also the effects of learning or training.

Acknowledgments

Prof. Seiji Ogawa (PI)
Tohoku Fukushi University / Gachon University

Prof. Yousuke Kawachi
Tohoku Fukushi University

Dr. Uk-Su Choi
National Institute of Information and Communications Technology

Dr. Daehun Kang
Tohoku Fukushi University

Chichiro Abe
Tohoku Fukushi University

Yuki Otomo
Tohoku Fukushi University

This study was supported by the MEXT-Supported program for the Strategic Research Foundation at Private Universities, 2014-2018

(697 / 750 words)

Title: Measurement of task-induced high frequency band signals by ultra-high temporal resolution imaging

Author: Yul-Wan Sung, Daehun Kang, and Seiji Ogawa

(Synopsis) (later…)

(Purpose) Functional MRI studies have focused on slow signal changes dominated by vasculature dynamics. Recent advances in MRI technique have made With improvement of MR imaging, the imaging technique with high temporal resolution has been suggested. In the previous study, inverse imaging with multiple echoes was suggested to improve temporal resolution by 10 ms [1]. In this study, we investigated task-based change in high-frequency MR signal by using the imaging technique.

(Methods) (Pulse sequence & image reconstruction) A typical GRE sequence with multiple echoes was modified to obtain radial trajectories. Each session consisted of consecutive three scans: initial dummy scan for steady-state magnetization (20 sec.), reference scan, and projection scans in order. The image reconstruction was discussed in the previous study [1].

(fMRI protocol) To derive the activation in BOLD signal in the primary visual area, a checkerboard pattern flickering at 8 Hz was used. Each session consisted of initial period of 20 s and 4 repetitions of stimulus period of 20 s and resting period of 20 s as shown in Figure 1(a). Thus, it took 180 s for a single session. 4 sessions were performed to a subject.

(Data acquisition) Six healthy volunteers participated in this study. Informed and written consent was obtained in accordance with the Declaration of Helsinki. All MRI experiments were performed using a 3T Skyra-fit system (Siemens Healthcare GmbH, Erlangen, Germany) with a standard, 16-channel head matrix coil. For imaging, multi-echo projection sequence was used with three TEs of 4.0, 5.3, 6.7 ms, TR of 10 ms, FA of 8°, FOV of 220 mm, in-plane resolution of 3.4 mm, slice thickness of 5.0 mm, and BW of 2kHz/pixel. A single slice was located including the calcarine sulcus of a brain. The orientation angles were 0°, 120°, and 60° in order of TEs.

(Analysis) The BOLD activation was detected by general linear model (GML) analysis, with which a map of beta was obtained. A voxel with the highest beta value and adjacent eight voxels were selected as a region of interest (10.2 x 10.2 x 5.0 mm^3, ROI) in the posterior area of a brain. To evaluate the change in frequency bands by visual stimulus, we investigated the power spectrum density (PSD) in six bands and nine periods which were defined in Table 1 and in Figure 1(b), respectively. To normalize PSDs, the criterion was selected to the PSD value obtained from the initial period of each session. For the statistical analysis, paired t-test was performed between PSDs of stimulus and resting periods.

(Results) Among 24 sessions obtained from 6 subjects, 2 sessions were rejected due to a large motion. 88 pairs of stimulus and resting periods from 22 sessions were used for analysis. Figure 2 showed examples of the reconstructed image and the BOLD-based activation map by visual stimulus. The average in beta on ROIs was 1.376 ± 0.375 (mean $\pm$ standard deviation). As shown in Figure 3, normalized PSDs depending on the presence of stimulus were compared in the six frequency bands. On the stimulus period, the band #1 as BOLD signal showed the increase in PSD with the significance as expected ($p<0.001$). In contrast, the PSDs in band #2 and #5 tended to decrease with a little significance ($p<0.2$). The other bands showed no significant change or increase related with stimulus.

(Discussion) We tried the ultra-high sampling measurement for a single slice, whose sampling ratio was 100 Hz. Based on a hypothesis that the local and periodic potential variation might influence on the spin coherence and the MR signal, we investigated the high-frequency signals on functional MRI with the imaging technique. If the

hypothesis works, the larger potential variation accelerates dephasing of the spin coherency and makes MR signal lower. In this study, the high frequency bands were defined by referring to those in electroencephalography (EEG). PSDs in the band #2 and #5 (i.e., delta and beta bands in EEG, respectively) tended to reduce on stimulus periods although it was with a statistically low significance. It was considered as some potential to monitor neuronal activation. To derive an obvious result, however, further study is required.

(Conclusion) Based on time courses with a sampling time of 10 ms, high-frequency signals were examined with a block-designed fMRI experiment. Some frequency bands showed slight tendency of decreasing in PSDs on stimulus period.

(Acknowledgements) This study was supported by the MEXT-Supported program for the Strategic Research Foundation at Private Universities, 2014-2018.

(References)

[1] (#2965@ISMRM2017)

Use the "Insert Citation" button to add citations to this document.

E-mail : sung@tfu-mail.tfu.ac.jp

Brian maps reflected in different imaging modalities

Yul-Wan Sung, Daehun Kang, Yousuke Kawachi, Seiji Ogawa

Kansei Fukushi Research Institute, Tohoku Fukushi University, Sendai, Japan

Introduction

1. Voxel-based morphometry (VBM) has been used for measurement of structural changes such as in grey matter of the brain in relation to sensory and cognitive function.
2. VBM has been mostly applied to T1-constrast MRI images. But the T1-constrast image does not carry absolute T1 values of the brain so that T1-constrast MRI images may be less sensitive to changes in cortical structures than T1-absolute-value images.
3. **Aims:** (1) To compare the sensitivities of T1-weighted images and T1-absolute-value images in VBM analysis to the estimation of brain plasticity changes (2) To examine whether brain areas identified by VBM analysis based on the T1-absolute-value image show changes in T1-value.

Method

(*Subjects*) Twenty-four college students with musical training experiences of 6 to 12 years for playing wind instruments were participated. (*Data measurements*) 3 T MRI scanner (Skyra-fit, Siemens) was used. T1-weighted images were acquired by 3D MPRAGE pulse sequence. For T1-absolute value images four scans were performed by GRE pulse sequence. Two of them were for B1 field correction by double angel method and the other two were for estimation of T1-value. In the two scans for B1 field correction, a long TR of 20 seconds was used, which was 4 times longer than the T1 of cerebrospinal fluid (CSF), with flip angles of 45 or 90 degrees each. In the other two scans for T1-value estimation, two TRs of 0.8 seconds or 1.6 seconds were used. T1-absolute-value images were estimated from these two T1 contrast images after B1 field corrected. (*Data analysis*) MRI data were analyzed using VBM8 implemented in SPM 12.

Results

1. Brain maps with grey matter volume showing correlation with musical training years were estimated from both the T1-weighted image and the T1-absolute value image.
2. The brain map estimated by T1-weighted image showed an area in the superior temporal gyrus (Figure 1).
3. The brain map by T1-absolute-value image showed several brain areas across the frontal, temporal and parietal gyri (Figure 2) with including the area in the superior temporal gyrus estimated by T1-weighted image.
4. A brain map with T1-absolute value showing correlation with musical training years were also estimated from the T1-absolute-value image. An area in the right frontal gyrus showed significant correlation with musical training years with indicating that T1-value decreases with increase of musical training years (Figure 3).

Results

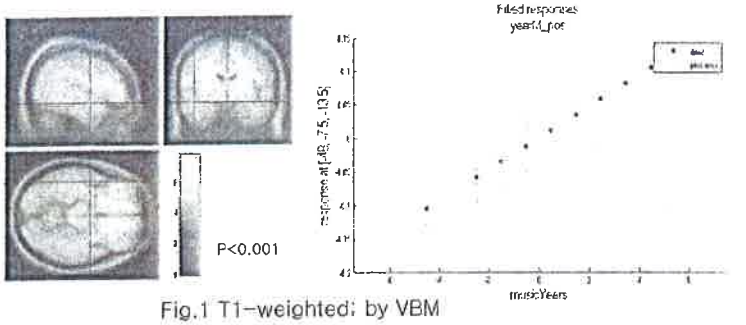


Fig.1 T1-weighted: by VBM

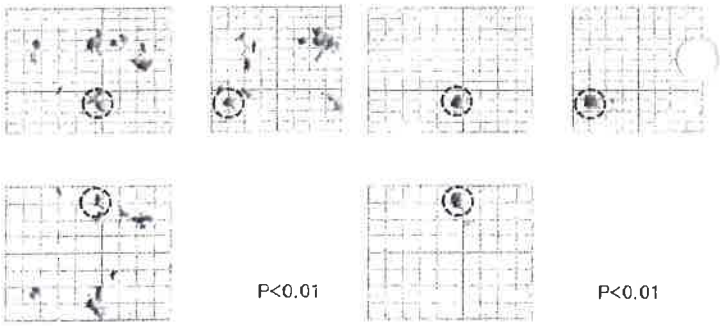


Fig.1 T1-absolute-value vs T1-weighted: by VBM

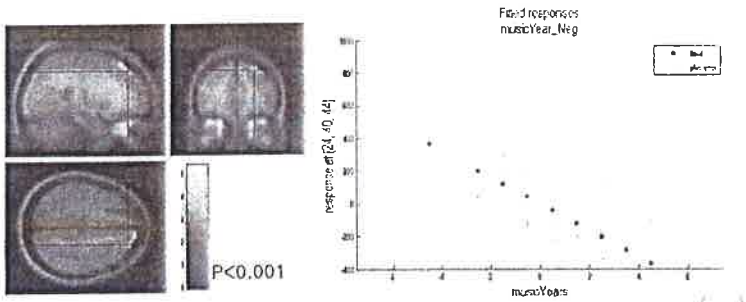


Fig.3 T1-absolute-value

Discussion/Conclusion

1. Grey matter volume changes by musical training were found.
2. T1-absolute-value image includes intrinsic information of cortical structure changes and may reflect higher sensitivities to learning or training effects.
3. T1-absolute-value images are more sensitive to brain structural changes than T1-weighted images.
4. The T1-absolute-value map also supports this by showing that additional information for cortical structural changes can be obtained from T1-absolute-value images.
5. Difference between processing modalities for the same image should be further examined.

Acknowledgements

This research was supported by MEXT-Supported Program for the Strategic Research Foundation at Private Universities, 2014-2018.

謝辞

Functional brain networks reflecting human characteristics

Yul-Wan Sung[1], Yousuke Kawachi[1], Daehun Kang[1], Chihiro Abe[1], Yuki Otomo[1] Seiji. Ogawa[1]

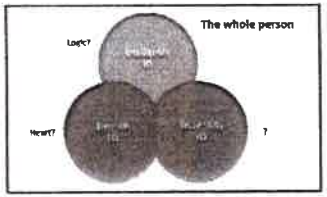
[1]Kansei Fukushi Research Institute, Tohoku Fukushi University, Sendai, Japan

172.09

Background

A human being can be described by diverse human characteristics of feeling, thinking, and behaving. Brain function underlies those characteristics, and thus it is expected to be possible to evaluate the characteristics describing an individual by measuring brain function. Measurement of human characteristics by fMRI usually requires the related tasks to the characteristics but it is very difficult for some characteristics. In this study we attempted:

1) to identify functional brain networks of resting state fMRI corresponding to various psychometric variables reflecting human characteristics by which we can describe an individual comprehensively, 2) to design SVM to estimate those characteristics through MRI data.



Methods

[Subjects]

153 college students: resting state fMRI

[Psychological tests]

A set of 130 psychometric variables (SQ, IQ, EQ) related to social quotients (ability), intelligence quotients and emotion quotients.

Methods

[MRI measurements]

Siemens 3T, Skyra-fit

1. Voxel-based morphometry (VBM)

T1 MPRAGE, 1x1x1 mm^3

2. Resting state fMRI

TR 1s, Sices 34, FA 70, Matrix 64x64, 3.4x3.4x3.4mm^3

Number of volumes 480, MB-EPI sequence

[Data analysis]

(Functional network identification reflecting psychometric variables)

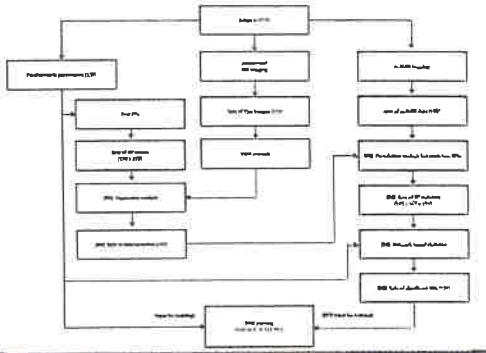
(1) ROI-based network analysis

1) 163 ROIs localized on the basis of AAL template and psychometric variables ($p = 0.05$, corrected), (VBM, SPM)

2) Simple regression analysis for each psychometric variable ($p = 0.005$, corrected), (GraphVar)

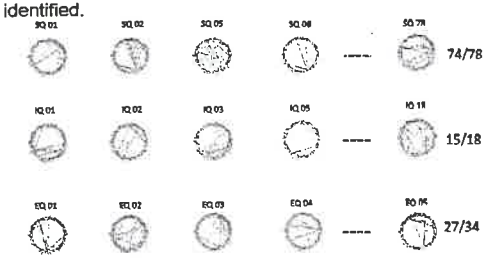
(2) Multiple class Support Vector Machine

Design of 8 classes SVM (LIBSVM)



Results

1. Functional networks (128) for 116 psychometric variables were identified.



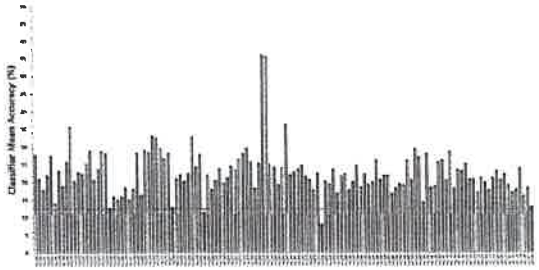
Results

An example of identified networks: a SQ variable of the Positive towards Others.



1. One SVM classifier was designed for each network.
2. 123 SVM classifiers among those for 128 functional networks were significant.
3. 123 SVM classifiers were corresponding to 111 psychometric variables (Fig.1)

(Some of parameters had two classifiers)



Discussion and Conclusion

1. A set of 128 functional networks of cognition/behavior were identified by rs-fMRI, which span a variety of human characteristics explained by psychometric variables.
2. 123 multiple-class SVM classifiers corresponding to 111 psychometric variables were derived.
3. The results demonstrate that we can identify functional areas or networks of the brain not only by tb-fMRI but also by rs-fMRI.
4. They also demonstrates that we can evaluate cognition/behavior and develop biomarkers for a wide variety of human characteristics using the 111 dimensions of the data obtained from a single rs-fMRI scan.
5. The data and classifiers may also be applied to longitudinal studies or studies evaluating educational, training, or career development programs.

Acknowledgements

Supported by MEXT-Supported Program for the Strategic Research Foundation at Private Universities, 2014-2018 .

15th European Congress of Psychology, July 11-14, 2017, Amsterdam

An fMRI study of the relationship between neuroticism and neural responses to infant emotional faces

Katsuko NIWANO[1], Ayahito ITO[2], Motoko TANABE[3], Yosuke SATO[3], Toshikatsu FUJII[2]

1. Faculty of Education , Tohoku Fukushi University, Sendai, Japan
2. Kansei Fukushi Research Institute, Tohoku Fukushi University , Sendai, Japan
3. Faculty of Health Science , Tohoku Fukushi University , Sendai, Japan

Introduction

- Infant facial expressions provide an important cue to elicit emotional and behavioral responses from a caregiver.
- Recent studies revealed personality traits are stable predictors of maternal behavior. However, little is known about the influence of female personality traits on discriminating infant facial expressions.
- It has been reported that lower levels of neuroticism are associated with better cognitive function later in life. We predicted that neuroticism would correlate with neural activations to infant emotional stimuli.
- The purpose of the present study was to investigate neuroticism-related differences in nulliparous females' neural response to infant emotional faces using fMRI.

Methods

【Participants】

55 healthy, right-handed nulliparous females (mean age = 20.2 years, age range = 20–21 years) with no childcare experience.

【Personality assessment】

Neuroticism was measured before the fMRI experiment with the Maudsley Personality Inventory (MPI).

【fMRI acquisition】

3T MRI (MAGNETOM Skyra, Siemens)

SPM 8 (Wellcome Department of Imaging Neuroscience, London, UK)

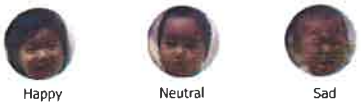
【Region-of-Interest (ROI) analysis】

We performed region of interest (ROI) analyses for the dorsal anterior cingulate cortex (dACC), the fusiform gyrus, and the nucleus accumbens using the MarsBaR software (Brett et al., 2002). Each ROI was anatomically defined and derived from Individual Brain Atlases using the SPM software (IBA SPM) (Alemán-Gómez et al., 2006) implemented in the WFU PickAtlas (Wake Forest University, Winston-Salem, NC) (Maldjian et al., 2003, 2004).

【Stimuli and tasks】



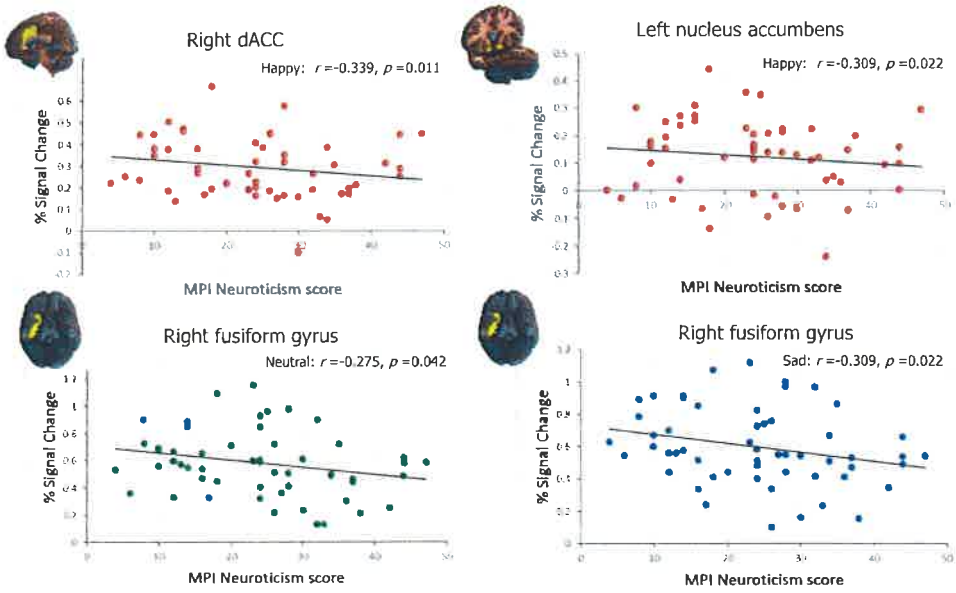
Participants were presented with 72 photographs of unknown four infant faces expressing three kinds of emotions (happy, neutral, and sad) in randomized counter-balanced order, and they were asked to rate each face on an 8-point scale of happy to sad to assess the perceived affect level during the scan.



Examples of infant facial expressions used as stimuli

Results

- The mean score (SD) of the 55 subjects on the neuroticism scores : 24.16 (10.91).
- We carried out correlation analyses of the relationships between the neuroticism scores and the activity of the dACC, the fusiform gyrus, and the nucleus accumbens .
- Neuroticism score negatively correlated with the activities of the right dorsal anterior cingulate cortex (dACC) and the left nucleus accumbens while the subjects viewed happy faces. The score also negatively correlated with the activity of the right fusiform gyrus while viewing neutral faces, and with that of the left fusiform gyrus while viewing sad faces.



Discussion and Conclusions

- The results demonstrated that nulliparous women with lower neuroticism showed increased activation in the dACC and the nucleus accumbens, which are thought to participate in the brain reward system, suggesting that they consider an infant happy face to be a reword.
- Nulliparous women with higher neuroticism exhibited reduced activation in the fusiform gyrus while viewing neutral or sad infant faces probably because it is difficult for them to rate infant ambiguous or negative facial expressions.
- Our findings indicate that in the nulliparous women, the neuroticism scores are well correlated with the activity of the right dACC, left nucleus accumbens, and right fusiform gyrus contingent upon the type of emotion expressed in infant stimuli.

Acknowledgments

This work was supported by Grant-in-Aid for Scientific Research (C) (15K04081 to K.N.) from the Japan Society for the Promotion of Science (JSPS) and MEXT-Supported Program for the Strategic Research Foundation at Private Universities.

Age-related reduction of cognitive dissonance

Ayahito Ito[1], Yousuke Kawachi[1], Iori Kawasaki[2], Toshikatsu Fujii[1]

[1]Kansei Fukushi Research Institute, Tohoku Fukushi University

[2]Department of Behavioral Neurology and Cognitive Neuroscience, Tohoku University Graduate School of Medicine

Introduction

- When individuals are forced to choose between similarly preferable alternatives, a negatively arousing cognitive conflict occurs, and the preference attitudes toward the chosen and rejected alternatives diverges.
- This phenomenon, often referred to as "cognitive dissonance", is of interest in psychological and decision neuroscience research.
- The dorsal anterior cingulate cortex (dACC) is involved in representing the cognitive conflict induced by difficult-choice tasks.
- Previous studies have shown age-related decline of the dACC function. However, whether the heightened activity of the dACC regarding cognitive conflict and choice-induced preference change that occur in young subjects also occur in the elderly is unknown.
- To address this question, we used functional magnetic resonance imaging (fMRI) and a modified free-choice paradigm.

Materials and Methods

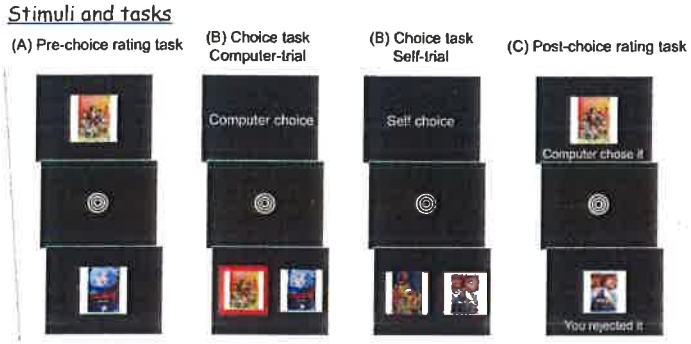
Participants

14 young participants (7 females; mean age 20.29 years)

14 elderly participants (6 females; mean age 65.86 years)

MMSE scores of elderly participants confirmed that they had normal cognitive function (29.06±1.61)

Stimuli and tasks



Rating task (A, C)
During the pre-choice rating task, 192 DVD images were presented successively in randomized order. Each DVD image was presented for 3500 ms, and the subjects were asked to rate their preference for each image on an eight-point scale (1 = not liked at all and 8 = liked very much).

Choice task (B)
During the choice task, a cue indicating the trial to be performed (either a computer-trial or a self-trial) was presented for 1500 ms, and after a brief delay of 500 ms, a pair of DVD images were displayed for 5000 ms.

In the self-trials, the subjects were asked to choose the image that they preferred.

In the computer-trials, the subjects were asked to choose images surrounded by a red square that were randomly chosen by the computer.

The self- and computer-trials were randomly arranged. According to the pre-choice rating scores, pairs of DVD images were determined.

Experimental conditions of the choice task (B)
1) Self-Easy condition, 2) Self-Difficult condition
3) Comp-Easy condition, 4) Comp-Difficult condition (control condition)

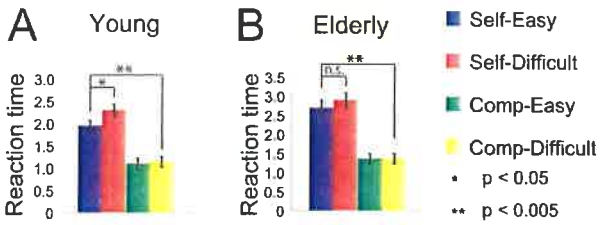
Based on the literature, we classified trials into Easy or Difficult conditions (Izuma et al., 2010).
Easy condition: trials in which one item was rated 5 or more, the other item was rated 4 or less, and the difference in scores was greater than 3 were classified as Easy conditions.

Difficult condition: trials in which both items were rated as 5 or more and the difference between the scores was less than 2 (i.e., 1 or 0) were classified as Difficult conditions.

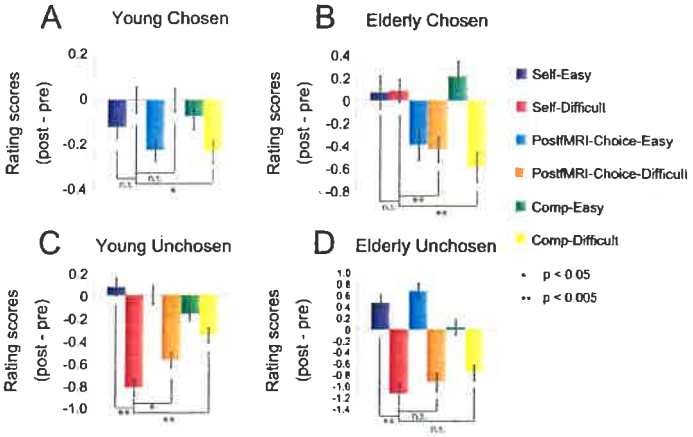
Data acquisition and analysis

3T MRI (MAGNETOM Verio, Siemens)
SPM8 (Wellcome Department of Imaging Neuroscience, London, UK)

Results-Reaction times during the choice task

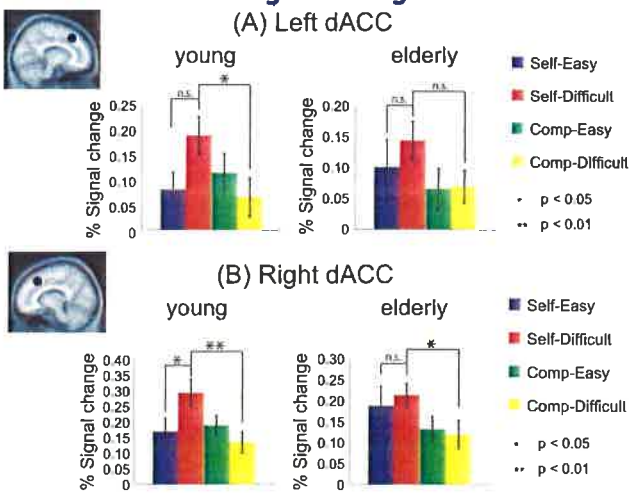


Results-Behavioral data on the preference change



PostfMRI-Choice-Easy and PostfMRI-Choice-Difficult condition (New control condition)
After the post-choice rating task, the participants were asked to indicate their true preferences for alternatives shown in the computer trials during the choice task. For easy and difficult pairs, according to their true preferences, we classified the alternatives (blue and orange colored bars).

Results- % signal change in the dACC



Discussion and conclusion

- Only in young participants, behavioral data confirmed the existence of cognitive dissonance and preference change for the alternatives.
- The imaging data also revealed that the right dACC displayed greater activity for difficult choices than for easy choices only in young participants. We did not observe such effects in the elderly participants.
- These results suggest that elderly people likely feel less cognitive conflict when confronted with difficult choices, and this age-related decrease in cognitive dissonance leads to a reduction in choice-induced preference change.
- If we had not divided the control conditions into Easy and Difficult trials, we might have reported that both elderly and young participants exhibited choice-induced preference change. Thus, our procedure is important to detect genuine "cognitive dissonance".

Acknowledgments
We thank Yul-Wan Sung and Daehun Kang for assistance in collecting and analyzing data. This work was partly supported by the MEXT-Supported Program for the Strategic Research Foundation at Private Universities.

The effect of childcare training on the perception of infant's emotional facial expression

Ayahito Ito[1], Katsuko Niwano[2], Motoko Tanabe[3], Yosuke Sato[3], Toshikatsu Fujii[1]

[1]Kansei Fukushi Research Institute, Tohoku Fukushi University
[2]Faculty of Education , Tohoku Fukushi University
[3]Faculty of Health Science , Tohoku Fukushi University

Introduction

• In many developed countries, the number of infants who experience non-parent childcare is increasing, and the role of preschool teachers is becoming more important. Thus, developing effective curriculums to cultivate preschool teachers is necessary to provide better support for infants.

• However, little attention has been paid to the effects of childcare training on students who study to become preschool teachers.

• As a first step in this research, we used functional magnetic resonance imaging (fMRI) to investigate whether and how childcare training affects brain responses to infants' facial expressions among young females studying to become preschool teachers.

• The main purpose of the present study was to investigate whether and how the amygdalae, the fusiform gyri, and the ventral striatum contribute to reflecting the effects of childcare training on perceptions of infants' facial expressions.

Materials and Methods

Participants

Experimental group
25 young participants who attended a four-week childcare training session (age range, 20-21 years; mean age, 20.13 years)

Control group
21 young participants participants who did not attend the four-week childcare training session (age range, 20-21 years; mean age, 20.14 years)

Stimuli and tasks



24 happy faces, 24 neutral faces, and 24 sad faces were employed as experimental stimuli. The subjects were asked to rate each face based on how happy or sad it was using an 8-point scale.

Examples of stimuli



Happy face Neutral face Sad face

Experimental conditions
• type of facial expression
1. happy condition (left)
2. neutral condition (middle)
3. sad condition (right)
• time point of data collection
1. Before childcare training
2. After the childcare training

We collected behavioral and neuroimaging data before and after the training period for both the experimental and control groups.

Data acquisition and analysis

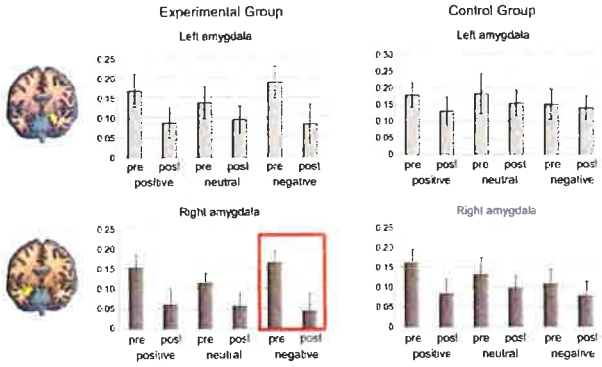
3T MRI (MAGNETOM Skyra, Siemens)
SPM 8 (Wellcome Department of Imaging Neuroscience, London, UK)

Region-of-Interest (ROI) analysis

We performed region of interest (ROI) analyses for the amygdala, the fusiform gyrus, and ventral striatum using the MarsBaR software (Brett et al., 2002). Each ROI was anatomically defined and derived from Individual Brain Atlases using the SPM software (IBASPM) (Alemán-Gómez et al., 2006) implemented in the WFU PickAtlas (Wake Forest University, Winston-Salem, NC) (Maldjian et al., 2003, 2004).

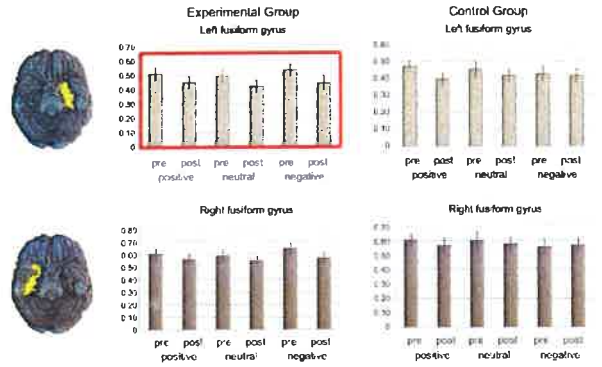
The purpose of this ROI analysis was to elucidate whether the activity in each ROI reflected the effects of the childcare training.

Results- % signal change in the amygdalae



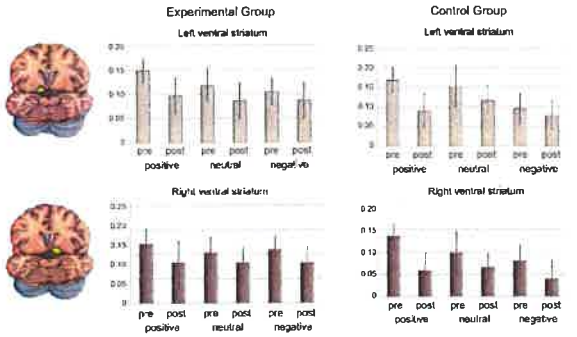
The percentage signal change in the sad condition from the "post" was significantly lower than from the "pre" in the experimental group only.

Results- % signal change in the fusiform gyri



For the left fusiform gyrus in the experimental group, we found significant main effect of the time point of the data collection.

Results- % signal change in the ventral striatum



We found no significant main effects.

Discussion and conclusion

• The present study investigated whether and how childcare training affected brain responses to infants' facial expressions among nulliparous young females studying to become preschool teachers.

• In the experimental group only, a direct comparison of the activity of the right amygdala between the first and second rating tasks revealed a significant reduction specifically for sad faces. This finding suggest that the experimental-group-specific reduction of the right amygdala activity was associated with intense childcare training.

• The left fusiform gyrus exhibited a valence-independent reduction in activity in the second fMRI scan. Perhaps the function of the left fusiform gyrus would be sophisticated by multiple interactions with infants during childcare training. As for the VS, we did not find any significant effects and group differences in the analyses and childcare-training-related activity change. One possible explanation for this is that habituation effect does not easily occur in the VS compared with in the amygdala.

Acknowledgments
We thank Yul-Won Sung for his help in collecting the data. This work was partly supported by a Grant-in-Aid for Scientific Research C# (15K04081 to K.N.) from the Japan Society for the Promotion of Science and MEXT-Supported Program for the Strategic Research Foundation at Private Universities.

The 31th International Congress of Psychology, July 24-29, 2016, Yokohama

Relationship between regional brain responses to infant faces and personality traits in young female adults

Katsuko NIWANO[1], Ayahito ITO[2], Motoko TANABE[3], Yosuke SATO[3], Toshikatsu FUJII[2]

1. Faculty of Education , Tohoku Fukushi University, Sendai, Japan
2. Kansei Fukushi Research Institute, Tohoku Fukushi University , Sendai, Japan
3. Faculty of Health Science , Tohoku Fukushi University , Sendai, Japan

Introduction

- Infant facial expressions provide an important cue to elicit emotional and behavioral responses from a caregiver.
- Recent studies revealed personality traits are stable predictors of maternal behavior. However, little is known about the influence of female personality traits on discriminating infant facial expressions.
- The orbitofrontal cortex (OFC) and ventromedial prefrontal cortex (vmPFC) are thought to play an important role in the modulation of social behavior.
- The purpose of the present study was to investigate the relationship between OFC and vmPFC responses to infant emotional faces and individual differences of conscientiousness, which is one of the Big Five personality traits, in nulliparous young women.

Methods

【Participants】

55 healthy, right-handed nulliparous females (mean age = 20.2 years, age range = 20–21 years) with no childcare experience.

【Personality assessment】

All subjects completed the Japanese adaption of 70-item Five Factor Inventory (2008), which yields independent measures of conscientiousness, neuroticism, extraversion, openness to experience, and agreeableness.

【fMRI acquisition】

3T MRI (MAGNETOM Skyra, Siemens)

SPM 8 (Wellcome Department of Imaging Neuroscience, London, UK)

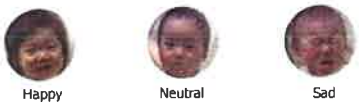
【Region-of-Interest (ROI) analysis】

We performed region of interest (ROI) analyses for the dorsal anterior cingulate cortex (dACC), the insula, the OFC, and vmPFC using the MarsBaR software (Brett et al., 2002). Each ROI was anatomically defined and derived from Individual Brain Atlases using the SPM software (IBA SPM) (Alemán-Gómez et al., 2006) implemented in the WFU PickAtlas (Wake Forest University, Winston-Salem, NC) (Maldjian et al., 2003, 2004).

【Stimuli and tasks】



Participants were presented with 72 photographs of unknown four infant faces showing various emotions (happy, neutral, and sad) in randomized counter-balanced order, and they were asked to rate each face on an 8-point scale of happy to sad to assess the perceived affect level during the scan.

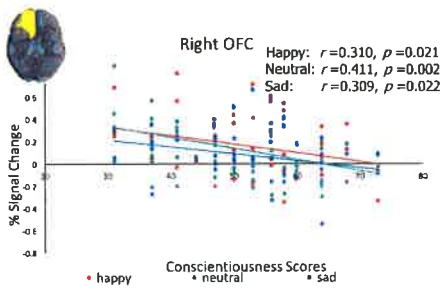


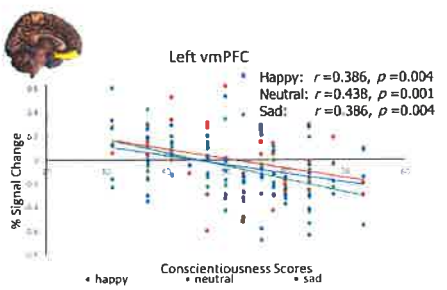
Examples of infant facial expressions used as stimuli

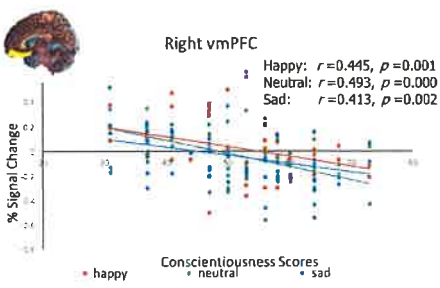
Results

- The mean scores (SD) of the 55 subjects on the conscientiousness scores : 51.58 (10.94).
- We carried out correlation analyses of the relationships between the conscientiousness scores and the activity of the bilateral OFC and the bilateral vmPFC.
- The conscientiousness scores were negatively correlated with the activity of both the bilateral OFC and the bilateral vmPFC while viewing any kinds of emotional infant faces.









Discussion and Conclusions

- Our data showed the significant negative correlations between individual scores on conscientiousness and both the bilateral OFC and the bilateral vmPFC activation in response to infant emotional faces.
- Previous fMRI studies have found that maternal-motivation-specific brain regions include the OFC and the vmPFC which relate to affect, reward, and decision making.
- The people with high conscientiousness scores are sensitive to discipline, organization and achievement orientation (Goldberg, 1993). The participants with high conscientiousness might process infant stimuli composedly and show relatively low activations of the OFC and the vmPFC.
- Our results suggest that exposure to infant emotional expression evokes increased activation of the OFC and the vmPFC in nulliparous young women with low conscientiousness scores.

Acknowledgments

This work was supported by Grant-in-Aid for Scientific Research (C) (15K04081 to K.N.) from the Japan Society for the Promotion of Science (JSPS) and MEXT-Supported Program for the Strategic Research Foundation at Private Universities.

The 39th Annual Meeting of JNS, July 20-22, 2016, Yokohama

Behavioral inhibition system relates to the responses of the dorsal anterior cingulate cortex and the orbitofrontal cortex to infant emotional faces

行動抑制システムと乳児の顔に対する背側前帯状皮質及び眼窩前頭皮質の反応の関連

Katsuko NIWANO[1], Ayahito ITO[2], Motoko TANABE[3], Yosuke SATO[3], Toshikatsu FUJII[2]

庭野賀津子[1] ・ 伊藤文人[2] ・ 田邊素子[3] ・ 佐藤洋介[3] ・ 藤井俊勝[2]

1 Faculty of Education , Tohoku Fukushi University / 東北福祉大学教育学部

2 Kansei Fukushi Research Institute, Tohoku Fukushi University / 東北福祉大学感性福祉研究所

3 Faculty of Health Science , Tohoku Fukushi University / 東北福祉大学健康科学部

Introduction

- Infant facial expressions provide an important cue to elicit emotional and behavioral responses from a caregiver.
- Previous fMRI studies have found maternal neural responses to emotional infant stimuli in some brain regions, such as ACC, insula and OFC.
- The purpose of the present study was to investigate the relationship between brain responses to infant emotional faces and individual differences in motivational tendencies in nulliparous women.

Methods

【Participants】

55 healthy, right-handed nulliparous females (mean age = 20.2 years, age range = 20–21 years) with no childcare experience.

【Personality assessment】

All subjects completed the Japanese adaption of the Behavioral Inhibition System (BIS) / Behavioral Approach System (BAS) scales to determine individual differences in motivational tendencies.

【fMRI acquisition】

3T MRI (MAGNETOM Skyra, Siemens)

SPM 8 (Wellcome Department of Imaging Neuroscience, London, UK)

【Region-of-Interest (ROI) analysis】

We performed region of interest (ROI) analyses for the dorsal anterior cingulate cortex (dACC), the insula, and the orbitofrontal cortex (OFC) using the MarsBaR software (Brett et al., 2002). Each ROI was anatomically defined and derived from Individual Brain Atlases using the SPM software (IBA SPM) (Alemán-Gómez et al., 2006) implemented in the WFU PickAtlas (Wake Forest University, Winston-Salem, NC) (Maldjian et al., 2003, 2004).

【Stimuli and tasks】



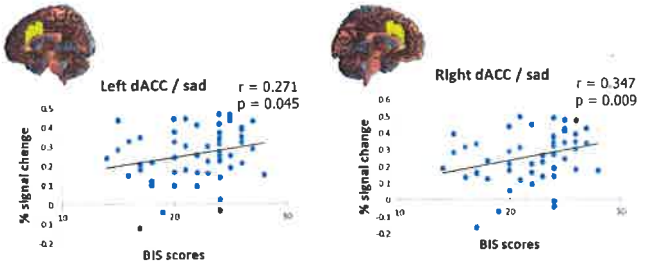
Participants were presented with 72 photographs of unknown four infant faces showing various emotions (happy, neutral, and sad) in randomized counter-balanced order, and they were asked to rate each face on an 8-point scale of happy to sad to assess the perceived affect level during scan.

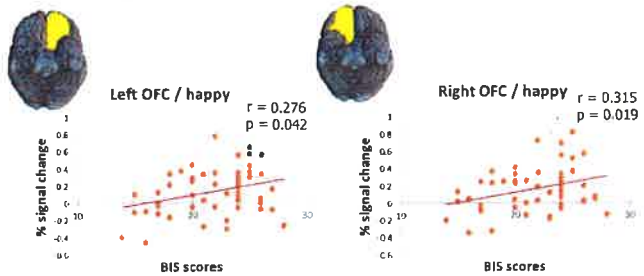


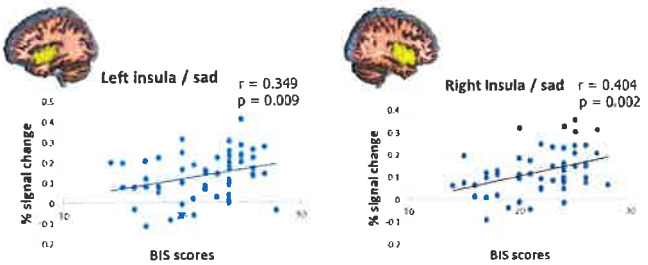
Examples of infant facial expressions used as stimuli

Results

- The mean scores (SD) of the 55 subjects on the BIS/BAS scales: 21.93 (3.5) for BIS, and 40.2 (4.7) for BAS.
- We carried out correlation analyses of the relationships between the BIS/BAS scores and the activity of (1) the dACC, (2) the insula, and (3) the OFC.
- The BIS scores were positively correlated with the activity of the bilateral dACC and the bilateral insula while viewing infant sad faces.
- The BIS scores were positively correlated with the activity of the bilateral OFC while viewing infant happy faces.
- No correlations were found between the BAS scores and the activity of these regions.







Discussion and Conclusions

- The results indicate that the BIS scores are well correlated with the activity of the dACC and the insula (viewing infant sad faces), and the OFC (viewing infant happy faces) of the nulliparous young women in response to the emotional infant stimuli.
- It is conceivable that people with high BIS scores are sensitive to signals of no reward, punishment, and novelty (Carver & White, 1994).
- One potential explanation for the greater activation of the dACC and the insula while viewing a sad infant face is that the dACC and the insula may play a role of processing negative infant affection, and the tendency is particularly strong among the nulliparous women with high BIS scores.
- The OFC has been considered as one of component regions of the brain's 'reward system'. Our findings suggest that the nulliparous women with high BIS scores tend to recognize a happy infant face as reward.

Acknowledgments

This work was supported by Grant-in-Aid for Scientific Research (C) (15K04081 to K.N.) from the Japan Society for the Promotion of Science (JSPS) and MEXT-Supported Program for the Strategic Research Foundation at Private Universities.

ICP 2016 YOKOHAMA

The 31st International Congress of Psychology

July 24-29, 2016
YOKOHAMA, JAPAN

PROGRAM

Congress Theme
Diversity in Harmony : Insights from Psychology



http://www.icp2016.jp/

performance: The Japanese version of Dickman Impulsivity Inventory
Yamamoto, Akira (Japan); Furumitsu, Isato; Imada, Sumio

Tuesday, July 26, 09:30 – 10:30
Exhibition Hall Poster4

PS26A-08-393 Identity developmental trajectories in adolescence and young adulthood: based on the five dimensional model
Hatano, Kai (Japan); Sugimura, Kazumi

PS26A-08-394 Is ambiguity tolerance an important factor that can distinguish between depression and anxiety?
Tomono, Takanari (Japan)

PS26A-08-395 Interpersonal sensitivity and privileged self as a risk factor for depression (1) :Re-examination of the factor structure of the Interpersonal Sensitivity/Privileged Self Scale
Muranaka, Masaki (Japan); Yamakawa, Itsuki; Sakamoto, Shinji

PS26A-08-396 Reliability and validity of the Japanese version of the ABbreviated Impulsiveness Scale
Kobashi, Mariko (Japan); Ida, Masanori

PS26A-08-397 Does defensive pessimism help anxious people to communicate with strangers? Defensive pessimism and state anxiety interact to predict the behavioral intention for smooth communication
Shimizu, Haruka (Japan); Nakashima, Ken'ichiro; Morinaga, Yasuko

PS26A-08-398 Transformative Process Concerning Hypervigilant Narcissism in University Students
Koya, Mayumi (Japan); Takano, Yasuyo

PS26A-08-399 Socioeconomic Status and Life Satisfaction Among Chinese Adolescents: Analyses of Self-esteem as a Mediator and Optimism as a Moderator
Zhou, Zongkui (China (People's Republic of China)); Chen, Wu

PS26A-08-400 Having features of both eating quickly and type A behavior pattern, it is a risk factor for obesity
Ogawa, Sayaka (Japan); Saigo, Tatsuo; Takeoka, Atsushi; Hamaguchi, Toyohiro; Shirabe, Susumu; Tayama, Jun

PS26A-08-401 Competitiveness as the reason Impulsiveness in non-linear psychology (Five-Factor Personality Model)
Basimova, Polina (Russia); Basimov, Mikhail

PS26A-08-402 Psychological features of professional qualities formation in pilots
Mukeyeva, Karina (Kazakhstan); Munaidarova, Bakhyt; Zhexembayeva, Zhadra; Oilybayeva, Laura; Taurbekova, Ainur; Abdulkarimova, Glyussya; Tlenbayeva, Aisha; Naurzalina, Danna; Li, Alexina

PS26A-08-403 Analysis of the Relationship Between Time Perspective and Difficulties in Emotional Regulation with Structural Equation Modeling among Turkish Undergraduate Students.
Bürhan, Pinar (Turkey); Bayram, Nuran

PS26A-08-404 The Relationship of Fear of Anger to Self-compassion and Self-criticism.
Hayashi, Tatsuya (Japan)

PS26A-08-405 Comparison of Emotion Regulation between high and low perceived criticism groups in Japanese university students
Naruse, Mayu (Japan); Jinnai, Ayane; Horiuchi, Satoshi; Sakano, Yuji

PS26A-08-406 The mediation effect of loneliness between negative affectivity and sexual problem in university students.
Jin, Eunju (Korea (Republic of Korea)); Hwang, Suk-hyun

PS26A-08-407 Exploratory factor analysis study : Relationship of Ambivalence over emotional expressiveness with emotion and personality variables
A-reum, Lee (Korea (Republic of Korea)); Hwang, Samuel S

PS26A-08-408 Interactive effects of interoceptive awareness and finitude salience on empathy
Takahama, Sachiko (Japan)

PS26A-08-409 Delay discounting: a changing state or a stable personality trait?
Malesza, Marta (Poland)

PS26A-08-410 Effects of the Clay-Work Combined with the Listening to the Music on the Mental States
Yamawaki, Mayumi (Japan)

PS26A-08-411 The effects of the quality of social relationships and emotion regulation ability on the happiness of introvert individuals
Gutierrez Cobo, Maria J (Spain); Cabello, Rosario; Fernandez- Berrocal, Pablo

PS26A-08-412 Development of the Japanese version of the Humiliation Inventory (HI-J)
Numata, Mami (Japan); Matsui, Yutaka (Japan); Hartling, Linda M (United States of America)

PS26A-08-413 Measuring Mindfulness in Daily Life
Blanke, Elisabeth S (Germany); Brose, Annette

PS26A-08-414 Reliability and validity of the Japanese version of the Trypophobia Questionnaire (TQ-J)
Imaizumi, Shu (Japan); Furuno, Manami; Hibino, Haruo; Koyama, Shinichi

PS26A-08-415 Does the non-dominant hand increase the frequency of draws in rock-paper-scissors?
Kushizaki, Masashi (Japan)

PS26A-08-416 The theoretic and empirical study of youth self-assessment
Toxanbayeva, Nurgul (Kazakhstan); Turdaliyeva, Sholpan; Smatova, Klara; Abisheva, Elmira; Alimbayeva, Saule; Ussenova, Sandugash

PS26A-08-417 The interaction of personality traits and environmental factors in the prediction of depression in Russian young adults
Kuznetsova, Valeriya (Russia); Knyazev, Gennady; Dorosheva, Elena; Bocharov, Andrey; Savostyanov, Alexander

PS26A-08-418 Specifics in Development of the Legal Consciousness of Law Students
Lukashova, Svetlana (Kazakhstan); Omirzhanov, Yesbol; Chongarov, Yerzhan; Baigelova, Nurgul

PS26A-08-419 Correlations between the brain responses of nulliparous females when viewing infants' facial expressions and their personality
Tanabe, Motoko (Japan); Niwano, Katsuko; Ito, Ayahito; Sato, Yosuke; Fujii, Toshikatsu

PS26A-08-420 Effects of collage execution in a group and subsequent sharing activity on participants' mood change and affiliative behavior
Takeuchi, Itsuko (Japan); Terasaki, Masaharu; Takei, Yuko; Kadota, Masako

PS26A-08-421 Impaired working memory in patients with borderline personality disorder: An ERPs study
Yi, Jinyao (China (People's Republic of China)); Liu, Ying; Zhong, Mingtian; Yao, Shuqiao

Tuesday, July 26, 15:30 – 16:30
Exhibition Hall Poster4

PS26P-12-396 Trait Respect Correlates Positively with Prosocial Behavior in Japanese University Students
Muto, Sera (Japan)

PS26P-12-397 PREDICTORS OF TREATMENT DROPOUT IN DEPRESSED OUTPATIENTS: THE ALTERNATIVE FIVE

31st International Congress of Psychology (ICP2016) | July 24-29, 2016, Yokohama

Correlations between the brain responses of nulliparous females when viewing infants' facial expressions and their personality

Motoko Tanabe[1], Katsuko Niwano[2], Ayahito Ito[3], Yosuke Sato[1], Toshikatsu Fujii[3]

[1]Faculty of Health Science, Tohoku Fukushi University
[2]Faculty of Comprehensive Welfare, Tohoku Fukushi University
[3]Kansei Fukushi Research Institute, Tohoku Fukushi University

Introduction

- Several fMRI studies have explored mother's brain response when viewing infants' facial expressions, but there are few studies focusing on young female's brain response.
- The Temperament and Character Inventory (TCI) was a personality measure originally developed by Cloninger et al. (1993).
- The purpose of this study was to investigate the correlations between the brain responses of young females when viewing infants' facial expressions and seven dimensional scores of the TCI.

Methods

【Participants】

55 healthy, right-handed nulliparous females (mean age = 20.2 years, age range = 20–21 years) with no childcare experience.

【Personality assessment】

All subjects completed the Japanese version of the Temperament and Character Inventory (TCI), which yields seven dimensional scores.

【fMRI acquisition】

3T MRI (MAGNETOM Skyra, Siemens)
SPM 8 (Wellcome Department of Imaging Neuroscience, London, UK)

【Region-of-Interest (ROI) analysis】

We performed region of interest (ROI) analyses for the amygdala , the orbitofrontal cortex (OFC), and the ventromedial prefrontal cortex (vmPFC) using the MarsBaR software (Brett et al., 2002). Each ROI was anatomically defined and derived from Individual Brain Atlases using the SPM software (IBASPM) (Alemán-Gómez et al., 2006) implemented in the WFU PickAtlas (Wake Forest University, Winston-Salem, NC) (Maldjian et al., 2003, 2004).

【Stimuli and tasks】



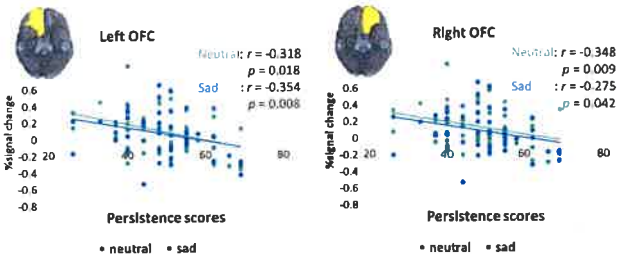
Participants were presented with 72 photographs of unknown four infant faces showing various emotions (happy, neutral, and sad) in randomized counter-balanced order, and they were asked to rate each face on an 8-point scale of happy to sad to assess the perceived affect level during the scan.

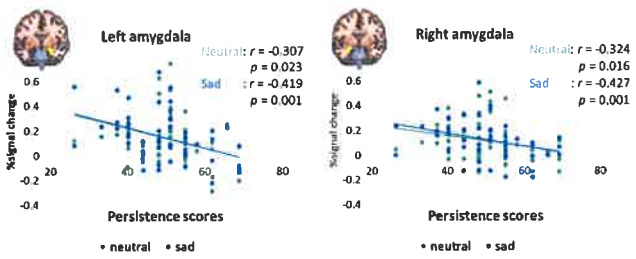


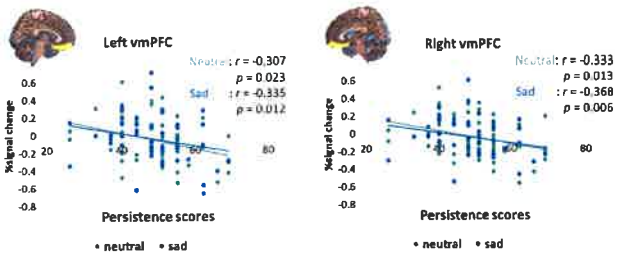
Examples of infant facial expressions used as stimuli

Results

- We carried out correlations analyses of the relationships between seven dimensional scores and the activations (1) the amygdala, (2) the OFC, and (3) the vmPFC.
- During the viewing of infants' sad and neutral faces, significant negative correlations were found between persistence scores, one of the TCI, and the responses of bilateral amygdala, bilateral OFC, and bilateral vmPFC.
- No significant correlations were found between the persistence scores and the activity these regions while the viewing of infants' happy faces.







Discussion and Conclusions

- The results showed that persistence scores in the TCI were negatively correlated with the activity of the amygdala, the OFC, and the vmPFC, while the subjects viewed sad and neutral faces.
- Previous studies have shown that the response of amygdala was related to negative emotion (Britton et al., 2008). The activation of the OFC was associated with the maternal positive mood (Nistschke et al., 2004). The response of the vmPFC was associated with sympathy to others (Janowski et.al., 2012).
- Our results suggest that patient people inhibit the activation of emotion-related regions when viewing sad faces.

Acknowledgments

This work was supported by Grant-in Aid for Scientific Research (C) (15K01428 to M.T. and 15K04081 to K.N.) from the Japan Society for the Promotion of Science (JSPS) and MEXT-Supported Program for the Strategic Research Foundation at Private Universities.

The effect of wearing a medical mask and sunglasses on perceiver's impression

Toshikatsu Fujii[1], Ayahito Ito[1], Rob Jenkins[2], Jet Sanders[2], Kazuki Yoshida[3], Yui Murakami[4], Shinya Sakai[4], Motoko Tanabe[5]

[1]Kansei Fukushi Research Institute, Tohoku Fukushi University
[2]Department of Psychology, University of York
[3]Department of Functioning and Disability, Faculty of Health Science, Hokkaido University
[4]Division of Health Sciences, Graduate School of Health Sciences, Hokkaido University
[5]Faculty of Health Science , Tohoku Fukushi University

Introduction

• Shading facial parts such as eyes, nose, or mouth is common practice in contemporary society. Face mask protects our noses and mouths against virus and pollen dust and sunglasses protect our eyes against sunlight (Horii 2014; Brown 2015).

• Previous psychological studies have investigated the effect of face mask and sunglasses on facial impression (Miyazaki and Kawahara, 2016; Terry et al., 1989).

• However, it remains largely unknown how the mask and sunglasses affect facial impression.

• In the present study, we investigated the effects of these items on 1) attractiveness, 2) trustworthiness, and 3) dominance of others' faces.

Materials and Methods

Participants

36 students of Tohoku Fukushi University (18 females; age range, 20-22 years; mean age, 20.75 years). After the subjects received a detailed description of the study, they provided their written informed consent in accordance with the Declaration of Helsinki, and the guidelines approved by the Ethical Committee of Tohoku Fukushi University. There was no significant difference in age ($t(34) = 1.085$, $p = 0.286$) between the female and male subjects.

Stimuli and tasks



naked condition　mask condition　sunglasses condition

Stimuli

Three sets each containing 20 female and 20 male naked faces, 20 female and 20 male faces with face mask, and 20 female and 20 male faces with sunglasses, and each set containing faces of 120 individuals.

Task

The experiment consisted of three tasks: an attractiveness rating, a trustworthiness rating, and a dominance rating tasks. The photographs were randomly presented using Psychopy2 (version 1.82) (Peirce, 2007, J Neurosci Methods; Peirce, 2009, Front Neuroinform).

The subjects were presented each photographs one at a time and asked to rate how attractive it was in the attractiveness rating task (1: most unattractive, 7: most attractive), how trustworthy it was in the trustworthiness rating task (1: most untrustworthy, 7: most trustworthy), and how dominant it was in the dominance rating task (1: most non-dominant, 7: most dominant) using 7-point Likert-scale.

Analysis

First, we divided female and male faces into two groups based on the scores of naked faces using median-split procedure.

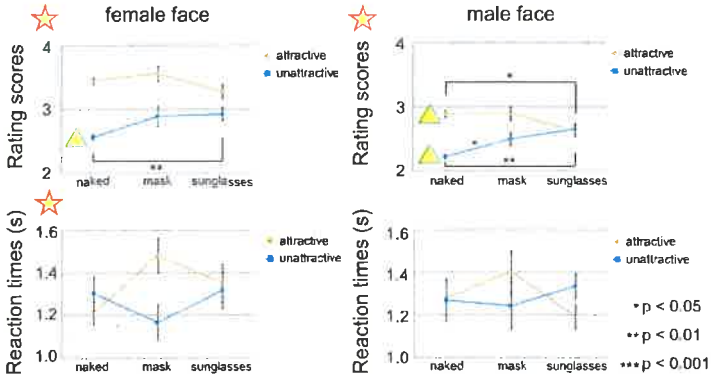
1. Attractive group and Unattractive group
2. Trustworthy group and Untrustworthy group
3. Dominant group and Non-dominant group

As for the rating scores and reaction times, we then conducted two-way repeated-measures analysis of variances (ANOVAs) with the type of the item (none, face mask and sunglasses) as a within-subject factor and the group difference (high group and low group) as a between-subject factor.

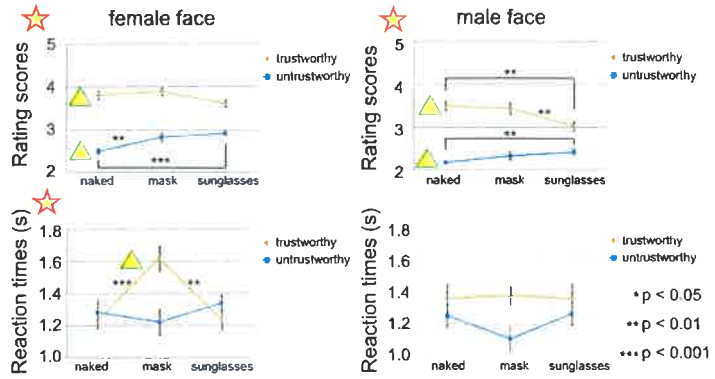
When we found significant interaction in the above two-way ANOVA (indicated by ☆), we conducted one-way ANOVAs with the type of the item (none, face mask and sunglasses) as the within-subject factor when interaction was significant.

When we found significant effect in the above one-way ANOVA (indicated by △), we conducted post-hoc t-tests with Bonferroni correction.

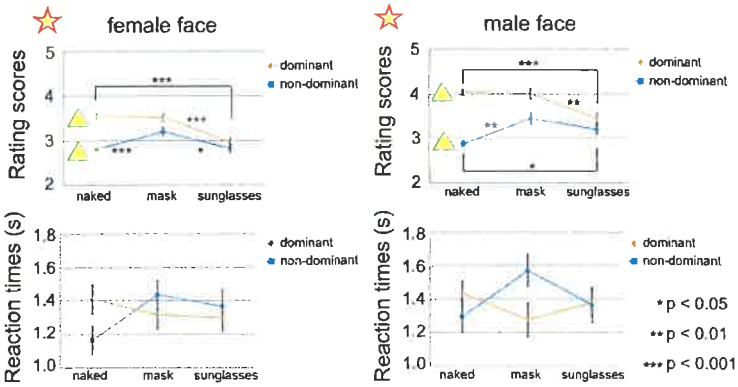
Results- Attractiveness



Results- Trustworthiness



Results- Dominance



Discussion and conclusion

• As for the attractiveness, the present results showed that wearing sunglasses increased facial attractiveness of unattractive faces irrespective of gender of face. The face mask increased the attractiveness of unattractive female faces.

• As for the trustworthiness, the present results showed that wearing sunglasses increased facial trustworthiness of untrustworthy faces irrespective of gender of face. The face mask increased the trustworthiness of untrustworthy female faces. Intriguingly, wearing sunglasses decreased facial trustworthiness of trustworthy male faces.

• As for the dominance, the present results showed that wearing facial mask increased facial dominance of non-dominant faces irrespective of gender of face. Intriguingly, wearing sunglasses decreased facial dominance of dominance faces irrespective of gender of faces.

• These results highlight the effects of facial mask and sunglasses on facial impression and suggest that these items play important role in the contemporary society beyond the original purposes.

E-mail : sung@tfu-mail.tfu.ac.jp

Interaction between high and low level areas and the temporal window for repetition suppression

Yul-Wan Sung[1], Uk Su Choi[2], Seiji Ogawa[1]

[1]Kansei Fukushi Research Institute, Tohoku Fukushi University, Sendai, Japan, [2]Neuroscience research institute, Inchon, Korea, Republic of

Introduction

The effect of perceptual expectation[1] on the attenuation of stimulus-induced neuronal response by repeated stimulation (repetition suppression) proposes that repetition suppression phenomenon is attributable to top-down modulation. However, in the top-down modulation systematic factors such as what high level areas are involved or temporal window the perceptual expectation is effective on the suppression phenomenon were not shown. To clarify those factors we used two short and long inter-stimulus intervals for the perceptual expectation paradigm of paired stimulation.

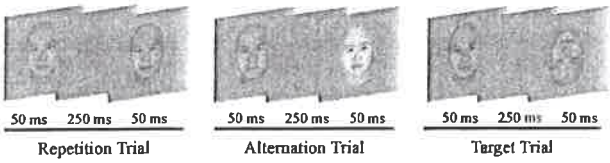
Method

[Subjects] Eleven subjects participated in the study. This study was approved by our Institutional Review Boards.

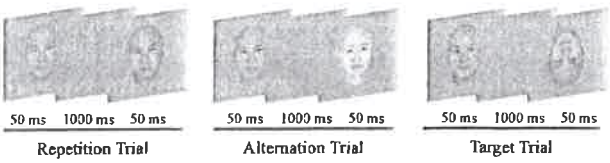
[Stimulus Design] A mixed block design: event-related design in stimulus blocks. Three trial conditions: repetition trial, alternation trial and target trial. Trials paired stimuli of face images with inter-stimulus interval (ISI). On-time of each image: 50ms. Repetition trial: a pair of two identical images. Alternation trial: a pair of different face images. Target trial: a pair of two identical images, the second face image with inverted one of the first. The main experiment: two experimental runs, ISI, 250ms or 1000ms. Each experimental run: repetition block, alternation block. Each block: repetition, alternation and target trials. Each block: 20 trials. The ratio of each trial in a block: [repetition block] 60% repetition trials (Rr), 20% alternation trials (Ra) and 20% target trials [alternation block] 20% repetition trials (Ar), 60% (Aa) alternation trials and 20% target trials.

[MRI measurment] 3-Tesla MRI scanner (Siemens Verio, German). Functional images: Gradient Echo (GE) single-shot echo planar image (EPI) sequence (TR = 2000ms, TE = 30ms, in-plane resolution = 3.4 x 3.4 mm2, slice thickness = 3 mm).

Exp1: ISI 250 ms

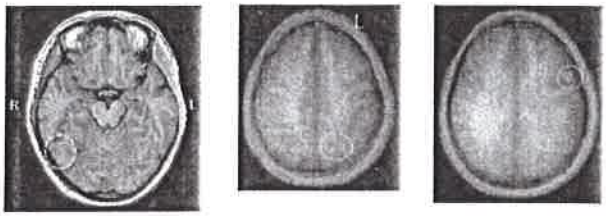


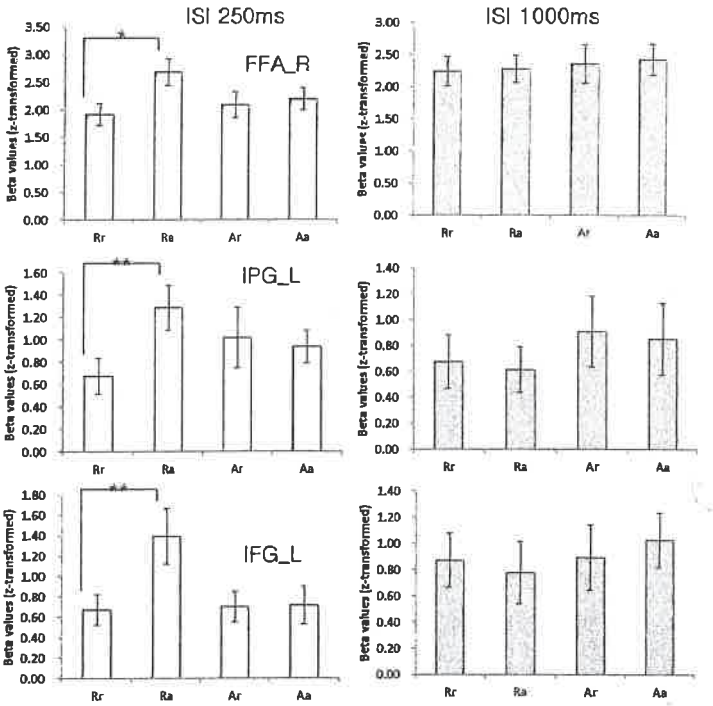
Exp2: ISI 1000 ms



Results

Brain areas responding to stimulus trials were found in occipital, temporal, parietal and frontal lobes with the contrast of all trial conditions versus the rest by whole brain analysis. Among these the right (FFA_R), the left inferior parietal gyrus (IPG_L) and the left inferior frontal gyrus (IFG_L) showed repetition suppression only for repetition block at 250ms ISI ($p = 0.01$, $p = 0.001$, $p = 0.001$), but no significant differences at 1000 ms ISI.





Conclusion

1. Repetition suppression/top-down modulation fade out at 1000 ms.
2. Two high-level areas are involved in repetition suppression related to perceptual expectation.

References

[1] Summerfield et al, Neural repetition suppression reflects fulfilled perceptual expectations. *Nat. Neurosci.* **11**, 1004–1006 (2008).

Acknowledgements

This research was supported by MEXT-Supported Program for the Strategic Research Foundation at Private Universities, 2014–2018.

A challenge for sub-millisecond fMRI

JSMRM 2016
PDF-043

Yul-Wan Sung[1], Daehun Kang[1] and Seiji Ogawa[1]
[1]*Kansei Fukushi Research Institute, Tohoku Fukushi University, Sendai, Japan*

Introduction

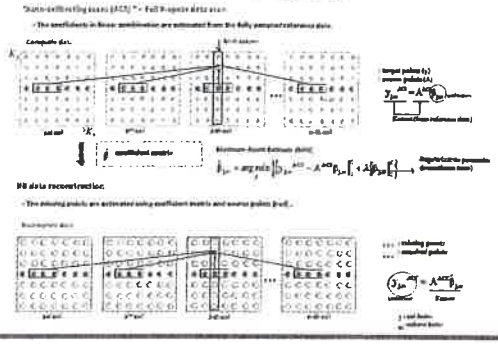
As advances of MRI technologies both in hardware and software, high spatial resolution imaging of hundred micrometer order came to be available. In the same way, temporal resolution also has been advanced. Whole brain acquisition in half a second came to be available by fast imaging technologies such as the Multiband EPI sequence. With inversing imaging technology even faster imaging up to several tenth milliseconds is possible though some deterioration of image quality should be tolerated.
In this study we are further challenge to get much faster imaging up to sub-millisecond.

Contents
(1) Inverse imaging technology: Principle of inverse imaging
(2) [illegible]ing sequence of TR 800 us
(3) Comparison of image quality between full k-space and INI for several conditions
(4) Examination of dynamic signal changes on the INI images
(5) Examination of dynamic signal changes on the INI images
(6) Summary

Methods

INI Reconstruction Inverse imaging technology: Principle of inverse imaging

Estimation of fitting coefficients in K-INI



Results

- **Pulse sequence**



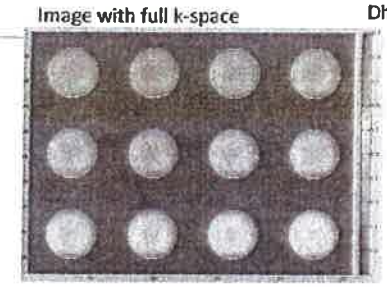
Full K-space TR 200ms

Full K-space TR = 200 ms
INI TR = 800 us
TE = 2.0, 2.8, 3.6, ... , 10.8 msec

Image reconstructed by 2D k-
INI method
- INI test within a k-space
- I[illegible]on.

Comparison of image quality

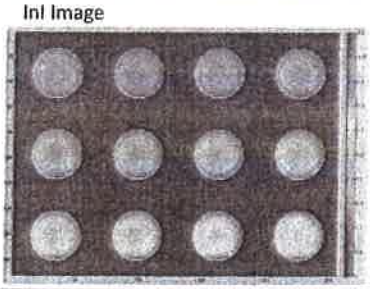
Image with full k-space



Difference Image between full k-space and INI



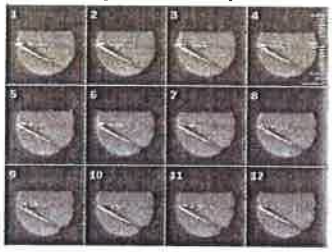
INI Image



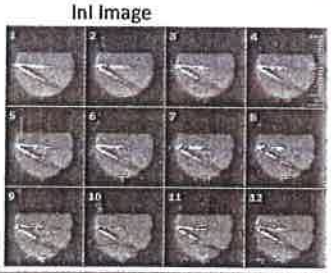
Summary
(1) INI images reproduce quite faithfully the original image of full k-space.
(2) The boundary in the difference images shows insufficient image quality for INI images.
(3) INI images reveal similar image quality to the original full k-space image except for the boundary.
(4) Dynamic signal changes can be detected on the INI images with sub-millisecond sampling time.
(5) The site in which dynamic signal changes occur is not precise.

Examination of dynamic signal

Image with full k-space



INI Image



Discussion and Conclusion

1. The results demonstrate that acquiring image with sub-millisecond sampling rate is possible.
2. Further improvement of image quality is needed especially for measuring dynamic signal changes.
3. One of the methods to improve the image quality is to add additional sampling lines, which will be a trade-off with temporal resolution.

Acknowledgements: This study was supported by MEXT-Supported program for the Strategic Research Foundation at Private Universities, 2014-2018, and JSPS KAKENHI Grant Number 26350995.

JSMRM 2016
PDF-014

Comparison of voxel-based morphometry (VBM) analysis and absolute T1 value analysis

Daehun Kang, Yul-Wan Sung, and Seiji Ogawa
Kansei Fukushi Research Institute, Tohoku Fukushi University, Sendai, Japan

Purpose

- **Cortical structural information** of the human brain
  - has been known to be related with the **plasticity change**.
- **Voxel-based morphometry (VBM) based on T1-weighted images**
  - T1-weighted images has been used for anatomical imaging
  - Easy to obtain it by a single scan (usually, MPRAGE or FLASH pulse sequence)
  - However, it is not appropriate to reflect intrinsic characteristics of cortical structure.
- **T1 absolute value** (T1 map) can reflect the change in tissue (Mezer, A., et al., 2013).
- Purpose
  - To compare the sensitivity from T1-weighed image and T1 map when evaluating the brain plasticity change through anatomical quantity

Methods

- Data measurement
  - 3T MRI (Skyra-fit, Siemens)
  - T1-weighted imaging by 3D MPRAGE pulse sequence
    - 1 mm^3 isotropic voxel
  - T1 imaging by GRE pulse sequence with two different TRs
    - 2 mm^3 isotropic voxel
    - corrected by B1+ map
    - (obtained by double angle method)
- Subjects
  - 24 college students trained for wind musical instruments
  - Mean of training years (8.40 ± 2.16 years)
- Co-registration
- The correlations with training years
  - T1-based VBM vs. MPR-based VBM


Fig. T1 map


Fig. MPR image

Results

- **Regions correlated with training years in VBMs based T1 map and T1-weighted images**

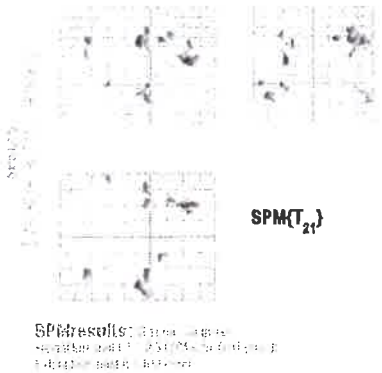


Fig. Correlation map from T1-based VBM (p<0.01, uncorrected)



Fig. Correlation map from MPR-based VBM (p<0.01, uncorrected)

- VBM for T1 map revealed more brain areas than that for T1-weighted image. The brain areas identified by the T1-weighted image were almost included in those by the T1 map
- T1-based VBM showed more sensitivity

Conclusion

- It was expected that the results could be similar to each other in VBM analysis, because T1 map is a kind of T1-weighted image.
- However, T1-value-based VBM analysis seemed to be sensitive to brain plasticity change.
- Difference between processing modalities for the same image should be further examined.

- **Acknowledgements**: This study was supported by MEXT-Supported program for the Strategic Research Foundation at Private Universities, 2014-2018, and JSPS KAKENHI Grant Number 26350995.

Brain plasticity changes by playing wind instruments and piano

Yul-Wan Sung[1], Daehun Kang[1], Yosuke Kawachi[1], Seiji. OGAWA[1]
[1]Kansei Fukushi Research Institute, Tohoku Fukushi University, Sendai, Japan

709.01

Background

Neuroimaging studies have showed plasticity changes in the human brain by training or learning. For musical training the plasticity change was observed in musical genres such as piano playing, violin playing or singing. However, when one person has experiences playing several musical instruments, differences in the plasticity change between musical instruments are not yet known well.

Aim

To examine plasticity changes in the brain by musical training in wind instruments.

Methods

[Subjects]

Twenty-four subjects : VBM
Sixteen subjects: resting state fMRI
Average training years:
Music instruments 8.9, Piano 9.1

[MRI measurements]

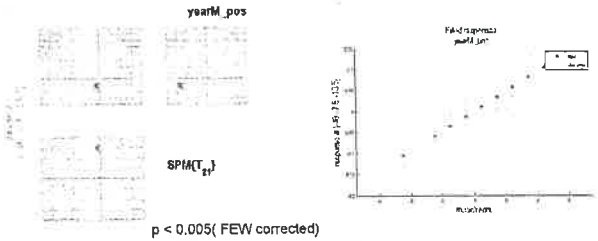
Siemens 3T, Skyra-fit
1. Voxel-based morphometry (VBM)
T1 MPRAGE, 1x1x1 mm^3
2. Resting state fMRI
TR 1s, Sices 34, FA 70, Matrix 64x64
3.4x3.4x3.4mm^3
Number of volumes 480
MB-EPI sequence

[Data analysis]

1. VBM: SPM
2. Resting state fMRI: Conn

Results

VBM



p < 0.005(FEW corrected)

Left superior temporal gyrus(STG)

Resting state fMRI: Postcentral Gyrus as a seed;
Wind instrument training years



Seed:Right Postcentral Gyrus (p = 0.000001, p-FWE)



Seed:Left Postcentral Gyrus (p = 0.000016, p-FWE)

Resting state fMRI: Postcentral Gyrus as a seed;
Piano training years



Seed:Right Postcentral Gyrus (p = 0.00002, p-FWE)

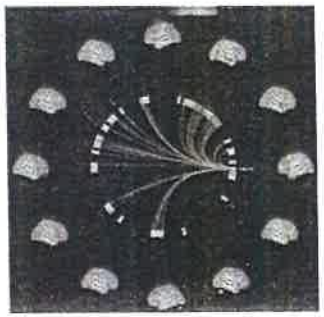


Seed:Right Postcentral Gyrus (p = 0.000014, p-FWE)

Results

Resting state fMRI: STG as a seed :

Wind instruments and Piano training years



Wind instruments



Piano

- The areas shown correlation with only the wind instrument training: the left supramarginal gyrus (SMG), the left frontal pole (FP) and the bilateral paracingulate cortices (Para-CC).

- The areas shown correlation with only the piano training: the superior division of the right lateral occipital cortex and caudate nucleus.

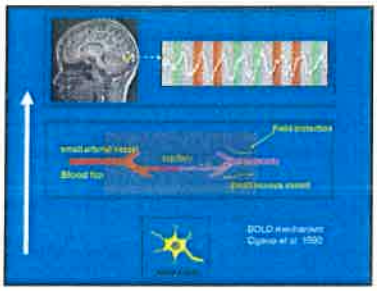
Discussion and Conclusion

- SMG is a part of the somatosensory association cortex, which interprets tactile sensory data. The core function of the FP is known as processing of the cognitive branching that enables multiple tasks. Para-CC is involved in social cognition. These, with the correlation of postcentral gyrus with precentral gyrus for wind instruments training years, suggest that ***the training of wind instruments affects brain functions related to somatosensory, multiple tasks and social cognition.***
- The caudate nucleus and lateral occipital cortex are known to be involved in working memory, and the caudate nucleus is also known to be involved in motor processing. These suggest that ***piano training affects working memory and motor function.***
- Those results, together, indicate that brain plasticity change is related specifically to the playing styles as well as the musical instrument per se.

Acknowledgements
Supported by MEXT-Supported Program for the Strategic Research Foundation at Private Universities, 2014-2018 , and JSPS KAKENHI Grant Number 26350995

Microscopic Functional Structures seen through fMRI Signals

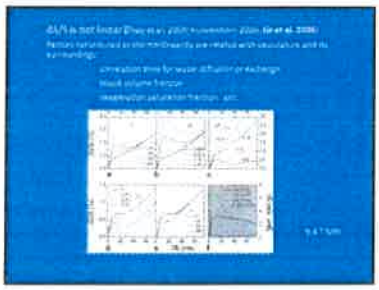
Tohoku Fukushi University, Japan
Yulwen Sung





Contents

1. fMRI (BOLD) and functional resolution
2. A new approach to estimate functional microstructure
   (Logic and experiment for the TE-dependence of $R2^*$)
3. Supporting data for verification
   (1) High spatial frequency effects
   (Effects of image distortion by high threshold susceptibility at FFA and PPA)
   (2) Signal amplitude dependence
   (3) Imaging artifact
4. Summary



Multi-echo imaging: three echo images

1. fMRI (BOLD) and function resolution

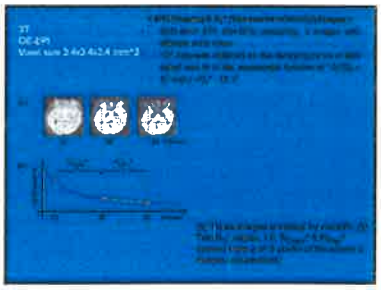
Hypothesis

(a) Different arrangements of vessels would represent different TE-dependence of $R2^*$

(b) Different neuronal circuits would result different arrangements of vessels in a voxel

→

TE-dependent $R2^*$ would reflect the difference of neuronal circuits.



Multi-echo imaging: three echo images

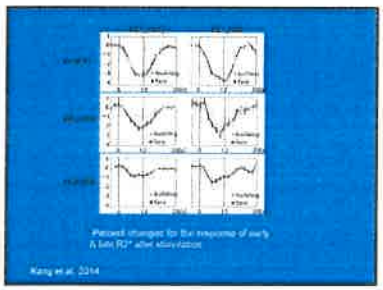
(Hypothesis test)
By assuming independence of $\Delta R2^*$ on TE and stimulus, tested it

$\gamma = \Delta R2^*_{early} / \Delta R2^*_{late}$
$= 1$

$\gamma_{face} = \gamma_{other}$?

But the difference at FFA and PPA might have been from some artifacts unrelated with neuronal information?

Acknowledgements:
- Collaborators:
  Daehun Kang
  Seiji Ogawa
- Supported by MEXT-Supported Program for the Strategic Research Foundation at Private Universities, 2014-2016, and
  JSPS KAKENHI Grant Number 26350995 & 25330173



Percent changes for the response of early & late $R2^*$ after stimulation

Kang et al. 2014

The imaging artifact related with acquisition duration and $R2^*$ is negligible.

→

The difference of γ at FFA and PPA was not by the imaging artifact !

Summary of the experiment

(1) FFA and PPA: $\gamma_{face} \neq \gamma_{building}$
→ $\Delta R2^*$ is TE dependent
→ neuronal circuits responding to the face and building are different

(2) V1: $\gamma_{face} = \gamma_{building}$
→ $\Delta R2^*$ is not TE dependent
→ neuronal circuits responding to the face and building are not different

5. Summary
- It is possible to estimate the microstructural information in a brain area by multi-echo EPI imaging
- Nonlinearity property of $R2^*$ on TE reflects neuronal circuits differences
- Further study:
  Clarification of the relation of γ with neuronal sources
- Limitations

E-mail : uschoi@gachon.ac.kr

Brain plasticity seen in musicians of wind instruments

Uk Su Choi[1], Yul-Wan Sung[2], Jun-Young Chung[1], Seiji Ogawa[2]

[1]Neuroscience research institute, Inchon, Korea, Republic of, [2]Kansei Fukushi Research Institute, Tohoku Fukushi University, Sendai, Japan

Introduction

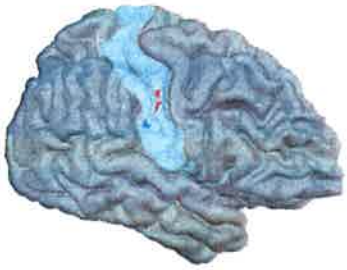
Anatomical and functional changes in the human brain by musical training have been studied noninvasively by MRI. White matter and gray matter changes were measured by structural MRI imaging, diffusion weighted imaging (DWI) for white matter and, cortical thickness and voxel based morphometry (VBM) for gray matter. Studies on white matter reported that musicians showed different fractional anisotropy (FA) maps in several brain areas compared with non-musicians [1]. In addition to white matter, gray matter of musicians also showed different cortical volume or cortical thickness in music related brain areas such as Heschl's sulcus and bilateral intraparietal sulcus (IPS) compared with those of non-musicians [2]. Changes in brain function and functional connectivity have been also reported in musicians. Functional changes were observed mainly in auditory-motor areas which played crucial role in musical activities [3]. Most of the above studies were for musicians of orchestra such as pianist or violinists. In this study we examined brain structural and functional changes on music playing group who played wind instruments. We expected that anatomical changes in mouth related brain areas and functional connectivity of those areas with other music related brain areas would be different from non-music playing group. To find the anatomical differences in mouth related areas, we compared the cortical thickness maps between music playing group and non-music playing group. Functional connectivity was examined by resting state fMRI.

Method

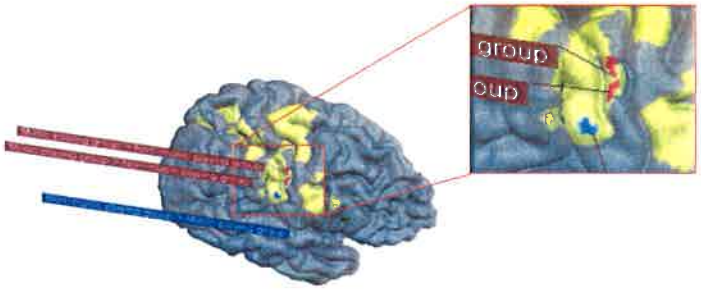
Fourteen music playing subjects (with experiences of more than 6 years) and fourteen non-music playing subjects participated in this study. All subjects were scanned two sessions which included anatomical image (T1) and resting state functional MRI (rsfMRI). The anatomical images were acquired using following parameters: repetition time = 1900 ms, echo time = 2.52 ms, matrix size = 256 x 256, in-plane resolution = 1 x 1 mm2, slice thickness = 1 mm. rsfMRI data were acquired using following parameters: repetition time = 2000 ms, echo time = 30 ms, matrix size = 64 x 64, in-plane resolution = 3.4 x 3.4 mm2, slice thickness = 3.4 mm. In resting state fMRI session, subjects were lied in a bed and tried to think nothing with closed eyes. Data were analyzed using Brainvoyager QX (Brain Innovation B.V., Maastricht, The Netherlands). Cortical thickness of segmented images was measured using laplace method, individually [4]. Those cortical thickness maps were normalized in cortically aligned cortex mesh. The cortical thickness maps of musicians and control group were calculated for group comparison. Each cortical thickness maps were compared by paired t-test. All resting state functional images were analyzed by spatial independent component analysis (ICA) using fastICA algorithm [5]. Individual ICA maps were normalized to group ICA maps.

Results

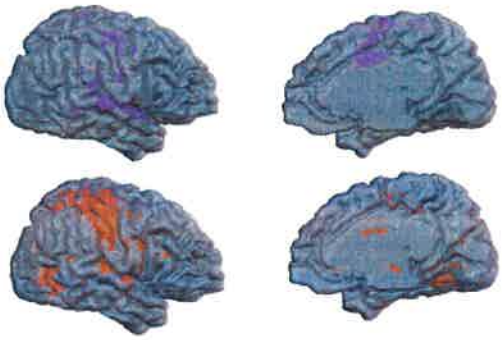
Brain areas in right hemisphere were significantly different in cortical thickness between musicians and non-musicians. Among those areas, two areas were located in postcentral gyrus (somatosensory areas). One is known to be related to the lip and the other is to the tongue. The lip related area, which was located in the anterior part of precentral gyrus (BA 3), was thicker in musicians and the tongue related area, which was located in the posterior part of postcentral gyrus (BA 3), was thinner in musicians. Among forty components by spatial ICA in musicians, a sensory motor related resting state network (RSN) which included those two areas was found. This RSN also included precentral gyrus (BA 6), postcentral gyrus (BA3), inferior frontal gyrus (BA9) and nferior parietal lobule (BA 40). The RSN including the lip and tongue related areas was not found from non-musicians.



Somatosensory area and a difference map of cortical thickness. Red is the area in which the music playing group is thicker than the non-music playing group. Blue is the area in which the music playing group is thinner than the non-music playing group. Those areas with different cortical thickness values are included in the postcentral gyrus in cyan color. Both thicker and thinner areas are statistically significant ($p < 0.005$, uncorrected).



New network in the music playing group. Red and blue areas are included in the new network in yellow ($p < 0.05$, corrected).



SMNs of the music playing group and the non-music playing group. Purple is the area of SMN for the music playing group and orange is the area of SMN for the non-music playing group ($p < 0.05$, corrected). The SMN of the music playing group contains the thicker area but the SMN of the non-music playing group contains both thicker and thinner areas.

Conclusion

Our findings demonstrate that playing wind instruments modify sensory areas related to the lip and tongue anatomically and functionally.

Acknolegements

This study was supported by the MEXT-Supported program for the Strategic Research Foundation at Private Universities, 2014-2018.

References

[1] Moore E, Schaefer RS, Bastin ME, Roberts N, Overy K (2014), 'Can Musical Training Influence Brain Connectivity? Evidence from Diffusion Tensor MRI', Brain Sciences, vol 4, no 2, pp 405–427

[2] Foster NEV, Zatorre RJ (2010), 'Cortical structure predicts success in performing musical transformation judgments', NeuroImage, vol 53, no 1, pp 26–36

[3] Baumann S, Koeneke S, Meyer M, Lutz K, Jäncke L (2005), 'A Network for Sensory-Motor Integration', Annals of the New York Academy of Sciences, vol 1060, no 1, pp 186–188

[4] Jones SE, Buchbinder BR, Aharon I (2000), 'Three-dimensional mapping of cortical thickness using Laplace's Equation', Human Brain Mapping, vol 11, no 1, pp 12–32

[5] Hyvärinen A, Oja E (2000), 'Independent component analysis: algorithms and applications', Neural Networks, vol 13, no 4–5, pp 411–430

OHBM 2015 #4161

Investigation of microscopic functional specificity for attention in peripheral visual field

Daehun Kang[1,2], Satoshi Shioiri[2], Yul-Wan Sung[1], and Seiji Ogawa[1]

[1]*Kansei Fukushi Research Center, Tohoku Fukushi University, Sendai, Japan*

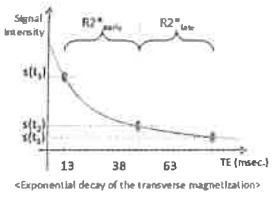
[2]*Graduate School of Information Sciences, Tohoku University, Sendai, Japan*

Purpose

- The "spotlight" effect of the visual attention (Brefczynski and DeYoe, 1999)
- The microscopic functional specificity of neuronal clusters in a voxel was investigated for multiple stimuli in the previous study
  - "Microscopic information of an area can be estimated from stimulus-induced susceptibility changes" (Kang et al., 2014)
- Purpose
  - To investigate the microscopic functional specificity of visual attention in human primary visual area

Methods

- Data measurement
  - 3T MRI (Verio, Siemens)
  - 3-echo-train EPI pulse sequence; TE = 13, 38, & 63 msec
  - TR = 2 sec., Voxel size = 3.4 mm^3, 20 slices
  - MPRAGE pulse sequence; T1- weighted anatomy imaging
  - 5 healthy subjects
- Derivation of two R2* & γ
  - *At each voxel,* $S(t) = S_0 \cdot \exp(-R_2^* \cdot t)$
  - $R^*_{2,early} = -(\ln S(t_2) - \ln S(t_1))/(t_2 - t_1)$
  - $R^*_{2,late} = -(\ln S(t_3) - \ln S(t_2))/(t_3 - t_2)$
  - $\gamma = \left(\frac{\Delta R^*_{2,late}}{R^*_{2,base,late}}\right) \Big/ \left(\frac{\Delta R^*_{2,early}}{R^*_{2,base,early}}\right) = \%R^*_{2,late} / \%R^*_{2,early}$
  - cf) $BOLD(\%) = \frac{\Delta S}{S_{base}}$



<Exponential decay of the transverse magnetization>

- Visual stimulation



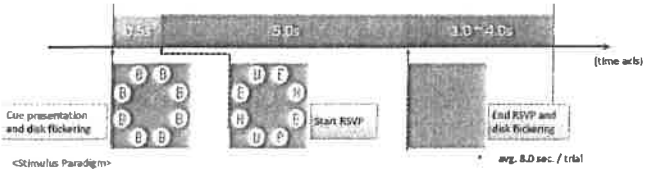
<Main stimulation>



<Disk flickering>



<Rapid serial visual presentation (RSVP)>



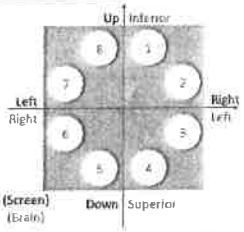
<Stimulus Paradigm>

- avg. 8.0 sec. / trial

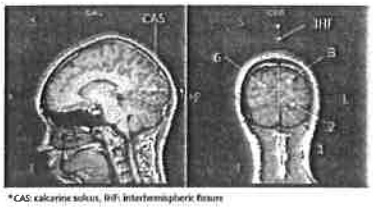
- **Acknowledgements**: This study was supported by MEXT-Supported program for the Strategic Research Foundation at Private Universtities, 2014-2018 and JSPS KAKENHI Grant No. 25330173 & 26350995.

謝辞

Results



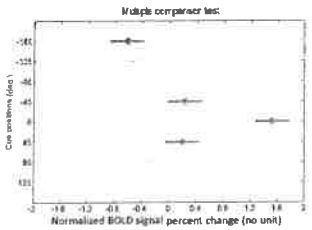
(a) Stimulus on screen & the corresponding location in the primary visual area



*CAS: calcarine sulcus, IHF: interhemispheric fissure
(b) Example of part of 8 ROIs

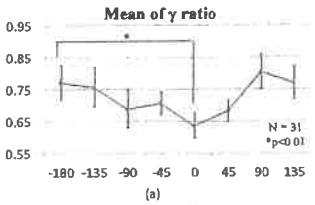
- Eight locations at a brain as ROIs
  - Statistical validness & anatomical reasonableness were considered
  - Statistical condition: cued > un-cued, un-cued > 0, & $p<0.05$
  - Anatomical criterion: Retinotopic location in the primary visual area

- **BOLD response**

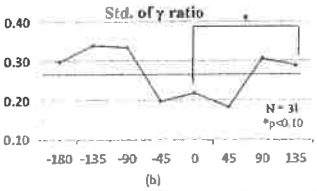


- Conventional BOLD
  - one-way ANOVA: $F(248,7)=3.28$, $p=0.002$
- Z-normalized BOLD at each location
  - $z = (x - \mu)/\sigma$
  - one-way ANOVA: $F(248,7)=32.87$, $p<10^{-5}$
  - To compensate a local characteristic of each location
- BOLD response: attended >> non-attended

- **γ-ratio evaluation**



(a)



(b)

- γ-ratio
  - one-way ANOVA test: $F(240,7)=1.33$, $p<0.24$
  - Low significant difference
  - Basically the microscopic functional specificity is supposed to be similar in primary visual area.
- The significant difference of γ-ratio
  - t-test between attended and non-attended cases
  - It implies the possibility of the existence of the specific neuronal circuit related with attention modulation
- Difference in standard deviation of γ-ratio
  - More stable γ-ratio from attended areas

Conclusion

- Attention in the primary visual area
  - Modulating BOLD signals
  - In each location, neuronal populations contributing to BOLD signals might be almost same, assessed by the similar values in microscopic functional specificity
  - But, it seems like the small neuronal population related directly with attention exists

Robustness of microscopic functional structures estimated by dynamic magnetic susceptibility change

1717

Yulwan Sung, Daehun Kang and Seiji Ogawa

Kansei Fukushi Research Institute, Tohoku Fukushi University, Sendai, Japan

Introduction

The functional units of the human brain comprise many neuronal populations (or circuits) that work together, although not always in the same manner. Functional magnetic resonance imaging (fMRI) observations of functional areas of the human brain show that they can be activated by multiple stimuli but using conventional fMRI, it is difficult to discriminate the fMRI response evoked in a specific neuronal population from that in another because of the limited spatial resolution of 27–125-mm3 voxels with 3-Tesla MRI as well as the properties of the fMRI signal produced by magnetic susceptibility, which is smoothed across vessels and surrounding tissues in a voxel. In the previous report, we proposed a novel method for obtaining the microscopic information related to a functional area, in which multiecho echo-planar imaging (ME-EPI) was used to measure stimulus-induced (dynamic) changes in magnetic susceptibility of an area depending on echo-time. However, it was not evaluated whether the dynamic magnetic susceptibility change was affected by magnetic susceptibility in the resting (static) state. Static magnetic susceptibility may be affected by other factors than neuronal activation and also different between brain areas.

Previous study: microscopic information of an area can be estimated from stimulus-induced susceptibility changes (Kang et al., Magn. Reson. Imaging vol. 32, pp. 1031-1036)

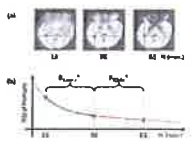
Study aim: To prove further the proposed method in the previous study by evaluating the relation between static and dynamic magnetic susceptibility.

Previous study

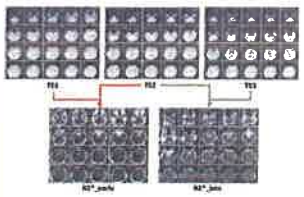
Assumption: ΔR2* is independent on TE and stimulus:

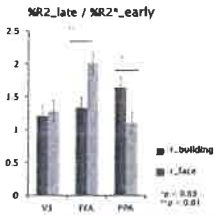
(1) γ = %R2*_late / %R2*_early = 1

(2) γ_s1 = γ_s2 --> neuronal circuits to two stimuli are the same



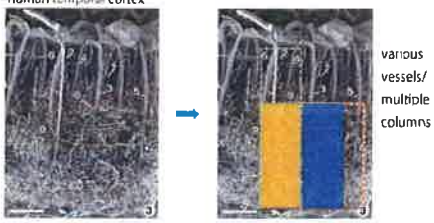
$S(TE) = S0(T1) \cdot \exp(-R2^* \cdot TE)$





Vasculature

human temporal cortex



various vessels/ multiple columns

Results

γ_f ≠ γ_b --> different neuronal circuits in FFA and PPA

Methods

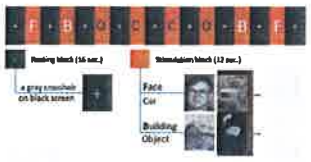
(M.1) All MRI experiments were performed using a Verio system (Siemens, Germany) with a standard, 12-channel head matrix coil operating at 3 Tesla. For functional imaging, ME-EPI sequence was used with TR of 2 sec., three TEs of 13, 38 and 63 ms, 90 degree flip angle, 220 mm field of view, 64 × 64 mm matrix size, and 3.4 mm slice thickness with 0.5 mm gaps. Twenty slices parallel to the AC-PC were acquired for each volume.

(M.2) From the equation of $S(TE) = S0 \cdot \exp(-R2^* \cdot TE)$, where S0 is the signal at TE = 0 and R2* is the transverse relaxivity (= 1/T2*), two R2* values, i.e., R2*_early and R2*_late, were derived from the TE1 and TE2 images and from the TE2 and TE3 images, respectively. As well, the magnetic susceptibility feature after activation was estimated on the basis of the ratio of %R2*_late relative to %R2*_early.

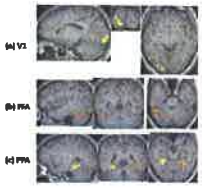
(M.3) Twelve subjects were participated.

(1) An MRI scan of 240 seconds: face, building, object and car conditions

(2) Data at TE2 (TE = 38 msec.) used to localize regions of interest (ROIs)



Stimulation protocol

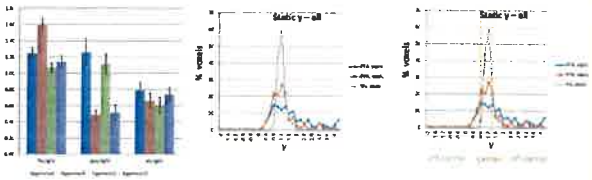


Static γ : ratio of R2*_early and R2*_late at resting state

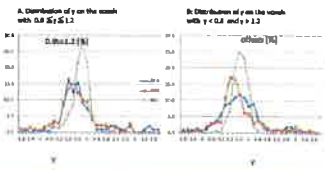
Dynamic γ : ratio r of percent signal change for R2*_early and R2*_late

Distribution of static γ : grouped to the center (0.8< γ <1.2) and off-center (γ <0.8, γ >1.2)

Distribution of dynamic γ : at each voxel of the groups in V1, FFA and PPA



No difference between distributions for the dynamic γ of the center and the off-center : not affected by specific voxels with high susceptibility



Supplementary Experiment

Signal amplitude dependence

(Phantom experiment)

1) To examine a trivial case that γ is proportional to response signal amplitude of neurons.

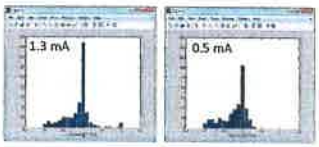
If this is true, γ does not reflect the difference in neuronal circuits.

2) Two levels of current, 0.5mA and 1.3mA, were used in a phantom model



Activation map by current flowing.

Red for positive and green is for negative.



For both two levels of current, most of voxels the gamma values γ = 1.

In the most of voxels R2* is not dependent on TE.

Thus, the difference in gamma is not just dependent on the current amplitude.

Conclusion It was proved that γ at the previous study had been not affected by specific voxels with high magnetic susceptibility. The proposed method can be used to probe microscopic functional structure in a brain area.

Acknowledgements: This study was supported by JSPS KAKENHI Grant No. 25330173 & 26350995 and MEXT-Supported program for the Strategic Research Foundation at Private Universities, 2014-2018.

Regional difference in characteristics for top-down modulation in the ventral visual stream

Yul-Wan SUNG[1], Hyoun. YOON[2], Uk-Su CHOI[3], *Seiji. OGAWA[1]
[1]Touhoku Fukushi Univ., Sendai, Miyagi, Japan; [2]Daegu Cyber Univ., Daegu, Korea, Republic of; [3]Neurosci. Res. Inst., Gachon Univ. of Med. and Sci., Incheon, Korea, Republic of

792

Background

Top-down modulation to low level areas from high cognitive areas has been reported in number of electrophysiology studies. In particular, ventral visual stream has shown area-specific characteristics such as center-peripheral specialization and categorical specialization. In terms of center-peripheral specialization, lateral areas supposed to be more sensitive to center vision and facial like stimuli, whereas medial areas to peripheral vision than building stimulation. There is a possibility that ventral visual stream has similar regional differences in characteristics for top-down modulation.

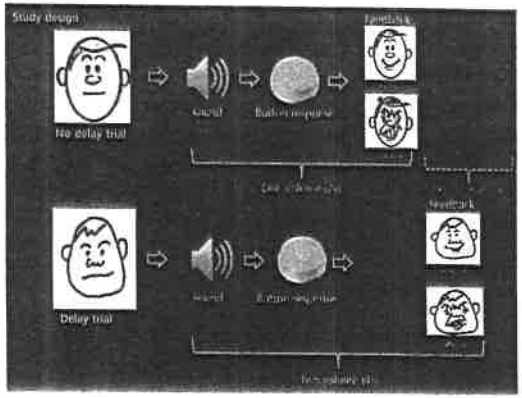
Aim

To examine a possible difference in top-down modulation depending on areas in the ventral visual region.

Methods

[Subjects]
25 subjects
[MRI measurements]
(fMRI) GE-EPI
Rrepetition time = 2000 ms, Echo time = 30 ms, Matrix size = 64 x 64, In-plane resolution = 3.4 x 3.4 mm2, Slice thickness = 3.4 mm.
Flip angle = 90
[Data analysis]
Deconvolution analysis was performed to estimate hemodynamc response function.
The onset for the analysis was chosen as the onset of sound.
The hypothesis is that feedback is working on the test faces when participants hear the sound.
Brainvoyage QX was used for the analysis.

Methods



visual and auditory categorization paradigm

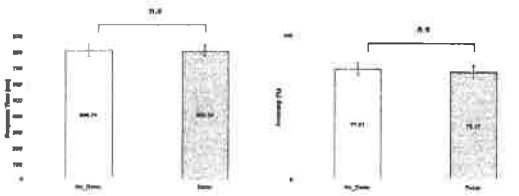
- button press according to the combinations
  : positive faces – rising FM tones
  negative faces – falling FM tones
- no prior information given

Stimulus trials
Non-Delay(7s):
Face (1s) – Sound – Button- Face (1s) –rest (2-4 s)
Dealy(7s):
Face (1s) - Sound – Button- delay (1s) -Face (1s)-rest(2-4s)

Non-delay and Delay trials repeated 20 times randomly in a scan. Scan time: 496 s

Results

Behavioral data: Delay vs Non-delay

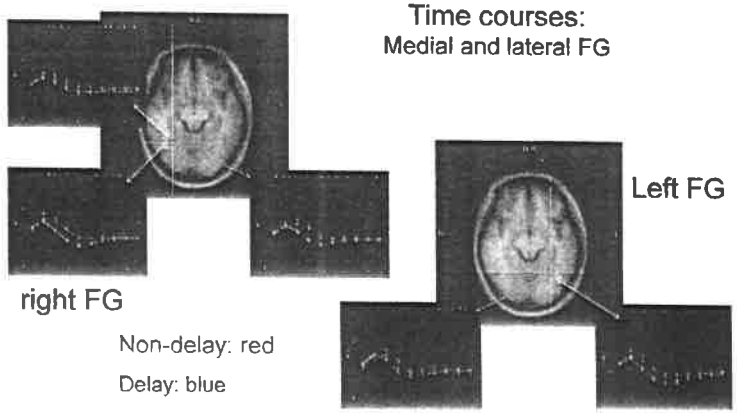


Response time:
No-significant difference

Accuracy:
No-significant difference

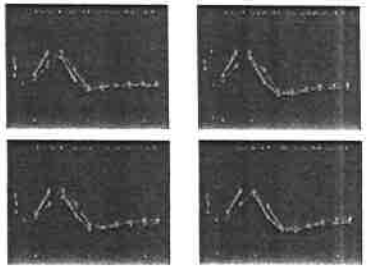
Results

Time courses:
Medial and lateral FG



Non-delay: red
Delay: blue

Time courses:
Fovea and peripheral V1



fMRI responses: the delayed feedback shown though the shifted time course at the medial fusiform gyrus (FG)

fMRI responses: the delayed feedback shown through the shifted time course at the fovea and peripheral areas of V1.

Discussion and Conclusion

- The fMRI response is considered from feedback because the onset was for the sound.
- This difference in occipitotemporal region might reflect the different feedback characters in the lateral and medial areas of early visual cortices, which seem to be influenced by top-down modulation.
- This result indicates the area-specific differences to the feedback in the ventral region.

Acknowledgements
Supported-by-MEXT-Supported Program for the Strategic Research Foundation at Private Universities, 2014-2018

Morphological changes in cortical microstructure of the brain by short-term training

Yul-Wan Sung[1], Daehun KANG[1], U.-S. CHOI[2], S. OGAWA[1]

[1]Kansei Fukushi Institute, Tohoku Fukushi Universit, Sendai, Japan; [2]Neurosci. Res. Inst., Gachon Univ. of Med. and Sci., Incheon, Korea

816

Background

Most of the previous studies of neuroplasticity in system level by MRI were on long-term and intensive training such as music and physical exercise over years or months though few studies were over weeks. As for shorter timescales, several minutes of electrical and magnetic stimulation is known to cause morphological changes in the cortical microstructure of the brain. Some studies using diffusion-weighted MRI have demonstrated the microstructural changes in human. Recently a study reported microstructural changes in the motor area by short-term magnetic stimulation [Abe et al, PNAS 2012].

Aim

To examine whether the similar period of training not by electrical or magnetic stimulation but by typical functional tasks such as finger tapping would cause the same kind of microstructural changes in the cortex.

Methods

Subjects

Seven subjects

MRI measurements

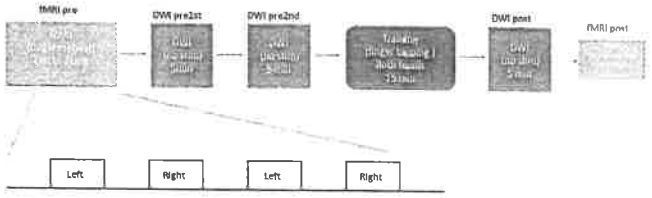
1. fMRI (GE-EPI)
TR 2s, Sices 17, FA 90, Matrix 64x64
2. Diffusion weighted imaging (DWI)
Unipolar gradient
Two b values in a scan: low and high b values, 300 s/mm^2 and 1200 s/mm^2, interleaved in a measurement scan, 50 volumes

Data analysis

1. Activation maps calculated by fMRI data
2. DWI data were evaluated on activation maps by fMRI.
3. All sampling point averaged

Methods

Experimental paradigm

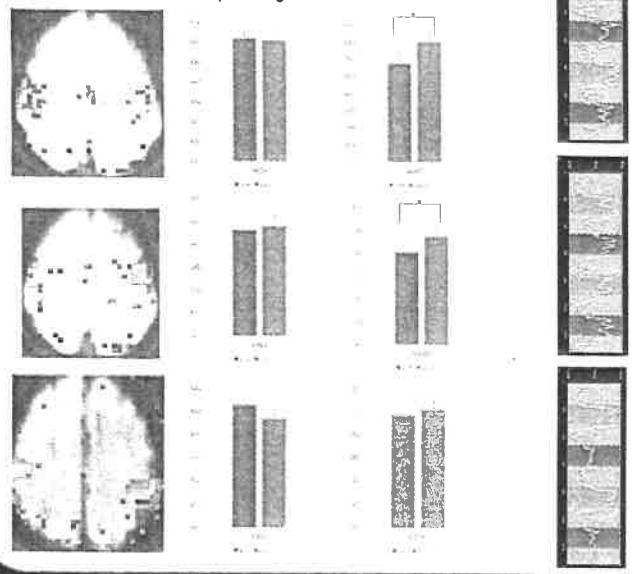


1. fMRI (GE-EPI) for localization
(rest 30 s stim 30 s) stim: finger tapping
2. Diffusion-weighted imaging (DWI)
DWI before and after training
(finger tapping with both hands: as fast as possible)
3. Two pre DWI scans: for control

Results

Motor areas: signal differences at pre- and post-training periods depending on b values

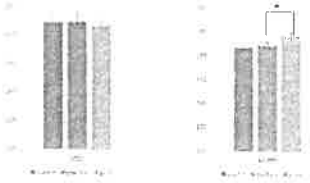
*: $p < 0.05$



Results

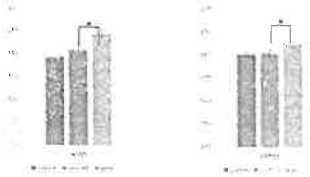
Motor areas: signal differences at pre- and post-training periods

Signal difference only for large b value

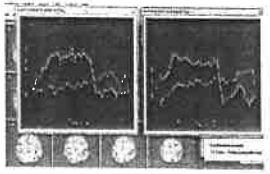


Motor areas: signal differences at pre- and post-training periods

Signal difference both in small and large b values



BOLD signal change at pre- and post-training period : at the same motor area shown significant difference in b 1200 (one subject) almost similar



T2 change at pre- and post-tralning period : at the same motor area shown significant difference in b 1200 (one subject): almost similar



Discussion and Conclusions

- Several motor areas showed statistically significant differences in DWI signals before and after the training but with no difference between two measurements before the training.
- Some areas of them showed the difference only for high b value and others for both low and high b values.
- These results suggest some microstructural changes by the training in the areas, especially the areas shown signal differences only for the high b value.
- This is parallel with the previous study used magnetic stimulation and shows the possibility of microstructural changes by a short period of tasks.
- In addition, the results give a caution about the evaluation of the data. The signal sources of the areas shown differences for both b values are considered to be large blood vessels rather than tissues.

Acknowledgements

Supported by MEXT-Supported Program for the Strategic Research Foundation at Private Universities, 2014-2018

Estimation of functional specificity of visual areas by a transverse relaxation profile

APCV 2014

Daehun Kang[1,2], Yulwan Sung[2] , Satoshi Shioiri[1], Seiji Ogawa[2]

[1] Tohoku University, Sendai, Japan, [2] Kansei Fukushi Research Institute, Tohoku Fukushi University, Sendai, Japan

Purpose

- Brain areas to study
  - The cognitively-specified category-selective areas on ventral region [1,2]
    - Fusiform face area (FFA)
    - Parahippocampal place area (PPA)
    - sensitive to "Face", "Building"
  - Basic visual areas on occipital region
    - such as primary visual area (V1)
    - insensitive to kinds of stimuli (as it has been known)
- Can the functional specificity to some stimuli of a brain part be identified ?
  - BOLD contrast (as conventional method of fMRI) [3] provides the signal change at a part of brain activated
  - However, it is difficult to know whether the area consists of **functionally heterogeneous neuronal populations**.
  - In previous study, high-resolution imaging technique was used [4]
- The proposed method to investigate the functional specificity to certain stimuli
  - MR Imaging : multi-echo-train echo-planar-imaging (me-EPI)
  - Data analysis : ratio of percent change between early & late R_2* in a voxel [5]

- References : [1] Choi U-S et al., Neuroreport 2013; 24: 53-7. [2] Grill-Spector K. Curr Opin Neurobio 2003; 13: 1-8. [3] Ogawa S et al., Biophys J 1993; 64: 803-12. [4] Grill-Spector K, Sayres R, Ress D. Nat Neurosci. 2006;9(9):1177-85. [5] D. Kang et al., Mag Res Imaging 2014 (online)
- Acknowledgements : [1] MEXT-Supported program for the Strategic Research Foundation at Private Universities, 2014-2018. [2] JSPS KAKENHI Grant Number 25330173 & 26350995

Methods

< MRI imaging & R_2* (transverse relaxivity) map >

- me-EPI producing 3 images with different echo times
- R2* map was obtained as the decaying curve of MRI signal was fit to the exponential function of "$S(t) = S_0(T_1) \cdot exp(-R_2^* \cdot t)$" **(Fig. 1)**

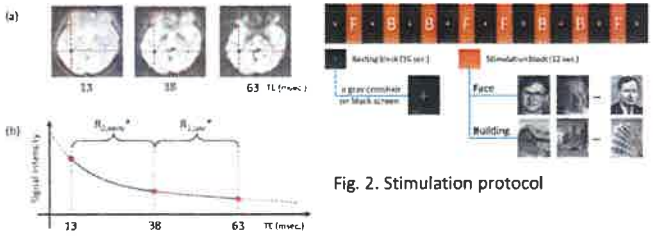


Fig. 1. (a) Three images provided by me-EPI. (b) Two R_2* values, i.e. $R_{2,early}$* & $R_{2,late}$* derived from 2 of 3 points of the above 3 images, respectively

Fig. 2. Stimulation protocol

< Functional experiment protocol >

- Total 240 sec. = 4 face blocks + 4 building blocks **(Fig. 2)**
- 8 different pictures / each block
- 1 sec. to each picture with of an inter-picture of 0.5 sec.

< Data analysis >

- Tool : Brain Voyager QX (Brain Innovation B.V., Postbus, The Netherlands) software.
- All image data from the functional session for each subject were preprocessed with Brain Voyager QX and motion correction, scan time correction, and high-pass filtering with a cut-off frequency of 0.005 Hz.
- Percent signal changes for $R_{2,early}$* and $R_{2,late}$* were calculated at the ROIs by the event-related-averaging option implemented in Brain Voyager.
- Ratios of the percent signal changes of $R_{2,late}$* to that of $R_{2,early}$*, i.e., " = $\%R_{2,late}$* / $\%R_{2,early}$* ", were derived at each condition and each area.

< Regions of Interest, ROIs >

- Criterion : Activations of image data of TE = 38 msec. (BOLD contrast)
- The ROIs defined are the followings:
  - Visual primary area (V1)
  - FFA & PPA by a conjunction analysis
  - FFA ; $BOLD_{face} > BOLD_{building}$ and $BOLD_{face} > BOLD_{rest}$
  - PPA ; $BOLD_{face} < BOLD_{building}$ and $BOLD_{building} > BOLD_{rest}$

< Imaging protocol >

- 3T MRI machine (Verio system, Siemens, Germany)
- Standard 12-channel head matrix coil
- Imaging parameters
  - TR 2000 msec., TEs 13, 38 & 63 msec.
  - Voxel resolution 3.4^3 mm^3 (cube) with 0.5 mm gaps, FOV 220^2 mm^2
  - 20 slices parallel to the AC-PC

Results

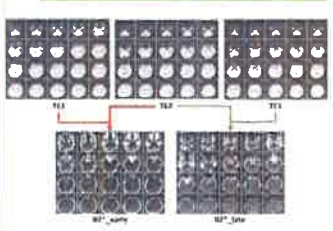


Fig. 3. Derivation of two R2* map

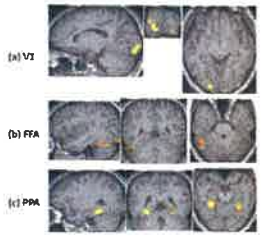


Fig. 4. ROI Localizations of V1, FFA & PPA

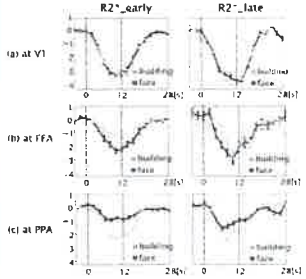


Fig. 5. Percent changes in the response of early & late R2* after stimulation

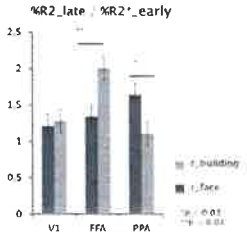


Fig. 6. Ratio of percent change of early & late R2*

- Fig. 5 shows event-related responses of two R_2* for different kinds of stimuli
- In Fig. 6, the ratio of R_2* percent changes indicates
  - The ratio to non-preferred stimuli is larger than the ratio to preferred stimuli at FFA & PPA
  - At V1, the significant difference in the ratios was not observed

Discussion & conclusion

- The aim of the present study was to investigate the heterogeneity in neuronal populations of category-selective areas.
- It is assumed that the higher heterogeneity would cause the more complex change in a signal decaying curve when a functionally-specific stimulus was applied.
- FFA & PPA as category-selective areas significantly presented different ratios to different kinds of stimuli.
- It is supposed that the proposed method can be used to examine the microscopic functional characteristics in a certain voxel

Supplement

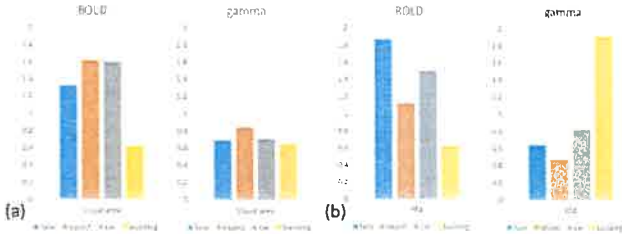
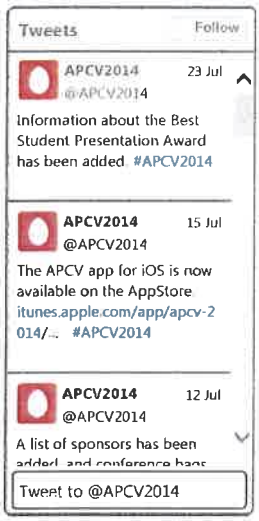


Fig. 7. BOLD versus ratio (γ, gamma) to various types of stimulus (a) at early visual area and (b) at FFA

- At early visual area, there are somewhat differences in BOLD contrast. However, their ratio did not show the significant difference.
- At FFA, in spite of various levels of BOLD, only building stimulus made a significant value in gamma.



Home
Program
Registration
Abstracts
To Presenters
Access
Committees
Sponsors



Best Student Presentation Award

The Best Student Presentation Award was given to the following students.

Winners of APCV 2014 Best Student Presentation Award

Mika Babe (Osaka University, Japan)
Title: Integration of multiple spatial frequency channels in V1 disparity detectors
Co-authors: Kota S. Sasaki & Izumi Ohzawa

Hideki Tamura (Toyohashi University of Technology, Japan)
Title: Relationship between brightness enhancement and self-luminosity of the glare illusion
Co-authors: Shigeki Nakauchi & Kowa Koida

Kenichi Yuasa (The University of Tokyo, Japan; Japan Society for the Promotion of Science (JSPS), Japan)
Title: The dilations and compressions of the interval-time perception caused by visual flickers and auditory flutters
Co-author: Yuko Yotsumoto

Program (Online Version)

You can see details of each session by clicking the time table below. Errors will be corrected in each case.

Program July 21 (Day 3)

Visual Recognition

P3-21 Estimation of functional specificity of visual areas by a transverse relaxation profile
Daehun Kang[1,2], Yulwan Sung[1], Satoshi Shioiri[2], Seiji Ogawa[1]
([1]Tohoku Fukushi University, Japan, [2]Tohoku University, Japan)

P3-22 Perceiving group-wide attractiveness for human faces
Hidekazu Yarimizu, Yoshitaka Makino, Jun Kawahara
(Chukyo University, Japan)

P3-23 The temporal dynamics of object detection between target and non-target response by using fragmented object contours
Kosuke Taniguchi
(Doshisha University, Japan)

P3-24 Dynamic face adaptation in facial expression judgment and its position specificity
Yu Ting Lew, Hong Xu
(Nanyang Technological University, Singapore)

P3-25 The effect of verbal overshadowing on face identification — A pilot study
Minje Kim[1], Kyongmee Chung[1], Woo Hyun Jung[2]
([1]Yonsei University, Korea, [2]Chungbuk National University, Korea)

P3-26 Positive eyes facilitate use of pigment and shape information from the rest of the face
Harold C H Hill[1], Sarah Shrimpton[2], Yumiko Otsuka[3], Mark D Shriver[4], Peter D Claes[5]
([1]University of Wollongong, Australia, [2]University of Dundee, UK, [3]UNSW Australia, Australia, [4]The Pennsylvania State University, USA, [5]Katholieke Universiteit Leuven, Belgium)

P3-27 Configural face processing in serial visual presentation
Jasmina Stevanov[2], Zorica Stevanov[1], Dejan Todorovic[1]
([1]University of Belgrade, Serbia, [2]Kyoto University, Japan)

P3-28 Visual field coverage of category selective regions in human visual cortex estimated using pRF mapping
Nathan Witthoft[1], Mai Nguyen[2], Sonia Poltoratski[3], Golijeh Golarai[1], Alina Liberman[4], Karen F LaRocque[1], Mary E Smith[4], Kalanit Grill-Spector[1]
([1]Stanford Unviersity, USA, [2]New York University, USA,[3]Vanderbilt University, USA, [4]University of California, Berkeley, USA)

P3-29 Importance of the stimulus intensity in perceptual adaptation
Dayi Jung, Euihyun Kwak, Kyongmee Chung
(Yonsei University, Korea)

Visual Attention, Awareness and Cognition

P3-30 Rapid and efficient processing of frequently-used meaningful visual symbols
Naoto Sakuma, Eiji Kimura, Ken Goryo
(Chiba University, Japan)

P3-31 Inhibition of return to eye gaze develops in teenage
Hui Fang Lin[1], Li Jingling[2], Chih Chien Lin[3], Chia Jui Tsai[4], Yen Ching Wu[3], Joung Kung Yih[3], Lin Me Chen[3], Wan Ru Tzeng[3], Mei Jung Chen[3]
([1]National Changhua University of Education, Taiwan, [2]China Medical University, Taiwan, [3]Taichung Veterans General Hospital, Taiwan,[4]Changhua Christian Hospital, Taiwan)

Society for Neuroscience 2014

Effects of signals originating from large blood vessels on BOLD signals of the fusiform face area

823.11

Yulwan SUNG[1], Jun-Young CHUNG[2], Seiji OGAWA[1,2]

[1]Kansei Fukushi Res. Institute, Tohoku Fukushi Univ., Sendai, Japan; [2]Neurosci. Res. Institute, Gachon Univ, Incheon, Korea

Introduction

The paramagnetic property of blood in BOLD imaging, in itself, is a short-range phenomenon located within a few tens of microns from an activated neuronal site. However, two factors make an undesirable contribution to BOLD-based fMRI signals, leading to an exaggeration of the spatial specificity and signal amplitude compared with those expected. One factor is the propagation of the bolus of oxygen-enriched blood by neuronal activation to the larger draining venous structures. Another is inflow effect. MRI signals are inherently sensitive to inflowing fully magnetized spins; therefore, hemodynamic changes, particularly in larger blood vessels, can create signal fluctuations that are coincident with neuronal activation due to the inflow effect. The fusiform face area (FFA) is known to play a pivotal role in face processing. The FFA is located in the ventral region, at the base of the brain, through which large vessels run. The location of the FFA via fMRI varies across subjects, although the average location is almost invariant across groups of subjects. If the variation in location is dependent on large blood vessels, then the signal of the FFA can be under- or overestimated. However, this issue has not been examined.

Aim: to investigate whether the FFA includes large blood vessels and/or whether inflow signals contribute to fMRI signals of the FFA.

Methods

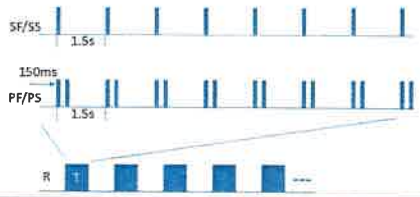
Visual stimulation

(1) Face and building pictures were used.

(2) Stimulus ontime of pictures was 50 ms.

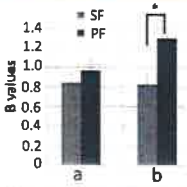
(3) Task blocks: 12 s and rest periods: 18 s.

(4) SF: face single, PF: face pair,
SS: building single, PS: building pair



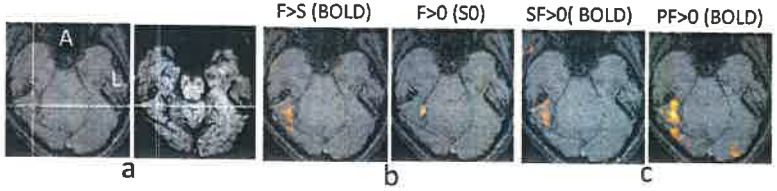


SWI-MIP images (across eight slices in sliding window mode). The dark lines in the slices represent large blood vessels.



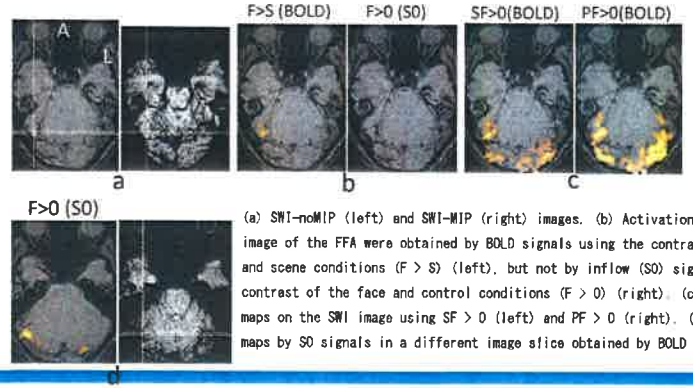
Averaged responses of the FFA in 10 subjects, and originated from random-effects BOLD signals using individual and group analyses. (a) Individual data, no significant differences were observed between SF and PF ($P = 0.39$, paired t-test). (b) Group data, PF was larger than SF ($P < 0.01$, paired t-test). Error bars: S.E.M.

1. Inflow signals appeared at the same slice



(a) SWI-noMIP (left) and SWI-MIP (right) images. (b) Activation maps on the SWI-noMIP of the FFA by BOLD signals using the contrast of the face and scene conditions (F > S) (left), and an activation site caused by inflow (S0) signals using the contrast of the face and control conditions (F > 0) (right). (c) Activation maps on the SWI image using SF > 0 (left) and PF > 0 (right)

2. Inflow signals appeared at a different slice



(a) SWI-noMIP (left) and SWI-MIP (right) images. (b) Activation maps on the SWI image of the FFA were obtained by BOLD signals using the contrast of the face and scene conditions (F > S) (left), but not by inflow (S0) signals using the contrast of the face and control conditions (F > 0) (right). (c) Activation maps on the SWI image using SF > 0 (left) and PF > 0 (right). (d) Activation maps by S0 signals in a different image slice obtained by BOLD signals.

Methods

3T MRI scanner (Siemens, Verio) was used for fMRI experiments.

(1) Susceptibility-weighted imaging (SWI) sequences was used to visualize large blood vessels

(2) Dual-echo gradient-echo EPI sequence was used to measure inflow signals.

$S(TE) = S0\ (T1) \cdot \exp(-TE/T2^*) \longrightarrow$

$S0 = \exp[[\log(S(TE1)) - (TE1/TE2)\log(S(TE2))]/(1 - ET1/TE2)]$

where S0 reflects inflow effects; TE is the effective echo time; and T2* is the apparent transverse relaxation time. TE1 and TE2 were 13 ms and 38 ms respectively.

(3) For BOLD signals S(TE2)was used.

Results and Discussion

1. fMRI responses of the FFA of all participants (10 subjects) were not affected by inflow signals and also activation maps were not affected by large blood vessels (maps of two representative subjects were shown here).

2. The presence of large blood vessels and the activation by inflow effects around the FFA represent a warning that the evaluation of FFA responses via intersubject averaging may lead to a wrong direction (plot).

3. The results suggest that the consideration of the contribution of large blood vessels by the presented methods in parallel with the typical functional analysis would be needed for ensuring reliability.

This study was supported by JSPS KAKENHI Grant Number 26350995 & 25330173 and MEXT-Suproted program for the Strategic Research Foundation at Private Universities, 2014-2018.

Society for Neuroscience 2014

Functional differences in processing preferred and non-preferred stimuli at object selective areas. 550.04

Uk Su Choi[1], Yul-Wan Sung[2], Young Bo Kim[1], Zang-Hee Cho[1], Hyo Woon Yoon[3], S. Ogawa[2,1]

[1]Neurosci. research institute, Gachon Univ. of Med. and Sci., Incheon, Korea, Republic of; [2]Touhoku Fukushi Univ., Sendai, Miyagi, Japan; [3]Department of Art Therapy, Daegu Cyber University, Daegu, Republic of Korea

Introduction

Ventral visual stream is known as dedicated to processing of visual objects. The lower areas on the stream including the primary visual areas (V1) have a topographic organization corresponding to visual fields, called the retinotopy (Tootell et al. 1998). Neurons at the stream have small receptive fields in the lower level and large ones in the higher level (Serences and John T 2006). It is also known that some high-level visual areas show category-selectivity. Two well-known category-selective areas are fusiform face area (FFA), showing selectivity to faces, and parahippocampal place area (PPA), showing selectivity to scenes (Kanwisher, McDermott et al. 1997, Epstein and Kanwisher 1998, Epstein, Harris et al. 1999).

The two areas have shown not as much strong retinotopic maps as the primary visual field. The two areas have shown some invariance on some physical properties such as the stimulus size or stimulus position (Ewbank, Schluppeck et al. 2005, Carlson, Hogendoorn et al. 2011).

The properties of the category-selective areas of the large receptive field, invariance to those physical properties and weak retinotopy imply that a visual stimulus such as face or scene pictures should be processed and interpreted as one meaningful image rather than a set of different physical parts even in the case that the image contains other physical variations irrelevant to the category itself.

On the other hand, FFA and PPA show activation to non-preferred stimuli as well as preferred stimuli although responses to non-preferred stimuli are small compared to preferred stimuli. In addition, there are some characteristic differences between FFA and PPA, that is, FFA is located in the lateral side and PPA in the medial side of the ventral of the temporal cortex and also FFA is more related to center vision (Lerner, Hendler et al. 2006, Goesaert and Op de Beeck 2010, Baldassano, Iordan et al. 2012) and PPA is to peripheral vision (Nasr, Liu et al. , Epstein and Kanwisher 1998, Epstein, Harris et al. 1999, Carlson, Hogendoorn et al.). This throws a question how those areas process an image stimulus composed of two parts, one belonging to the preferred category and the other to a non-preferred category. In this study we examined the processing strategies for preferred and non-preferred stimuli in FFA and PPA through composite pictures.

Materials and Methods

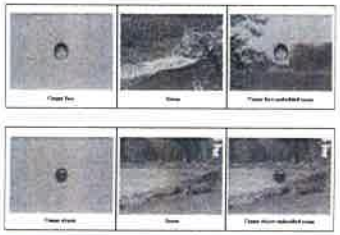
Subjects

Sixteen healthy volunteers(8 male, 8 female, age; 20-29) were participated. They were all university students. None of volunteers took medications that might affect brain function and had clinical or pathological history of neuropsychiatric disease.

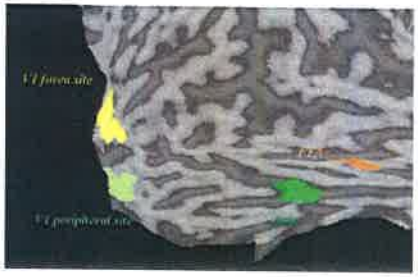
Experimental design

Before scanning, subjects were informed an information on the experiment out of the scanner. In a first experiment, three kinds of stimuli were used, a face picture at the center (F, visual field = 3.9°x3.9°), a scenery picture (S, visual field = 28°x21°) and a scenery picture with the face at the center (SF). A second experiment was composed of three kinds of stimuli, an object picture at the center (O, visual field = 3.9°x3.9°), a scenery picture (S, visual field = 28°x21°) and a scenery picture with the object at the center (SO). Each block lasted for 18 seconds and one trial lasted for 1 second. The total duration of the single run was 450 seconds. All blocks were randomly ordered. Subjects performed a one-back task, for the center and peripheral.

Stimulus

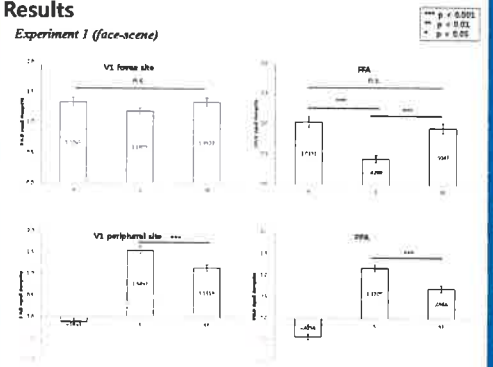


Target ROIs

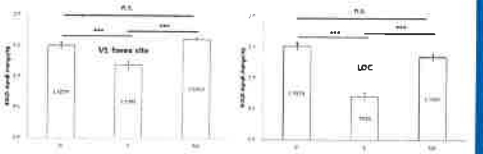


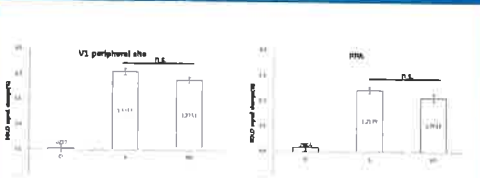
Results

Experiment 1 (face-scene)



Experiment 2 (object-scene)





1 FFA and PPA (face-scene)

(1) V1 fovea site and FFA showed the similar pattern
There were no significant differences between F and SF.
(2) V1 peripheral site and PPA showed similar pattern
There were significant differences S and SF

2 LOC and PPA (object-scene)

(1) V1 fovea site and LOC showed the similar pattern
There were no significant differences between F and SF.
(2) V1 peripheral site and PPA showed similar pattern
There were no significant differences S and SF

Conclusions

These indicate that FFA and PPA are different in the processing strategy for preferred and non-preferred stimuli. A composite picture seems to be interpreted as only the face at FFA but the face and scene pictures in the composite picture seem to be separately processed at PPA. The face signal to PPA may come from FFA when the invariance of PPA is considered.

This work was partly supported by MEXT-Supported program for the Strategic Research Foundation at Private Universities, 2014-2018, and National Research Foundation of Korea(NRF) Grant (2006-2005137)

E-mail : sung@tfu-mail.tfu.ac.jp

脳機能ネットワークによるヒト特性変化の推定

Estimation of changes in human traits through functional brain networks

Yul-Wan Sung, Yousuke Kawachi, Yuki Otomo, Seiji Ogawa

Kansei Fukushi Research Institute, Tohoku Fukushi University, Sendai, Japan

Introduction

1. Background: Previous studies reporting that brain function changes due to cognitive training, exercise, occupation, etc. are reflected as connectivity changes in functional brain networks.

2. Identification of functional brain networks related to human traits: Social Intelligence Quotient (SQ), Intelligence Quiotient (IQ), and Emotional Intelligence Quotient(EQ) using rs-fMRI.

3. Design of estimator for human traits on the basis of identified functional networks using eight classes support vector machine (SVM).

4. Longitudinal measurements of several subjects by rs-fMRI (about 36 months academic years: every 2 months on average).

Study aim:

5. To estimate functional plasticity related to human traits.

Method

(*Subjects*)

1. Functional network and estimator: one hundred and fifty-three subjects (college students) were participated.

2. Data of twelve subjects who have participated to the longitudinal experiments.

(*Data measurements*) Structural images and functional images were measured. Parameters for structural images were matrix size= 256 × 256, voxel size=1mm3, and number of slices=192. Parameters for functional fMRI measurements were repetition time = 1000 ms, echo time = 24 ms, matrix size = 64 × 64, in-plane resolution = 3.4 × 3.4 mm2, slice thickness = 3.4 mm, and number of volumes = 480. 3T MRI scanner (Skyra-fit, Siemens) was used. Brain ROIs for network identification: 163

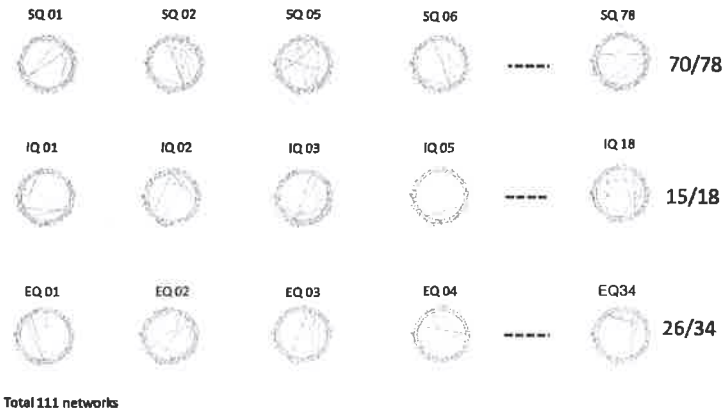
(Data Analysis)

Preprocessin: DPABI, SPM; Network analysis: GraphVar

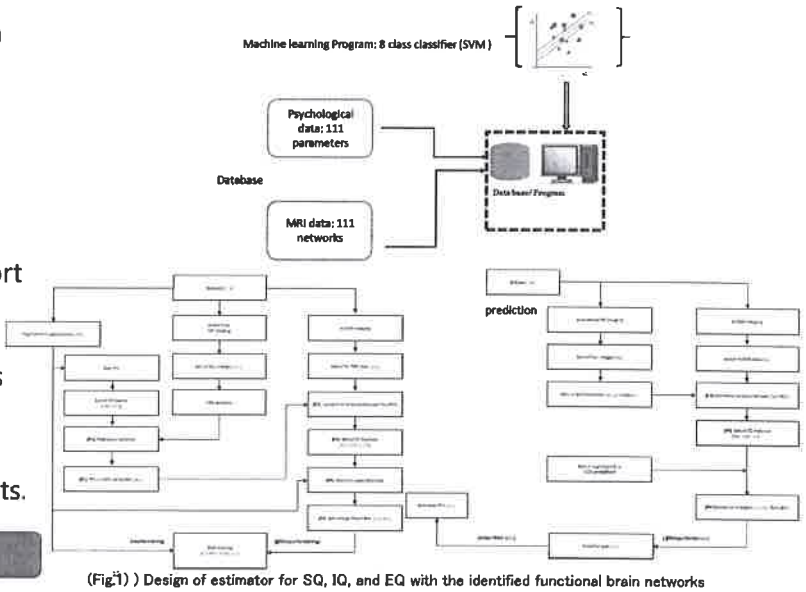
Estimator: Matlab & libSVM

Results

Total 111 networks and estimators reflecting human traits of SQ, IQ and EQ were identified: 70 from SQ, 15 from IQ, 26 from EQ.



Results



(Fig1)) Design of estimator for SQ, IQ, and EQ with the identified functional brain networks

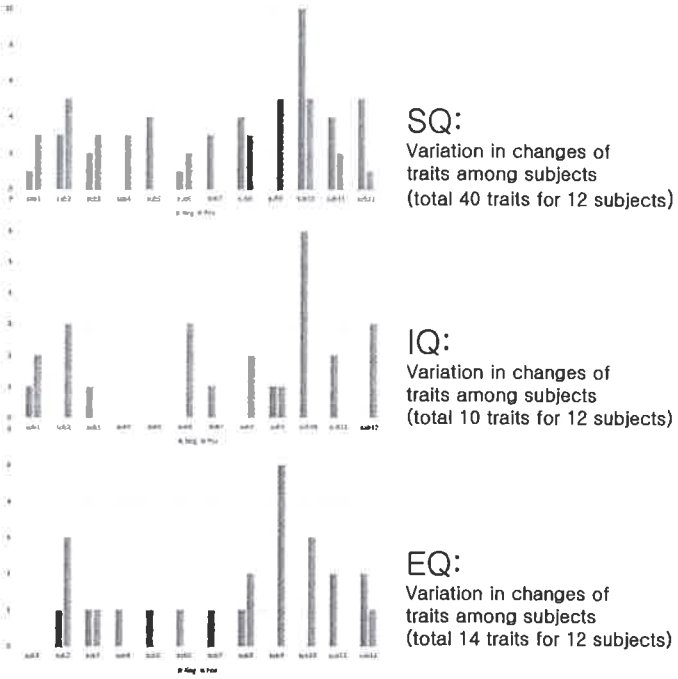


Fig2. Number of Human traits changed through 36 months per subject

Discussion/Conclusion

1.Changes of human traits through academic years could be measured by resting state fMRI.

2.Further examination should be made to clarify details affecting on the change, such as curriculum or college lifestyle.

3.Objective evaluation of education effects through fMRI data may be possible.

Acknowledgements

This research was supported by MEXT-Supported Program for the Strategic Research Foundation at Private Universities, 2014–2018.

E-mail : sung@tfu-mail.tfu.ac.jp

Estimation of specific functional brain areas reflecting individual characteristics

Yul-Wan Sung, Yousuke Kawachi, Yuki Otomo, Seiji Ogawa

Kansei Fukushi Research Institute, Tohoku Fukushi University, Sendai, Japan

Introduction

1. Most of fMRI studies were performed on the basis of a group level.
2. Recent some studies have challenged to identify functional brain areas and networks reflecting differences among individuals.

Study aim: to identify brain areas / functional networks that reflect individuality.

(1) Behavioral data of human traits related to Social Intelligence Quotient (SQ), Intelligence Quiotient (IQ), and Emotional Intelligence Quotient(EQ) and BivFive (NEO-PI-R).

(2) Derivation of a parameter differentiating individuals

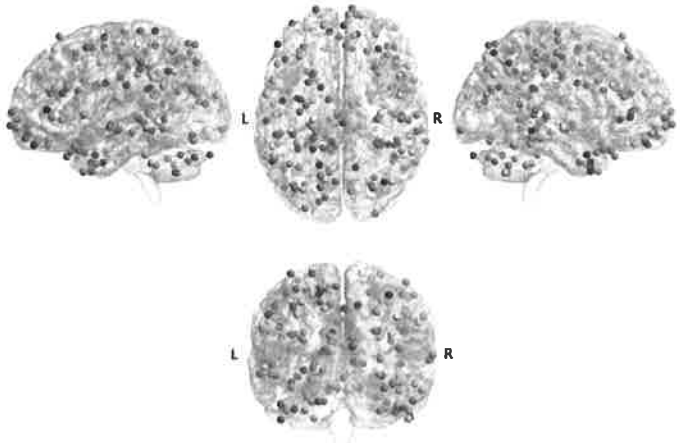
(3) Measurements of brain function by resting state fMRI

Method

(*Subjects*)
One hundred and twenty-one subjects (college students) were participated.
(Behavioral data measurements)
SQ, IQ, EQ, NEO-PI-R evaluation by the test batteries
(*MRI data measurements*) Structural images and functional images were measured. Parameters for structural images were matrix size= 256 × 256, voxel size=1mm3, and number of slices=192. Parameters for functional fMRI measurements were repetition time = 1000 ms, echo time = 24 ms, matrix size = 64 × 64, in-plane resolution = 3.4 × 3.4 mm2, slice thickness = 3.4 mm, and number of volumes = 480. 3T MRI scanner (Skyra-fit, Siemens) was used. Brain ROIs for network identification: 163
(Data Analysis)
Preprocessin: DPABI, SPM; Network analysis: GraphVar

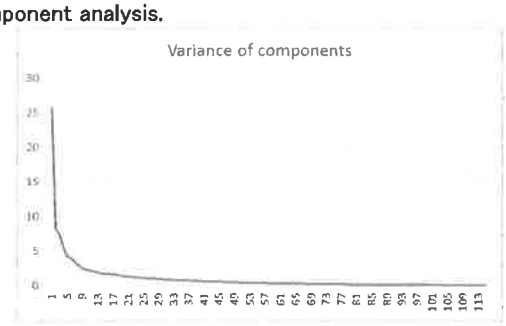
Method

Brain areas of 163 ROIs reflecting the human traits of SQ, IQ and EQ for identification of functional brain networks (Sung et al 2018)

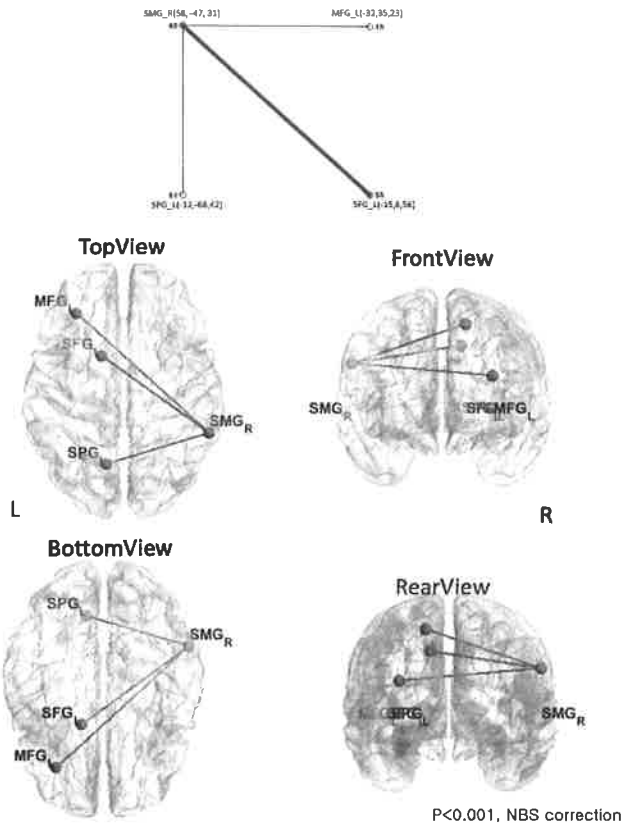


Results

A variable mostly differentiating individuals was derived through a principal component analysis.



(Fig.1) Variance of each principal component [%]



(Fig.2) Brain network/areas reflecting individuality

Discussion/Conclusion

1. A funtional brain network reflecting individuality was identified by rs-fMRI.
2. The functional network can explain individuality more than 25%
3. The interaction between the right SMG and left SFG is considered to reflect the individuality.
4. Functional roles of SMG and SFG should be examined more for the clarification of individuality represented on the brain.

Acknowledgements

This research was supported by MEXT-Supported Program for the Strategic Research Foundation at Private Universities, 2014–2018.

P11

E-mail : kikuchi.yutaro.s1@dc.tohoku.ac.jp

Quantification method of functional brain networks and estimation of network measure

Yutaro Kikuchi[1], Yul-Wan Sung[2], Seiji Ogawa[2]

[1]Graduate School of information Sciences, Tohoku University, Sendai, Japan
[2]Kansei Fukushi Research Institute, Tohoku Fukushi University, Sendai, Japan

Introduction

1. Psychological characteristics as well as brain disorders are reflected on functional brain networks derived from the resting state fMRI signals.
2. To evaluate functional brain networks, a measure is needed.
3. *Network measures from graph theory have been used but ea ch one reflects only an aspect of networks.*

In this study, we (1) **examined a quantification method of functional brain networks that uses edges of a network and a matrix composed of the edges to get eigen values as a network measure, and** (2) **a machine learning (Support Vector Regression) method to make the quantification robust.**

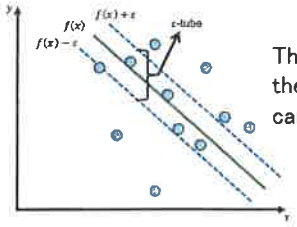
Method

Seventy functional brain networks of social intelligence quotient (SQ) and 153 subjects' data were used (Sung et al. 2018; JHBM2019 P13).



1. Adjacency matrices were made from edges and nodes of functional brain networks and then eigen values for the adjacency matrices were calculated.
2. The functional brain networks were evaluated by eigen values (Subjects' data for a network could be ordered by its eigen values.)

3. Support vector regression (SVR) was used for robust estimation of eigen values to variation of functional brain networks by physical and physiological noises in fMRI experiments.



The hyper parameter of SVR, ε,, specifies the epsilon-tube in left figure, and the ε, can be used to reduce noises.

Results

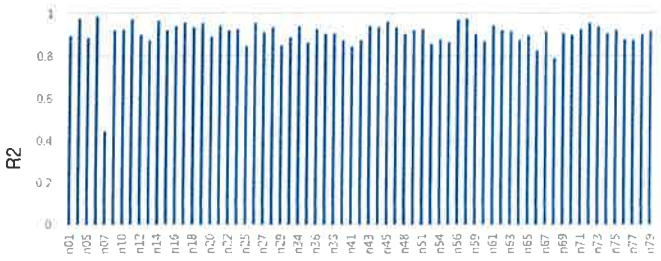


Figure 1. R2 score for training data of SVR for 70 networks with 130 subjects' training data set (with default hyper parameters of epsilon = 0.1, C = 1)

Results

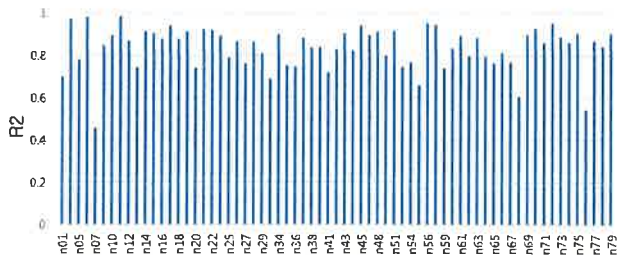


Figure 2. R2 score for 23 subjects' test data set

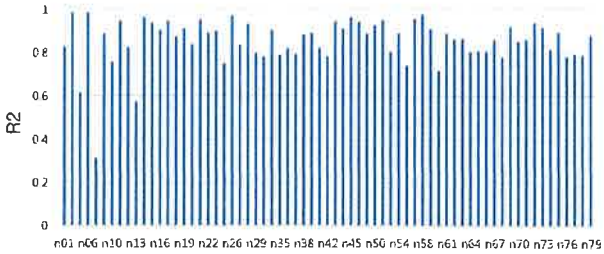
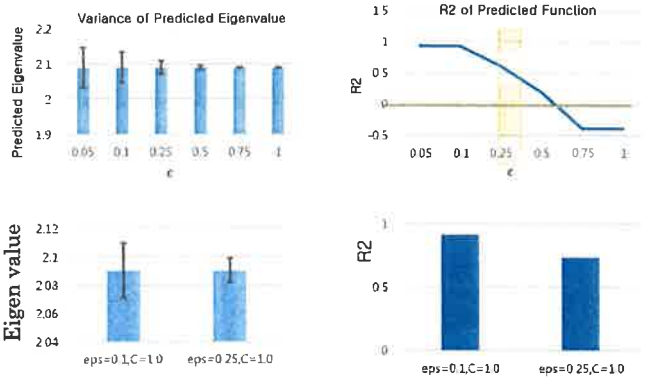


Figure 3. R2 score for 36 subjects' data set of a different experiment from that of the training and test data



An example network for robust derivation of eigen Values with repeated experiment data (8 times).



Discussion/Conclusion

1. We could **quantify a functional network by the eigen value of the adjacency matrix of the network.**
2. We could estimate **eigen values robust to measurement noises through SVR and parameter optimization.**
3. Trade-off between reduction of variation and R2 score should be further examined.
4. Other hyper parameters as well as ε will be examined in the future study.

Acknowledgements

This research was supported by MEXT-Supported Program for the Strategic Research Foundation at Private Universities, 2014–2018 and JSPS KAKENHI under Grant number 17K01993.

3EV-057

実行機能ネットワークの同定

The identification of network for executive functions

○ 阿部千裕[1] ・ 河地庸介[2]

1 東北大学大学院文学研究科，2 東北福祉大学総合福祉学部

背景

実行機能とは
課題目標に向けた思考や行動の制御を行う
高次の認知機能とされている
(Friedman et al,. 2016)

実行機能には以下の3つの構成要素からなるとされている



各要素を反映する認知課題間の高い相関関係と(Friedman et al., 2008)
各要素に関連する脳部位の重複がある(Reineberg et al., 2016)

- 目 的 -

Executive Function Network Test を作成し
実行機能の要素間に相互作用があるかどうかを検討した

方 法

参加者 大学生・大学院生31名
(mean age 20.43, SD=±3.08)

課 題 Executive Function Network Test

【刺激】 2～9のいずれかの数字

【Cue】 ● ：標的刺激の奇数・偶数判断
● ：標的刺激の5以下・6以上判断

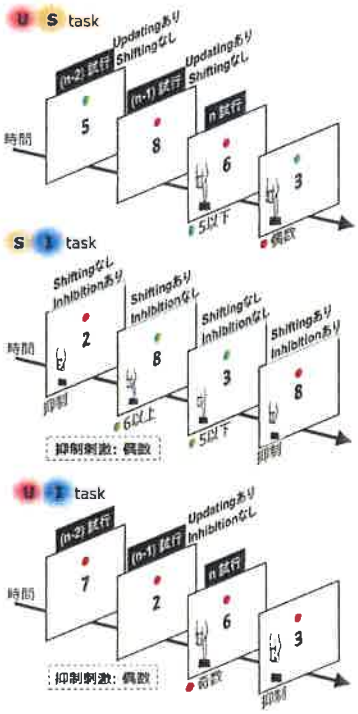
参加者はcueに従って標的刺激を速く正確に判断する

Updating
2あるいは1画面前の
標的刺激について解答する
2-back条件
(vs 0back条件)

Shifting
Cueの色に応じて判断を
切り替える
Switch条件
(vs no switch条件)

Inhibition
特定の標的のみ反応を
抑制する
No go条件 (vs Go条件)

Interaction taskの例



-- All tasks --

Simple task
● S ●

Interaction task
U S S ● U ●

指 標 各要素および2つの要素について、
個々人のベースラインRTを考慮して条件間RT差の差分値をスコアリング

U の場合

$$\frac{\text{Uあり} - \text{Uなし}}{\text{Uなし}}$$

U → S の場合

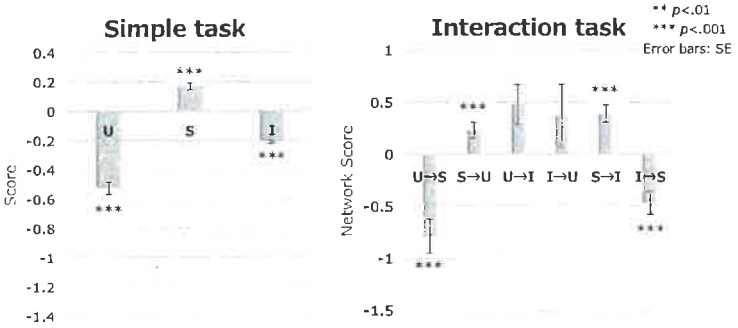
$$\frac{(\text{Uあり}-\text{Sなし}) - (\text{Sあり}-\text{Sなし})}{\text{Sあり}-\text{Sなし}}$$

Uなし

結 果

3要素と相互作用の各指標について
one-sample *t*検定（Bonferroni法による多重比較補正）によりゼロとの比較を行い、
各要素および要素間の効果を検討した

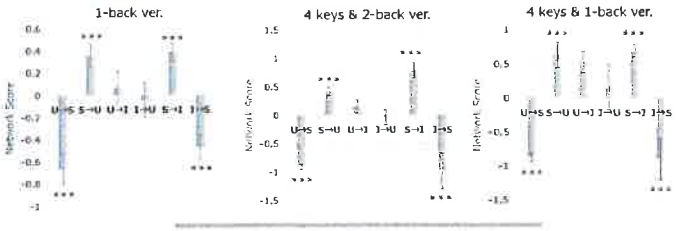
* $p<.05$
** $p<.01$
*** $p<.001$
Error bars: SE



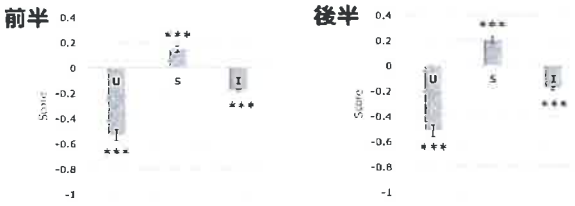
➢ 3要素すべてにおいて効果あり

➢ U S と S ● は互いに干渉を受ける

* ● ● の効果について、異なるバージョンの課題においても互いに干渉を受けない



また、相互作用の効果を正確に評価するために(Wang et al., 2015)、
3要素の各指標について各課題の前半と後半のスコアを比較し信頼性を検討した



Cronbachのα係数	Updating	Shifting	Inhibition
	0.89	0.65	0.82

➢ 3要素すべてにおいて比較的高い信頼性が示された

考 察



Updating 情報の更新 と Shifting 心的構えの切替
➢ 異なる認知機能を同時に用いるため互いに干渉を受けやすい(Baddeley, 1996)

Shifting 心的構えの切替 と Inhibition 行動抑制の有無に関する処理
➢ 類似した認知機能を同時に用いるため互いに干渉を受けた可能性がある

要素単独の効果のみならず、要素間相互作用が存在している

今後、Updating のみならず、課題の難易度や種類を調整し、
要素間相互作用の有無が一般的であるかの確認をしていく必要がある

謝辞：本研究はJSPS科学研究基盤研究C（16K00212）および東北福祉大学感性福祉研究所における文部科学省私立大学戦略的研究基盤形成支援事業（平成26年度～30年度）による助成を得て行われた。

pP2-082

実行機能ネットワークテストの考案

Measuring executive function network

○ 阿部千裕[1] ・ 河地庸介[2]

1 東北大学大学院文学研究科，2 東北福祉大学総合福祉学部

背景

実行機能とは
課題目標に向けた思考や行動の制御を行う
高次の認知機能とされている
(Friedman et al,. 2016)

実行機能には以下の3つの構成要素からなるとされている。



しかし、

各要素を反映する認知課題間の高い相関関係と(Friedman et al., 2008)
各要素に関連する脳部位間の重複がある(Reineberg et al., 2015)

- 目 的 -

Executive Function Network Test を作成し
実行機能の要素間に相互作用があるかどうかを検討した

方法

参加者 大学生・大学院生30名
(mean age 20.75, SD=±2.10)

課 題 Executive Function Network Test

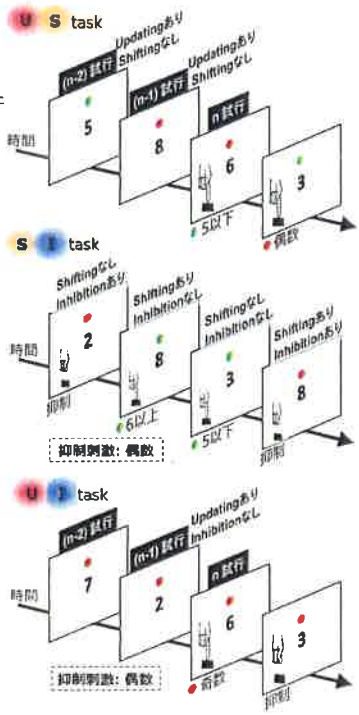
【刺激】 2～9のいずれかの数字
【Cue】 ● ：標的刺激の奇数・偶数判断
● ：標的刺激の5以下・6以上判断

参加者はcueに従って標的刺激を速く正確に判断する

Updating
2あるいは1画面前の
標的刺激について解答する
2-backあるいは1-back条件
(vs 0back条件)

Shifting
Cueの色に応じて判断を
切り替える
Switch条件
(vs no switch条件)

Inhibition
特定の標的のみ反応を
抑制する
No go条件 (vs Go条件)



-- All tasks --

Simple task
U S I

Interaction task
U S S I U I

指 標 各要素および2つの要素について、
個々人のベースラインRTを考慮して
条件間RT差の差分値をスコアリング

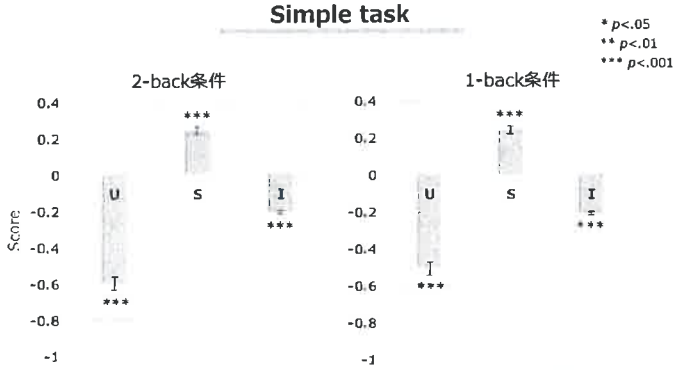
結果

3要素とネットワークの各指標について
one-sample t検定（Bonferroni法による多重比較補正）によりゼロとの比較を行い、
各要素の効果、および要素間の促進的・抑制的な効果を検討した

＊ Updating関連課題については 2-back条件 の指標を用いた

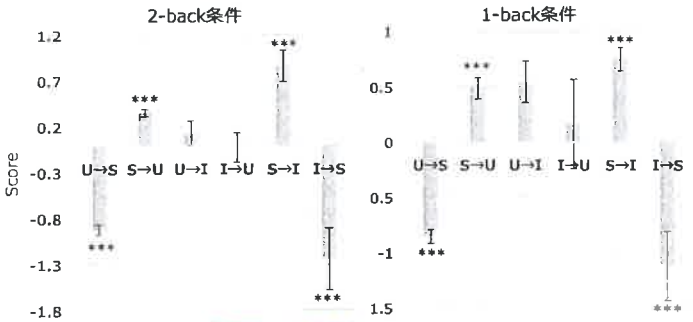
さらに、
Updating関連課題を 1-back条件 にすることで課題間の難易度を調整し、
2-back条件を用いた結果と同様の結果が得られるかを検討した

Simple task



➢ 課題の難易度に関係なく、3要素すべてにおいて効果あり

Interaction task



➢ U S と S I 間に抑制的効果あり
➢ 1-back条件においても2-back条件と同様の結果

考察

Executive Function Network Testにより、
実行機能の各要素単独の効果に加えて要素間相互作用を測定した



Updating 情報の更新 と Shifting 心的構えの切替
および
Shifting 心的構えの切替 と Inhibition行動抑制の有無に関する処理 は
互いに干渉を受けることが示された

➢ 要素単独の効果のみならず、要素間相互作用が存在している

実行機能を包括的に捉えるための新たな測定法として
Executive Function Network Testが有効である可能性が示された

今後、Updating のみならず、 Inhibition 関連課題の難易度や種類を調整し、
要素間相互作用の有無が一般的であるかの確認をしていく必要がある

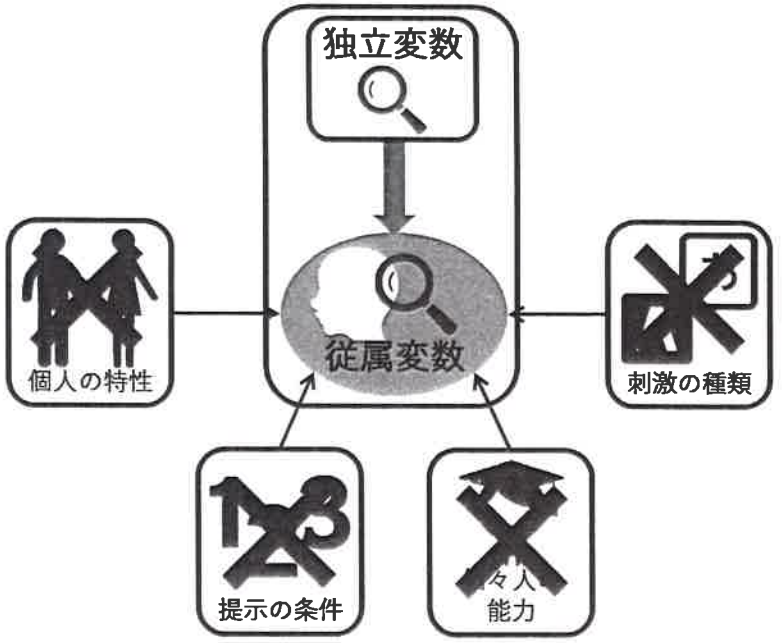
謝辞：本研究はJSPS科学研究基盤研究C（16K00212）および東北福祉大学感性福祉研究所における文部科学省私立大学戦略的研究基盤形成支援事業（平成26年度～30年度）による助成を得て行われた。

線形混合モデルでみるメタ記憶

大友ゆき・河地庸介
（東北福祉大学）

本研究は、JSPS科学研究費基盤研究C(RS150203, RS150601)および
東北福祉大学感性福祉研究所における文部科学省平成26年度採択
私立大学戦略的研究基盤形成支援事業(平成26年度～30年度)
による助成を得て行われた。





第一種の過誤（Type1 Error）



線形混合モデル
(Linear-Mixed Effect Model)

固定効果
(独立変数)

通常の分析方法では統制することが
難しい要因も同時にまとめて分析できる

より厳密な分析となり
第一種の過誤を低減

刺激提示
の条件

被験者1人ひとり
の特性

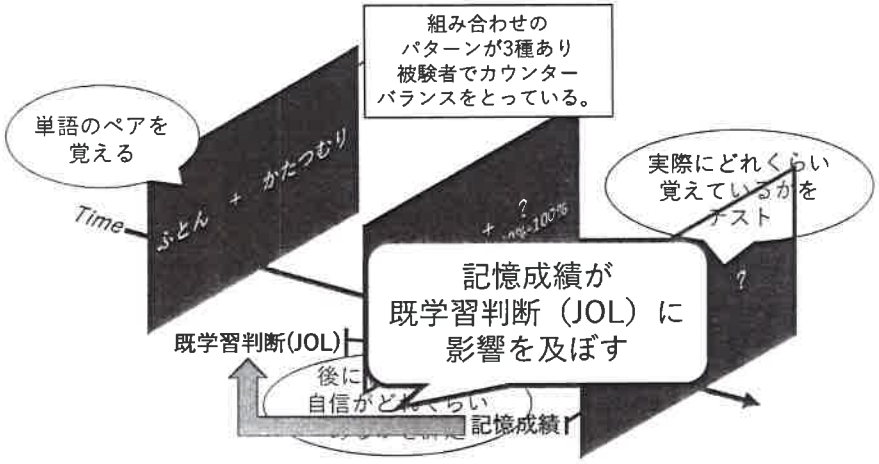
メタ記憶研究における分析

メタ記憶の精度を示す指標（Gamma等）を

実際のメタ記憶実験2種の結果を用いて
線形混合モデルを用いた分析を行い、
通常の分析結果との比較・検討を行う

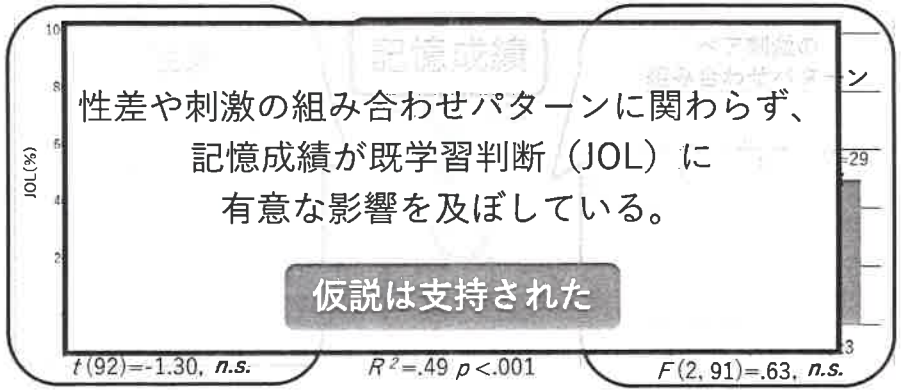
5%よりも大きく上昇 (Murayama et al., 2014)

方法：JOL判断



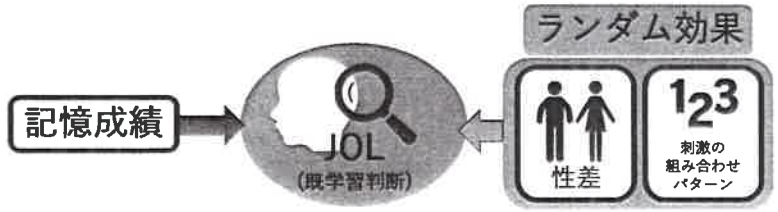
結果

t検定, 分散分析, 回帰分析の結果 (N=94)



結果

線形混合モデルの結果（N=94）



結果

線形混合モデルの結果（N=94）

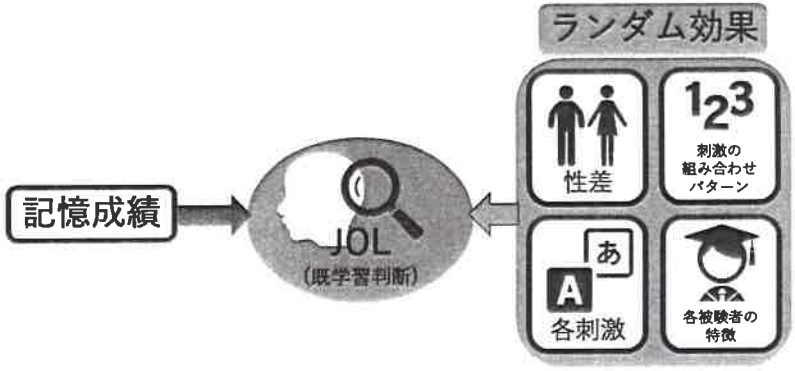
記憶成績が既学習判断（JOL）に
有意な影響を及ぼしている。

仮説は支持された

しかし、刺激の組み合わせパターンも
確信度評定（JOL）に影響を
及ぼしている可能性がある。

結果

線形混合モデルの結果（N=94）



結果

線形混合モデルの結果（N=94）

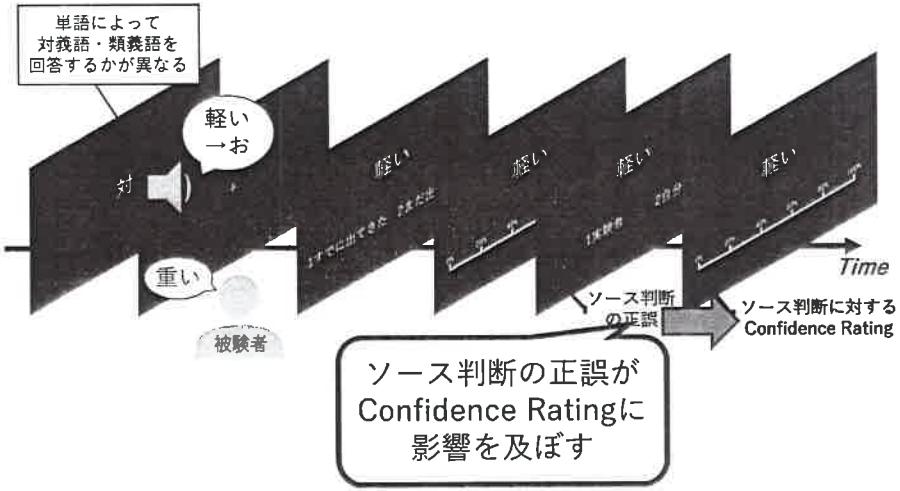
記憶成績が既学習判断（JOL）に
有意な影響を及ぼしている。

仮説は支持された

しかし、被験者の回答の特徴や記憶能力も
影響を及ぼしている可能性がある。

記憶成績

方法：ソースモニタリング判断



結果

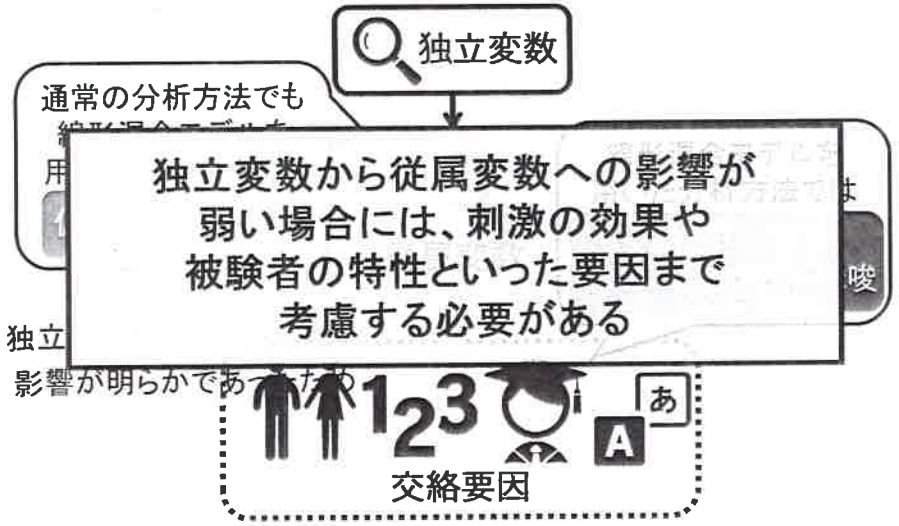
ソースモニタリング判断における

ソース判断の正誤が
ソース判断に対するConfidence Ratingに
有意な影響を及ぼしている。

仮説は支持された

しかし、被験者の回答の特徴や刺激の種類も
影響を及ぼしている可能性がある。

考察



結果

重回帰分析の結果 (N=94)

既学習判断（JOL）は、
性差や刺激の組み合わせパターンからは
影響を受けず、記憶成績からのみ
有意な影響を受ける。

仮説は支持された

性差

β=.03, *n.s.*

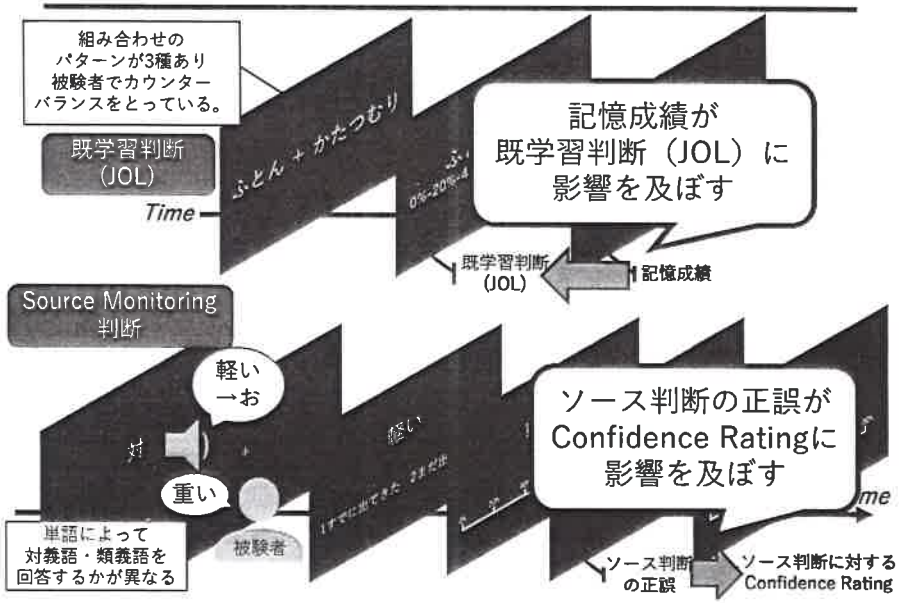
記憶成績

R^2=.50 p <.001

ペア刺激の組み合わせパターン

β=-.10, *n.s.*

方法



PA02

パーソナリティ特性が既学習判断 (Judgment of Learning: JOL)に及ぼす影響

大友ゆき[1]・河地庸介[1,2]
(1東北福祉大学感性福祉研究所、2東北福祉大学総合福祉学部)

背景

課題遂行後の成績に関する自己評価（確信）は認知的能力に加えてパーソナリティ特性に影響を受けると考えられている (Kröner et al., 2007)。

認知的能力
実際の記憶成績
etc...

パーソナリティ特性

メタ記憶

既学習判断
(Judgment of Learning: JOL)
学習した内容を後に想起できるか否かの判断

その他の要因
参加者の評価基準の個人差,実験刺激の種類 etc...

線形混合モデルを用いることで
従来の分析方法では困難な
JOLに影響を与える可能性のある要因も
同時にまとめて分析可能になる。

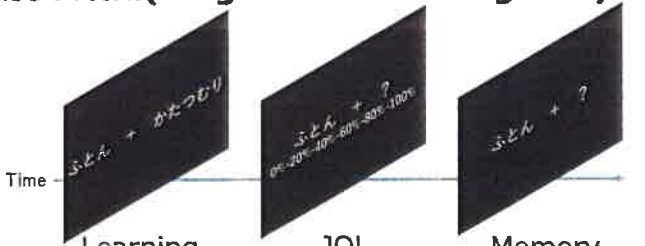
目的

**線形混合モデルを用いた分析を行い
自分自身の記憶についての評価(メタ記憶)
を正確に理解するための要因を検討する。**

方法

参加者
大学生・大学院生79名
男性14名(mean age 20.57, SD ±1.28),
女性65名(mean age 20.91, SD ±1.76)

既学習判断(Judgment of Learning: JOL)



Learning
関連がないように設定したペア単語を学習する
※ペアの組合わせパターンを3種作成

JOL
Confidence Rating
学習した単語を後のテストで思い出せる自信の程度を評定する

Memory Test
学習した単語を実際にどの程度覚えているかテストする

パーソナリティ特性の測定

NEO-PI-R(下仲ら, 2011)を用いた質問紙調査を実施

5つの因子
N：神経症傾向　E：外向性
O：開放性　A：協調性　C：誠実性

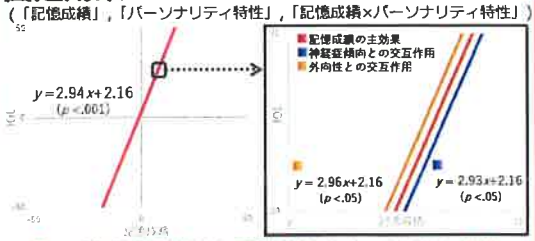
分析方法

統計解析ソフト R のパッケージ"lme4"および"lmerTest"を使用し**線形混合モデル**による分析を行った。

結果

固定効果

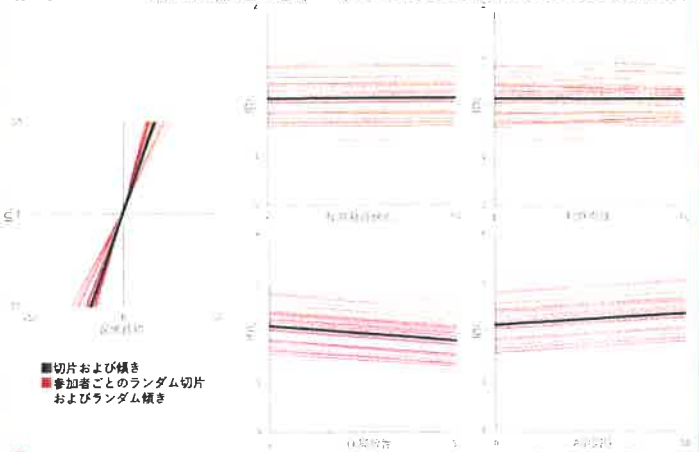
(「記憶成績」,「パーソナリティ特性」,「記憶成績×パーソナリティ特性」)



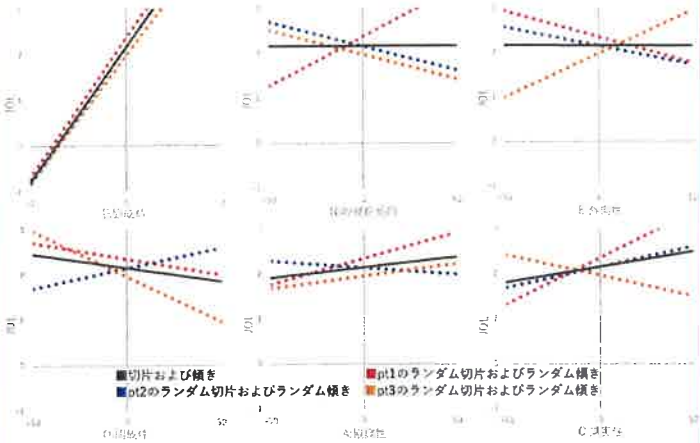
JOLは記憶成績および記憶成績とパーソナリティ特性(神経症傾向および外向性)の交互作用の影響を受ける。

ランダム効果

(「参加者, 刺激呈示順, ペア単語の組合せpt, 性別によって異なるJOLにおける基準値」,「記憶成績およびパーソナリティ特性に応じた参加者, 刺激, ペア単語の組合せpt, 性別ごとのJOLの変化量」)



各参加者の「JOL基準値(切片)」・「記憶成績に応じたJOL変化量(傾き)」・「パーソナリティ特性に応じたJOL変化量」が異なる。



各ペア単語の組合せptの「JOL基準値(切片)」・「記憶成績に応じたJOL変化量(傾き)」・「パーソナリティ特性に応じたJOL変化量(傾き)」が異なる。

考察



参加者/単語の組合せptごとの基準値・変化量
ランダム効果

パーソナリティ特性単体でJOLに影響するのではなく認知的能力との関連の中で影響する
→認知的能力は神経症傾向によってJOLを抑制する傾向がする
→認知的能力は外向性によってJOLを増幅する傾向がある

自分の記憶評価を正確に理解するためには
認知的能力とパーソナリティ特性の関連に加えて
参加者ごと/単語の組合せパターンごとのJOLの
基準値および変化量についても考慮する必要がある

謝辞：JSPS科学研究費基盤研究C(16K00212, 17K01993)および東北福祉大学感性福祉研究所における文部科学省私立大学戦略的研究基盤形成支援事業(平成26年度～30年度)による助成を得て行われた。

短期的訓練が実行機能に及ぼす影響

阿部 千裕[1]・河地 庸介[1,2]

[1]東北福祉大学感性福祉研究所，[2]東北福祉大学総合福祉学部福祉心理学科

JSPS科学研究基盤研究C（26350995）および東北福祉大学感性福祉研究所における
文部科学省私立大学戦略的研究基盤形成支援事業（平成26年度～30年度）による助成を得て
行われた。

背 景：実行機能とは

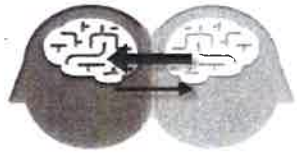
従来、種々の認知機能に関する
実証的・理論的研究が進められてきた

そして近年は
種々の認知機能を制御する高次の機能として
実行機能（Executive functions：EF）
(Damasio et al., 1994: Friedman & Miyake, 2017)
が注目されている

自分の思考や行動を
制御する際に不可欠な心的機能とされている
(Baddeley et al., 1974: Miyake et al,. 2000)

背 景：実行機能とは

EFの3要素

更新 (Updating)	切替 (Shifting)	抑制 (Inhibition)
		
Working memoryの追加や削除	心的な構えの切り替え	適切ではない反応の抑制

(Miyake et al., 2000; Friedman et al., 2016)

背 景：実行機能の低下と訓練

種々の精神障害（統合失調症、躁うつ病、ADHD等）における
EFの低下が報告されている
(for a review Snyder, Miyake, & Hankin, 2015)

他方で多くの認知機能は
訓練によりパフォーマンスが向上するといった
認知的可塑性が報告されている
(Dahlin et al., 2008)

➤ **EFの訓練によるパフォーマンスの向上は**
適応的行動を促すきっかけとなる可能性がある

背 景：実行機能の訓練

EFの各要素を反映する課題について
1か月以上の集中的訓練による課題成績の向上
(Dahlin et al., 2008; Basso et al., 2006)

他の認知機能の多くは
数十分単位の短期的訓練により課題成績が向上する
(Collie et al., 2003)

目 的

EFについても20～30分程度で課題成績が向上する可能性

➤ EF改善のための訓練時間に限界はあるのか

--- 本研究 ---

20～30分程度の訓練による
EF課題成績への効果

方 法

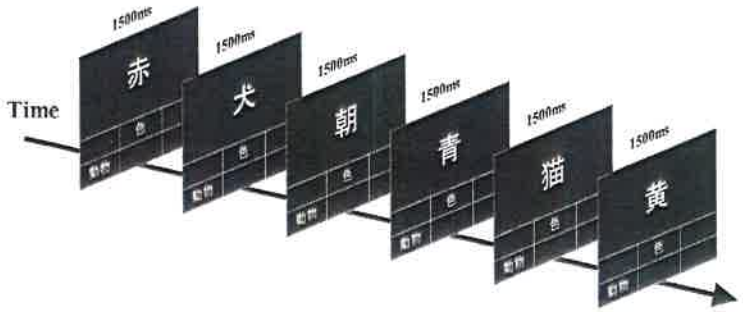
参加者： 大学生・大学院生24名
平均年齢21.38歳（SD=±1.96）

測定： 【更新】Keep track課題
【切替】Category switch課題
【抑制】Stop signal課題
(Friedman et al., 2008)

手続き： 各課題の試行を繰り返した
課題遂行の順番はカウンターバランスをとった

＊東北福祉大学研究倫理審査委員会の承認を得て実施した。

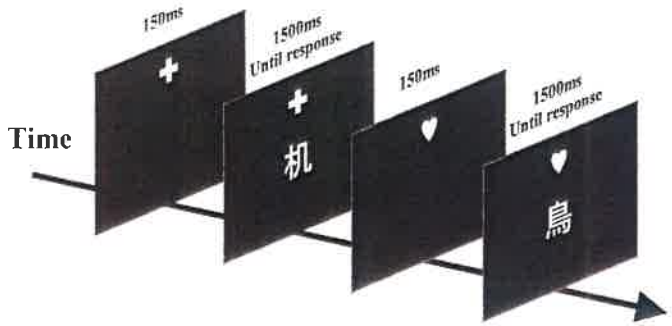
E F – 更新 課題



Keep track 課題

指標：単語の正解率（Accuracy (%)）
（カテゴリ2～4）

EF – 切替 課題

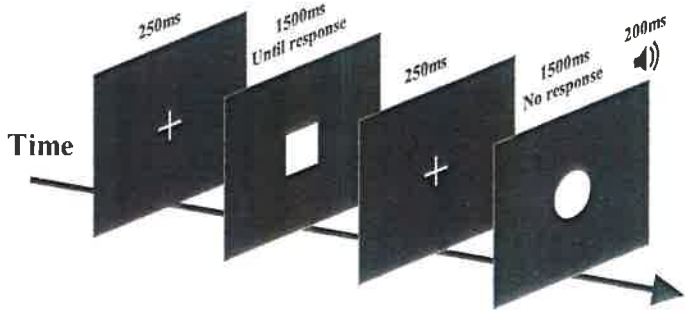


Category switch 課題

指標：判断基準を切り替えるのにかかった時間コスト (switch cost (ms))

（切り替えなし試行のRT－切り替えあり試行のRT）

EF – 抑制 課題

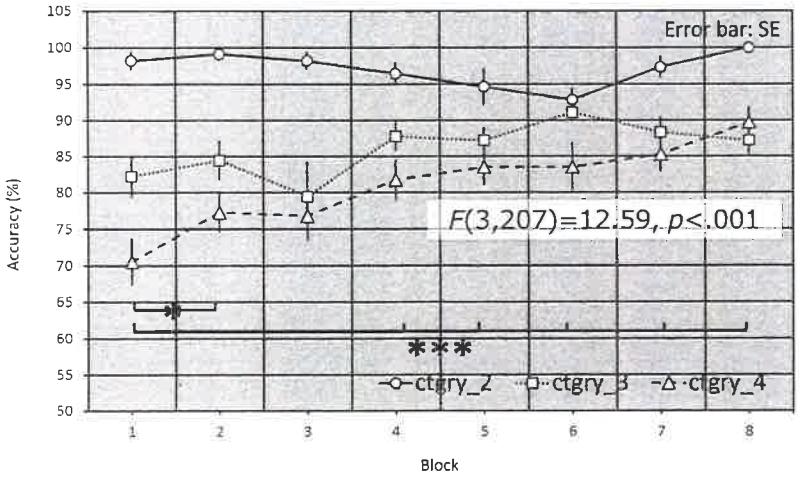


Stop signal 課題

指標：図形の判断に成功した音がない試行 (go trial) の反応時間 (RT (ms))

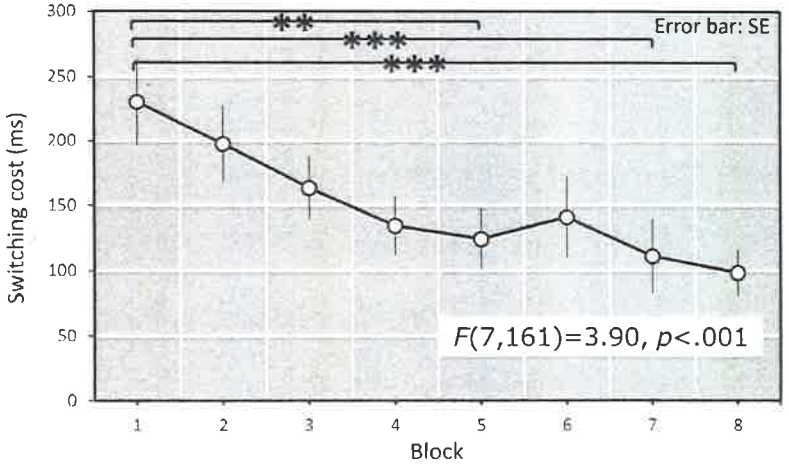
音が呈示されたときには判断をしない

結 果



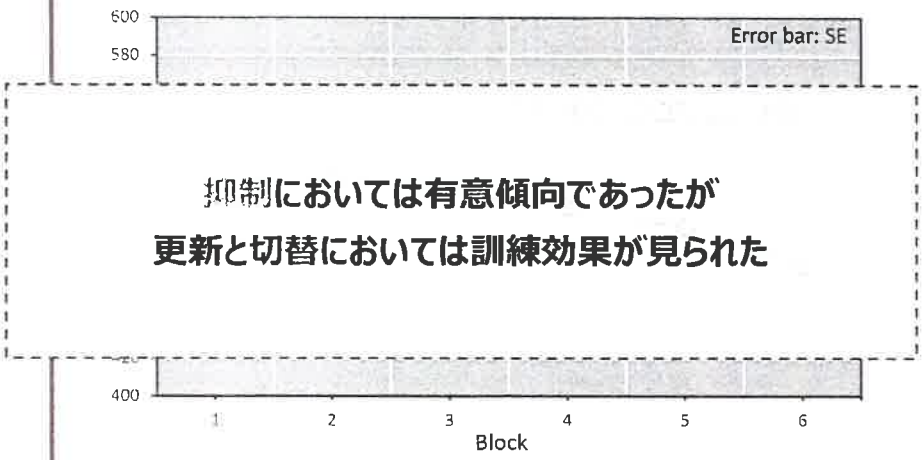
更新の訓練効果

結 果



切替の訓練効果

結 果



抑制においては有意傾向であったが
更新と切替においては訓練効果が見られた

抑制の訓練効果

考 察

課題成績向上率

((最終ブロックの指標-1ブロック目の指標)/ 1ブロック目の指標)×100

	更新	切替	抑制
			
先行研究 ：	約16%	約41%	約20%
本研究 ：	約18%	約57%	約10%

考 察

EFの短時間訓練効果の応用に向けて

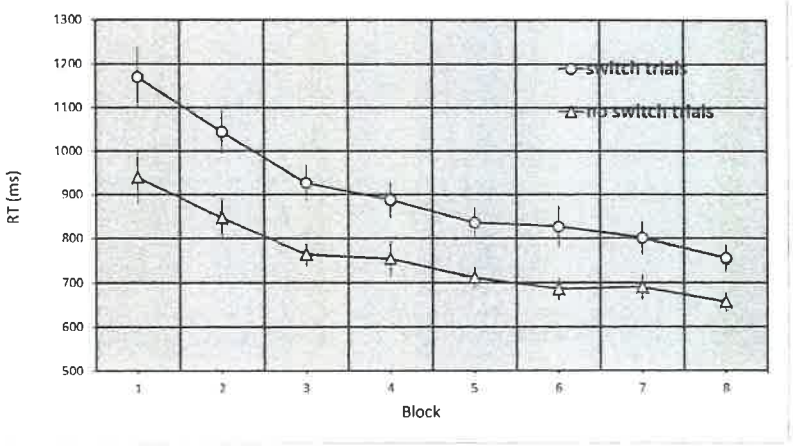
・訓練効果の持続性

・他の課題への転移(transfer)効果

➤ EF訓練が必要な患者への負担の減少

➤ 日常における適応的行動の早期的な改善

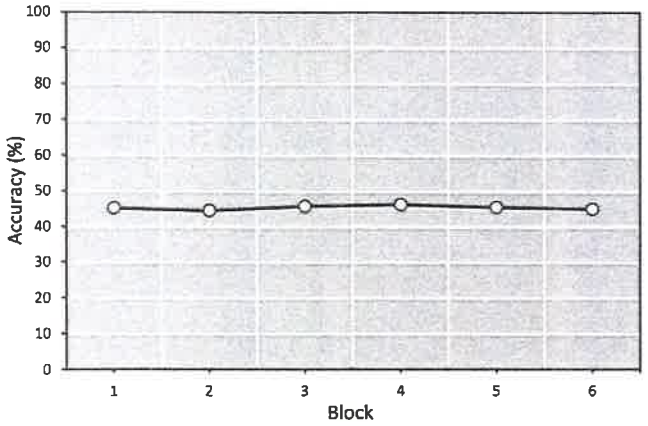
結 果 – 補足



切替の条件ごとのRT

➤ ほぼ平行のまま、反応がはやくなっていく

結果 – 補足



抑制の正解率（反応を抑制できた確率）

➤ 50%の正解率を保ったまま、RTが徐々に短くなっていく

結果 – 補足

ブロックごとの課題成績

EF tasks	Block 1 M (SD)	Block 2 M (SD)	Block 3 M (SD)	Block 4 M (SD)	Block 5 M (SD)	Block 6 M (SD)	Block 7 M (SD)	Block 8 M (SD)	% change	F statistic
Keep track task										
cigry(2) accuracy (%)	98.44 (4.22)	96.35 (6.88)	98.96 (3.53)	96.88 (5.53)	-	-	-	-	-1.59	0.59
cigry(3) accuracy (%)	90.28 (9.73)	93.4 (8.14)	95.49 (7.36)	96.88 (5.92)	-	-	-	-	7.31	3.21*
cigry(4) accuracy (%)	73.7 (16.06)	79.43 (14.21)	83.33 (10.69)	86.98 (10.08)	-	-	-	-	18.02	12.59***
Category switch task										
switch cost (ms)	230.5 (163.82)	197.48 (148.38)	163.29 (122.63)	134.21 (110.54)	124.18 (114.63)	140.75 (151.96)	110.96 (138.89)	98.42 (86.34)	57.3	3.91***
Stop-signal task										
go RT (ms)	523.34 (112.25)	516.22 (137.42)	507.42 (94.02)	499.9 (81.58)	489.48 (89.64)	468.56 (99.02)	-	-	10.47	2.2+

課題成績におけるブロック1との差

EF tasks	Block1 - Block2		Block1 - Block3		Block1 - Block4		Block1 - Block5		Block1 - Block6		Block1 - Block7		Block1 - Block8	
	Mean change score	% change	Mean change score	% change	Mean change score	% change	Mean change score	% change	Mean change score	% change	Mean change score	% change	Mean change score	% change
Keep track task														
cigry(2) accuracy (%)	-2.08	-2.12	0.52	0.53	-1.56	-1.59	-	-	-	-	-	-	-	-
cigry(3) accuracy (%)	3.13	3.46	5.21	5.77	6.6***	7.31	-	-	-	-	-	-	-	-
cigry(4) accuracy (%)	5.73*	7.77	9.64***	13.07	13.28***	18.02	-	-	-	-	-	-	-	-
Category switch task														
switch cost (ms)	33.03	14.33	67.21	29.16	96.29	41.77	106.32**	46.13	89.75	38.94	119.55***	51.86	132.08***	57.3
Stop-signal task														
go RT (ms)	7.12	1.36	15.92	3.04	23.44	4.48	33.86	6.47	54.78	10.47	-	-	-	-

メタ認知と自己成長主導性の関連性

大友 ゆき・阿部 千裕・河地 庸介
東北福祉大学

本研究は、JSPS科学研究費基盤研究C(16K00212)および
東北福祉大学感性福祉研究所における文部科学省平成26年度採択
私立大学戦略的研究基盤形成支援事業(平成26年度～30年度)
による助成を得て行われた。

背景



背景

自己成長主導性

成長には自らが率先して行うという意図・行動が必要である。
（Robitschek et al., 2004; 徳吉・岩崎, 2014）

自己成長主導性は質問紙でのみ測定されている概念であり、訓練等により向上させることは難しい

密接な関連が示唆されるメタ認知の観点からであれば、自己成長主導性向上の可能性を見出せるのでは？

（Shorey et al.,2007; 徳吉・岩崎, 2011）

背景

メタ認知

「認知についての認知」
（Donlosky & Metcalfe, 2010； Flavell, 1979）

メタ認知的知識

認知についての信念や
エピソードに基づいた知識。

メタ認知的活動

モニタリング

認知的活動の継続的な
進捗状況や現在の状態の
査定あるいは評価。

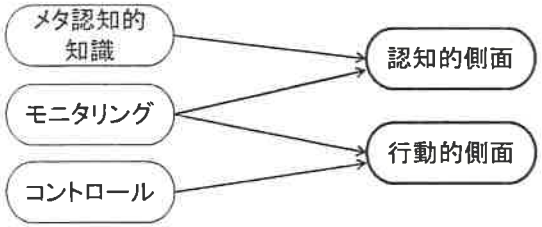
コントロール

進行中の認知的活動の
中断や変更などの調整機能。

目的

メタ認知と自己成長主導性が関連していることを
直接的に調査し、メタ認知のどの構成要素が
より自己成長主導性に影響を及ぼしているのか

＊仮説



方法：質問紙調査

対象：大学生 105名

（男性20名,女性85名,平均年齢20.63歳, *SD*=1.77）

成人用メタ認知尺度
（阿部・井田, 2010）

28項目からなる質問紙。
3つの下位因子がある。



自己成長主導性尺度Ⅱ
(PGIS-Ⅱ)
（徳吉・岩崎, 2014）

16項目からなる質問紙。
4つの下位因子がある。



※実験への参加や質問への回答は参加者の自由意思に基づいて行われた。
東北福祉大学 感性福祉研究所内にて、東北福祉大学研究倫理委員会の承認を得て実施された。

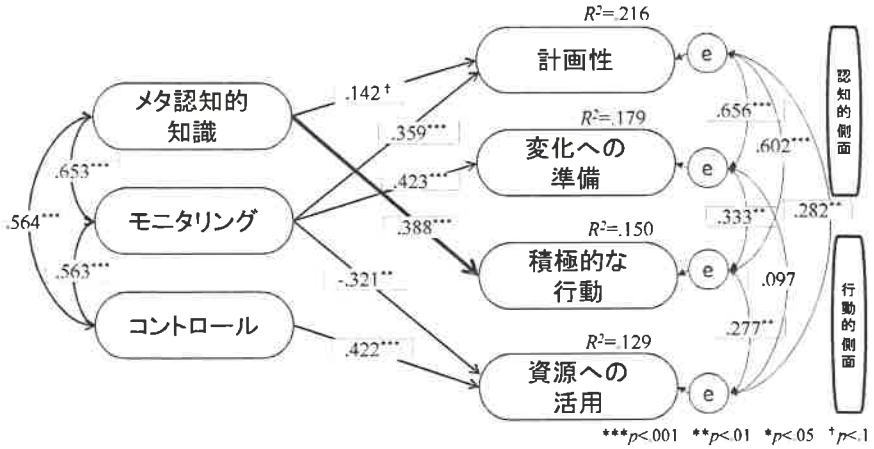
結果：相関分析

	メタ認知			自己成長主導性			
	メタ認知的知識	モニタリング	コントロール	計画性	変化への準備	積極的な行動	資源の活用
メタ認知的知識	1	.653***	.564***	**.456*** **	**.380*** **	.439**	.145
モニタリング		1	.563***	**.475*** **	**.439*** **	**.306** **	-.067
コントロール			1	.226*	.205*	**.215***	**.233***
計画性				1	.730***	.670***	.194*
変化への準備					1	.438***	.034
積極的な行動						1	.272**
資源の活用							1

***p<.001　**p<.01　*p<.05

仮説と関する部分のほとんどで正の相関が認められた。

結果：共分散構造分析



***p<.001　**p<.01　*p<.05　†p<.1

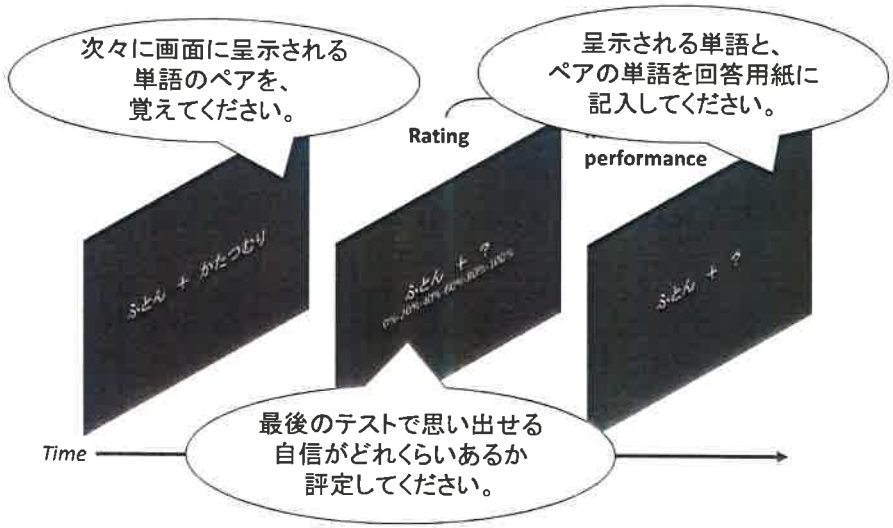
おおむね仮説は指示され、メタ認知的知識は
行動的側面にも影響することが明らかになった。

考察

メタ認知と自己成長主導性には関連があり、
メタ認知の異なる構成要素が自己成長主導性の
下位因子にそれぞれ影響していることが示された。

自己成長主導性を向上できる可能性があるメタ認知との関連を
さらに検討するために、行動指標によるメタ認知との関連性を調査する。

行動実験



行動実験

対象：大学生および大学院生　81名

（男性13名,女性68名,平均年齢20.73歳,*SD*=1.69）

既学習判断
(JOL：Judgment of Learning)
Nelson & Dunlosky (1992;2004)を参考

学習した記憶内容の再生可能性の程度評定と、
実際の再生成績からメタ記憶を測定する行動実験。

- Rating：再生可能性の程度評定値の平均
- Memory performance：実際の再生成績
- gamma：評定値と再生成績の相関

結果：相関分析

	JOL			自己成長主導性			
	Rating	Memory performance	gamma	計画性	変化への準備	積極的な行動	資源の活用
Rating	1	.665***	-.165	.213	.141	.135	.061
Memory performance		1	-.180	.046	.020	-.068	-.087
gamma			1	-.054	-.011	.043	-.059
計画性				1	.765***	.670***	.223*
変化への準備					1	.550***	.247*
積極的な行動						1	.330**
資源の活用							1

***p<.001　**p<.01　*p<.05

JOLと自己成長主導性では、いずれも相関が見られなかった。

考察

「自己の記憶についてのモニタリング」という側面の

メタ認知は自己成長主導性と関連しない。

しかし…

JOLではメタ認知の一部の側面しか測定できていない。

自己成長主導性の向上におけるメタ認知の活用のために
メタ認知のその他の側面に着目した行動指標を用いて
検討を続けている。

2-42

報酬を導く意思決定方略への依存
ーアイオワギャンブリング課題を用いた検討

○ 阿部千裕[1] ・ 河地庸介[1,2] ・ 北村康宏[3] ・ 成烈完[1] ・ 小川誠二[1]
1 東北福祉大学感性福祉研究所，2 東北福祉大学総合福祉学部，3 (公財)鉄道総合技術研究所

背景

不確実な状況下における意思決定は
過去に学習した方略により最適化される
(Maia & McClelland, 2004)

この学習が
意識的になされるのか否かについて
盛んに検討が進められている
(Bechara et al., 1997; Maia & McClelland, 2004)

特にVMPFC損傷患者において
不十分な学習に伴うリスク選好型意思決定が問題とされてきた

しかし、
多くの健常者における日常での問題は
方略の学習それ自体にあることは多くはなく、
方略を状況適応的に調節し、意思決定できるか否かにあると考える

ー目的ー

選択行動の傾向、意思決定までの時間の観点から

**学習した方略の有効性が変化する状況下での
当該方略への依存の検討**

方法

参加者： 大学生・大学院生60名 (mean age 20.75, SD=±2.10)
このうち、30名を**実験群 (Prior群)**
30名を**統制群 (Original群)** へと割り当てた。

課題：アイオワギャンブリング課題 (Bechara et al., 1994)
オリジナル版の課題をコンピュータ上で行えるように改変して用いた。

Original群の課題

100trials

	A	B	C	D
利益：損失	5:5	9:1	5:5	9:1
長期的損失	多い	多い	少ない	少ない

Prior群の課題

方略を学習させるために
Prior block を課した。

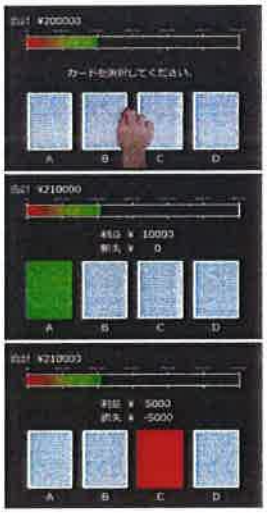
Prior block：A deckを選択し続けると
長期的な獲得金額は利益が多くなる

Prior block　40trials

	A	B	C	D
利益：損失	9:1	9:1	5:5	9:1
長期的損失	極端に少ない	多い	少ない	少ない

Original block　100trials

	A	B	C	D
利益：損失	5:5	9:1	5:5	9:1
長期的損失	多い	多い	少ない	少ない



教示： ゲームの目標
『できる限りお金を獲得すること あるいは
できる限りお金の損失を避けること』

＊カードの選択は自由に変更可能
＊いつ、どのくらい損失するかは不明
＊悪いカードの山がある
＊本物のゲームであるかのように振る舞う

指標： A deckの選択率(%)、選択反応時間:RT(ms)

	方略の学習		指標の比較				
Original群			Block1	2	3	4	5
Prior群	Prior block1	2	Block1	2	3	4	5

結果と考察

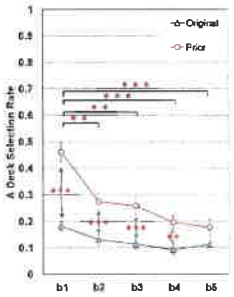
Error bars : SE
b : Original block, pb : Prior block
*** : p<.001, ** : p<.01, * : p<.05

A deckの選択率(%)

Prior群とOriginal群との有意差
➤ Prior blockにおける経験から
A deckを"good deck"と認識している

Aを選ぶ方略への依存が見られる

なお、Prior群と異なり、
Original群ではブロック間で有意な差はない

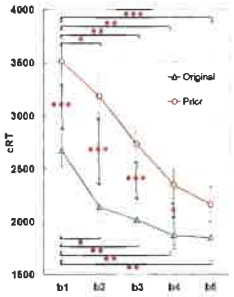


選択反応時間(ms)

Prior群とOriginal群との有意差
➤ Prior blockにおける経験が影響している

Original群のRTはb1からb2にかけて急激に短縮
➤ 方略の学習が急激に進み、選択肢を絞り込む

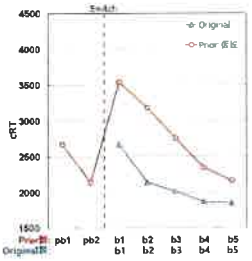
Prior群のRTは徐々に短縮していく
➤ 方略の学習が緩慢に進み、徐々に選択肢を絞り込む



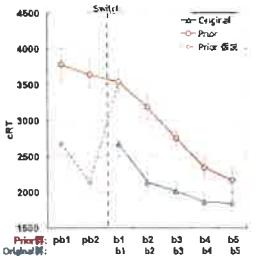
Prior群とOriginal群のRTの差異の検討

RTが方略の見直しを反映するなら、b1ではPrior block
よりも処理が増えるため **Prior block ＜ b1** になる

方略の見直しではない



【仮 説】Prior block の RT



【結 果】Prior block の RT

追加実験とまとめ

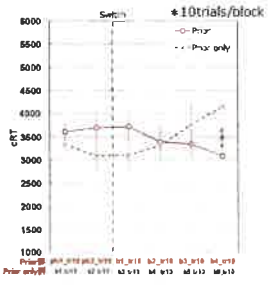
方略の見直しの必要がない **Prior only 課題**を遂行した群と
Prior群のRTの比較から、Aを選ぶ方略の見直しについて検討した。

Prior only課題：Prior blockのみの課題（合計金額が満額になった時点で試行数の打ち切りを行った）

Prior only群とPrior群のRTの差異

【Switch後】
Prior only群：徐々にRTが長くなっている
➤ Aの選択に確信がなく、
潜在的に選択肢を絞り込めていない

Prior群：徐々にRTが短くなっている
➤ Aを選択する方略を見直し、
選択肢を絞り込んでいる可能性



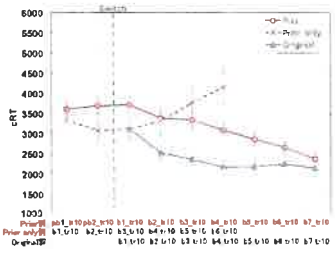
学習した方略が通用しない状況の意思決定

【方略が通用しなくなる（switchの）前後】
Aを選ぶ一方で、
潜在的に選択肢の絞り込みができていない

【Switch以降のPrior群RT＞Original群RT】
Aに確信がなく、
潜在的に絞り込めないことによる時間差

【Switch以降のPrior群RT＜Prior only群RT】
Aを選ぶ方略の見直しと
選択肢の絞り込みによる時間差

➤ **従来の方略の緩慢な見直しとともに、
従来の方略に確信がないにもかかわらず
他の選択肢の再検討をせず頼り続ける（依存）**



謝辞：本研究はJSPS科学研究基盤研究C（16K00212）および東北福祉大学感性福祉研究所における文部科学省私立大学戦略的研究基盤形成支援事業（平成26年度～30年度）による助成を得て行われた。

O3-5-06

統合失調型パーソナリティ傾向におけるメタ記憶の特徴

大友 ゆき・河地 庸介・阿部 千裕・成 烈完・松江 克彦・小川 誠二
東北福祉大学

本研究は、JSPS科学研究費基盤研究C(16K00212)および東北福祉大学感性福祉研究所における文部科学省平成26年度採択私立大学戦略的研究基盤形成支援事業(平成26年度～30年度)による助成を得て行われた。

演題発表に関連し、開示すべきCOI関係にある企業などはありません。

目 的

メタ記憶

自己の記憶のうち「覚えていること」または「覚えていないこと」を正確に認識する能力。

統合失調症

記憶しているか否かに関わらず「覚えていない」という認識が強い。
(Thuaire, Izaute & Bacon, 2012
McAnanama,2013 et al.)

統合失調症と連続性が仮定される
統合失調型パーソナリティではどうか？

健常者を対象とすることで、
統合失調症と統合失調型パーソナリティとの間に
メタ記憶の問題においても連続性がある可能性を検討

方 法

対象：健常成人　50名(男性4名,女性46名)

※実験への参加や質問への回答は参加者の自由意志に基づいて行われた。
東北福祉大学 感性福祉研究所内にて、
東北福祉大学研究倫理委員会の承認を得て実施された。

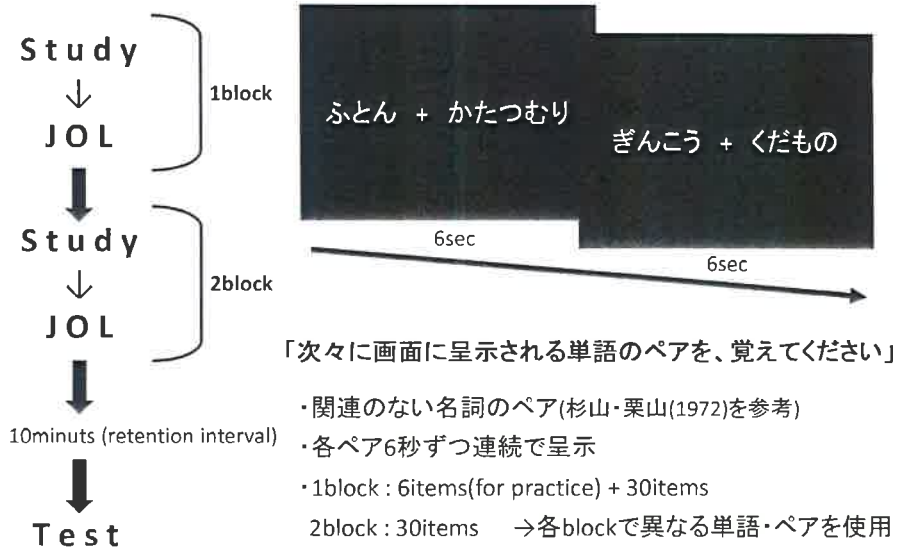
統合失調型パーソナリティ尺度 (SPQ-B)

統合失調型パーソナリティの包括的な評価を目的として作られた自己記入式の質問紙(伊藤ら,2008)。
→得点が高いほど、統合失調型パーソナリティ傾向あり

既学習判断 (JOL：Judgment of Leaning)

学習した記憶内容の再生可能性の程度評定と、実際の再生成績からメタ記憶を測定する行動実験。
→Nelson & Dunlosky (1992;2004)を参考

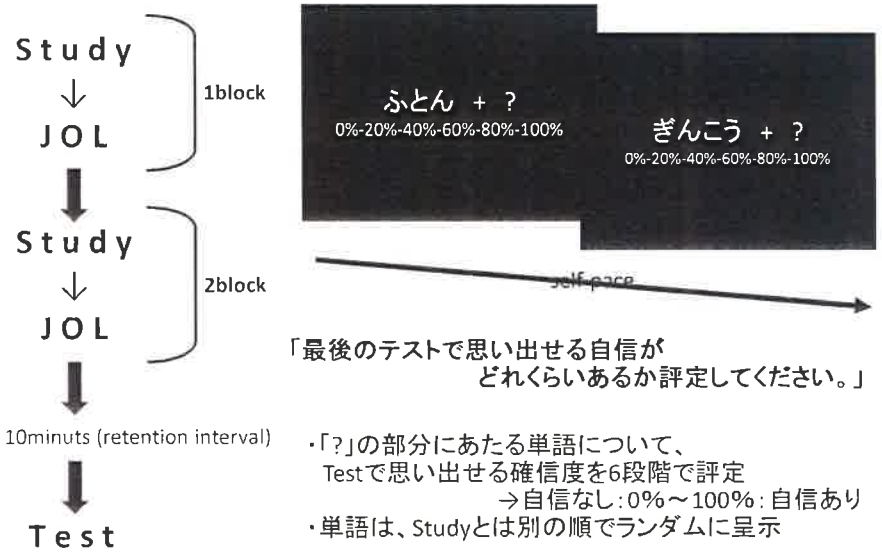
Study



「次々に画面に呈示される単語のペアを、覚えてください」

・関連のない名詞のペア(杉山・栗山(1972)を参考)
・各ペア6秒ずつ連続で呈示
・1block：6items(for practice) + 30items
2block：30items　→各blockで異なる単語・ペアを使用

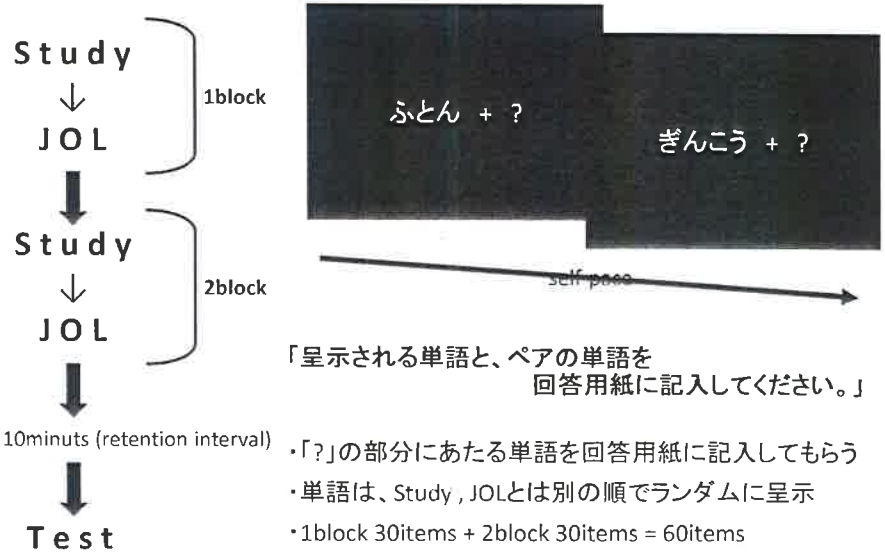
JOL



「最後のテストで思い出せる自信が
どれくらいあるか評定してください。」

・「?」の部分にあたる単語について、
Testで思い出せる確信度を6段階で評定
→自信なし：0%～100%：自信あり
・単語は、Studyとは別の順でランダムに呈示

Test



「呈示される単語と、ペアの単語を
回答用紙に記入してください。」

・「?」の部分にあたる単語を回答用紙に記入してもらう
・単語は、Study , JOLとは別の順でランダムに呈示
・1block 30items + 2block 30items = 60items

結　果

被験者ごとに以下の指標を算出

Correct answer	Testにおける正再生率(%)
mean JOL	全確信評定(%)の平均値

メタ記憶研究の指標(Schraw 2009)	
absolute accuracy	再生成績に関しての確信評定の精度
correlation	再生成績と確信評定の相関
bias	確信評定の過大・過小の程度
scatter	正答・誤答内での確信評定値の変動
discrimination	正答・誤答内での確信評定弁別の容易さ

相　関

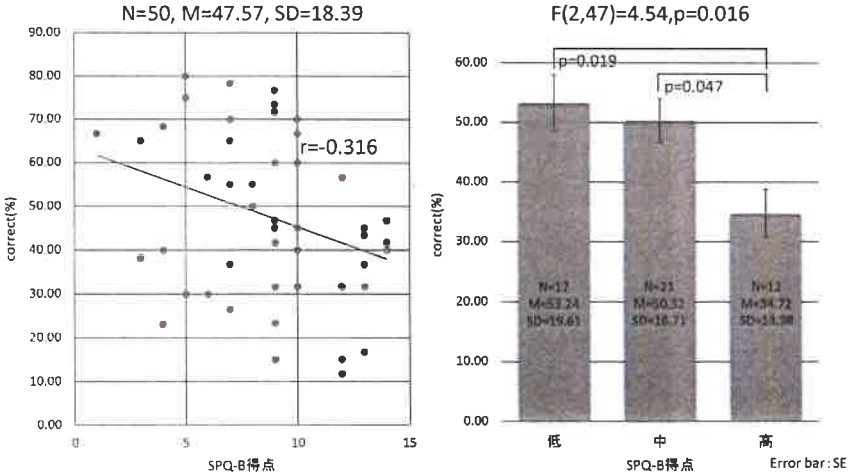
(N=50)

	correct	mean JOL	absolute	correlation	bias	scatter	discrimination	SPQ
correct	1	.623**	-.043	-.087	-.462**	.573**	.888**	**-.316***
mean JOL		1	-.101	.011	.405**	-.103	.634**	-.180
absolute			1	-.703**	-.064	-.147	-.386**	.247
correlation				1	.115	-.057	.211	-.176
bias					1	-.787**	-.320*	.165
scatter						1	.559**	-.230
discrimination							1	**-.355***
SPQ								1

**:1%水準で有意　*:5%水準で有意

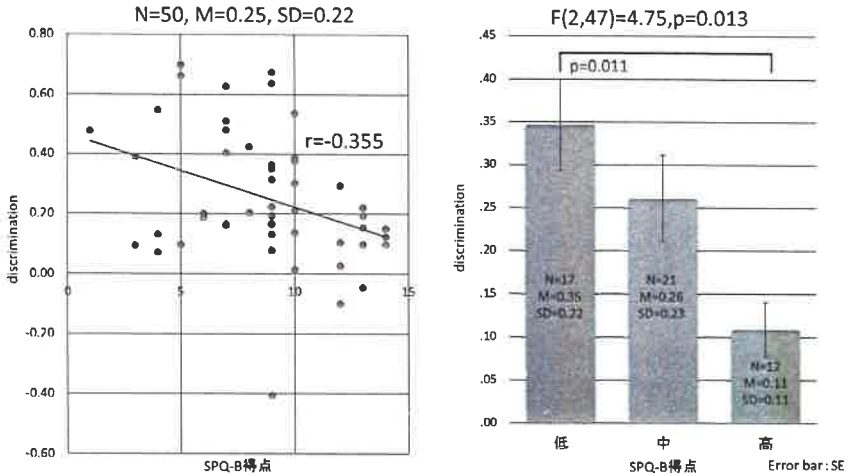
SPQ × correct answer, SPQ × discriminationについて
有意な相関があることが示された 。

correct answer



統合失調型パーソナリティ傾向が高いほど、正再生率が低くなる。

discrimination



統合失調型パーソナリティ傾向が高いほど、
再生成績の正答・誤答の弁別が困難である。

考　察

Correct answer × SPQ

統合失調型パーソナリティ傾向が高いと再生成績が低下する。
→統合失調症では記憶機能が
低下することが知られている(松井,2003;2004)。

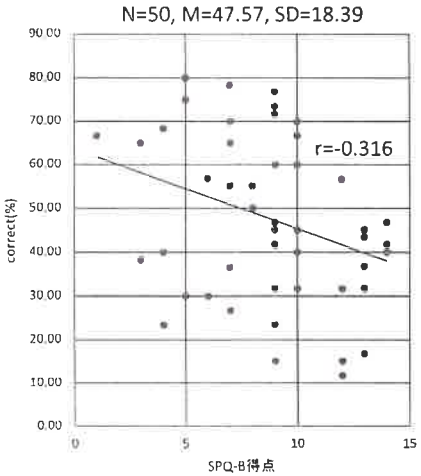
discrimination × SPQ

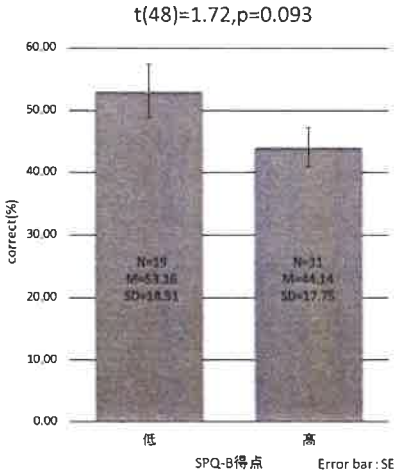
「覚えている」または「覚えていない」ことを容易に弁別する
というメタ記憶に問題があると考えられる。

統合失調症と連続性が仮定される
統合失調型パーソナリティにおいても
メタ記憶の低下が示された。

メタ記憶が統合失調症予測の1つの指標として期待できる。

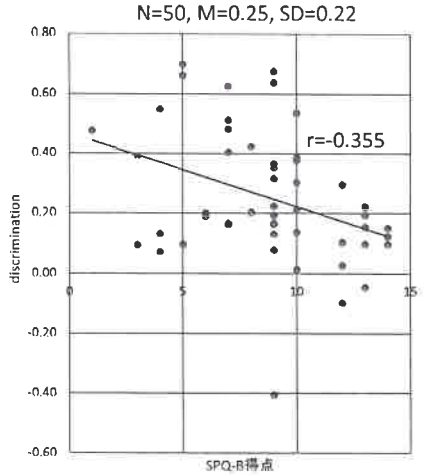
correct answer

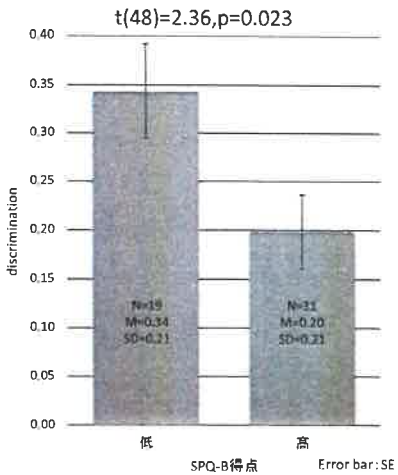




統合失調型パーソナリティ傾向が高いほど、正再生率が低くなる傾向がある。

discrimination





統合失調型パーソナリティ傾向が高いほど、
再生成績の正答・誤答の区別ができない。

Absolute accuracy = $1/N\sum_{i=1}^{N}(c_i - p_i)^2$

Ci：確信評定(0～100%)
pi:再生成績の正誤(0 or 100%)

Correlation = γ　※SPSSにて計算

Bias = $1/N\sum_{i=1}^{N}(c_i - p_i)$

Ci：確信評定(0～100%)
pi:再生成績の正誤(0 or 100%)

Scatter = $1/N[N_c\,var(c_{correct}) - N_i\,var(c_{incorrect})]$

$var(c_{correct})$:正答itemの確信評定変動
$var(c_{incorrect})$:誤答itemの確信評定変動

Discrimination = $1/N[\sum_{i=1}^{N_i}(c_{i\ correct}) - \sum_{i=1}^{N_i}(c_{i\ incorrect})]$

N：item数
N_c:正答item数
N_i：誤答item数

$C_{i\ correct}$:正答itemの確信評定
$C_{i\ incorrect}$：誤答itemの確信評定

相関(N=49)

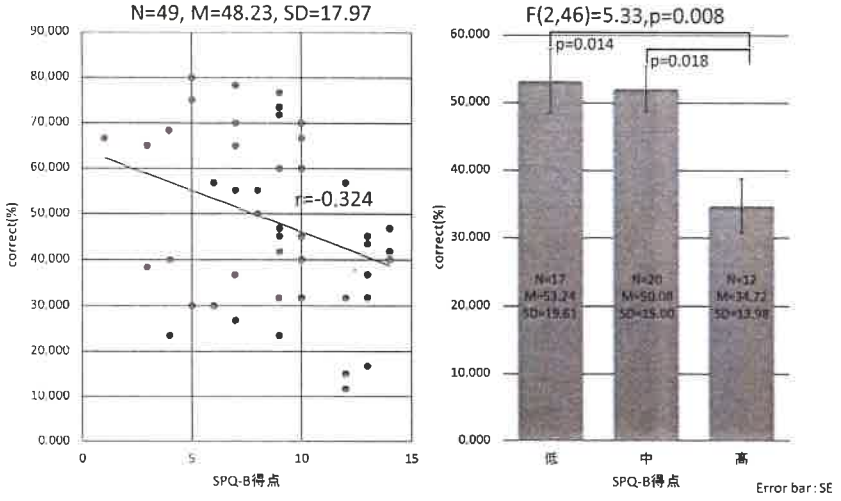
(N=49)

	correct	mean JOL	absolute	correlation	bias	scatter	discrimination	SPQ
correct	1	.616**	-.063	-.093	-.443**	.533**	.892**	-.324*
mean JOL		1	-.111	.010	.434**	-.165	.646**	-.180
absolute			1	-.705**	-.054	-.188	-.462**	.249
correlation				1	.118	-.065	.230	-.176
bias					1	-.796**	-.285*	.166
scatter						1	.475**	-.243
discrimination							1	-.388**
SPQ								1

**：1%水準で有意　*：5%水準で有意

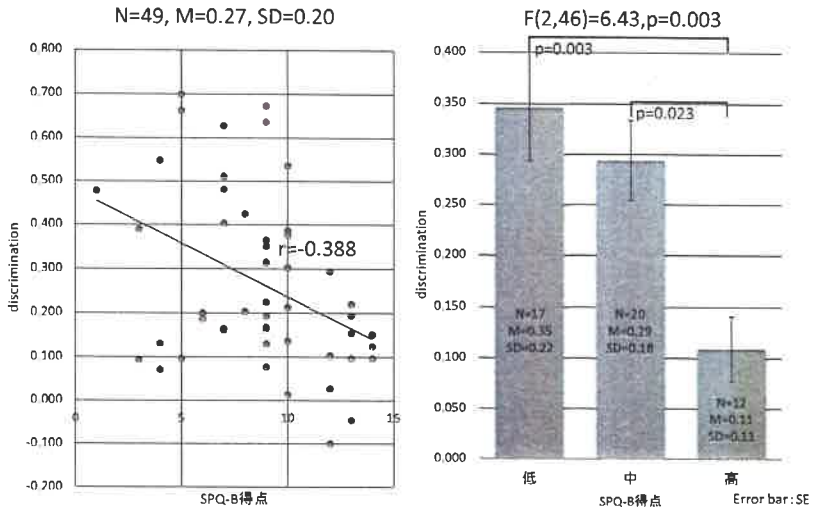
N=50の場合と、同様の結果が得られた。

correct answer(N=49)



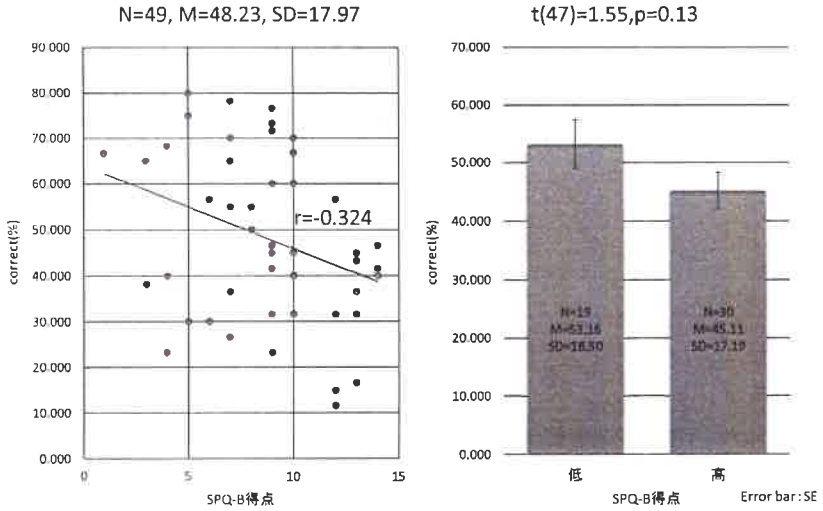
N=50の場合と同様の結果が得られた。

discrimination(N=49)



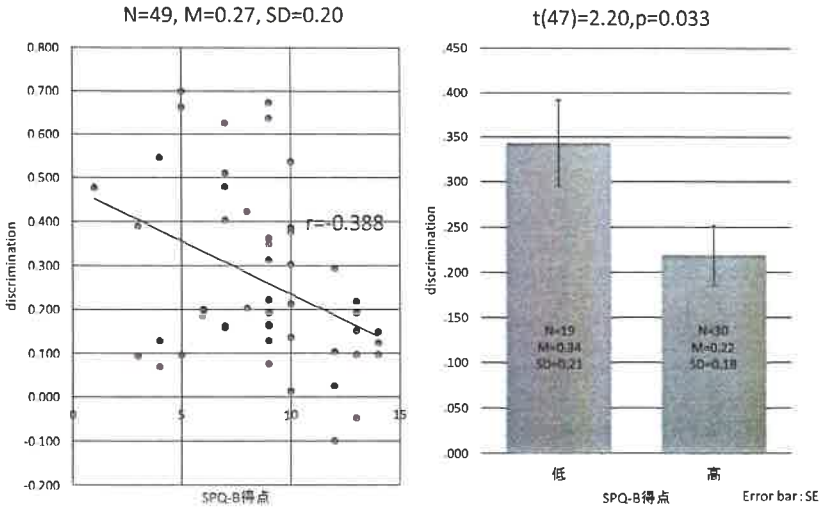
N=50の場合と同様の結果が得られた。

correct answer(N=49)



N=50の場合は、有意な傾向が見られたが、
N=49場合は、有意な差は見られなかった。

discrimination(N=49)



N=50の場合と同様の結果が得られた。

O3-5-03

統合失調型パーソナリティの個人差が注意の下位機能間の相互作用に及ぼす影響

河地 庸介[1]・阿部 千裕[2]・成 烈完[1]・松江 克彦[3]・小川 誠二[1]

1. 東北福祉大学 感性福祉研究所
2. 東北福祉大学大学院 総合福祉学研究科
3. 東北福祉大学 健康科学部

JSPS科学研究費基盤研究C（16K00212）および東北福祉大学感性福祉研究所における文部科学省私立大学戦略的研究基盤形成支援事業（平成26年度～30年度）による助成を得て行われた。

演題発表に関連し、開示すべきCOI関係にある企業などはありません。

はじめに－３機能と統合失調症－

注意は以下の３つの機能からなるとされている。
(Posner & Petersen, 1990; Fan, McCandliss, Sommer, Raz, & Posner, 2002)

喚起: 予測される刺激に対して反応準備を高める機能

定位: 複数の選択肢からある情報を選択する機能

実行制御: 情報が競合する状況を解決する機能

実験方法は同様であることから
対象者への治療の影響等も考えられる。

はじめに－注意の３つの機能－

注意は以下の３つの機能からなるとされている。
(Posner & Petersen, 1990; Fan, McCandliss, Sommer, Raz, & Posner, 2002)

喚起: 予測される刺激に対して反応準備を高める機能

定位: 複数の選択肢からある情報を選択する機能

実行制御: 情報が競合する状況を解決する機能

目　的

健常者のもつ
統合失調症様の体験をしやすい特性が
（統合失調型パーソナリティ特性）
注意機能に及ぼす影響を検討する。

Experiment

被験者: 健常成人51名 (M = 21.26, SD = 2.90)

質問紙: 統合失調型パーソナリティ尺度 (SPQ-B, 伊藤ら, 2008)

— 認知・知覚（陽性症状様体験）、対人関係（陰性症状様体験）、 解体様体験の下位尺度からなる。

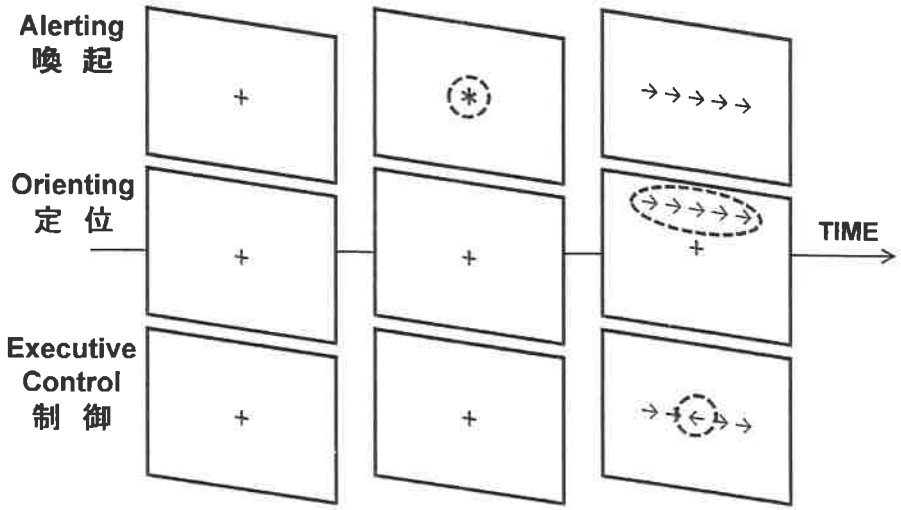
実験課題: Attention Network Test (ANT Fan et al., 2002)



参加者には書面および口頭によるインフォームドコンセントを行った。
本研究は東北福祉大学研究倫理審査委員会の承認を得て実施した。

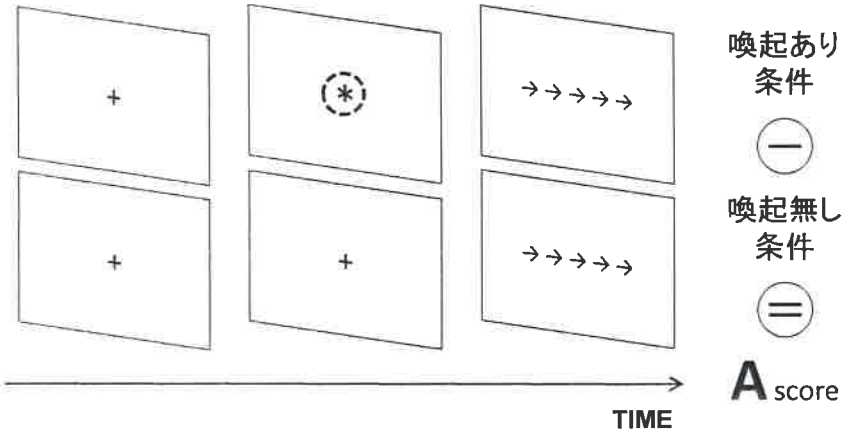
Attention Network Test (ANT)

(Fan, McCandliss, Sommer, Raz, & Posner, 2002; Wang et al., 2016)



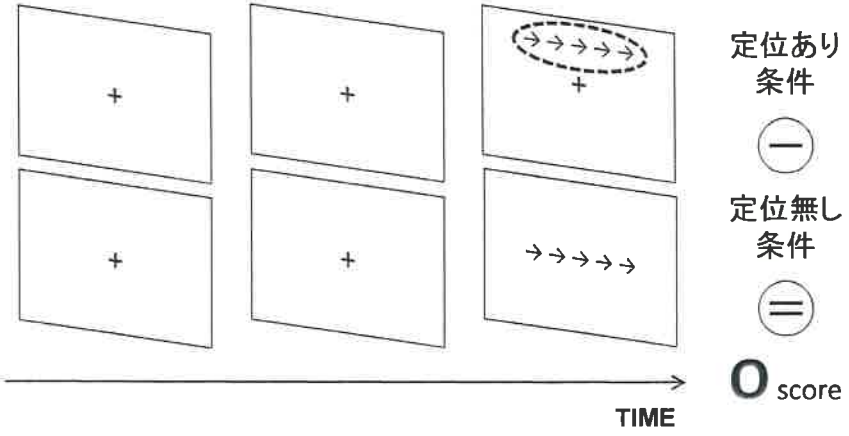
ANT – 喚起機能指標

(Fan, McCandliss, Sommer, Raz, & Posner, 2002; Wang et al., 2016)



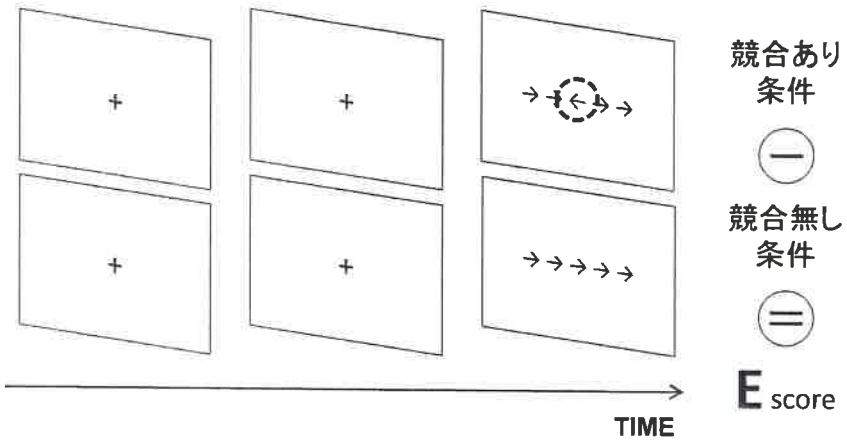
ANT – 定位機能指標

(Fan, McCandliss, Sommer, Raz, & Posner, 2002; Wang et al., 2016)



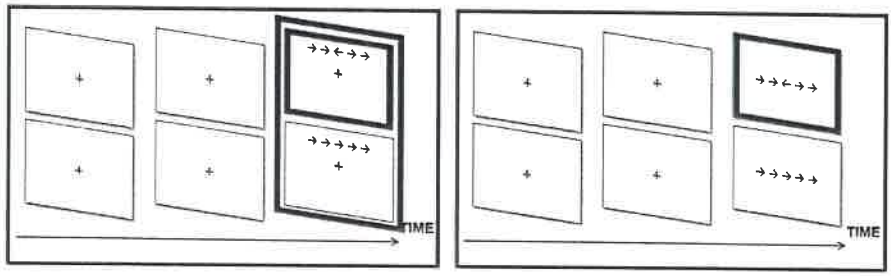
ANT – 制御機能指標

(Fan, McCandliss, Sommer, Raz, & Posner, 2002; Wang et al., 2016)



ANT – 定位から制御への影響（O to E）

(Fan, McCandliss, Sommer, Raz, & Posner, 2002; Wang et al., 2016)



「注意の定位によって、遅延する注意の制御」を評価する

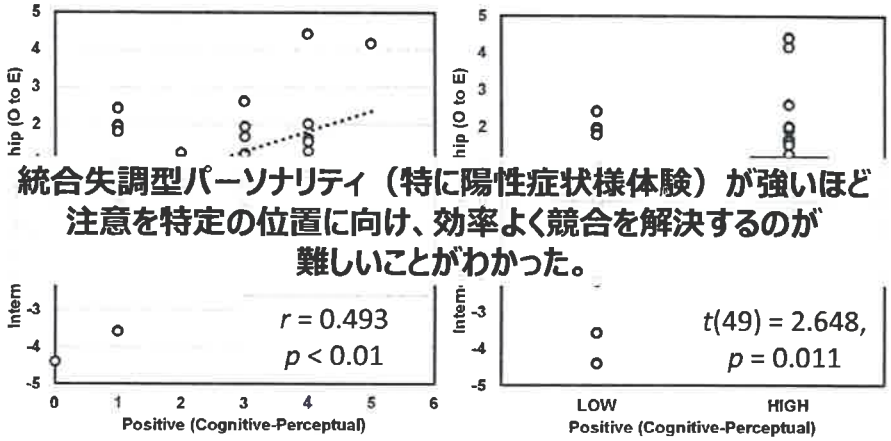
Results Correlation analysis

	A	O	E	A to O	O to A	A to E	E to A	O to E	E to O
Posi	.227	-.170	.047	.059	.130	-.060	-.049	.493**	.306*
Nega	.038	-.041	.037	.289*	-.078	-.252	.028	.109	.181
Diso	-.141	.010	-.040	.145	.012	-.104	-.044	.237	.038
SPQ	.053	-.090	.022	.247	.019	-.209	-.026	.377**	.245

先行研究に従って、
まずSPQの全体得点との有意な相関に着目した。

「定位から制御機能への影響」を表す指標と
全体得点、特に陽性症状様体験との相関が有意であった。

Results Correlation analysis & *t* test



**統合失調型パーソナリティ（特に陽性症状様体験）が強いほど
注意を特定の位置に向け、効率よく競合を解決するのが
難しいことがわかった。**

Conclusion

健常者であっても
統合失調型パーソナリティ特性の強さに応じて
定位と制御機能間の関係に影響が出ることがわかった。

健常者を対象とした本研究と
患者を対象とした先行研究の結果を考慮すると、
定位・実行制御機能に問題がある可能性が高いと考える。

03-5-09

実行機能と統合失調型パーソナリティの関係

Relationship between executive functions and schizotypal personality traits

阿部千裕・河地庸介・成烈完・松江克彦・小川誠二

東北福祉大学

JSPS科学研究基盤研究C（26350995）および東北福祉大学感性福祉研究所における
文部科学省私立大学戦略的研究基盤形成支援事業（平成26年度～30年度）による助成を得て行われた。
演題発表に関連し、開示すべきCOI関係にある企業などはありません。

背景 – 定義

適応的な生活で特に重要かつ
一般知能とは独立した認知機能とされる

実行機能（Executive functions）

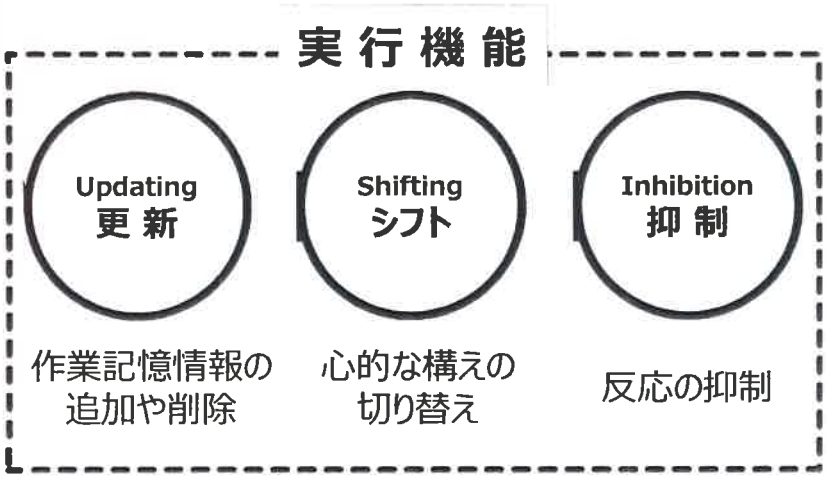
(Damasio, et al., 1994: Friedman, et al., 2006)

に注目する。

…自分自身の思考や行動を制御する心的機能

(Baddeley et al., 1974: Miyake et al,. 2000)

背景 – 定義



(Miyake et al., 2000)

背景 – 問題

統合失調症および統合失調型パーソナリティ特性と実行機能に関する知見は多く報告されている

	Updating	Shifting	Inhibition
統合失調症	*	*	*
統合失調型パーソナリティ特性	△	*	△

*：関連あり △：不一致

(Donohoe et al., 2006: Kane et al., 2016: Gooding et al., 1999: O'Leary et al., 2000: Ettinger et al., 2014)

しかし、Miyake et al. (2000)の分類に基づいて統合失調型パーソナリティ特性と実行機能3要素すべてを測定している研究はほぼ皆無に等しい

目的

健常者を対象として
統合失調症との連続性が仮定される
パーソナリティ特性の実行機能への影響の検討

方法

対象者：健常成人50名（平均年齢20.9歳±1.57）

対象者には本研究について書面および口頭によるインフォームドコンセントを行った。

質問紙：統合失調型パーソナリティ尺度（伊藤ら, 2008）
Schizotypal Personality Questionnaire: SPQ-B

1) 認知・知覚（陽性様症状）
2) 対人関係（陰性様症状）
3) 解体（解体様症状）

行動実験：実行機能を測定する3つの課題

東北福祉大学研究倫理審査委員会の承認を得て実施した。

方法 – Updating 課題



Updating (Keep track) 課題

指標：単語の正解率（Accuracy (%)）

方法 – Shifting 課題

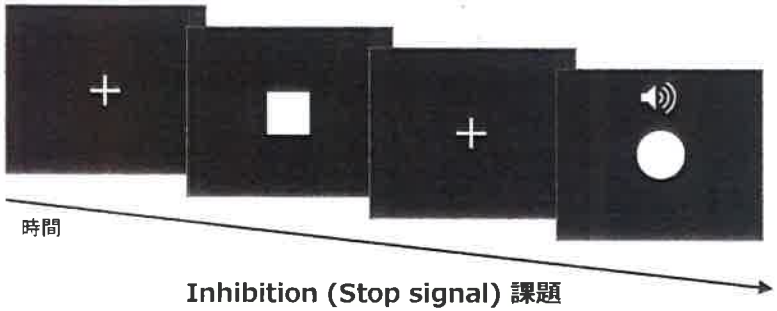


Shifting (Category switch) 課題

指標：判断基準を切り替えるのにかかった
時間コスト(Switch cost (ms))

（切り替えなし試行のRT－切り替えあり試行のRT）

方 法 – Inhibition 課題



Inhibition (Stop signal) 課題

指標：図形の判断に成功した試行 (go trial) の反応時間 (RT (ms))

結 果

SPQ（3つの下位項目＋全体得点）と実行機能3要素間の相関

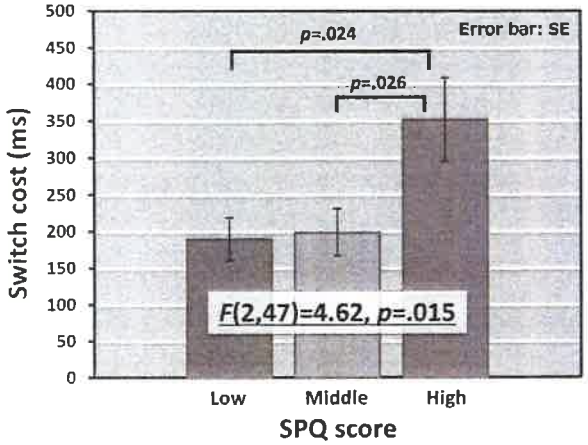
		Updating		Shifting		Inhibition		
		Category_ 3 accuracy	Category_ 4 accuracy	Accuracy average	Switch cost average	Accuracy average	All go RT SD	All go RT mean
認知・知覚 (陽性機症状)	相関係数	.032	.178	.097	.170	.005	-.148	-.070
対人関係 (陰性機症状)	相関係数	.077	.043	.186	.186	-.174	-.240	-.124
解体 (解体機症状)	相関係数	.069	.154	.069	.157	-.137	-.010	-.011
統合失調型パーソナリティ尺度	相関係数	.043	.104	.244	.341*	-.171	-.302*	-.175

*p<.05

SPQの全体得点とshiftingのswitch cost averageに有意な相関が見られた

結 果

SPQの全体得点とshifting課題間の関連



SPQの得点が高いと、心的な構えの切り替えが長くなる

考 察

Updatingとshiftingについての
先行研究の結果が一貫していないように、
統合失調型パーソナリティ特性との関連を確認することはできなかった

実行機能においてshiftingのみが統合失調型パーソナリティ特性と統合失調症の連続性を示唆する